WARWICK
THE UNIVERSITY OF WARWICK

A Thesis Submitted for the Degree of PhD at the University of Warwick

Permanent WRAP URL:

http://wrap.warwick.ac.uk/153956

Copyright and reuse:
This thesis is made available online and is protected by original copyright.
Please scroll down to view the document itself.
Please refer to the repository record for this item for information to help you to cite it.
Our policy information is available from the repository home page.

For more information, please contact the WRAP Team at: wrap@warwick.ac.uk

warwick.ac.uk/lib-publications

Nitrile-oxide/dipolarophile cycloaddition polymers derived from renewable feedstocks

By
Nyle Owen Saul Jones

A thesis submitted for the degree of

Doctor of Philosophy in Chemistry

Supervisor: Professor Andrew Clark

Department of chemistry,

University of Warwick, UK

September 2020

Table of Contents

List of Figures

List of Equations

List of Schemes

List of Tables

Acknowledgments

Firstly, I would like to thank my supervisor Professor Andrew Clark for his support and guidance throughout my time studying at the University of Warwick. I'd also like to thank him for helping me to restart my MChem project part way through the year and for providing me with the funding to carry out my PhD research project.

The office and laboratory have always been busy with multiple different groups and I would like to thank everyone from the Clark, Rourke, Chan, and Clarkson group for their help and for making my work life incredibly enjoyable. I'd particularly like to thank Stuart Henry and Jivan Badhan for their friendship both in and out of work.

The technical staff at Warwick do an amazing job and I thank them all for their help and services. The NMR team, Dr Ivan Prokes and Mr Robert Perry for all their help with high resolution and variable temperature NMR. The mass spectroscopy team run by Dr Lijiang Song, particularly for his help in analysing the aldoxime and oximoyl chloride compounds. Dr Daniel Lester for maintaining the polymer analysis equipment, training me to use them and analyse the results. Mr David Hammond for maintaining the thermal analysis equipment. James Town is another person I would like to thank for his help with MALDI-TOF sample preparation and analysis.

I thank all my family for their love and support throughout the PhD, especially my Mum and Kenny for putting up with me whilst I finished writing this thesis. Finally, I would like to thank Rachel Kerr for her love, support, and lifts into university, I wouldn't have been able to do this without all three of those things.

Declaration

The work presented in this thesis was carried out by the author at the university of Warwick between October 2016 and March 2020, it has not been submitted for a degree at another institution. Where work has been compared to literature results it has been acknowledged and referenced, other previously reported results and ideas have also been acknowledged and referenced.

Nyle Owen Saul Jones

Abstract

Polytriazoles formed by 1,3-dipolar cycloaddition have been widely reported in literature, including some derived from renewable feedstocks. The analogous nitrile oxide-alkyne cycloaddition has received limited attention as a polymerisation technique. This work explores the application of 1,3-dipolar nitrile oxide cycloadditions to the synthesis of renewably derived polymers.

Initial studies were carried out using commercially available dipolarophiles to assess the reproducibility of a polymerisation technique taken from a literature source. The polymerisation technique used molecular sieves as a mildly basic additive to form nitrile oxides from oximoyl chlorides *in situ*. After the technique was shown to successfully form polyisoxazolines, it was applied to dialkene and dialkyne acetamide monomers, these were used to model the behaviour of intended fatty acid derived monomers. Polyisoxazoles and polyisoxazolines were formed with low numbers of repeat units, attempts were therefore made to optimise the polymerisation conditions. Optimisation studies showed that a longer reaction time was required, moving forward this finding was applied to later polymerisations.

Dialkene and dialkyne monomers were derived from palmitic, stearic, oleic, linoleic and linolenic acid. They were used along with a di(oximoyl chloride) premonomer to form polyisoxazoles and polyisoxazolines. Unsaturated fatty chains demonstrated an ability to allow crosslinking to occur through cycloaddition with the *cis*-alkene. Finally, oximoyl chloride and dialkene monomers were derived from vanillin and used in conjunction with the fatty acid derived dipolarophiles to form bio-derived polyisoxazoles. Vanillin was also used to form a difunctional monomer which allowed for the formation of homopolymers by a solvent free polymerisation method.

Abbreviations

3 Å MS	3 Å molecular sieves
4 Å MS	4 Å molecular sieves
$CDCl_3$	Deuterated chloroform
Đ	Dispersity
DCM	Dichloromethane
DEGDA	Di(ethylene glycol) diacrylate
DEGDMA	Di(ethylene glycol) dimethacrylate
DMA	Dynamic mechanical analysis
DMF	Dimethyl formamide
DMSO	Dimethyl sulfoxide
DSC	Differential Scanning Calorimetry
EGDA	Ethylene glycol diacrylate
ES-MS	Electron Spray – Mass Spectroscopy
Et_2O	Diethyl Ether
EtOAc	Ethyl acetate
EtOH	Ethanol
GPC	Gel permeation chromatography
Hex.	Hexane
IR	Infrared Spectroscopy
min	Minutes
m.p.	Melting Point
M_n	Number Average Molar Mass
M_w	Mass Average Molar Mass
NMM	*N*-methylmorpholine
NMR	Nuclear Magnetic Resonance
NO	Nitrile Oxide(s)
OC	Oximoyl chloride
PEGDA	Poly(ethylene glycol) diacrylate
Pet.	Petroleum ether
PMMA	Polymethylmethacrylate
ppt.	Precipitate
PS	Polystyrene
RT	Room Temperature
RU	Repeat Unit
TEA	Triethylamine
T_g	Glass Transition Temperature
TGA	Thermogravremetric Analysis
THF	Tetrahydrofuran
TLC	Thin layer chromatography

1.0 Introduction

The petrochemical boom following the Second World War has led to an ever-increasing dependence on fossil fuels for energy and organic chemicals. Cheap organic chemical by-products from the petrochemical industry are the foundation on which our polymer materials industry is built. These materials are not only used for their structural properties (clothing, building materials, etc.) but also for more sophisticated applications (medicinal, electronics etc.). Oil reserves are being depleted and extraction methods becoming more expensive and dangerous,[1] consequently renewable alternatives to fossil fuel feedstocks are becoming more advantageous. As the majority of fossil fuels are used in the energy sector there has been extensive research towards possible alternatives, these include nuclear,[2,3] biomass,[4] and solar power[5] among many others. Biomass is, however, the major alternative feedstock for organic chemicals and the materials industry.[6]

Biomass is biological material sourced from plants and animals. Usually feedstocks for renewable materials are derived from plant matter in the form of wood, algae, carbohydrates, agricultural waste, and lipids. Biomass can be used directly as building materials or undergo modification to be used as bioplastics, which are polymeric materials derived from these sources. The focus of this work will be on vegetable oil and vanillin derived bioplastics.

1.1 Historical use and production of materials

Natural biosynthesis produces a plethora of macromolecules that are essential to the structure of all living organisms. Humans have used these renewable macromolecules as a source of fuel, shelter, food, and clothing throughout our history. Use of natural materials has become more sophisticated over the centuries and by the mid-19th century it had changed from one of application to modification. The Victorian era saw the first commercial thermoplastics in the form of cellulose acetates **1.1**[7] and nitrates **1.2**,[8–10] whilst vulcanization of poly-isoprene (natural rubber) **1.3** led to elastomers[11] (Figure 1-1). These initial man-made polymers all came from renewable feedstocks.

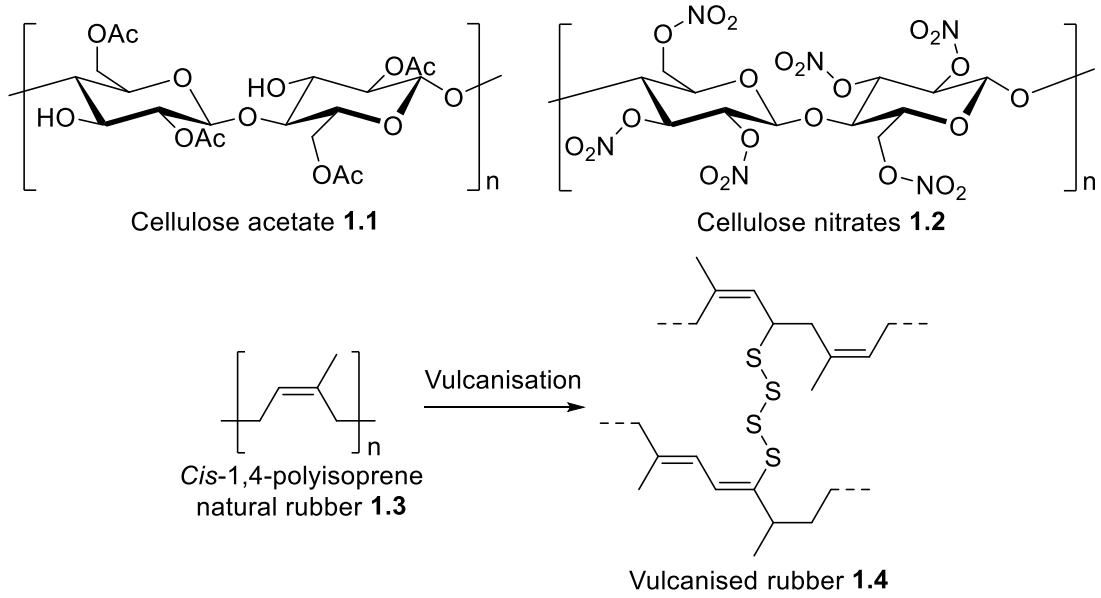

Figure 1-1: Structures of early man-made polymers

Following the Second World War fossil fuels, particularly oil, became the major feedstock for a tremendous diversity of cheap organic chemicals. The "Plastic Age" in which we are currently living was borne out of this availability of cheap, varied, and numerous monomers. Renewable polymers were still present as an industry although holding a significantly reduced market share, which continued to decrease as investment in non-renewable materials increased throughout the 20th century.

Towards the end of the 20th century public perception of petrochemicals began to shift as it became apparent that our dependence on fossil fuels for energy and materials was not sustainable. Petrochemical fuel dominance has been sustained by its economic advantage over renewable energy; however, as fossil fuels become scarcer their

economic advantage will dwindle. Cheap petrochemical derived chemicals are a by-product of the petrochemical fuel refining process, as our reliance on these fuels reduces so will the abundance of readily available chemicals.

Reproduction of the long chain alkanes present in crude oil has been attempted from biomass,[12] whist this would be useful for fuel and solvent synthesis, the small hydrocarbon by-products used in materials synthesis would not be present. Rather than attempting to reproduce crude oil most research investigates methods of adapting renewable substances to replace crude oil as the feedstock for materials synthesis. Like crude oil, biomass must be refined to isolate specific chemicals for use in materials synthesis, this is achieved using a bio-refinery which separates chemicals through physical, chemical and biochemical mechanisms.[13] Renewable polymers have been formed from bio-derived chemicals using two approaches; forming known monomers for conventional polymer synthesis or developing new bio-derived polymer structures.

1.2 Renewable feedstocks

The major aim behind renewable materials research is to derive polymeric materials from renewable feedstocks with minimal environmental impact. Biomass has received the most attention during investigations into renewable feedstocks for polymer production. Carbon dioxide has also been investigated as a renewable feedstock for polymer synthesis as it has the added benefit of reducing atmospheric carbon.

1.2.1 Carbon dioxide derived polymers

Humanities dependence on fossil fuels has resulted in raised levels of atmospheric carbon, mostly in the form of CO_2 which acts as a greenhouse gas. These gases are having a noticeable warming effect of global temperatures. Processes that use gaseous carbon to form valuable products are therefore highly sought after. Using a huge variety of catalysts, CO_2 has been converted into useful small chemicals such as methanol, carboxylic acids, dimethyl carbonate and urea.[14–17] In recent years CO_2 derived polymers (polycarbonates, polyurethanes, polyureas and polyesters) have been investigated, in the synthesis of these polymers CO_2 has been used both to form polymerizable building blocks and directly as a co-monomer.[18]

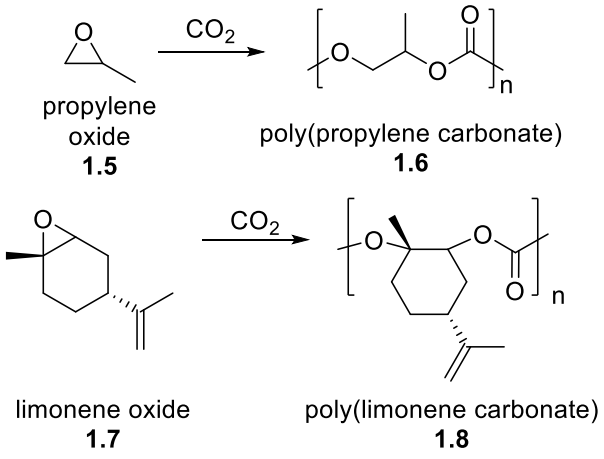

Figure 1-2: Synthesis of CO_2 derived polycarbonates

A focus of carbon dioxide derived polymers has been on polycarbonates, which can be formed by direct use of CO_2 as a comonomer in ring opening copolymerisation. When used with propylene oxide **1.5**, a non-renewable monomer, this method has enabled up to 50 % of polymer mass to be derived from CO_2.[19] The method has also been applied to renewably derived epoxides such as limonene oxide **1.7**, leading to

renewable CO_2 derived poly(limonene carbonate) **1.8**.[20–22] Polycarbonates have also been formed *via* CO_2 derived polymerisable carbonate building blocks. These building blocks have been used as comonomers for ring opening polymerisations and in step-growth polymerisations (Figure 1-3).[18]

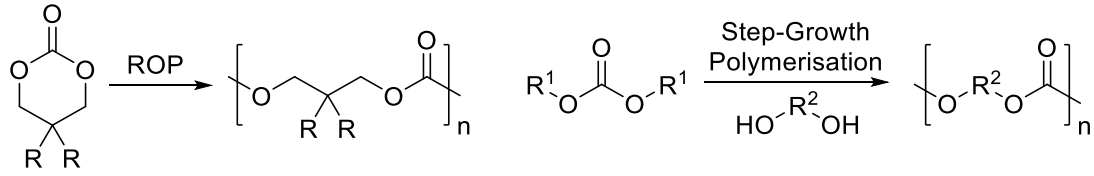

Figure 1-3: CO_2 derived polymerisable building blocks

1.2.2 Biomass resources

Biomass can be sourced from animals and vegetables, both sources have been used extensively throughout human history to provide food, fuel, clothing and shelter. Historically animal biomass provides wool,[23] silk,[24] leather,[25] gelatin,[26] carbon black,[27] resins,[28] fats and waxes,[29] through well-established processes. Modern work using animal biomass has focused on the modification of chitin and chitosan,[30] proteins,[31] and cellulose whiskers from molluscs to synthesise renewable polymers.[31]

Vegetable biomass is split into 3 categories: wood, annual plants and algae. Traditionally wood has been used directly as a fuel, building material and in paper manufacturing. Recent wood research has focused on the modification of 4 components which are present in all species, cellulose, hemicellulose, lignin, and polyphenols. Wood also contains species specific compounds, these can be small molecules like terpenes and steroids, or polymeric molecules such as poly-isoprene **1.3** and suberin.[32] Annual plants (e.g. grains) have a primary use as food although they have also begun to be used as feedstocks for chemicals and bio-fuels. Annual plants have similar core structural components as wood however starch, vegetable oils and saccharides can be isolated from substances annual plants provide. The third category algae are a form of marine vegetable biomass. It is an interesting precursor to materials that can be grown in bulk industrial conditions whilst taking on substantial amounts of atmospheric carbon.[33] Species of algae can provide polysaccharides which have been exploited as a source for polyelectrolyte materials.[34]

1.2.3 Carbohydrate derived materials

Cellulose, hemi-cellulose, chitin, sugars and starch are all carbohydrates and are some of the most abundant sources of renewable carbon. Carbohydrates are defined by four groups, monosaccharides, disaccharides, oligosaccharides and polysaccharides. These groups are used by living organisms for structural purposes (chitin/cellulose) and as an energy source (sugars/starch).

1.2.3.1 Cellulose

Cellulose **1.9** forms the largest component of the structural lignocellulosic framework of plant cell walls, as such it is the most common natural polymer on the planet. Its structural properties rely on a semi-crystalline highly regular polysaccharide composition (Figure 1-4).

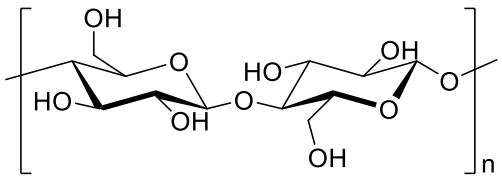

Cellulose **1.9**

Figure 1-4: β-1,4-linked D-glucose polysaccharide structure of cellulose.

This natural bio-polymer was the basis of early polymer work with the formation of acetates and nitrates[7–10] (Figure 1-1). Another widely used cellulose **1.9** derived polymer is cellophane, which (depending on coatings) is biodegradable.[35] Focus of recent cellulose research has been on modification of bulk cellulose to form functionalized macromolecules,[36] modification of fibre surfaces for composite materials,[37] use as nanofibers in composites,[38] and applications of bacterial cellulose.[39]

1.2.3.2 Chitin

Chitin **1.10** is a structural polysaccharide that is found in the exoskeletons and carapaces of crustaceans, reptiles and insects, as well as in fungal cell walls.[40–43] It is the second most abundant bio-polymer after cellulose **1.9** and a major waste product of the fishing industry. Deacetylation of chitin **1.10** gives chitosan **1.11**, an easily functionalisable bio-polymer. Chitin **1.10** and chitosan **1.11** can be used directly or modified to make performance chemicals, packaging materials, and membranes.[42]

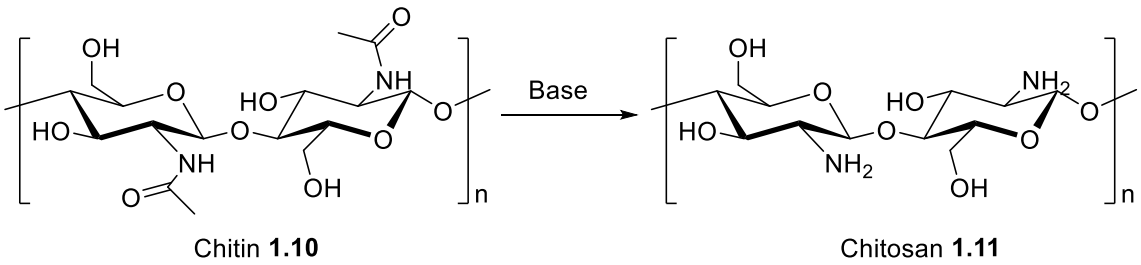

Figure 1-5: Structure of chitin and chitosan derived from fungal cell walls and animal biomass[43]

1.2.3.3 Starch

Like cellulose **1.9**, starch is a biodegradable polysaccharide formed of glucose units, these units however are joined by α-glucosidic bonds.[44] There are two microstructures of starch, linear amylose **1.12**, which reaches molecular weights in the hundred thousand Da, and branched amylopectin **1.13**, which is predicted by light scattering analysis to reach molecular weights above a million Da (Figure 1-6).[45] The ratio of amylose to amylopectin varies between crop sources. Starch is a promising renewable material, it is abundant, cheap and found in many annual crops, it is particularly interesting as a feedstock for biodegradable materials.[46] During the extrusion process starch can undergo multiphase transitions, microstructure and mechanical properties therefore depend on the processing conditions.[47–50]

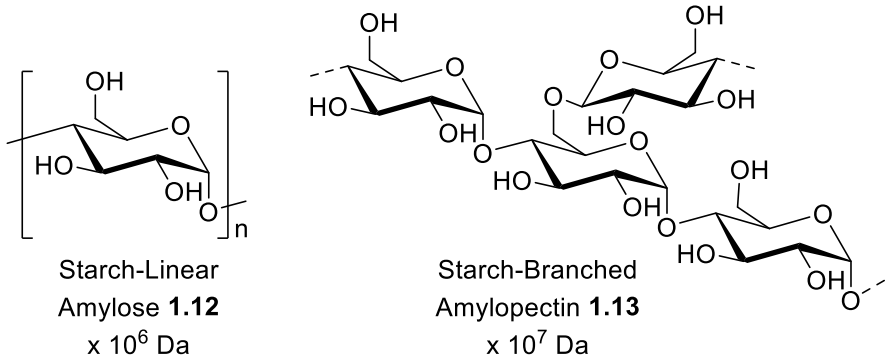

Figure 1-6: Two microstructures of starch

To improve starch's material performance, it has been used to form composites with other bio-degradable natural materials. Starch composites have particularly focused on biodegradable films and packaging. Mechanical properties of starch are improved using cellulose **1.9** fibres, Wallerdorfer *et al.* reported a four-fold increase in tensile strength of thermosplastic wheat starch when reinforced by fibres.[51] Blending of starch with other natural polymers such as proteins also can improve material properties,[52] starch and gelatine composites have been found to form better gas barriers than pure

cellulose films.[53–57] Some starch composites have functionality, Amjad *et al.*[58,59] reported that composites with pomegranate peel introduced antimicrobial functionality[60] whilst also improving the films tensile strength, Young's modulus and stiffness. Bio-degradable foams can also be derived from starch to replace the tradition packaging foams (PS, PU, PE etc.).[61] Starch is not only used as a feedstock for renewable packaging, it can also be used to form drug delivery materials.[62]

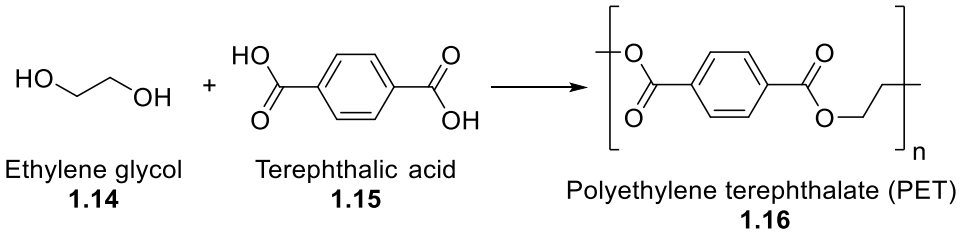

Figure 1-7: Synthesis of polyethylene terephthalate (PET)[63,64]

Instead of using starch directly to form polymers, it can be converted to form monomers already used in petrochemically derived polymers. Ethylene glycol **1.14** used as a comonomer in the production of poly(ethylene terephthalate) (PET) **1.16** can be derived from starch although this is a complex multi-step process.[19,63,64] The other comonomer (terephthalic acid **1.15**) is derived from petrochemical sources although there has been significant recent research in methods of forming it from biomass feedstocks.[63,64] Whilst manufacture of the monomers may be complex, the significant benefit of this direction of research is that the polymerisation processes and polymer properties are identical to well-studied petrochemical derived polymers..

1.2.3.4 Hemi-cellulose

Hemi-cellulose **1.17** is a polysaccharide that is present in both annual and perennial plants at 20 – 30 % by weight, it contains shorter chains than cellulose giving it a more amorphous physical structure. Unlike cellulose, hemi-cellulose contains a mixture of sugars which vary in structure (linear or branched) between different plant species.[65] A variety of techniques are used to extract hemicellulose from biomass, with its composition being dependent on the methods used.[66,67]

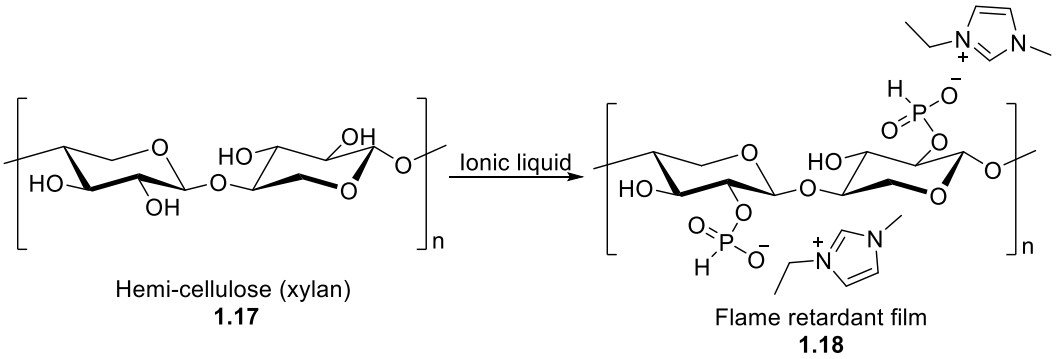

Figure 1-8: Flame retardant films formed from hemi-cellulose[68]

The free hydroxyl groups of hemi-cellulose **1.17** give it a wide scope for functionalisation. Like cellulose **1.9**, hemi-cellulose **1.17** has been acetylated for use in film formation, this was first carried out in 1949.[69] It has gone on to be used directly or modified for the synthesis of films and coating which have found applications in packaging, food-additives, wound dressings and drug delivery.[65,70] In a recent example of hemicellulose's versatility, Kuroda *et al.* reported on its treatment with phosphonate ionic liquids, resulting in flame retardant thermoplastics **1.18**.[68]

Hemi-cellulose is also a renewable source of small molecules. Hydrolysis and dehydration of hemi-cellulose can result in furfural, a promising starting point for bio-derived polymers.[71] Furfural is a five membered aromatic aldehyde that can be converted to form a huge range of chemicals with different functionalities, some of which are already used as monomers in the polymer industry (Figure 1-9).[71]

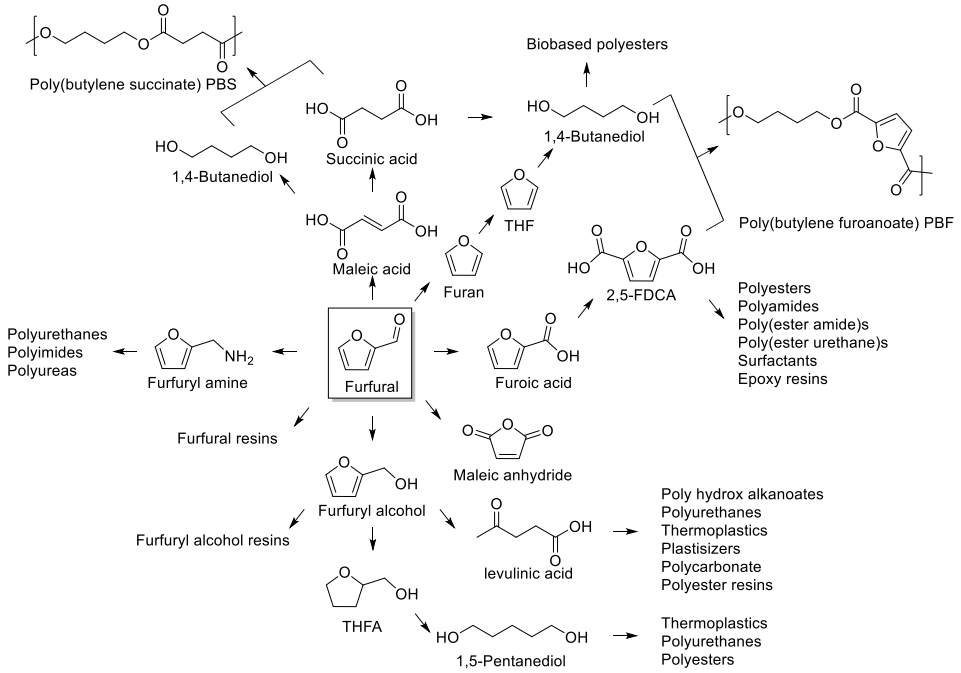

Figure 1-9: Applications of furfural in small molecule/monomer synthesis[71]

1.2.4 Lignin derived materials

Another component of plant cell walls, lignin **(**Figure 1-10**)**, has an irregular branching phenolic structure[72] that contains 30% of non-fossil carbon on earth.[73] Due to the interwoven nature of lignocellulose industrial isolation of cellulose **1.9** and hemicellulose **1.17** gives lignin as a by-product, which has traditionally been burnt as fuel.[74] To isolate cellulose **1.9** the papermaking industry developed the Kraft processing method. It is a delignification processes that isolates cellulose **1.9** and gives black liquor as a by-product, a solution which contains water soluble sulphonated lignin fragments.[72,75,76] Through the LignoBoost process purification of lignin from black liquor has been achieved on a large scale.[77] The organosolv process is a more recently developed alternative to the Kraft process that produces both higher quality paper pulp and higher quality lignin.[78–80] Furthermore, biomass refineries are expected to produce significant quantities of lignin whilst isolating cellulose **1.9** and hemicellulose **1.17** through steam explosion processing. Isolation by steam explosion gave higher purity lignin than recovery from black liquor.[81]

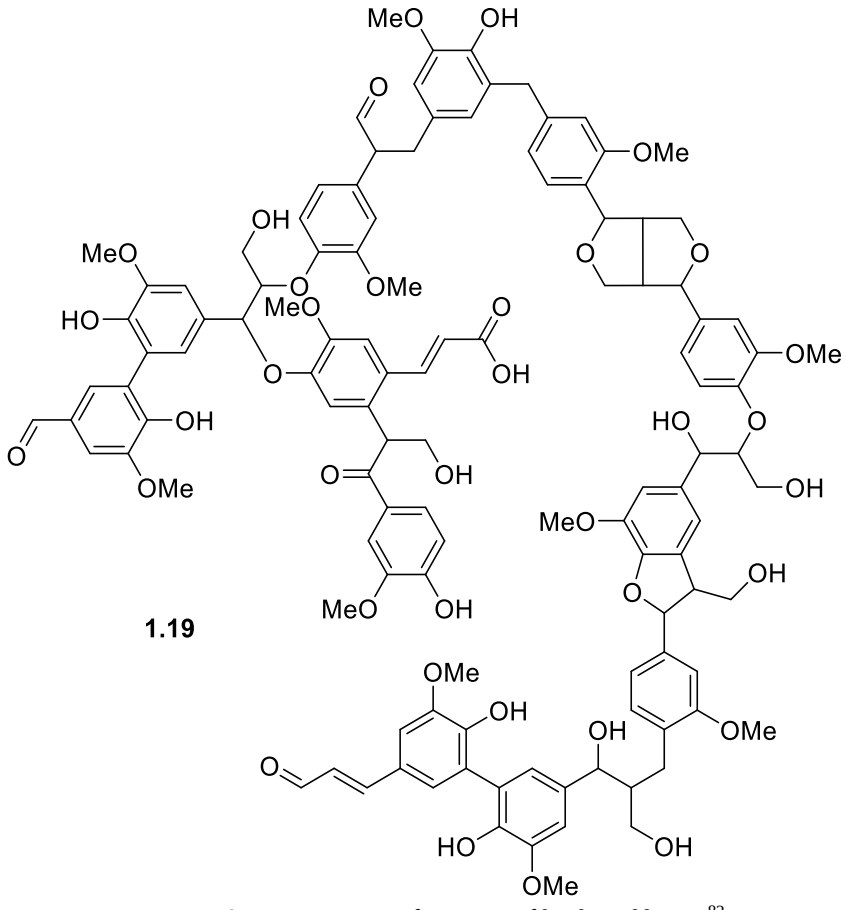

Figure 1-10: Representation of a section of hardwood lignin.[82]

Lignin and its derivatives have well established low value roles as cement additives, adhesives, binders and dispersants.[83,84] To increase the value of lignin feedstocks it has been explored as a macromonomer and a polymer additive.[85,86] Lignin composites are expected to improve the structural properties of polyolefins, with higher molecular weight and chemically modified lignin having better compatibility.[87] Polylactide (PLA) is an established biodegradable polymer derived from lactic acid that suffers from poor thermal and mechanical properties.[88] Chung *et al.*[89] described methods of improving the compatibility of lignin and PLA, whilst Spiridon *et al.*[90] reported improved thermal stability and mechanical properties of lignin/PLA copolymers relative to PLA.

In materials synthesis lignin has been reported to have many applications beyond use as a composite or copolymer. Investigations have been carried out on improving lignin's potential as an adhesive feedstock, particularly as a phenol formaldehyde replacement in the manufacturing of wood composites (plywood, chipboard, etc.).[91,92] Lignin has also been reported to have applications in waste management, acting as flocculants and absorbents.[93–96] Further applications of lignin have explored its use in battery energy storage and in hydrogels for the biomedical sector.[97]

Lignin has a range of applications in its biopolymer form, its true value however is in the wealth of renewable aromatic molecules contained within it. Aromatic compounds are the basis of many routine and specialised materials, from polystyrene to Kevlar. Most aromatic compounds used by industry are derived from petrochemical feedstocks in the form of benzene, toluene, xylene, and cumene.[98] Biomass is the only alternative source of renewable aromatic molecules, with lignin as the most readily available feedstock.[98] Although the isolation of aromatic compounds from lignin has received extensive attention[99] the only commercial process is the production of vanillin **1.20** (Figure 1-11) from lignosulphonates.[100,101]

1.3 Vanillin

Vanillin (4-hydoxy-3-methoxybenzaldehyde, **1.20**), is the major component extracted from the vanilla orchid, *Vanilla planifolia*,[102] it is responsible for vanilla extract's distinctive aroma and taste. Due to the expense of growing and extracting from *Vanilla planifolia* only 1% of industrially used vanillin **1.20** is produced this way, mainly for food and cosmetic applications. To meet industrial demand for vanillin **1.20** it is derived from other sources. In the late 1930's vanillin **1.20** was first produced on an industrial scale using waste lignin from the paper industry.[103] During the petrochemical boom that followed the Second World War guaiacol **1.21**, a petroleum derivative, became the economically preferable feedstock.[104] Currently two companies produce most of the world's vanillin **1.20**, Salvay-Rhodia producing 85% from petroleum sources and Borregaard producing the majority of the rest from lignin.[105]

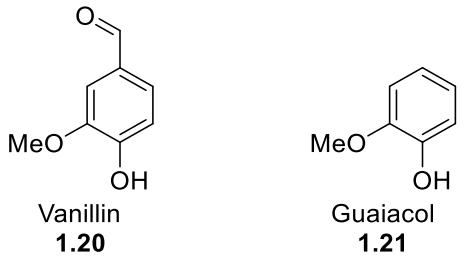

Figure 1-11: Structure of vanillin **1.20** and guaiacol **1.21**

In recent decades significant improvements have been made in the methods for the extraction of phenolic compounds from lignin. These have been brought about by better understanding of the lignin depolymerisation mechanism which has led to increased yields and purity.[106–113] These new depolymerisation techniques have focused on the use of alkali media with O_2 to produce vanillin **1.20**.[82,114] Although others methods have been developed using acidic conditions,[115] ionic liquids,[116] microwaves,[6] and biotechnologies.[117] Traditionally vanillin **1.20** has been used as an additive in the food and pharmaceuticals industry.[118,119] The recent improvements in the production of vanillin **1.20** from lignin however has made it a promising platform chemical for the renewable materials industry.

Polymers have been formed from vanillin **1.20** using three approaches. Direct use of a functionalised vanillin monoaromatic monomer (**1.22**, Figure 1-12)[120]. Use of a diaromatic monomer formed by coupling of two vanillin derivatives before

functionalisation (**1.23**, Figure 1-12).[121] Introducing vanillin **1.20** or vanillin derivatives onto a pre-formed polymer to alter its properties (**1.24**, Figure 1-12).[122–124]

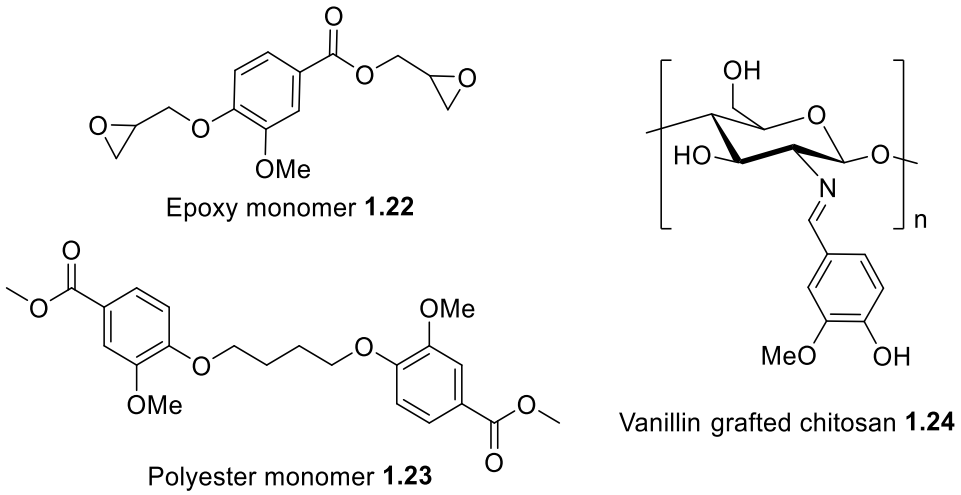

Figure 1-12: Examples of the use of vanillin in monomer and polymer formation

Vanillin **1.20** is easily functionalised through the phenol and aldehyde, furthermore lignin depolymerisation processes can use harsh oxidative or reductive conditions leading to diols and carboxylic acids (Figure 1-13).[125,126] The same oxidations and reductions can be purposefully carried out to introduce sites for modification.[126] The diol **1.27** has been used directly to synthesis polyesters.[127] Modification of compounds **1.25** – **1.27** has resulted in a variety of monomers in the form of difunctionalised epoxy monomers (e.g. **1.22**, Figure 1-12),[120] dialkenes, diamines and dicarboxylic acids, as well as dicarbonate esters for ring opening polymerisations. [98,105,126]

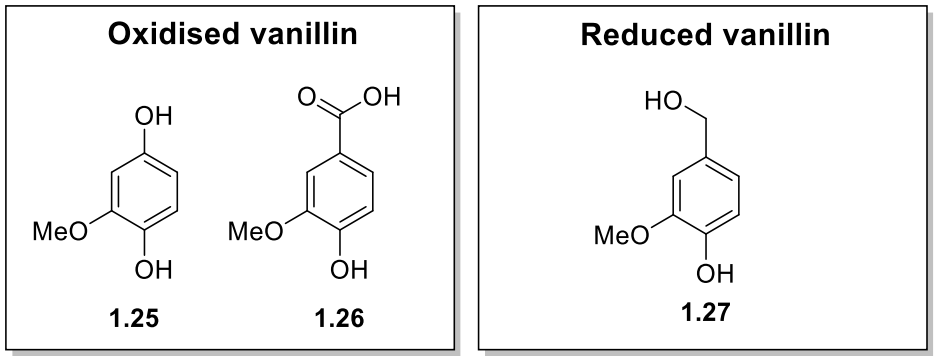

Figure 1-13: Oxidised and reduced vanillin products of some lignin depolymerisation processes.

Diaromatic monomers have been formed by linking two vanillin **1.20** molecules or derivatives together before introducing monomer functionality. Aufo *et al.*[128] reported the formation of dialkene **1.28** and its subsequent conversion to epoxide monomer **1.29**, a possible renewable alternative to bisphenol A diglycidyl ether **1.30** a major epoxide monomer used by industry and derived from hazardous bisphenol-A (BPA).

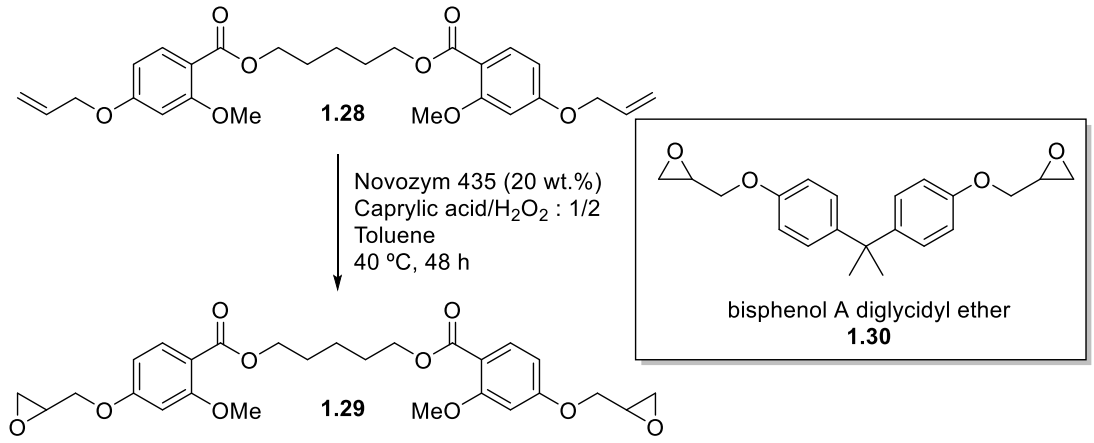

Figure 1-14: Synthesis of diaromatic vanillin derived epoxide monomer[128]

The method of linking vanillin **1.20** through the phenolic group or by an aldehyde derivative has been used to form a variety of monomers.[129–133] Bisvanillin **1.31** has also been formed by Fe(II) or enzyme promoted oxidative coupling.[134] Amarasekara *et al.*[135] demonstrated that oxidative coupling of vanillin **1.20** could be followed by electrochemical reduction of the aldehyde. The resulting polymer **1.32** was estimated to have a M_n around 10 kDa and analysis by TGA indicated thermal stability to 300 ºC. Amarasekara *et al.*[136] also went on to show how the reaction of bisvanillin **1.31** with diamines formed Schiff base polymers **1.33**. These polymers **1.33** had lower thermal stability than the previously reported polymers **1.32**[135] but did show an ability to chelate metal ions.

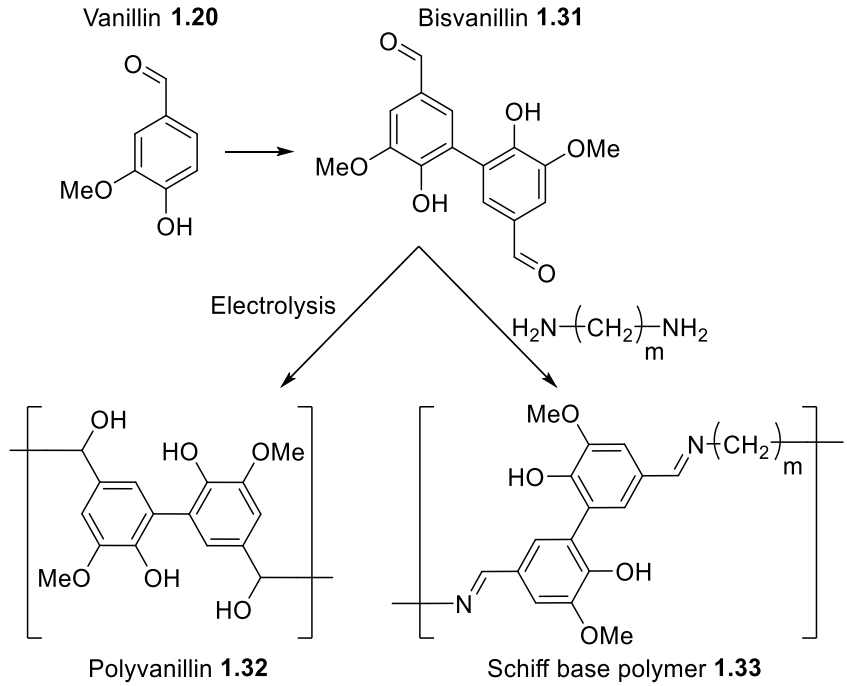

Figure 1-15: Vanillin derived polymers *via* bisvanillin **1.31**[135,136]

Vanillin **1.20** and its derivatives have been grafted onto pre-existing polymers to alter their physical characteristics and functionality. The amine group of chitosan **1.11** has allowed for easy vanillin functionalisation through the formation of Schiff bases. Vanillin functionalised chitosan **1.24** (Figure 1-12) forms strong gels, a property attributed to H bonding which leads to a self-organised lamella phase.[123,124] Chitosan films modified with vanillin **1.24** were reported to have improved tensile strength and optical properties,[122] they also had reduced vapour transmission and antifungal properties on *Aspergillus flavus*[122] and *Canidad albicans*.[123] Renbutsu *et al.*[137] grafted vanillin derived acrylates onto chitosan *via* reductive amination. The functionalised chitosan **1.34** had improved solubility in several organic solvents and were reported to crosslink by free radical polymerisation when exposed to UV light (Figure 1-16).

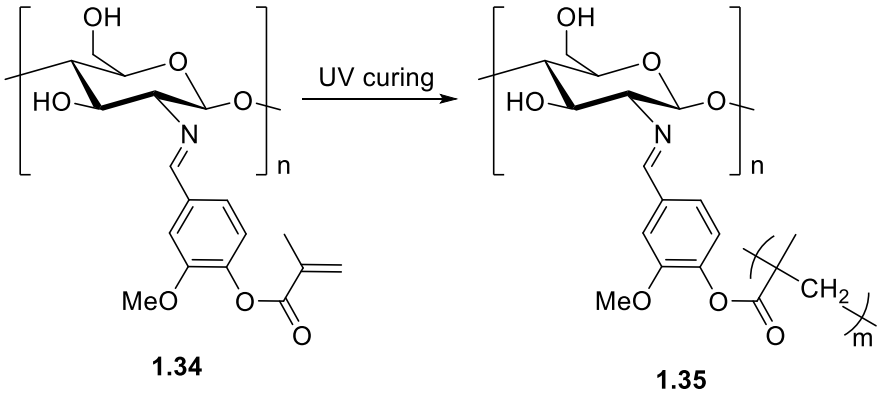

Figure 1-16: Curing of chitosan functionalised by methacrylic vanillin

1.4 Vegetable Oils

Lipids are biological fats and oils that dissolve in non-polar solvents, they are present in the cell membranes of all living organisms.[138] These oils are particularly prevalent in nuts and seeds and have been exploited by humans for thousands of years. Typically, at room temperature plant lipids are liquid, thus they are known as vegetable oils. They are mostly made up of triglycerides, which are an ester of glycerol and fatty acid chains (Figure 1-17). The fatty acid component varies between plant species, season and growing condition, which significantly affects the chemical and physical properties of the vegetable oil.[139,140] Depending on the fatty acid chains, triglycerides present a range of possible sites for chemical modification,[141] those most commonly exploited are the alkene, allylic, and carbonyl functionalities (Figure 1-17). Some vegetable oils (e.g. castor oil) contain fatty acids bearing easily modified hydroxyl or epoxide functionalities, such as ricinoleic **1.41** and vernolic acid **1.42** (Figure 1-18).

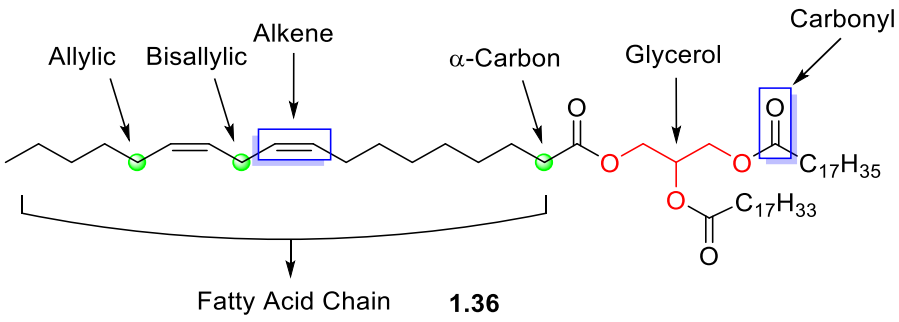

Figure 1-17: Representation of a triglyceride, highlighting functionalities for possible chemical modification.

Fatty acid structure varies in chain length and level of unsaturation, some fatty acids also contain other functional groups (Figure 1-18). Characterisation of fatty acids is denoted numerically, for example oleic acid **1.39** is 18:1 indicating it is 18 carbons long with 1 alkene bond. To retain the correct viscosity warm blooded organisms and those that exist at higher temperatures generally have shorter saturated chains in their triglycerides (14:0 myristic acid).[142] Conversely, cold-blooded and marine organisms that exist at lower temperatures have a higher proportion of longer polyunsaturated fatty acid chains (20:5 Eicosapentaenoic acid). Vegetable oils predominantly contain medium length fatty acid chains with limited levels of unsaturation (Table 1-1).[143] The fatty acid composition of triglycerides is determined by fatty acid methyl ester (FAME) analysis.[143,144]

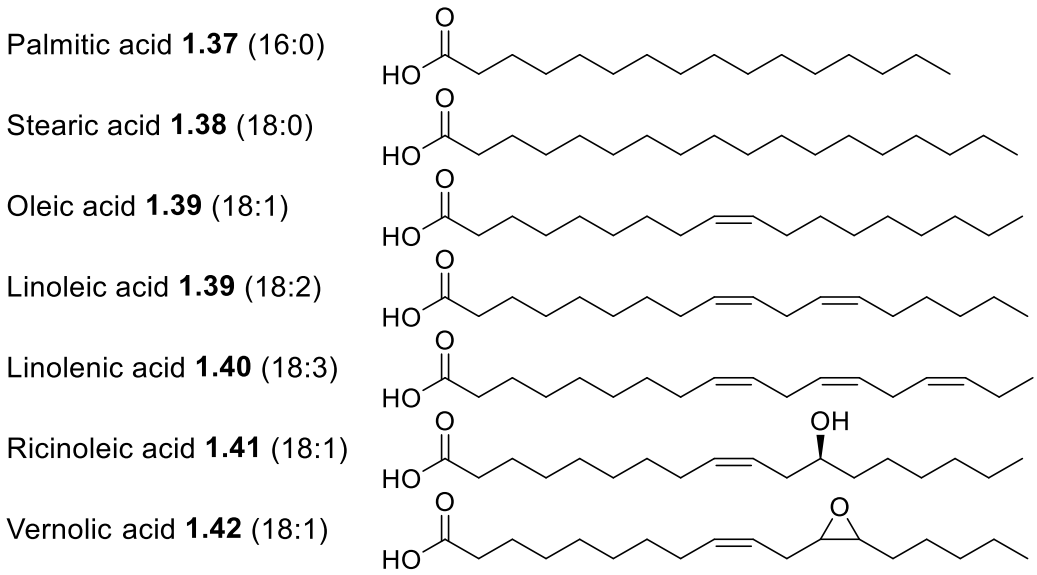

Figure 1-18: Typical fatty acids present in vegetable oil.

Plant Oil	Fatty acid composition / %[a]				
	C16:0	C18:0	C18:1	C18:2	C18:3
Canola	4	2	64	19	9
Cocoa Butter	26	34	35	-	-
Corn	13	3	31	52	1
Cottonseed	23	2	17	56	-
Grapeseed	7	4	16	72	>0.5
Linseed	6	3	17	14	60
Olive	10	2	78	7	2
Palm	44	4	39	11	-
Rapeseed	4	2	62	22	10
Safflower[a]	7	3	14	75	-
Sesame	9	6	41	43	-
Soybean	11	4	23	53	-
Sunflower	6	5	65	26	-

[a]Composition varies significantly between species, growing conditions, and extraction methods.

Table 1-1: Fatty acid composition of a range of common vegetable oils, determined by FAME analysis.[143,144]

Plant lipids are widely used by industry due to their ease of modification, low toxicity, and renewable nature. Their use ranges from biofuels and materials to food and cosmetics. Global production of plant oils for 2019/2020 was 207.5 million metric tonnes,[145] with palm (75.7 mil.), soybean (56.7 mil.), rapeseed (27.0 mil.) and sunflower oil (20.6 mil.) making up the majority.[146] As such they are a readily available feedstock for renewable materials.

Polymers have been derived from vegetable oils following two strategies. One approach is direct polymerisation of triglycerides using function groups that are

already present in the fatty acid chain (e.g. alkenes, epoxides and alcohols). The second method involves modification of vegetable oils to introduce functionality and allow for the formation of a variety of polymers. The second tactic can involve isolating the fatty acids or derivatives as the feedstock for monomer synthesis by reactions at the carbonyl.

1.4.1 Reactions at the allylic carbon

The allylic carbon in unsaturated fatty acids is prone to autoxidation, this is particularly prevalent in poly unsaturated chains with multiple bis-allylic carbons.[147] Highly unsaturated triglycerides, known as drying oils, have been used for coatings for thousands of years. Due to labile bis-allylic hydrogens these oils self-polymerise in an oxidative atmosphere, forming a dry film (Figure 1-19).[148] Drying oils can be used directly as coatings, such as linseed oil finishing on wood, or included in paints and coatings as film formers.[149] Metal soaps, often cobalt or manganese compounds, are normally included to reduce film drying time, these are added in small amounts along with other additives to alter the film's properties.[150]

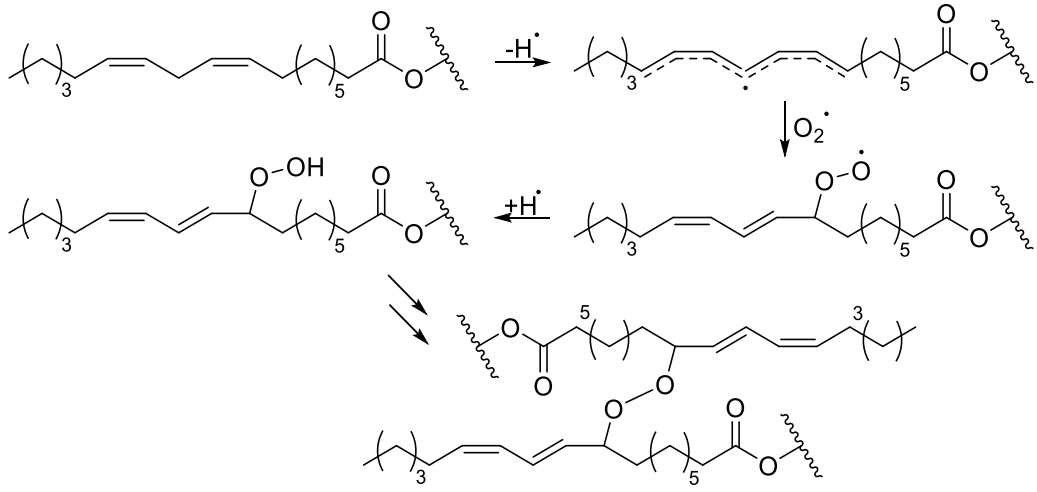

Figure 1-19: Representation of the autoxidation reaction of the drying oils (polyunsaturated triglycerides)

The lability of allylic hydrogens has also been used to incorporate functionalities into the fatty acid chain. Hydroxyl groups have been introduced at this site. Once multiple hydroxyl groups are present the triglyceride can be used as a feedstock for polyurethanes and polyesters. Cadiz *et al.*[151,152] introduced allylic alcohols into sunflower oil **1.44**. Acrylate groups were incorporated using these alcohols and the subsequent monomers **1.46** underwent free radical polymerisation to give cross-linked

materials **1.47**.[151] A second study converted allylic alcohols **1.45 to** phosphinites, a sigmatropic rearrangement then resulted in phosphine oxide groups **1.49** which gave the resulting cross-linked material **1.51** flame-retardant properties (Figure 1-21).[152]

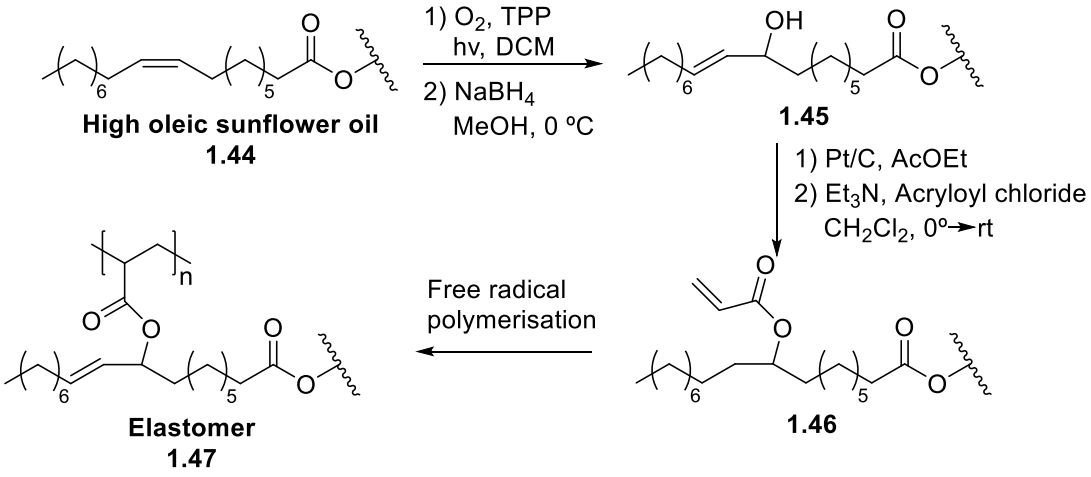

Figure 1-20: Introduction of allyilic alcohols into sunflower oil and subsequent formation of polyacrylate.

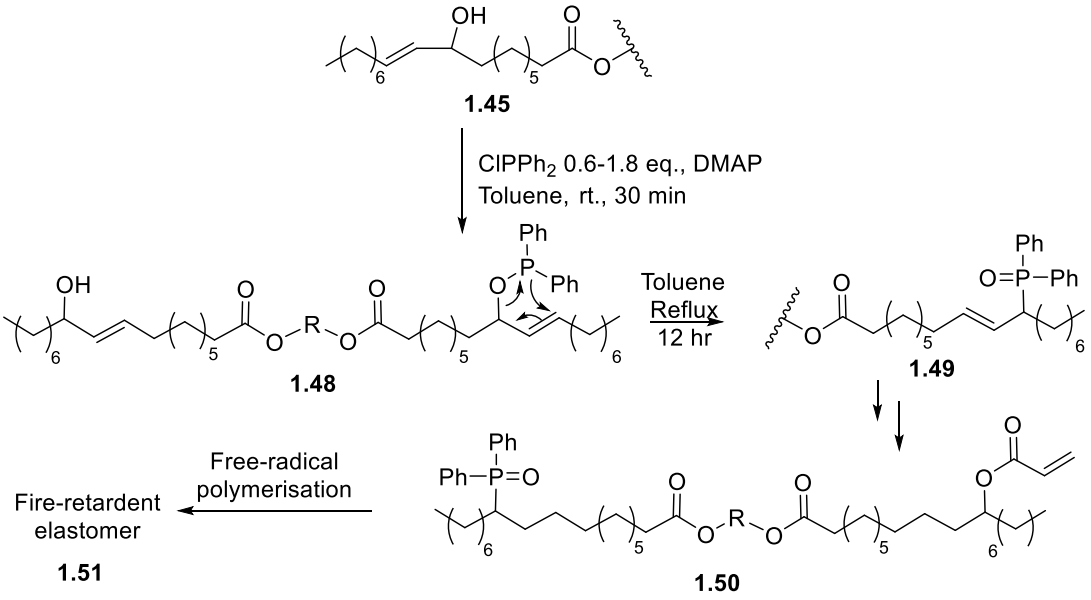

Figure 1-21: Synthesis of sunflower oil derived fire retardant materials

The formation of allylic bromides by Wohl-Ziegler bromination is a well-established process that has been used during the formation of a variety of vegetable oil derived isocyanate monomers.[153,154] Traditionally Wohl-Ziegler bromination has used ozone depleting CCl_4 as the solvent. Using fatty acid methyl esters Winker *et al.*[155] demonstrated high yields and conversion of bromination could be achieved using cyclohexane. The brominated esters were then used to form polymers by two different

methods. As with previous studies[153,154] the allylic bromine atom was used as a leaving group to introduce different functionality, in this case a secondary amine was formed and used to synthesise polyamides.[155] The second method used the brominated esters as initiators for atom transfer radical polymerisation (ATRP) of methyl methacrylate, showing good control of molecular weight.[155]

1.4.2 Reactions at the Alkene

The alkene of unsaturated triglycerides is exploited commercially *via* a range of methods. Most commonly by hydrogenation, the reduction of the unsaturated fatty acid chains to completely saturated has been widely applied in the food industry since its realisation in 1902.[156]

Unsaturated triglycerides and their derivatives are available for olefin metathesis, which splits the fatty acid chain at the double bond with regeneration of C=C in both products. The metathesis process generally uses a Grubbs catalyst and has been used for both monomer preparation and as a polymerisation technique.[157] A simple application of metathesis has been reported with drying oils. Erhan *et al.* reported a reduction in the drying time of unmodified soybean oil by 42% with the inclusion of 5% by weight of self-metathesized soybean oil.[158]

1.4.2.1 Epoxidation of triglycerides

The ability to epoxidise unsaturated fatty acid chains is one of the most useful reactions in triglyceride-based materials chemistry. Epoxidised vegetable oils are industrially important platform chemicals that have applications in the synthesis of plasticisers, coatings, resins, PVC stabilisers, and lubricants.[159–162] Epoxidation of olefins is most often achieved using peroxide containing compounds, peracids.[163] For industrial processes the more volatile peracids such as peracetic acid are favoured, as they can be generated *in situ* and by-products are easily removed.[164] Epoxidation using peracids however does have several issues that need improving.[163] Metal catalysts have been investigated; they were found to reduce the need for excess peroxide and reduced competing reactions.[165] Enzymes have also been found to be viable environmentally friendly alternatives to the peroxide method.[166]

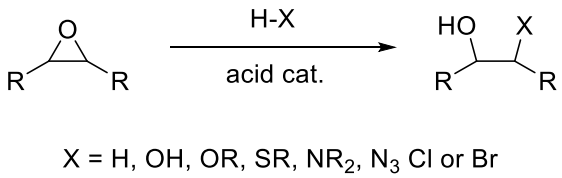

Figure 1-22: Nucleophilic ring opening of epoxides

Epoxidised vegetable oils readily undergo nucleophilic ring opening due to ring strain, allowing for the inclusion of most nucleophiles such as alcohols, amines, and halogens (Figure 1-22). These ring-opened triglycerides can be used directly in polymer synthesis or further modified to form monomers with different functionalities. A common example is the use of epoxidised triglycerides to form polyol monomers for polyurethane synthesis.[167–172] Nucleophilic ring opening of epoxidised triglycerides can be used to directly to form polyethers.[161,162,173,174] These polyethers can be formed using a low equivalence of cationic initiator to induce self-polymerisation[175] or by copolymerisation often with a difunctional or cyclic co-monomer.[176]

Previously Clark *et al.*[174] has reported on the production of polyethers by the copolymerisation of epoxidised vegetable oils with THF, catalysed by a Lewis acid. The polyethers terminated with hydroxyl groups to leave polyols which were used as macromonomers along with a diisocyanate to form polyurethanes. Polyurethanes formed from the THF-(epoxidised palm oil) copolymers showed improved mechanical properties compared to those formed directly from ring-opened epoxidised palm oil.

1.4.3 Reactions at the carbonyl

Whilst many vegetable oils are used directly by industry, others undergo reactions at the carbonyl to form fatty acids or derivatives and glycerol **1.52**, an industrially useful by-product.[177,178] These are well established industrial processes that generally produce fatty acids, fatty esters or fatty amides (Figure 1-23) as platform chemicals. The fatty acids and their derivatives can be used in materials synthesis using the functionalities described in sections 1.4.1 and 1.4.2.

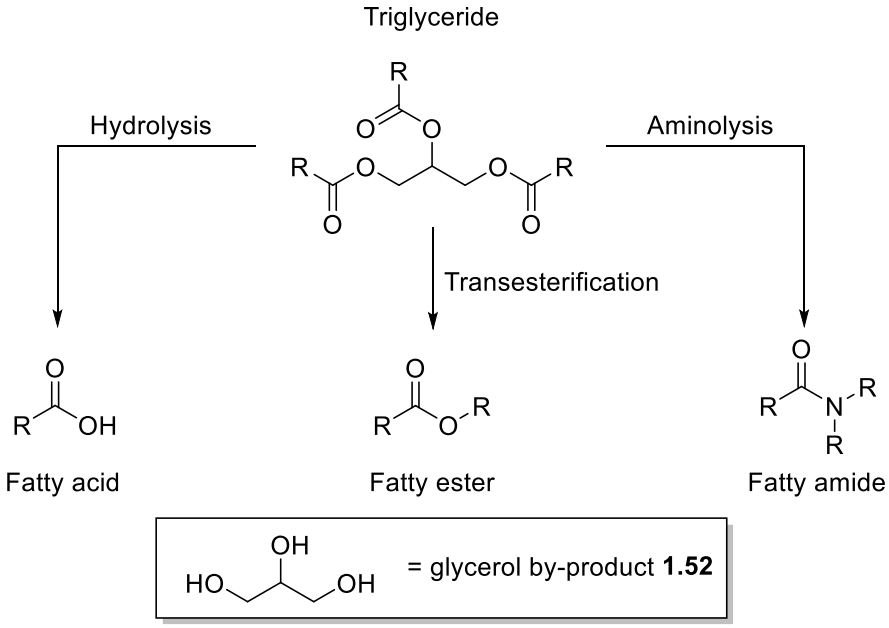

Figure 1-23: General products of reactions at the triglyceride carbonyl

1.4.3.1 Hydrolysis

The ester functionality of a triglyceride is susceptible to nucleophilic substitution due to a labile glycerol **1.52** leaving group. The hydrolysis of triglycerides can therefore be achieved at moderate temperatures with water or steam, resulting in free fatty acids and glycerol **1.52**.[179] This reaction is widely used by industry to produce fatty acids for use in the production of soaps, pharmaceuticals, cosmetics, and a range of other products.[180] Miscibility of the vegetable oils and water is the main limiting factor, which has led industry to use superheated steam hydrolysis of triglycerides as the primary method of commercial fatty acid production.[181] Cheaper alternative processes have been investigated, these use solid acid catalysts that would allow for lower temperatures and a continuous process.[182]

1.4.3.2 Transesterification

Transesterification of triglycerides is another industrial important reaction of vegetable oil. It is used to form simple alkyl esters for use as fuels or to introduce functionality for use as performance chemicals. The reaction is generally promoted using alkali catalysts, although the use of acid and enzyme catalysts along with microwave irradiation has also been investigated.[183–186]

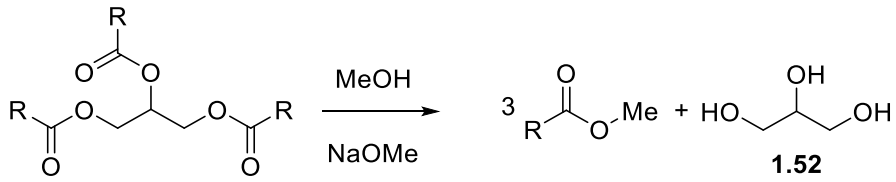

Figure 1-24: Methyl ester biodiesel synthesis

Vegetable oils as biofuels have received significant interest as an alternative to petroleum. Global biodiesel production for 2018 was 33.6 billion litres.[187] Vegetable oils cannot be used directly as biodiesel due to their higher viscosity and low volatility.[188,189] Transesterification to methyl and ethyl fatty acid esters modifies the properties to be closer to conventional diesel. Biodiesel yields are typically increased with the use of alkali catalysts (Figure 1-24). The remaining glycerol **1.52** can be removed, although its presence reduces crystallisation temperature allowing for biodiesels use in colder climates.[190]

Functionality for performance chemicals can be introduced by glycerolysis. Reaction of triglycerides with different ratios of glycerol **1.52** produces mono and di-glycerides (Figure 1-25).[191] These hydroxy bearing products have a direct use, mostly as surfactants, in many industries as well being open to further modification.

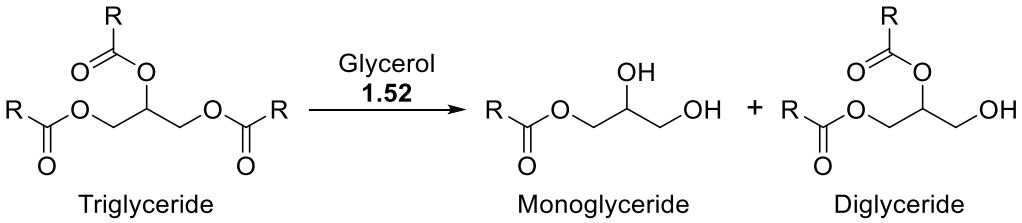

Figure 1-25: Glycerolysis of triglycerides

1.4.3.3 Aminolysis

Triglycerides can be converted to fatty amides via aminolysis, early studies by Gast et al.[192] reported direct formation of fatty amide diols from linseed oil using sodium methoxide catalysts (Figure 1-26). In industry however this process is often multi-stepped with fatty acid or fatty ester intermediates.[193] Industry has traditionally produced fatty amides by reaction of fatty acids with ammonia at high temperatures and pressures (~200 ºC, 345-600 kPa).[194] Like transesterification, recent studies have shown direct aminolysis of triglycerides can be achieved with microwave irradiation or a variety of alkali, acid and biological catalyst.[193,195–200] As with the early studies by Gast[192] aminolysis is often carried using ethanolamine or diethanolamine **1.53**.[201]

The resulting fatty amide alcohols have an amphiphilic nature and are important surface activating agents.[202] They also have analgesic, anti-inflammatory, anticonvulsant, and anti-depressant properties.[203]

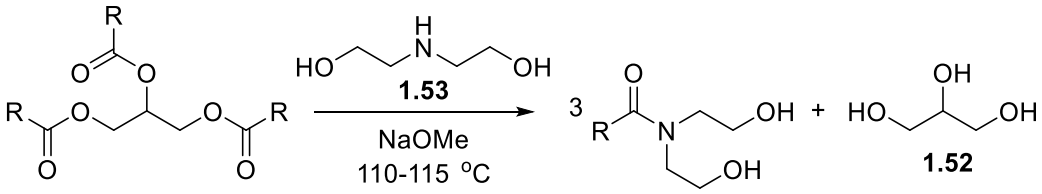

Figure 1-26: Aminolysis of a triglyceride with diethanolamine **1.53**[192]

1.4.3.4 Carbonyl modification for materials synthesis

Removal of glycerol **1.53** by nucleophilic substitution is a common first step in deriving monomers from vegetable oils, it is particularly prevalent in the formation of polyols which can be used in the synthesis of polyurethanes. Mono-glyceride polyols and fatty amide diols have been used along with diisocyanates to form polyurethane resins and blown foams.[204–207] By introducing functionality through the carbonyl the fatty chain is generally left unaltered during polymerisation and acts as a plasticizer, this property has allowed the formation of thermoplastic polyurethanes.[171]

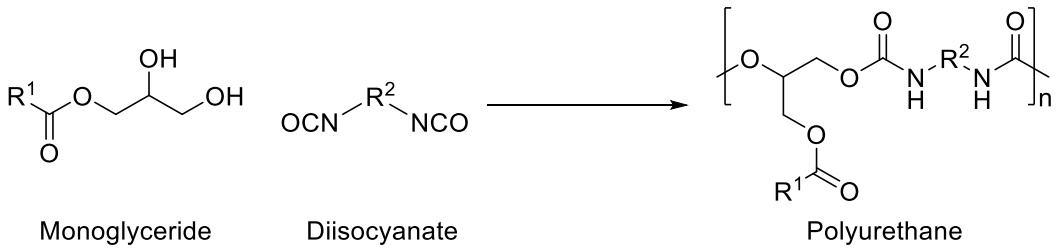

Figure 1-27: Polyurethane synthesis

Palanisamy *et al.* formed water-blown polyurethane foams using diethanol fatty amides derived from karanja and castor oil along with methylene diphenyl diisocyanate.[208,209] Karanja oil derived foams were found to have good compression and flexural strength that were dependent on foam density.[208] Prior to aminolysis of castor oil the alkenes were epoxidised and ring opened, forming secondary alcohols to increase cross-linking.[209] The castor oil derived foams had higher density and lower mechanical strength than the respective karanja oil foams, although in both studies the foam properties were highly dependent on the composition of the foam formulation.

1.5 1,3-Dipolar cycloadditions

Cycloadditions between 1,3-dipole systems and dipolarophiles (traditionally alkenes or alkynes) have been known for over 100 years, but it was not until the mechanistic work of Prof. Rolf Huisgen in 1963 that these reactions were described in detail.[210,211] Systematic analysis of these cycloaddition reactions by Huisgen has led them often being described as "Huisgen cycloadditions." Huisgen defined these cycloadditions as occurring between a multiple bond dipolarophile and a 1,3-dipole, *a*-*b*-*c*, where *a* has an electron sextet and thus a formal positive charge, whilst *c* has an unshared pair of electrons leading to a negative charge (Figure 1-28). The cycloaddition creates two σ-bonds whilst removing two π bonds, leading to an uncharged five-membered ring. After extensive debate in the 1960's between Huisgen and Firestone,[212] the cycloadditions were determined to proceed by a concerted mechanism and not a diradical mechanism.[213]

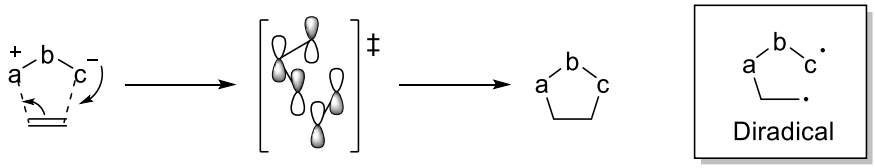

Figure 1-28: Mechanisms proposed by Huisgen (*left*) and Firestone (*right*)

The 1,3-dipoles fall into two categories, the allyl dipoles and the propargyl/allenyl dipoles.[214] An electron sextet on a carbon, nitrogen or oxygen is not stable and so the dipoles must have resonance stabilisation that would allow for octet structures (Figure 1-29). To allow this the central atom *b* of the allyl anion type can be nitrogen, oxygen or sulfur, whereas in the propargyl/allenyl anion type it can only be nitrogen. Huisgen indicated 16 parent dipoles, 12 allyl type and 6 propargyl/allenyl type (Figure 1-30).

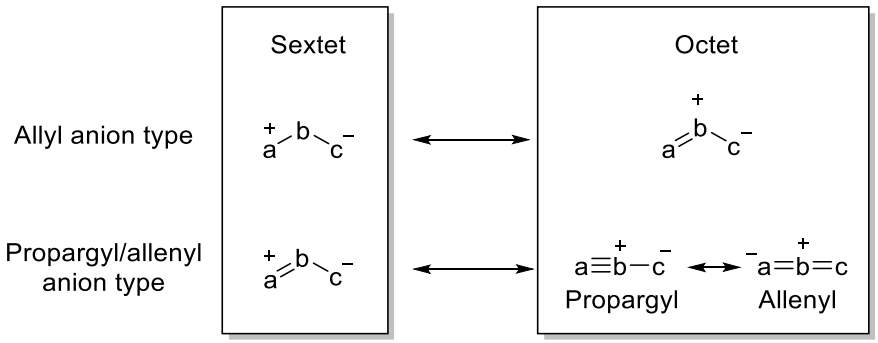

Figure 1-29: Example resonance structures of 1,3-dipoles

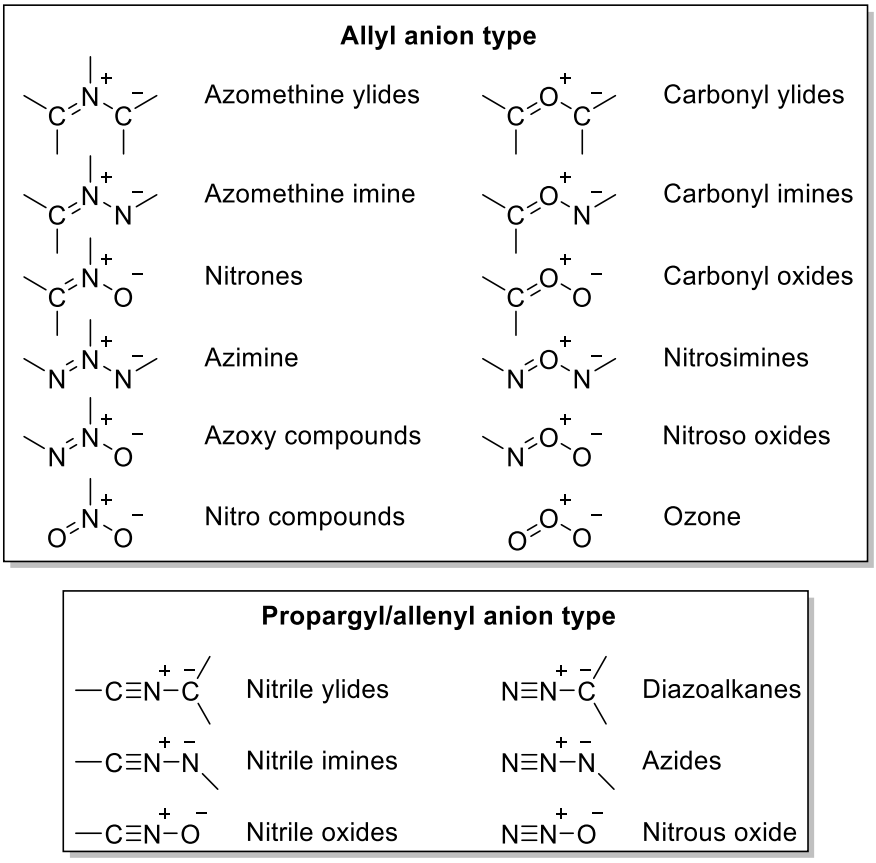

Figure 1-30: Parent 1,3-dipoles identified by Prof. Rolf Huisgen[211] shown in their octet resonance form.

Transition states of concerted Huisgen cycloadditions are directed by frontier molecular orbitals, with the dipole LUMO interacting with the dipolarophile HOMO and/or the dipolarophile LUMO interacting with dipole HOMO.[214] These interactions determine the rate of reaction as well as the stereochemistry of the resulting five-membered rings. Sustman described three types of 1,3-dipolar cycloadditions that depend on the relative energies of dipole and dipolarophile frontier molecular orbitals, with dominant interactions occurring between molecular orbitals of the most similar energy (Figure 1-31).[215,216]

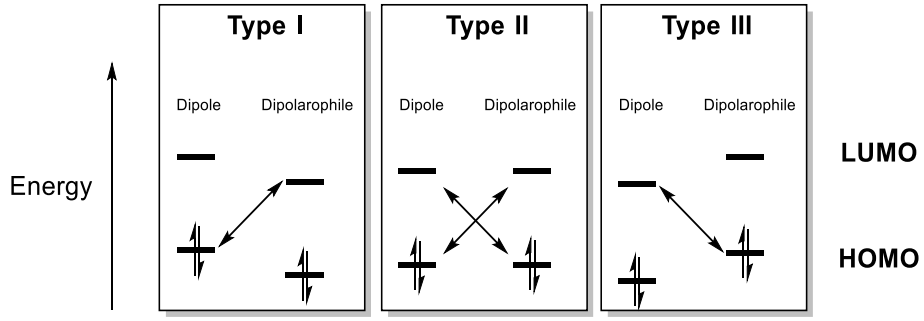

Figure 1-31: Three types of frontier molecular orbital interactions between 1,3-dipoles and dipolarophiles.[214,216]

Type I cycloadditions are directed by interactions between the dipole HOMO and the dipolarophile LUMO, azomethine imines and azomethine ylides generally react by this method.[214] Type II reactions have similar HOMO and LUMO energies for both dipole and dipolarophile, these reactions therefore can be directed by the interaction of all the frontier molecular orbitals. Nitrones generally undergo cycloaddition by type II interactions whilst nitrile oxides are considered type II but on the borderline with type III due to low HOMO energies. Type III are directed by interactions between dipole LUMO and dipolarophile HOMO, Huisgen cycloadditions of ozone are examples of this type. The reactivity of a dipole with a dipolarophile can be assessed using second order perturbation theory and the simplified equation which assumes only HOMO-LUMO interactions determine reactivity (Equation 1-1). The smaller the HOMO-LUMO gap of the reacting orbitals the larger the reduction in energy (ΔE) and therefore the more favourable the reaction is.

$$\Delta E \propto \frac{c_{HOMO} c_{LUMO}}{E_{HOMO} - E_{LUMO}}$$

Equation 1-1: Simplified second order perturbation theory equation, (ΔE = change in energy on cycloaddition, c = atomic orbital coefficient, E = energy of frontier molecular orbital)

Regioisomers formed by cycloaddition are also determined by the HOMO-LUMO ineteractions.[214] The energy change during cycloaddition relates to interorbital overlap (Equation 1-2), with a larger change in energy driving orientation.[217] Stabilisation during the transition state plays an important role, alignment of orbital coefficients of similar magnitudes increases stabilisation (Figure 1-32), which raises the numerator value in Equation 1-2 increasing the overall change in energy.

$$\Delta E = \frac{(C_1^1 \cdot C_a \cdot \gamma_{1a} + C_3^1 \cdot C_b \cdot \gamma_{3b})^2}{E_1} + \frac{(C_a^1 \cdot C_1 \cdot \gamma_{1a} + C_b^1 \cdot C_3 \cdot \gamma_{3b})^2}{E_2}$$

Equation 1-2: Approximation of energy change (ΔE) during cycloaddition, E_1= energy gap between $LUMO_{dipol}$ and $HOMO_{dipolarophile}$; E_2 = energy gap between $HOMO_{dipole}$ and $LUMO_{dipolarophile}$; C = HOMO orbital coefficient; C^1 = LUMO orbital coefficient; a,b,1,3 = interaction sites on dipole and dipolarophile (Figure 1-32), γ = resonance integral.[217]

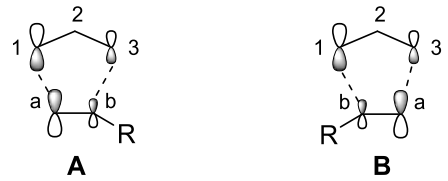

Figure 1-32: Representation of frontier orbital interaction during a 1,3-dipolar cycloaddition, with orbital size relating to the magnitude of orbital coefficients, **A** is more stable than **B**.[217]

Frontier molecular orbital energies and coefficients can be altered dramatically by substituents on the dipole or dipolarophile, thus altering the type of interaction present during cycloaddition (type I, II or III).[215] Electron withdrawing substituents lower orbital energies, affecting the LUMO more than the HOMO, the orbital coefficient remains smaller at the substituted end of the dipolarophile (Figure 1-33).[217] Electron donating substituents conversely raise the orbital energies, affecting the HOMO more than the LUMO, the dipolarophile orbital coefficient of the HOMO remains larger at the unsubstituted end although this is reversed in the LUMO.

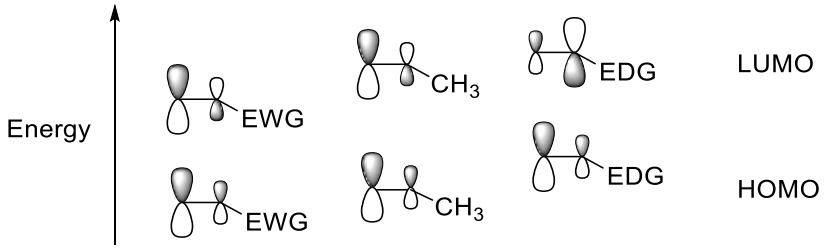

Figure 1-33: Substituent affects on dipolarophile HOMO LUMO energies and magnitude of orbital coefficients

Substituents can be used separately or in combination to improve orbital energy overlap and increase reaction rate or control stereochemistry. Furthermore, metal Lewis acids can alter frontier orbital energies as well as atomic orbital coefficients, they are therefore used as stereoselective catalysts in some 1,3-dipolar cycloadditions.[214] A particularly widespread application of this is the copper catalysed azide-alkyne click reaction.

1.6 Click chemistry reaction

In 1998 Sharpless coined the term click chemistry, describing a method of carbon-carbon linkage often mediated by a heteroatom. By 2001 a full definition of click chemistry required reactions to be modular, wide in scope, high yielding, and create only inoffensive by-products.[218] The reactions had to be stereoselective with simple reaction conditions and benign or easily removed solvents. The *sine qua non* for click reactions is a high thermodynamic driving force, typically greater than 84 kJ mol^{-1}, as this allows for mild reaction conditions. Fusion processes are considered the best form of click chemistry, as they are entirely atom efficient. The most common examples of click reactions are cycloadditions, nucleophilic substitutions, non-aldol carbonyl chemistry and addition to carbon-carbon multiple bonds (e.g. epoxide formation). Click chemistry has found applications in a range of fields including materials science, bio-conjugation chemistry and drug discovery[219].

1.6.1 Azide-Alkyne cycloadditions

Huisgen 1,3-dipolar cycloadditions have become the preeminent reaction in click chemistry, in particular the copper (I) catalysed cycloadditions between azides and alkynes.[220] They proceed stereospecifically in aqueous solvent at room temperature to form 1,4-disubstituted 1,2,3-triazole pentacyclic rings in high yields (Figure 1-34). The 1,5-disubstuted isomer can also be achieved using ruthenium catalysts.[221] These dependable cycloadditions have been applied extensively across chemical and biological fields, in drug discovery, carbohydrate chemistry, and polymer synthesis as well as in proteomics and DNA research.[222,223]

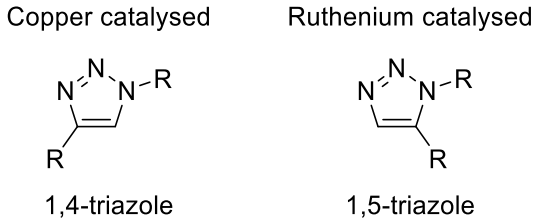

Figure 1-34: Triazole rings formed by copper and ruthenium catalysed azide-alkyne cycloadditions

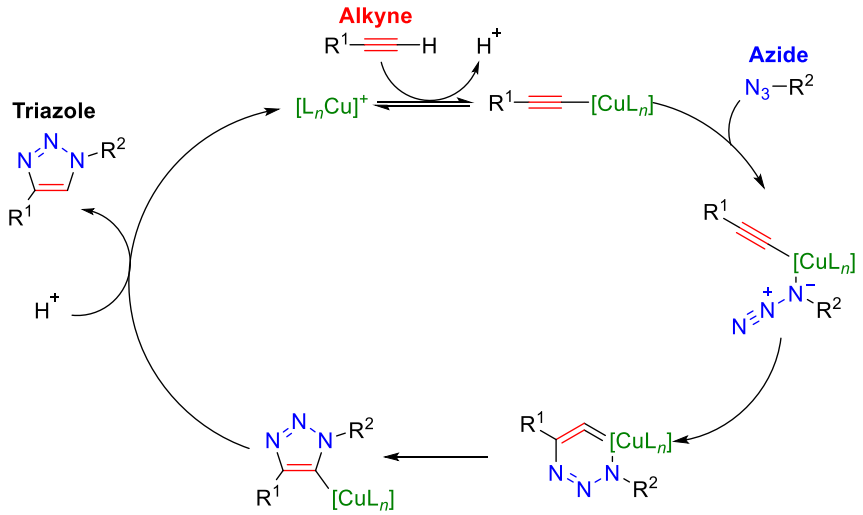

Figure 1-35: Mechanism of copper catalysed azide alkyne cycloaddition proposed by Sharpless *et al.*[224]

The mechanism proposed by Sharpless *et al.* requires one catalytic copper ligand per cycle, which initially forms a copper (I) acetylide.[224] Rather than undergoing a concerted cycloaddition, a stepwise incorporation of the azide moiety *via* a six membered ring was proposed (Figure 1-35). More recently Folkin *et al.*[225] have investigated the mechanism and determined that cycloaddition occurs by a dinuclear copper intermediate (Figure 1-36). The initial copper complex forms a weak π interaction, a second copper compound then causes it to rearrange into a copper (I) acetylide with the second copper now having the π interaction with the acetylide. The π bound copper then reversible coordinates to the azide, which undergoes subsequent nucleophilic attack from the β-carbon of the acetylide. In the resulting complex the copper centres are equivalent, there is therefore equal probability of ejecting [Cu]^a or [Cu]^b during ring closure.

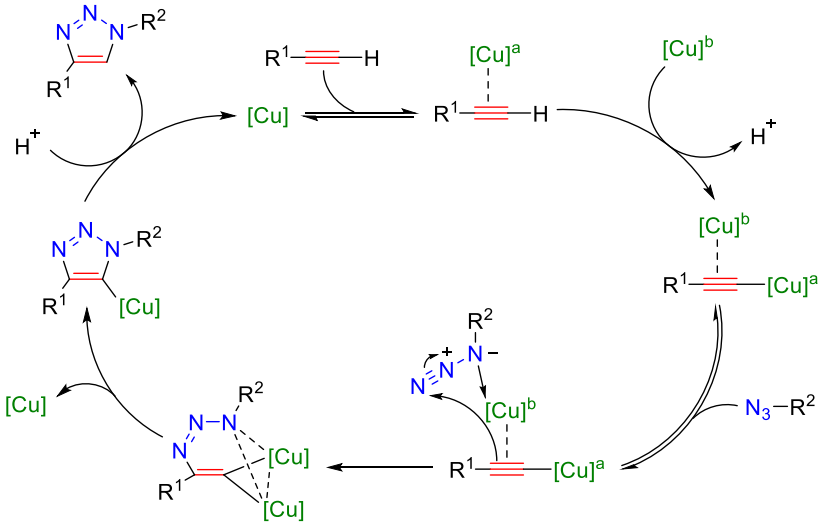

Figure 1-36: Copper catalysed azide alkyne mechanism proposed by Fokin *et al.*[225]

The presence of a copper catalyst results in some limitation for azide based click chemistry as they can be toxic[226] and mediate further reactions in aqueous systems.[227] They can be particularly damaging in bio-conjugation systems, where unstabilised Cu catalysts fragment oligonucleotides and polysaccharides.[228,229] Uncatalysed azide-alkyne cycloadditions have been performed, however higher temperatures are required and racemic mixtures can be formed in chiral systems.[230,231] The azide moiety required for this cycloaddition also presents issues due to its highly toxic and explosive nature.[232]

1.6.2 Polytriazoles

Copper catalysed azide-alkyne cycloaddition chemistry has been widely applied to material synthesis, within this field it has been used in the realisation and functionalization of linear, cyclic and star polymers as well as dendrimers and block copolymers.[233,234] Azide-alkyne cycloadditions have been applied to polymer and materials chemistry using a variety of methods, those most often encountered are the functionalisation of pre-existing polymers and by formation of polymers directly through cycloaddition reactions.

By incorporating an azide or alkyne group into the repeat unit of a polymer it becomes easily functionalisable by copper catalysed cycloadditions. Functionalised polymers can go on to act as macromonomers that can undergo cross-linking or form various structures (e.g. brushes).[235] This method has also been used to create polymers with particular functionality and has seen widespread use in biomedical applications.[236] Liu *et al.* demonstrated the formation of triazole bearing polymers for applications as anion exchange resins.[237] An azide group was first introduced to commercially available poly(2,6-dimethy phenylene oxide), from this a triazole was formed and subsequently alkylated using methyl iodide (Figure 1-37). The anion exchange membrane **1.54** showed comparable highest hydroxide conductivity (20 mS/ cm at room temperature) to many reported in literature.

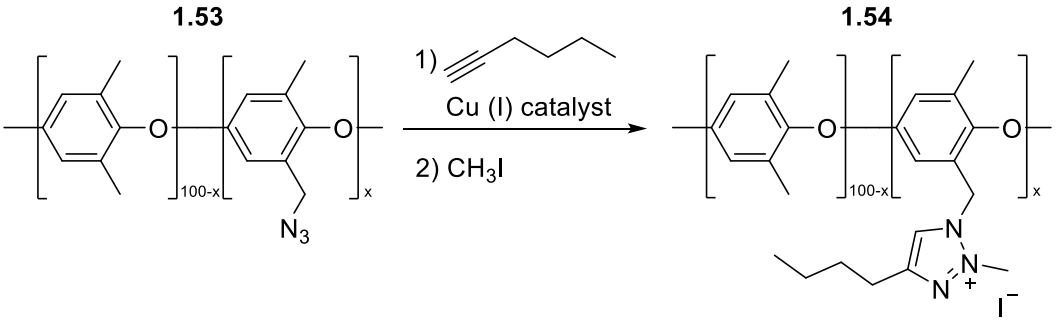

Figure 1-37: Anionic exchange membrane formed by triazole functionalisation of a polymer.[237]

Polytriazoles have been formed through step growth polymerisations using double click reactions of diazides and dialkynes.[238] Dual functional monomers have also been employed to form homopolymers, Xie *et al.* used monomer **1.55** to synthesise hyperbranched polytriazoles **1.56** (Figure 1-38).[239] The step growth cycloaddition polymerisation can be carried out with a high level of control over stereochemistry and chain length, Hughes *et al.* demonstrated this with a study into potential peptidomimetic compounds.[240] Protection of the alkyne with trimethylsilyl stops the polymerisation after each Huisgen cycloaddition, the alkyne was then deprotected to allow for the inclusion of the next repeat unit. Whilst Hughes *et al.*[240] used this level of control to form oligomers for peptidomimetic studies, others have applied it to the formation of highly controlled polymers.[241,242]

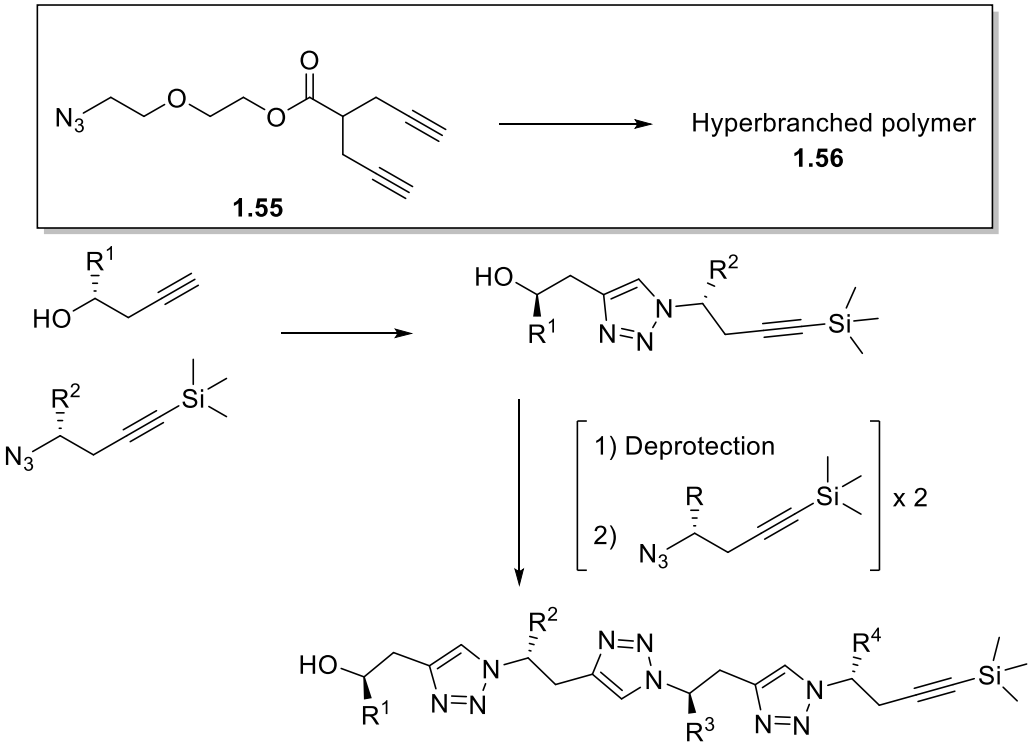

Figure 1-38: Formation of hyperbranched polytriazoles (*top*), controlled synthesis of triazoles (*bottom*).

Bio-“click”-polymers have been derived from vegetable oils using azide-alkyne cycloadditions. Shah *et al.* used epoxidised vegetable oils to introduce azide and alkyne functionalities into the triglycerides.[243,244] Bio-polytriazoles were synthesised *via* two methods, copper catalysed and solvent free thermal non-catalysed polymerisations. The solvent free thermal process was found to be more favourable than the copper catalysed polymers. The non-catalysed process resulted in narrower thermal decomposition profile, more homogeneous cross-linking, and lower glass transition temperatures (T_g) as no catalyst was trapped within the system.

Narine *et al.*[245] have also derived bio-polytriazoles from vegetable oils using solvent and catalyst free conditions. Physical properties of the polymers were severely affected by hydrogen bonding between carbonyls and hydrogen in the triazole ring. They went on to reported biomedical applications of these fatty acid derived polytriazoles.[246] Three amphiphilic polytriazoles were formed with different densities of triazole along the polymer backbone, as triazole density increased hydrophobicity decreased. The polytriazoles had antimicrobial properties, which increased as hydrophobicity decreased. It was believed that the amphiphilic nature of the polymers caused cell membrane disruption leading to bacterium death.

1.6.3 Polyisoxazolidines

The formation of polytriazoles by copper catalysed azide-alkyne cycloadditions has demonstrated the utility of 1,3-dipolar cycloadditions in polymer formation.[247,248] An alternative catalyst free 1,3-dipolar cycloaddition using nitrones (Figure 1-30) and dipolarophiles has also been explored as a step-growth polymerisation method.[249,250] Ritter and Vretik reported the formation of a polyisoxazolidine from bis-nitrone and bis-maleimide monomers.[251] The polymerisation required anaerobic conditions and long reaction times (2 days), however even with these conditions side reactions occurred leading to polymers with low molecular weights and high dispersity’s. A key feature of these polymerisations is the formation of isoxazolidines throughout the backbone of the polymer, these heterocycles may allow access to post-polymerisation modification through the formation of β-lactams.[249,252]

1.7 Nitrile oxide cycloaddition reactions

The field of "click" polymers has focused heavily on polytriazoles formed *via* 1,3-dipolar cycloadditions between azides and alkynes.[248] Although effective, the formation of polytriazoles has significant drawbacks, particularly the large scale use of azides, which is extremely dangerous due to their explosive and toxic nature.[253] The reaction also requires a metal catalyst for high conversions and stereoselectivity. The analogous 1,3-dipolar cycloaddition using nitrile oxides (Figure 1-39) proceeds well at ambient temperatures without the need for a catalyst.[254] The uncatalysed cycloaddition has high regioselectivity, generally forming the 3,5-isomer as the major product.[255] Nitrile oxide Huisgen cycloadditions are used widely in small molecule synthesis and have been applied to the functionalisation of pre-formed polymers.[256] These reactions have seen limited use in the direct formation of polymers (polyisoxazoles and polyisoxazolines)[254,256,257] and no publications known to me relate to their use in forming renewably derived polymers.

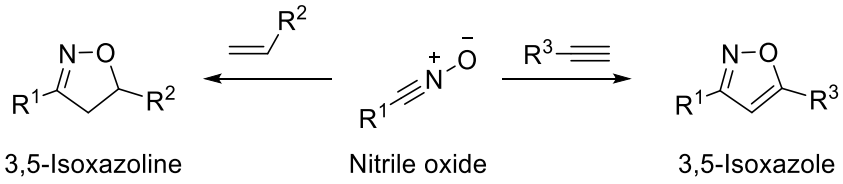

Figure 1-39: Products of 1,3-dipolar cycloadditions of nitrile oxides with alkenes and alkynes

Nitrile oxides are ambiphilic dipoles (type II), the HOMO of the dipole can overlap with the LUMO of the dipolarophile or the HOMO of the dipolarophile can overlap with the LUMO of the dipole.[214] The rate of cycloaddition can therefore be increased by electron withdrawing and electron donating substituents on the dipolarophile, as both will reduce the energy gap between the HOMO and LUMO.[215] The reaction generally proceeds by interactions between the nitrile oxide LUMO and the dipolarophile HOMO. When using monosubstituted dipolarophiles the cycloaddition is highly regioselective as the oxygen orbital coefficient has better overlap with the substituted end of the dipolarophile, leading to the 3,5-isoxazole almost exclusively (e.g. **1.58** Figure 1-40).[217] The 3,4-isoxazole **1.59** can be formed using strong electron withdrawing groups (SO_2R/NO_2) on the dipolarophile, this causes the cycloaddition to proceed through interactions between the nitrile oxide HOMO and the dipolarophile LUMO. Regioiselectivity can also be directed by steric hinderance effects,[210] this

further increases the general regioselectivity towards 3,5-isomers, with addition of less hindered oxygen to the more hindered substituted carbon being the preferable route.

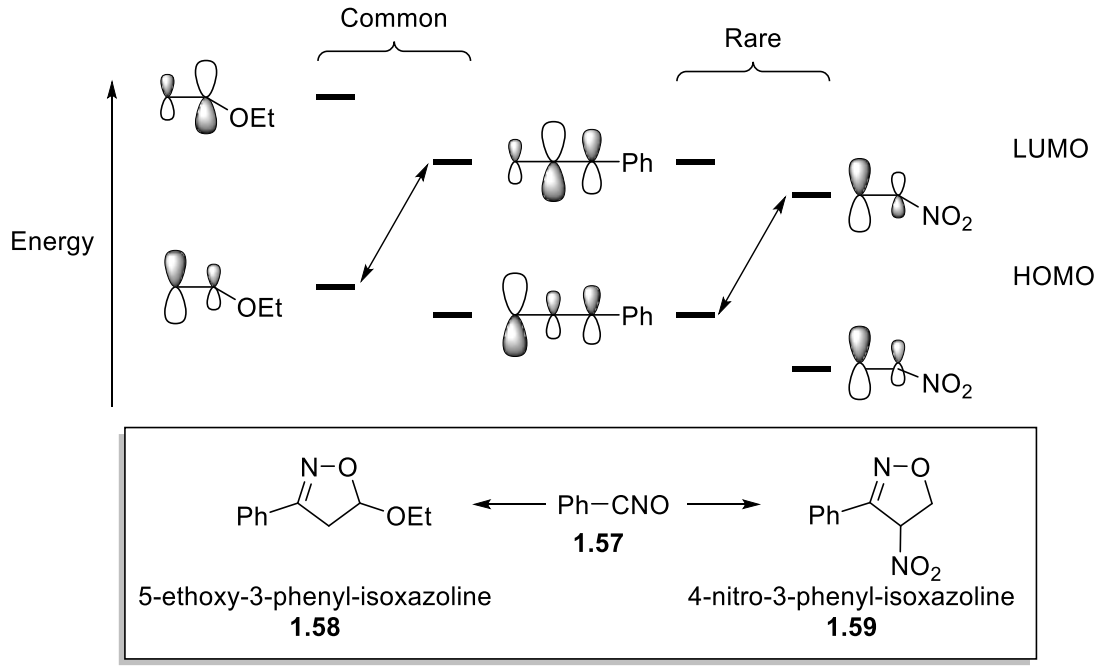

Figure 1-40: Substituent effects on the formation of isoxazoline isomers.

1.7.1 Nitrile oxides

Nitrile oxides are isomeric with cyanates and isocyanates, with very early literature suggesting the cyclic structure **1.60 (**Figure 1-41).[258] Energy calculations and optical data however indicated nitrile oxides have a linear structure. The octet stabilised structure **1.61a** is the generally accepted representation although it is important to note that the structure is more accurately described as a hybrid of resonance forms **1.61a – e** (Figure 1-41).

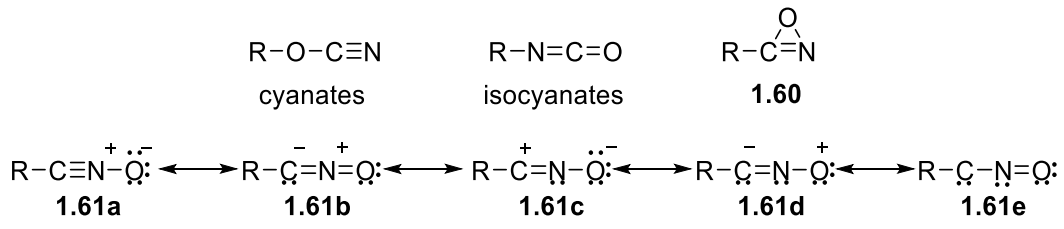

Figure 1-41: Nitrile oxide isomers *(top)* and resonance structures *(bottom).*[258]

Nitrile oxides are highly reactive, with low molecular weight compounds such as fulminic acid (HCNO) being potentially explosive, this is not an issue with higher molecular weight compounds.[258] Due to their reactivity most nitrile oxides will

spontaneously dimerise to form furoxans,[259] although a range of other products may be formed depending on reaction conditions (Figure 1-42).[217] For this reason nitrile oxides are generally formed *in situ*.

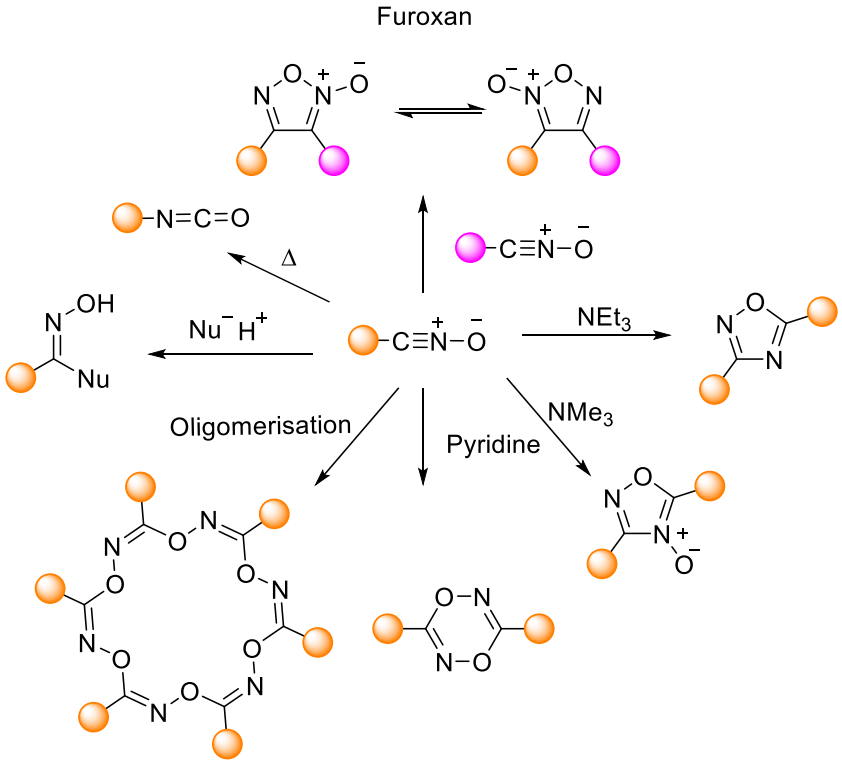

Figure 1-42: Possible reactions of nitrile oxide in the absence of suitable dipolarphiles[217]

Most nitrile oxides are only stable at temperatures below 0ºC, at room temperature the half-life of aliphatic nitrile oxides is seconds to minutes, whilst aromatic nitrile oxides is minutes to days.[260] Sterically hindered nitrile oxides do not dimerise as readily and can be studied in solutions. With enough steric hindrance nitrile oxides are stable at room temperature, although they can still rearrange to isocyanates at raised temperatures.[261] They are also susceptible to nucleophilic addition, reacting with a range of nucleophiles to form hydroximic acids. The stability of aromatic nitrile oxides are effected by substituents on the ring but it is not particularly pronounced.[258,262,263] Both electron withdrawing and electron donating groups stabilise nitrile oxides whilst in the *para* position, but electron withdrawing groups destabilise nitrile oxides in the *ortho* position.

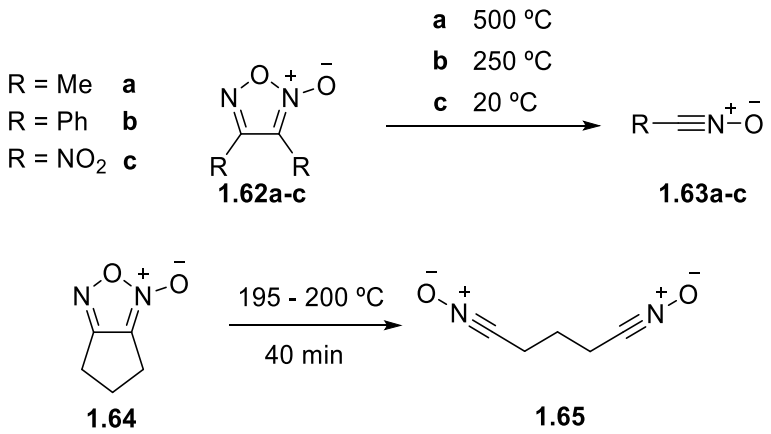

Figure 1-43: Thermolysis of furoxans to regenerate nitrile oxides[264,265]

The major limitation with nitrile oxide cycloadditions is the propensity to form furoxans. Nitrile oxides can be regenerated from furoxans by flash vacuum pyrolysis at 500 – 600 ºC.[266] If the furoxan is suitably strained by bulky or cyclic substituents nitrile oxides can be regenerated by prolonged heating in solvent at lower temperatures (20–257ºC) (Figure 1-43).[267,265] These nitrile oxides can then be used in cycloaddition reactions, to achieve a decent yield of isoxazole or isoxazoline, excess dipolarophile is required as due to the high temperatures required the regenerated nitrile oxides quickly isomerise to form isocyanates.[264,265,267–269]

To avoid the formation of furoxans and other by-products nitrile oxides are general formed *in situ*, this has been done by a variety of different methods but the most often encountered is dehydrohalogenation of oximoyl chlorides (hydroxamic acid chlorides).[270] The benefit of this method is that the nitrile oxide can be derived from a large catalogue of aldehydes through fast high yielding reactions, hence conversion of aromatic aldehydes to aldoximes is followed by chlorination using electrophilic chlorine sources (NCS, Cl_2, etc.).[271–274] Decomposition of these oximoyl chlorides to nitrile oxides can be achieved either by promotion with a base or thermally, giving HCl as the by-product (Figure 1-44).

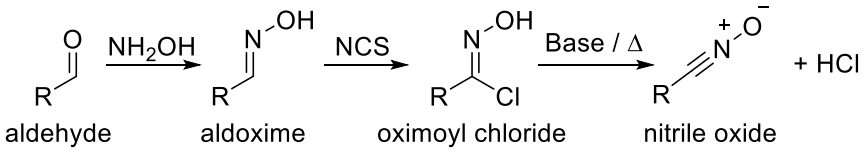

Figure 1-44: Formation of oximoyl chloride and subsequent decomposition to nitrile oxide.

1.7.2 Isoxazoles and isoxazolines

Nitrile oxides undergo 1,3-dipolar cycloadditions with alkynes and alkenes to form isoxazoles and isoxazolines (4,5-dihydroisoxazole) respectively. Monosubstituted dipolarophiles react faster than disubstituted, with terminal alkenes being more susceptible than terminal alkynes to cycloaddition.[258] The reaction intermediates are controlled by frontier molecular orbitals, generally resulting in the 3,5-isomers as the major product when reacting with monosubstituted dipolarophiles (Figure 1-45).

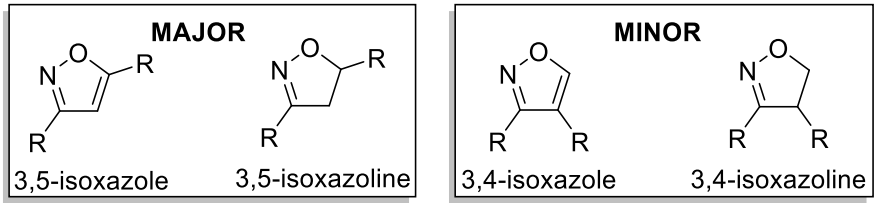

Figure 1-45: Disubstituted isoxazole and isoxazoline rings

Isoxazoles are weakly basic aromatic five membered heterocycles with similar properties to pyridine, they can form hydrogen bonds through the nitrogen if a suitable electrophilic proton is present.[275] The ring structure is resistant to strong acids and oxidising agents, with electrophilic substitution reactions occurring in the 4-position.[217] As weak bases isoxazoles readily undergo *N*-alkylation to form quaternary salts.[276] Nucleophilic attack of isoxazoles generally causes fragmentation of the ring structure and so is rarely seen in the literature.[217]

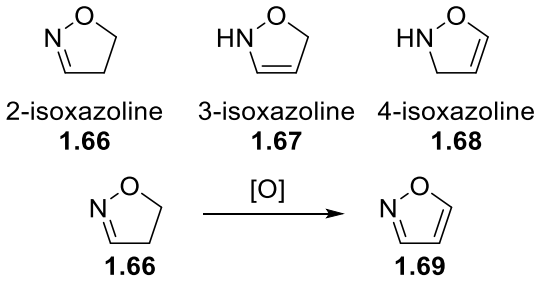

Figure 1-46: Isoxazoline isomers *(top)*, dehydrogenation of isoxazoline to form isoxazole *(bottom).*

There are three isomeric forms of isoxazolines with 2-isoxazolines **1.66** the most commonly encountered in literature, it is also more stable and versatile than **1.67** and **1.68** (Figure 1-46).[217] Although forming in a similar manner to isoxazoles, the lack of aromatic character in isoxazolines gives them different properties and reactivity. Isoxazolines are easily dehydrogenated to aromatic isoxazoles with a range of oxidising agents (Figure 1-46).[217] This aromatisation reaction is particularly important

as isoxazolines are easier to form by 1,3-dipolar cycloadditions than isoxazoles.[258] Isoxazolines are however stable to oxidation with peracids.[277] Isoxazolines are susceptible to thermal or base mediated fragmentation, cycloreversions have also been observed at 600-650ºC under flash-vacuum conditions.[217]

Arguably the most important property of isoxazoles and isoxazolines is their ability to undergo selective reductive cleavage. Depending on the reaction conditions the N-O bond of the heterocycle can be cleaved to unmask β-aminoenones, β-amino alcohols or di-ketones (Figure 1-47) along with a range of other systems.[278–293] Isoxazolines undergo selective reductive cleavage more readily than isoxazoles, with full ring cleavage being achieved using $LiAlH_4$, borane complexes and sodium in ethanol.[217] They have also been reported to be reduced without cleavage using sodium borohydride giving an isoxazolidine.[294]

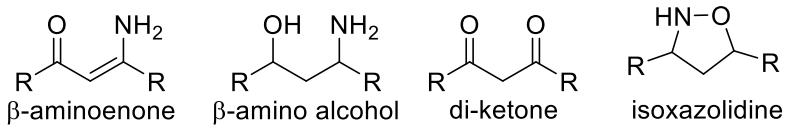

Figure 1-47: Example of products of isoxazole and isoxazoline reduction

Isoxazoles and isoxazolines are widely used in small molecule synthesis due to their properties and ease of synthesis making them good linkage groups. These properties have made isoxazoles and isoxazolines important groups in pharmaceutical products, with isoxazoles as the 33rd most common ring in currently marketed drugs.[295] They are also common in naturally occurring medicinal chemicals, natural isoxazolines and their derivatives have been investigated as anti-cancer agents.[296]

1.7.3 Polyisoxazoles and polyisoxazolines

Cycloaddition of nitrile oxides with dipolarophiles is analogous to the azide alkyne 1,3-dipolar cycloaddition used widely in modern polymer chemistry.[254] Like the triazole forming reactions nitrile oxide cycloadditions can be used to functionalise pre-existing polymer chains or used directly to form polyisoxazoles and polyisoxazolines. Due to nitrile oxides ability to dimerise, significantly fewer polyisoxazoles and polyisoxazolines than polytriazoles are reported in literature.[254,257]

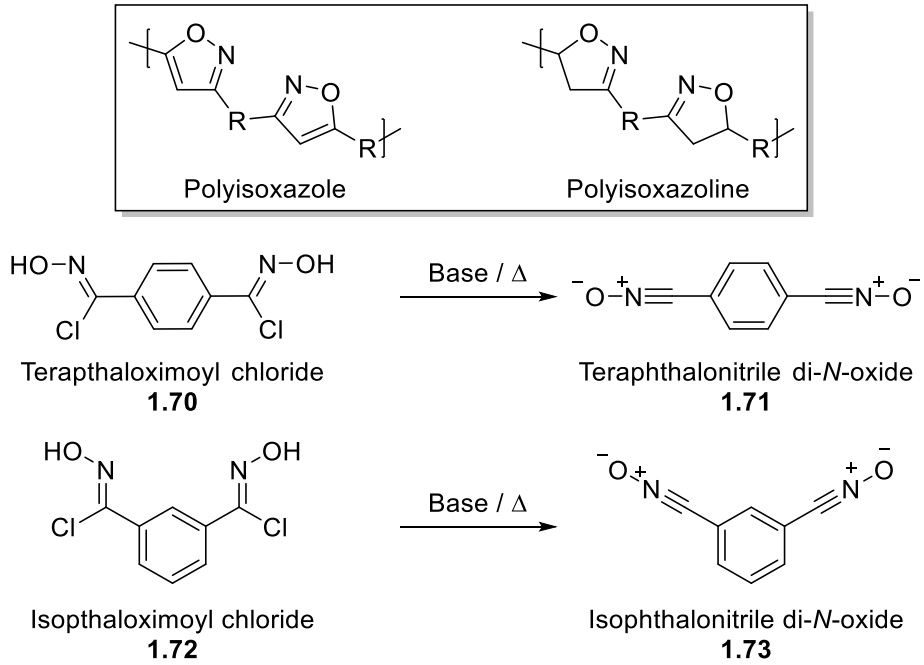

Figure 1-48: Representation of polyisoxazole and polyisoxazoline (*top)*, typical nitrile oxide precursors used to form nitrile oxide monomer *in situ* (*bottom*).

Early work on nitrile oxide cycloaddition polymers was carried out in the 1960's and 70's[297–304] after Huisgen's[210,211] extensive studies on 1,3-dipolar cycloadditions. These studies generated di(nitrile oxide) bearing compounds from oximoyl chlorides with the use of base or by thermal decomposition. It was noted that teraphthalonitrile di-*N*-oxide **1.71** could be generated before polymerisation and stored unchanged for multiple days, unlike isophthalonitrile di-*N*-oxide **1.73** which dimerised rapidly and so must be formed *in situ*.[301] These studies generally gave medium to high yields of polymers (50–100%) with high thermal stability (>200ºC) and some evidence of semi-conductor properties.[257] Semi-conductor properties of polyisoxazolines reported in early work[304] were later investigated by Mahrous.[305–309] Polyisoxazolines were synthesised using **1.70** and dialkenes, generating the nitrile oxide **1.71** *in situ* by refluxing in toluene[309] to give low molecular weight polymers (M_w = 5 kDa).[306] The competing nitrile oxide dimerisation reaction was also investigated by Overberger and Fujimoto, and intentional homopolymerisation of **1.71** resulted good yields of polyfuroxans (89 %) as a yellow solid.[300]

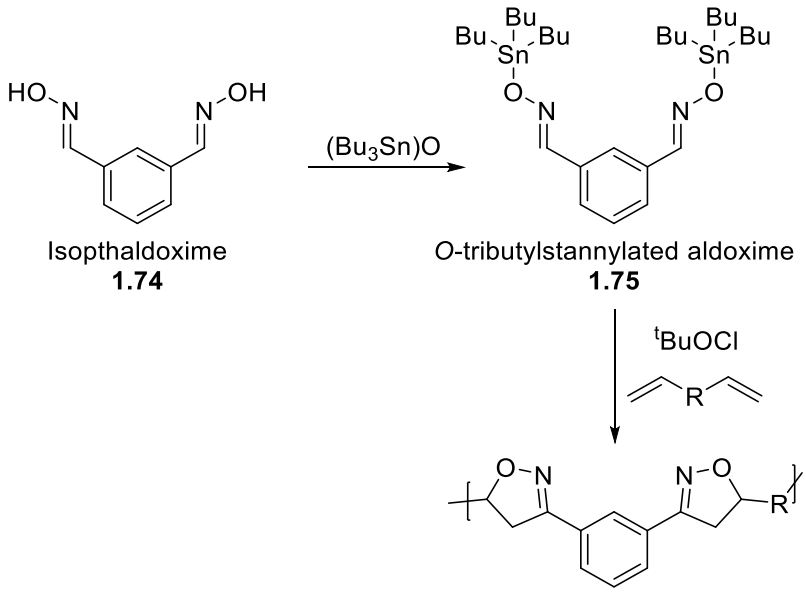

Figure 1-49: Polyisoxazoline formed by *via* an *O*-tributylstannylated aldoxime **1.75** intermediate.[310]

After the wave of initial research, examples in literature dwindled, particularly literature relating to polyisoxazoles. Later polymerisations have trialled different methods of forming polyisoxazolines. Takenouchi *et al.*[311] reported on the solid phase formation of isoxazoline oligomers, believing the controlled addition method could be applied to polyisoxazoline synthesis. Moriya and Endo[310] investigated polyisoxazole synthesis from isophthaldoxime **1.74** using an *O*-tributylstannylated aldoxime **1.75** intermediate (Figure 1-49). With the introduction of tert-butylhypochlorite (^{t}BuOCl), nitrile oxide **1.73** was formed at room temperature and underwent cycloaddition polymerisation with dialkene comonomers, resulting in polymers with number average molecular weights (M_n) around 10 kDa and narrow dispersity's ($Đ$ = 1.01 – 1.23). Cheng and Li[312] investigated the application of a one-pot copper catalysed method to polyisoxazoline synthesis, forming the polymer directly from dialdehydes in a "double click" reaction (Figure 1-50). Polymerisations were regioselective, forming the 3,5-isoxazole at medium yields (46 – 78 %). The polymers had narrow dispersity's (between 1.08 and 1.13) with number average molecular weights (M_n) between 7.7 kDa and 9.2 kDa. As had been noted in previous publications[310] the polyisoxazoles derived from **1.71** have low solubility due to their high crystallinity which may cause them to precipitate during polymerisation.

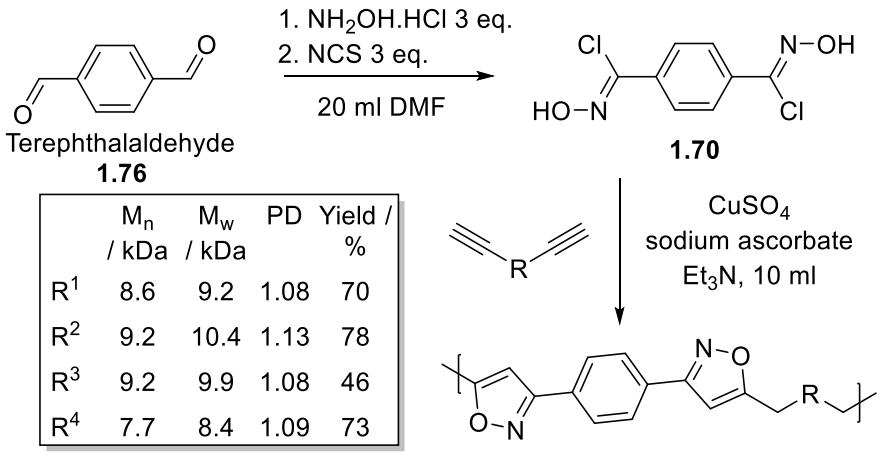

	M_n / kDa	M_w / kDa	PD	Yield / %
R^1	8.6	9.2	1.08	70
R^2	9.2	10.4	1.13	78
R^3	9.2	9.9	1.08	46
R^4	7.7	8.4	1.09	73

Figure 1-50: One-pot copper catalysed polyisoxazole synthesis.[312]

Although molecular sieves are known for their absorbent properties they can also be used to promote organic transformations.[313,314] They are mildly basic and have been reported to promote nitrile oxide cycloadditions due to the slow degradation of oximoyl chlorides reducing dimerisation reactions.[315,316] With this in mind Takata *et al.* investigated the use of molecular sieves to generate di(nitrile oxides) *in* situ for polyisoxazole and polyisoxazoline synthesis (Figure 1-51).[317] They reported good yields of polymers (80–99%) from a variety of dipolarophiles, although the polymers had a mixed range of molecular weights and dispersity's (M_n = 1200 – 9100, $Đ$ = 1.3 – 2.0), with polyisoxazoles performing worse than polyisoxazolines. A following report showed that modification of the dialkyne monomers gave access to much higher molecular weight polyisoxazoles (M_n = 11.7 kDa, $Đ$ = 1.8).[318]

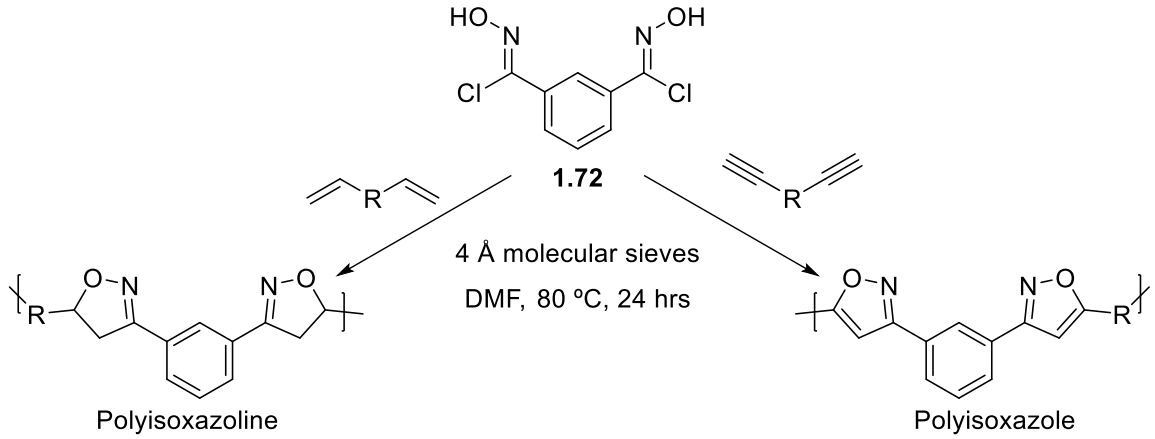

Figure 1-51: Synthesis of polyisoxazolines and polyisoxazoles mediated by molecular sieves.[317]

To demonstrate the masked functionality of polyisoxazoles they were reportedly ring opened by reductive cleavage using Fe(II) and $LiAlH_4$ to give poly(β-aminoenones) and poly(β-amino alcohols) respectively (Figure 1-52).[318] Destruction of the

heteroaromatic ring reduced glass transition temperatures for the polymers. The functionality of poly(β-amino alcohols) was then assessed by cross-linking them with aldehydes and isocyanates (Figure 1-52). Dialdehydes cross-link the poly(β-amino alcohol) through imine formation. Diisocyanates can cross-link the poly(β-amino alcohol) through two reactions, isocyanates can react with the amine to form urea groups whilst the hydroxyl group reacts with isocyanates to form urethane groups.

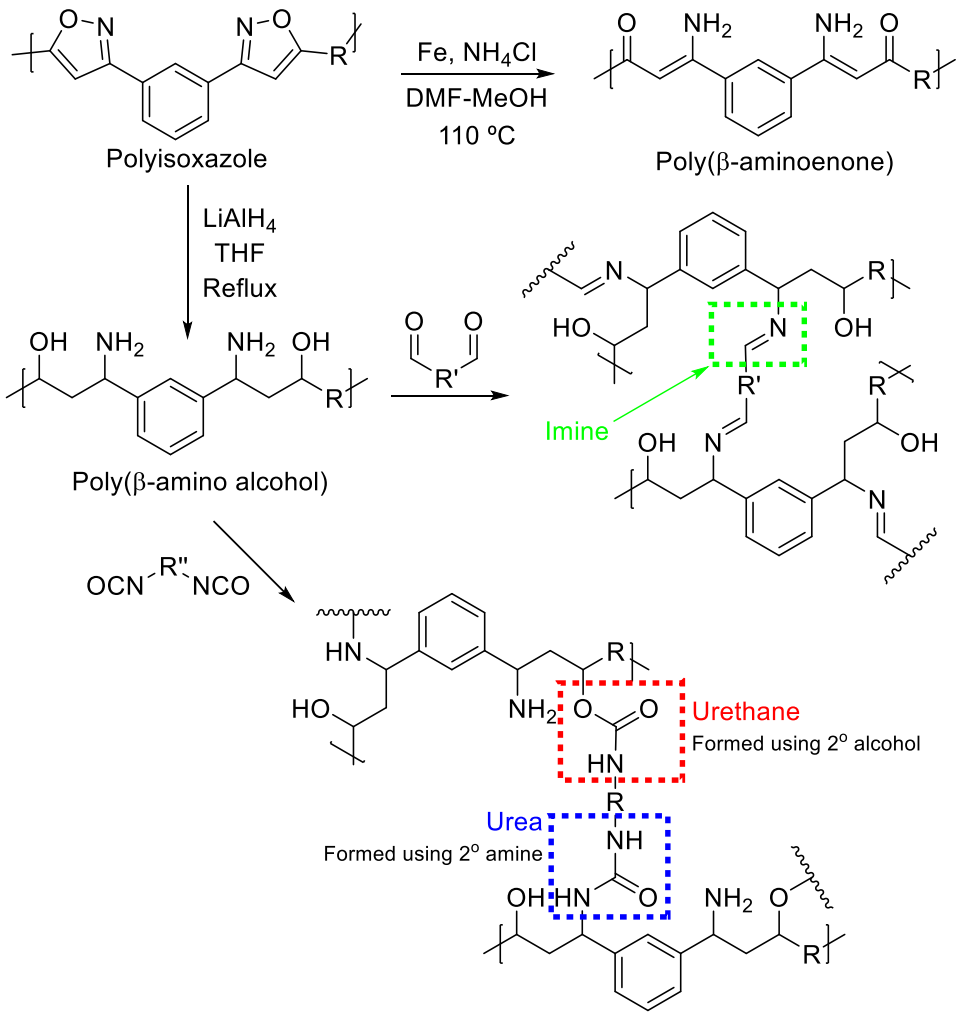

Figure 1-52: Reductive cleavage of polyisoxazoles and subsequent cross-linking.[318]

1.8 Research Aims

The work of Takata *et al.*[317,318] demonstrated a mild, high yielding polymerisation method that gave access to polyisoxazoles and polyisoxazolines. The isoxazole and isoxazoline rings found throughout the polymer have interesting properties and have been shown to allow for post polymerisation modification. There has been limited research on these types of polymers and I have seen no evidence of bio-derived nitrile oxide cycloaddition polymers. It is therefore the aim of this work to investigate the polymerisation method reported by Takata *et al.*[317,318] and apply it to the production of renewably derived polyisoxazoles and polyisoxazolines from vegetable oils (dipolarophiles) and vanillin derivatives (dipoles).

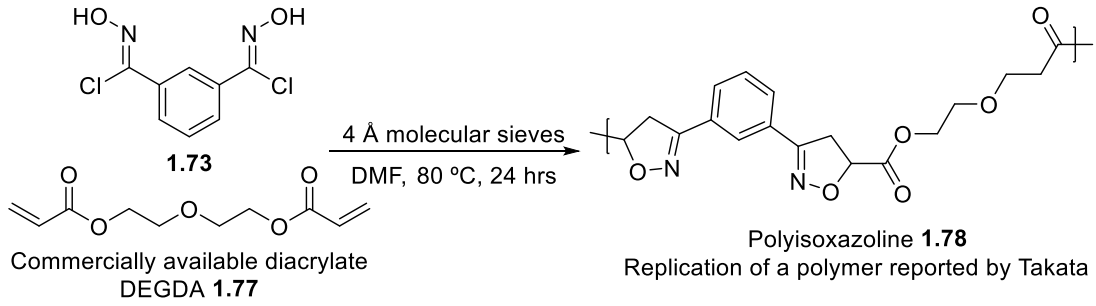

Figure 1-53: Reproduction of a polyisoxazole synthesis performed by Takata *et al.*[317]

Consequently, in chapter 2 the polymerisation conditions described by Takata *et* al.[317] are investigated using commercially available diacrylate dipolarophiles and isophthalonitrile di-*N*-oxide **1.73** (Figure 1-53). Two of Takata's reactions are reproduced and analysed by GPC, TGA and DSC to allow comparison with the literature results.[317] The polymer structure is also assessed using ^{1}H and ^{13}C NMR, IR, and MALD-TOF spectroscopy. The effect of monomer structure and monomer ratios on polymerisation and polymer characteristics is then explored using the same analysis techniques. In chapter 3 acetamide dipolarophile monomers are studied to determine how different methods of incorporating dipolarophilic groups into vegetable oil derivatives would effect polymerisation and polymer properties (Figure 1-54).

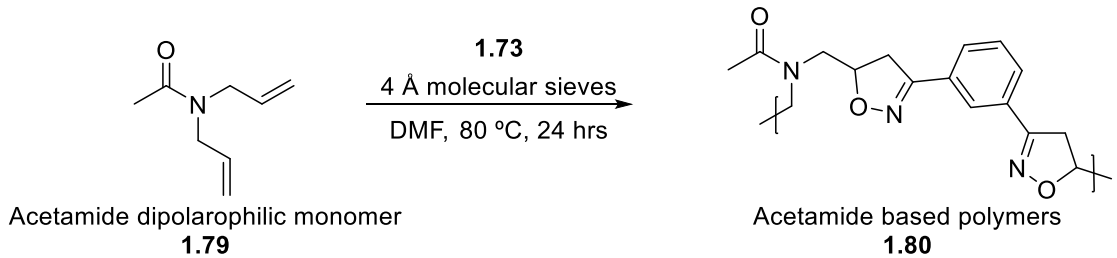

Figure 1-54: Example polymerisation of acetamide based dipolarophilic monomers.

After some evidence of incomplete polymerisation, optimisation of polymerisation conditions is attempted in chapter 4. Using a monofunctional nitrile oxide precursor **1.81** and a dialkyne **1.82**, a range of reaction conditions are trialled and conversion of alkyne to isoxazole **1.83** is assessed by ^{1}H NMR integrals (Figure 1-55). The most successful cycloaddition conditions are then applied to a polymerisation reaction between isophthalonitrile di-*N*-oxide **1.73** and the dialkyne and compared to "Takata's conditions."[317]

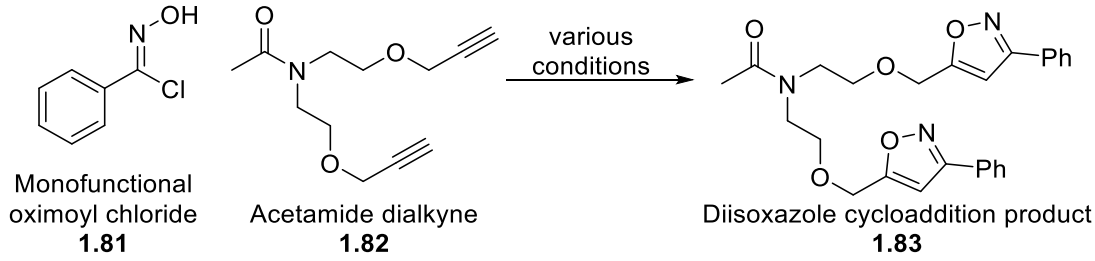

Figure 1-55: Cycloaddition reaction used to optimise isoxazole synthesis conditions

The improved polymerisations conditions are then applied to fatty acid derived dipolarophilic monomers and isophthalonitrile di-*N*-oxide **1.73** in chapter 5. Cross-linking using the internal *cis* alkene of unsaturated fatty acids is explored as well as a brief study into post polymerisation modification by heterocycle reductive cleavage.

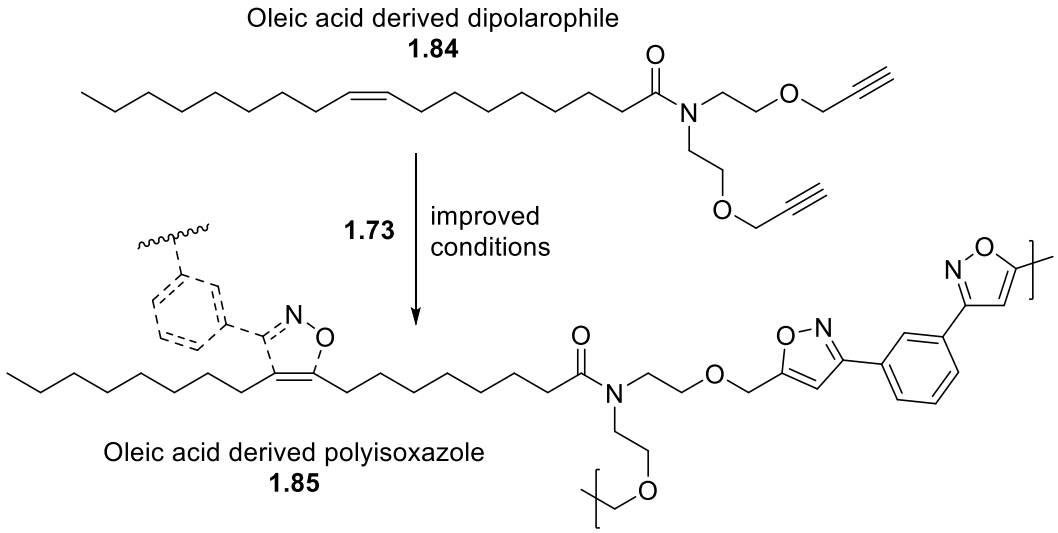

Figure 1-56: Fatty acid derived dipolarophile and it's polymerisation with isophthalonitrile di-*N*-oxide **1.73**, indicating the *cis* alkene as a possible site for cross-linking.

In chapter 6 a range of aromatic oximoyl chlorides are formed with different ring substituents to assess how they effect oximoyl chloride stability and so inform a decision on a renewable aromatic aldehyde feedstock (Figure 1-57). Following this vanillin **1.20** is explored as a renewable feedstock for dinitrile *N*-oxide monomers

1.86. These vanillin derived dipole monomers and a fatty acid derived dipolarophile are used to form renewably derived polyisoxazoles. Vanillin **1.20** is also investigated as a feedstock for dipolarophilic monomers **1.87**, allowing the formation of a completely vanillin derived polyisoxazole. Finally, a vanillin derived dual functional monomer **1.88** is used for solvent-based and solvent-free homopolymerisations.

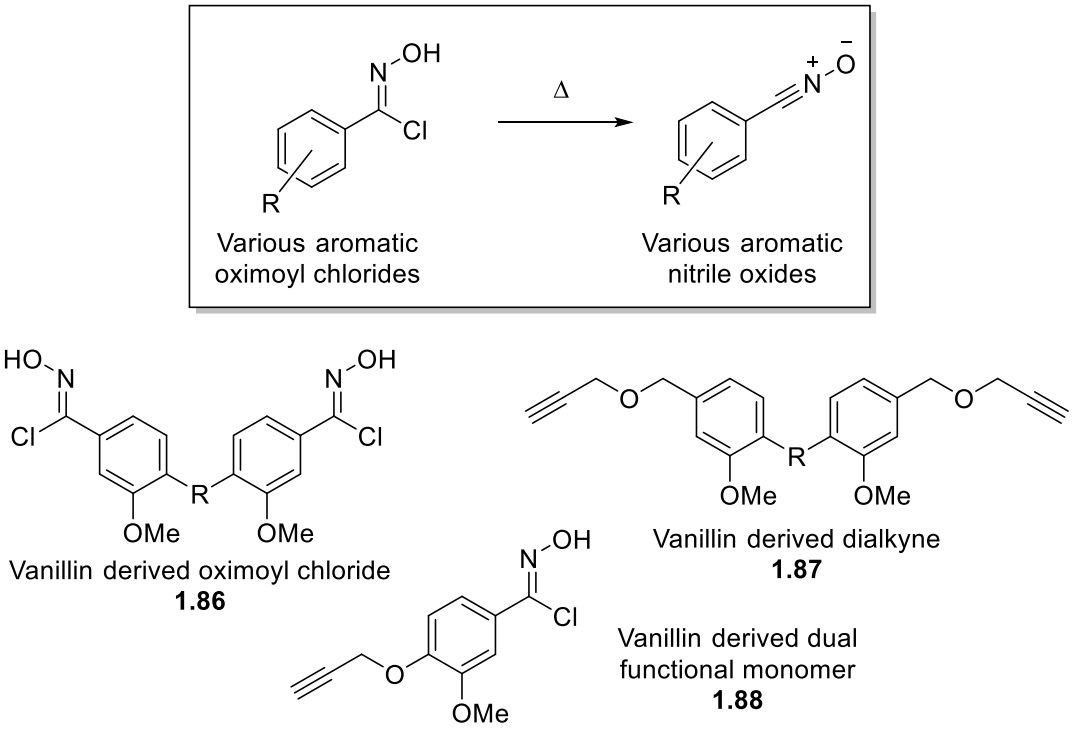

Figure 1-57: Thermal stability analysis of different aromatic oximoyl chloride (*top boxed*); vanillin derived oximoyl chlorides, dipolarophiles and dual functional monomers.

2.0 Polyisoxazolines synthesised from commercial dipolarophile monomers.

2.1 Introduction

Click chemistry is an efficient method for producing polymers and it has seen extended use in the formation of polytriazoles.[247,319,320] Whilst these polymerisations have been successful, they do have significant drawbacks, the azide monomers can be explosive and toxic.[247] They also require copper catalysts to be regioselective, although even with a catalyst the reactions can be slow.[321] The analogues Huisgen cycloadditions to form isoxazole rings are used widely throughout the world of small molecule synthesis due to their high yield and regioselectivity,[321] they have however received limited attention as a method for polymerisation.[322] This "click" reaction replaces the azide monomer with a nitrile oxide and does not require a catalyst to proceed regioselectively, while the stereochemistry of the newly formed isoxazole ring is directed strongly by frontier molecular orbitals and steric interactions.[213,214] Most nitrile oxides are not explosive and can also perform Huisgen cycloadditions with alkenes to form isoxazolines. The major drawback with using nitrile oxides is their ability to dimerise and form furoxans if a suitable dipolarophile is not present to capture the dipole.[258,323] For this reason, nitrile oxides must be formed *in situ*.

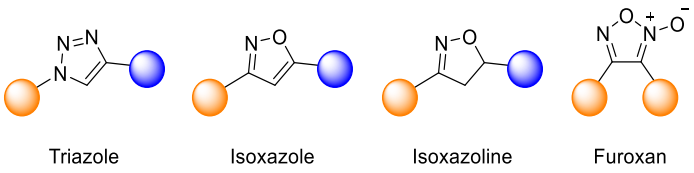

Figure 2-1: Heterocycles formed by Huisgen cycloadditions and the product of nitrile oxide dimerisation.

Literature on the formation of polyisoxazoles *via* nitrile oxides is limited[322], Li and Cheng published a paper on polyisoxazole synthesis that used a copper catalyst like in polytriazole synthesis.[312] Takata *et al*. however published a series of papers on polyisoxazoles and polyisoxazolines where the synthesis method utilised molecular sieves as a mild base,[317,318] achieving polyisoxazoles without the use of transition metal catalysts. They recorded higher yields than Li in general, although with lower molecular weights for comparable compounds.

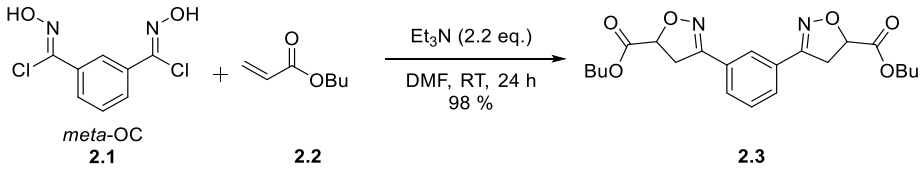

Scheme 2-1: Reaction of bifunctional nitrile *N*-oxide precursor *meta*-OC **2.1** and butyl acrylate **2.3**.[317]

Takata *et al.*[317] began investigating the possibility of efficient polyisoxazoline synthesis by studying the preparation of an isoxazoline using a bifunctional nitrile *N*-oxide precursor (*meta*-OC, **2.1**) and butyl acrylate (Scheme 2-1). The reaction used an excess of butyl acrylate and supposedly gave one 3,5-isoxazoline diastereomer **2.3** in a high yield (98 %). Encouraged by this initial study, polymer reactions were trialled using the bifunctional oximoyl chloride **2.1** as the nitrile *N*-oxide precursor and diethylene glycol diacrylate (DEGDA, **2.4**) as a dipolarophile (Scheme 2-2). A variety of conditions were investigated by altering base, solvent, temperature, and time. The most successful conditions used 4 Å MS as the base in DMF at 80 ºC for 24 hours (1g, Table 2-1). This method gave a 99 % yield of polymer **2.5** with the highest M_n (9.1 kDa) and M_w (14.9 kDa). Longer reaction times (1h, Table 2-1) and higher temperatures (1i, Table 2-1) resulted in lower molecular weights and yields, believed to be caused by retrocycloaddition.

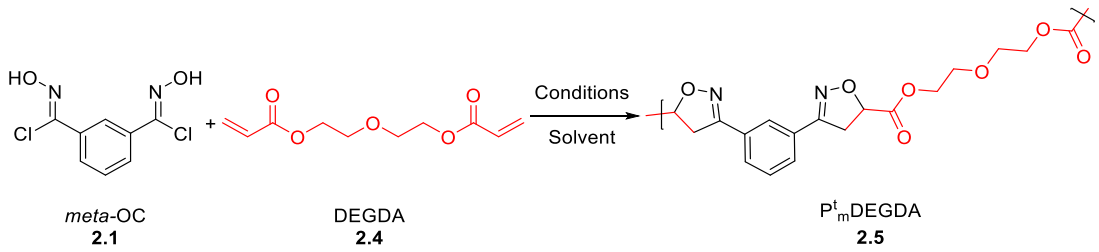

Scheme 2-2: Conditions trial for "click polymerisation" between *meta*-OC **2.1** and DEGDA **2.4**.

Entry	Base	Solvent	Temp / °C	Time / d	Mn / kDa	Mw / kDa	*Đ*	Yield / %
1a	-	Toluene	120	1	3.7	5.5	1.5	24
1b	NaOH	$CHCl_2/H_2O$	rt	1	3.4	4.6	1.3	99
1c	Et_3N	DMF	rt	1	4.2	5.7	1.4	60
1d	KF	DMF	rt	1	4.6	6.5	1.4	60
1e	KF	DMF	rt	5	5.3	7.8	1.5	67
1f	MS 4Å	DMF	rt	7	6.0	8.6	1.4	90
1g	MS 4Å	DMF	80	1	9.1	14.9	1.6	99
1h	MS 4Å	DMF	80	8	6.0	8.6	1.4	86
1i	MS 4Å	DMF	100	1	6.7	10.1	1.5	89

Table 2-1: Effect of varying conditions on Mn, Mw, *Đ* & yield of P^t_mDEGDA **2.5**.[317]

Takata *et al.*[317] then used the optimised conditions (4 Å MS, DMF, 80 ºC, 24 hrs) with a series of both alkene and alkyne dipolarophiles. Removal of the molecular sieves by filtration followed by precipitation in MeOH furnished the desired polymers. Polymers were successfully formed using a range of dialkene dipolarophiles (99 % yields), although at lower molecular weights than with DEGDA **2.4**. Reaction of DEGDA **2.4** with terepthalohydroximoyl dichloride **2.6**, resulted in lower molecular weights than when *meta*-OC **2.1** was used as the nitrile oxide precursor (Scheme 2.3, ΔMn = −5.8 kDa, ΔMw = −10.0 kDa). Use of terminal alkynes instead of alkenes as dipolarophiles led to lower yields (80 – 90 %) and lower molecular weights presumably as alkynes are less susceptible to dipolar cycloaddition.[258]

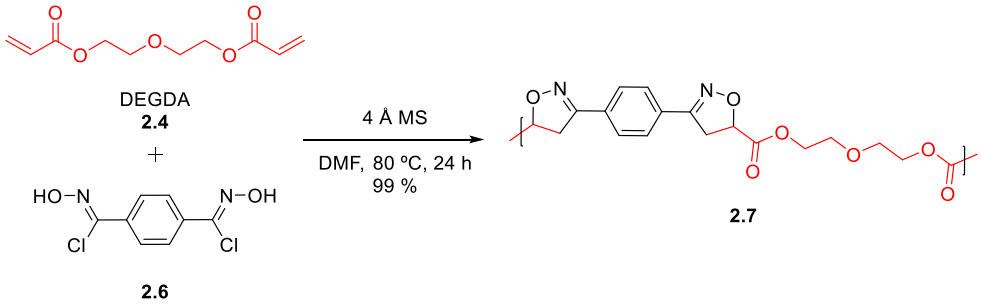

Scheme 2-3: Polymerisation of terepthalohydroximoyl dichloride **2.6** and DEGDA **2.4**.[317]

In a following paper in 2009 Takata *et al.*[318] improved on the polyisoxazole molecular weights by using different dialkyne monomers. The inclusion of an ether before the terminal alkyne significantly increased the molecular weight of the polyisoxazoles. Polyisoxazoles were then ring opened to unmask β-aminoenones and β-amino alcohols which allowed for further post polymerisation modification (Figure 2-2).

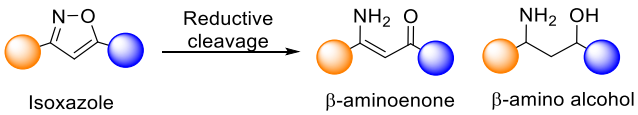

Figure 2-2: Unmasked functionalities by reductive cleavage of isoxazole rings.

2.2 Aims and Objectives

The method employed by Takata *et al*.[317,318] to produce polyisoxazoles and polyisoxazolines formed polymers with masked functionalities in the heterocyclic backbone. The overall aim of our work is to form similar polymers using monomers derived from renewable feedstocks. The field of nitrile oxide – dipolarophile polymerisation is small and unexplored, therefore, to increase our understanding of how these polymerisations proceed and the structure of the resulting polymers, investigations using commercially available dipolarophiles were initially carried out.

- We initially re-examined the reported reactions of Takata *et al.*[317] by preparing polyisoxazolines from *meta*-OC **2.1** and the dipolarophiles DEGDA **2.4** and DEGDMA **2.8** (Figure 2-3). Polymer thermal properties were determined, as well as a more thorough characterisation of the resulting polymer structures than was previously published.
- Other commercial monomers, EGDA **2.9** and PEGDA **2.10** (Figure 2-3) were used as dipolarophiles to investigate the effect of spacing of the isoxazoline moieties within the polymer structure.
- Due to competing side reactions to produce furoxans the effect of differing stoichiometry of monomers upon the end group chemistry, molecular weight, and thermal properties of polymers was also undertaken.

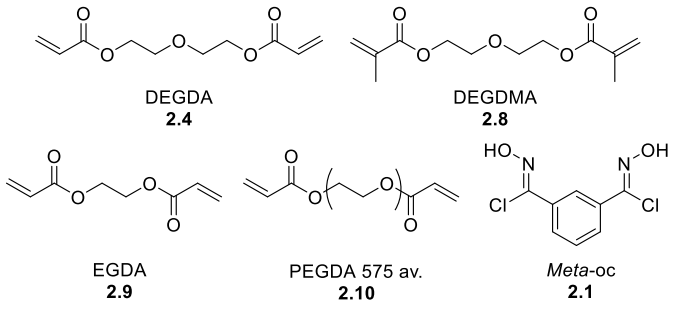

Figure 2-3: Monomers used for polyisoxazoline investigations in chapter 2.

2.3 Does the published method work? Comparison and characterisation of known literature polyisoxazolines.

Unhindered nitrile oxides are extremely reactive and as such must be formed *in situ*, often by the degradation of an oximoyl halide using heat or base. Aromatic nitrile oxides are more stable than aliphatic nitrile oxides,[260] therefore they are less likely to undergo unwanted side reactions during polymerisation. Takata *et al.*[317] published a viable way of forming polyisoxazolines and polyisoxazoles from the aromatic nitrile oxide *meta*-OC **2.1** and a range of dipolarophiles. As this was a relatively unexplored area of research it was deemed prudent to replicate some of Takata's reactions and compare the resulting polymers with those reported in the literature[317] as well as take the opportunity to characterise the polymers in greater detail.

Commercially available diethylene glycol diacrylate (DEGDA), **2.4**, and diethylene glycol dimethacrylate (DEGDMA), **2.8**, were chosen for comparison to reactions from Takata's 2008 paper[317] (Scheme 2-4).

Nomenclature of polymers in this thesis: Polymers will be given a code as well as an Arabic numeral reference (e.g. P^{t}_{m}DEGDA-1 (**2.5**)).

P represents a polymer (**P**$^{t}_{m}$DEGDA-1)

Superscript denotes method used for polymerisation ($P^{\mathbf{t}}_{m}$DEGDA-1)

P^{t} = Thermal procedure of Takata (24 hours)

P^{o} = Optimised polymerisation procedure

P^{t2} = Thermal procedure of Takata (48 hours)

P^{sf} = Solvent free procedure

Subscript denotes the nitrile oxide precursor ($P^{t}_{\mathbf{m}}$DEGDA-1)

m = *meta*-OC **2.1**

Abbreviation represent the dipolarophile monomer (P^{t}_{m}**DEGDA**-1)

Arabic numeral after a hyphen represent the ratio of dipolarophile to nitrile oxide precursor used (P^{t}_{m}DEGDA-**1**).

P^t_mDEGDA-1 is therefore a polymer formed by Takata's thermal method using *meta*-OC (**2.1**) and DEGDA (**2.4**) in a 1 : 1 ratio.

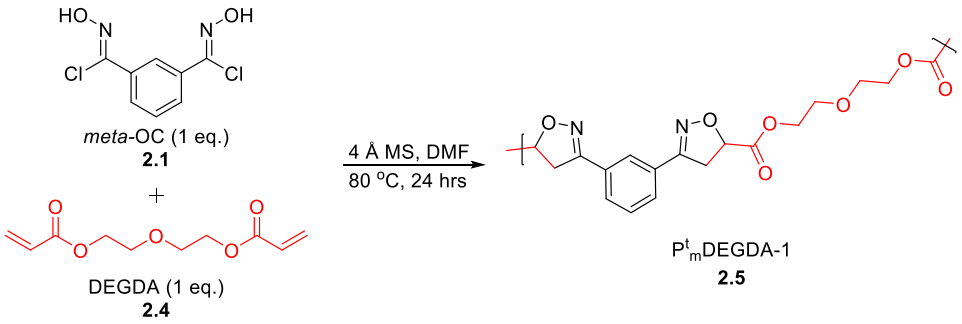

Scheme 2-4: Synthesis of polyisoxazoline P^t_mDEGDA-1 **2.5**

2.3.1 Synthesis of nitrile oxide precursor – *meta*-OC **2.1**

Nitrile precursor monomer *meta*-OC **2.1** was synthesised from isopthalaldehyde **2.11** in two steps (Scheme 2-5). Isopthalaldehyde **2.11** was dispersed in ethanol and water with sodium acetate and hydroxylamine hydrochloride at RT for 4 hours. The resulting white precipitate was filtered and washed with cold ethanol, leaving the dioxime **2.12** as a white solid in 71 % yield. The dioxime **2.12** was dispersed in DMF with *N*-chlorosuccinimide (NCS) at RT for 2 hours after which it was quenched with water and extracted with EtOAc. The dioximoyl chloride **2.1** (*meta*-OC) was purified by recrystallisation from toluene to give a white solid in 84 % yield.

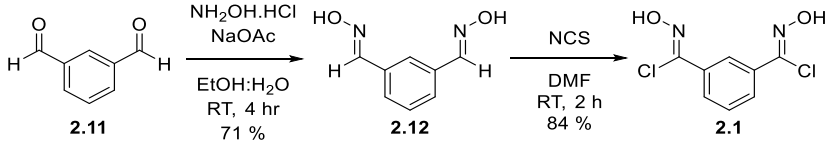

Scheme 2-5: Two-step synthesis pathway to form aromatic dioximoyl chloride *meta*-OC **2.1**

Crystals of *meta*-OC **2.1** were grown from acetone and analysed by x-ray crystallography to determine the relative conformation of the oximoyl chloride functional groups as well as whether the *syn*-(*Z*)- or *anti*-(*E*)-stereoisomers were preferred. In general oximoyl chlorides prefer the (*Z*)-conformation,[324,325] but the (*E*)-forms can be accessed by photoisomerisation of related acetates followed by hydrolysis. We wished to determine the stereochemistry of the groups because it is known that (*E*)-oximoyl chlorides typically decompose to their corresponding nitrile oxides at a slower rate than the corresponding (*Z*)-conformations (~6×10^7).[274] The crystal structure of *meta*-OC **2.1** (Figure 2-4) was confirmed as the *bis*-(*Z*)-

conformation and included a hydrogen bond between the OH group of the oximoyl chloride and the carbonyl of the solvent of crystallisation acetone. It is likely a similar hydrogen bonding interaction may occur with the carbonyl of DMF, the solvent used in our polymerisation reactions.

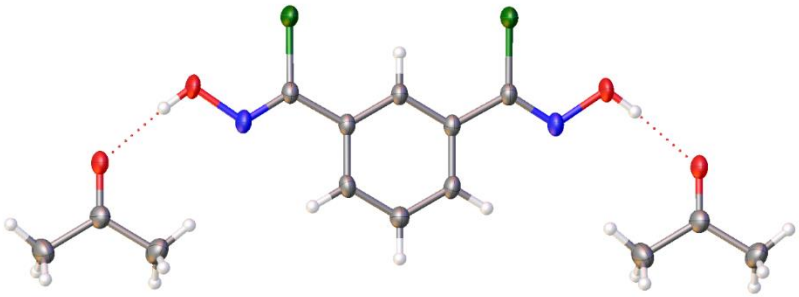

Figure 2-4: X-ray crystal structure of *meta*-OC **2.1**, shown coordinated to two acetone molecules.

2.3.2 Thermal analysis of nitrile oxide precursor – *meta*-OC **2.1**

The original work of Takata[317] utilised a temperature of 80 °C to facilitate polymerisation *via* the thermal degradation of the oximoyl chlorides by loss of HCl. The thermal characteristics of the nitrile oxide precursor *meta*-OC **2.1** were therefore briefly investigated. Complete conversions to the desired nitrile oxide *meta*-NO **2.13** by double elimination of HCl from *meta*-OC **2.1** was expected to produce a mass loss of 31 %. The TGA revealed a very gradual mass loss beginning around 100 °C. The temperature of complete HCl elimination (T_E) however did not occur until 217 °C (Figure 2-5). DSC evaluation of *meta*-OC (**2.1**) showed two strong exothermic peaks at 167 °C and 190 °C attributed to HCl elimination and nitrile oxide dimerization of *meta*-NO (**2.13**) respetively, these peaks began to appear around 125 °C before the melting point interrupts the enthalpic rise.

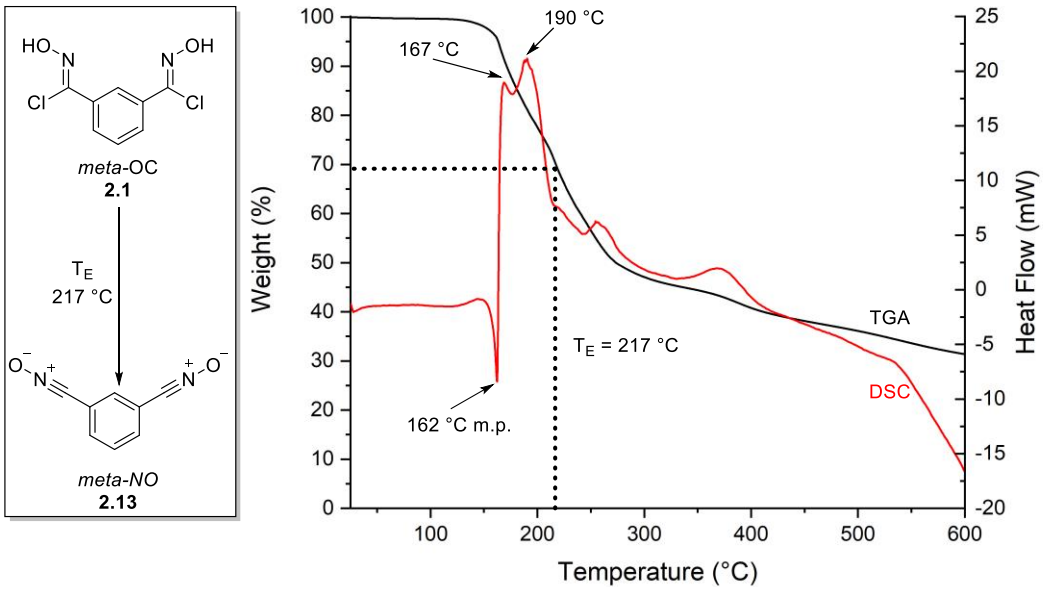

Figure 2-5: Thermal decomposition of *meta*-OC **2.1** to *meta*-NO **2.13** (*left*); Thermal degradation of *meta*-OC **2.1** (– TGA, – DSC) carried out at a heating rate of 10 °C min^{-1} under a N_2 atmosphere (*right*).

2.3.3 Synthesis of P^t_mDEGDA-1 **2.5** and P^t_mDEGDMA-1 **2.14**

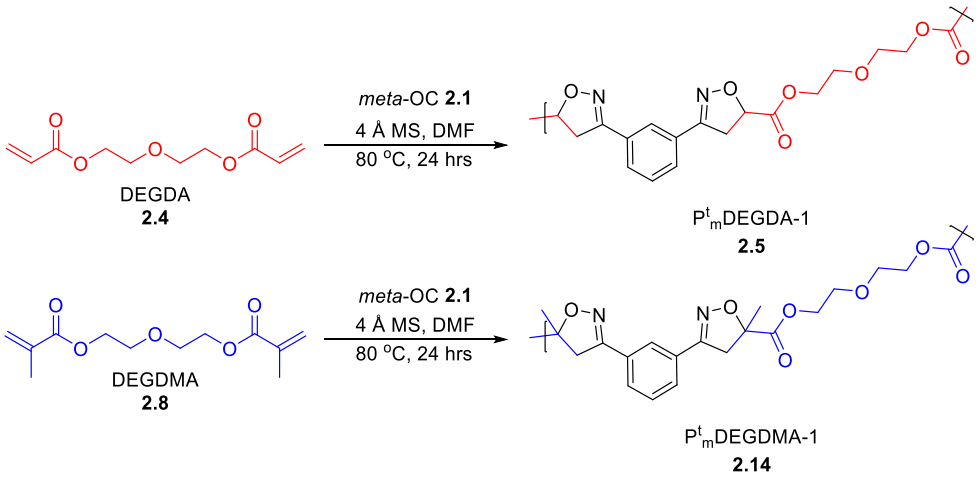

Scheme 2-6: Synthesis of P^t_mDEGDA-1 **2.5** and P^t_mDEGDMA-1 **2.14** using Takata's conditions.[317,318]

Polyisoxazolines were formed by the method employed by Takata *et al.*[317] This protocol was initially tested with DEGDA **2.4** and DEGDMA **2.8** (Scheme 2-6). The dipolarophiles (1 eq.) were dispersed in DMF (1 M) along with *meta*-OC **2.1** (1 eq.) and unactivated 4 Å molecular sieves (1.6 g / mmol of nitrile oxide precursor) for 30 minutes at room temperature, the temperature was then increased to 80 °C for 24 hours. Stirring was kept low (50 RPM) to reduce destruction of the molecular sieves, making their removal in the work up of the polymers easier. After 24 hours at 80 °C the mixture was diluted with $CHCl_3$ and filtered to remove the sieves, which were washed with additional $CHCl_3$ to collect any residual polymer. The organic filtrate was precipitated

into methanol. The precipitate was collected and washed with methanol to leave a light brown solid. To ensure an accurate yield was recorded the precipitate was removed from the filter paper by dissolving with $CHCl_3$, which was then reduced *in vacuo* to leave a foam. The polymeric foams were P^t_mDEGDA-1 **2.5** and P^t_mDEGDMA-1 **2.14**, formed from DEGDA **2.4** and DEGDMA **2.8** respectively. The foams were soluble in $CHCl_3$ and their structures could be confirmed by 400MHz ^{1}H NMR.

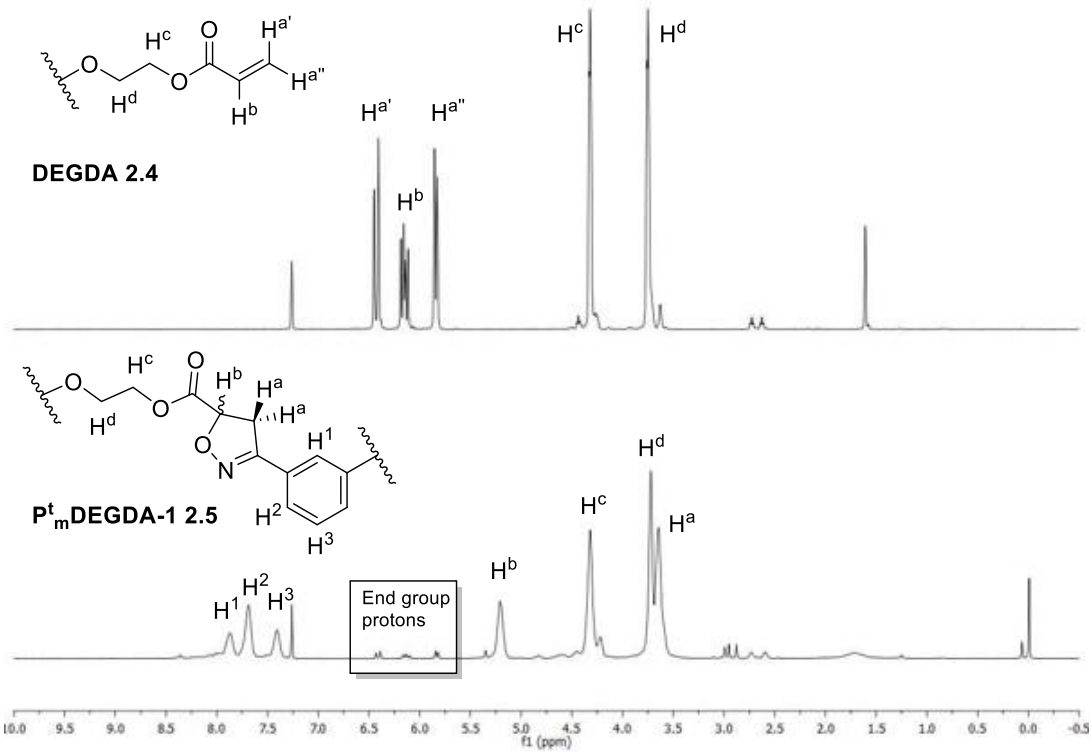

Figure 2-6: 400 MHz ^{1}H NMR of DEGDA **2.4** (top) and P^t_mDEGDA-1 **2.5** (bottom).

P^t_mDEGDA-1 **2.5**: Successful polymerisation was evident by the reduction of the signals of the alkene protons (5.5 – 6.5 ppm) in the monomer **2.4** as well as the incorporation of aromatic signals above 7.26 ppm (Figure 2-6). The 3,5-disubstituted isoxazoline ring in the polymer P^t_mDEGDA-1 **2.5** was confirmed by the signal at 5.21 ppm which corresponds to the H^b resonance in the isoxazoline ring. The signal corresponding to the H^a protons overlaps with protons from the glycol backbone of DEGDA at around 3.64 ppm, it could therefore not be used to estimate molecular weight by end group analysis. By comparing the integrals of the residual alkene signal at 6.13 ppm (H^b-end group) with the signal at 5.21 ppm in the polymer (H^b-polymer) it was possible to estimate that the polymer contained an average of 16 repeat units (6.2 kDa), (assuming acrylate end groups).

P$^{t}_{m}$DEGDMA-1 **2.14**: Similar observations were recorded in the 400MHz ^{1}H NMR of P$^{t}_{m}$DEGDMA-1 **2.14**, namely the reduction of the signals for the alkene protons at 5.56 and 6.11 ppm (Figure 2-7). The additional methyl substitution in the 3,5,5-trisubstituted isoxazoline ring compared to P$^{t}_{m}$DEGDA-1 **2.5** leads to the signals for the protons represented by H^{a} to be in different environments (doublets at 3.89 ppm and 3.24 ppm, $^{2}J_{HH}$ coupling of 16.5 Hz). The signal for the methyl group (H^{b}) shifts from 1.94 ppm in the monomer, where it is proximal to an alkene, to 1.70 ppm in the polymer where it is adjacent to the isoxazoline ring. Comparing the integrals of the isoxazoline signals at 3.89 ppm and 3.24 ppm with those relating to the residual end groups at 6.11 ppm and 5.56 ppm, it was possible to estimate that the polymers contained an average of 16 repeat units (6.7 kDa), (assuming acrylate end groups).

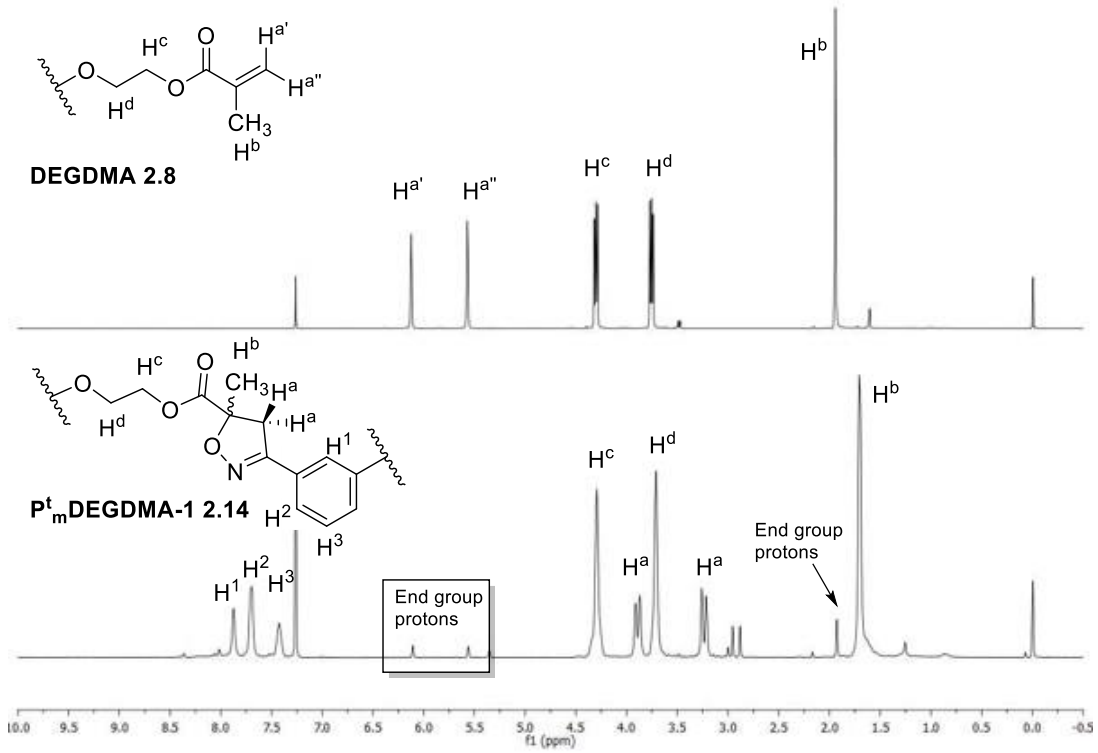

Figure 2-7: ^{1}H NMR of DEGDMA **2.8** (top) and P$^{t}_{m}$DEGDMA **2.14** (bottom).

2.3.4 Comparison of results to those published by Takata *et al.*[317]

To allow comparison between our recent work and the work done by Takata *et al.*[317] the yield, thermal analysis and molecular weight data was displayed against each other in Tables. Our work is denoted by "Jones" in the tables whilst the work by Takata *et al.*[317] is referred to by "Takata". The molecular weight and thermal data for

P$^{t}_{m}$DEGDA-1 **2.5** and P$^{t}_{m}$DEGDMA-1 **2.14** were compared to the analogous data reported in Takata's 2008 paper[317] to determine the reproducibility of the method described (Table 2-2). The thermal analysis data was similar to that recorded by Taketa *et al.*[317], however, there were significant differences in yields and molecular weight as determined by GPC analysis.

Entry	Polymer		Yield / %	T_g / °C	M_n / kDa	M_w / kDa	$Đ$
2a	P$^{t}_{m}$DEGDA-1 **2.5**	Jones	70	73	7.5[a]	13.4[a]	1.8[a]
2b[317]	P$^{t}_{m}$DEGDA-1 **2.5**	Takata	99	74	9.1[b]	14.9[b]	1.6[b]
2c	P$^{t}_{m}$DEGDMA-1 **2.14**	Jones	84	72	6.3[a]	13.0[a]	2.1[a]
2d[317]	P$^{t}_{m}$DEGDMA-1 **2.14**	Takata	99	58	4.2[b]	5.4[b]	1.3[b]

[a] DMF eluent, estimated by GPC against PMMA standards, [b] $CHCl_3$ eluent, estimated by GPC against PS standards

Table 2-2: Comparison of yield, thermal analysis and molecular weight to literature values.[317]

Yields of P$^{t}_{m}$DEGDA-1 **2.5** and P$^{t}_{m}$DEGDMA-1 **2.14** were lower in our hands compared to those reported by Takata.[317] During the work up of the reactions the polyisoxazoles were precipitated into methanol and collected by filtration. Mass spectroscopic analysis of the methanol filtrate revealed masses equivalent to trimer (**2.15**) and tetramer (**2.16** & **2.17**) oligomers (Figure 2-8), which would account for the reduced yield (assuming less low molecular weight oligomers were produced in the Takata study[317]).

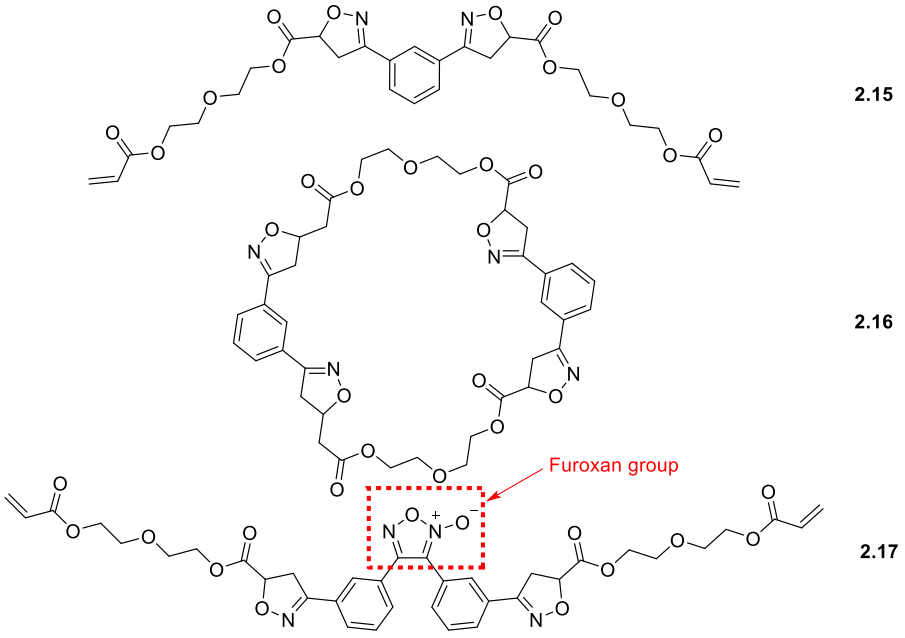

Figure 2-8: 3- and 4-membered oligomers of P$^{t}_{m}$DEGDA **2.5**.

Interestingly because the mass spectrometric analysis indicated equal ratios of monomers incorporated into the oligomers (**2.16** & **2.17**) combined with the fact that nitrile oxides are too reactive to remain as end groups, these materials must be cyclic or contain a furoxan link caused by nitrile oxide dimerization (Figure 2-8). This interpretation was confirmed by analysis of the filtrate by 300 MHz ^{1}H NMR analysis which indicated a low ratio of alkene signals (5.5 – 6.5 ppm) relative to aromatic signals (7.3 – 8.0 ppm), suggestive of significant levels of cyclic structures (**2.16)**.

2.3.4.1 Thermal analysis comparison

To polyisoxazoline's glass transition temperatures (T_g) were analysed by DSC under N_2 at a heating rate of 10 °C min^{-1}. Polymers (**2.5** & **2.14**) were first heated to 100 ºC, cooled to –100 ºC then heated to 300 ºC, T_g's were determined from the second heating step. P$^{t}_{m}$DEGDA-1 **2.5** had a similar T_g to that recorded by Takata[317] (3a & 3b, Table 2-3, P$^{t}_{m}$DEGDA-1 **2.5** $\Delta T_g = -1$ °C). The T_g of P$^{t}_{m}$DEGDMA-1 **2.14** was significantly higher than Takata's[317] (3c & 3d, Table 2-3, P$^{t}_{m}$DEGDMA-1 **2.14** $\Delta T_g = +14$ °C). Estimation of the molecular weight of P$^{t}_{m}$DEGDMA-1 **2.14** by 400MHz ^{1}H NMR and GPC suggested larger polymers than those reported by Takata. This increased size is a possible cause of the measured higher T_g.

Entry	Polymer		T_g / °C	T_5 / °C	T_{20} / °C
3a	P$^{t}_{m}$DEGDA-1 **2.5**	Jones	73	230	275
3b[317]	P$^{t}_{m}$DEGDA-1 **2.5**	Takata	74	253	260
3c	P$^{t}_{m}$DEGDMA-1 **2.14**	Jones	72	258	280
3d[317]	P$^{t}_{m}$DEGDMA-1 **2.14**	Takata	58	268	278

Table 2-3: Comparison of thermal analysis of P$^{t}_{m}$DEGDA-1 and P$^{t}_{m}$DEGDMA-1 to literature values.[317]

Thermal analysis of the polymers by TGA revealed some difference in the T_5 and T_{20} values, the temperature at which 5 % and 20 % of the initial weight has been lost, as those reported in literature.[317] Initial degradation (T_5) began at a lower temperature for P$^{t}_{m}$DEGDA-1 **2.5** compared to Takata's[317] (3a & 3b, Table 2-3, P$^{t}_{m}$DEGDA-1 **2.5** $\Delta T_5 = -23$ °C, $\Delta T_{20} = +15$ °C). While values were closer when comparing P$^{t}_{m}$DEGDMA-1 **2.14** to the values given in the paper[317] (3c & 3d, Table 2-3, P$^{t}_{m}$DEGDMA-1 **2.14** $\Delta T_5 = -10$ °C, $\Delta T_{20} = +2$ °C).

2.3.4.2 GPC analysis comparison

While both polymers were soluble in $CHCl_3$ (the same eluent used for GPC analysis by Takata[317]), the column set up for the GPC at Warwick was different and included TEA as an additive. The additive may have been the cause of the significant difference seen in results, in particular the significantly lower molecular weights than calculated *via* 400MHz ^{1}H NMR end group analysis (4a vs 4b; 4d vs 4f, Table 2-4).

Changing the eluent to DMF with ammonium tetrafluoroborate (NH_4BF_4) as the stabilisation additive provided results in agreement with end group analysis. As previously mentioned (section 2.3.4.1), the higher molecular weight could be the cause for the higher T_g of P^t_mDEGDMA-1 **2.14** compared to literature[317] (3c & 3d, Table 2-3, ΔT_g = +14 °C).

Entry	Polymer		GPC eluent	M_n / kDa	M_w / kDa	$Đ$
4a	P^t_mDEGDA-1 **2.5**	Jones	$CHCl_3$	1.9[a]	7.2[a]	3.8[a]
4b	P^t_mDEGDA-1 **2.5**	Jones	DMF	7.5[b]	13.4[b]	1.8[b]
4c[317]	P^t_mDEGDA-1 **2.5**	Takata	$CHCl_3$	9.1[b]	14.9[b]	1.6[b]
4d	P^t_mDEGDMA-1 **2.14**	Jones	$CHCl_3$	3.3[b]	9.8[b]	3.0[b]
4e	P^t_mDEGDMA-1 **2.14**	Jones	DMF	6.3[b]	13.0[b]	2.1[b]
4f[317]	P^t_mDEGDMA-1 **2.14**	Takata	$CHCl_3$	4.2[b]	5.4[b]	1.3[b]

[a] Estimated by GPC based on PS standards, [b] estimated by GPC based on PMMA standards

Table 2-4: Comparison of molecular weight estimated by GPC against different standards using different eluents.

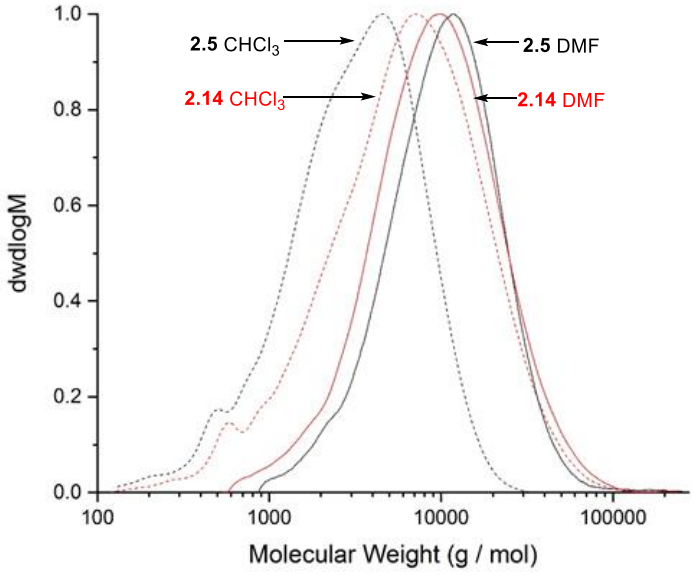

Figure 2-9: GPC plot of P^t_mDEGDA-1 **2.5** (--- $CHCl_3$, – DMF) and P^t_mDEGDMA-1 **2.14** (--- $CHCl_3$, – DMF)

2.3.5 Structural analysis using MALDI-TOF-MS and IR spectroscopy

Takata did not publish detailed structural studies of his polymers to determine the type of end group or the presence of furoxan linkages. To gain a better understanding of the structure of these polyisoxazolines, MALDI-TOF analysis of P^t_mDEGDA-1 **2.5** and P^t_mDEGDMA-1 **2.14** was performed using a Bruker Daltonix – autoflex™ speed MALDI-TOF instrument. P^t_mDEGDA-1 **2.5** presented 9 distinct repeating peaks in the MALDI spectrum, (Figure 2-11 is a section of the MALDI spectrum containing the repeating masses). The masses have been labelled 1 – 10, the repeating unit relating to the dipolarophile (DEGDA **2.4**) will be referred to as A and the di(nitrile oxide) unit **2.13** as B (Figure 2-10). When at the end of a polymer chain it, the unit A can be terminated as either an acrylate, a carboxylic acid or an alcohol group-(see later).

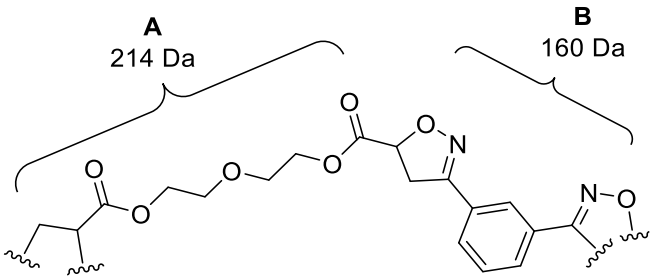

Figure 2-10: A – dipolarophile derived polymer section, B – nitrile-oxide derived polymer section.

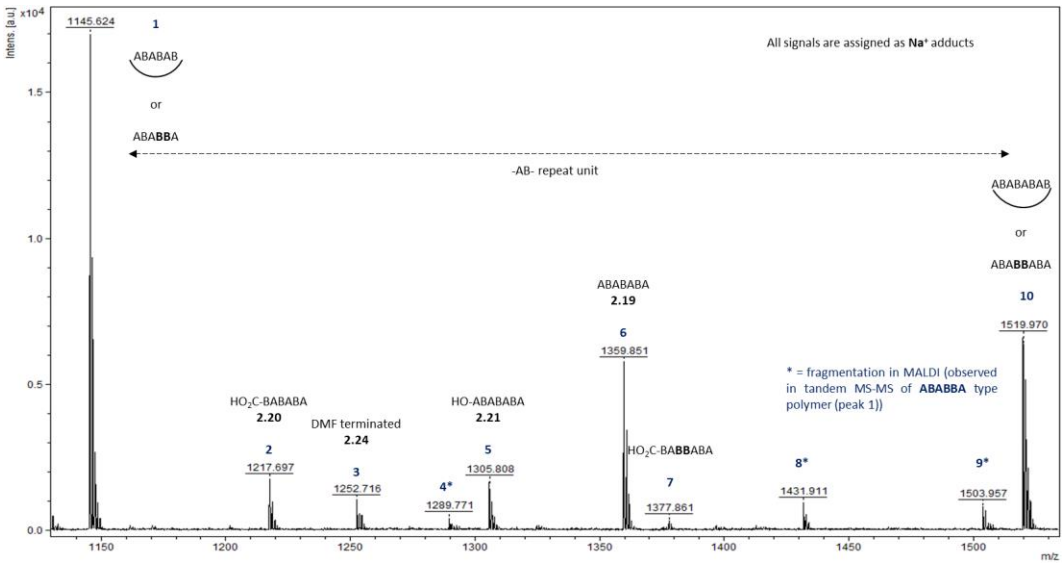

Figure 2-11: Section of P^t_mDEGDA-1 **2.5** MALDI-TOF spectra

P^t_mDEGDA-1 **2.5**: The repeat unit (374 Da) can be observed in the spectrum (masses 1 → 10). Mass 1 at 1145.624 Da contains equal ratios of dipolarophile (A) and nitrile oxide (B). As described for the oligomers in section 2.3.4, the equal ratios are caused

by the polymer either adopting a cyclic structure or by dimerisation of nitrile oxides groups *via* a furoxan link.

Tandem MS-MS analysis of peak 1(Figure 2-12) showed significant fragmentation arising from groups lost by the decomposition of the isoxazoline ring, with the major fragment being caused by the loss of an AB unit. As the mass of DEGDA **2.4** and *meta*-NO **2.13** is conserved during polymerisation it is not possible to tell whether the AB unit was lost from an end group or by decomposition of two isoxazoline rings removing a section from a cyclical polymer. The next most abundant decompositions are caused by the loss of a B unit (160 Da) and A(2B) unit (534 Da). Once again, the loss of an A(2B) unit (532 Da) could occur in a cyclical polymer or in a linear polymer with a penultimate furoxan link (ABABBA). The loss of the singular B unit (160 Da) however is indicative of a cyclical polymer as nitrile oxide B cannot remain as a chain end due to its reactivity, it could therefore only be lost by the decomposition of two isoxazoline rings.

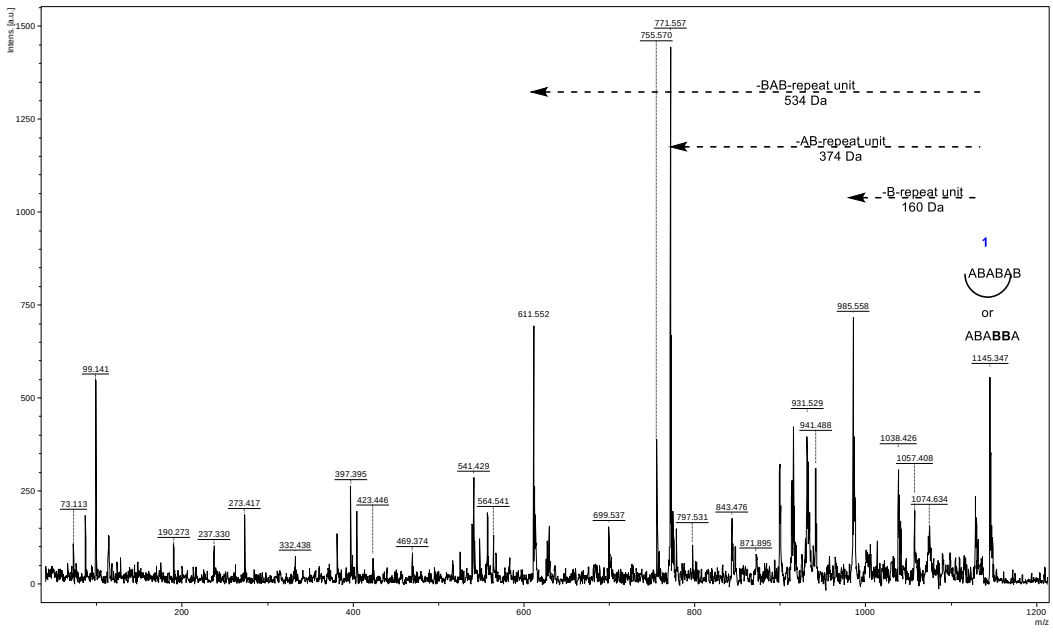

Figure 2-12: Tandem MS-MS analysis of peak 1 from **2.5** (1146 Da)

Infrared analysis supported a linear structure, with weak absorptions at 1606 cm^{-1} and 1574 cm^{-1} associated to a furoxan link (Figure 2-13). The formation of these furoxan links lowers the desired 1:1 reacting stoichiometry of nitrile oxide : alkene functional groups during polymerisation and consequently leads to the relatively small number of repeat units observed in the polymers. The Tandem MS-MS analysis and the IR

analysis suggests that the $(AB)_n$ polymer chains are a combination of linear chains containing furoxan links (minor) and cyclical polymers caused by back biting (major).

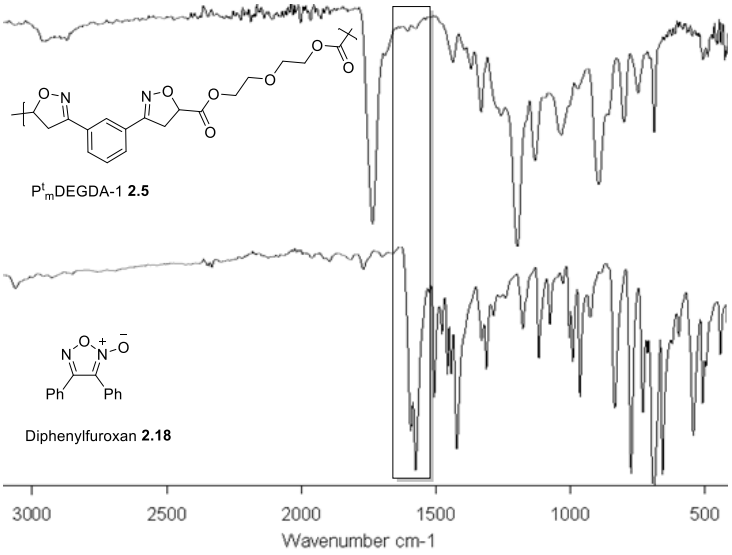

Figure 2-13: IR spectra of P^t_mDEGDA-1 **2.5** and Diphenyl furoxan **2.18**.

The second most abundant repeating unit corresponds to mass 6 (1359.851 Da) and is assigned as the ABABABA structure **2.19** with the terminal alkenes of the acrylate groups intact, (Figure 2-14). At lower molecular weights (<2.3 kDa) the signals corresponding to the repeat units $(AB)_n$ are more abundant than those containing DEGDA termination $(AB)_n$-A. At higher molecular weights (>2.3 kDa) however this trend switches, supporting the conclusion that cyclic $(AB)_n$ compounds are more common than furoxan containing $(AB)_n$ chains. As the chain length increases back biting becomes less common and furoxan formation becomes the predominate cause of $(AB)_n$ polymers, leading to less $(AB)_n$ compounds relative to $(AB)_n$-A chains.

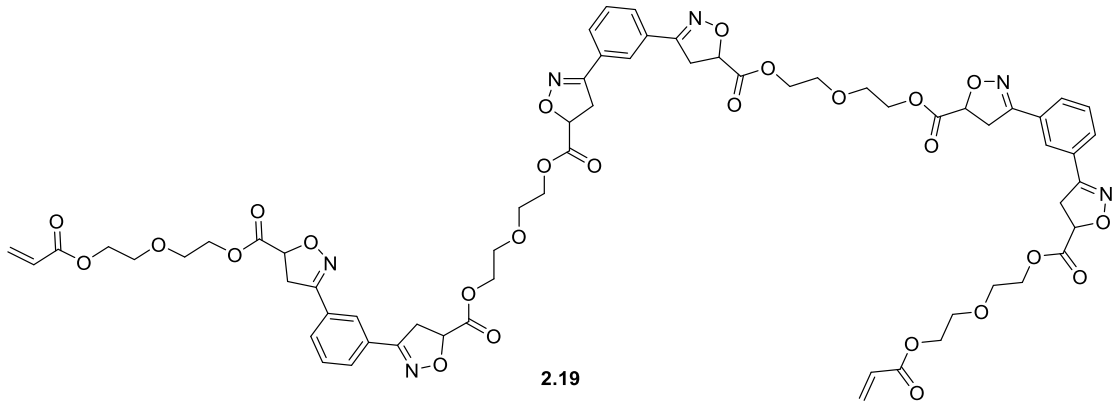

Figure 2-14: Peak 6 (A + 1 : B) polymer structure, **2.19**.

The units corresponding to the peaks 2 (**1217.697**), 5 (**1305.808**), and 7 (**1377.861**) relate to alcoholic and acidic end groups (Figure 2-15). These have been caused by degradation of DEGDA's **2.5** prior to MALDI analysis. Hydrolysis of DEGDA's **2.5** ester results in acrylic acid **2.22** and 2-(2-hydroxyethoxy)ethyl acrylate **2.23** (Figure 2-16), if this happened before or during polymerisation it would have terminated chain growth, hydrolysis could have also occurred after polymerisation. The presence of peak 7 ($(AB)_n$-B-CO_2H) requires a furoxan link in the growing polymer chain, which further infers that furoxan links are also present in the $(AB)_n$ chains.

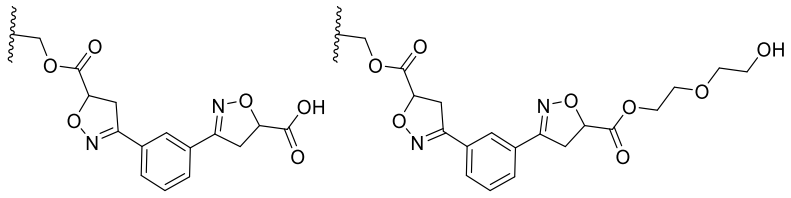

Figure 2-15: Acrylic acid terminated polymer (**2.20**, *left*), 2-(2-hydroxyethoxy)ethyl acrylate terminated polymer (**2.21**, *right*).

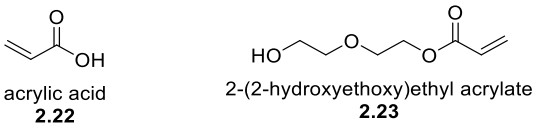

Figure 2-16: Hydrolysis products of DEGDA **2.4**.

Peak 3 (**1252.716**) relating to a highly unusual addition of the DMF solvent onto a oximoyl chloride end group (Figure 2-17) is of particular interest. It is unclear how this occurs and as to whether it plays a catalytic role in the polymerisation propagation, like in the Vilsmeier–Haack reaction,[326] or whether it terminates the chain end by stopping a nitrile oxide forming. This unusual end group structure was proposed after the analysis of a product from a small molecule reaction described in section 3.4. Analysis of this product (section 3.4) by ^{1}H and ^{13}C 500 MHz NMR allowed for the tentative assignment of peak 3 as having the end group structure **2.24**.

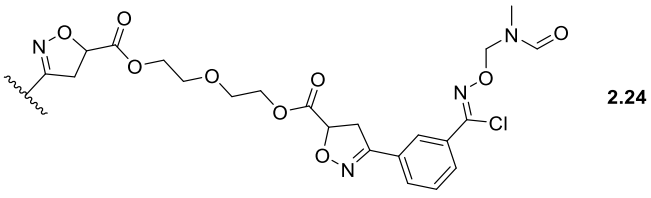

Figure 2-17: DMF addition onto the chain end.

The less abundant repeating units corresponding to peaks 4 (**1289.771**) 8 (**1431.911**) and 9 (**1503.957**) are caused by fragmentation of $(AB)_4$ and $(AB)_4$-A during the analysis by MALDI-TOF (this fragmentation pattern was observed in the tandem MS-MS of $(AB)_n$ units (Figure 2-12)). Peaks 4 and 9 relate to the breaking of the isoxazoline ring at the weak N-O bond followed by loss of the radical fragment **2.25** (Figure 2-18) from $(AB)_4$ and $(AB)_4$-A respectively. Peak 8 however is caused by the unzipping of the DEGDA chain and a loss of **2.26** from $(AB)_4$, once again indicating a cyclical polymer.

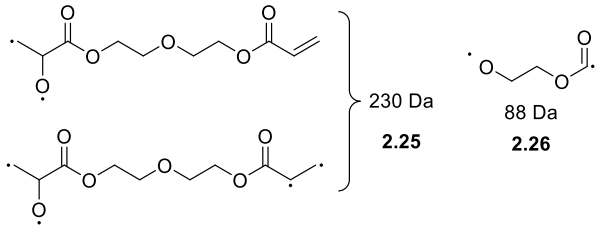

Figure 2-18: Radical molecules **2.25** and **2.26** lost by MALDI-TOF initiated degradation of P^t_mDEGDA-1 **2.5**.

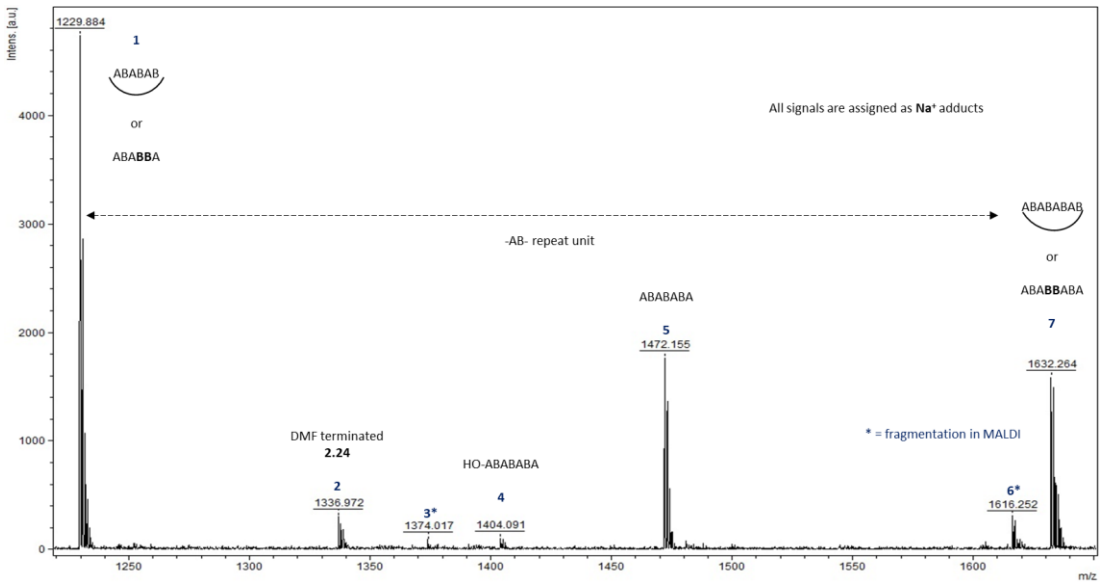

Figure 2-19: Section of P^t_mDEGDMA-1 **2.14** MALDI-TOF spectra.

P^t_mDEGDMA-1 **2.14**: P^t_mDEGDMA-1 **2.14** had fewer repeating peaks observed in its MALDI-TOF spectra, (Figure 2-19) than P^t_mDEGDA-1 **2.5**. Peaks 1(**1229.884**) and 7 (**1632.264**) correspond to the $(AB)_n$ structures. There was no evidence of molecules where the addition to methacrylic acid (decomposition of DEGDMA) had occurred although peak 4 (**1404.091**) does relate to the alcohol end group caused by the hydrolysis of a DEGDMA unit. As with P^t_mDEGDA-1 **2.5** there was evidence (peak 2) for the addition of DMF to a terminal oximoyl chloride unit, as demonstrated by the

stereotypical chlorine isotopic mass distribution. Peaks 3 and 6 were degradation peaks caused by decomposition of the isoxazoline ring in the same manner as with P^t_mDEGDA-1 **2.15** (Figure 2-18, **2.25**). Peak 5 corresponds to the $(AB)_n$-A polymer. IR analysis of P^t_mDEGDMA-1 **2.14** also revealed weak adsorptions around 1600 cm^{-1} and 1575 cm^{-1} that could relate to the occurrence of furoxan rings.

2.4 Effect of glycol chain length on polymer properties

By altering the glycol chain length of the dipolarophilic monomer the effect of the proximity of dipolarophilic groups upon the thermal properties of the polymers was investigated. Commercially available ethylene glycol diacrylate (EGDA **2.9**) and polyethylene glycol diacrylate (PEGDA **2.10**) were used and the results compared with those already described for DEGDA **2.4** (Figure 2-20). EGDA **2.9** and PEGDA **2.10** were chosen to study the extremes of glycol chain length

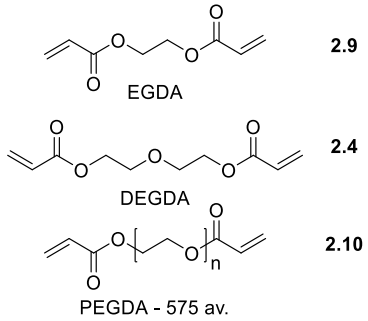

Figure 2-20: Commercially available dipolarophiles used in the study

2.4.1 Analysis of polymers containing variable glycol chain lengths

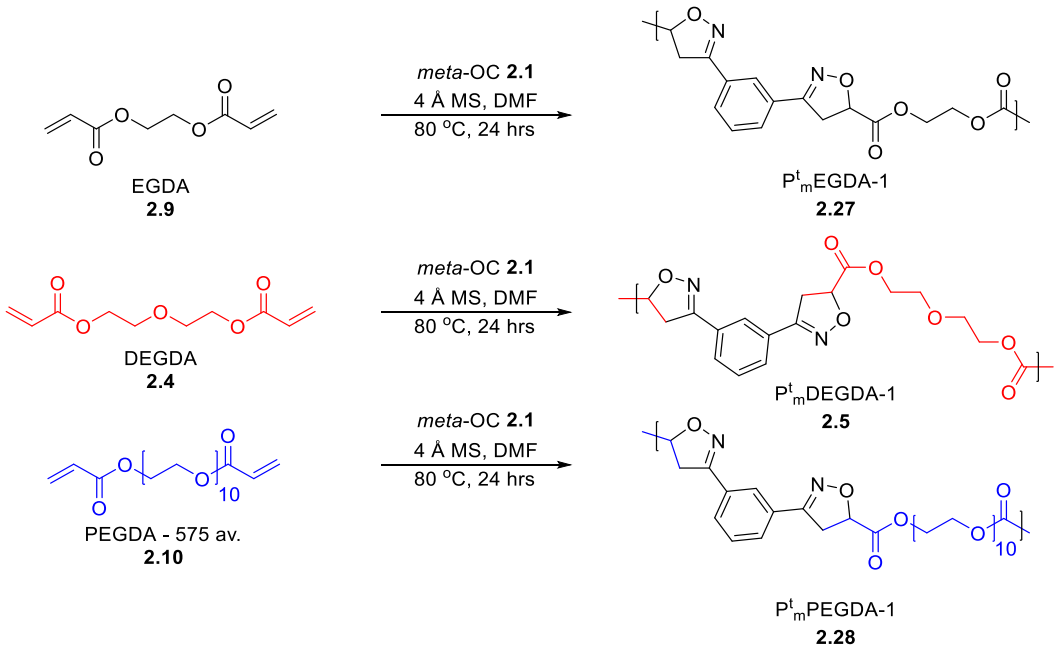

Scheme 2-7: Synthesis of polyisoxazolines with different glycol chain lengths.

Following the same polymerisation and work up procedure described in section 2.3.3, P^t_mEGDA-1 **2.27** and P^t_mPEGDA-1 **2.28** were synthesised in 48 % and 43 % yields

respectively (Scheme 2-7). P$^{t}_{m}$EGDA-1 **2.27** was a hard brown solid whilst P$^{t}_{m}$PEGDA-1 **2.28** was a soft brown wax. End group analysis using 400 MHz ^{1}H NMR allowed estimation of polymer sizes with both P$^{t}_{m}$EGDA-1 **2.27** and P$^{t}_{m}$PEGDA-1 **2.28** estimated having an average of 8 repeat groups, predicting molecular weights of 2.8 kDa and 6.5 kDa respectively.

Entry	Polymer	NMR calc.	M_n[a] / kDa	M_w[a] / kDa	$Đ$[a]	RU[b] M_n	RU[b] M_w	Yield / %
5a	P$^{t}_{m}$EGDA-1 **2.27**	8	3.9	5.4	1.4	12	16.5	48
5b	P$^{t}_{m}$DEGDA-1 **2.5**	16	7.5	13.4	1.8	20	36	70
5c	P$^{t}_{m}$PEGDA-1 **2.28**	8	10.8	22.4	2.1	14.5	30.5	43

[a] Estimated by GPC based on PMMA standards, [b]Calculated by division of GPC data by the repeat unit (RU) molecular weight

Table 2-5: Comparison of yield and polymer size (as determined by NMR and GPC) between polyisoxazolines containing different glycol chain lengths.

GPC analysis of the three polymers in DMF using a PMMA standard is highlighted for comparison (Table 2-5, Figure 2-21). The extent of polymerisation was determined by dividing the GPC molecular weight estimations by the repeat unit (RU) molecular weight, 330 Da, 374 Da, and 735 Da for P$^{t}_{m}$EGDA-1 **2.27**, P$^{t}_{m}$DEGDA-1 **2.5** and P$^{t}_{m}$PEGDA-1 **2.28** respectively. Analysis by both 400 MHz ^{1}H NMR and GPC indicated that P$^{t}_{m}$DEGDA-1 **2.5** had the highest number of repeat units, suggesting that spacing between dipolarophilic groups in the monomer may influence the achievable extent of polymerisation. A similar trend was seen in the isolated yield of the three polyisoxazolines, with less precipitate being collected for P$^{t}_{m}$EGDA-1 **2.27** and P$^{t}_{m}$PEGDA-1 **2.28** relative to P$^{t}_{m}$DEGDA-1 **2.5**.

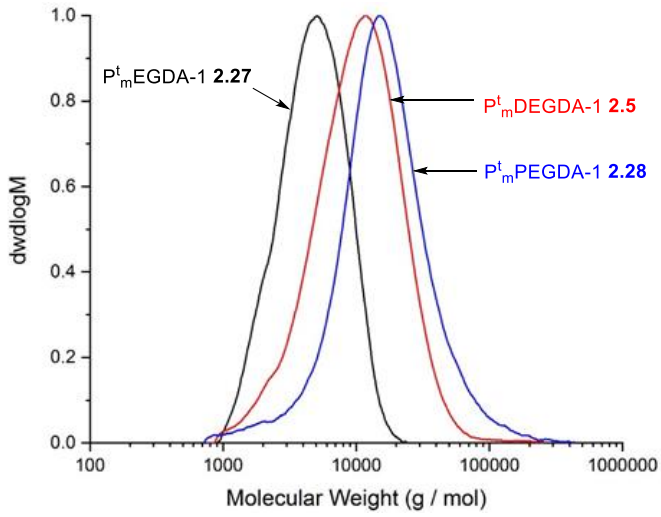

Figure 2-21: GPC plot of P$^{t}_{m}$EGDA-1 **2.27**, P$^{t}_{m}$DEGDA-1 **2.5**, and P$^{t}_{m}$PEGDA-1 **2.28**.

Glass transition temperatures followed the expected trend with lower T_g's for the more flexible acrylates (Table 2-6). P^t_mEGDA-1 **2.27** had the highest (T_g = 102 °C), followed by P^t_mDEGDA-1 **2.5** (T_g = 73 °C) with P^t_mPEGDA-1 **2.28** (T_g = −8 °C) being considerably lower. This shows the physical properties of the polyisoxazolines can be tuned by changing the chain length separating the heterocyclic rings.

Entry	Polymer	T_g / °C	T_5 / °C	T_{20} / °C
6a	P^t_mEGDA-1 **2.27**	102	224	278
6b	P^t_mDEGDA-1 **2.5**	73	230	275
6c	P^t_mPEGDA-1 **2.28**	-8	250	327

Table 2-6: Thermal analysis of P^t_mEGDA-1 **2.27**, P^t_mDEGDA-1 **2.5**, and P^t_mPEGDA-1 **2.28.**

The polymers T_5 thermal stability also increased with the increase in acrylate flexibility (Table 2-6). P^t_mEGDA-1 **2.27** (6a, Table 2-6, T_5 = 224 °C, T_{20} = 278 °C) and P^t_mDEGDA-1 **2.5** (6b, Table 2-6, T_5 = 230 °C, T_{20} = 275 °C) had similar thermal stability and degradation patterns unlike P^t_mPEGDA-1 **2.28** (6c, Table 2-6, T_5 = 250 °C, T_{20} = 327 °C) which had a higher thermal stability than the shorter glycol chain polymers. This is most likely caused by the large polyethylene glycol (PEG) composition of P^t_mPEGDA-1 **2.28**. The thermal stability of PEG increases with molecular weight with PEG_{400} reported to begin degradation around 250 ºC.[327,328]

2.5 Polymers using non-stoichiometric ratios of monomers

One of the major issues with using nitrile oxides as monomers is their ability to dimerise and form furoxans.[259,262,329] If this occurs during polymerisation it propagates polymer growth but reduces the ratio of dipole (type B monomer) to dipolarophile (type A monomer), leading to premature termination and low molecular weights. Analysis of the polyisoxazolines by MALDI-TOF-MS (section 2.3.5) revealed masses containing equal ratios of dipolarophile A and dipole B. As nitrile oxides cannot remain as chain ends due to their reactivity it suggests that the polymers were terminating as cyclical oligomers or that furoxans were forming. Infrared analysis provided evidence of furoxan formation with weak adsorptions around 1600 cm^{-1} and 1575 cm^{-1}. As stated above the occurrence of furoxans would cause non-stoichiometric ratios of dipolarophile to dipole. To investigate this effect further polymerisations were carried out, varying the ratios of dipolarophiles (EGDA **2.9**, DEGDA **2.4**, PEGDA **2.10** and DEGDMA **2.8**) relative to nitrile oxide precursor *meta*-OC **2.4** (Scheme 2-8).

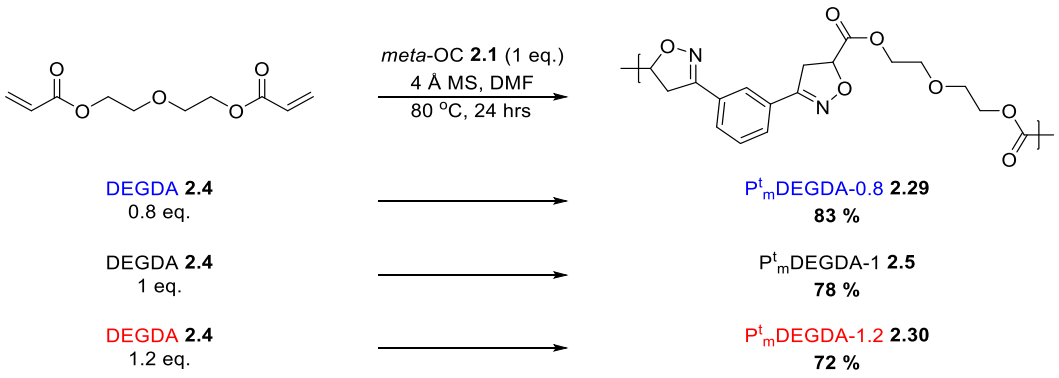

Scheme 2-8: Synthesis of polyisoxazolines using different ratios of monomers

In the following discussion the ratio of dipolarophile relative to nitrile oxide (A : B) is indicated by a number at the end of the polymer abbreviation, hence, P^t_mDEGDA-1.2 **2.30** refers to a polyisoxazoline formed using 1.2 equivalents of DEGDA **2.4** relative to *meta*-OC **2.1**.

2.5.1 Properties of polymers produced using differing ratios of monomers.

If the nitrile oxide reactive centre in *meta*-OC **2.1** (monomer B) can react with itself (e.g. B + B → BB to give a furoxan) then this process competes with the desired

cycloaddition (A + B → AB). Furoxan formation removes nitrile oxide reactive centres in the growing polymer chain, leading to polymers preferentially terminated by an A monomer. This will have the effect of lowering the molecular weight of the observed step growth polymers by diverging the ratio of reactive monomer groups away from the desired 1:1 ratio (see the Carothers equation, equation 2.1). If furoxan formation is prevalent during polymerisation increasing the amount of *meta*-OC **2.1** (monomer B) relative to monomer A, should cause the stoichiometry of reactive groups in both monomers A and B to approach 1:1. The exact ratios of A:B to ensure the largest molecular weights will be dependent upon the relative rates of A + B → AB and B + B → BB and whether the B + B ↔ BB process is reversible.

$$X_n = \frac{1 + r}{1 + r - 2rp}$$

Equation 2.1: Non-equimolar Carothers equation, X_n = number average degree of polymerisation, r = stoichiometric ratio of monomers, p = conversion

Entry	Polymer	T_g / °C	T_5 / °C	T_{20} / °C	M_n[a] / kDa	M_w[a] / kDa	$Đ$[a]	Yield / %
7a	P^t_mEGDA-0.8 **2.31**	108	174	263	4.7	8.5	1.8	60
7b	P^t_mEGDA-1 **2.27**	102	205	268	3.9	5.4	1.4	49
7c	P^t_mEGDA-1.2 **2.32**	118	168	244	3.2	5.1	1.5	56
7d	P^t_mDEGDA-0.8 **2.29**	76	230	266	8.8	18.1	2.1	83
7e	P^t_mDEGDA-1 **2.5**	73	229	274	7.5	13.4	1.8	78
7f	P^t_mDEGDA-1.2 **2.30**	58	243	286	6.0	9.6	1.6	72
7g	P^t_mPEGDA-0.8 **2.33**	-6	250	332	13.0	29.2	2.2	79
7h	P^t_mPEGDA-1 **2.28**	-8	250	327	10.8	22.4	2.1	43
7i	P^t_mPEGDA-1.2 **2.34**	-8	243	327	10.3	21.1	2.1	30
7j	P^t_mDEGDMA-0.8 **2.35**	83	234	277	8.1	19.0	2.4	72
7k	P^t_mDEGDMA-1 **2.14**	74	254	278	6.3	13.0	2.1	84
7l	P^t_mDEGDMA-1.2 **2.36**	72	253	276	6.2	10.6	1.7	84

[a] DMF used as eluent, estimated by GPC based on PMMA standards.

Table 2-7: Thermal analysis and GPC data for polyisoxazoles

Analysis of the molecular weights of the polymers produced from reaction with the 4 monomers EGDA, DEGDA, PEDGDA and DEGDMA (monomers A) and *meta*-OC **2.1** (monomer B) indicate a steady decrease in molecular weight with increasing monomer A concentration. As expected from the analysis above the highest molecular weight polymers were observed using a 0.8:1.0 ratio of A:B monomers (7a, 7d, 7g &

7j, Table 2-7). In addition, (with the exception of EGDA 7c) dispersity's and T_g drop as the amount of dipolarophile A is increased (Table 2-7).

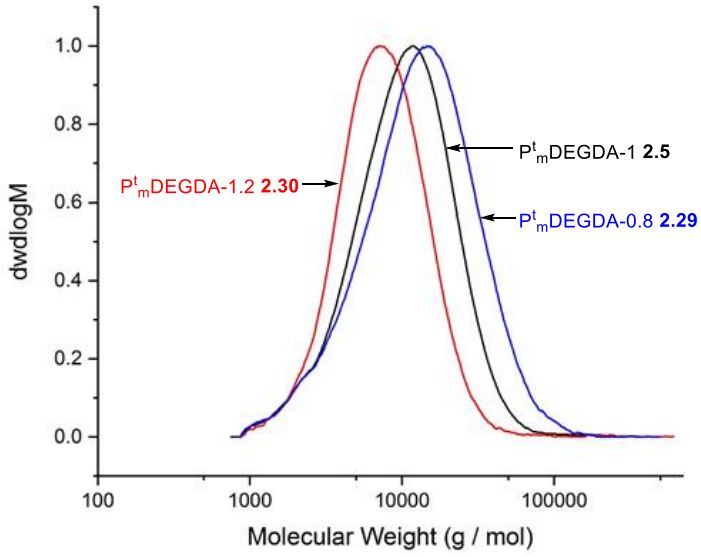

Figure 2-22: GPC plot of P^t_mDEGDA-0.8 **2.29**, P^t_mDEGDA-1 **2.5**, and P^t_mDEGDA-1.2 **2.30**

Thermal analysis of the polyisoxazolines show no clear trend in thermal stability. In the P^t_mDEGDA series initial mass loss (T_5) and secondary mass loss (T_{20}) was similar for the three different ratios P^t_mDEGDA-0.8 **2.29** (8a, Table 2-8, T_5 = 230, T_{20} = 266), P^t_mDEGDA-1 **2.5** (8b, Table 2-8 T_5 = 229, T_{20} = 274), and P^t_mDEGDA-0.8 **2.30** (8c, Table 2-8, T_5 = 243, T_{20} = 286). Given the molecular weight differences between the three polymers this indicates that the polymer chain size has negligible effects on thermal stability.

Entry	Polymer	T_g / °C	T_5 / °C	T_{20} / °C
8a	P^t_mDEGDA-0.8 **2.29**	76	230	266
8b	P^t_mDEGDA-1 **2.5**	73	229	274
8c	P^t_mDEGDA-1.2 **2.30**	58	243	286

Table 2-8: Thermal analysis of non-equimolar P^t_mDEGDA series.

Unlike thermal stability, glass transition temperature shows a strong correlation to the equivalents of dipolarophile used. As the equivalents of DEGDA **2.4** used increased, the T_g reduced. P^t_mDEGDA-1.2 **2.30** (8c, Table 2-8, T_g = 58 °C) had a much lower T_g than P^t_mDEGDA-1 **2.5** (8b & 8c, Table 2-8, $\Delta T_g = -15$ °C) which is presumably linked to the much lower molecular weight (7e & 7f, Table 2-7, $\Delta M_n = -1.5$ kDa, $\Delta M_w = -3.8$ kDa). Given the molecular weight difference (7d & 7e, Table 2-7, $\Delta M_n = -1.3$

kDa, ΔM_w = −4.7 kDa) a surprisingly small increase in T_g was observed between **2.5** and **2.29** (8a & 8b, Table 2-8, ΔT_g = −3 °C).

2.5.2 Analysis of polyisoxazolines using 400 MHz ^{1}H NMR

The 400 MHz ^{1}H NMR spectra of the three DEGDA derived polymers **2.29**, **2.5** and **2.30** are shown in Figure 2-23 and are similar below 5.5 ppm. However, upon increasing the amount of *meta*-OC **2.1** (monomer B) relative to dipolarophile (monomer A) the levels of acrylate end groups (peaks in the range 5.75 – 5.50 ppm) decreases. P^t_mDEGDA-1.2 **2.30** had a higher ratio of these protons relative to the polymer backbone protons than P^t_mDEGDA-1 **2.5**. This suggests termination of the polymers at lower chain growth which agrees with GPC analyses and the Carothers equation. P^t_mDEGDA-0.8 **2.29** does not have any shifts indicative of terminal alkenes, suggesting cyclic polymers are formed exclusively *via* backbiting of the nitrile oxide. The formation of the cyclical polymers could be the cause of the small increase in T_g of **2.29** compared to **2.5** even though **2.29** was shown to have a higher molecular weight by GPC (7d & 7e, Table 2-7).

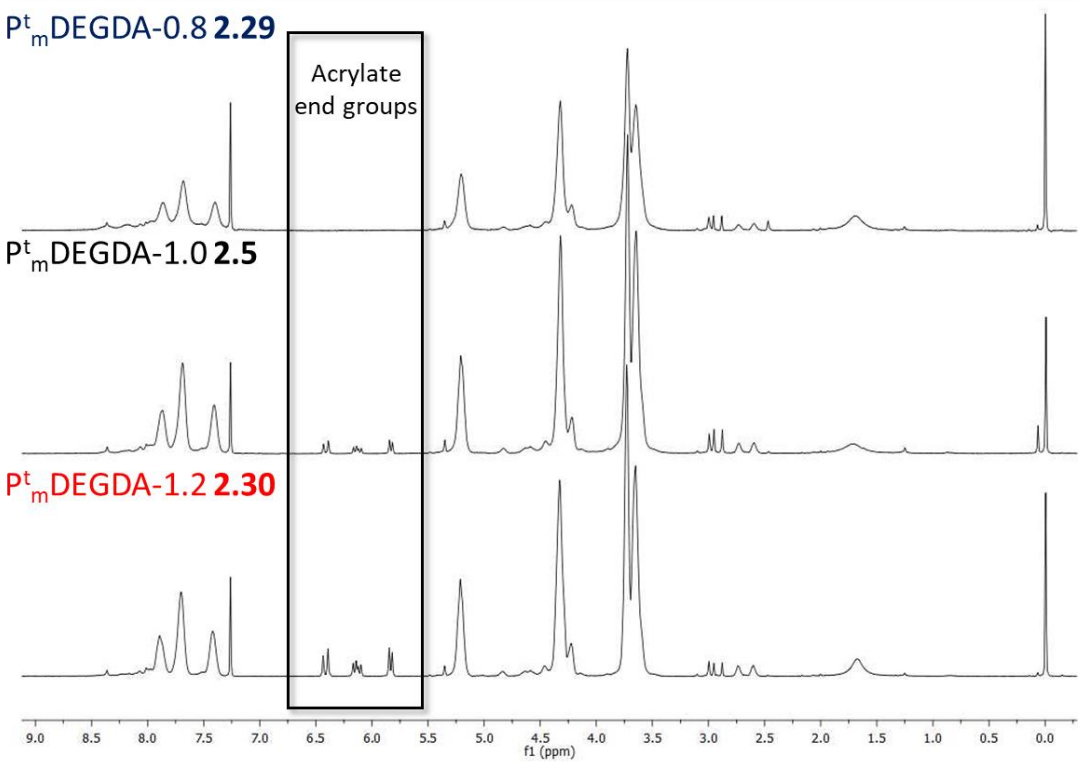

Figure 2-23: 400 MHz ^{1}H NMR spectra (P^t_mDEGDA-0.8 **2.29**, P^t_mDEGDA-1 **2.5**, and P^t_mDEGDA-1.2 **2.30**)

2.5.3 Analysis of polyisoxazolines using MALDI-TOF-MS and IR

If the conclusions from the analysis in the previous section are correct then one would assume that P^t_mDEGDA-1.2 **2.30** should be made up of preferentially ABABABA type polymers with acrylate end groups, while P^t_mDEGDA-0.8 **2.29** should be mainly cyclic $(AB)_n$ or linear polymers of type $(AB)_n$ where there is significant furoxan formation (B-B linkages). If furoxan formation is prevalent then $(AB)_n$-B chains should also be apparent in the MALDI-TOF spectrum of P^t_mDEGDA-0.8 **2.29**. The effects of changes in dipolarophilic monomer ratio on polymer structure were investigated by MALDI-TOF analysis, focussing on the P^t_mDEGDA series (**2.5**, **2.29**, **2.30**, Figure 2-24). Full analysis of the MALDI of P^t_mDEGDA-1 **2.5** was presented in section 2.3.5.

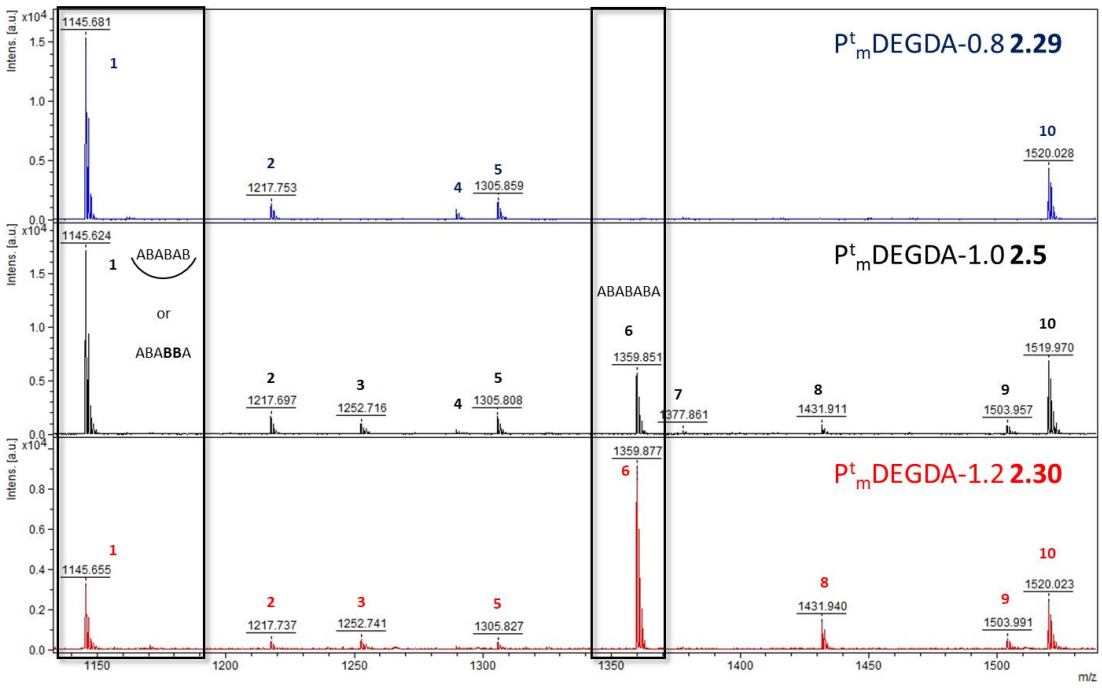

Figure 2-24: Section of MALDI-TOF spectra (P^t_mDEGDA-0.8 **2.29**, P^t_mDEGDA-1 **2.5**, and P^t_mDEGDA-1.2 **2.30**)

The MALDI-TOF-MS spectra of P^t_mDEGDA-1.2 **2.30** is similar to that of P^t_mDEGDA-1 **2.5**, but with no weak peak 7 at 1377.86 (Figure 2-24). The most significant difference is the decrease in the intensity of the $(AB)_n$ type polymers (peaks 1 and 10, Figure 2-24) relative to the linear $(AB)_n$-A type polymer (peak 6). The increase in abundance of dipolarophile (monomer A) during this polymerisation would reduce the occurrences of nitrile oxide dimerization to form furoxans and intramolecular cycloaddition to form cyclical polymers (peaks 1 and 10), resulting in

greater number of linear $(AB)_n$-A polymers (peak 6). The reverse should be true for the P^t_mDEGDA-0.8 **2.29** and in fact there are no peaks for a linear not-furoxan containing material at all (peak 6).

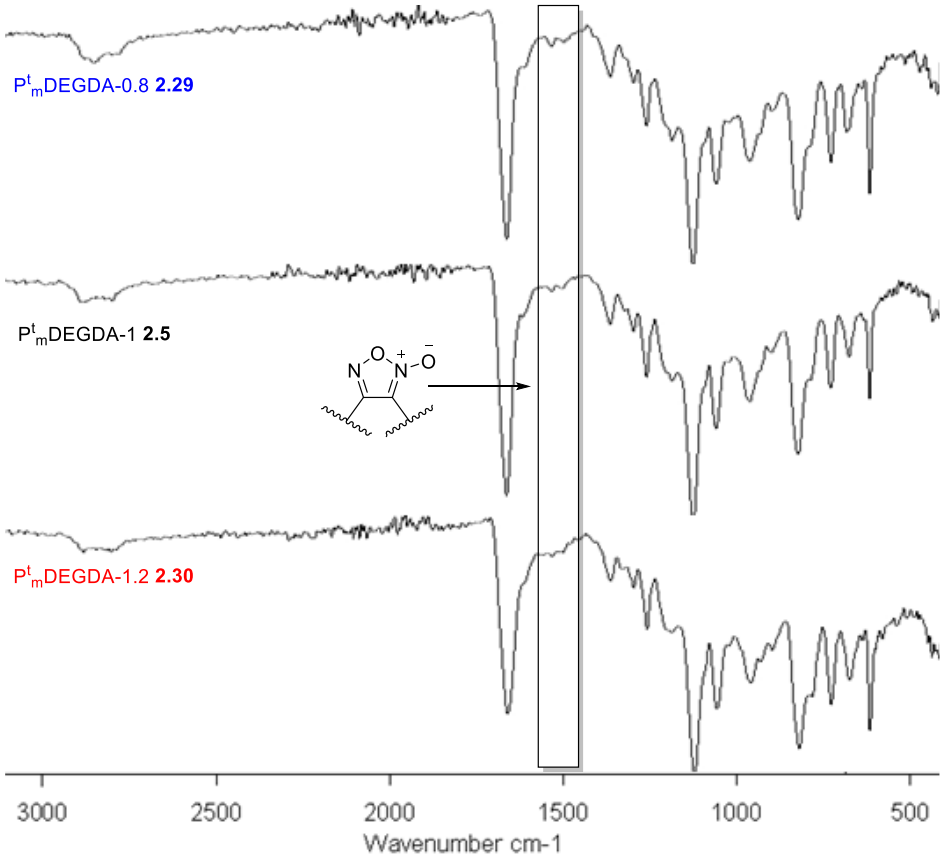

Figure 2-25: IR spectra of P^t_mDEGDA-0.8 **2.29**, P^t_mDEGDA-1 **2.5**, and P^t_mDEGDA-1.2 **2.30**

P^t_mDEGDA-0.8 **2.29** has significantly less repeating peaks in the MALDI spectrum, with only peaks 1, 2, 4, and 5 remaining from the spectrum of P^t_mDEGDA-1 **2.5** (Figure 2-24). There is no longer a peak relating to an uneven ratio polymer $(AB)_n$-A with A groups terminating both ends of the polymer, therefore there are no peaks that depend on additions to it or degradations of it. Using excess *meta*-OC **2.1** (B) for the polymerisation seems to have a much greater effect on polymer structure than using excess dipolarophile (A). As peak 6 was no longer present, the linear ABABABA structure was completely removed from the polymer. Only cyclical polymer chains contained a genuine alternating AB structure, or linear polymers containing a furoxan link (ABABBA) are present. Examination of the 400 MHz ^{1}H NMR spectrum of P^t_mDEGDA-0.8 **2.29** showed no peaks corresponding to a terminal alkene suggesting that linear polymers containing a furoxan link (ABABBA) are not abundant. Excess

nitrile oxide therefore promoted cyclisation over furoxan formation. The lack of any peaks relating to an $(AB)_n$-B type polymer also indicates that cyclisation is the major cause of $(AB)_n$ polymers not furoxan links. If furoxan links were the major cause, multiple furoxan links may be expected to be seen within the same polymer chain.

In summary, both MALDI-TOF-MS and 400 MHz ^{1}H NMR analysis of the P^t_mDEGDA (**2.5**, **2.29**, **2.30)** series indicates that excess nitrile oxide (**2.29**) likely leads to cyclical polymers preferentially. IR analysis (Figure 2-25) does indicate that some dimerisation to form furoxan links may occur within these cyclic structures, with an observed increase in absorptions around 1600 cm^{-1} and 1575 cm^{-1} as the equivalents of DEGDA **2.4** decreases.

2.6 Summary and conclusion

Nitrile-oxide – alkene cycloaddition polymers were synthesised from *meta*-OC **2.1** and commercially available dipolarophiles *via* a mildly basic thermally promoted method pioneered by Takata *et al.*[317] Initial tests to assess the reproducibility of Takata's work using DEGDA **2.4** and DEGDMA **2.8** as the dipolarophile were successful in forming similar polymers to those reported in the literature.

Investigations into the effect of changing the dipolarophilic monomer glycol chain length were carried out using EGDA **2.9** and PEGDA **2.10**. There was a strong correlation between the separation of the dipolarophilic groups in the monomer and glass transition temperature.

Polyisoxazoles formed using varying ratios of the monomers were studied. Performing polymerisations with excess dipolarophile (monomer A) relative to *meta*-OC **2.1** (monomer B), e.g. P^{t}_{m}DEGDA-1.2 **2.30**, led to lower molecular weights, T_g's and acrylate terminated linear polymers preferentially. On the other hand, increasing the ratio of the equivalents of *meta*-OC **2.1** (monomer B) e.g. P^{t}_{m}DEGDA-0.8 **2.29**, increased the molecular weight and T_g's but led to cyclic polymers or furoxan linkages preferentially.

3.0 Polymerisation of acetamide dipolarophiles

3.1 Introduction

In Chapter 2 we reported the successful nitrile-oxide / dipolarophile cycloaddition polymerisation of commercial dialkenes[318,330] to give polyisoxazolines. Furthermore, it was demonstrated how the monomer structure effected the resulting polymer properties. The ultimate intention of the research is to derive polyisoxazolines and polyisoxazoles from renewable sources, specifically using vegetable oils as the feedstock for dipolarophilic monomers. Dipolarophilic groups (those containing alkenes and alkynes) therefore need to be prepared from renewable feedstocks. Production of fatty amides from vegetable oils is a well-established method of breaking apart triglycerides and introducing functionality, with the added benefit of producing the industrially useful by-product glycerol **3.1** (Figure 3-1).[331–333]

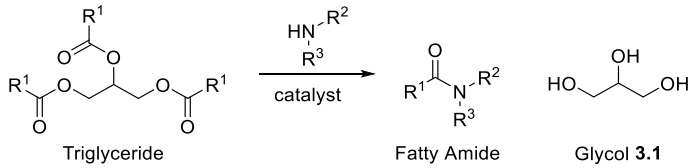

Figure 3-1: Aminolysis of triglycerides to form fatty amides and glycerol **3.1**.

The structure of tertiary amides can be complicated by the possibility of rotamers caused by restricted rotation around the C-N bond.[334] Restricted rotation is caused by the delocalisation of the N lone pair into the C=O bond giving the C-N bond partial double bond character. Kemitz and Lowel[335] calculated that acetamide **3.2** has partial doubled bond structure around the C-N bond with resonance structure B contributing 28% to the overall structure of the amide bond (Figure 3-2). Rotation can be further restricted if desired by the introduction of bulky groups (R^1, R^2, R^3 Figure 3-1) causing steric clashing, this can trap a compound in a particular orientation (*cis* or *trans* amide if $R^2 \neq R^3$), a method that has been used in attempts to synthesise compounds stereoselectively.[336]

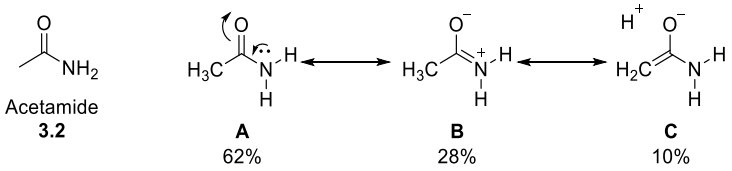

Figure 3-2: Resonance forms of acetamide **3.2**

Amide restricted rotation can produce distinct separate environments in NMR analysis.[334] For example the methyl protons of the common solvent DMF **3.3** resonate at different frequencies (^{1}H NMR $CDCl_3$: 2.96 ppm and 2.88 ppm)[337], the methyl *cis* to the oxygen resonates upfield of the *trans* methyl (Figure 3-3).[334] In *N,N*-diethylformamide **3.4** however the N-CH_2 group *cis* to the oxygen resonates downfield of the *trans* N-CH_2 group. Assignment of *cis* and *trans* as upfield and downfield is therefore not consistent and caution must be used if making assignments in other molecules.

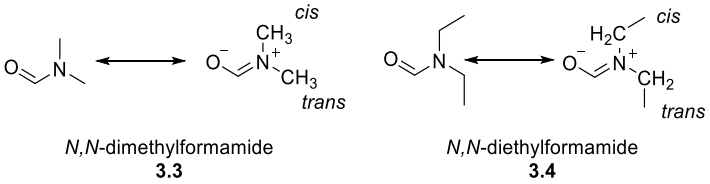

Figure 3-3: Resonance forms of DMF **3.3** and DEF **3.4**

3.2 Aims and objectives

Work in the previous chapter demonstrated the viability of Takata's[318,330] method of polyisoxazoline synthesis and revealed methods of tailoring the polymer properties using different dipolarophilic monomers. The intention is to source the monomers from vegetable oils which requires dipolarophilic groups to be introduced, this could be achieved by aminolysis to form fatty amides (Figure 3-1). Before exploring renewable amides we first needed to ensure that the amide functionality was tolerated in the new polymerisation process. A range of amide monomers **3.5 – 3.8** were prepared. Polymers were produced using these model monomers and the materials studied in order to inform which dipolar acceptor should be introduced into vegetable oil derived monomers.

- Model dipolarophilic acetyl amide monomers (**3.5** – **3.8**) were synthesised and characterised.
- The model monomers **3.5 – 3.8** (block A) and *meta*-OC **2.1** (block B) were reacted in a 8:1 ratio to make discrete ABA compounds to study their structure and spectroscopic properties to help in characterising more complex polymeric materials prepared later.
- Polymers were made using the model amide monomers (**3.5** – **3.8**) and *meta*-OC **2.1**. They were characterised spectroscopically where possible and their physical and thermal properties explored.

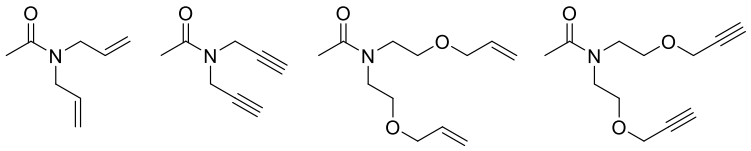

Figure 3-4: Model acetyl amide dipolarophilic monomers

3.3 Synthesis of acetamide monomers

Rather than deriving monomers from vegetable oils (due to their complex NMR spectra) an initial study was carried out on models with 4 different dipolarophilic end groups. Dialkenes (**3.5** and **3.7**) and dialkynes (**3.6** and **3.8**) were prepared with acetyl groups in place of a fatty acid chain in order to simplify the analysis (Figure 3-5). In section 2.4 the spacing between isoxazoline rings was found to have a significant effect on the physical characteristics of polymers. The model monomers were therefore designed with different spacing between dipolarophilic groups.

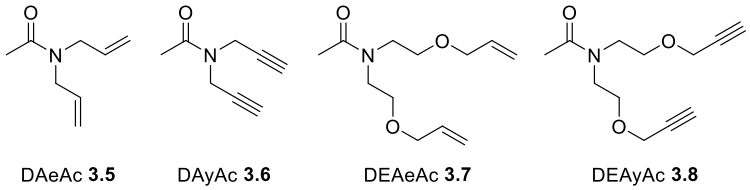

Figure 3-5: Model acetyl amide dipolarophilic monomers

Nomenclature of novel amide monomers in this thesis: monomers will be given a code as well as an Arabic numeral reference (e.g. DEAeAc **3.7**).

D represents a difunctional monomer (**D**EAeAc).

E or lack thereof refers to the inclusion of an ether linkage in monomer (D**E**AeAc).

The dipolarophilic group is signified by **Ae** for alkene or **Ay** for alkyne (DE**Ae**Ac).

Ac denotes the acetyl group (DEAe**Ac**) in later chapters (5 and 6) **Ac** will be replaced by the fatty acid chain used to form the monomer.

3.3.1 Synthesis of non-ether containing monomers **3.5** and **3.6**

N,*N*-Diallylacetamide (DAeAc **3.5**) was synthesised by drip-feeding diallylamine into ice cold acetic anhydride **3.9** over the course of an hour. The temperature was then raised to 100 °C for 2 hours followed by fractional distillation under reduced pressure to give a colourless liquid **3.5**, 85 %.

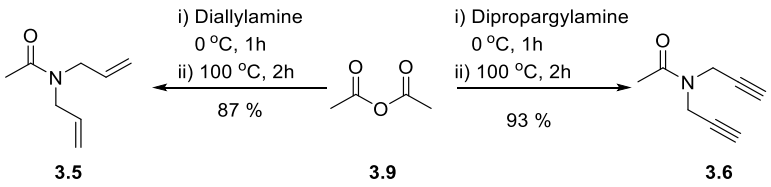

Scheme 3-1: Synthesis of DAeAc **3.5** and DAyAc **3.6** from acetic anhydride.

Synthesis of *N*,*N*-di(prop-2-yn-1-yl)acetamide (DAyAc **3.6**) was prepared in a similar manner to DAeAc **3.5** although on a much smaller scale due to the expense of dipropargylamine. During purification of DAeAc **3.5** some fractions of DAeAc **3.5** were discarded as they also contained an impurity, which slightly reduced the yield. DAyAc **3.6** synthesis was carried out on a smaller scale and so the reaction was worked up in a different manner to avoid this issue. Once complete the reaction was taken into water and extracted with $CHCl_3$. The organic extraction was reduced to leave a crude dark brown liquid, purification through a silica plug gave a pale yellow liquid **3.6**, 93 %. The product DAyAc **3.6** had a similar R_f to dipropargylamine, so the reaction was monitored by mass spectrometry rather than TLC.

3.3.2 Synthesis of ether containing monomers **3.7** and **3.8**

DEAeAc **3.7** and DEAyAc **3.8** were formed from the diol **3.11**. The diol intermediate **3.11** itself was formed by dropwise addition of acetic anhydride **3.9** into a cooled solution of diethanolamine **3.10** in THF with the mixture allowed to come to room temperature overnight. Mass spectrometric analysis indicated that this resulted in three products with different levels of acetyl capping (Scheme 3-2, **3.11 – 3.13**). Acetic acid formed in the reaction was removed *in vacuo.* To selectively remove the ester-based acetyl groups the residue was taken into MeOH with potassium carbonate and refluxed for 2 hours to leave a pale yellow oil **3.11**, 49 %.

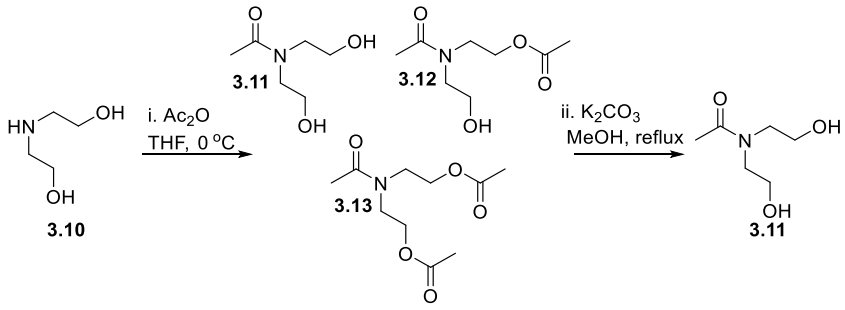

Scheme 3-2: Synthesis of diol intermediate **3.11**

The dipolarophilic monomers DEAeAc **3.7** and DEAyAc **3.8** were formed by dispersing diethanolamide **3.11** and sodium hydride in THF at −78 °C. Dropwise addition of the appropriate bromide and purification through a silica plug gave DEAeAc **3.7** and DEAyAc **3.8** as pale yellow oils, 59 % and 40 % respectively.

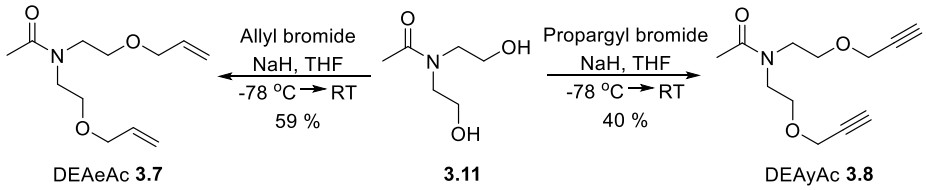

Scheme 3-3: Synthesis of DEAeAc **3.7** and DEAyAc **3.8** from amide **3.11**

Characterisation was undertaken for the dipolarophilic acetyl amide monomers (**3.6 – 3.8**) using ^{1}H and ^{13}C NMR, ES-MS and IR. Proton and carbon NMR revealed rotamers due to restricted rotation around the amide bond (Figure 3-6). In 2016 Aitken *et al*[338] noted a barrier to rotation of 75.6 kJ mol^{-1} for **3.11**, correcting a previous erroneous publication. Using VT-NMR we calculated a similar rotational barrier of 75.7 kJ mol^{-1} for the related DEAyAc **3.8** (appendix B).

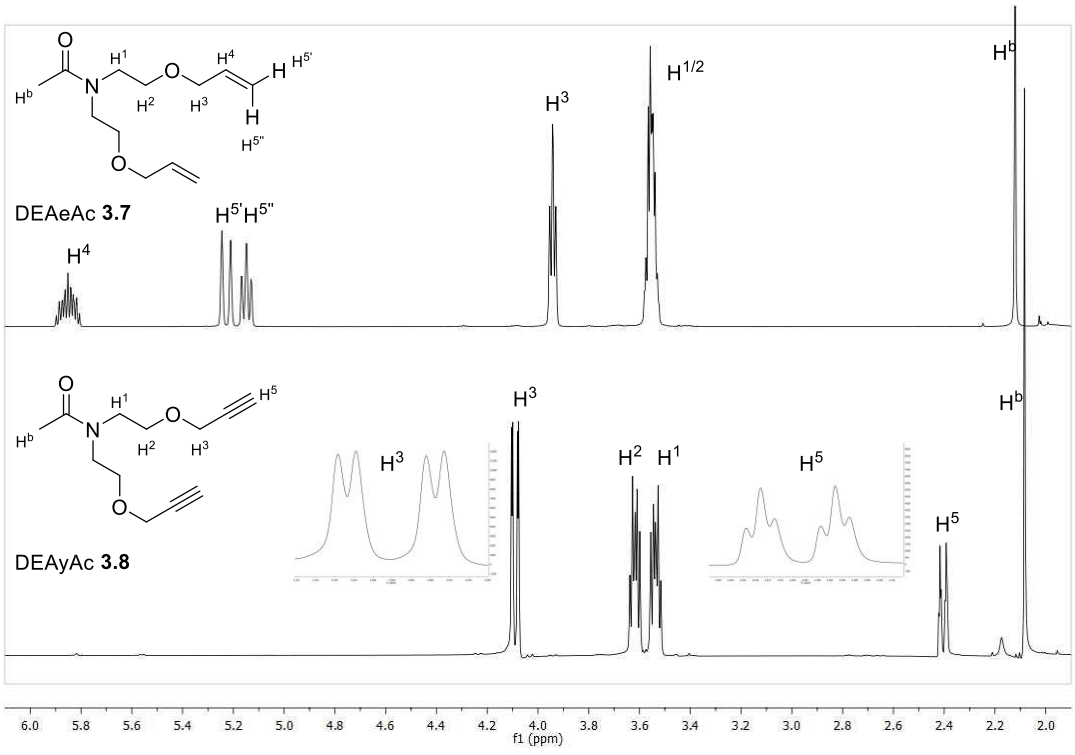

Figure 3-6: ^{1}H 500 MHz NMR spectra of DEAeAc **3.7** (*top*) and DEAyAc **3.8** (*bottom*).

In the 500 MHz ^{1}H NMR spectra the separate chemical environments of the two chains (c*is* and *trans* relative to the acetamide methyl group) are more obvious in the dialkyne monomers (**3.6** and **3.8**). In the ^{1}H spectrum of DEAyAc **3.8** the environments represented by H^3 (**3.8**, Figure 3-6) occur as two doublets (J^4 = 2.5 Hz) at 4.10 ppm and 4.08 ppm. The protons represented by H^5 (**3.8**, Figure 3-6) are present as two triplets (J^4 = 2.5 Hz) at 2.42 ppm and 2.39 ppm. In the 500 MHz ^{1}H spectrum of DEAeAc **3.7** the two environments of the terminal alkene protons (H^4 & H^5, **3.7**, Figure

3-6) overlap with the vicinal (^{3}J) splitting of the alkenes but are clear in the 125 MHz ^{13}C NMR spectrum (Figure 3-7). The further from the amide carbonyl the smaller the difference in chemical shifts. The terminal alkyne proton rotamers of DAyAc **3.6** have a difference of 41.7 Hz (2.30 ppm and 2.22 pm) whereas DEAyAc **3.8** (H_5, Figure 3-6) have a difference of 12.1 Hz (2.42 ppm and 2.39 ppm). The same trend is also apparent in the ^{13}C spectra of the monomers (Figure 3-7).

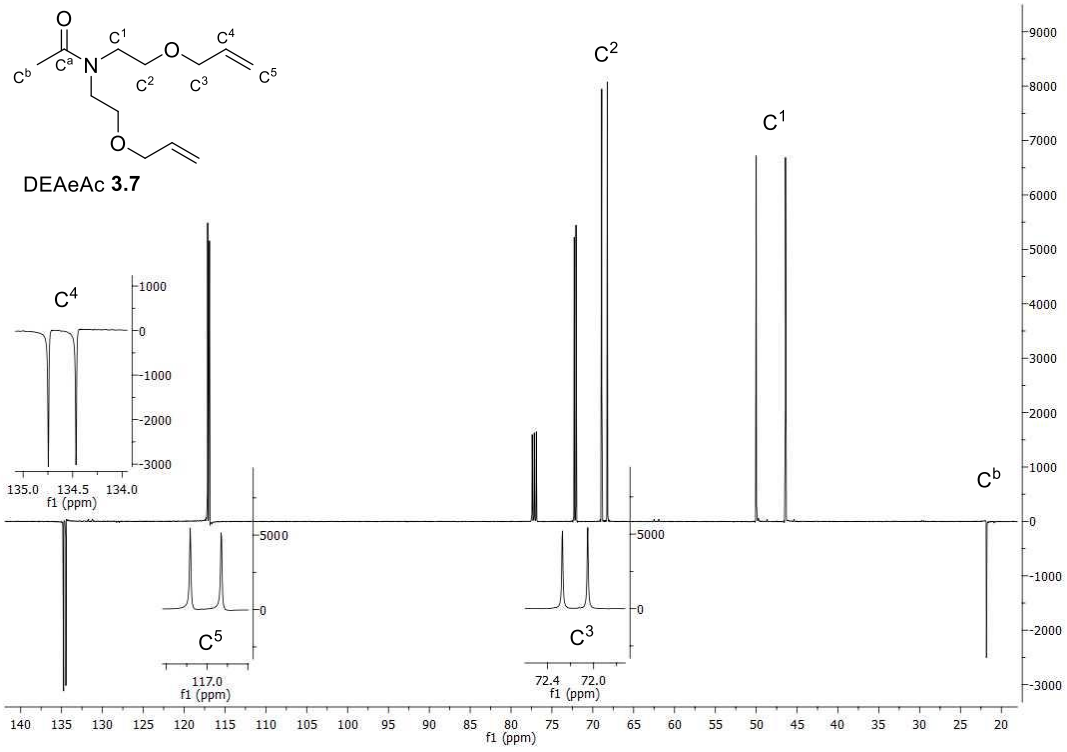

Figure 3-7: ^{13}C 500 MHz NMR spectrum of DEAeAc **3.7**

3.3.3 Thermal Characterisation of Model Monomers

The thermal stability of the monomers (**3.5 – 3.8**) was analysed by TGA (Figure 3-8) in order to determine their stability at the polymerisation temperature of 80 ºC. As in chapter 2 the monomers were heated at 10 ºC min^{-1} from 25 – 600 ºC under N_2. The monomers (**3.5 – 3.8**) all showed thermal stability above 80 ºC and were therefore suitable for heated polymerisation reactions.

Entry	Monomer	T_5 / °C	T_{20} / °C	W_{600} / %
1a	DAeAc **3.5**	127	164	0
1b	DAyAc **3.6**	133	170	0
1c	DEAeAc **3.7**	199	233	0
1d	DEAyAc **3.8**	240	285	19

Table 3-1: Thermal analysis of model dipolarophile monomers

The lower molecular weight monomers, DAeAc **3.5** and DAeAc **3.6**, have a sharp decline in weight, beginning around 120 ºC, reaching complete weight loss by 210 ºC. As the weight loss is complete in one sharp step it appears to be caused by evaporation rather than degradation. The higher molecular weight ether containing monomers DEAeAc **3.7** and DEAyAc **3.8**, have higher boiling points than their comparable smaller monomers (**3.5** and **3.6**). Weight loss occurs in two steps for DEAeAc **3.7** and multiple steps for DEAyAc **3.8** suggesting it is decomposition-based weight loss rather than evaporation. The dialkyne **3.8** is more thermally stable than the dialkene **3.7**, and may undergo a reaction at elevated temperatures forming a more stable compound as weight loss does not reach 100 % below 600 ºC (W_{600} = 19 %, 1d, Table 3-1).

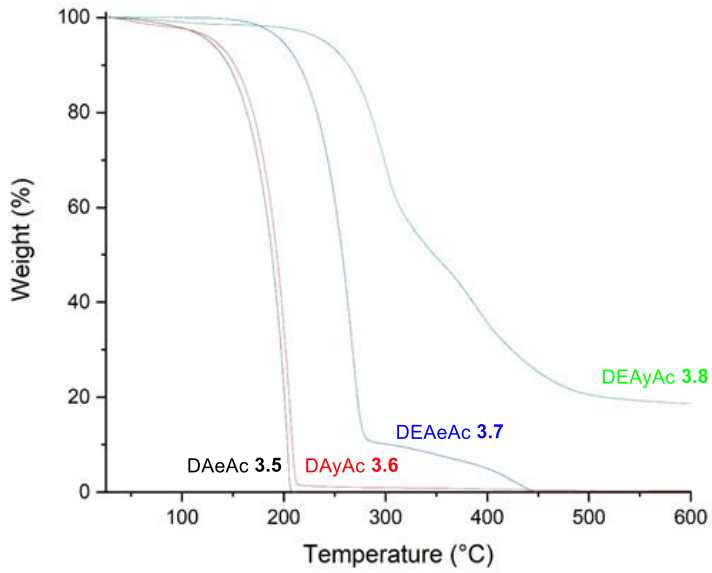

Figure 3-8: TGA of model dipolarophile monomer (– DAeAc **3.5**, – DAyAc **3.6**, – DEAeAc **3.7**, – DEAeAc **3.8**) carried out at a heating rate of 10ºC min^{-1} under a N_2 atmosphere.

3.4 Oligomer synthesis

In order to unambiguously obtain spectroscopic data to help analyse the novel polymers we first prepared discrete ABA oligomers **3.14 – 3.17**.

Nomenclature of novel oligomers in this thesis: oligomers will be given a code as well as an Arabic numeral reference (e.g. O_mDAeAc-ABA **3.14**).

O represents an oligomer (**O**$_m$DAeAc-ABA)

*Subscript 'm' denotes the nitrile oxide precursor meta-OC **2.1*** **(**O$_{\mathbf{m}}$DAeAc-ABA)

Abbreviation represents the dipolarophile monomer (O$_m$**DAeAc**-ABA)

The composition of the oligomer is indicated by ABA or ABABA where A refers to a dipolarophile unit and B refers to a nitrile oxide unit (O$_m$DAeAc-**ABA**)

O$_m$DAeAc-ABA **3.14** is therefore an oligomer constituting of 2 DAeAc **3.5** units and 1 *meta*-NO **2.13** unit.

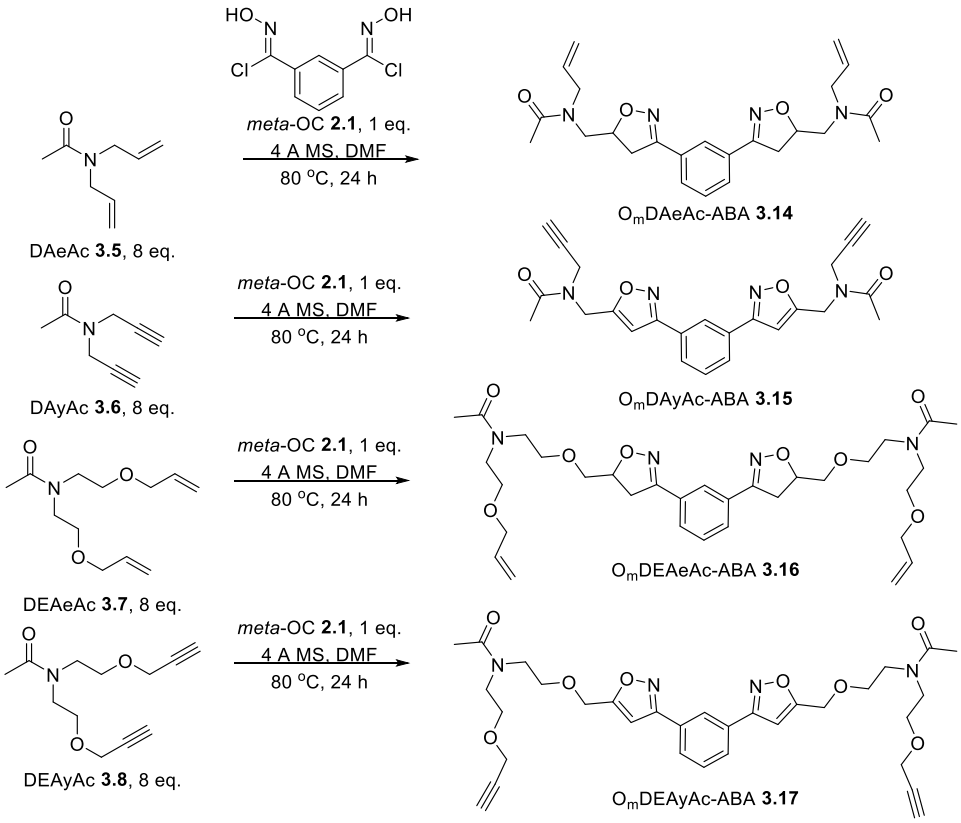

Scheme 3-4: Synthesis of ABA oligomers (**3.14** – **3.17**)

The oligomers (**3.14** – **3.17**, Scheme 3-4**)** were synthesised using similar conditions to the polymerisations in chapter 2, although at a lower molarity and with a large excess

of dipolarophile (**3.5** – **3.8**). Dipolarophile (**3.5** – **3.8**, 8.8 mmol, 8 eq.) and *meta*-OC **2.1** (1.1 mmol, 1 eq.) were stirred in DMF (0.1 M) with 4Å MS at RT for 30 mins before the temperature was increased to 80 °C for 24 hrs. After which the reaction mixture was poured into water and extracted with $CHCl_3$. The organic layers were combined and washed with water and brine, dried with $MgSO_4$ and reduced *in vacuo*. Using column chromatography, the excess dipolarophile monomer (**3.5** – **3.8**) was recovered, followed by ABA oligomers (**3.14** – **3.17**). During the purification of 3 of the oligomers a small amount of ABABA oligomer (**3.18** – **3.20**, Figure 3-9) was also recovered.

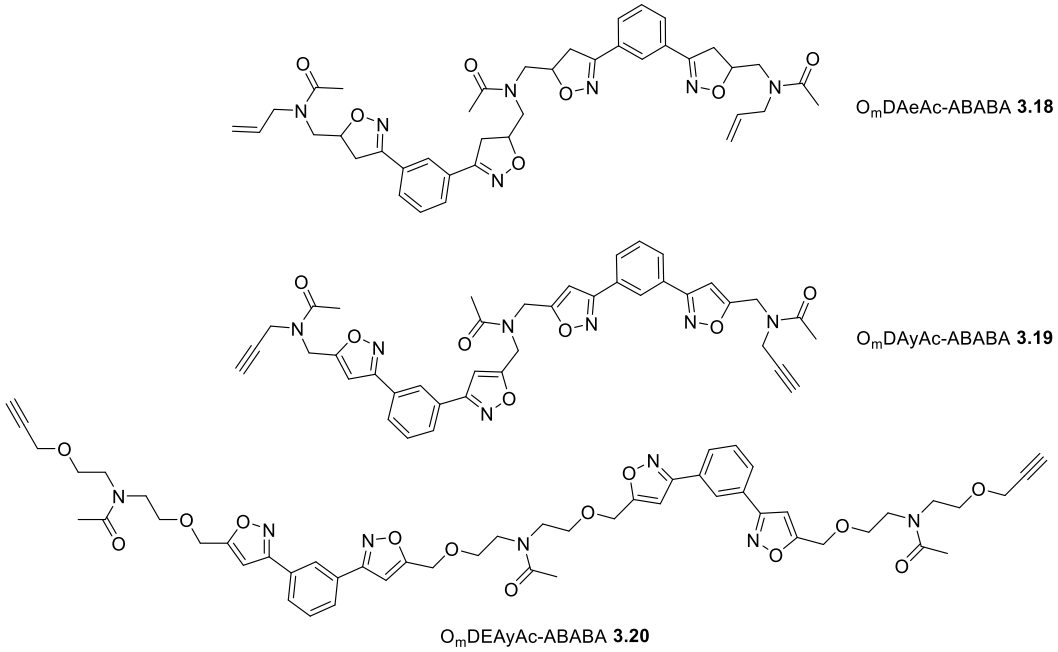

Figure 3-9: ABABA oligomers (**3.18** – **3.20**)

The purification of O_mDAeAc-ABA **3.14**, O_mDAyAc-ABA **3.15**, O_mDEAeAc-ABA **3.16** and O_mDEAyAc-ABA **3.17**, revealed significant differences in the polarity of the oligomers. In 100 % EtOAc the oligomers that contained an ether link (**3.16** & **3.17**) had considerably lower R_f's (2c & 2d, Table 3-2) than their related lower molecular weight ABA oligomers (2a & 2b, Table 3-2). The ether link therefore increased interaction with silica, signifying a more polar molecule.

Entry	Oligomer	R_f in EtOAc
2a	O_mDAeAc-ABA **3.14**	0.15
2b	O_mDAyAc-ABA **3.15**	0.55
2c	O_mDEAeAc-ABA **3.16**	0.05
2d	O_mDEAyAc-ABA **3.17**	0.20

Table 3-2: Calculated R_f values for oligomers **3.14** – **3.15** using EtOAc as eluent.

By comparing the isoxazoline and the isoxazole ring containing oligomers ring polarity can be examined. Isoxazoline **3.14** (2a, Table 3-2) has a lower R_f than isoxazole **3.15** (2b, Table 3-2), a difference also seen between **3.16** and **3.17** (2c & 2d, Table 3-2). This suggests that isoxazolines are more polar than isoxazole rings. The reduced polarity of the isoxazole ring is caused by the aromatic nature of the ring, which uses a lone pair of electrons from the oxygen to ensure the 6 electron Hückel aromaticity. This lone pair is conjugated within the ring lowering the molecules dipole with respect to the analogous isoxazolines and furthermore as the lone pair is conjugated it can no longer take part in intermolecular interactions.

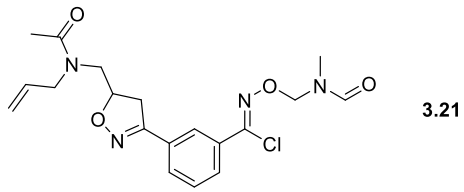

3.21

Figure 3-10: Fourth fraction recovered during the purification of **3.17**

During the purification of O_mDAeAc-ABA **3.14** a fourth fraction was recovered. Analysis by mass spectrometry indicated that the compound contained a chlorine atom due to its stereotypical isotopic pattern. The 500 MHz ^{1}H and 125 MHz ^{13}C NMR spectra confirmed the structure of **3.21** (Figure 3-10). Rather than forming the desired compound (**3.14**), *meta*-OC **2.1** had decomposed unsymmetrically to form 1 isoxazole ring. The other oximoyl chloride had not decomposed but instead added a DMF molecule (see section 2.3.5). As discussed in the previous chapter it was unclear as to whether DMF was acting catalytically in a similar way to a Vilsmeier-Haack reaction[326,339] or whether the inclusion of DMF was irreversible. The discovery of **3.21** in a small discrete molecule allowed for the tentative assignment of peak 3 in the MADLI-TOF spectrum of P^t_mDEGDA-1 **2.5** (Section 2.3.5). Equivalent compounds to **3.21** were not found in the purification of the other oligomers (**3.14** – **3.16**) or in the MALDI-TOF spectra of any of the polymers in this or following chapters.

3.5 Oligomer analysis

The ABA oligomers (**3.14** – **3.17**) were analysed by MS, NMR, IR, and GPC. Characterisation of the oligomers would allow for more accurate analysis of the related polymers. Due to the small amount of ABABA oligomers recovered (**3.18** – **3.20**) they were only analysed by MS, NMR and GPC.

3.5.1 MS and GPC analysis of oligomers (**3.14** – **3.20**)

Mass spectrometric analysis of the oligomers **3.14** – **3.17** allowed confirmation of the ABA type structure as well as identifying the ABABA compounds (**3.18** – **3.20**). It was not possible to obtain an x-ray crystal structure of any of the oligomers (**3.14** – **3.20**) as they were all waxy solids. The accurate mass of each oligomer (**3.14** – **3.20**) did however allow for a more accurate interpretation of the GPC. As the intended polymers contain an unorthodox linking unit (isoxazole / isoxazoline) they cannot reasonably be compared to the normal PMMA or PS standards used in GPC. Analysing the ABA and ABABA oligomers (**3.14** – **3.20**) of known molecular weight by GPC therefore gave a base line for small oligomeric standards for the later analysis of polymers. Using DMF as the eluent the oligomers (**3.14** – **3.20**) molecular weight was estimated by GPC against PMMA standards (Table 3-3).

Entry	Oligomer	Exact Mass / Da	GPC Peak / Da[a]	Peak Inflation / ×
3a	O_mDAeAc-ABA **3.14**	438	973	2.2
3b	O_mDAyAc-ABA **3.15**	430	1877	4.3
3c	O_mDEAeAc-ABA **3.16**	614	1601	2.6
3d	O_mDEAyAc-ABA **3.17**	608	1949	3.2
3e	O_mDAeAc-ABABA **3.18**	737	1817	2.5
3f	O_mDAyAc-ABABA **3.19**	725	2778	3.8
3g	O_mDEAyAc-ABABA **3.20**	989	2821	2.9

a – GPC estimated using DMF as eluent against PMMA standards.

Table 3-3: GPC estimation inflation of molecular weight compared to the exact mass of oligomers (**3.14 – 3.20)**

The data shows that in general for the alkene derived oligomers (3a, 3c, and 3e, Table 3-3) GPC estimates inflate the real molecular weight by a factor of approximately 2.5. The discrepancy is larger for the alkyne derived oligomers (3b, 3d, 3f and 3g, Table 3-3), approximately 4.0 for non-ether containing **3.15** and **3.19** and approximately 3.0 for the ether containing oligomers **3.17** and **3.20**.

3.5.2 IR analysis of the oligomers (**3.14** – **3.17**)

The IR spectra of the ABA oligomers **3.14** – **3.17** confirmed the key functional groups in the molecules. The alkene containing compounds **3.14** and **3.16** have adsorptions at 3075 and 3079 cm^{-1} respectively which relate to the C-H stretching of the terminal alkene. The dialkyne containing oligomers **3.15** and **3.17** have adsorptions at higher frequencies (3288 and 3286 cm^{-1}) caused by the shorter C-H bond of the terminal alkyne. Alkynes **3.15** and **3.17** also contained weak C≡C stretching adsorptions around 2100 cm^{-1}. The presence of these absorptions in any future polymerisations would allow us to determine these end groups would be present. The C=C stretching of the terminal alkene in the isoxazoline oligomers (**3.14** and **3.16**) was not visible beneath the strong C=O stretch of the amide at (1628 cm^{-1} and 1647 cm^{-1}). Due to the strong carbonyl stretch it was not possible to distinguish the C=N adsorption of the heterocyclic ring for both the isoxazolines (**3.14** and **3.16**) and the isoxazoles (**3.15** and **3.17**). Isolated oximes generally have weak adsorptions it is therefore probable that the C=N-O bonds in the heterocyclic rings also have weak transmittance and are hidden by the carbonyl of the amide bond. Furthermore, isolated isoxazolines are known to have weak adsorptions[340] around 1600 cm^{-1} and are therefore hidden in IR spectra of **3.15** and **3.17** by the carbonyl stretch. The compounds (**3.14** – **3.17**) all show an adsorption around 800 cm^{-1} due to the *meta*-disubstituted benzene ring and around 1200 cm^{-1} for the C-O bond in the heterocyclic ring. Ether containing oligomers **3.16** and **3.17** have strong adsorptions at 1100 and 1098 cm^{-1} respectively.

3.5.3 ^{1}H NMR analysis of the ABA membered oligomers (**3.14** – **3.17**)

Analysis of the monomers **3.5** – **3.8** by ^{1}H and ^{13}C NMR had revealed restricted rotation caused by the amide. At least two separate species were identified in the spectra of the ABA isoxazole oligomers **3.15** and **3.17** which are likely due to restricted rotation around the amide bond **3.15a** → **3.15b** (Figure 3-11), but could also be due to restricted rotation around the heterocyclic-aryl bond **3.15a** → **3.15c**, although this is likely to be rapid on the NMR timescale. For the isoxazolines **3.14** and **3.16** two diastereomers (*syn* and *anti*, Figure 3-11) are also possible which will complicate the analysis. Protons in a *meta*-disubstituted benzene rings normally present as a singlet (H^1), doublet (H^2) and a triplet (H^3) (Figure 3-11), in the oligomers

(**3.14** – **3.17**) however they occurred as overlapping signals due to the different environments of rotamers and / or diastereomers.

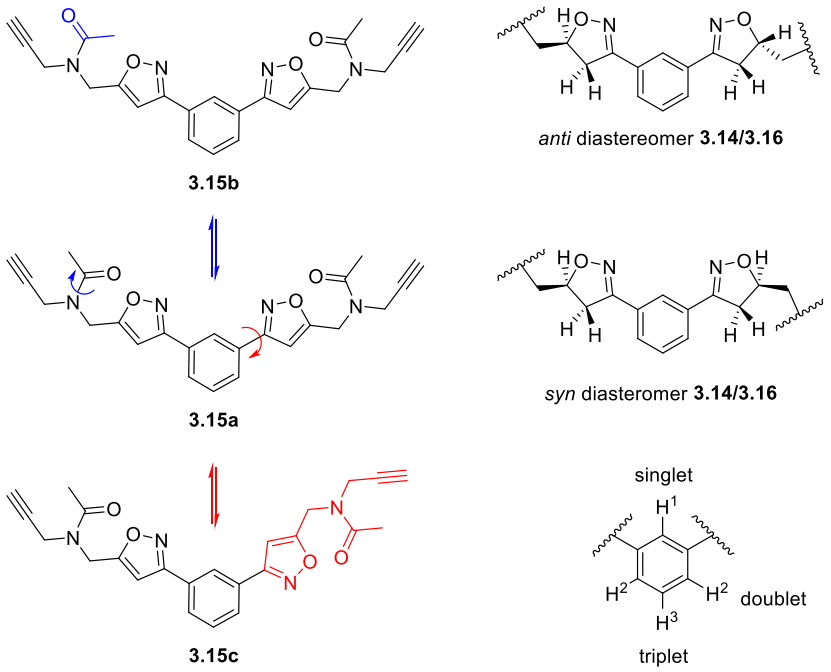

Figure 3-11: Sources of restricted rotation in the oligomers (*left*), diastereomers of *meta*-isoxazoline groups (*top right*), proton assignment of *meta*-disubstituted benzene ring (*bottom right)*

3.5.3.1 ^{1}H NMR analysis of isoxazole ABA oligomers **3.15** and **3.17**

Evidence of both a major and a minor species in a ratio of 0.6 : 0.4 (presumably amide rotamers) was present in the ^{1}H NMR spectrum of O_mDAyAc-ABA **3.15** (Figure 3-12). The isoxazole proton at 6.6 ppm (H^3, **3.15**, Figure 3-12), (which should occur as a singlet), was clearly apparent as two singlets at 6.61 ppm and 6.60 ppm respectively. There was also a slightly upfield shoulder for the signal at 4.82 ppm suggestive of two species for the CH_2 next to the isoxazole ring H^1 (**3.15**, Figure 3-12) which was confirmed by HSQC showing two CH_2 carbon environments at 43.4 ppm and 40.8 ppm. Similarly the propargylic CH_2 neighbouring the terminal alkyne $H^{1'}$ (**3.15**, Figure 3-12) occurred as two doublets (^4J = 2.5 Hz) and the terminal alkyne protons $H^{3'}$ (**3.15**, Figure 3-12) occurred as two triplets (^4J = 2.5 Hz), the downfield triplet at 2.36 being the major rotamer with the minor isomer obscured by the acetamide methyl signals at 2.27 ppm and 2.26 ppm.

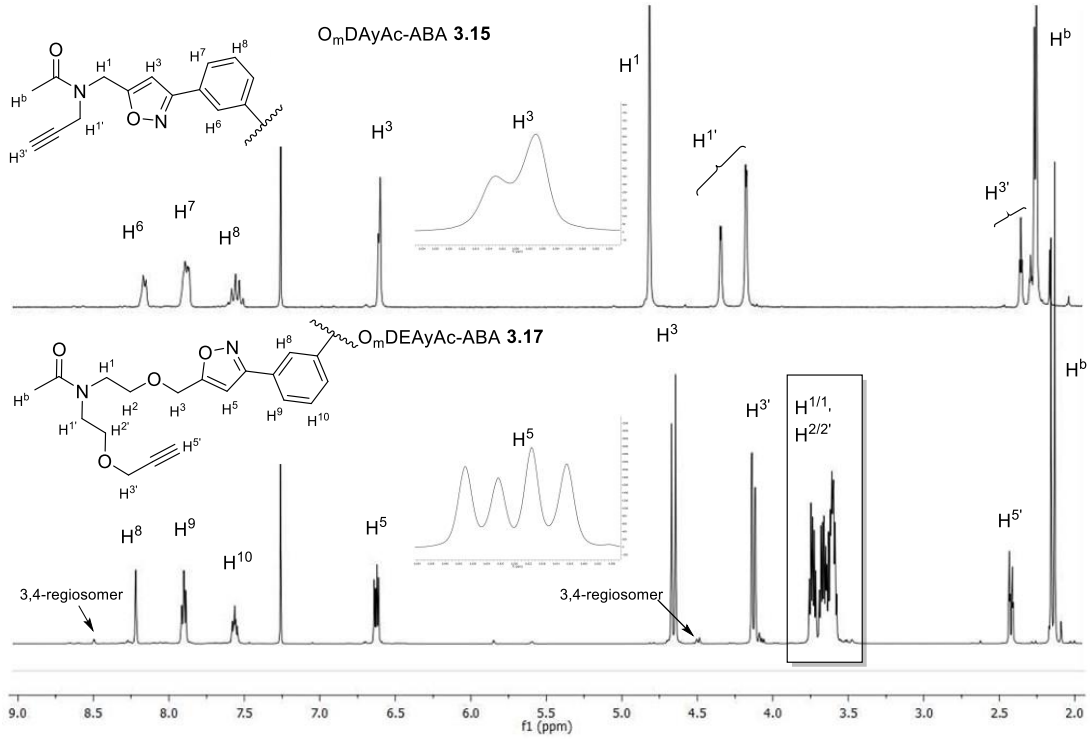

Figure 3-12: 500 MHz ^{1}H NMR spectra of **3.15** and **3.17**

As expected the 500 MHz ^{1}H NMR spectra of O_mDEAyAc-ABA **3.17** is similar to **3.15**, the inclusion of the ether introduced new environments between 3.5 ppm and 3.8 ppm, it also shifted some of the other environments (**3.17**, Figure 3-12). The rotamer ratio was reduced to 0.55 : 0.45 whilst the number of distinct environments increased from two to four, this was most obvious with the isoxazole proton H^5 (**3.17**, Figure 3-12) and in the ^{13}C NMR spectrum. When **3.17** was dissolved in d-DMSO for variable temperature analysis, the number of distinct rotamer environments in the ^{1}H NMR spectrum reduced back to two. Trace amount of 3,4-disubstituted cycloaddition product (Figure 3-13) was also detected in the ^{1}H NMR spectrum of **3.17** (Figure 3-12). The minor 3,4-regioisomer was apparent as two shifts in the spectrum at 8.45 ppm and 4.50 ppm, both of which appeared as doublets due to rotamers. The downfield shift (8.45 ppm) related to the proton on the 3,4-isoxazole ring, the other shift at 4.50 ppm was caused by the CH_2 next to the 3,4-isoxazole ring (Figure 3-12, Figure 3-13).

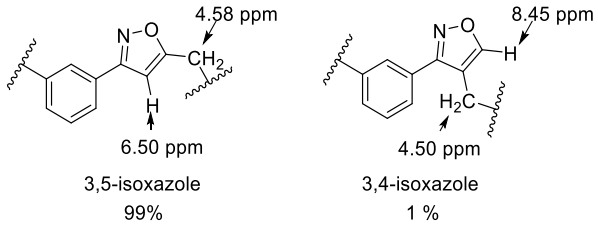

Figure 3-13: Regioisomers of isoxazoles

3.5.3.2 ^{1}H NMR analysis of isoxazoline ABA oligomers **3.14** and **3.16**

The ^{1}H NMR spectra of the isoxazoline oligomers (**3.14** and **3.16**, Figure 3-14) were more complicated than the isoxazole oligomers (**3.15** and **3.17**) as cycloaddition onto the terminal alkene formed diastereomers (Figure 3-11). The combination of the isoxazoline diastereomers and rotamers resulted in overlapping environments in the 500 MHz ^{1}H NMR spectra, particularly with the CH_2 environments between 3.4 ppm and 3.0 ppm for O_mDAeAc-ABA **3.14** (Figure 3-14). Due to the overlapping environments in **3.14**'s ^{1}H NMR spectrum the rotamer ratio (0.75 : 0.25) is only clear for the methyl protons of the acetamide groups H^b (**3.14**, Figure 3-14). Variable temperature ^{1}H NMR in d-DMSO (*insert*, **3.14**, Figure 3-14) showed the occurrence of rotamers more clearly as did the ^{13}C NMR spectrum.

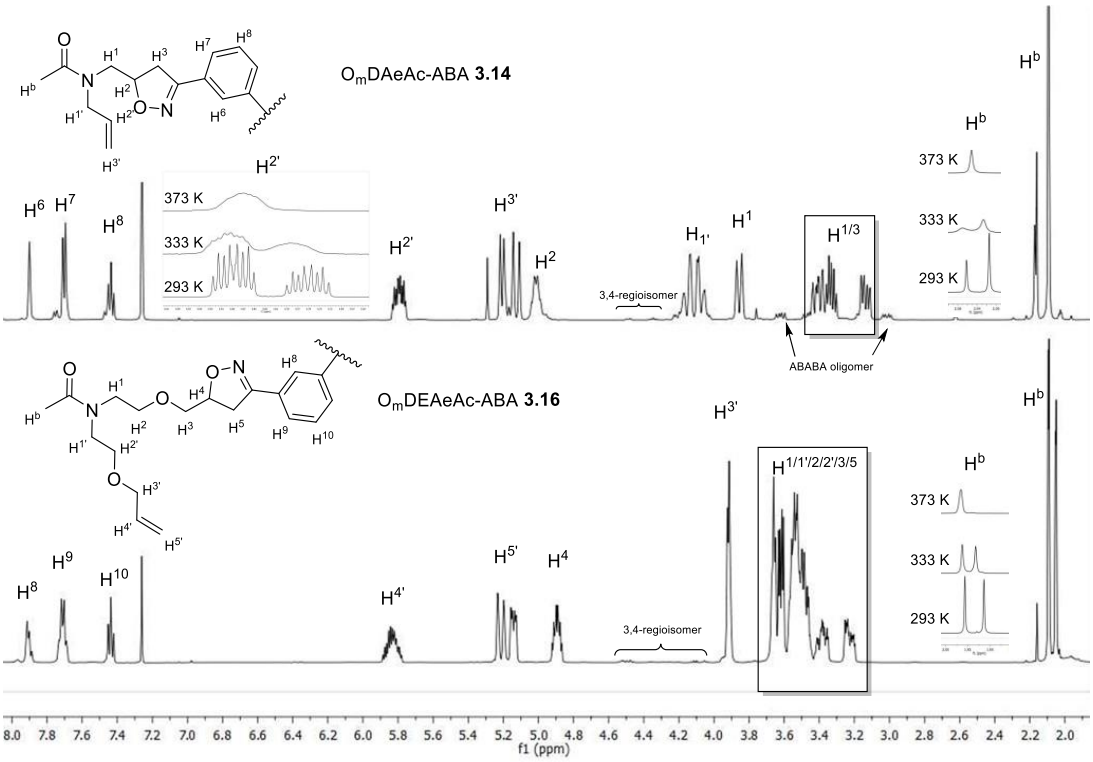

Figure 3-14: 500 MHz ^{1}H NMR spectra of **3.14** and **3.16**

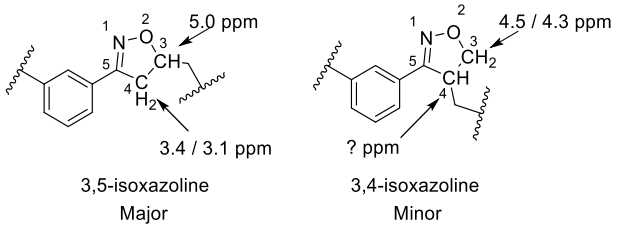

Figure 3-15: Regioisomers of isoxazoline O_mDAeAc-ABA **3.14**

As with the isoxazole oligomers **3.15** and **3.17,** minor amounts of the 3,4-isoxazoline regioisomer were formed during the synthesis of oligomers **3.14** and **3.16** (Figure 3-15). The minor regioisomer was apparent as two shifts in the spectrum of **3.14** (Figure 3-15) at 4.5 ppm and 4.3 ppm (Figure 3-14), these shifts were caused by the CH_2 in the ring. The CH in the 4 position on the ring (Figure 3-15) is unclear in the spectrum of **3.14** (Figure 3-14) as was expected to occur between 3 ppm and 4 ppm. Chemical shifts also occurred at 3.6 ppm and 3.0 ppm, as demonstrated later these shifts related to the larger oligomer O_mDAeAc-ABABA **3.18**.

Inclusion of the ether link in O_mDEAeAc-ABA **3.16** further complicated the 500 MHz ^{1}H NMR spectrum (**3.16**, Figure 3-14) with CH_2 environments between 3.7 ppm and 3.4 ppm. The rotamer ratio (0.55 : 0.45) could still be determined using the methyl shift of the acetamide (H^b, **3.16**, Figure 3-14). As with the isoxazole oligomers **3.15** and **3.17** the difference in rotamer ratio decreased with the inclusion of the ether link, the number of environments also increased from two to four when $CDCl_3$ was used as solvent. This reduced back to two environments when dissolved in d-DMSO for variable temperature analysis (*insert*, **3.16**, Figure 3-14). The minor 3,4-regioisomer was present in the ^{1}H spectrum of **3.16**, although at slightly different chemical shifts.

3.5.3.3 Ratio of isomers and variable temperature studies

The ratio of the major to minor rotamers in the compounds **3.14** – **3.17** could be estimated using the methyl shifts of the acetyl groups (H^b, Figure 3-12, Figure 3-14). The non-ether containing oligomers **3.14** and **3.15** exhibited rotamer ratios of 0.75 : 0.25 and 0.6 : 0.4 respectively, while the ratios for ether containing compounds **3.16** and **3.17** were lower (0.55 : 0.45). The smaller difference in rotamer ratio for **3.16** and **3.17** was likely caused by the greater distance between the isoxazoline ring and the acetyl group. The isoxazole ring (**3.15**, 0.6 : 0.4) has less of an effect on rotamer ratio than the isoxazoline (**3.14**, 0.75 : 0.25) for the lower molecular weight oligomers. As

the heterocyclic rings are freely rotating this difference could be caused by the methyl group interacting with either the greater electron charge density on the oxygen of the isoxazoline or by steric clashing with the non-planar hydrogens of the ring. With the larger oligomers (**3.16** and **3.17**) the increased distance between the heterocyclic ring and the amide group reduced the effect that the isoxazoline ring had on orientation.

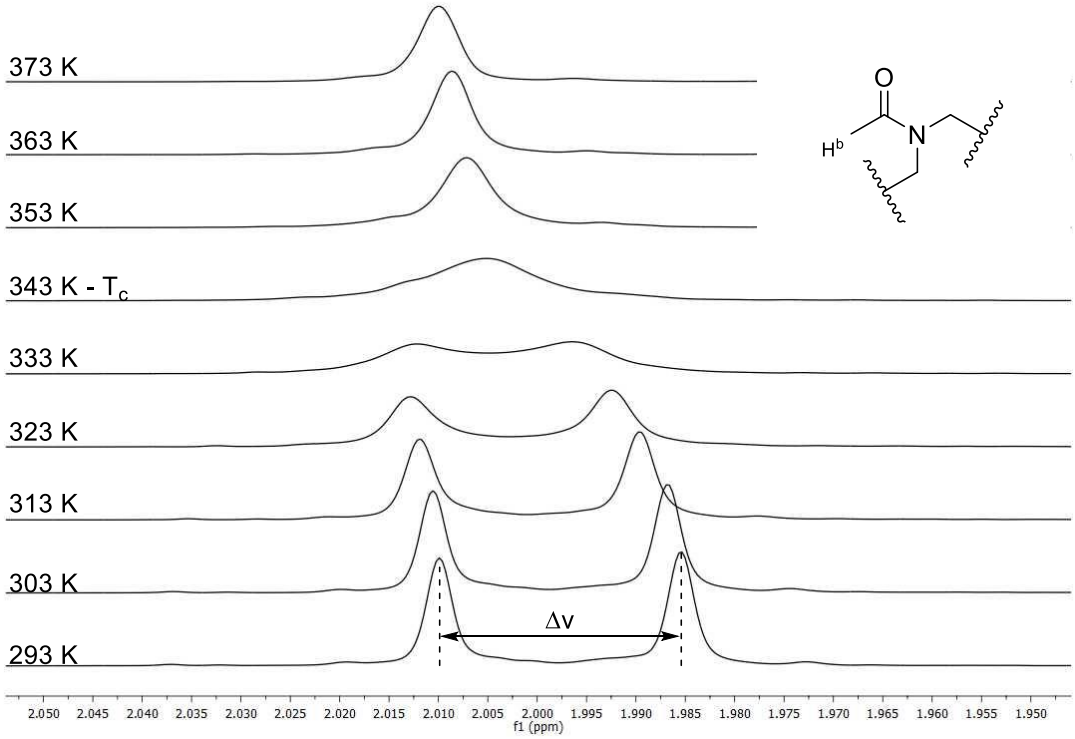

Figure 3-16: Variable temperature ^{1}H NMR of O_mDEAyAc-ABA **3.17** focussed on the acetamide environment.

Barriers to rotation were analysed by variable temperature ^{1}H NMR and calculated using Equation 3-1. Proton NMR analysis was performed on the oligomers at 10 K intervals between 293 K and 373 K (Figure 3-16). The frequency separation of the acetamide shift (H^b, Figure 3-16) at room temperature was taken as Δv. The temperature of coalescence (T_c) was taken as the first temperature at which the ^{1}H NMR spectrum showed one peak for the acetyl protons (H^b). Unfortunately, when dissolved in d-DMSO the acetamide rotamer shifts (H^b) for O_mDAyAc-ABA **3.15** appeared as one shift at 293 K, other environments however were present as distinct rotamers. The CH_2 environment next to the isoxazole ring (H^1, Figure 3-12) gave the cleanest coalescence and so was used to determine the barrier to rotation of **3.15**. As analysis was carried out at 10 K intervals the barriers to rotation are estimates with a degree of error of ± 1.3 kJ mol^{-1} (±0.3 kcal mol^{-1}).

$$\frac{\Delta G\ddagger}{RT_c} = 23 + \ln\frac{T_c}{\Delta v}$$

$$\Delta G\ddagger = RT_c(23 + ln\frac{T_c}{\Delta v})$$

Equation 3-1: Barrier to rotation equation ΔG‡ = free energy of activation, R = gas constant, T_c = temp coalescence, ΔV = frequency separation at 293 K.

Oligomer O_mDAeAc-ABA **3.14** (4a**,** Table 3-4) had the highest barrier to rotation (ΔG‡), which was similar to the dialkyne monomer DEAyAc **3.8** (4a & 4e, Table 3-4). Isoxazole O_mDAyAc-ABA **3.15** (4b, Table 3-4) had the lowest barrier to rotation, although the use of the CH_2 (H^1, **3.15**, Figure 3-14) shift instead of the acetamide (H^b, Figure 3-16) shift may be the source of its low calculated barrier to rotation. Considering the error in ΔG (±1.3 kJ mol^{-1}/±0.3 kJ mol^{-1}), the oligomers **3.14** – **3.17** barriers to rotation were very similar and little changed from DEAyAc **3.8**.

Entry	Compound	T_c / K	Δv	ΔG / kJ mol^{-1} [a]	ΔG / kcal mol^{-1} [b]	Ratio in $CDCl_3$
4a	O_mDAeAc-ABA **3.14**	353	23.5	75.5	18.0	0.25 : 0.75
4b	O_mDAyAc-ABA **3.15**	353	73.8	72.1	17.2	0.40 : 0.60
4c	O_mDEAeAc-ABA **3.16**	343	21.5	73.5	17.6	0.45 : 0.55
4d	O_mDEAyAc-ABA **3.17**	343	12.3	75.1	17.9	0.45 : 0.55
4e	DEAyAc **3.8**	353	21.5	75.7	18.1	0.50 : 0.50

a-±1.3 kJ mol^{-1} b-±0.3 kcal mol^{-1}

Table 3-4: Monomer (**3.8**) and oligomer (**3.14** – **3.17**) rotamer ratios and barriers to rotation.

3.5.4 ^{1}H NMR analysis of the ABABA oligomers (**3.18** – **3.20**)

ABABA oligomers were recovered for both non-ether containing compounds O_mDAeAc-ABABA **3.18** and O_mDAyAc-ABABA **3.19** and the larger ether containing isoxazole compound O_mDEAyAc-ABABA **3.19**. Analysis of these larger oligomers by 500 MHz ^{1}H and 125 MHz ^{13}C NMR revealed how environments changed as they moved away from dipolarophilic end groups.

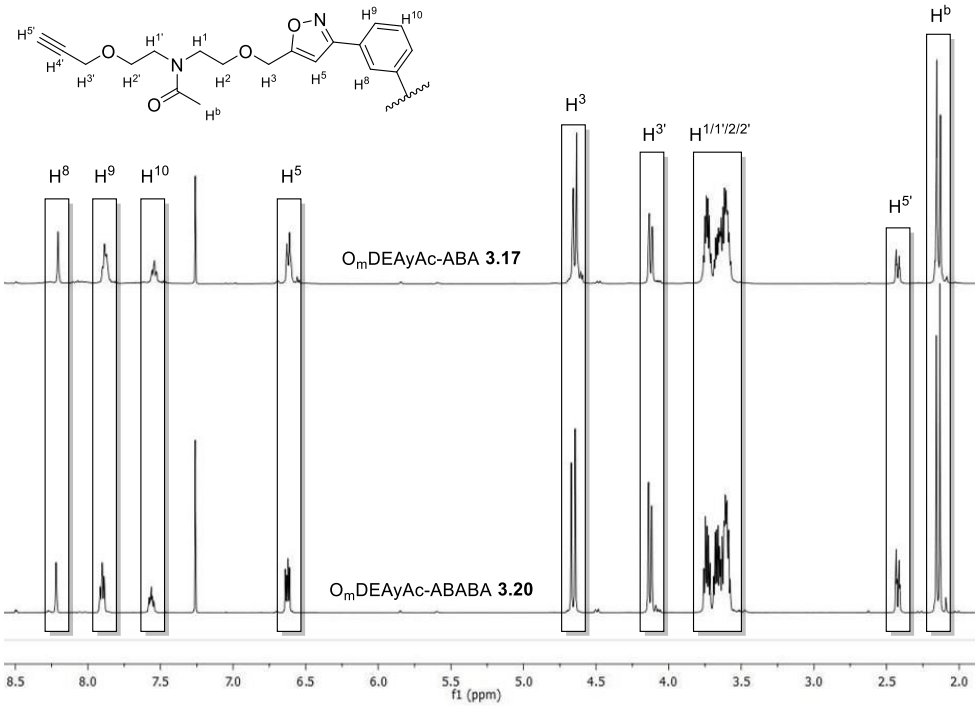

Figure 3-17: 500 MHz ^{1}H NMR spectra of **3.17** (*top*) and **3.20** (*bottom*)

Very little difference was observed when comparing the 500 MHz proton NMR spectra of ABABA isoxazole oligomers O_mDAyAc-ABABA **3.19** and O_mDEAyAc-ABABA **3.20** to the ABA membered isoxazole oligomers O_mDAyAc-ABA **3.15** and O_mDEAyAc-ABABA **3.17** (Figure 3-17). Indicating that there will be little change in environment chemical shifts as they move away from the end group during polyisoxazole synthesis.

Interestingly the 500 MHz ^{1}H NMR spectrum of the O_mDAeAc-ABABA **3.18** is different enough to the O_mDAeAc-ABA **3.14** (Figure 3-18) that we can distinguish between the two isoxazoline environments (the terminal environment 1and the internal environment 2. This suggests that it should be possible to identify the terminal environment 1 type of isoxazoline in any prepared polymers.

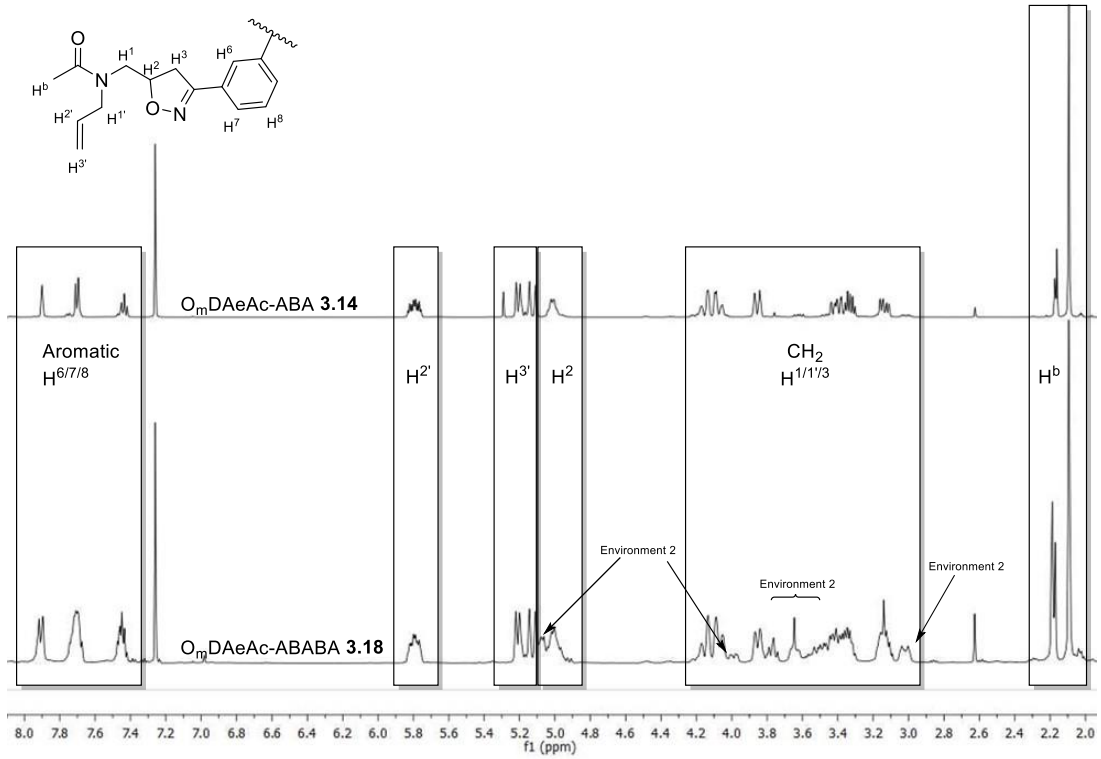

Figure 3-18: 500 MHz ^{1}H NMR spectra of O$_m$DAeAc-ABA **3.14** (*top*) and O$_m$DAeAc-ABA **3.18** (*bottom*).

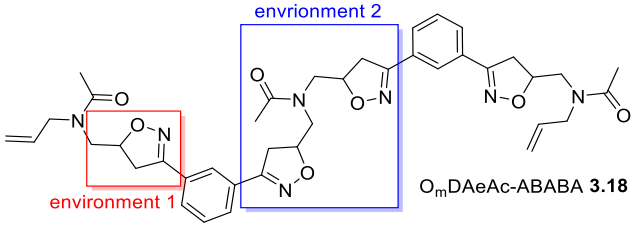

Figure 3-19: Different isoxazoline environments of O$_m$DAeAc-ABABA **3.18**

3.5.5 Thermal analysis of ABA oligomers (**3.14** – **3.17**)

The model repeat ABA units **3.14** – **3.17** were studied by TGA to determine any difference in the thermal stability of isoxazoline and isoxazole rings. Thermal analysis of the model ABA repeat units **3.14** – **3.17** revealed that initial degradation (T_5) was affected by the nature of the amide link with the greater T_5 found for ether derived compounds **3.17** (295 ºC) and **3.18** (302 ºC) compared to the shorter chain derivatives **3.14** (282 ºC) and **3.15** (280 ºC). However, the overall degradation profile was directed by the heterocyclic ring. The non-ether linked chained oligomers **3.14** and **3.15** (5a & 5b, Table 3-5) had similar T_5's (ΔT_5 = 2 ºC) but appreciably different T_{20}'s (ΔT_{20} = 40 ºC). A comparable relationship occurred with the ether containing oligomers **3.16** and **3.17** (5c & 5d, Table 3-5), although the difference in overall degradation did not occur until a later stage (**3.16** and **3.17**, ΔT_5 = 7 ºC, ΔT_{20} = 5 ºC, ΔT_{40} = 47 ºC).

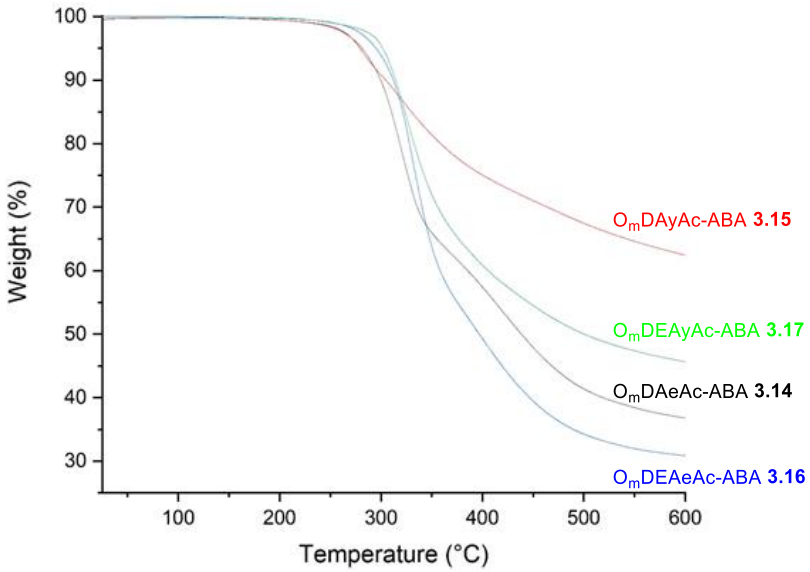

Figure 3-20: TGA of model oligomers (O_mDAeAc-ABA **3.14**, O_mDAyAc-ABA **3.15**, O_mDEAeAc-ABA **3.16**, O_mDEAyAc-ABA **3.17**) carried out at a heating rate of 10ºC min^{-1} under a N_2 atmosphere.

Residual weight of the isoxazoline O_mDAeAc-ABA **3.14** at 600 ºC was considerably lower than corresponding isoxazole O_mDAyAc-ABA **3.15** (5a & 5b, Table 3-5, ΔW_{600} = 25 %) indicating different decomposition pathways for isoxazole and isoxazoline rings. A similar trend was observed for isoxazoline O_mDEAeAc-ABA **3.16** and oxazole O_mDEAyAc-ABA **3.17**.

Entry	Oligomer	T_5 / ºC	T_{20} / ºC	W_{600} / %
5a	O_mDAeAc-ABA **3.14**	282	319	37
5b	O_mDAyAc-ABA **3.15**	280	359	62
5c	O_mDEAeAc-ABA **3.16**	295	328	30
5d	O_mDEAyAc-ABA **3.17**	302	333	46

Table 3-5: Thermal stability of 3 membered oligomers (3.14 – 3.17) determined by TGA

3.6 Acetamide based model polymers (**3.22 – 3.25**)

Once the oligomers **3.14** – **3.20** had been characterised (section 3.5), the dipolarophilic monomers **3.5** – **3.8** were used with *meta*-OC **2.1** to form polymers. The polymerisation method and work up was the same as employed in chapter 2. *Meta*-OC **2.1** (1 eq.) and dipolarophiles (**3.5** – **3.8**, 1 eq.) were slowly stirred in DMF along with 4 Å MS at 80 ºC for 24 hrs. The polymers were collected by precipitation into methanol. Polymer nomenclature was the same as in chapter 2, although no number was required as the polymerisations were all carried out stoichiometrically. This meant that P^t_mDAeAc **3.22** denoted a polymer formed from *meta*-OC **2.1** and DAeAc **3.5** using Takata's[318,330] thermal polymerisation method.

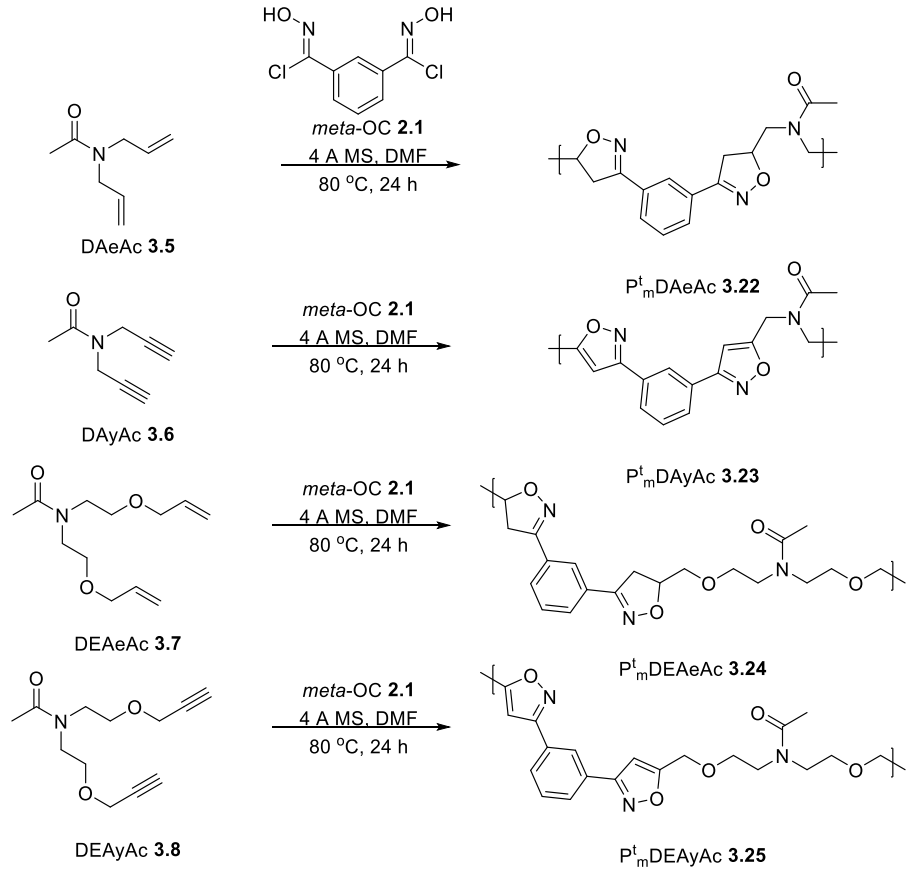

Scheme 3-5: Polymers **3.22** – **3.25** synthesised from model monomers **3.5** – **3.8** and *meta*-OC **2.1**

As with the polymers in chapter 2 the methanol filtrate was analysed, revealing low molecular weight oligomers and evidence of undecomposed oximoyl chloride. The presence of these oligomers in the filtrate could account for the low yields of polymer. The yield of polymers was even lower for the non-ether containing polymers (**3.22**, 62 % and **3.23**, 64 %) than those that with ether linkages (**3.24**, 76 % and **3.25**, 78 %).

Entry	Polymer	NMR Calc. repeat units	Yield / %
6a	P^t_mDAeAc **3.22**	13	62
6b	P^t_mDAyAc **3.23**	16	64
6c	P^t_mDEAeAc **3.24**	10	76
6d	P^t_mDEAyAc **3.25**	10	78

Table 3-6: Yields of **3.22** – **3.25** and number of repeat units calculated by NMR end group analysis

The polymers (**3.22** – **3.25**) were soluble in $CDCl_3$ and were therefore analysed by 500 MHz ^{1}H and 125 MHz ^{13}C NMR. Interpretation of the carbon and proton spectra was unproblematic as the oligomers (**3.14** – **3.20**) had been previously assigned (section 3.5). As expected the end group signals (terminal alkene and alkyne) associated with the dipolarophile were reduced in intensity and the signals corresponding to the heterocycles (isoxazoline and isoxazole) were increased relative to the oligomers (**3.14**

– **3.17**). Polyisoxazoles **3.23** and **3.25** had spectra similar to their respective ABA oligomers **3.15** and **3.17** (section 3.5.3.1), with only changes in the intensity of alkyne related environments. The spectra of polyisoxazolines **3.22** and **3.24** (Figure 3-21) however had significant changes from their ABA oligomers **3.14** and **3.16** (section 3.5.3.2). This change was anticipated from the ^{1}H NMR analysis of O_mDAeAc-ABABA **3.18** in section 3.5.4, where internal (environment 1) and external (environment 2) environments were observed in spectrum.

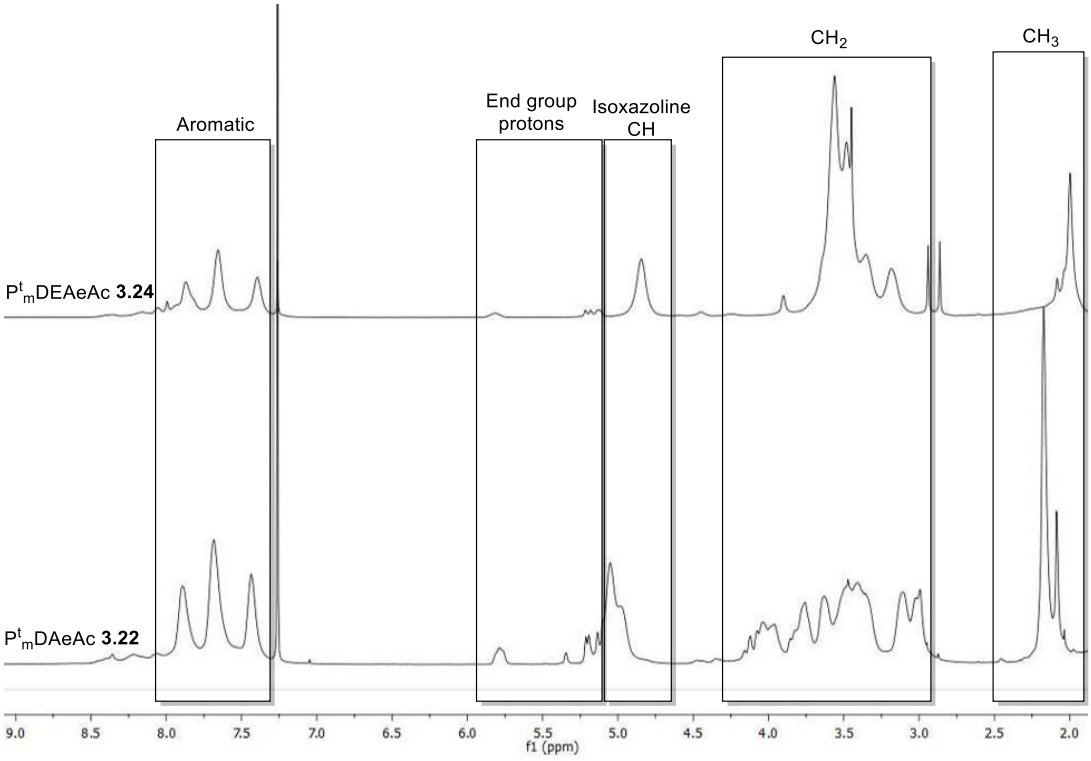

Figure 3-21: 500 MHz ^{1}H NMR spectra of P$^{t}_{m}$DAeAc **3.22** (*bottom*) and P$^{t}_{m}$DEAeAc **3.24** (*top*)

The number of repeat units in the average polymer chain was determined by end group analysis using the proton NMR spectra, this method assumes that the polymer chain has a regularly repeating linear structure with dipolarophiles as end groups. Due to the complex overlap of environments for the polyisoxazolines **3.22** and **3.24** (Figure 3-21), the calculation of polymer conversion by ^{1}H NMR was done using the alkene environment at 5.8 ppm and the aromatic peak at 7.4 ppm. As with oligomers, 500 MHz ^{1}H NMR spectra of the polyisoxazoles (**3.23** and **3.25**) were less complex. The terminal alkyne proton environments at 2.4 ppm could be compared with the isoxazole proton at 6.6 ppm to determine conversion. Number of repeat units calculated by NMR end group analysis (Table 3-6) indicates that the non-ether containing polymers (**3.22**

13 RU and **3.23** 16 RU) had a greater average number of repeat units in a chain than the ether containing polymers (**3.24** 10 RU and **3.25** 10 RU).

3.6.1 MALDI-TOF analysis of model polymers (**3.22 – 3.25**)

Samples of the polymers (**3.22** – **3.25**) were prepared for MALDI-TOF analysis using DMF doped with NaI (0.1 mg ml^{-1}). The samples were dissolved in the doped DMF (10 mg ml^{-1}). The matrix (DCTB) was also dissolved in separate doped DMF (40 mg ml^{-1}). Equal volumes (10 µl) of the two DMF solutions were mixed, a sample of the resulting mixture was placed on ground steel plate and dried in a vacuum oven at 25 °C and 0.01 atm for 30 minutes. Three of the polymers (**3.22**, **3.23** and **3.25**) presented clear MALDI-TOF spectra, unfortunately $P^t_mDEAeAc$ **3.24** did not, even with multiple attempts. Heterocycle comparisons were therefore made between P^t_mDAeAc **3.22** and P^t_mDAyAc **3.23**. Effects of the ether link on polymer structure were determined by comparisons between polyisoxazoles **3.23** and **3.25**. As in chapter 2 and section 2.5 the dipolarophile unit was denoted by A and the *meta*-NO **2.13** unit by B.

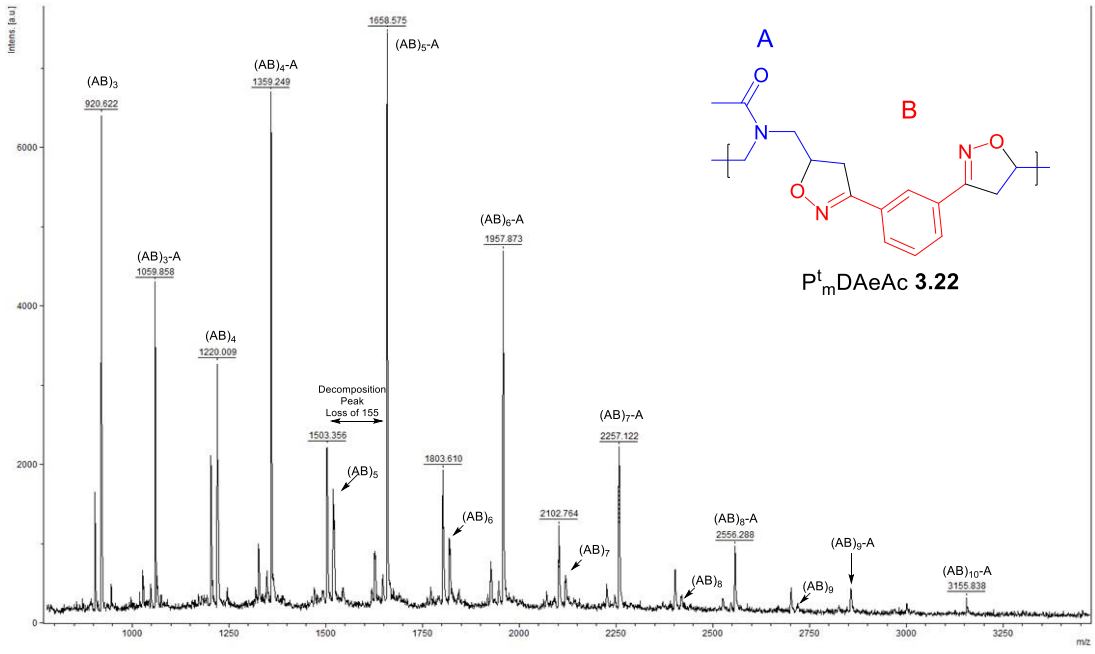

Figure 3-22: MALDI-TOF spectrum of P^t_mDAeAc **3.22**

P^t_mDAeAc **3.22**: Analysis of the polyisoxazoline **3.22** by MALDI-TOF (Figure 3-22) revealed the regular occurrence of polymers containing equal numbers of A and B units $(AB)_n$ as well as chains with an $(AB)_n$-A structure. Some $(AB)_3$ oligomers are present with molecular weights below 1000 Da, the intensity was higher than the

$(AB)_3$-A oligomer at 1059.9 Da. This difference in intensity however could be due MALDI-TOF analysis being more sensitive to lower molecular weight compounds. At higher molecular weights, the relationship is reversed with the $(AB)_n$-A chains registering a higher intensity. End group analysis by ^{1}H NMR estimates the average chain to contain 13 RU, the MALDI spectrum however does not report any P^t_mDAeAc **3.22** chains above 3155.8 Da, $(AB)_{10}$-A. Cyclisation would increase the ^{1}H NMR estimation without increasing molecular weight, this discrepancy might therefore infer that cyclisation was the major contributor to the $(AB)_n$ chains as opposed to dimerisation of nitrile oxides to form furoxans. The discrepancy may also be caused by the analysis technique being more sensitive to low molecular weight compounds. As with the polyisoxazolines in chapter 2 the MALDI spectra contained peaks that related to the decomposition of the polymer during MALD-TOF analysis, most notably a strong peak that related to a loss of 155 Da from (AB)-A chains, caused by the decomposition of the isoxazoline ring (**3.26**, Figure 3-23).

Figure 3-23: Major MALDI-TOF decomposition fragments of **3.22** and **3.23**

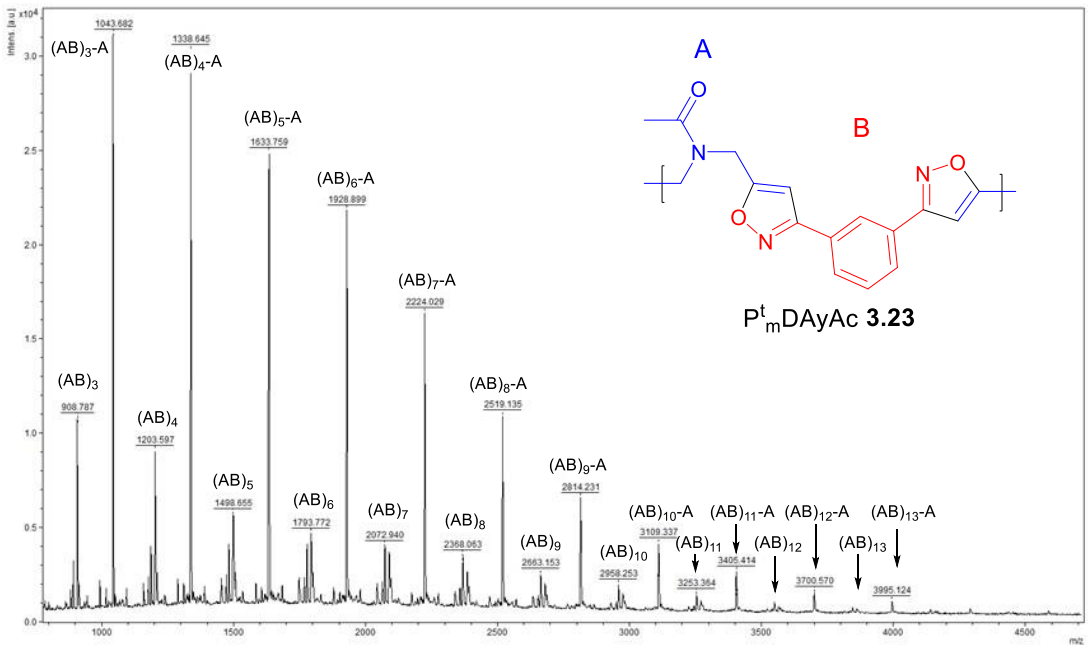

Figure 3-24: MALDI-TOF spectrum of P^t_mDAyAc **3.23**

P$^{t}_{m}$DAyAc **3.23**: Unlike **3.22** the polyisoxazole **3.23** MALDI-TOF (Figure 3-24) spectrum contained $(AB)_n$-A chains at higher intensities than $(AB)_n$ at all molecular weights. This indicated that the polyisoxazoles were less susceptible to form cyclical polymers or contain furoxan links than their polyisoxazoline equivalents. The major decomposition peak apparent in the spectrum was caused by the loss of 151 Da from $(AB)_n$-A chains, relating to the breaking of an isoxazole ring (**3.27**, Figure 3-23).

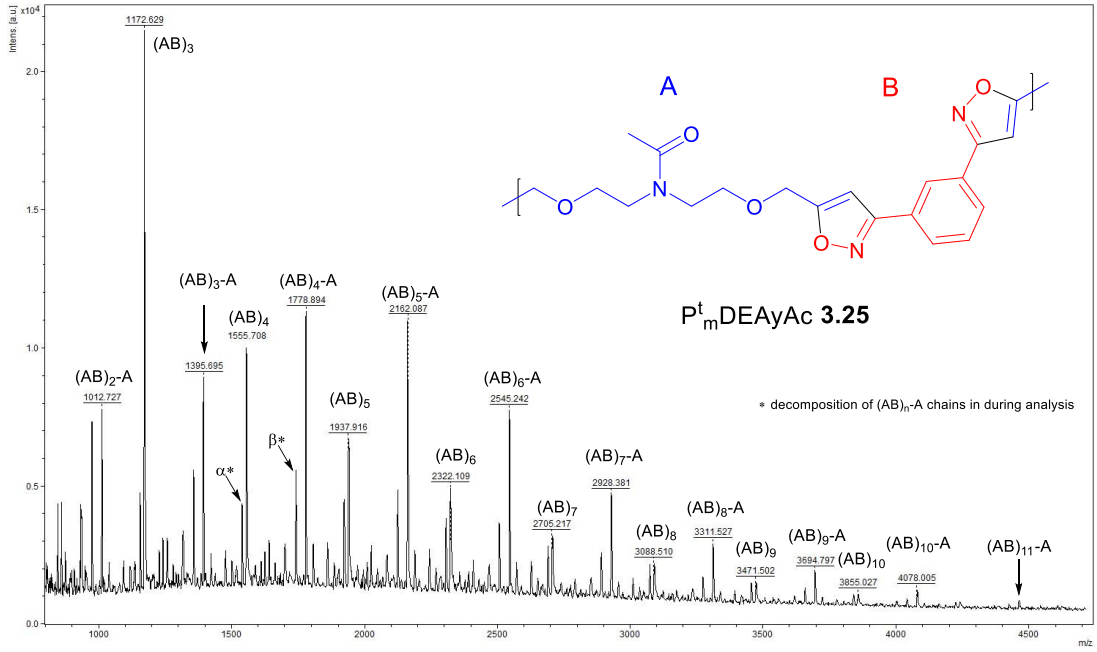

Figure 3-25: MALDI-TOF spectrum of P$^{t}_{m}$DEAyAc **3.25**

P$^{t}_{m}$DEAyAc **3.25**: At low molecular weight (<1500 Da) the MALDI-TOF spectrum of **3.25** (Figure 3-25) shows a greater abundance of $(AB)_n$ oligomers compared to $(AB)_n$-A, with a particularly intense $(AB)_3$ peak at 1172.629 Da. The relationship changes as molecular weight increases (>1500 Da) with $(AB)_n$-A chains becoming more intense than $(AB)_n$. In the MALDI-TOF spectrum of **3.25** chains are found up to at least $(AB)_{11}$-A (4465.905 Da). Analysis was only carried out up to 5000 Da and so any higher molecular weight chains were not observed. Apart from the $(AB)_n$ and $(AB)_n$-A peaks there are several repeating degradation peaks in the spectrum of **3.25**, with major degradation peaks (α - Figure 3-25) relating to the loss of **3.28** (Figure 3-26) by cleavage of the weak N-O bond. A second major degradation (β - Figure 3-25) may have related to the decomposition of the ether bond and the loss of either **3.31** or **3.32 (**Figure 3-26**)**, similar degradations weren't apparent in the spectra of **3.22** (Figure 3-22) and **3.23** (Figure 3-24).

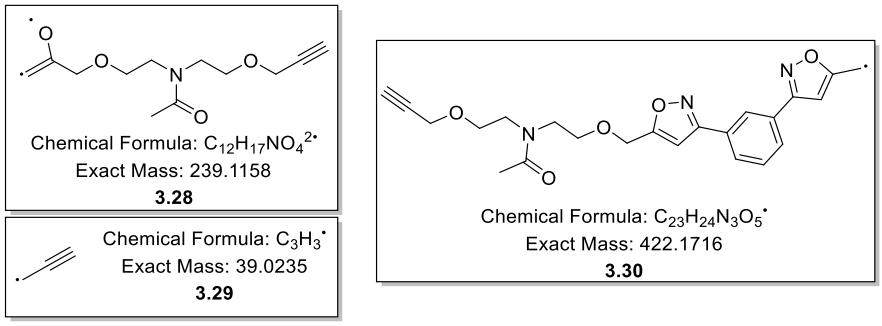

Figure 3-26: Major MALDI-TOF decomposition fragments of **3.25**

3.6.2 GPC analysis of model polymers (**3.22 – 3.25**)

Polyisoxazolines and polyisoxazoles are uncommon polymers and as such there are not standards which they can be compared against for GPC analysis. In order to gain a better understanding of the real molecular weight of the polymers (**3.22** – **3.25**), oligomers (**3.14** – **3.20**) of known molecular weight were analysed by GPC to set a baseline for polymer analysis (section 3.5.1). The methanol filtrate collected during polymerisation was also analysed by GPC. The compounds and polymers were run using DMF as the eluent against PMMA standards.

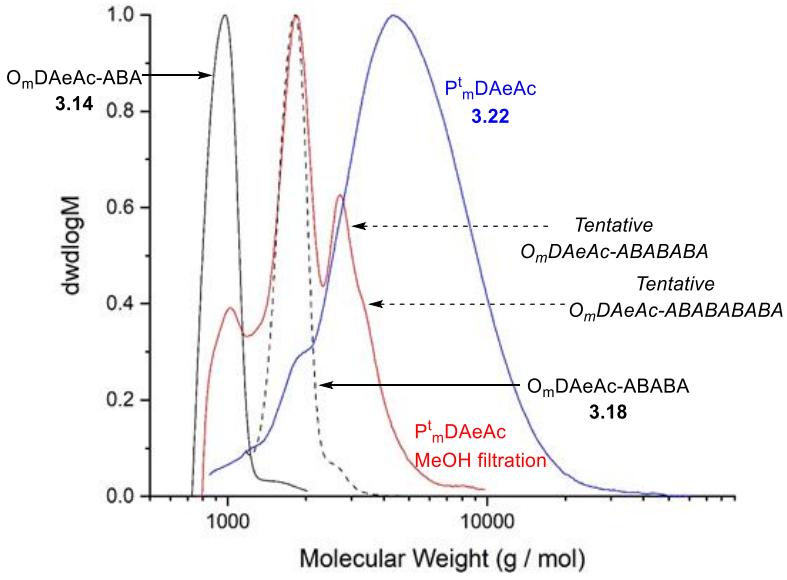

Figure 3-27: GPC plot of O_mDAeAc-ABA **3.14**, O_mDAeAc-ABABA **3.18**, P^t_mDAeAc-filtrate, P^t_mDAeAc **3.22**.

Entry	Polymer	M_n[a] / kDa	M_w[a] / kDa	$Đ$[a]	RU / Da	RU M_n[b]	RU M_w[b]
7a	P^t_mDAeAc **3.22**	3.9	5.7	1.5	299.3	13.0	19.0
7b	P^t_mDAyAc **3.23**	4.4	6.5	1.5	295.3	14.9	22.0
7c	P^t_mDEAeAc **3.24**	6.5	10.3	1.6	387.4	16.8	26.6
7d	P^t_mDEAyAc **3.25**	5.9	8.7	1.5	383.4	15.4	22.7

[a] Estimated by GPC based on PMMA standards, [b] Calculated by division of GPC estimated by RU MW

Table 3-7: GPC estimations of polymers **3.22** – **3.25**

In section 3.5.1 we concluded that the polymer molecular weight data obtained by GPC (Table 3-7) was likely an overestimation of the real molecular weight, with polyisoxazoles inflated to a greater extent than polyisoxazolines. By plotting the GPC curves of the respective oligomers, filtrates and polymers over one another a real appreciation for the growth in molecular weight can be had. The full plot of polyisoxazoline **3.22** shows the extent of polymerisation relative to the oligomers and methanol filtrate (Figure 3-27). The plot of the methanol filtrate indicates that it contains mostly O_mDAeAc-ABABA oligomers **3.18**.

Estimates from GPC data suggested that polymers P^t_mDEAeAc **3.24** and P^t_mDEAyAc **3.25** derived from the ether monomers DEAeAc **3.7** and DEAyAc **3.8** had higher molecular weights and repeat units (7c & 7d, Table 3-7) than the corresponding polymers P^t_mDAeAc **3.22** and P^t_mDAyAc **3.23** (7a & 7b, Table 3-7). Furthermore, the GPC plot of **3.23** (Figure 3-28) has lower molecular weight shoulders leading to the peak at 5.1 kDa, these shoulders are indicative of oligomers. The plot of P^t_mDEAyAc **3.25** (Figure 3-28) is smooth with no shoulders before the peak at 7.2 kDa inferring less lower molecular weight oligomeric species.

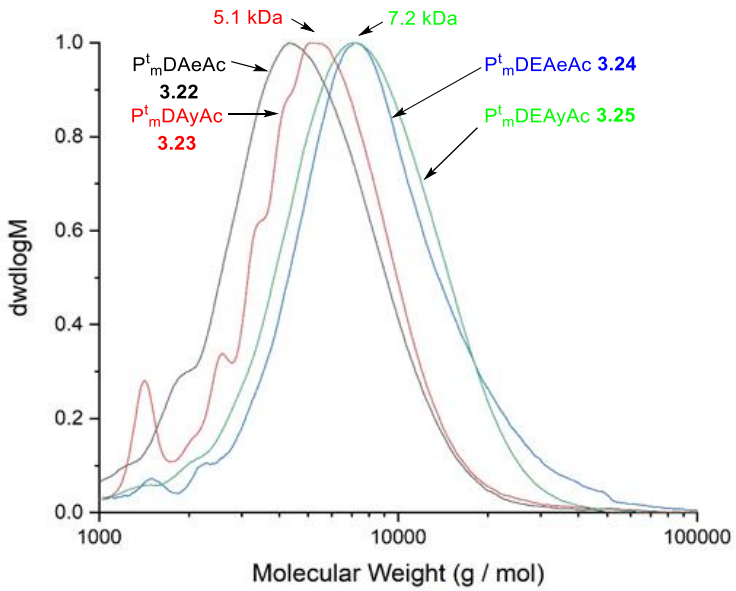

Figure 3-28: GPC plot of P^t_mDAeAc **3.22**, P^t_mDAyAc **3.23**, P^t_mDEAeAc **3.24**, P^t_mDEAyAc **3.25**.

In section 2.4 P^t_mDEGDA-1 **2.5** achieved a greater degree of polymerisation than P^t_mEGDA-1 **2.27**, indicating that spacing between dipolarophilc groups effects the molecular weight. Ether containing monomers **3.7** and **3.8** have 9 atoms between the dipolarophilic groups, the same as DEGDA **2.4**, and reached higher numbers of repeat

units than **3.5** and **3.6**, which only have 3 atoms between the dipolarophilic groups (similar to EGDA **2.9**).

3.6.3 Thermal analysis of the model polymers (**3.22 – 3.25**)

The model polymers (**3.22 – 3.25**) physical properties were assessed by thermal analysis using TGA to ascertain thermal stability and DSC to determine glass transition temperature (T_g). Thermal stability was measured by heating the polymers from 25 ºC to 600 ºC at 10 ºC / min under nitrogen.

Entry	Polymer	T_g / °C	T_5 / °C	T_{20} / °C	W_{600} / %
8a	P^t_mDAeAc **3.22**	124	233	300	59
8b	P^t_mDAyAc **3.23**	112	251	349	62
8c	P^t_mDEAeAc **3.24**	67	226	318	52
8d	P^t_mDEAyAc **3.25**	51	249	339	57

Table 3-8: Thermal analysis of the model polymers (**3.22 – 3.25**) by DSC and TGA

Initial decomposition (T_5) of the polymers (**3.22 – 3.25**, Table 3-8) occurred at lower temperatures than their respective oligomers (**3.14 – 3.17**, section 3.5.5) but at similar temperatures to the polyisoxazoles in chapter 2. Unlike with the oligomers (**3.14 – 3.17**), initial decomposition temperature was dictated by the heterocycle rather than the inclusion of the ether link, with polyisoxazolines (8a & 8c, Table 3-8) beginning to decompose at lower temperatures than polyisoxazoles (8b & 8d, Table 3-8). Residual weight at 600 °C (W_{600}) increased for polymers **3.22**, **3.24** and **3.25** compared to their isolated oligomers (**3.22**, **3.24** and **3.25)**, but remained the same for P^t_mDAyAc **3.23** (**3.15** and **3.23**, W_{600} = 62 %).

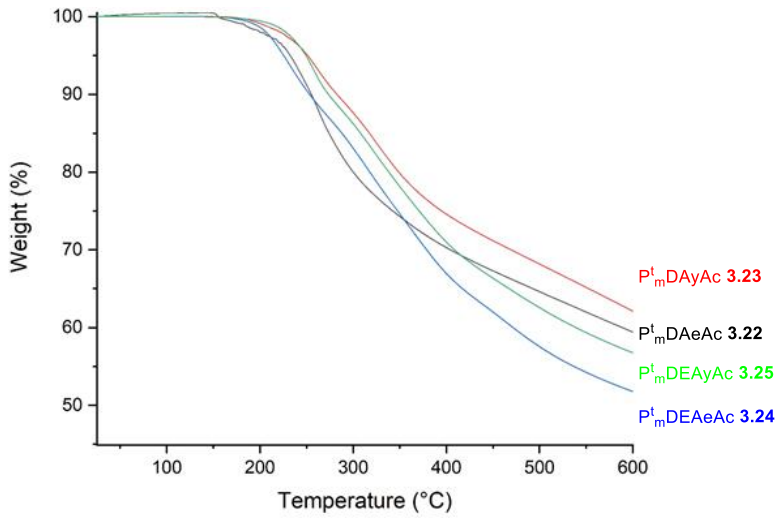

Figure 3-29: TGA of model polymers (P^t_mDAeAc **3.22**, P^t_mDAyAc **3.23**, P^t_mDEAeAc **3.24**, P^t_mDEAyAc **3.25**) carried out at a heating rate of 10ºC min^{-1} under a N_2 atmosphere.

To establish the T_g's of the polymers (**3.22 – 3.25**) were heated under N_2 then cooled before heating again, it was on the second heating that the T_g was recorded (Table 3-8). After an initial tests, polymer **3.22** and **3.23** were studied between 0 °C and 150 °C whilst ether containing polymer s **3.24** and **3.25** were analysed between −100 °C and 100 °C. The work in section 2.4 showed that the longer the glycol chain between the *meta*-isoxazoline groups (Figure 3-30) the lower the T_g, this was shown to hold true for the model polyisoxazolines (**3.22** and **3.24**) and polyisoxazoles (**3.23** and **3.25**). As expected from the work in section 2.4 the ether containing polymers (8c & 8d, Table 3-8, **3.24** T_g = 67 ºC and **3.25** T_g = 51 ºC) resulted in lower T_g's than their non-ether containing counterparts (8c & 8d, Table 3-8, **3.22** T_g = 124 ºC and **3.23** T_g = 112 ºC) that were only separated by 3 atoms.

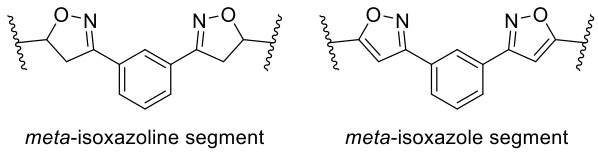

Figure 3-30: *Meta*-isoxazoline and *meta*-isoxazole segment of the polymers

There was a difference in T_g between the comparable polyisoxazoles (**3.23** and **3.25**) and polyisoxazolines (**3.22** and **3.24**). The polyisoxazoles were expected to have higher T_g's as the aromatic heterocycles have a more planar structure which would presumably allow for more regular packing and π stacking interactions than their isoxazoline counterparts. The T_g's as determined by DSC however revealed the polyisoxazolines (8a & 8c, Table 3-8, **3.22** T_g = 124 ºC and **3.24** T_g = 67 ºC) to have higher T_g's than the analogous polyisoxazoles (8b & 8d, Table 3-8, **3.23** T_g = 112 ºC and **3.25** T_g = 51 ºC). During the purification of the oligomers (section 3.4) it was noted that the isoxazolines (**3.14** and **3.16**) were considerably more polar than the isoxazoles (**3.15** and **3.17**). Intermolecular interactions caused by the greater polarity of the repeating isoxazoline could therefore have a greater effect on raising T_g than the better packing associated with the planar isoxazole.

3.7 Summary and conclusion

Dipolarophilic amide model monomers (e.g. DEAyAc **3.8**) were successfully synthesised with an acetyl group in place of a long alkyl fatty acid chain. Analysis of the monomers by both ^{1}H and ^{13}C NMR revealed rotamers caused by the amide bond, splitting the NMR environments of the non-acetyl atoms (Figure 3-31). The different rotamer environments were more distinct in the di-alkyne derived monomers than the di-alkene ones. The chemical shift difference for corresponding atoms in the respective *cis* and *trans* chains reduced as the distance from the amide group increased.

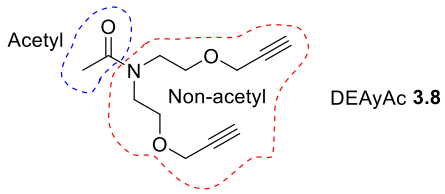

Figure 3-31: Model dipolarophilic monomer DEAyAc **3.8**

ABA oligomers **3.14** – **3.17** (Figure 3-32) were formed using the model monomers **3.5** – **3.8** (A) and *meta*-OC **2.1** (B). During the purification additional ABABA oligomeric compounds **3.18** – **3.20** were recovered. TLC of the oligomers revealed that isoxazoline heterocycles **3.14** and **3.16** were substantially more polar than isoxazole rings **3.15** and **3.17**. The oligomers **3.14** – **3.20** were characterised fully to give insight into polymer structures at a later date. Thermal analysis of the oligomers **3.14** – **3.17** by TGA indicated that the isoxazole ring was more stable than the isoxazoline ring at elevated temperatures.

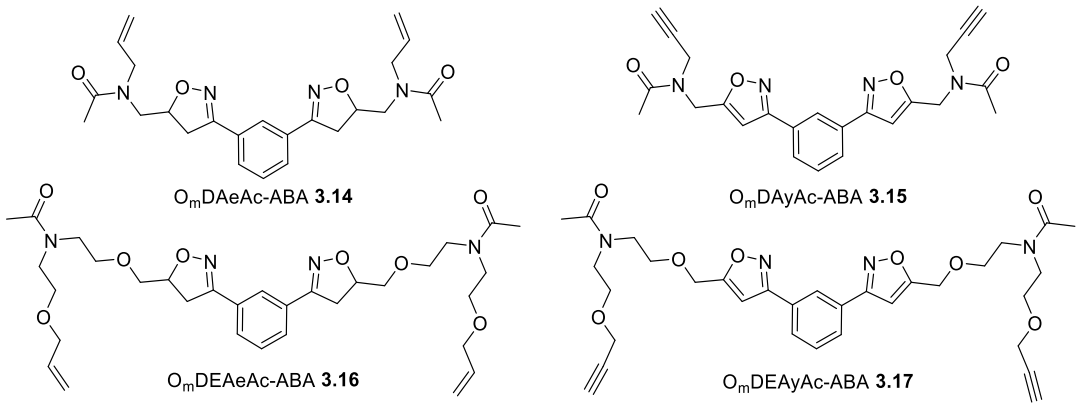

Figure 3-32: Acetamide ABA oligomers **3.14** – **3.17**.

Polymers **3.22** – **3.25** (Figure 3-33) were made from the model monomers **3.5** – **3.8** and *meta*-OC **2.1**. The ether containing monomers **3.7** and **3.8** produced polymers with higher yields than the monomers **3.5** and **3.6** with a smaller distance between reactive groups. End group analysis by 500 MHz ^{1}H NMR suggested that non-ether containing polymers **3.22** and **3.23** were comprised of a greater number of repeat units than their ether containing counterparts **3.24** and **3.25**. MALDI-TOF analysis revealed that the polyisoxazoline P^{t}_{m}DAeAc **3.22** had a greater propensity towards forming $(AB)_{n}$ chains than polyisoxazole P^{t}_{m}DAyAc **3.23**. It also indicated that the inclusion of an ether linkage increased the occurrence of $(AB)_{n}$ chains. GPC analysis suggested that the larger monomers **3.7** and **3.8** resulted in greater degrees of polymerisation than the lower molecular weight monomers **3.5** and **3.6**. Thermal analysis of the polymers **3.22** – **3.25** indicated that they were less thermally stable than the oligomers. It also revealed that the polyisoxazolines **3.22** and **3.24** had higher T_{g}'s than their related polyisoxazoles **3.23** and **3.25**.

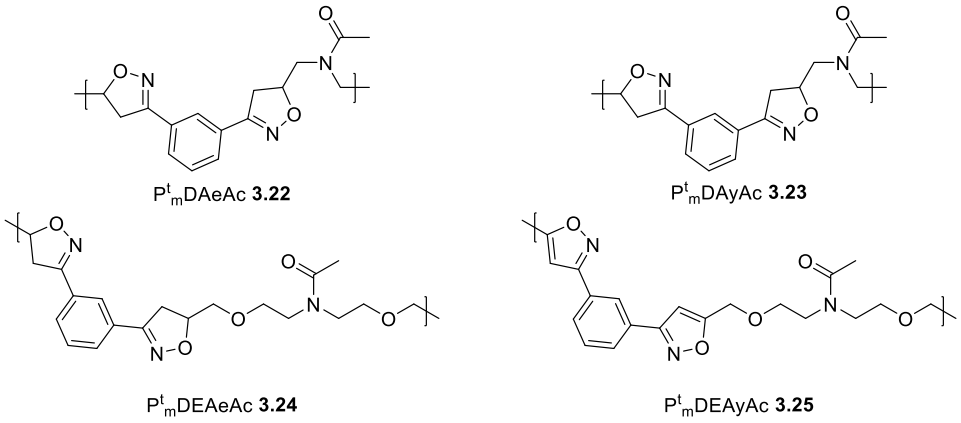

Figure 3-33: Acetamide polymers **3.22** – **3.25**.

The study of the model monomers **3.5** – **3.8** and their ability to form polymers **3.22** – **3.25** showed some important differences between the type of dipolarophilic reactive group. The smaller non-ether containing monomers **3.5** and **3.6** resulted in polymers **3.22** and **3.23** with lower yields and less repeat units. They did however have significantly higher glass transition temperatures. The ether containing monomers **3.7** and **3.8** gave polymers **3.24** and **3.25** with higher yields and more repeat units on average. Polyisoxazolines **3.22** and **3.24** were less thermally stable than polyisoxazoles **3.23** and **3.25** but had higher glass transition temperatures. These

polymers were all formed using Takata's[318,330] thermal polymerisation method and whilst polymers were formed, the molecular weights estimated by GPC were an inflation of the real molecular weight. The polymers were therefore terminating at low numbers of repeat units using Takata's[318,330] method, it was believed that this method could be improved upon to form higher molecular weight polyisoxazoles and polyisoxazolines.

4.0 Optimisation of polymerisation conditions

4.1 Introduction

The field of "click" polymers has focused heavily on polytriazoles formed *via* 1,3-dipolar cycloadditions between azides and alkynes.[233,234,243,244,247,320] The analogous 1,3-dipolar cycloaddition between nitrile oxides and unsaturated carbons has received far less attention, with limited evidence of polyisoxazoles and polyisoxazolines[254,257] in the literature. Polymers formed in this work so far (chapters 2 and 3) followed the procedure published by Takata *et al*[317] but only achieved low molecular weights.

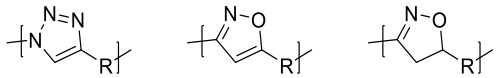

Figure 4-1: Polymers formed by 1,3-dipolar cycloadditions

4.1.1 Nitrile oxide – alkyne cycloadditions

Whilst polymers formed by nitrile oxide-dipolarophile cycloadditions are rare, they are used significantly in the field of small molecule synthesis and as such there has not been a strong focus on increasing yields and limiting side reactions as purification could always be performed. Most literature examples do not record yields over 90 % or use a significant excess of dipolarphile compared to nitrile oxide precursor. This is not acceptable for step-growth polymerisation. Nitrile oxide cycloadditions have been carried out under a range of conditions; the different methods are generally focused on novel methods for nitrile oxide generation. Three main themes appear; base promoted, metal-catalysed, and thermally promoted.[295,341–354] These methods are used separately and in combination.

4.2 Aims and Objectives

Polymers were formed in chapters 2 and 3 following Takata's[317] polymerisation method. Whilst successful the polymers did have low molecular weights, possibly caused by back-biting of the chain or nitrile oxide side reactions lowering the stoichiometry of reagents. There was also some evidence of unreacted oximoyl chloride monomer in the ^{1}H NMR of some polymers.

Using DEAyAc **3.8** and a mono-functional oximoyl chloride **4.1**, cycloaddition reaction conditions will be studied and optimised to achieve a higher conversion of alkyne to isoxazoles. The optimised conditions will then be applied to polymerisation reactions in an attempt to increase polymer growth compared with the method used in previous chapters.

- Synthesise and characterise hydroxybenzimidoyl chloride **4.1** (benz-OC).
- Investigate the 1,3-dipolar cycloaddition reaction between benz-OC **4.1** and DEAyAc **3.8**, characterising the products and by-products.
- Optimise the cycloaddition between a DEAyAc **3.8** and benz-OC **4.1**.
- Trial the most successful method for polymer synthesis and compare it to the method used in chapters 2 and 3.

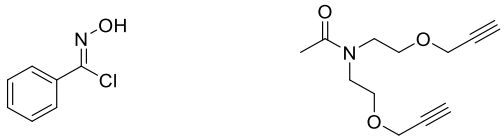

Benz-OC **4.1** DEAyAc **3.8**

Figure 4-2: Small molecules used in optimisation study.

4.3 Synthesis of monofunctional oximoyl chloride **4.1**.

For the optimisation studies, a simple monofunctional nitrile oxide precursor **4.1** was derived from benzaldehyde **4.2**. To form benz-OC **4.1**, benzaldehyde **4.2** was dispersed in ethanol and water with sodium acetate and hydroxylamine hydrochloride for 30 minutes. The mixture was taken up in EtOAc, washed, dried and purified through a silica plug to give benzaldoxime (benz-O) **4.3** as a white solid, 60 %. This white solid **4.3** was dispersed in DMF with NCS for 2 hours after which it was quenched with water and extracted with EtOAc. The organic extraction was washed repeatedly with water, dried and reduced *in vac*uo leaving a crude solid. Purification *via* column chromatography resulting in a cream solid, with a yield of 73 %.

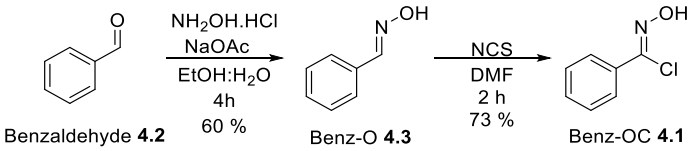

Scheme 4-1: synthesis pathway to form benz-OC **4.1**.

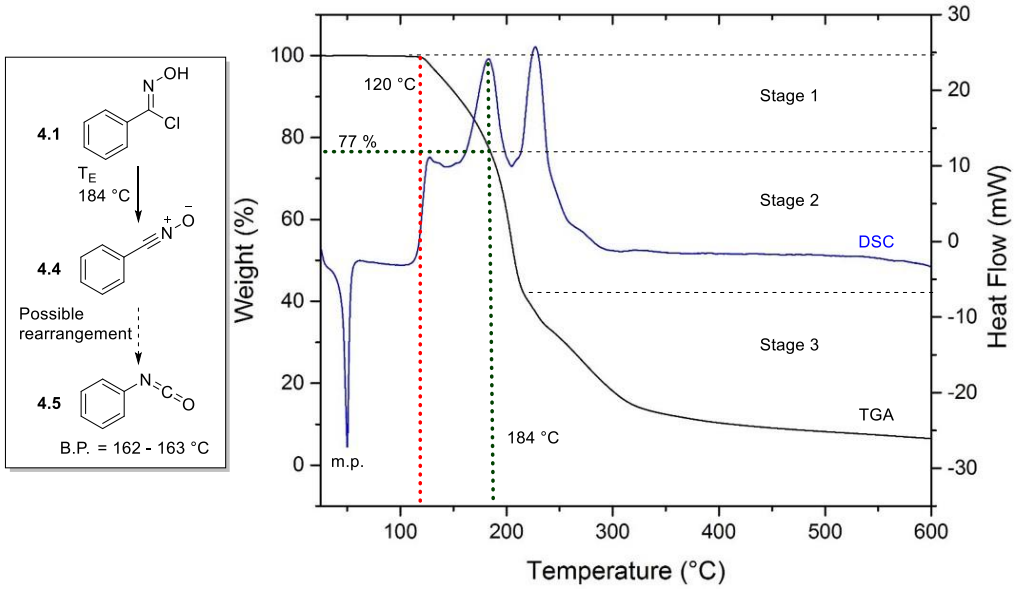

Figure 4-3: Thermal decomposition of *benz*-OC **4.1** to *meta*-NO **4.4** and possible subsequent rearrangement to phenyl isocyanate **4.5** (*left*); Thermal degradation of *meta*-OC **4.1** (– TGA, – DSC) carried out at a heating rate of 10 °C min^{-1} under a N_2 atmosphere (*right*).

Characterisation of benz-O **4.3** and benz-OC **4.1** using data gathered by 500 MHz ^1H and ^{13}C NMR, melting point, mass spectroscopy and infrared spectroscopy matched literature data.[355,356] Thermal analysis of benz-OC **4.1** using TGA (Figure 4-3) reveals very gradual mass loss begins above 90 °C but it is not until 120 °C that the weight obviously begins to drop (T_1 = 123 °C). Like *meta*-OC **2.1** (section 2.3.2), the

temperature at which benz-OC **4.1** was completely converted to nitrile oxide **4.4** (T_E) was determined by weight loss. Complete conversion of benz-OC **4.1** to **4.4** was expected to cause a 23 % weight loss. Using the TGA plot (Figure 4-3) the T_E of benz-OC **4.1** was found to be 184 °C, which aligned with the first DSC peak (stage 1, Figure 4-3). Weight loss continues past this point (stage 2, Figure 4-3), this may be caused by thermally driven nitrile oxide rearrangement, leading to the formation and subsequent evaporation of phenyl isocyanate **4.5**[261] which has a boiling point of 165 °C.[357] The second DSC peak relates to the third stage of mass loss (stage 3, Figure 4-3) which may have been caused by furoxan thermolysis (diphenyl furoxan **2.18** thermolysis reported at 250 °C)[265] and subsequent evaporation.

The initial temperature of degradation supplied by TGA (gradual mass loss above 90 °C) is in agreement with studies in deuterated DMF. Benz-OC **4.1** was suspended in deuterated DMF and analysed by 400 MHz ^{1}H NMR spectroscopy, initially at room temperature. The temperature of the solution was then raised incrementally by 10 °C for an hour at a time. It was not until the solution spent an hour at 100 °C that any change was evident in the ^{1}H NMR spectrum. The new peak was barely perceptible, temperature was increased to 110 °C to push the degradation to completion. Decomposition of benz-OC **4.1** was slow at 110 °C, taking 4 days to reach complete decomposition.

4.4 Conversion investigation using Takata's thermal method

Compounds formed in the optimisation investigation will be referred to using the following nomenclature. When DEAyAc **3.8** has been capped by one isoxazole group it will be referred to as once capped DEAyAc (OCAc) **4.6**, when it has been capped twice it will be referred to diisoxazole acetamide (DIAc) **4.7** (Figure 4-4).

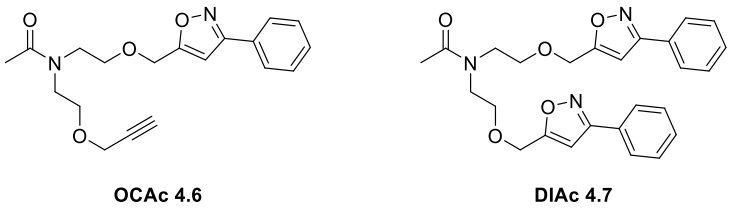

Figure 4-4: DEAyAc **3.8** cycloaddition products of the optimisation reaction, OCAc **4.6** and DIAc **4.7**.

Reaction progress was determined by comparing peak intensities in proton NMR spectra. Integrations of the chemical shifts caused by the isoxazole group (H^b, Figure 4-5, 6.5 ppm) and the terminal alkyne (H^d, Figure 4-5, 2.4 ppm) were compared and presented as a percent of conversion to isoxazole. The conversion was corroborated using the shift of the CH_2 next to the isoxazole (H^a, Figure 4-5, 4.6 ppm) and the peak at 4.1 ppm caused by the CH_2 proximal to the alkyne (H^c, Figure 4-5). Mass spectroscopy was used to establish whether residual alkyne peaks related to OCAc **4.6** only or also unreacted DEAyAc **3.8**.

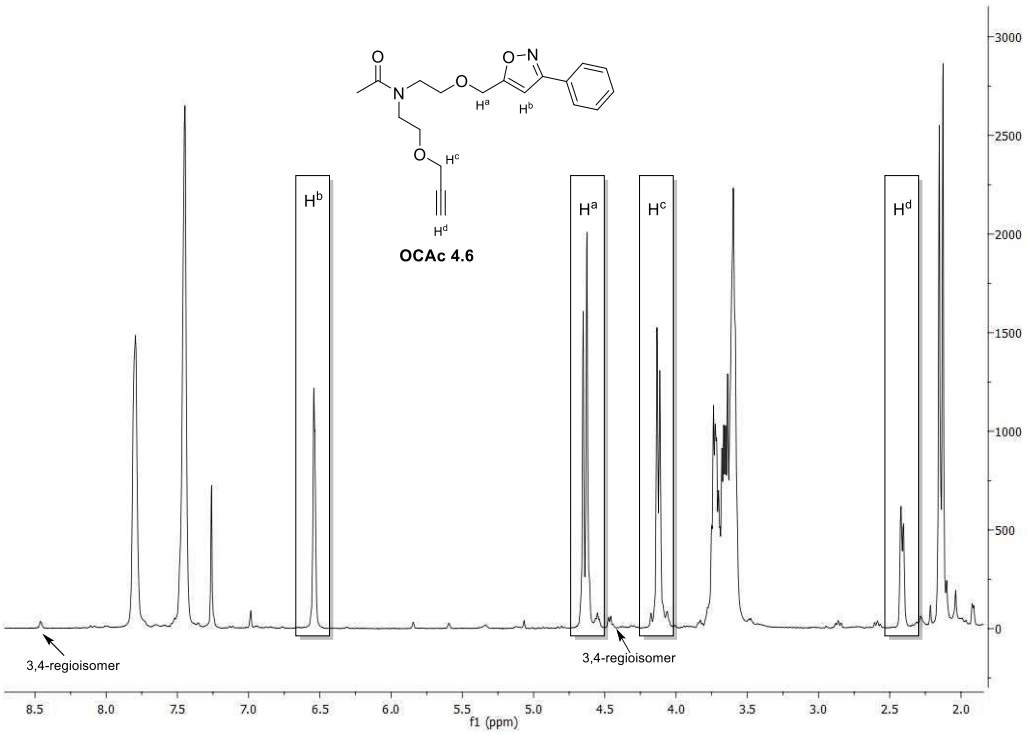

Figure 4-5: ^1H NMR spectrum of OCAc **4.6** showing different alkyne and isoxazole environments.

As with the formation of isoxazoles in chapter 3, cycloadditions were not entirely regioselective, small peaks at 8.45 ppm and 4.50 ppm (Figure 4-5) related to the minor 3,4-isoxazoles regioisomer (Figure 4-6). It is the minor product by a large margin, forming at less than 4% of the total isoxazole.

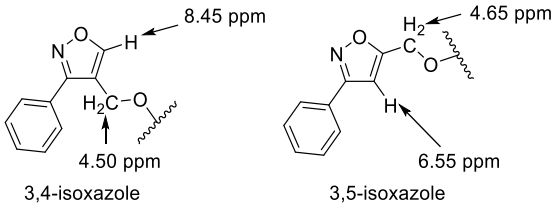

Figure 4-6: Isoxazole regioisomers of benzonitrile-*N*-oxide **4.1** / DEAyAc **3.8** cycloaddition products.

4.4.1 Setting a baseline for the optimisation investigation method

A baseline for the investigation into isoxazole synthesis was set by following Takata's molecular sieve based method of polymerisation.[317] DEAyAc **3.8** and two equivalents of benz-OC **4.1** were dispersed in DMF with 4 Å MS. To determine the rate at which this reaction progressed, samples were taken, and conversion examined with ^{1}H NMR. The reaction was initially left at room temperature for 1 hour and a sample taken to determine if the reaction occurred without heat. Following this the temperature was raised to 80 °C. Samples were taken once an hour for 6 hours and the reaction was quenched after 24 hours at 80 °C. To remove DMF for ^{1}H NMR analysis the samples and final reaction mixture were poured into water and extracted with multiple washes of $CHCl_3$. The organic layers were combined, dried, and reduced *in vacuo* to leave a crude mixture of compounds which were analysed by ^{1}H NMR.

Monitoring the reaction revealed that nitrile oxide formation and subsequent cycloaddition occured at room temperature (32 % conversion, Figure 4-7). After 3 hours at 80 °C (81 % conversion, Figure 4-7) the reaction seemed to be reaching its furthest extent, with little increase in isoxazole formation between this sample and that taken after 6 hours, (3 hr 80 ºC and 6 hr 80 ºC, Figure 4-7, $\Delta_{conv.}$ = 3%). After 6 hours at 80 ºC there was however still a small peak above 10 ppm associated with the wandering OH environment of the oximoyl chloride **4.1** (Figure 4-8). This peak can be seen to move between 8.5 ppm and 11 ppm in different samples as it concentration changes. After 24 hours the conversion of alkyne to isoxazole was at 89 % and the OH

peak was no longer visible indicating complete decomposition of the oximoyl chloride **4.1**, which led to the optimisation experiments being run for 24 hours.

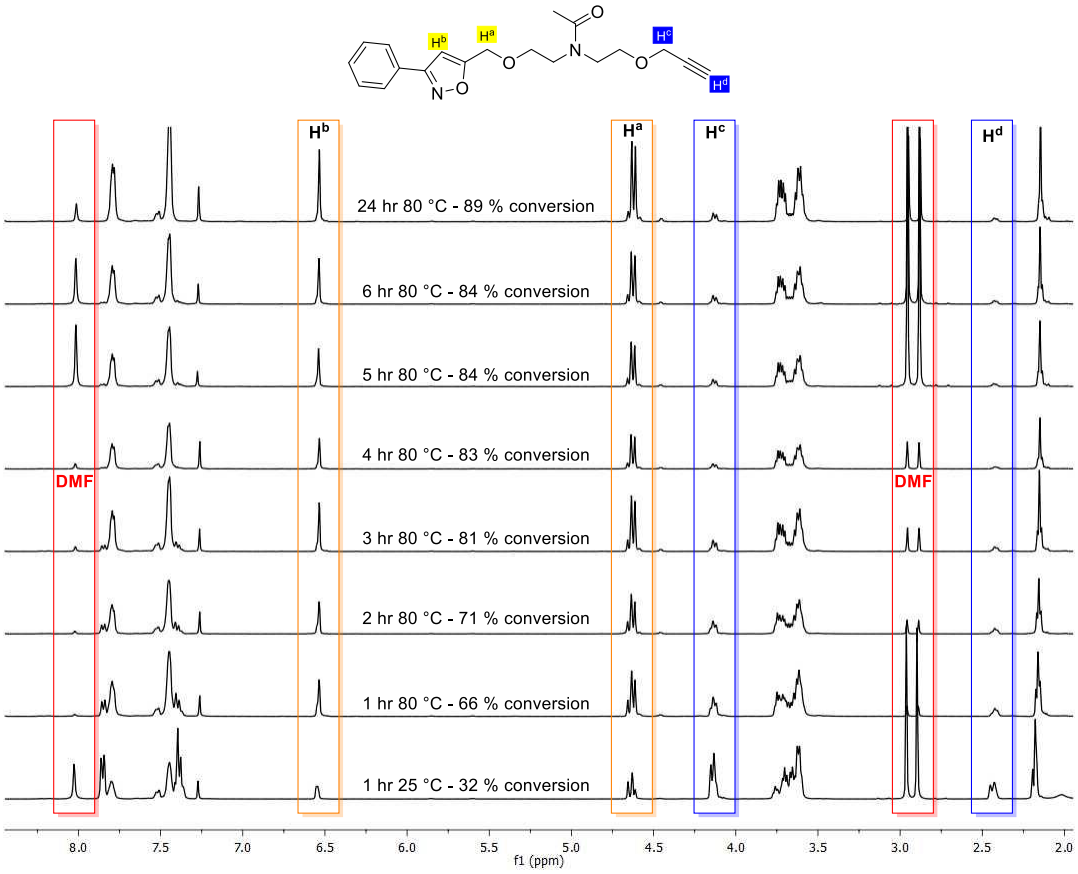

Figure 4-7: ^{1}H NMR spectra of samples taken during the baseline study for the optimisation investigation

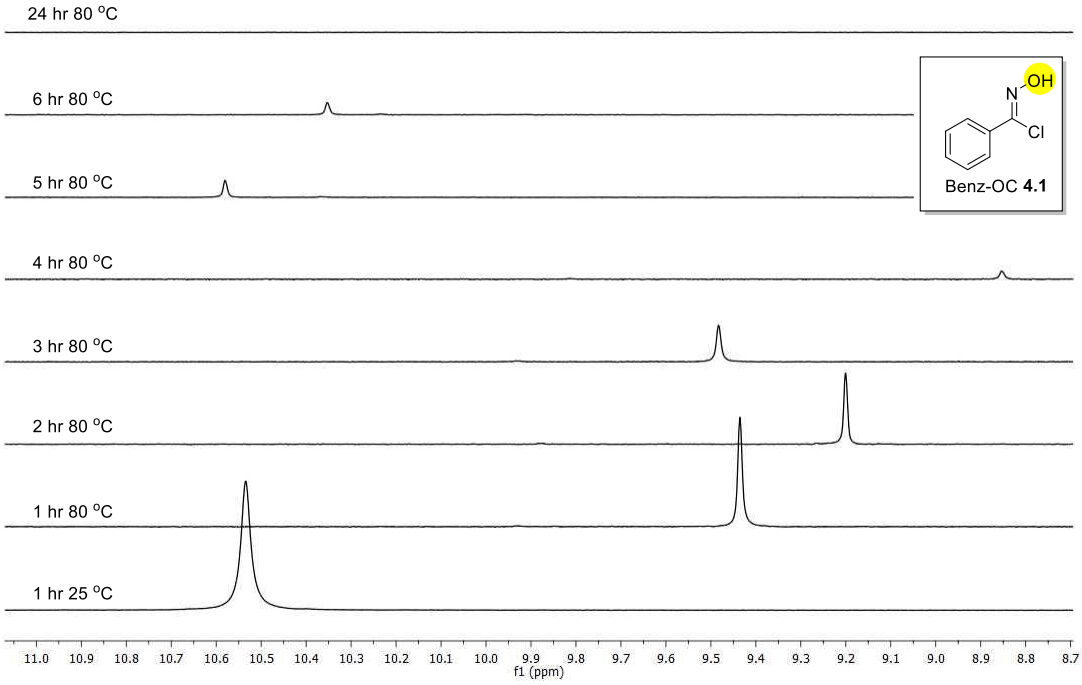

Figure 4-8: Chemical shift of benz-OC **4.1** hydroxy group in different samples.

The crude product recovered after 24 hours at 80 ºC contained a mixture of compounds. DEAyAc **3.8** had undergone cycloaddition once or twice with benz-OC **4.1**, giving OCAc **4.6** and DIAc **4.7** respectively. Mass spectroscopy indicated no residual DEAyAc **3.8**. Separating the crude mixture *via* column chromatography revealed diphenyl furoxan **2.18** as the major by-product (6 % recovered from column). As expected dimerisation was therefore the major side reaction of benzonitrile oxide **4.4** (Figure 4-9).

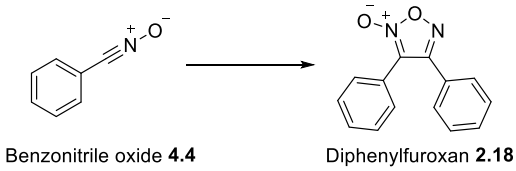

Figure 4-9: Benzonitrile oxide **4.4** dimerisation to form diphenylfuroxan **2.18**.

Thermal analysis of isolated DIAc **4.7** by TGA showed increased thermal stability compared to DEAyAc **3.8** (ΔT_{10} = 32 ºC, Figure 4-10). By comparing DIAc **4.7** to diphenylfuroxan **2.18** thermal analysis also indicated that the isoxazole ring is more thermally stable than the furoxan ring (ΔT_{10} = 45 ºC, Figure 4-10). This difference in decomposition may allow identification of furoxan links in the polymers if they are

present. It may have also been the cause for the lower thermal stability of the polymers in chapter 3 compared to their oligomers.

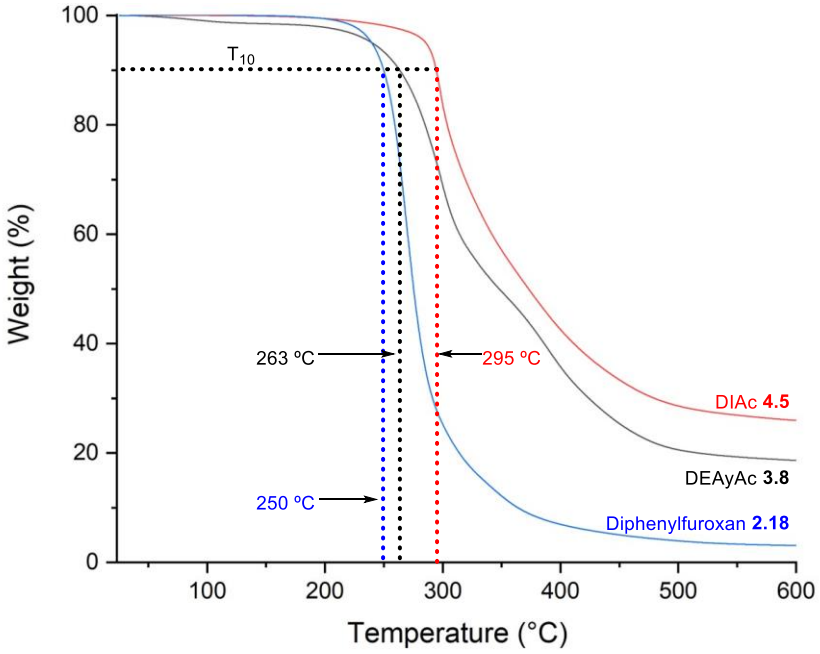

Figure 4-10: TGA analysis of DEAyAc **3.8**, DIAc 4.7 and diphenylfuroxan 2.18

During the initial investigation and the optimisation study the samples and reactions were quenched with water and then extracted to remove DMF for ^{1}H NMR analysis. As the calculated conversions were dependent on comparison between environments in DEAyAc **3.8**, OCAc **4.6** and DIAc **4.7** the compounds were tested for their water solubility. Pure samples of the **3.8** and **4.7** were separately dissolved in DMF and introduced to water. The water was then extracted with multiple washes of $CHCl_3$ which were combined. Unlike with the regular work up, the combined organic phases were washed extensively with water to remove DMF, then dried thoroughly. The recovered yield for both compounds was 98 %, mass loss was more likely to have been caused during transfer between vessels as opposed to compound water solubility.

4.5 Optimisation of 1,3-dipolar nitrile oxide cycloadditions

For the optimisation reactions DEAyAc **3.8** and two equivalents of benz-OC **4.1** were dispersed in a solvent with an additive for 24 hours. To ensure that alkyne to isoxazole conversions calculated from ^{1}H NMR analysis were reproducible the baseline reaction (DMF, 4 Å MS, 80 ºC) was done in triplicate. The reactions reached 87.2 %, 86.7 %, and 87.7 % conversion, averaging at 87.2 % with a standard deviation of 0.49. The narrow standard deviation indicated high reproducibility for these reactions, allowing confidence in the conversions calculated for other cycloaddition methods.

4.5.1 Cycloaddition method trial

Using the DEAyAc **3.8** and benz-OC **4.1** a range of nitrile oxide-alkyne cycloaddition methods were trialled, including a solvent and additive free method (1b, Table 4-1) and a more environmentally benign solvent based method (1e, Table 4-1). Literature methods generally used a significant excess of either alkyne or oximoyl chloride followed by purification.[295,341–354] As stoichiometric equivalents of these functional groups were used in this study most literature methods seemed unsuitable. Copper catalysed methods, (similar to the polymerisation method employed by Li and Cheng),[312] were shown be successful in the literature.[352] A copper catalysed method was therefore trialled, however it resulted in a low isoxazole conversion (1c, Table 4-1). Another more environmentally benign method was trialled in water using Oxone and KCl (1d, Table 4-1), this had the benefit of using the oxime **4.3** rather than oximoyl chloride **4.1**, unfortunately it only had a moderate yield which would not be applicable to step-growth polymerisation. From this initial examination it was evident that 4 Å MS method (1a, Table 4-1) used in chapters 2 and 3 was the most promising route to optimise.

Entry	Solvent	Temperature / °C	Additive	Conversion / %
1a	DMF	80	4 Å MS	87
1b	–	80	–	55
1c	DMF:Water 1:1	40	copper (II) sulphate / sodium ascorbate[312]	57
1d[a]	Water	25	Oxone© / KCl[349]	68
1e	Acetone:Water 1:1	25	NaOH	23

a-oxime **4.3** was used rather than benz-oc **4.1**.

Table 4-1: Conditions used to trial methods of nitrile oxide-alkyne cycloaddition .

4.5.2 Investigation of the molecular sieve method

As the most successful method from the initial trial, optimisations were carried out on thermally promoted method of using DMF and 4 Å MS as a basic additive. From the sampled reaction in section 1.4, cycloaddition was known to occur at room temperature. A range of temperatures were therefore trialled. Performing the reaction in DMF at 80 °C with 4 Å MS had already given an average conversion of 87 % (2b, Table 4-2). Increasing the temperature to 100 °C reduced the conversion isoxazole slightly, albeit within experimental error (2a, Table 4-2), whilst lower temperatures, 60 ºC and 25 °C, gave unexpected results (2c & 2d, Table 4-2). Performing the reaction at 25 ºC (2d, Table 4-2) gave a lower conversion than the heated reactions (2a & 2b, Table 4-2). The lowest conversion however was found at 60 °C (2c, Table 4-2), where mass spectroscopy detected significant residual DEAyAc **3.8**. High conversion at 25 ºC was believed to have been due to slow dehalogenation of benz-OC **4.1**, which reduced nitrile oxide dimerisation as less nitrile oxide was present in the reaction at one time. Furthermore at 25 °C competing nitrile oxide side reactions, such as dimerisation, are known to be slow or may not occur at all.

Entry	Solvent	Temperature / °C	Additive	Conversion / %
2a	DMF	100	4 Å MS	86
2b[a]	DMF	80	4 Å MS	87
2c	DMF	60	4 Å MS	80
2d	DMF	25	4 Å MS	85

a-1a Table 4-1

Table 4-2: Molecular sieve (4 Å) method trialled over a range of temperature

The 4 Å molecular sieves were next investigated to determine how they were affecting the reaction. Removing any additive from the reaction led to a low conversion (38 %, 3a, Table 4-3), even at 100 ºC, the temperature at which benz-OC **4.1** degrades in DMF (section 1.3). To understand whether it was the drying effect or basicity of the 4 Å MS that promoted formation of DIAc **4.7**, cycloadditions were carried out in the presence of $MgSO_4$, TEA and a combination of them both, (3b-e, Table 4-3). Conversions were low compared to the 4 Å MS themselves (Table 4-2). TEA was trialled at 80 ºC and 25 ºC to determine if conversion could be increased by reducing the rate of side reactions whilst using a stronger base to promote oximoyl chloride decomposition. The conversion at 25 ºC (63 %, 3d, Table 4-3) was lower than at 80 ºC (67 %, 3c,

Table 4-3). A reduction in temperature would slow isoxazole formation as well as the side reactions, TEA therefore may have been too strong a base and caused a high concentration of nitrile oxide that dimerised to form furoxans. The highest conversion was achieved with the combination of $MgSO_4$ and TEA (71 %, 3e, Table 4-3) but this was still lower than for just 4 Å MS.

Entry	Solvent	Temperature / °C	Additive	Conversion / %
3a	DMF	100	–	38
3b	DMF	80	$MgSO_4$	66
3c	DMF	80	TEA	67
3d	DMF	25	TEA	63
3e	DMF	80	$MgSO_4$ / TEA	71

Table 4-3: Conditions used to investigate the effect of molecular sieves on nitrile oxide-alkyne cycloaddition

Molecular sieve pore size was next investigated. Using 3 Å MS at 80 ºC was found to be effective, giving a higher conversion of 89% (4a, Table 4-4). Molecular sieves are made from alumina, silica, and metal oxides in a ratio of 2 : 1 : 1, the alumina and metal oxides outweigh the silica giving molecular sieves slightly basic characteristics. The difference between 4 Å and 3 Å molecular sieves derives from the metal oxides used, 4 Å MS contain Na_2O exclusively whereas 3 Å MS contain K_2O and Na_2O at a 2 : 1 ratio. To determine if it was the pore size or chemical differences that caused a higher conversion with 3 Å MS, reactions were carried out using the components of the two types of molecular sieves rather than the sieves themselves (4b & 4c, Table 4-4). This was performed using KOH and NaOH in the place of KO and NaO. Although not as effective as 3 Å MS themselves, the 3 Å MS model (83 %, 4c, Table 4-4) was more effective than the 4 Å MS model (75 %, 4b, Table 4-4). KOH (pK_b = -0.7) is marginally more basic than NaOH (pK_b = -0.6), this slight difference in basicity could be the cause of the better conversion with 3 Å MS.

	Solvent	Temperature / °C	Additive	Conversion / %
4a	DMF	80	3 Å MS	89
4b	DMF	80	4 Å MS Model	75
4c	DMF	80	3 Å MS Model	83
4d	DMF	25	3 Å MS	96

Table 4-4: Investigation into the use of different molecular sieves

The 4 Å MS resulted in a high conversion at 25 ºC as the rate of oximoyl chloride decomposition and nitrile oxide side reactions were limited. As 3 Å MS are slightly

more basic than 4 Å MS, without being as basic as TEA, they were trialled at 25 ºC. It was believed 3 Å MS would marginally increasing oximoyl chloride decomposition without effecting the rate of side reactions. This resulted in an extremely high alkyne to isoxazole conversion of 96 % (4d, Table 4-4). Replication in triplicate to ensure its accuracy resulted in an average conversion of 95.3 % with a standard deviation of 1.8.

4.5.3 Solvent trials with 3 Å molecular sieves

As it appeared 3 Å MS produced the highest conversion, conditions and solvents were next tested using them as the basic additive. The reaction was tested in a range of common solvents at 80 °C and 25 ºC. Conversion of alkyne to isoxazole in other solvents was poor at 80 ºC (5a-e, Table 4-5) when compared to DMF (5f, Table 4-5), with chloroform and THF achieving the highest conversion at 84 % (5b & 5e, Table 4-5). At 25 ºC (5g-k, Table 4-5) conversion improved for all solvents except EtOAc (5g, Table 4-5), which suggests the low conversions in EtOAc was due to low reactivity rather than nitrile oxide side reactions. It improved dramatically for chloroform and EtOH resulting in a conversion of 93 % and 94 % respectively (5h & 5i, Table 4-5). The high conversion in EtOH is encouraging for green applications.

	Solvent	Temperature / ºC	Additive	Conversion / %
5a	EtOAc	80	3 Å MS	71
5b	$CHCl_3$	80	3 Å MS	84
5c	EtOH	80	3 Å MS	79
5d	Acetone	80	3 Å MS	78
5e	THF	80	3 Å MS	84
5f[a]	DMF	80	3 Å MS	89
5g	EtOAc	25	3 Å MS	47
5h	$CHCl_3$	25	3 Å MS	93
5i	EtOH	25	3 Å MS	94
5j	Acetone	25	3 Å MS	89
5k	THF	25	3 Å MS	90
5l	DMF	25	3 Å MS	95[b]

a-4a Table 4.4, b-average of reaction done in triplicate

Table 4-5: Conditions used to investigate the solvent effect on 3 Å MS mediated NOAC.

4.6 Trialling the optimised conditions for polymerisation

From the optimisation studies it was evident that the use of 3 Å MS in DMF at room temperature gave the highest conversion of alkyne to isoxazole and so were considered the optimised conditions. Chloroform and ethanol afforded similar conversions, however as previous literature has reported on solubility issues with polyisoxazoles,[317] DMF was used in the trial polymerisations.

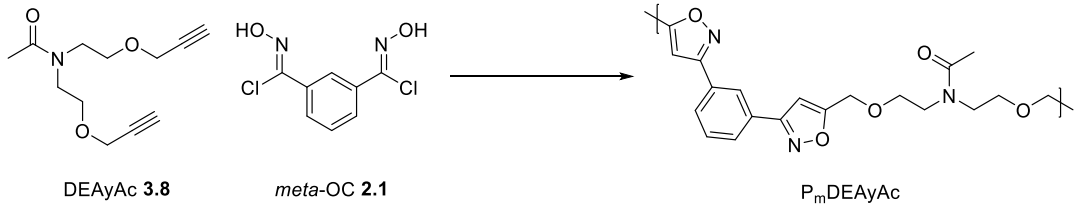

Figure 4-11: Polyisoxazole formed from DEAyAc **3.8** and *meta*-OC **2.1**

Polyisoxazoles were formed using DEAyAc **3.8** and the nitrile oxide precursor from previous chapters (*meta*-OC **2.1**). To determine whether the optimisation of the small molecule coupling translated to an optimisation of the polymerisation method, polymers were formed using the thermal method[317] (P^t), (used in chapters 2 and 3), and the optimised method (P^o). Polymer nomenclature will follow the same rules as in chapters 2 and 3. Where samples have been analysed, the number of hours at which the sample was taken follows the dipolarophilic monomer. Thus P^o_mDEAyAc-24 would refer to a sample of polymer formed using the "optimised" conditions taken after 24 hours.

4.6.1 Sampled "optimised" polymerisation trial

Molar equivalents of DEAyAc **3.8** and *meta*-OC **2.1** were dispersed in DMF (0.5 M) along with molecular sieves. The solution was either heated to 25 °C or 80 °C depending on the method. A sample of each solution was taken every 24 hours and analysed by GPC. The reactions were stopped when GPC did not record an increase in polymer size from the last sample.

Although the optimised conditions (3 Å MS, RT) worked for small molecule synthesis they did not appear to work well for polymerisations (P^o_mDEAyAc). After 14 days (P^o_mDEAyAc-336) the M_n and M_w were lower than P^t_mDEAyAc-24 and the reaction

was stopped (Table 4-6). Subsequent work, detailed in chapter 6, revealed the cause of why this difference in reactivity occurred between benz-OC **4.1** and *meta*-OC **2.1**.

	Optimised Conditions P^{o}_{m}DEAyAc			Takata's Conditions P^{t}_{m}DEAyAc		
Time / hours	M_n	M_w	*Đ*	M_n	M_w	*Đ*
24	1000	1300	1.3	2400	4100	1.7
48	1200	1500	1.3	3200	5800	1.8
72	1200	1800	1.4	3500	6500	1.9
168	1600	2200	1.4	-	-	-
240	1900	2700	1.4	-	-	-
336	2200	3100	1.4	-	-	-

Table 4-6: GPC estimations of samples taken from polymerisations using the ooptimised conditions and the original thermal conditions.

Analysis of results using Takata's thermal method (P^{t}_{m}DEAyAc, Table 4-6) provided insight into achieving higher molecular weights. It was apparent that the polymerisation method used in chapters 2 and 3 took longer than 24 hours, with a significant difference in molecular weight between P^{t}_{m}DEAyAc-24 and P^{t}_{m}DEAyAc-48 (Table 4-6). The reaction was practically complete after 48 hours with very little difference in molecular weight between P^{t}_{m}DEAyAc-48 and P^{t}_{m}DEAyAc-72 (Table 4-6). The molecular weight estimated by GPC after 48 hours (P^{t}_{m}DEAyAc-48) was lower than that given in chapter 3 after 24 hours (P^{t}_{m}DEAyAc **3.27**) as the P^{t}_{m}DEAyAc-48 sample had not been precipitated into methanol to remove low molecular weight oligomers.

4.6.2 Optimised polymerisation analysis

Polymers were once again formed using the two different methods and were worked up in the same manner as the polymers in chapter 2 and 3. P^{o}_{m}DEAyAc **4.8** was formed by dispersing molar equivalents of DEAyAc **3.8** and *meta*-OC **2.1** in DMF along with 3 Å MS at 25 ºC, then worked up after 14 days (336 hours) to leave the polymer **4.8** as a brown solid (9 %). P^{t2}_{m}DEAyAc **4.9** was formed using the same method as P^{t}_{m}DEAyAc **3.27** (chapter 3) except for being left to react for 48 hours rather than 24 hours. P^{t2}_{m}DEAyAc **4.9** was a brown solid (86 %) after drying *in vacuo*.

During the work up of polymers **4.8** and **4.9** they were precipitated into methanol in order to remove DMF. Previous work had shown that this step also removed low molecular weight oligomers. The low yield of the optimised polymer (9%, 6a, Table

4-7) indicates that few higher molecular weight chains were formed even after 14 days of polymerisation. End group analysis by proton NMR revealed that the polymeric precipitate **4.8** contained an average of 9 RU's, polymerisation was therefore achieved but with a low yield. The yield of $P^{t2}{}_m$DEAyAc **4.9** (86 %, 6b, Table 4-7) was higher than $P^{t}{}_m$DEAyAc **3.27** (78 %, 6c, Table 4-7), signifying that the longer polymerisation time reduced the number of small methanol soluble oligomers. End group analysis using the proton NMR spectrum suggested that the average chain of **4.9** also contained more repeat units than **3.27**.

Entry	Polymer	Polymerisation Time / days	Temp. / ºC	Additive	Yield / %	RU NMR
6a	$P^{o}{}_m$DEAyAc **4.8**	14	25	3 Å MS	9	9
6b	$P^{t2}{}_m$DEAyAc **4.9**	2	80	4 Å MS	86	14
6c	$P^{t}{}_m$DEAyAc **3.27**	1	80	4 Å MS	78	10

Table 4-7: Polymerisation conditions, yield and RU by ^{1}H NMR for $P^{o}{}_m$DEAyAc **4.8** and $P^{t2}{}_m$DEAyAc **4.9**

Entry	Polymer	M_n	M_w	*Đ*
7a	$P^{o}{}_m$DEAyAc **4.8**	4100	6300	1.5
7b	$P^{t2}{}_m$DEAyAc **4.9**	9100	14200	1.5
7c	$P^{t}{}_m$DEAyAc **3.27**	5900	8700	1.5

Table 4-8: GPC estimates of polymers formed from DEAyAc **3.8** and *meta*-OC **2.1** using different conditions.

GPC estimates of the polymer molecular weights were carried out in DMF against PMMA standards. The results could be directly compared, even though they were probably overestimations (section 3.5, as the polyisoxazoles had the same structure. The "optimised" conditions (**4.8**) resulted in molecular weight estimates (7a, Table 4-8, M_n = 4100, M_w = 5900) that were considerably lower than the thermally promoted method $P^{t2}{}_m$DEAyAc **4.9** (7a & 7b, Table 4-8, ΔM_n = 5000, ΔM_w = 7900). The milder "optimised" conditions also did not improve dispersity with both **4.8** and **4.9** having the same *Đ* (1.5). Furthermore, the GPC plot of $P^{o}{}_m$DEAyAc **4.8** revealed that it contained considerable amounts of the ABA oligomer **3.17** (Figure 4-12). Using the thermally promoted conditions for 48 hours (**4.9**) rather than 24 hours (**3.27**) significantly increased the molecular weight of the polymers (7b & 7c, Table 4-8, ΔM_n = 3200, ΔM_w = 5500) without effecting the dispersity (1.5).

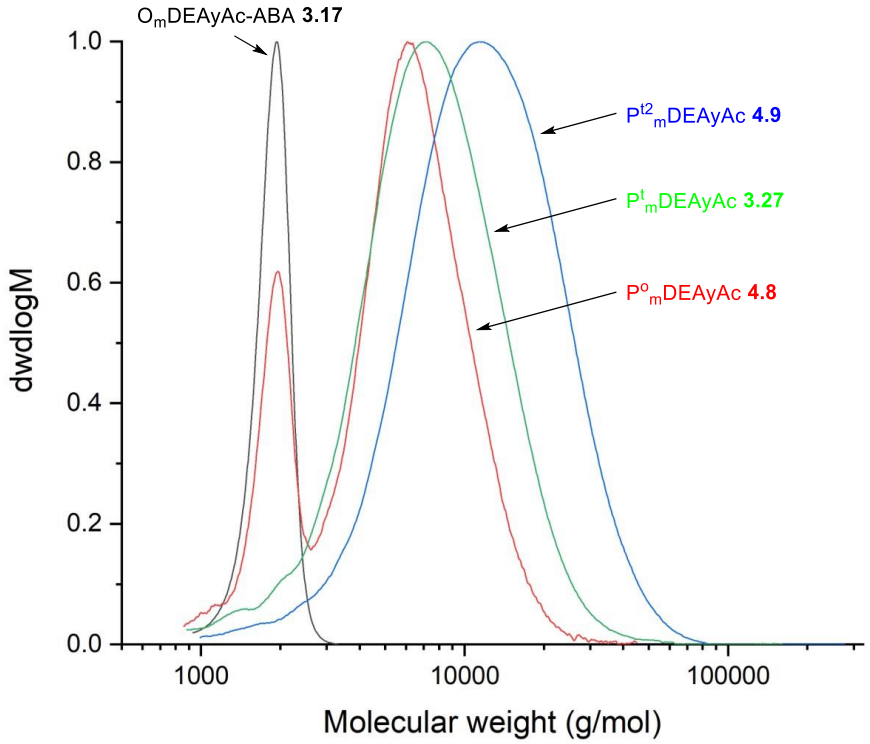

Figure 4-12: GPC estimate plots of oligomers and polymers formed from DEAyAc **3.8** by different methods.

Investigations into the molecular weight of the polyisoxazoles (**3.27**, **4.8** and **4.9**) showed large differences that depended on the method of polymerisation used. The polymers had the same structure however which gave an opportunity to investigate how molecular weight effected the thermal properties of polyisoxazoles. To achieve this glass transition temperatures (T_g) and thermal stability were analysed using DSC and TGA respectively. Analysis of the polymers revealed that the thermal properties of polyisoxazoles are not strongly affected by molecular weight. Polymer thermal stability and T_g hardly changed between **4.8** and **4.9** (8a & 8b, Table 4-9, ΔT_g = +1 ºC, ΔT_5 = -7 ºC, ΔT_{20} = +3 ºC) even though **4.9** had much higher molecular weight chains (8a & 8b, Table 4-8, ΔM_n = 5000, ΔM_w = 7900). Thermal properties of **3.27** and **4.9** were also practically identical (8b & 8c, Table 4-9, ΔT_g = 0 ºC, ΔT_5 = +3 ºC, ΔT_{20} = +1 ºC).

Entry	Polymer	T_g / ºC	T_5 / ºC	T_{20} / ºC
8a	P^{o}_{m}DEAyAc **4.8**	50	253	335
8b	P^{t2}_{m}DEAyAc **4.9**	51	246	338
8c	P^{t}_{m}DEAyAc **3.27**	51	249	339

Table 4-9: Thermal properties of P^{o}_{m}DEAyAc **4.8** and P^{t2}_{m}DEAyAc **4.9**

4.7 Summary and conclusion

Monofunctional oximoyl chloride, benz-OC **4.1**, was synthesised and used along with DEAyAc **3.8** to investigate small molecule nitrile oxide/alkyne cycloaddition reactions. The polymerisation conditions used in chapters 2 and 3 were first investigated. This gave an 86 % overall conversion of alkyne to isoxazole in 24 hours. For polymerisations, the conversion should ideally be higher and so methods of isoxazole synthesis were investigated. The use of 4 Å MS at 80 ºC in DMF was shown to be the most successful method of isoxazole synthesis from the initial study. This method was therefore examined further and optimised.

From the optimisation work it was found that the highest conversion of alkyne to isoxazole was achieved using 3 Å MS at 25 ºC in DMF. The "optimised" conditions achieved an average conversion of 95 % when performed in triplicate. It was believed that the lower temperature, but slightly more basic molecular sieves, reduced side reactions whilst maintaining a good rate of oximoyl chloride decomposition to nitrile oxide. The method was also successful in a range of other solvents with conversions of 89 % to 94 % in THF, acetone, $CHCl_3$ and EtOH. The conversion of 94 % in EtOH was encouraging for green applications of the reaction.

The "optimised" conditions were assessed as a polymerisation method (P^o). As the conditions were milder than the previous polymerisation method used in chapters 2 and 3, the rate of polymerisations was assessed using GPC and compared to the harsher previously used conditions (P^t). GPC sampling of the reaction showed that even after 14 days the molecular weight of the polymer formed using the "optimised" conditions ($P^o{}_m$DEAyAc-336) was still lower than the harsher conditions after 1 day ($P^t{}_m$DEAyAc-24). The study did however show that extending the reaction time from the harsher conditions from chapters 2 and 3 was advantageous.

Polymers were made using the original conditions but over 48 hours ($P^{t2}{}_m$DEAyAc **4.9**) and compared to $P^t{}_m$DEAyAc **3.27** from chapter 3. Analysis showed a large increase in molecular weight between **4.9** and **3.27**, but no change in dispersity. Thermal analysis also revealed that thermal stability and glass transition temperature were not strongly affected by molecular weight. The "optimised" conditions were also

used to form a polymer over 14 days (P^{o}_{m}DEAyAc **4.8**), work up of the polymer by precipitation into methanol returned a low yield of a low molecular weight polymer.

Although the 'optimised' conditions for small molecule synthesis were not successful for polymer synthesis a method of increasing polyisoxazole molecular weight was determined. Consequently, in the work moving forwards polymerisations were undertaken using the same conditions as chapter 2 and 3 however over 48 hours rather than 24 hours.

5.0 Fatty acid derived polymers

5.1 Introduction

A variety of dipolarophilic monomers were examined in chapter 3 to determine how to best design monomers derived from vegetable oil feedstocks. It was found that either monomers DEAeAc **3.7** and DEAyAc **3.8** (Figure 5-1) resulted in polymers with higher yields and molecular weights but lower glass transition temperatures than DAeAc **3.5** and DAyAc **3.6** (Figure 5-1). The work also indicated that dialkene monomers **3.5** and **3.7** (Figure 5-1) led to more cyclical or furoxan containing polymer chains than the dialkyne monomers **3.6** and **3.8** (Figure 5-1). DEAyAc **3.8** was determined to be the best acetamide dipolarophilic monomer for nitrile-oxide/dipolarophile cycloaddition polymerisation, whilst DAeAc **3.5** was found to produce polymers with the highest glass transition temperature. Polymerisation conditions used in chapters 2 and 3 were then investigated and improved in chapter 4.

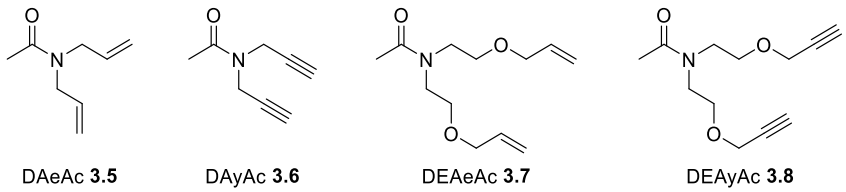

Figure 5-1: Acetamide monomers used for polymerisation study in chapter 3

5.1.1 Vegetable oils

Vegetable oils are mostly made up of triglycerides, which are an ester of glycerol and fatty acid chains (Figure 5-2). The fatty acid component varies between plant species, season and growing condition, changes in the fatty acid chain significantly affect the chemical and physical properties of the vegetable oil.[139,140] They predominantly contain medium length fatty acid chains with limited levels of unsaturation (Figure 5-2).[143] Triglycerides, particularly those with unsaturated fatty chains, have multiple functionalities that can be used for chemical modification. The ester groups have been widely exploited, with hydrolysis and transesterification being extensively used to form industrially important products.[177,178]

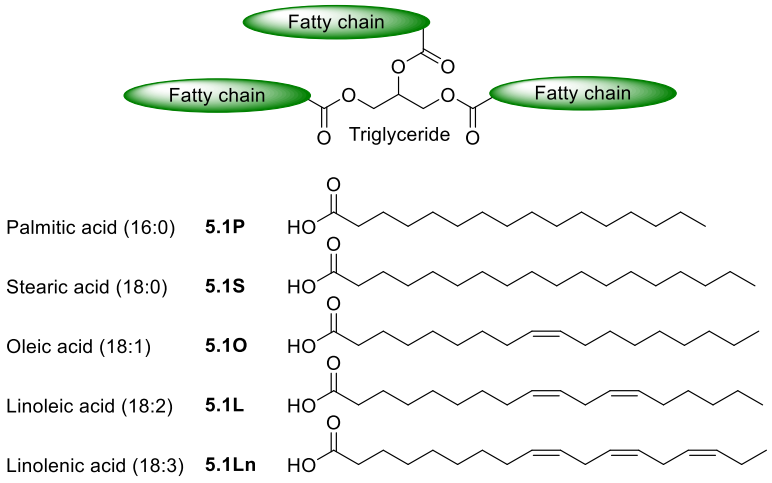

Figure 5-2: Triglyceride structure (*above*) five most common fatty acids in vegetable oils (*below*)

Amides can also be formed from triglycerides by aminolysis of the ester, this has been mediated by sodium methoxide, enzymes, or microwave irradiation.[193,195–200] Aminolysis is often carried using mono- and diethanolamine.[201] The resulting diol derived fatty amides have an amphiphilic nature and are important surface activating agents.[202] They also have analgesic, anti-inflammatory, anticonvulsant, and anti-depressant properties.[203] The inclusion of hydroxyl groups allows for further modification, a route that has been used in the formation of polymers from vegetable oil derivatives. Palanisamy *et al.* forming water-blown polyurethane foams from castor oil.[208,209]

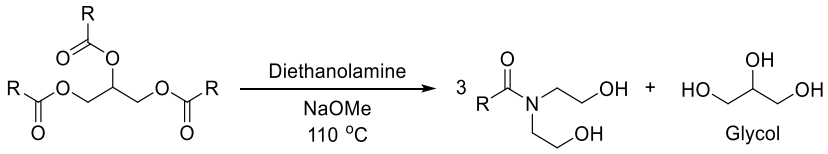

Scheme 5-1: Aminolysis of a triglyceride with diethanolamine

5.1.2 Reductive cleavage of isoxazole rings

The ability to functionalise isoxazole and isoxazoline rings is well established. The heterocyclic rings themselves are weakly basic[275] and resilient to strong acids.[217] Isoxazoles are stable under oxidation reactions whilst isoxazoline rings are resilient to oxidation by peracids[277] but can be dehydrogenated to form isoxazoles.[217] Isoxazole rings can undergo electrophilic aromatic substitution reactions to further functionalise the ring, whilst the α proton at C_5 (Figure 5-3) is slightly acidic and has been exploited in substitution reactions.[217] Most importantly however the heterocycles can be

selectively ring opened by reductive cleavage to produce a range of exposed functional groups[278–293] which could be exploited for post polymerisation modification.

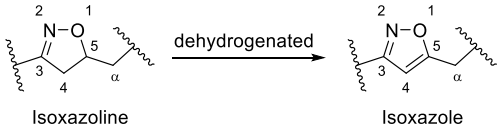

Figure 5-3: Isoxazole and isoxazoline rings (numbered)

Using reductive cleavage Takata *et al.* performed post polymerisation modifications on polyisoxazoles.[318] After an initial trial of reagents, polyisoxazoles were ring opened using iron and $LiAlH_4$ based reductive cleavage methods (Figure 5-4). The $LiAlH_4$ method contradicts many literature examples which report that $LiAlH_4$ produces aziridines (Figure 5-4) from isoxazoles[278] not β-amino alcohols. Takata *et al.*[318] went on to crosslink the poly(β-amino alcohol)s using dialdehydes and diisocyanates.

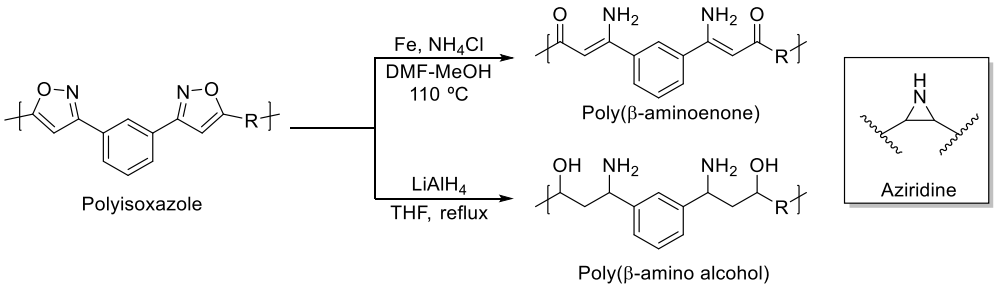

Figure 5-4: Reductive cleavage of polyisoxazoles by Takata *et al.*[318] (*left*), aziridine ring (*right*)

5.2 Aims and objectives

Dipolarophilic monomers were derived from free fatty acids, a renewable feedstock. Different dipolarophilic groups were shown to affect polymerisation and polymer properties in chapter 3. The ether containing dialkyne group (DEAyR) **5.2** was determined to result in the highest polymerisation yields and so was introduced to the fatty acids. The fatty acid chain was expected to reduce glass transition temperature relative to the acetamide polymers in chapter 3, dialkene (DAeR) fatty amide monomers **5.3** were therefore also studied as this group resulted in the highest T_g in polymers in chapter 3. The alkene functionality in the side-chain of some fatty acid derivatives may compete in cycloaddition to the desired alkene and alkyne reaction points. Crosslinking through the *cis* alkene in the monomers derived from these unsaturated fatty acids was also explored, using ether containing dialkene (DEAeR) fatty amide monomers **5.4** for comparison with the DEAyR monomers **5.2**. Post polymerisation modification was investigated with attempts to ring open isoxazoles using the methods employed by Takata.[318]

- Five fatty acids **5.1** were used as the feedstock for the preparation of dipolarophilic monomers with the DAeR **5.3** and DEAyR **5.2** group.
- Small molecule models were formed from fatty acid derivatives and spectroscopic properties investigated.
- Fatty acid derived dialkyne (DEAyR) **5.2** and dialkene (DAeR) **5.3** monomers were used to form polymers with *meta*-OC **2.1**.
- Dialkene monomers (DEAeR) **5.4** were formed from stearic and oleic acid.
- Stearic and oleic acid derived monomers of 5.2 – 5.4 were used to investigate the effect of potential crosslinking in polymers derived from unsaturated fatty acids.
- Small molecule models were used to investigate isoxazole reductive cleavage for application in post polymerisation modification.

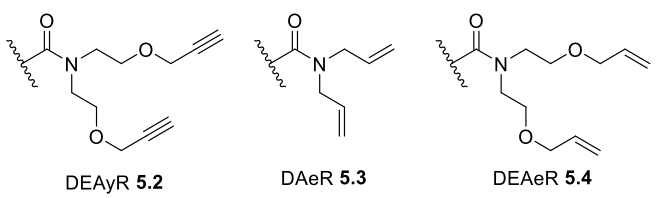

Figure 5-5: Dipolarophilic groups introduced into fatty acids for monomer preparation

5.3 Fatty acid derived monomer synthesis

Vegetable oils are primarily comprised of medium length fatty acid chains with low levels of unsaturation, these are predominantly palmitic, P (C16:0), stearic, S (C18:0), oleic, O (C18:1), linoleic, L (C18:2), and linolenic, Ln (C18:3). To increase the scope of the research, dipolarophilic monomers were derived from these five most common fatty acids (**5.1P-Ln**) found in vegetable oils rather than the triglycerides themselves. This would allow for the findings to be applied across multiple vegetable oils.

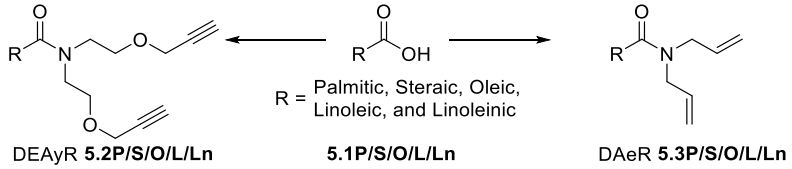

Figure 5-6: Dipolarophilic monomers derived from five fatty acids

The free fatty acids (P (C16:0), S (C18:0), O (C18:1), L (C18:2), and Ln (C18:3) **5.1P-Ln** were converted into two different dipolarophilic monomers (Figure 5-6). The ether linked alkyne group DEAyR **5.2P-Ln** (Figure 5-6) were prepared as they were shown to be the best monomers in chapters 3. The fatty acid chains of the monomers were predicted to significantly reduce glass transition temperature of the polymers relative to their acetamide counterparts in chapter 3, dialkene monomers DAeR **5.3P-Ln** (Figure 5-6) were therefore also produced as they had the highest T_g in chapter 2. The nomenclature for the monomers remained the same as in chapter 2 with the fatty acid replacing 'Ac'. Each type of compound is given an Arabic numeral followed by the fatty acid from which it was derived. DEAyS **5.2S** therefor refers to an ether linked dialkyne derived from stearic acid.

5.3.1 Synthesis of dialkyne fatty amide monomers

As with the ether containing monomers **3.7** and **3.8** in chapter 3, the fatty acid derived dialkynes were formed in two steps. First fatty amide diols **5.6** were formed followed by an alkylation to introduce the dipolarophilic groups. The amides were synthesised *via* labile (ethyl carbonic) anhydride intermediates **5.5** to allow for milder reaction conditions with the aim of reducing ester formation (Figure 5-7).

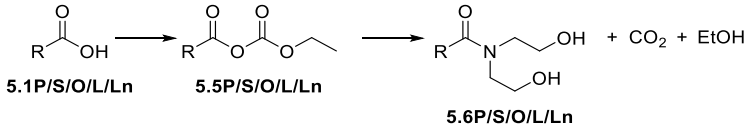

Figure 5-7: Diethanolamide synthesis from fatty acids *via* an ethyl carbonic anhydride intermediate

To form the diol compounds **5.6P-Ln**, the respective fatty acids were dissolved in solvent along with *N*-methylmorpholine and stirred in an ice bath for 5 minutes. Unsaturated fatty acids **5.1O**, **5.1L** and **5.1Ln** were soluble in THF at RT and also when cooled. Palmitic **5.1P** and stearic acid **5.1P** however were sparingly soluble in THF at RT and completely crashed out when cooled, Et_2O was therefore used as the solvent for these reactions. After 5 minutes ethyl chloroformate was added dropwise and the reaction stirred for 30 minutes. *N*-methylmorpholine hydrochloride formed as a white precipitate which could be filtered off to leave the fatty anhydride in the filtrate. Unsaturated anhydrides **5.5O**, **5.5L** and **5.5Ln** remained dissolved in THF and could be used directly for the next step. Saturated anhydrides **5.5P** and **5.5S** however partly crashed out of Et_2O, the mixtures were therefore reduced *in vacuo* to leave white solids. These solid anhydrides **5.5P** and **5.5S** were taken into $CHCl_3$ for the next step of the reaction. The anhydride solutions were added dropwise to diethanolamine and TEA in DMF. Due to the anhydride-based leaving group, amide formation was fast with the reaction being complete between 2 and 3 hours, after which it was quenched with 2 M HCl and extracted with Et_2O. The organic extract was washed with water and brine, followed by drying and reduction *in vacuo* to leave crude products. The saturated fatty amide diols were purified by recrystallisation from Et_2O to leave pure white solids (**5.6P** 55%, **5.6S** 64 %). Purification by column chromatography of the unsaturated fatty amide diols gave pure colourless oils (**5.6O** 86 %, **5.6L** 78%, **5.6Ln** 59%).

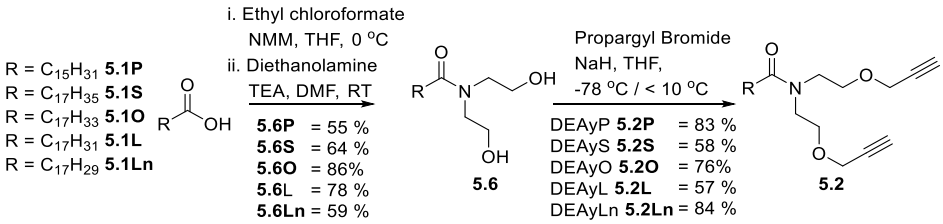

Scheme 5-2: Synthesis of dialkyne fatty amides **5.6P-Ln**

Ether linked dialkyne monomers **5.2P-Ln** were synthesised from diethanol fatty amides **5.6P-Ln** using the same method as in chapter 3 to leave crude yellow solids

for the saturated dialkynes **5.2P** and **5.2S** and yellow oils for the unsaturated monomers **5.2O**, **5.2L** and **5.2Ln**. Purification by column chromatography resulted in white solids (DEAyP **5.2P** 83 %, DEAyS **5.2S** 58 %) and colourless oils (DEAyO **5.2O** 76 %, DEAyL **5.2L** 57 % and DEAyLn **5.2Ln** 84 %).

5.3.2 Synthesis of dialkene fatty amide monomers

Due to the solvation issues surrounding the saturated fatty acids **5.1P** and **5.1S** in the synthesis of **5.2P** and **5.2S**, the dialkene fatty amides **5.3P**-**Ln** were formed following a different procedure that went *via* an acyl chloride intermediate **5.7**. The acyl chloride intermediates **5.7P-Ln** were reacted with diallyl amine without further purification. To achieve fatty acyl chlorides **5.7**, the desired fatty acid **5.1** was placed under nitrogen in dry toluene with catalytic DMF. The mixture was then heated to reflux before dropwise addition of oxalyl chloride. It was stirred at reflux for 3 hours before being cooled to room temperature and left stirring overnight. For the saturated fatty compounds **5.7P** and **5.7S** the mixture could be filtered at this stage to remove any residual fatty acid **5.1P** and **5.1S**. The unsaturated fatty acids **5.1O**, **5.1L** and **5.1Ln** were soluble in toluene and so could not be removed in this way. Solvent and HCl was removed from the acyl chlorides **5.7P-Ln** *in vacuo.*

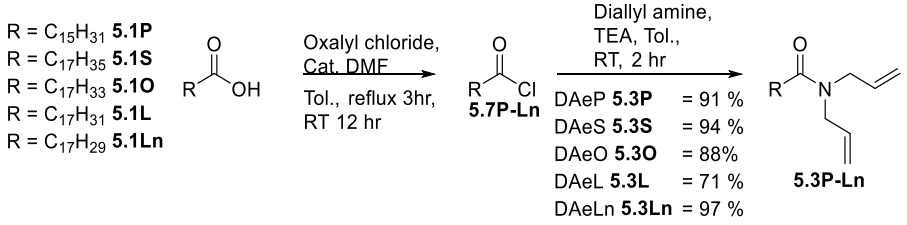

Scheme 5-3: Synthesis of fatty acid derived dialkene monomers **5.3P-Ln**

Without further purification acyl chlorides **5.7P-Ln** were taken into dry toluene and added dropwise to a solution of diallylamine and TEA in dry toluene. Monitoring of the reaction showed that it had reached completion 2 hours after the end of dropwise addition. It was quenched with 2M HCl then extracted with Et_2O. The organic layer was washed with water and brine then dried, finally the solvent was removed *in vacuo* to leave saturated compounds as a pure white solid (DAeP **5.3P** 91 %, DAeS **5.3S** 94 %) and the unsaturated dialkenes **5.3O-Ln** as crude yellow oils. Purification through a silica plug resulted in pure colourless liquids (DAeO **5.3O** 88 %, DAeL **5.3L** 71 % and DAeLn **5.3Ln** 97 %).

5.3.3 Monomer analysis

Characterisation of the fatty acid derived monomers was achieved after analysis with infrared, ^{1}H and ^{13}C NMR, mass spectroscopy and melting point where appropriate. Proton and carbon NMR spectra of monomers **5.2(P-Ln)** and **5.3(P-Ln)** were similar to the spectra of their respective monomers **3.5** and **3.8** in chapter 3, the only difference being the addition of signals relating to the fatty acid chains (H^{a-r}, Figure 5-8).

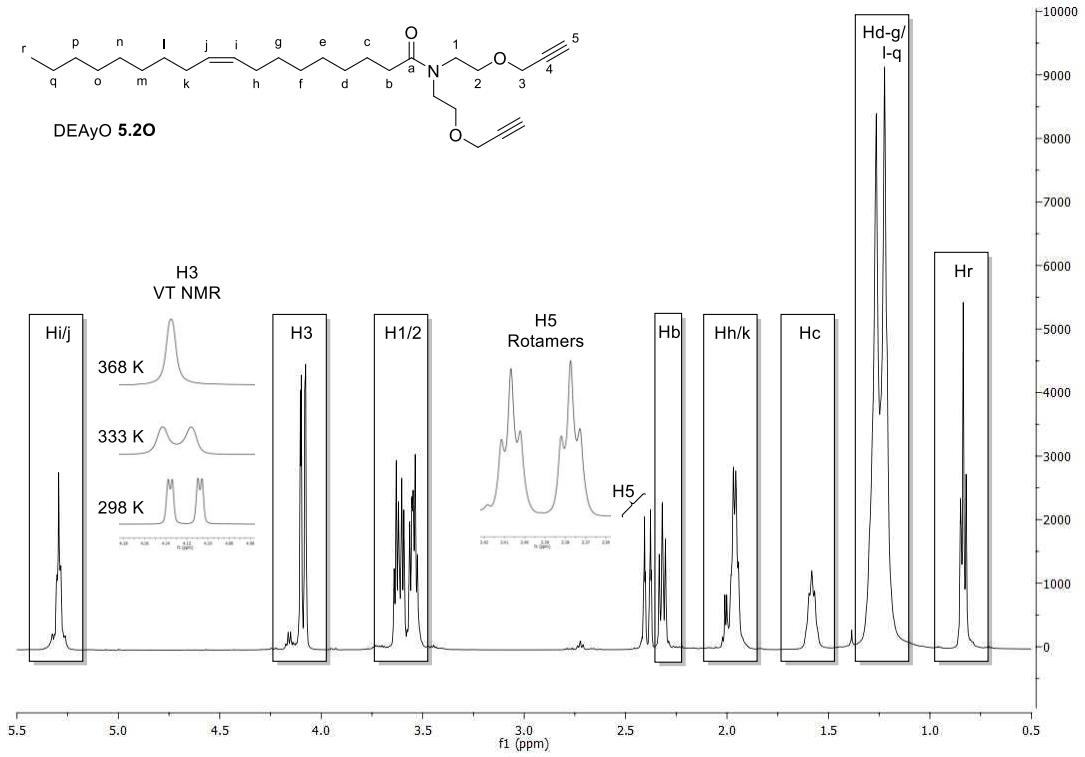

Figure 5-8: ^{1}H NMR spectrum of DEAyO **5.2O**, VT ^{1}H NMR of H3 proton (*insert*)

Like the dipolarophilic monomers in chapter 3, ^{1}H and ^{13}C NMR spectra of **5.2(P-Ln)** and **5.3(P-Ln)** revealed rotamers caused by restricted rotation around the amide C-N bond.[334] Split environments were only present in modified sections of each molecule (H^{1-5}, Figure 5-8) and not the fatty chains (H^{a-r}, Figure 5-8). Variable temperature ^{1}H NMR of DEAyO **5.2O** established that peaks coalesced at raised temperatures (*insert* Figure 5-8/appendix D). Using Equation 3-1 (section 3.5.3 a barrier to rotation of 76.5 kJ mol^{-1} (18.3 kcal mol^{-1}) was calculated for DEAyO **5.2O**, which was similar to the acetamide monomer DEAyAc **3.8** in section 3.3.2 (75.7 kJ mol^{-1}/18.1 kcal mol^{-1}).

As polymerisations were to be carried out at 80 ºC over 2 days the monomers thermal stability was analysed by TGA (Table 5-1). Both dialkyne **5.2P-Ln** and dialkene

monomers **5.3P-Ln** showed thermal stability well above the required 80 ºC. As with the acetamide monomers (section 3.3.3) the dialkynes left a residue at 600 ºC (1a-e, Table 5-1) whereas the dialkenes did not (1f-j, Table 5-1). The degradation profile of acetamide dialkene DAeAc **3.5** was not reported in chapter 3 as **3.5** evaporated at raised temperatures. Fatty acid derived dialkenes **5.3P-Ln** were less volatile and showed a two steps degradation profile (DAeO **5.3O**, Figure 5-9). Like the acetamide dialkyne DEAyAc **3.8** the degradation of the dialkyne monomers **5.2P-Ln** occurred as one step (DEAyO **5.2O**, Figure 5-9).

	Monomer	T_5 / ºC	T_{20} / ºC	W_{600} / %
1a	DEAyP **5.2P**	321	364	11
1b	DEAyS **5.2S**	322	362	10
1c	DEAyO **5.2O**	321	369	10
1d	DEAyL **5.2L**	328	380	8
1e	DEAyLn **5.2Ln**	299	370	10
1f	DAeP **5.3P**	262	308	0
1g	DAeS **5.3S**	304	351	0
1h	DAeO **5.3O**	289	332	0
1i	DAeL **5.3L**	306	351	1
1j	DAeLn **5.3Ln**	267	333	1

Table 5-1: Thermal stability analysis of dipolarophilic monomers **5.2** and **5.3** by TGA

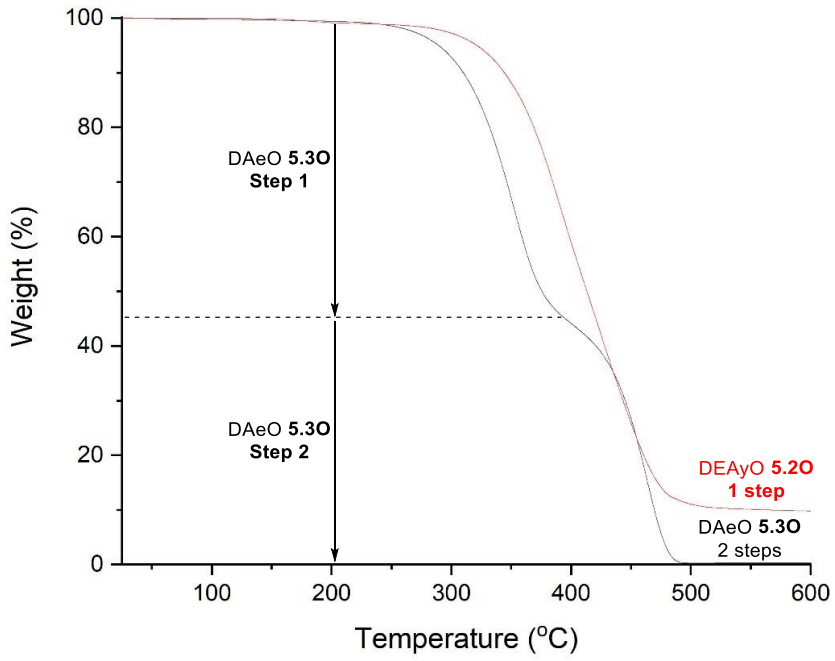

Figure 5-9: TGA of DEAyO **5.2O** and DAeO **5.3O** performed at a heating rate of 10ºC min^{-1} under a N_2.

5.4 Exploring the fatty acid chain

The dipolarophilic groups (Figure 5-10) were investigated in depth in chapter 3. To understand how the introduction of long aliphatic chains will affect polymer behaviour and analysis the fatty acid chains were investigated. To do this an oligomer was synthesised using excess DEAyS **5.2S** and *meta*-OC **2.1** and analysed, synthesis and nomenclature was the same as for the ABA oligomers in chapter 3. Unsaturation in the oleic chain was also investigated using methyl oleate and benz-OC **4.1** (chapter 4).

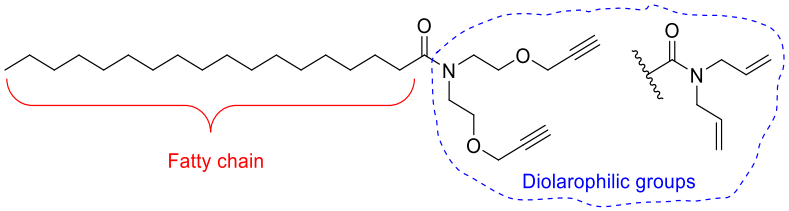

Figure 5-10: Depiction of stearic acid derived dialkyne and dialkene dipolarophile monomers

5.4.1 Oligomer synthesis and analysis (O_mDEAyS-ABA **5.8**)

In order to understand how the inclusion of the fatty acid chain would affect polymer analysis an ABA oligomer was formed using an excess of DEAyS **5.2S** and *meta*-OC **2.1** in the same manner as in section 3.4. Purification was achieved *via* column chromatography through a silica plug, excess DEAyS **5.2S** was recovered from the column followed by the desired 3 membered oligomer O_mDEAyS-ABA **5.8** (48 %).

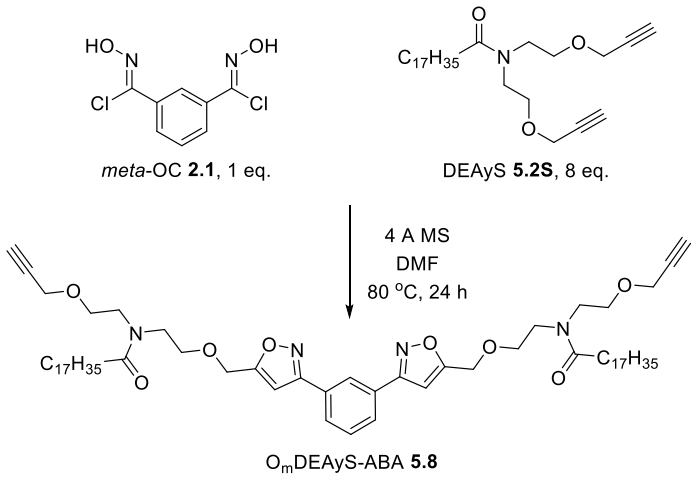

Scheme 5-4: Synthesis of O_mDEAyS-ABA **5.8**

Analysis of O_mDEAyS-ABA **5.8** by 500 MHz ^{1}H and 125 MHz ^{13}C NMR gave similar spectra to the related acetamide oligomer O_mDEAyAc-ABA **3.17** characterised in chapter 3, the only major difference being the signals relating to the aliphatic fatty

chain (H^{a-r}, Figure 5-11). Proton NMR analysis of **5.8** revealed a smaller difference in the ratio of major to minor rotamers (0.55 : 0.45) than **3.17** ((0.6 : 0.4), section 3.5.3). Using variable temperature ^{1}H NMR (*insert*, Figure 5-11/appendix D) a barrier to rotation of 75.2 kJ mol^{-1} (18.0 kcal mol^{-1}) was calculated for O_mDEAyS-ABA, this was similar to **3.17** (75.1 kJ mol^{-1}/17.9 kcal^{-1}, section 3.5.3).

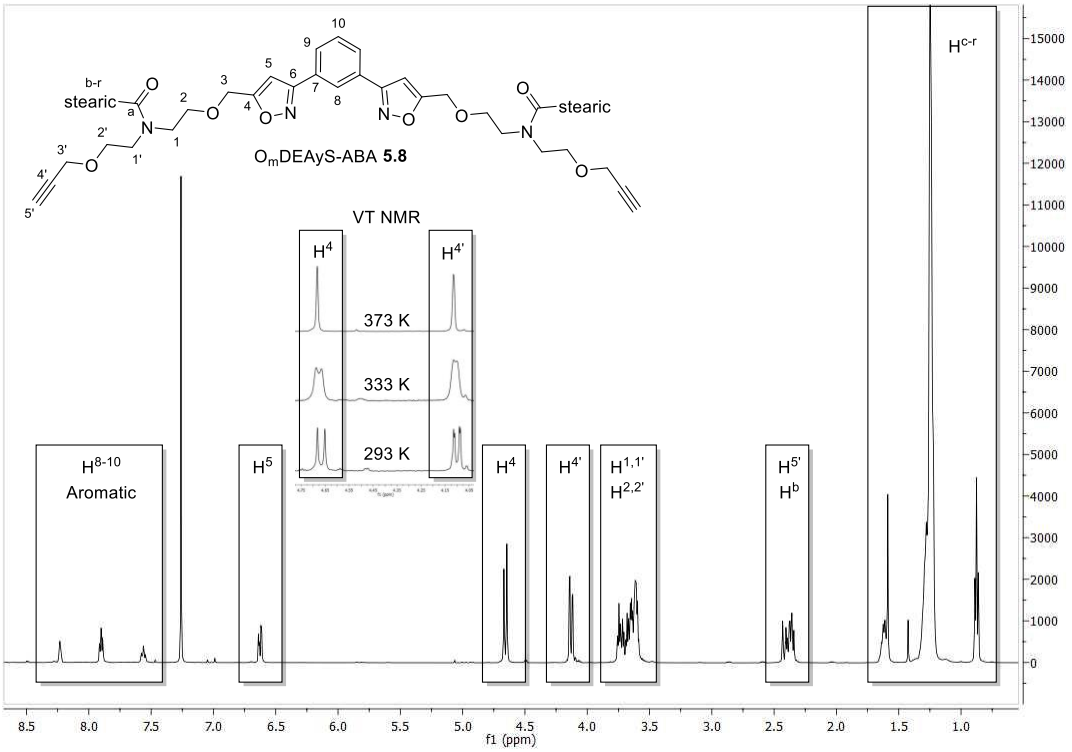

Figure 5-11: ^{1}H NMR spectrum of O_mDEAyS-ABA **5.8**, VT NMR of H^4 and $H^{4'}$ environments (*insert*)

	Exact Mass	GPC Peak	Peak inflation
DMF	1055.54	874	0.8
$CHCl_3$		1275	1.2

Table 5-2: GPC estimate inflation of OmDEAyS-ABA **5.8** in DMF and $CHCl_3$

In chapter 3 the molecular weight of the ABA oligomers was shown to be overestimated by GPC analysis. To investigate how the fatty acid chain effected the polymers molecular weight estimations O_mDEAyS-ABA **5.8** was analysed by GPC (Table 5-2). The molecular weight of **5.8** was underestimated when DMF was used as the eluent against PMMA standards. O_mDEAyS-ABA **5.8** was rerun using $CHCl_3$ as the eluent against PMMA standards, which overestimated the molecular weight. The difference in estimations may have been caused by solvent polarity, with the more polar DMF causing the fatty acid chains to constrict and fold back on themselves

reducing the compounds hydrodynamic radius. The less polar $CHCl_3$ however would solvate the long non-polar chains causing a larger hydrodynamic radius. As the polymer grows these fatty acid chains will form a substantial component of it, which may affect the suitability of DMF as eluent for analysis.

5.4.2 Cycloaddition to internal dipolarophiles

The oleic fatty acid chain contains an internal *cis* alkene bond. According to literature these internal alkenes can undergo cycloaddition with a nitrile oxide, although at a much slower rate than terminal dipolarophilic groups.[258] To test the reactivity of the internal dipolarophile methyl oleate **5.9** was reacted with benz-OC **4.1**. Molar equivalents of the compounds were dissolved in DMF and stirred along with 4 Å MS at 80 ºC for 24 hours. The mixture was diluted with $CHCl_3$ and filtered to remove the molecular sieves. The filtrate was washed with water and brine, then dried and reduced *in vacuo* to leave a crude oil. Column purification through a silica plug resulted in a low yield of isoxazoline compound **5.10** as a pure colourless oil (8 %).

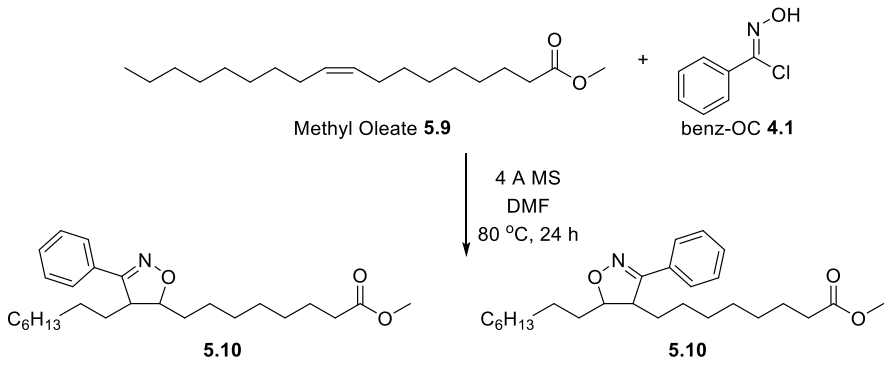

Scheme 5-5: Synthesis of isoxazoline **5.10** using benz-OC **4.1** and methyl oleate **5.9**

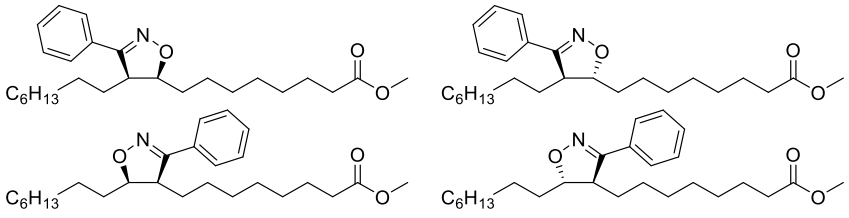

Figure 5-12: Stereoisomers of isoxazoline **5.10.**

NMR analysis revealed a complicated mixture of diastereomers and regioisomers (Figure 5-12), caused by there being limited regiospecific driving force for Huisgen cycloadditions between NO and the internal alkene.[210,323] The proton next to the oxygen in the isoxazoline ring was split into two multiplets 4.50 and 4.45 ppm (H^1,

Figure 5-13), in the ^{13}C spectra this was split between four environments from 86.7 – 85.5 ppm (C^1, Figure 5-13 *insert*). The other proton in the isoxazoline ring experienced a larger difference in environments between the regioisomers with multiplets at 3.40 and 3.25 ppm (H^2, Figure 5-13). The larger difference may be caused by whether the proton was *cis* or *trans* to the oxygen of the isoxazole ring. The carbon environments were also split by a greater degree with two environments around at 52.69 ppm and 52.63 ppm, whilst the other two at 48.47 ppm and 48.39 ppm (C^2, Figure 5-13 *insert*).

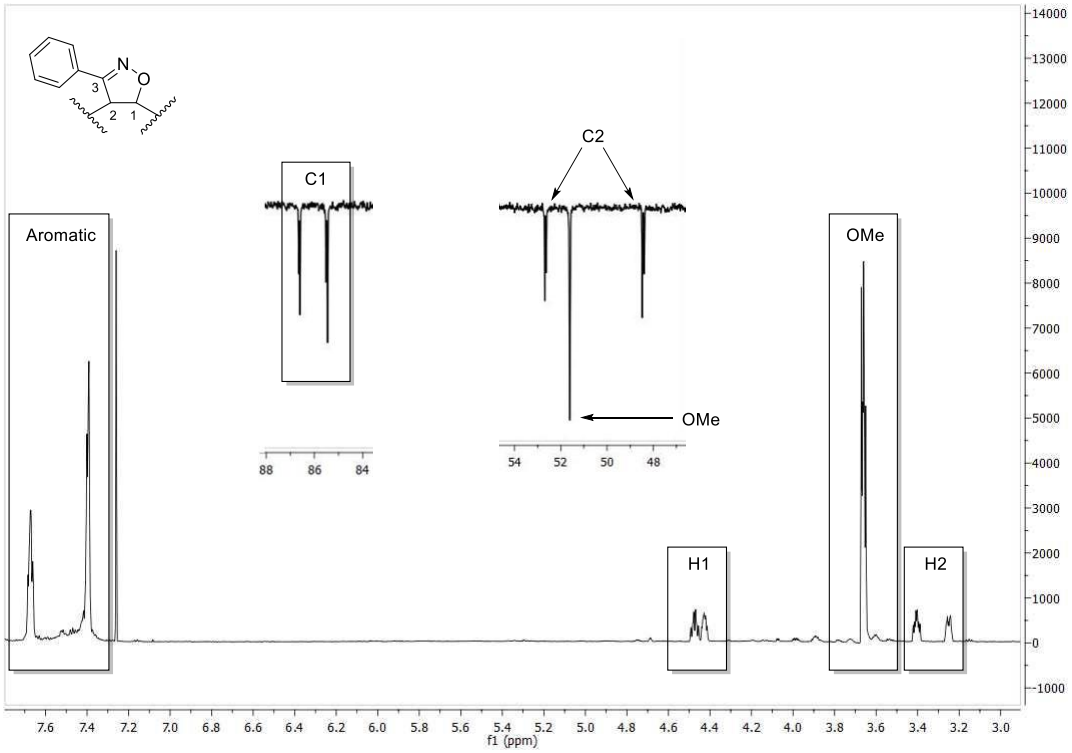

Figure 5-13: A section of the ^1H NMR spectrum of **5.10**, ^{13}C NMR sections (*inserts*)

The low yield of **5.10** (8 %) indicated that whilst isoxazoline formation is possible, it is not particularly prevalent or fast. Polymerisation of the monomers derived from unsaturated fatty acids was therefore likely to primarily progress *via* the desired cycloaddition with the terminal dipolarophiles. Crosslinking through the internal alkene of unsaturated fatty acid monomers however will be a minor side reaction that could alter the polymer properties. Assessment of the level of cross-linking by ^1H NMR analysis will be difficult due to overlapping signals in the ^1H NMR spectrum, particularly in polyisoxazolines. It may be possible to detect cross-linking environments *via* the ^{13}C spectra although it would require concentrated samples.

5.5 Fatty acid derived polyisoxazole synthesis and analysis

Polymers were formed using *meta*-OC **2.1** and the two variants of the fatty amide dipolarophilic monomers **5.2P/S/O/L/Ln** and **5.3P/S/O/L/Ln**, using the improved polymerisation technique from chapter 4. The dipolarophilic monomers **5.2** or **5.3** (1 eq.) and *meta*-OC **2.1** (1 eq.) were dissolved in DMF and stirred at room temperature along with 4 Å MS for 30 minutes. The temperature was then raised to 80 ºC for 48 hours, after which the mixture was diluted with $CHCl_3$ and filtered to remove molecular sieves. The filtrate was reduced *in vacuo* to leave a polymeric residue in DMF. The residue was taken back into minimal $CHCl_3$ and added dropwise to methanol, causing a precipitate to form, which was collected and washed with methanol. To ensure that the total yield was recorded the polymeric precipitate was removed from the filter paper using warm $CHCl_3$, which was then reduced *in vacuo* to leave the polymeric product.

Nomenclature for the polymers was described in section 2.3. Polymers made using Takata's[317] thermal conditions (over 48 hours) were denoted by a superscript 't2', as with the monomers the Arabic numeral was followed by the fatty acid code. $P^{t2}{}_m$DEAyS **5.11S** therefore refers to a polymer made using the 48 hour method from *meta*-OC **2.1** (1 eq.) and DEAyS **5.2S** (1 eq.).

5.5.1 Fatty acid derived polyisoxazole synthesis with analysis by ^{1}H and ^{13}C NMR

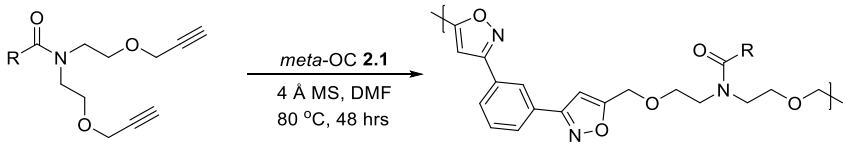

DEAyP **5.2P**
DEAyS **5.2S**
DEAyO **5.2O**
DEAyL **5.2L**
DEAyLn **5.2Ln**

$P^{t2}{}_m$DEAyP **5.11P** = 87 %
$P^{t2}{}_m$DEAyS **5.11S** = 84 %
$P^{t2}{}_m$DEAyO **5.11O** = 80 %
$P^{t2}{}_m$DEAyL **5.11L** = 76 %
$P^{t2}{}_m$DEAyLn **5.11Ln** = 71 %

Scheme 5-6: Synthesis of fatty acid derived polyisoxazoles **5.11P/S/O/L/Ln**

Polymers were initially formed using molar equivalent of *meta*-OC **2.1** and dialkynes **5.2P-Ln**. Polyisoxazoles **5.11P-Ln** all formed as malleable light brown solids. The longer reaction times gave similar yields for the fatty polyisoxazoles (3a-e, Table 5-3) as the acetamide equivalent (3f, Table 5-3) from chapter 4. The similar yields may not

signify a similar degree of polymerisation however as the aliphatic chains of the fatty amide polymers may cause oligomers with a low number of repeat units to precipitate when dropped into methanol. Analysis of the methanol filtrate by mass spectroscopy revealed 2AB and 2A2B oligomers, this was the same as the analysis of the filtrate from $P^{t2}{}_m$DEAyAc **4.8** workup.

	Polymer	Yield / %	NMR RU
3a	$P^{t2}{}_m$DEAyP **5.11P**	87	8.5
3b	$P^{t2}{}_m$DEAyS **5.11S**	84	10
3c	$P^{t2}{}_m$DEAyO **5.11O**	80	6
3d	$P^{t2}{}_m$DEAyL **5.11L**	76	5
3e	$P^{t2}{}_m$DEAyLn **5.11Ln**	71	3
3f	$P^{t2}{}_m$DEAyAc **4.8**	86	14

Table 5-3: Yield and estimated number of repeat units for fatty acid derived polyisoxazoles **5.11P/S/O/L/Ln**

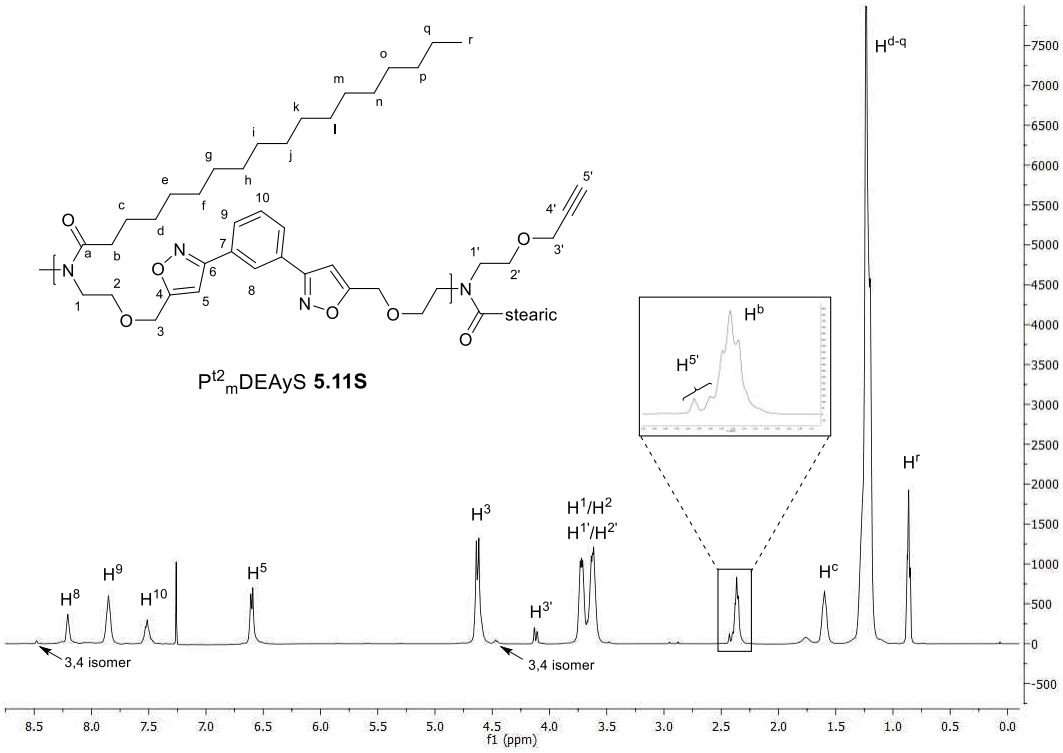

Figure 5-14: ^{1}H NMR spectrum of $P^{t2}{}_m$DEAyS **5.11S**.

The oligomer work in section 5.4 and acetamide polyisoxazole synthesis in chapter 3 made analysis of the ^{1}H and ^{13}C NMR spectra of the fatty polyisoxazoles **5.11P-Ln** much easier. The proton and carbon environments were similar to those reported for $P^t{}_m$DEAyAc **3.27**, the only difference being the inclusion of signals relating to the fatty acid chains (a-r, Figure 5-14). Strong aliphatic environments from the fatty acid chains (H^b, Figure 5-14) meant that the terminal alkyne environment ($H^{5'}$, Figure 5-14) could

not be used for end group analysis. End group analysis could still be achieved using the CH_2 groups proximal to the isoxazole ring (H^3, Figure 5-14) and terminal alkyne ($H^{3'}$, Figure 5-14). The large integration of the aliphatic chains (H^{d-q}, Figure 5-14) reduced the accuracy of end group analysis as the terminal alkyne protons ($H^{3'}$, Figure 5-14) were extremely close to the baseline. Over the fatty amide series (3a-3e, Table 5-3), the number of repeat units predicted by ^{1}H NMR reduced as unsaturation in the fatty chain increased. Crosslinking using the internal alkene of the fatty chain may have been the cause as it would remove nitrile oxide equivalents from the reaction whilst not reducing the amount of terminal alkyne present. Evidence of crosslinking however could not be determined in the ^{1}H NMR spectra of **5.11O**, **5.11L** or **5.11Ln**, it was however indicated in the ^{13}C NMR spectra. Like the methyl oleate derived isoxazoline **5.9**, cross-linked polyisoxazoles **5.11O-Ln** have very weak signals around 48 ppm and 86 ppm relating to CH environments (Figure 5-15).

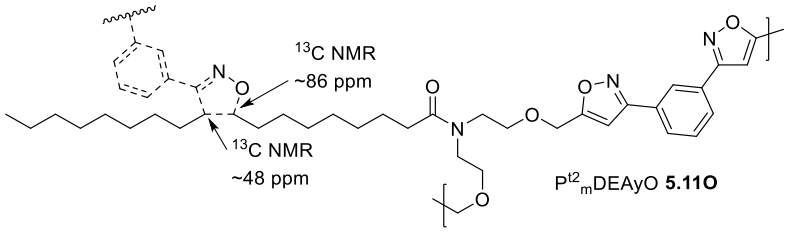

Figure 5-15: Representation of **5.11O** with chemical shifts of crosslinking environments in ^{13}C NMR spectrum.

5.5.2 Analysis of P$^{t2}_m$DEAyR **5.11P-Ln** by GPC

	Polymer	$CHCl_3$			DMF		
		M_n / kDa	M_w / kDa	*Đ*	M_n / kDa	M_w / kDa	*Đ*
4a	P$^{t2}_m$DEAyP **5.11 P**	4.8	11.9	2.5	4.6	9.6	2.1
4b	P$^{t2}_m$DEAyS **5.11 S**	4.8	12.7	2.7	4.2	7.4	1.8
4c	P$^{t2}_m$DEAyO **5.11 O**	5.6	19.4	3.4	4.4	16.1	3.7
4d	P$^{t2}_m$DEAyL **5.11 L**	6.3	33.6	5.3	7.2	63.4	8.8
4e	P$^{t2}_m$DEAyLn **5.11 Ln**	4.3	16.5	3.9	7.5	72.3	9.6
4f	P$^{t2}_m$DEAyAc **4.8**	-	-	-	9.1	14.2	1.5

Table 5-4: GPC estimates for fatty acid derived polyisoxazoles **5.11P/S/O/L/Ln**

The molecular weight achieved by polymerisations was estimated by GPC using both $CHCl_3$ and DMF as the eluent. For the saturated and oleic derived polymers (4a-c, Table 5-4) GPC estimations were as expected, with those run in $CHCl_3$ resulting in larger estimations than those run in DMF. For the more unsaturated polymers (4d & 4e, Table 5-4) however the relationship was reversed, using DMF as the eluent

resulted in incredibly high M_w estimations (>60 kDa) which led to high dispersity values. Compared to the 500 MHz ^{1}H NMR end group analysis the M_w's estimated in DMF for **5.11L** and **5.11Ln** were unrealistic, even taking into account the possibility of crosslinking occurring in **5.11O/L/Ln** which could be the cause of the high M_w and *Đ* estimations in both solvents.

Fatty polyisoxazoles (4a-e, DMF, Table 5-4) were estimated to have lower M_n's than the acetamide polyisoxazole (4f, DMF, Table 5-4) in DMF. Studies using oligomers O_mDEAyS-ABA **5.8** and O_mDEAyAc-ABA **3.17** had shown GPC estimates in DMF were underestimated and overestimated respectively. This is therefore the probable cause for the significant difference in M_n estimates between **5.11P-Ln** and **4.8**.

5.5.3 Thermal analysis of $P^{t2}{}_m$DEAyR **5.11P-Ln** by TGA and DSC

	Polymer	T_g / ºC	T_5 / ºC	T_{20} / ºC
5a	$P^{t2}{}_m$DEAyP **5.11P**	6	272	323
5b	$P^{t2}{}_m$DEAyS **5.11S**	5	279	327
5c	$P^{t2}{}_m$DEAyO **5.11O**	-1	255	321
5d	$P^{t2}{}_m$DEAyL **5.11L**	3	253	336
5e	$P^{t2}{}_m$DEAyLn **5.11Ln**	6	247	345
5f	$P^{t2}{}_m$DEAyAc **4.8**	51	246	338

Table 5-5: Thermal analysis data for fatty acid derived polyisoxazoles **5.11P/S/O/L/Ln**

Polyisoxazoles **5.11P-Ln** thermal characteristics were assessed by TGA and DSC. Thermal stability was analysed by TGA, heating the polymers from 25 °C to 600 °C at 10 °C / min under nitrogen. As with previous chapters the polymers **5.11P-Ln** had lower thermal stability than their respective monomers **5.2P-Ln**. Polyisoxazoles formed from saturated fatty acids (5a & 5b, Table 5-5) had a higher thermal stability than those derived from unsaturated fatty acids (5c-5e, Table 5-5). In chapter 3 isoxazole rings were found to be more stable than isoxazoline rings, if crosslinking has occurred in polyisoxazoles **5.11O/L/Ln** then they would contain isoxazolines, reducing their thermal stability but an increased T_g would be expected.

Glass transition temperatures (T_g) were determined using DSC, the polymers were heated at 10 °C / min to 100 °C then cooled to -100 °C, following this they were heated through to 300 °C at 20 °C / min. Glass transition temperatures were taken on the second heating step. T_g's of the polyisoxazoles (Table 5-5) were also indicative of crosslinking. Normally T_g would decrease as unsaturation increased in the fatty acid

chains as they are more kinked, reducing their ability to pack. The reduction in T_g can be seen between the saturated polyisoxazoles **5.11P** and **5.11S** and the oleic derived polymer **5.11O** (Figure 5-16). As unsaturation in the monomer increases from **5.11O** to **5.11Ln** T_g increased, this was presumably caused by greater amounts of crosslinking occurring between the fatty acid chains as unsaturation increases. Terminal alkynes are more susceptible to cycloadditions than the internal alkenes found in the fatty acid chains. Crosslinking was therefore low between oleic chains as terminal alkynes were more prevalent and more reactive than its singular internal alkene. As the number of internal alkenes increased the opportunity to crosslink increased leading to higher T_g's for $P^{t2}{}_m$DEAyL **5.11L** and $P^{t2}{}_m$DEAyLn **5.11Ln** (Figure 5-16).

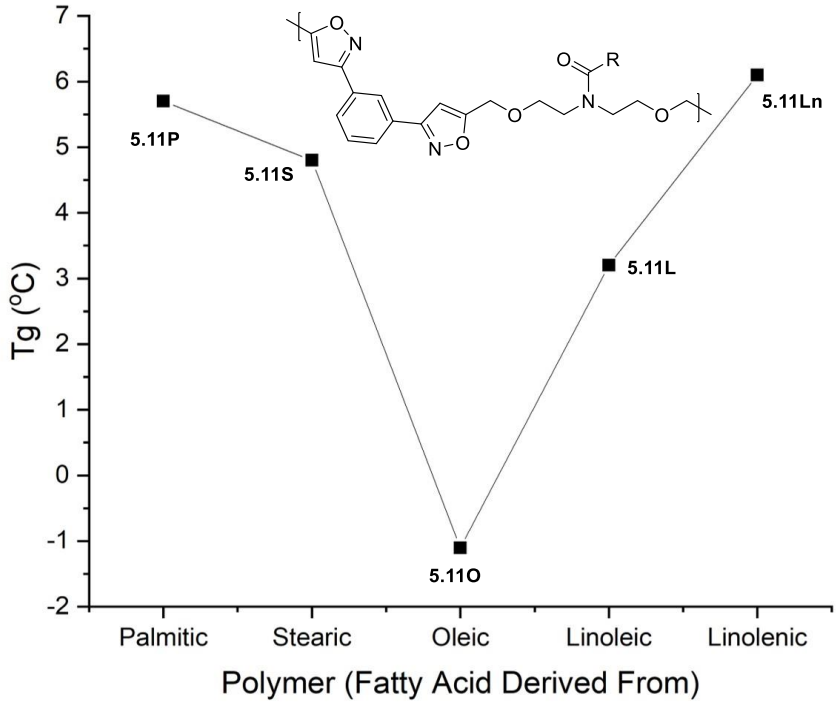

Figure 5-16: Glass transition temperatures (T_g) of fatty acid derived polyisoxazoles **5.11P/S/O/L/Ln**.

5.5.4 Analysis of $P^{t2}{}_m$DEAyR **5.11P-Ln** by MALDI-TOF

MALDI-TOF analysis of polyisoxazoles **5.11P-Ln** was carried out between 800 Da and 4500 Da (appendix D). Due to the inclusion of *cis*-alkenes in the unsaturated chains, polymers derived from oleic **5.11O**, linoleic **5.11L** and linolenic acid **5.11Ln** could form more structures than in chapters 2 and 3. Mass peaks in the MALDI spectra therefore can refer to different linear, cyclical and cross-linked structures (Figure 5-17). The clearest indication of cross-linking is the presence of $(AB)_n$-B peaks in the

MALDI-TOF spectra as $(AB)_n$ peaks have been previously shown to relate to cyclical and furoxan containing polymers. Cross-links are not definitively described by the presence of $(AB)_n$-B peaks however as they could also refer to the presence of cyclical-furoxan and double furoxan polymer chains.

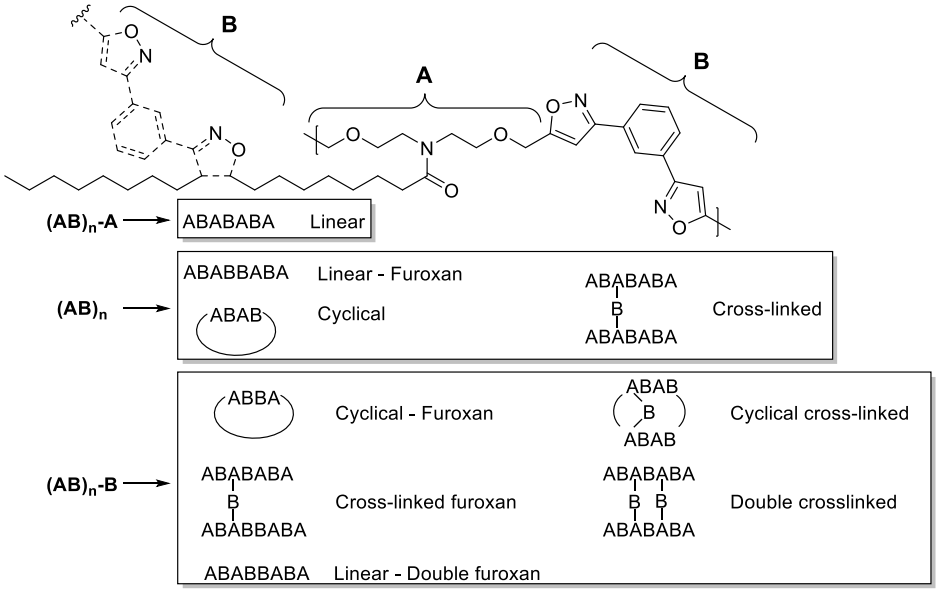

Figure 5-17: Possible polymeric structures of $(AB)_n$, $(AB)_n$-A, and $(AB)_n$-B

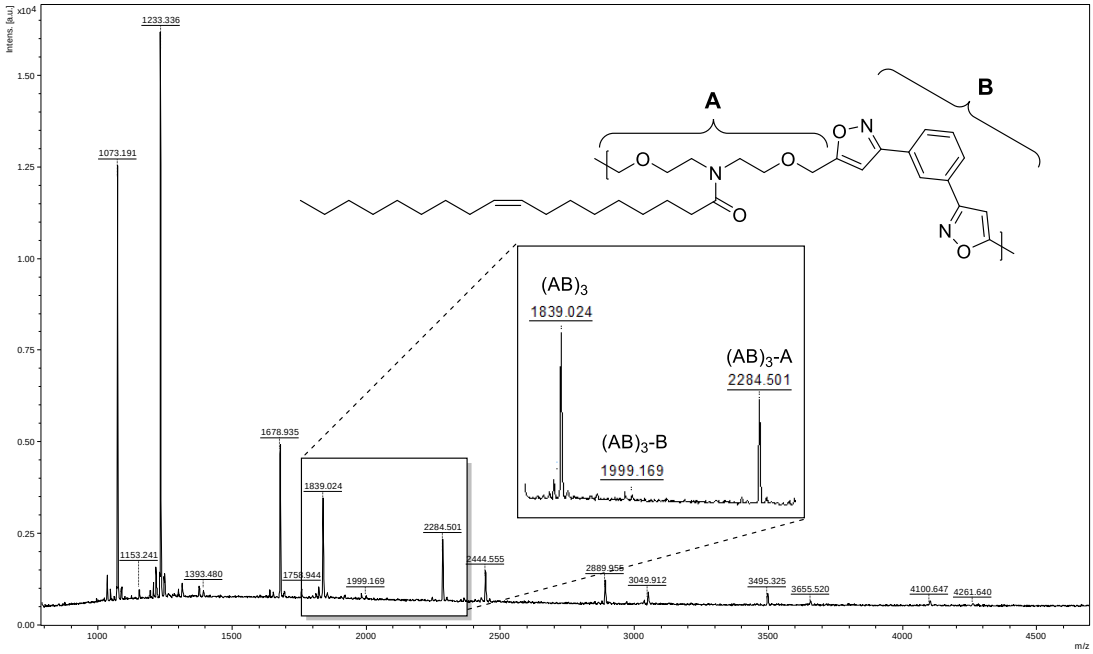

Figure 5-18: MALDI-TOF spectrum of $P^{t2}{}_m$DEAyO **5.11O**, focus on the n=3 chains (*insert*)

The intensity of peaks in the MALDI-TOF spectrum of saturated fatty acid derived polymers **5.11P** and **5.11S** indicated that they formed more $(AB)_n$-A chains than $(AB)_n$. The unsaturated fatty acid derived polyisoxazoles **5.11O**, **5.11L** and **5.11Ln** however had higher intensities for $(AB)_n$ chains than $(AB)_n$-A at all numbers of repeat

units. As unsaturation increased in the fatty chain the intensity of peaks relating to $(AB)_n$ chains increased relative to $(AB)_n$-A chains. It was also found that the intensity and occurrence of $(AB)_n$-B chains increased with unsaturation, $(AB)_n$-B chains were only found to n = 3 for $P^{t2}{}_m$DEAyO **5.11O** (Figure 5-18) but up to n = 5 for $P^{t2}{}_m$DEAyLn **5.11Ln**. The analysis of polyisoxazoles **5.11O-Ln** by MALDI-TOF is indicative of cross-linking occurring using the *cis*-alkenes in the fatty acid chains, which agrees with the trend in glass transition temperatures.

5.6 Fatty acid derived polyisoxazolines

Using the same polymerisation method as section 5.5 polyisoxazolines **5.12P-Ln** were synthesised using molar equivalents of *meta*-OC **2.1** and fatty dialkene amides **5.3P-Ln**. The polymeric yields reduced as unsaturation in the fatty acid chain increased (Scheme 5-7), the same trend was seen in the fatty polyisoxazoles **5.11P-Ln**.

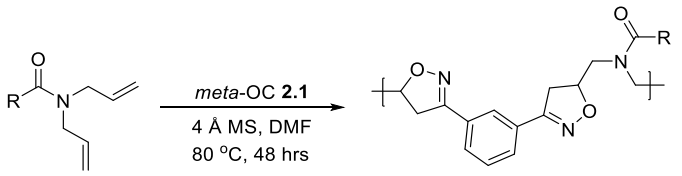

DAeP	**5.3P**		$P^{t2}{}_mDAeP$	**5.12P** = 83 %
DAeS	**5.3S**		$P^{t2}{}_mDAeS$	**5.12S** = 87 %
DAeO	**5.3O**		$P^{t2}{}_mDAeO$	**5.12O** = 77 %
DAeL	**5.3L**		$P^{t2}{}_mDAeL$	**5.12L** = 74 %
DAeLn	**5.3Ln**		$P^{t2}{}_mDAeLn$	**5.12Ln** = 72 %

Scheme 5-7: Synthesis of fatty acid derived polyisoxazolines **5.12P/S/O/L/Ln**.

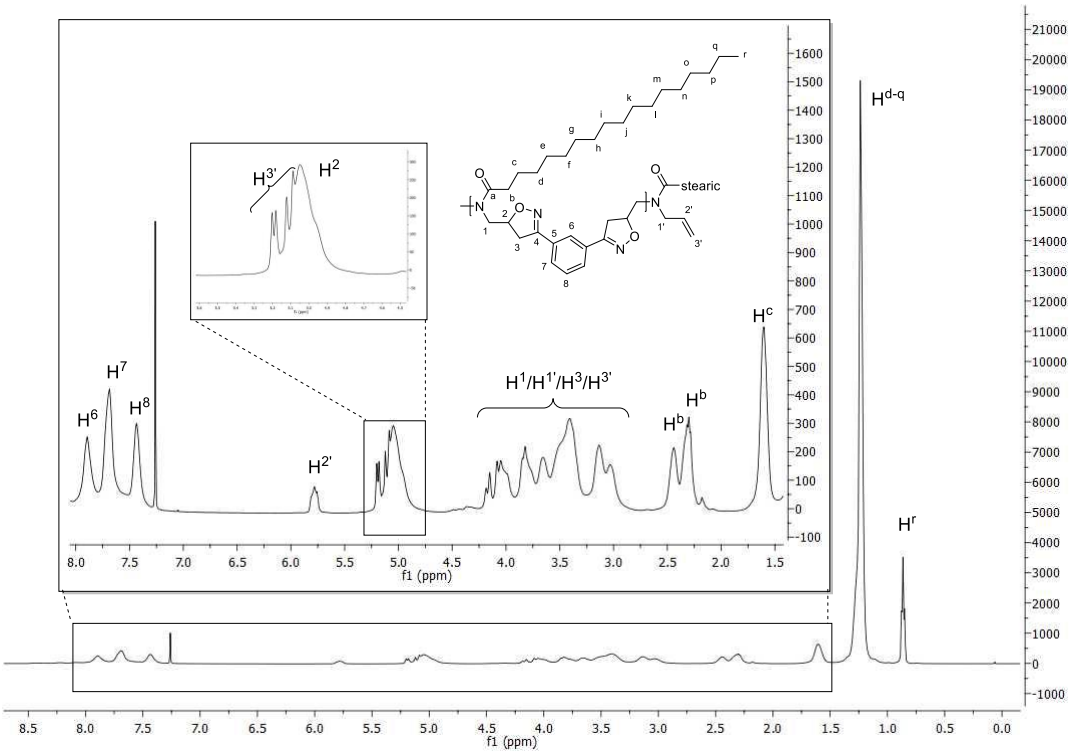

Figure 5-19: ^{1}H NMR spectrum of $P^{t2}{}_mDAeS$ **5.1**; regions between 1.5 and 8.0 ppm shown in more detail (*insert*).

Characterisation of a $P^t{}_mDAeAc$ **3.24** in chapter 3 helped in the interpretation of the 500 MHz ^{1}H and 125 MHz ^{13}C NMR spectra of polyisoxazolines **5.12P-Ln**. Like **3.24** the fatty acid derived polyisoxazoles **5.12** presented rotameric environments in the ^{1}H NMR, this was most clearly demonstrated in the first CH_2 environment of the fatty

chain (H^b, Figure 5-19). As with the polyisoxazolines in chapter 3, end group analysis was more difficult than the respective polyisoxazoles and was calculated using the terminal alkene and an aromatic proton ($H^{2'}$ & H^8, Figure 5-19). The large integration of aliphatic groups caused further issues as the alkene end group environments gave relatively weak signals. The error in end group analysis (Table 5-6) was therefore thought to be high. Like the unsaturated polyisoxazoles **5.11O-Ln**, there is evidence of crosslinking in the ^{13}C spectra of **5.12O-Ln** with very weak signals around 46 ppm and 86 ppm relating to CH environments.

	Polymer	Yield / %	NMR RU
6a	$P^{t2}{}_m$DAyP **5.12P**	83	17
6b	$P^{t2}{}_m$DAyS **5.12S**	87	8
6c	$P^{t2}{}_m$DAyO **5.12O**	77	31
6d	$P^{t2}{}_m$DAyL **5.12L**	74	8.5
6e	$P^{t2}{}_m$DAyLn **5.12Ln**	72	7

Table 5-6: Yield and estimated average number of repeat units for **5.12P/S/O/L/Ln**.

5.6.1 Analysis of $P^{t2}{}_m$DAeR **5.12P-Ln** by GPC

	Polymer	$CHCl_3$			DMF		
		M_n / kDa	M_w / kDa	$Đ$	M_n / kDa	M_w / kDa	$Đ$
7a	$P^{t2}{}_m$DAyP **5.12P**	4.0	11.0	2.7	1.7	5.5	3.2
7b	$P^{t2}{}_m$DAyS **5.12S**	4.0	8.6	2.1	0.5	1.4	3.1
7c	$P^{t2}{}_m$DAyO **5.12O**	4.9	14.6	3.0	3.0	13.5	4.4
7d	$P^{t2}{}_m$DAyL **5.12L**	5.9	16.7	2.8	7.1	69.1	9.7
7e	$P^{t2}{}_m$DAyLn **5.12Ln**	5.5	14.0	2.5	7.1	88.5	12.4

Table 5-7: GPC estimates for fatty acid derived polyisoxazolines **5.12P/S/O/L/Ln**.

The molecular weight of polyisoxazolines **5.12P-Ln** was estimated by GPC using both $CHCl_3$ and DMF as the eluent. DMF was expected to be a better solvent for $P^{t2}{}_m$DAeR **5.12P-Ln** polymers than $P^{t2}{}_m$DEAyR **5.11P-Ln**, as O_mDAeAc-ABA **3.14** (R_f = 0.15 in EtOAc) was indicated to be more polar than O_mDEAyAc-ABA **3.17** (R_f = 0.20 in EtOAc) in chapter 3. It was immediately obvious however that DMF was not a suitable eluent for analysis of the polyisoxazolines **5.12P-Ln**, severely underestimating the number average molecular weight (M_n) of the polymers (7a-e, DMF, Table 5-7). The lack of the ether link therefore may have had an unanticipatedly large effect on reducing the polarity of the **5.12P-Ln** relative to **5.11P-Ln** making DMF a poor eluent for GPC analysis. Also as with the polyisoxazoles **5.11P-Ln**,

estimations of M_w became exceedingly high for the unsaturated polyisoxazoles using DMF as eluent (7c-e, DMF, Table 5-7). GPC analysis of **5.12P-Ln** using $CHCl_3$ as eluent gave more reasonable estimations of molecular weight that aligned closer to the ^1H NMR estimations. The unsaturated polymers (7c-e, $CHCl_3$, Table 5-7) were estimated to have higher molecular weights than saturated polymers (7a & 7b, $CHCl_3$, Table 5-7), presumably due to cross-linking.

5.6.2 Thermal analysis of $P^{t2}{}_m$DAeR **5.12P-Ln** by TGA and DSC

Thermal characteristics of polyisoxazolines **5.12P-Ln** were assessed by TGA and DSC (Table 5-8). Thermal stability was analysed by TGA, heating the polymers from 25 °C to 600 °C at 10 °C / min under nitrogen. Thermal stability of polyisoxazolines **5.12P-Ln** followed the same trends as the fatty acid derived polyisoxazoles **5.11P-Ln**. Saturated fatty acids derived polyisoxazolines (8a & 8b, Table 5-8) had higher thermal stability than unsaturated fatty acid derived polymers (8c-e, Table 5-8). The polymers (**5.12P-Ln**) also had lower thermal stability than their respective monomers (**5.3P-Ln**). As in chapter 3, polyisoxazolines **5.12P-Ln** were less thermally stable than their respective polyisoxazoles **5.11P-Ln**, (5a, Table 5-5 & 8a, Table 5-8, $\Delta T_5 = -28$ °C).

	Polymer	T_g / ºC	T_5 / ºC	T_{20} / ºC
8a	$P^{t2}{}_m$DAyP **5.12P**	82	244	316
8b	$P^{t2}{}_m$DAyS **5.12S**	76	245	318
8c	$P^{t2}{}_m$DAyO **5.12O**	74	223	303
8d	$P^{t2}{}_m$DAyL **5.12L**	56	216	309
8e	$P^{t2}{}_m$DAyLn **5.12Ln**	64	210	322

Table 5-8: Thermal analysis for fatty acid derived polyisoxazolines **5.12P/S/O/L/Ln**.

Polyisoxazoles **5.12P-Ln** were analysed by DSC to determine their glass transition temperatures (T_g). As the polyisoxazolines **5.12P-Ln** were predicted to have higher T_g's than the polyisoxazoles **5.11P-Ln**, they were heated at 10 °C / min to 150 °C then cooled to 0 °C, following this they were heated through to 300 °C at 20 °C / min. Glass transition temperatures (T_g) were taken on the second heating step. As expected the T_g's of **5.12P-Ln** were considerably higher than their respective polyisoxazoles **5.11P-Ln** (5a, Table 5-5 & 8a, Table 5-8, $\Delta T_g = 76$ °C). A shorter flexible chain between the heterocycles was the major cause of the increased T_g's for **5.12P-Ln** relative to **5.11P-Ln**, although isoxazoline ring (instead of isoxazole) likely increased the T_g further. Crosslinking was less evident from the T_g's of polyisoxazolines **5.12P-Ln** (Figure

5-20). Glass transition temperature's (T_g) reduced from **5.12O** to **5.12L** which would be expected if no/limited crosslinking occurred, with the more kinked unsaturated fatty chain reducing the polymers ability to pack chains together. T_g only begins to increase from **5.12L** to **5.12Ln** (8d & 8e, Table 5-8, ΔT_g = 8°C) where significant unsaturation is present in the fatty chain.

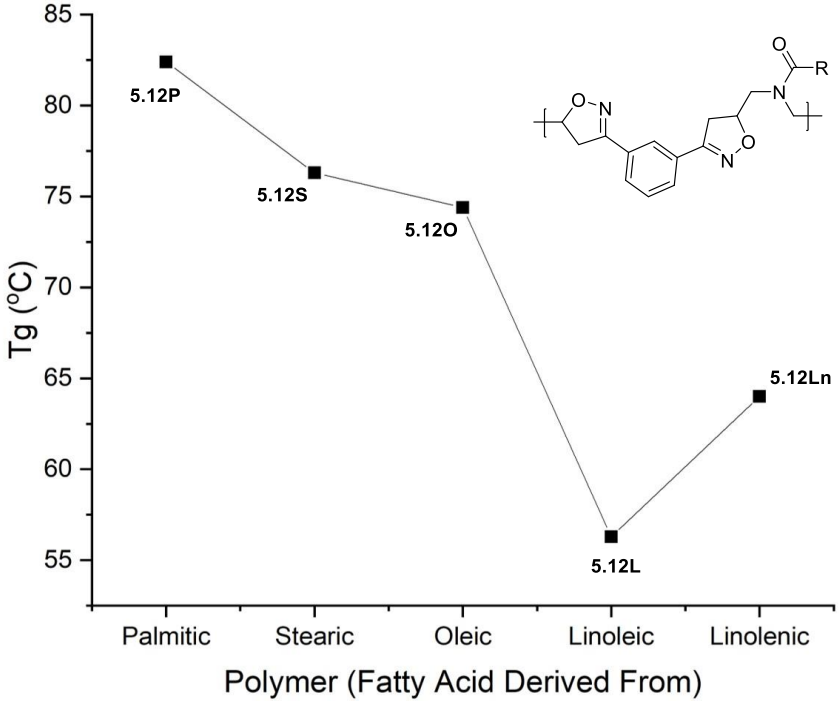

Figure 5-20: Glass transition temperatures (T_g) of fatty acid derived polyisoxazolines **5.12P/S/O/L/Ln**.

The increase in T_g was seen between the oleic and linoleic derived polyisoxazoles (5c & 5d, Table 5-5) whereas with the polyisoxazolines it was first seen between the polymers derived from linoleic and linolenic fatty acids (8d & 8e,Table 5-8). Terminal alkenes are more reactive towards Huisgen cycloadditions than terminal alkynes,[258] there was therefore less opportunity (greater rate difference) for the nitrile-oxide to undergo cycloaddition with the internal *cis*-alkenes of the unsaturated fatty chain during polyisoxazoline synthesis. It was not until internal *cis* alkenes had a numerical advantage over the terminal alkenes (DAeLn **5.3Ln**) that cross-linking could occur to a significant degree and increase T_g.

5.6.3 Analysis of $P^{t2}{}_m$DAeR **5.12P-Ln** by MALDI-TOF

MALDI-TOF analysis of polyisoxazolines **5.12P-Ln** was carried out between 800 Da and 4500 Da. The spectra of **5.12P-Ln** (appendix D) were generally of lower quality

than the polyisoxazoles **5.11P-Ln**. Like the polyisoxazoles **5.11P-Ln**, the spectra of saturated polyisoxazolines **5.12P** and **5.12S** had stronger intensities for peaks relating to $(AB)_n$-A chains than $(AB)_n$ chains, whilst intensities for the unsaturated polyisoxazolines **5.12O-Ln** were stronger for $(AB)_n$ than $(AB)_n$-A chains. Possibly due to the low quality of the spectra of unsaturated polyisoxazolines **5.12O-Ln**, $(AB)_n$-B peaks were only observed up to n = 3. This indicated that cross-linking has occurred, it does not however show how increasing amounts of unsaturation in the fatty chain affects the extent of cross-linking in the polymer.

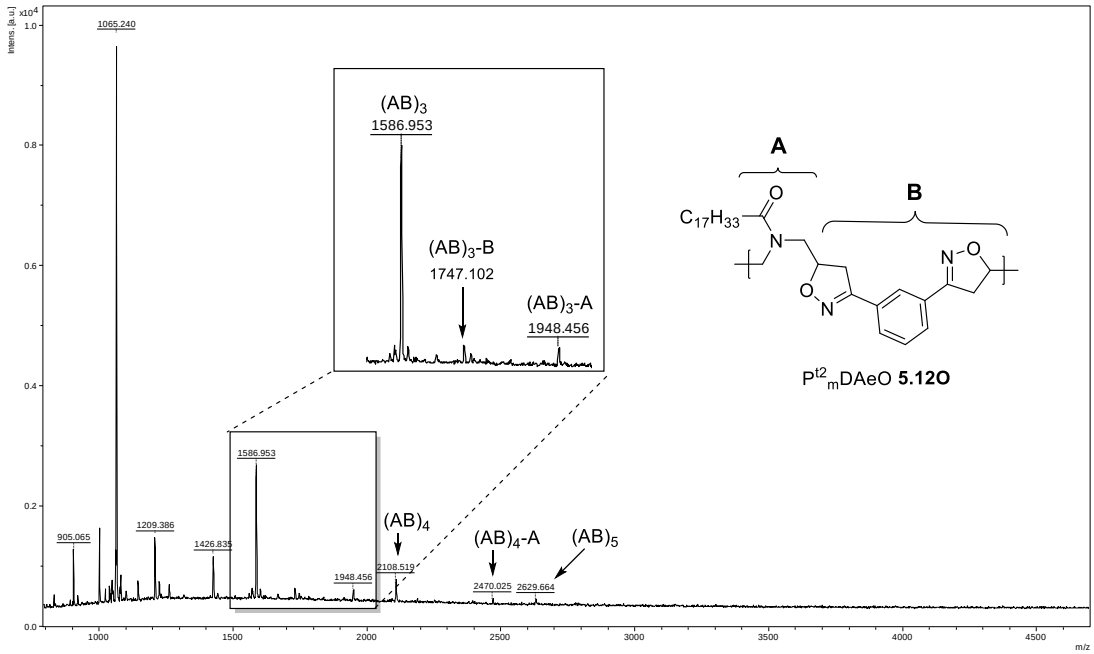

Figure 5-21: MALDI-TOF spectrum of P^{t2}_mDEAyO **5.12O**, focus on the n=3 chains (*insert*)

5.7 Ether containing dialkene fatty amide monomer synthesis

Analysis of polymers **5.11P-Ln** and **5.12P-Ln** indicated that crosslinking was more prolific during polymerisation when using the unsaturated dialkyne monomers **5.2O-Ln** than the unsaturated dialkene monomers **5.3O-Ln**. To investigate the difference in crosslinking, polymers were needed to be formed using an excess of *meta*-OC **2.1**. As dialkynes **5.2S-Ln** contained ether linkages and the dialkenes **5.3S-Ln** did not, they could not be directly compared. Ether linked dialkenes DEAeS **5.4S** and DEAeO **5.4O** were therefore synthesised from stearic and oleic diol fatty amides **5.6S/O** using allyl bromide and the same procedure as the dialkyne monomer synthesis in section 5.3.1 (Scheme 5-8). Dialkene monomers DEAeS **5.4S** and DEAeO **5.4O** were purified by column chromatography to give colourless oils 98 % and 76 % respectively. Characterisation of the monomers **5.4S/O** was achieved using analysis data from 500 MHz ^{1}H and ^{13}C NMR, infrared, and mass spectroscopy.

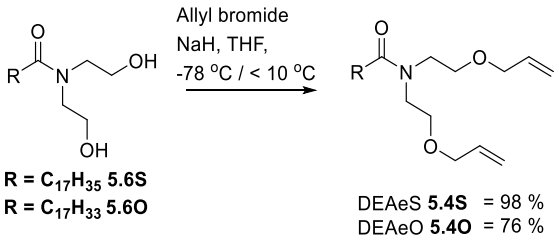

Scheme 5-8: Synthesis of ether-linked dialkene monomers derived from stearic and oleic acid.

Thermal analysis of dialkenes DEAeS **5.4S** and DEAeO **5.4O** (9c & 9d, Table 5-9) by TGA showed similar thermal properties to the dialkyne monomers (9e & 9f, Table 5-9). There was little difference in the thermal stability of stearic and oleic variants for the ether containing compounds (9c-f, Table 5-9), which were more thermally stable than the non-ether containing dialkenes (9a & 9b, Table 5-9). Unlike the smaller dialkene monomers (9a & 9b, Table 5-9), **5.4S/O** also left a residue at 600 °C, although not as much as the dialkyne compounds (9c & 9e, Table 5-9, ΔW_{600} = 7 %).

	Monomer	T_5 / °C	T_{20} / °C	W_{600} / %
9a	DAeS **5.3S**	304	351	0
9b	DAeO **5.3O**	289	332	0
9c	DEAeS **5.4S**	315	351	3
9d	DEAeO **5.4O**	323	358	3
9e	DEAyS **5.2S**	322	362	10
9f	DEAyO **5.2O**	321	369	10

Table 5-9: Thermal analysis of stearic and oleic acid derived dipolarophile monomers.

5.8 Polyisoxazolines from DEAeS **5.4S** and DEAeO **5.4O**

Before investigating the effect of excess nitrile oxide on polymer properties polyisoxazolines were formed using equal molar ratios of *meta*-OC **2.1** and ether linked dialkenes DEAeS **5.4S** and DEAeO **5.4O**. The polymerisation method was the same as in section 5.5, resulting in $P^{t2}{}_mDEAeS$ **5.13S** and $P^{t2}{}_mDEAeO$ **5.13O** as malleable brown solids with a yield of 87 % and 83 % respectively.

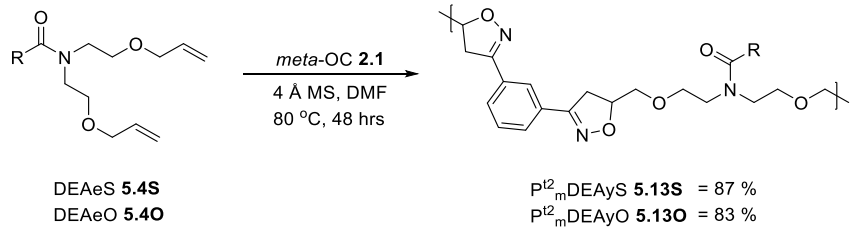

Scheme 5-9: Synthesis of fatty acid derived polyisoxazolines **5.13S** and **5.13O**.

Polyisoxazolines $P^{t2}{}_mDEAeS$ **5.13S** and $P^{t2}{}_mDEAeO$ **5.13O** were characterised using the same methods as the polymers in section 5. GPC analysis was performed using $CHCl_3$ as the eluent as DMF had shown poor suitability for the polyisoxazolines **5.12P-Ln** in section 5.6.1. Analysis by GPC against PMMA standards estimated that the stearic derived polyisoxazoline **5.13S** had much higher molecular weight than the oleic derived polyisoxazoline **5.13O**, this was corroborated by 500 MHz ^{1}H NMR end group analysis (10c & 10d, Table 5-10). Unlike **5.11O** and **5.12O**, both the ^{1}H and ^{13}C NMR of **5.13O** showed no evidence of crosslinking.

	Polymer	Yield / %	NMR RU	M_n / kDa	M_w / kDa	*Đ*
10a	$P^{t2}{}_mDAeS$ **5.12S**	87	8	4.0	8.6	2.1
10b	$P^{t2}{}_mDAeO$ **5.12O**	77	27	4.9	14.6	3.0
10c	$P^{t2}{}_mDEAeS$ **5.13S**	87	17	6.0	16.7	2.8
10d	$P^{t2}{}_mDEAeO$ **5.13O**	83	7	3.1	9.5	3.0
10e	$P^{t2}{}_mDEAyS$ **5.11S**	84	10	4.8	12.7	2.7
10f	$P^{t2}{}_mDEAyO$ **5.11O**	80	6	5.6	19.4	3.4

Table 5-10: Polymer analysis of stearic and oleic acid derived polymers

GPC estimated that the stearic derived polyisoxazoline **5.13S** (10c, Table 5-10) had a higher molecular weight average than either of the steric derived polymers in sections 5.5 and 5.6 (10a & 10e, Table 5-10). Oleic derived polyisoxazoline **5.13O** (10d, Table 5-10) however had a lower molecular weight average than the oleic derived polymers in sections 5.5 and 5.6 (10b & 10f, Table 5-10).

Thermal analysis of $P^{t2}{}_mDEAeS$ **5.13S** and $P^{t2}{}_mDEAeO$ **5.13O** by TGA (11c & 11d, Table 5-11) revealed them to have more similar thermal stability to the polyisoxazoles **5.11S** and **5.11O** (11e & 11f, Table 5-11) than the non-ether containing polyisoxazolines **5.12S** and **5.12O** (11a & 11b, Table 5-11). Indicating that the inclusion of the ether link in the monomer had a greater effect on thermal stability than the heterocyclic ring. This finding differs from chapter 3 where thermal stability was aligned with the heterocyclic ring rather than the inclusion of the ether link. The effect of the heterocyclic ring is however seen with glass transition temperature, with $P^{t2}{}_mDEAeS$ **5.13S** having a much higher T_g than $P^{t2}{}_mDEAyS$ **5.11S** (11c & 11e, Table 5-11, ΔT_g = +26 ºC).

	Polymer	T_g / ºC	T_5 / ºC	T_{20} / ºC
11a	$P^{t2}{}_mDAeS$ **5.12S**	76	245	318
11b	$P^{t2}{}_mDAeO$ **5.12O**	74	223	303
11c	$P^{t2}{}_mDEAeS$ **5.13S**	31	267	339
11d	$P^{t2}{}_mDEAeO$ **5.13O**	5	250	324
11e	$P^{t2}{}_mDEAyS$ **5.11S**	5	279	327
11f	$P^{t2}{}_mDEAyO$ **5.11O**	-1	255	321

Table 5-11: Thermal analysis of stearic and oleic acid derived polymers

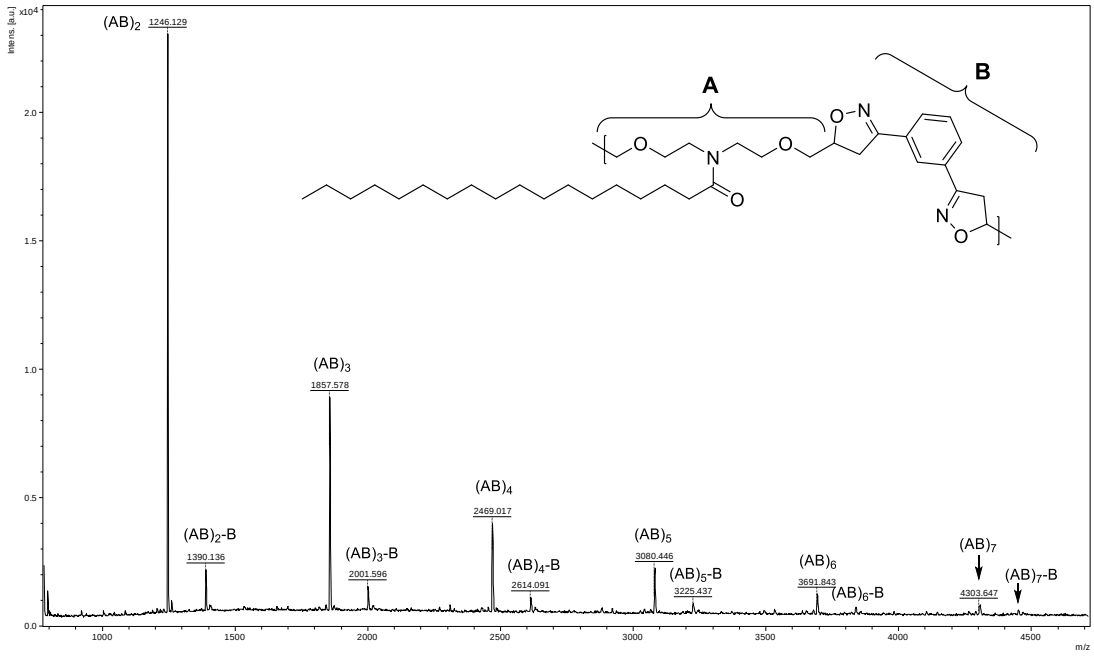

Figure 5-22: MALDI-TOF spectrum of $P^{t2}{}_mDEAeS$ **5.13S**.

MALDI-TOF analysis of polyisoxazolines $P^{t2}{}_mDEAeS$ **5.13S** and $P^{t2}{}_mDEAeO$ **5.13O** indicated a strong preference for forming $(AB)_n$ chains rather than $(AB)_n$-A (Figure 5-22; Figure 5-23). Saturated polyisoxazoline $P^{t2}{}_mDEAeS$ **5.13S** appeared to

exclusively form $(AB)_n$ and $(AB)_n$-B chains (Figure 5-22). In chapter 3 MALDI-TOF analysis of the acetamide polymers did not give a clear spectrum for $P^t_mDEAeAc$ **3.26**. Analysis of the other acetamide polymers however indicated that polyisoxazolines had a greater preference for forming $(AB)_n$ compounds over polyisoxazoles. The ether linked polyisoxazole $P^t_mDEAyAc$ **3.27** also formed more $(AB)_n$ chains than the shorter chained polyisoxazole P^t_mDAyAc **3.24**. It may be therefore that the combination of ether link and isoxazoline drives the polymer to exclusively form $(AB)_n$ and $(AB)_n$-B chains. Unexpectedly however the MALDI spectrum of P^{t2}_mDEAeO **5.13O** includes $(AB)_n$-A, although at lower intensities than the $(AB)_n$ chains (Figure 5-23).

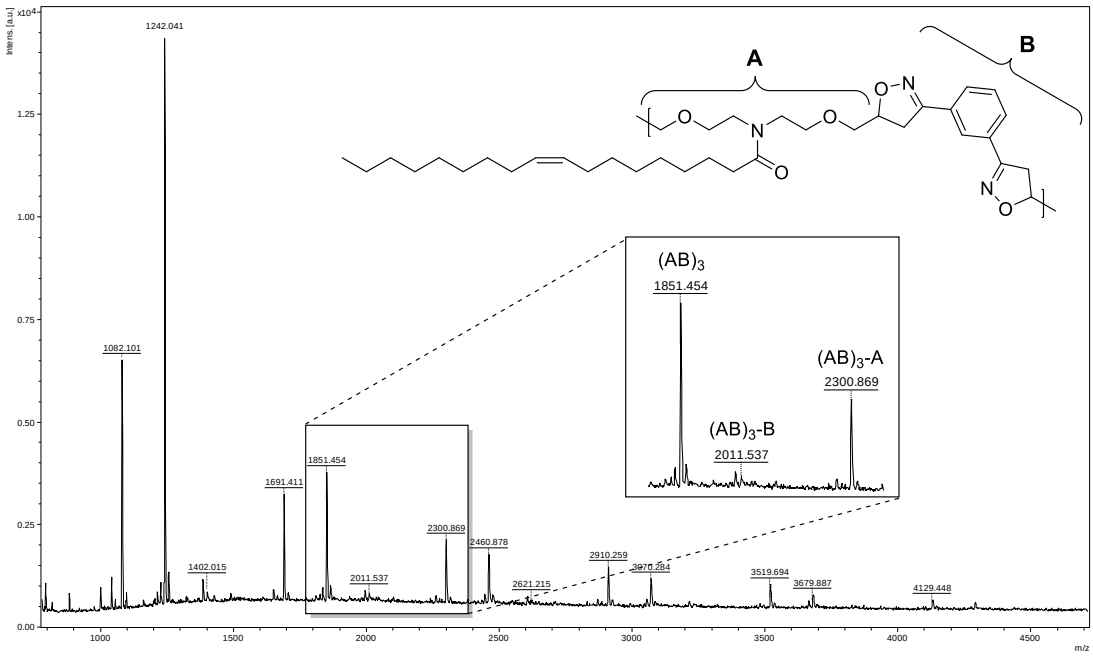

Figure 5-23: MALDI-TOF spectrum of P^{t2}_mDEAeO **5.13O**.

5.9 Polymers from non-stoichiometric ratios of monomers

To assess how different dipolarophilic groups **5.2-5.4** affected the extent of cross-linking in polymers, polymerisations were carried out using an excess of nitrile oxide precursor *meta*-OC **2.1** relative to stearic and oleic derived dipolarophilic monomers (**5.2-5.4)S/O**. In chapter 2 a similar study was done using commercially available diacrylates. This study indicated that excess nitrile oxide marginally increased glass transition temperature and led to the formation of $(AB)_n$ polymers almost exclusively. It was expected that excess nitrile oxide would form cyclical/furoxan containing stearic derived polymers with a marginal increase in their T_g relative to the respective polymers in sections 5.5-5.7. The oleic derived polymers however were predicted to have higher T_g's than their respective polymers in sections 5.5-5.7 due to increased crosslinking *via* the *cis*-alkene of the fatty chain.

5.9.1 Fatty acid derived polymers formed using excess *meta*-OC **2.1**

Polymers **(5.14 – 5.16)S/O** were synthesised from fatty acid derived dipolarophiles monomers (0.8 eq.) and excess *meta*-OC **2.1** (1 eq.) using the method described in section 5.5. Using the same nomenclature as in chapter 2, the ratio of dipolarophile relative to *meta*-OC **2.1** was presented as an Arabic numeral after the dipolarophile code. $P^{t2}{}_m$DAeS-0.8 **5.14S** therefore refers to a polymer formed using *meta*-OC **2.1** (1 eq.) and DAeS **5.3S** (0.8 eq.) using extended thermal conditions.

Scheme 5-10: Synthesis of polymers formed with uneven ratios of monomers

5.9.2 Assessment of cross-linking by ^{13}C and DSC analysis

The 500 MHz ^{13}C NMR spectra of both $P^{t2}{}_m$DAeO-0.8 **5.14O** and $P^{t2}{}_m$DEAyO-0.8 **5.16O** indicated cross-linking had occurred with weak signals around 86 ppm and 48 ppm. Like $P^{t2}{}_m$DEAeO **5.13O** the spectrum of $P^{t2}{}_m$DEAeO-0.8 **5.15O** did not show any evidence of cross-linking in 500 MHz ^{13}C NMR spectrum. This indicated that cross-linking in $P^{t2}{}_m$DEAeO-0.8 **5.15O** was limited compared to **5.14O** and **5.16O**,

Glass transition temperature (T_g) was a significant indicator of the extent of cross-linking in the unsaturated polymers **5.11O/L/Ln** and **5.12O/L/Ln** in sections 5.5 and 5.6. The polymers **(5.14 – 5.16)S/O** were analysed by DSC to determine how excess nitrile oxide had affected the polymer T_g's.. The stearic derived polymers (14a, 14c, 14e, Table 5-12) were used as a base line for any changes in T_g of the oleic derived polymers (14b, 14d, 14f Table 5-12). It was predicted that cross-linking would be most prevalent in the oleic derived polyisoxazole, (resulting in the greatest increase in Tg compared to stearic derived polymer), as terminal alkynes are less reactive than terminal alkenes in cycloaddition reactions.

	Polymer	T_g / ºC	ΔT_g / ºC
14a	$P^{t2}{}_m$DAeS-0.8 **5.14S**	86	+10
14b	$P^{t2}{}_m$DAeO-0.8 **5.14O**	84	+10
14c	$P^{t2}{}_m$DEAeS-0.8 **5.15S**	29	-2
14d	$P^{t2}{}_m$DEAeO-0.8 **5.15O**	15	+10
14e	$P^{t2}{}_m$DEAyS-0.8 **5.16S**	12	+7
14f	$P^{t2}{}_m$DEAyO-0.8 **5.16O**	8	+9

Table 5-12: T_g of polymers **(5.14 – 5.16)S/O** (*left*), difference to polymers formed from stoichiometric ratios of monomers (*right*)

Glass transition temperature (T_g) of both non-ether linked polyisoxazolines **5.14S** and **5.14O** increased by 10 ºC which suggests that there was a limited increase in cross-linking between $P^{t2}{}_m$DAeO **5.12O** and $P^{t2}{}_m$DAeO-0.8 **5.14O**. Ether linked stearic derived polyisoxazoline $P^{t2}{}_m$DEAeS-0.8 **5.15S** had a reduction in T_g (14c, Table 5-12). Analysis of **5.15S** by GPC and MALDI-TOF (appendix D) had suggested that it was mostly formed of low repeat unit cyclical chains, this may have reduced the polymers ability to pack leading to a reduction in T_g. A 10 ºC increase in T_g was recorded for $P^{t2}{}_m$DEAeO-0.8 **5.15O** which may indicate cross-linking had occurred, although no evidence of this was found in the ^{13}C NMR spectrum. Due to the suspected conformational change of $P^{t2}{}_m$DEAeS-0.8 **5.15S** it was not a reliable base-line for assessing cross-linking in **5.15O**. Polyisoxazole $P^{t2}{}_m$DEAyO-0.8 **5.16O** was the only polymer that gave an indication of increased cross-linking. Excess nitrile oxide caused the T_g of $P^{t2}{}_m$DEAyO-0.8 **5.16O** to increase by 9 ºC (14f, Table 5-12), which was 2 ºC more than the baseline of $P^{t2}{}_m$DEAyS-0.8 **5.16S** (14e, Table 5-12). As expected, the dialkyne monomer DEAyO **5.2O** appeared to show a higher propensity to form cross-linked polymers than the dialkene monomers DEAyO **5.3O** and DEAyO **5.4O**.

5.10 Post polymer modification investigation

Takata *et al.*[318] took advantage of the masked functionalities of isoxazole rings for post polymerisation modifications. After a trial of different reductive cleavage techniques Takata *et al.*[318] used an iron based method to convert polyisoxazoles to poly(β-aminoenones) and used $LiAlH_4$ to produce poly(β-amino alcohols). The poly(β-amino alcohols) were then crosslinked using aldehydes and isocyanates.

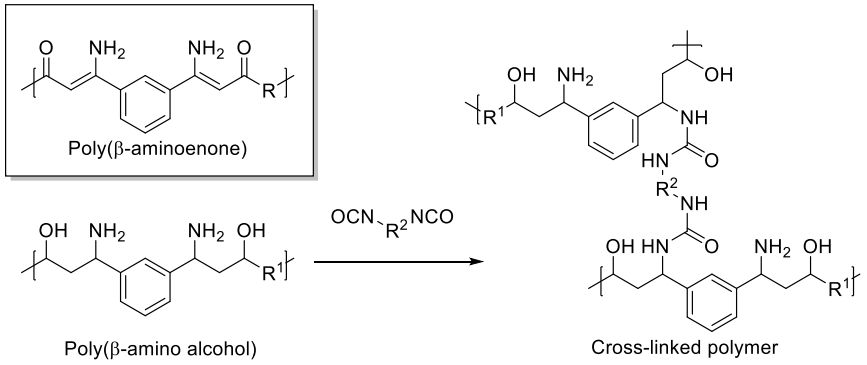

Figure 5-24: Polyisoxazole reductive cleavage products described by Takata[318] and subsequent cross-linking.

To determine whether similar reductive cleavage reactions could be performed on the fatty acid derived polymers, Takata's[318] methods were trialled on models. Research on the $LiAlH_4$ method in literature indicated a consensus that it achieved reductive cleavage with isoxazolines but when applied to isoxazoles it produced aziridines and it trialled with DIAc **4.5** from chapter 4.[278] The Fe based method was found to be successful outside of Takata's work[283] and so was trialled with a more representative model of fatty acid derived polyisoxazoles (O_mDEAyS-ABA **5.8**).

5.10.1 Reductive cleavage of isoxazoles with $LiAlH_4$

The diisoxazole **4.5** from the optimisation study in chapter 4 was used as the model for investigating the reductive cleavage of isoxazoles using $LiAlH_4$ under Takata's conditions.[318] DIAc **4.5** was placed under N_2 before dry THF was added and the solution cooled in an ice bath. $LiAlH_4$ (4M in Et_2O) was added slowly, temperature was then raised to reflux for 24 hours. Following this the reaction was cooled in an ice bath and quenched with saturated $NaSO_4$ solution and extracted with DCM. The organic layers were dried with $MgSO_4$ and reduced *in vacuo* to leave a crude red oil.

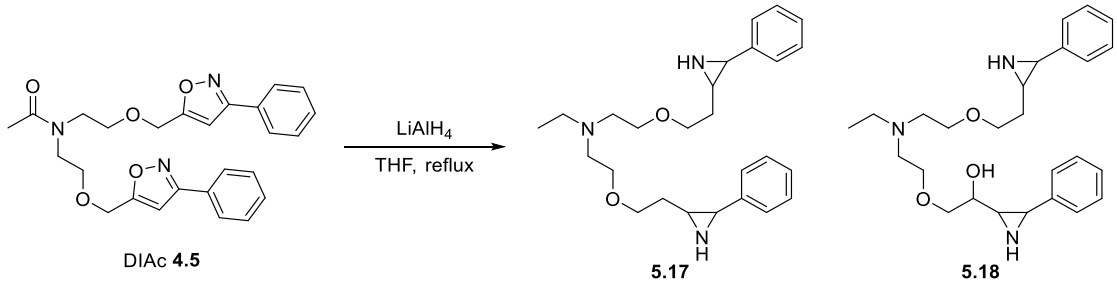

Scheme 5-11: Reduction of DIAc **4.5** using $LiAlH_4$

Analysis of the crude oil by mass spectroscopy revealed two masses, 424.4 Da and 440.4 Da, which related to protonated **5.17** and **5.18** respectively (Scheme 5-11). Analysis of the crude product by 500 MHz ^{1}H and ^{13}C NMR agreed with the mass spectroscopic analysis. The trial of $LiAlH_4$ as a reductive cleavage reagent for isoxazoles therefore did not agree with Takata but formed the more commonly reported aziridine.[278] Takata *et al.*[318] may have also formed a polyaziridine rather than the poly(β-amino alcohols) reported. A proof of the formation of poly(β-amino alcohols) was it's ability to crosslink using both a dialdehyde and diisocyanate driven by amine reactions. After crosslinking with the dialdehyde and diisocyanate Takata *et al.*[318] reported evidence of imine and urea formation respectively. As aziridines are established crosslinkers[358] and can undergo ring opening polymerisation,[359] it may be that a polyaziridine was formed by Takata *et al.*[318] and underwent crosslinking reactions similar to those anticipated (Figure 5-25).

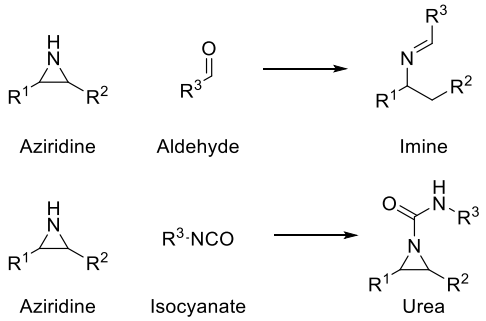

Figure 5-25: Potential crosslinking reactions of aziridine.

5.10.2 Reductive cleavage of isoxazoles with iron

Isoxazole reductive cleavage using iron is well established in the literature and results in a variety of different products depending on how the reaction is worked up.[282,360] Following Takata's method[318] and a similar reductive cleavage method that was

applied to a small molecule,[283] iron was trialled as reductive cleavage reagent using the model of stearic derived polyisoxazole O_mDEAyAc-ABA **5.8** from section 5.4.

This method was trialled under aerobic conditions by stirring **5.8**, iron powder and NH_4Cl in MeOH and DMF at 110 ºC. The mixture was initially clear and colourless with the iron powder mostly attached to the magnetic follower, after 2 hours the mixture was opaque with a deep orange colour. The reaction was monitored by TLC and 300 MHz ^{1}H NMR, samples were taken after 24, 48 and 72 hours but analysis showed no change from the starting material **5.8**. After 72 hours the reaction was cooled to room temperature then diluted with DCM. The mixture was filtered through a celite pad topped with silica. The organic filtrate was washed with 1M HCl followed by water and brine. The organic layer was dried with $MgSO_4$ and reduced *in vacuo* to recover a white solid. Analysis by mass spectroscopy and 300 MHz ^{1}H NMR indicated that the starting material **5.8** had been recovered with no evidence of ring opening.

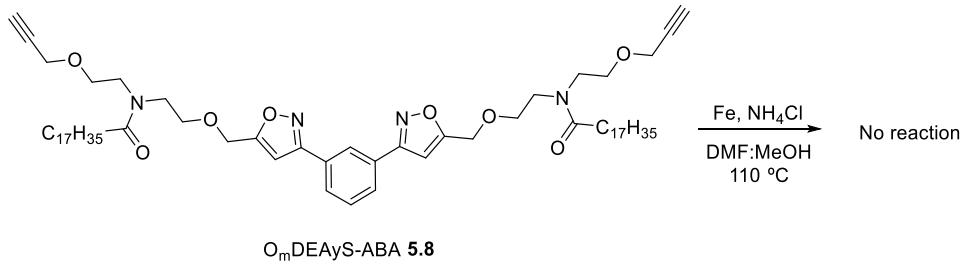

O_mDEAyS-ABA **5.8**

Scheme 5-12: Isoxazole reductive cleavage attempt using an iron based method.

Conditions were not specified as aerobic or anaerobic in either of the literature sources for the iron reductive cleavage method.[283,318] The reaction was therefore redone under anaerobic condition using dry solvents. As with the aerobic conditions the reaction mixture begins as a clear colourless solution with the iron powder attached to the magnetic follower. After 24 hours at 80 ºC the reaction mixture was still clear but with a slight orange tint. A sample was taken and analysis by TLC and 300 MHz ^{1}H NMR, no change could be seen from the starting material **5.8**. The reductive cleavage mechanism using iron requires water for the final step,[292] water was therefore added to the reaction which caused the mixture to become green. After 4 hours the reaction was cooled to room temperature and worked up in the same manner as the aerobic reductive cleavage trial. Analysis of the recovered white solid by mass spectroscopy and ^{1}H NMR revealed that once again only starting material had been recovered with no evidence of ring opening.

5.11 Summary and conclusion

Dipolarophilic monomers were derived from the five most common fatty acids found in vegetable oils. Dialkyne and dialkene monomers were produced as they were predicted to form polymers with different physical characteristics. As expected, the fatty acid derived polymers **5.11**, **5.12** and **5.13** had significantly lower T_g's than their related acetyl-based model polymer **3.24**, **3.26** and **3.27** in chapter 3. As reported in chapter 3 the polyisoxazoles **5.11P/S/O/L/Ln** had significantly lower T_g's than the polyisoxazolines **5.12P/S/O/L/Ln**, this was mostly caused by the ether link in the polyisoxazoles **5.11P/S/O/L/Ln**. Crosslinking was more evident with the polyisoxazoles derived from unsaturated fatty acids **5.11O/L/Ln** than in the related polyisoxazoline compounds **5.12O/L/Ln**. This was believed to be due to terminal alkynes being less reactive towards cycloaddition reactions than terminal alkenes.

To investigate the effect of end groups on crosslinking stearic and oleic derived polymers were formed using excess nitrile oxide to encourage crosslinking in oleic derived polymers. No strong trends were found in this work, although there was an indication that alkynes were more susceptible to crosslinking than the related alkene monomers.

An investigation into post-polymer modification was carried out using reactions taken from Takata's polyisoxazoline reductive cleavage paper.[318] The two methods that were trailed were unsuccessful. Literature sources predicted that the $LiAlH_4$ based method would fail to make a β-amino alcohol[278] but supported the iron based method.[283] The failure of the iron based method may therefore be due to other functional groups in the compound such as the combination of the amide and ether link. Further study is being done on the reductive cleavage of these fatty acid derived isoxazole compounds.

6.0 Vanillin derived oximoyl chlorides

6.1 Introduction

Previous chapters have looked at using different dipolarophiles, from commercially available diacrylates to fatty acid derived monomers, whilst polymerisations have all used the same nitrile oxide precursor, *meta*-OC **2.1**. To make a truly renewably derived nitrile oxide-dipolarophile cycloaddition polymer a nitrile oxide precursor must be derived from a renewable feedstock.

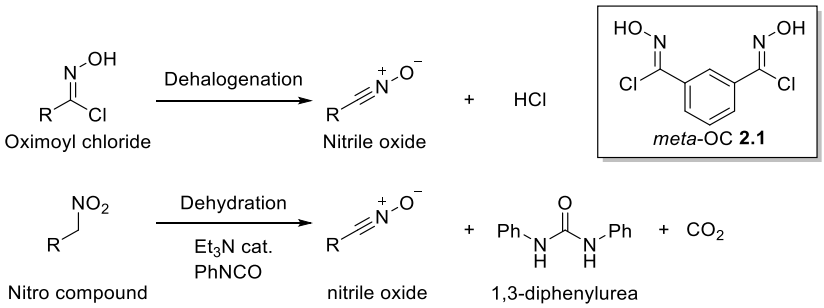

Figure 6-1: Methods of nitrile oxide synthesis; *meta*-OC **2.1** shown in box.

Due to their reactivity nitrile oxides must be formed in situ, the two of the most common methods used to achieved this are dehalogenation of an oximoyl chloride or dehydration of nitro compounds (Mukaiyama-Hoshino method) (Figure 6-1).[217] The Mukaiyama-Hoshino method is not atom efficient, producing a 1,3-diphenylurea by-product,[217] it is therefore is not suitable for polymerisations. Oximoyl chlorides are easily formed from aldehydes by a two-step synthesis,[272] whilst their dehalogenation is a more atom efficient method of generating nitrile oxides, only creating HCl as the by-product (depending on conditions).

6.1.1 Nitrile oxide stabilisation

Nitrile oxides are generally short-lived reactive species which undergo a variety of reactions in the absence of a suitable dipolarophile. The half-life of aliphatic nitriles is significantly lower than aromatic nitrile oxides, it can be increased with bulky substituents on the α-carbon of aliphatic compounds or in the *ortho* position of aromatic compounds.[258,260]

Aromatic nitrile oxides are more stable than aliphatic nitrile oxides due to the increased number of resonance contributions that can be considered to describe their structures (Figure 6-2). These resonance contributions have formal charges *ortho* and *para* to the nitrile oxide, consequently both electron withdrawing and electron donating substituents should stabilise nitrile oxides in these positions. There has been limited investigation into such substituent effects, those reported have focussed on the kinetics of nitrile oxide cycloaddition and have shown substituents to have negligible effects on the rate of this reaction.[262,263,361,362] These studies have indicated that aromatic nitrile oxides are stabilised by electron donating groups *para* to the nitrile oxide, whilst electron withdrawing groups have been reported to increase the rate of reactions when *para* or *meta* to nitrile oxides.[262,263,361,362]

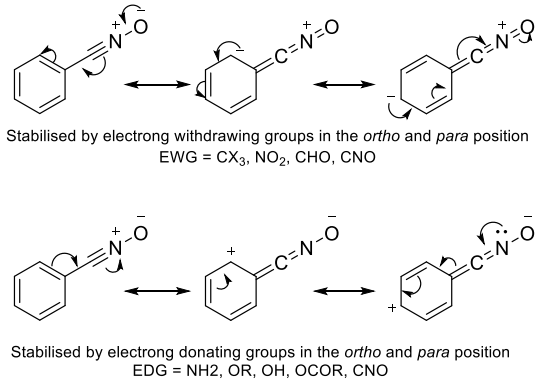

Figure 6-2: Resonance forms of aromatic nitrile oxides.

6.2 Aims and objectives

Polyisoxazoles and polyisoxazolines were formed using renewably derived dipolarophiles in chapter 5. To make a truly renewably derived nitrile oxide/dipolarophile cycloaddition polymer the nitrile oxide monomer must also be derived from a renewable source. In chapters 2 – 5 nitrile oxide monomers have been formed *in situ* from petroleum derived *meta*-OC **2.1**. To discover a viable renewable aromatic aldehyde feedstock, initially the stability of a range monofunctional aromatic oximoyl chlorides was investigated. One such renewable aromatic aldehyde is vanillin **6.1** and this was chosen as a renewable aromatic feedstock. Nitrile oxide precursors were derived from vanillin and used to form bio-derived polyisoxazoles. Vanillin was also explored as a feedstock for dipolarophile monomers and dual functional monomers to form completely vanillin derived polyisoxazoles.

- Aromatic oximoyl chlorides were synthesised with a range of ring substituents. The effect of ring substituents on oximoyl chloride stability was assessed using TGA.
- The correlation between oximoyl chloride thermal stability and reactivity in cycloaddition reactions was determined by a conversion study.
- Vanillin **6.1** was chosen as viable renewable aromatic aldehyde feedstock and used to form oximoyl chloride pre-monomers.
- The vanillin derived oximoyl chlorides were used along with DEAyS **5.2S** to form fully bio-derived polyisoxazoles and compared to $P^{t2}{}_{m}$DEAyS **5.11S**.
- Vanillin **6.1** was then explored as a feedstock for dipolarophile monomers.
- Polyisoxazoles formed from vanillin derived dipole and dipolarophile were characterised.
- Finally, a dual functional monomer containing both an alkyne and an oximoyl chloride was derived from vanillin and used to form homopolymers in the standard solvent based conditions and in a solvent free synthesis.

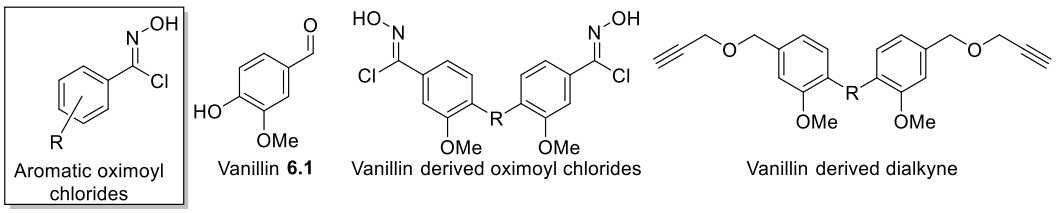

Figure 6-3: Monomer types derived from renewable vanillin for use in polyisoxazole synthesis.

6.3 The effect of substituents on the formation of nitrile oxides.

The stability of aromatic nitrile oxides is affected by substituents on the ring. It was believed that this would also influence the stability of oximoyl chlorides and alter the ease with which decomposition to nitrile oxides could be achieved. To study the effect of aromatic ring substituents on nitrile oxide formation, a variety of oximoyl chlorides were synthesised and their thermal stability tested by thermal gravimetric analysis.

6.3.1 Synthesis of oximoyl chlorides

Oximoyl chlorides **6.4a-j** were synthesised with electron donating and withdrawing groups at various positions on the aromatic ring (Scheme 6-1;Table 6-1). An oximoyl chloride **6.4i** was also formed from terephthalaldehyde **6.2i** (Figure 6-4), which allowed for a comparison with *meta*-OC **2.1** and gave an insight into the electronic effects of oximoyl chlorides and nitrile oxides on each other within a ring.

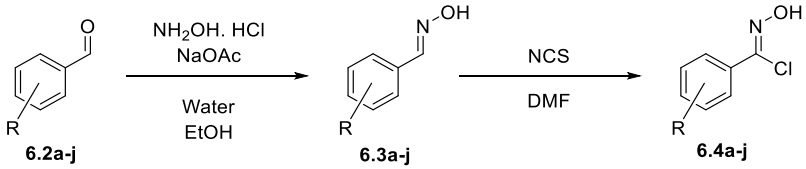

Scheme 6-1: aromatic aldoxime and oximoyl chloride synthesis

Entry	R	**6.3** Yield / %	**6.4** Yield / %[a]
1a	2-OMe **a**	92	78[b]
1b	3-OMe **b**	89	88
1c	4-OMe **c**	53	73
1d	4-F **d**	89	96
1e	4-CF_3 **e**	91	97
1f	3,4-OMe **f**	96	94
1g	3,4,5-OMe **g**	93	94
1h	4-AcO-3-OMe **h**	30	92
1i	4-CHO **i**	76	72
1j	4-OH-3-OMe **j**	83	-

a- evidence of some chlorination on the aromatic from NMR. b-evidence of furoxan formation (12 % impurity).

Table 6-1: Yield of aldoxime and oximoyl chloride synthesis

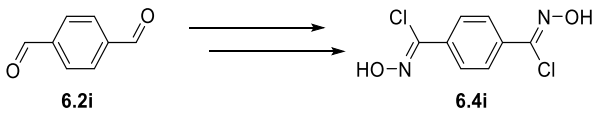

Figure 6-4: Synthesis of terephthalaldehyde derived **6.4i**

The oximes **6.3a-j** were formed using a similar method to *meta*-OC **2.1** (section 2.3.1) and benz-OC **4.1** (section 4.3) synthesis (Scheme 6-1;Table 6-1; Figure 6-4). Trisubstituted aldehyde **6.2g** was insoluble in the ethanol : water mixture at room temperature and so the reactions were heated to reflux to increase solubility. Acetyl bearing aldehyde **6.2h** was also sparingly soluble but was not heated due to the risk of hydrolysing the ester. To protect the ester, **6.3h** was synthesised using a stoichiometric ratio of reactants at room temperature overnight. In some reactions a white precipitate formed which allowed these oximes to be collected by Büchner filtration giving a pure white solid (**6.3a/g/i**). Oximes **6.3b/c/d/e/f/h** were poured into water and extracted with EtOAc, these required further purification by recrystallisation or column chromatography which resulted in white solids except for 3-methoxy benzaldoxime **6.3b** which was a clear oil.

As with *meta*-OC **2.1** and benz-OC **4.1**, oximoyl chlorides **6.4** were formed by taking the aldoximes **6.3** into DMF, then introducing NCS in five parts over the course of one hour to reduce the risk of thermal runaway. This was sufficient for the majority of the oximoyl chlorides (**6.4b-i**), but 2-methoxy benzoximoyl chloride **6.4a** generated the nitrile oxide in situ resulting in furoxan **6.5** (Figure 6-5). To form **6.4a**, NCS was added in 10 parts over 2 hours with careful monitoring of temperature, never allowing it to exceed 40 °C and reducing solvent *in vacuo* at 30 °C.

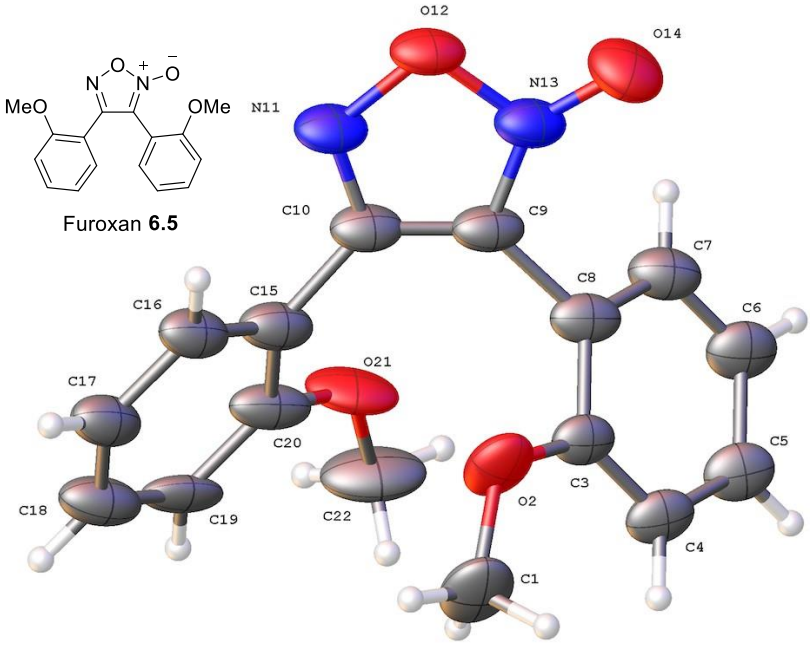

Figure 6-5: Solid state structure of 3,4-bis(2-methoxyphenyl) furoxan **6.5** determined by X-ray crystallography.

The chlorination step proceeded well to form oximoyl chlorides with small amounts of impurities. In some cases, the impurities could be removed by recrystallisation (**6.4c/f/g**) it was however not possible to remove impurities where chlorination of the aromatic ring occurred. More electron rich aromatics increased the occurrence of ring chlorination. Purification of **6.4h** and **6.4j** was not possible as recrystallisation and column chromatography caused decomposition of the oximoyl chloride. Oximoyl chloride **6.4h** only contained minor levels of impurities (< 5 %) and so was used for thermal analysis directly. Even with attempts to reduce side reactions and decomposition, (as with **6.4a**), the synthesis of **6.4j** resulted in the oximoyl chloride as a minor fraction relative to impurities, any thermal analysis data would not be accurate.

6.3.2 Thermal analysis of oximoyl chlorides

To investigate the effect that different substitutes had on the formation of nitrile oxides the oximoyl chlorides were analysed by TGA. At elevated temperatures oximoyl chlorides degrade to form nitrile oxides, releasing gaseous HCl. The oximoyl chlorides (**2.1**, **4.1**, **6.4a-i**) were heated at 10 °C min^{-1} and the temperature at which the percentage weight loss reached the calculated weight loss of complete oximoyl chloride degradation (T_E) were compared (Table 6-2).

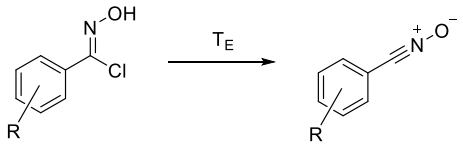

2.1/4.1/6.3a-i

Figure 6-6: Thermal decomposition of oximoyl chloride to nitrile oxide, T_E = complete degradation temperature

Entry	R	T_5 / ºC	T_{10} / ºC	T_E/ ºC
2a	2-OMe **6.4a**	132	150	178
2b	3-OMe **6.4b**	160	180	200
2c	4-OMe **6.4c**	135	164	194
2d	4-F **6.4d**	158	171	188
2e	4-CF_3 **6.4e**	176	190	199
2f	3,4-OMe **6.4f**	166	183	202
2g	3,4,5-OMe **6.4g**	228	248	258
2h	4-AcO-3-OMe **6.4h**	177	200	216
2i	4-CClNOH **6.4i**	183	190	219
2j	H **4.1**	138	154	184
2k	3-CClNOH **2.1**	163	171	213

Table 6-2: Thermal analysis of oximoyl chlorides **2.1**, **4.1**, and **6.4a-i** by TGA

Thermal analysis of the oximoyl chlorides shows that some substituent groups have a strong effect on the temperature at which the oximoyl chloride degrades to form nitrile oxide. Having either electron withdrawing or electron donating substituents on the ring increased the T_E relative to benz-OC **4.1** except for **6.4a** (2-methoxy group) where the T_E was lower (2a & 2j, Table 6-2, $\Delta T_E = -8$ °C), presumably due to a degree of steric release on moving to the linear nitrile oxide. A strong electron donating group (OMe) in the *para* position **6.4c** had a similar effect on T_E as having a strong electron withdrawing group (CF_3) **6.4e** (2c & 2e, Table 6-2, $\Delta T_E = 5$ °C) the major difference was in their onset of degradation (2c & 2e, Table 6-2, $\Delta T_5 = 41$ °C). The temperature of onset of degradation (T_5) of **6.4a** and **6.4c** were lower than benz-OC **4.1** (2a & 2j, Table 6-2, $\Delta T_5 = -3$ °C; 2c & 2j, Table 6-2, $\Delta T_5 = -6$ °C), which indicates that electron donating groups in the ortho and para position slightly promote the onset of oximoyl chloride degradation relative to unsubstituted benz-OC **4.1**. The methoxy group in the *meta* position **6.4b** however increases the T_5 by 22 °C relative to benz-OC **4.1** and the strong electron withdrawing group **6.4e** increases it by 38 °C.

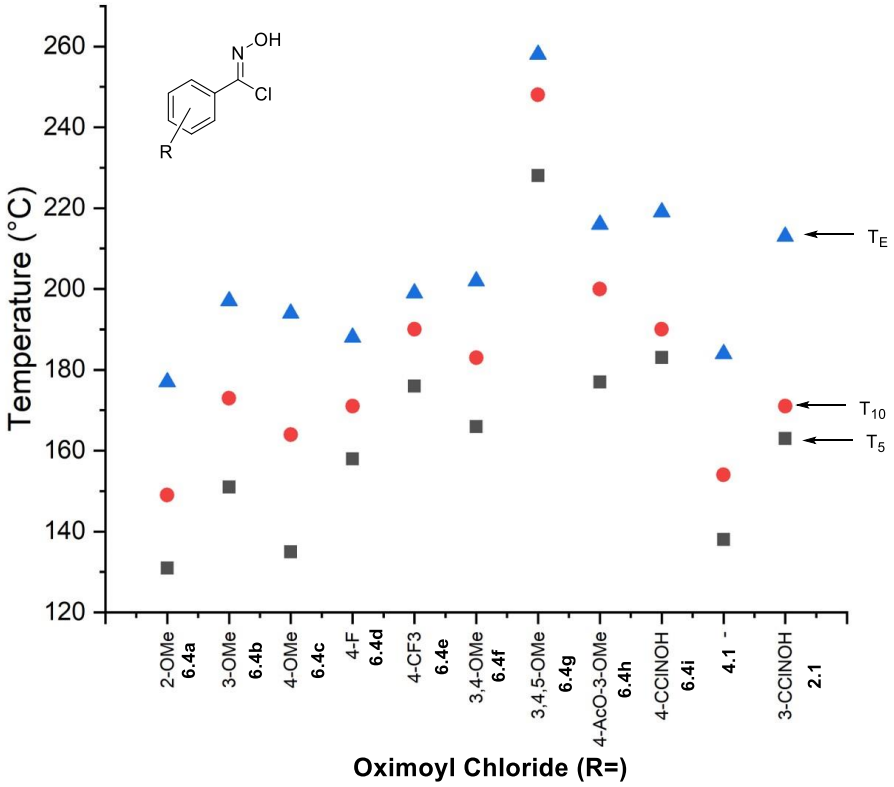

Figure 6-7: TGA summary of oximoyl chlorides *meta*-OC **2.1**, benz-OC **4.1**, **6.4a-i**

Increasing the number of substituents appears to increase oximoyl chloride stability, **6.4f** (3,4-OMe) has a higher T_5 and T_E than **6.4a-c** ($\Delta T_5 = 6$ °C, $\Delta T_E = 2$ °C), this effect

is further exemplified by **6.4g** (3,4,5-OMe) which was a considerably more thermally stable than any of the other compounds. Acetyl bearing **6.4h** (4-Ac-3-OMe) was more stable than **6.4f** (ΔT_E = 17 °C), possibly because the acetyl group in the para position is a weaker EDG than the methoxy group of **6.4f**. The oximoyl chloride group is electron withdrawing and has a greater stabilising effect in the para position (**6.4i**) compared to the meta position (*meta*-OC, **2.1**).

6.3.3 Conversion studies

In order to understand how the thermal degradation of oximoyl chlorides effected to their behaviour in a reaction, three oximoyl chlorides from section 6.3.2 were reacted with DEAyS **5.2S**. The reaction conditions were the same as initially used for the benz-OC **4.1** and DEAyAc **3.8** conversion studies in section 4.4, which would allow for tentative comparison with the reactivity of benz-OC **2.1**. The oximoyl chlorides (**6.4f-h**) were chosen as they had a range of T_E's.

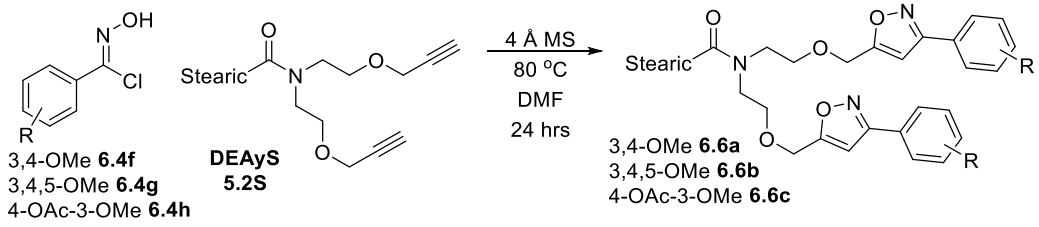

Scheme 6-2: Synthesis of diisoxazole DEAyS **5.2S** using **6.4f-g** to determine conversion

The conversion of the alkyne **5.2S** into isoxazoles **6.6a-c** was determined using 400 MHz ^{1}H NMR of the crude products, as in chapter 4. Due to the aliphatic chain of DEAyS **5.2S** it was not possible to use the shift at 2.4 ppm, (which related to the terminal alkyne proton), to measure conversions, instead it was calculated using the integral of the shift around 4.6 ppm (H^a, Figure 6-8), and comparing it to the integral of the shift around 4.1 ppm (H^c, Figure 6-8).

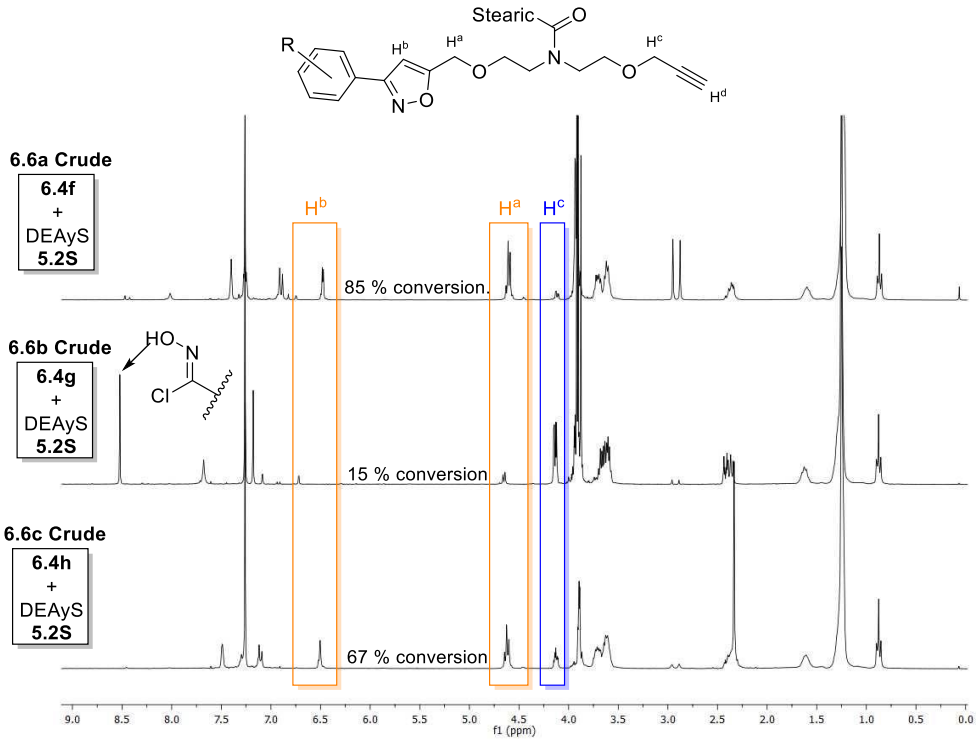

Figure 6-8: ^{1}H NMR spectra of crude product after reaction of **6.4f-h** with DEAyS **5.2S**

As expected, the calculated conversions (**6.6a-c,** Figure 6-8; 3a-c, Table 6-3) show a strong inverse correlation with oximoyl chloride thermal stability, (as T_E and T_5 increases the conversion of alkyne to isoxazoles reduces). Although not directly comparable, conversion of benz-OC **4.1** (the least thermally stable oximoyl chloride) and DEAyAc **3.8** to isoxazole using the same conditions in chapter 4 fits this trend (3d, Table 6-3).

Entry	Oximoyl chloride R =	T_5	T_{10}	T_E	Conversion to alkyne / %
3a	3,4-OMe **6.4f**	166	183	202	85 – **6.6a**
3b	3,4,5-OMe **6.4g**	228	248	258	15 – **6.6b**
3c	4-AcO-3-OMe **6.4h**	177	200	216	67 – **6.6c**
3d	H **4.1**	138	154	184	87[a]
3e	3-CClNOH **2.1**	163	171	213	-

a - Section 4.5 - average conversion of benz-OC **4.1**, DEAyAc **3.8**, 4 Å MS, DMF, 80 °C, 24 hrs.

Table 6-3: Thermal stability of oximoyl chlorides and their % conversion to isoxazoles after 24 hours

When it comes to designing novel nitrile oxide precursor monomers those with lower T_E's would be preferable as they will achieve a greater degree of conversion given the same time frame. However, a balance must be found as compounds with lower T_E's will have a higher risk of forming furoxan links if the nitrile oxides are forming too

quickly. Disubstituted oximoyl chlorides **6.4f** and **6.4h** (3a & 3c, Table 6-3) have similar T_E's to *meta*-OC **2.1** (3e, Table 6-3) and so monomers based on these structures would presumably have a similar reactivity. Dimethoxy **6.4f** has a lower T_E than *meta*-OC **2.1** (3a & 3e, Table 6-3, ΔT_E = − 11 °C), and a monomer based on this structure would presumably be more reactive. Vanillin **6.1,** a renewable source of aromatic aldehyde, can be used as the feedstock for **6.4f** and **6.4h**. Monomers with a similar T_E's to **6.4f** and **6.4h** can therefore presumably be formed by linking together two vanillin molecules by either an ether (similar to **6.4f**) or an ester (similar to **6.4h**), (Figure 6-9).

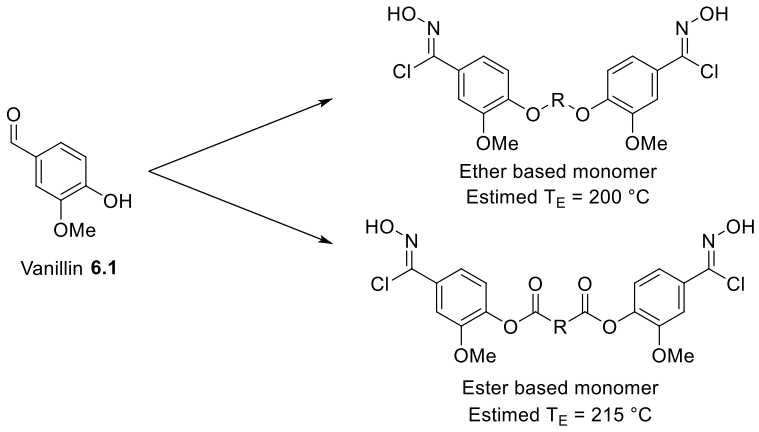

Figure 6-9: Nitrile oxide precursors derived from vanillin

The results of the conversion study also clarified the polymerisation issues discovered in section 4.6. During the optimisation trials using benz-OC **4.1** and DEAyAc **3.8** it was found that using milder conditions of 3 Å MS and 25 °C gave the highest conversion of 95 %. However, when these conditions were applied to a polymerisation reaction using *meta*-OC **2.1** instead of benz-OC **4.1** they gave a low yield (8 %) of low molecular weight polymers after 14 days. The conversion study in this chapter now sheds light onto this observation in that it has shown that oximoyl chloride reactivity relates to its T_E. Consequently, as benz-OC **4.1** has a considerably lower T_E than *meta*-OC **2.1** (3d & 3e, Table 6-3, ΔT_E = − 29 °C) the "optimised" conditions were appropriate to cause benz-OC **4.1** to decompose to nitrile oxide but not strong enough for the monomer precursor *meta*-OC **2.1.**

6.4 Renewably derived oximoyl chlorides

A completely renewably sourced polymer has been the aim throughout. Whilst the polymers in chapter 5 had renewably sourced dipolarophiles the nitrile oxide source originated from isophthalaldehyde **2.11**, a non-renewable feedstock. From the thermal study in section 6.3 vanillin **6.1** was chosen as an appropriate feedstock. Vanillin provides the required aromatic aldehyde as well as a phenol that could be used to form a di-functionalised molecules, from which di(oximoyl chloride) monomers could be synthesised with thermal stability similar to *meta*-OC **2.1**.

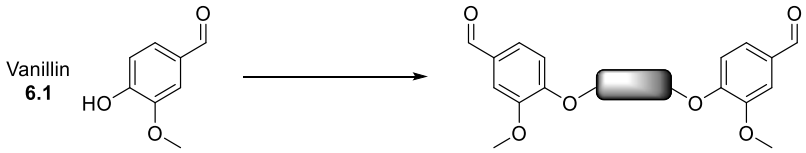

Figure 6-10: *Bis*-vanillin molecule linked *via* the phenol group.

The work in section 6.3 found that the type of substituents on the aromatic ring effected the T_E which was then found to relate to the conversion of oximoyl chloride to isoxazole. An ester group *para* to the oximoyl chloride **6.4h** gave a similar T_E to *meta*-OC **2.1** (3c & 3e, Table 6-3, ΔT_E = +3 ºC), suggesting that an ester linked vanillin derived oximoyl chloride would have a similar reactivity as a monomer. However, an ether group *para* to the oximoyl chloride **6.4f** decreased the T_E relative to *meta*-OC **2.1** (3a & 3e, Table 6-3, ΔT_E = −14 ºC), indicating an ether linked vanillin derived monomer would be expected to react faster than *meta*-OC **2.1** in polymerisation reactions.

6.4.1 Synthesis of renewable oximoyl chlorides

The ether linked vanillin **6.7a** was formed by refluxing vanillin **6.1** in acetone with K_2CO_3 and 1,4-dibromobutane for 48 hours (Scheme 6-3). The dialdehyde product **6.7a** was present as white precipitate that was collected by Büchner filtration, washing the precipitate with cold acetone and water left a pure white solid **6.7a** (72 %).

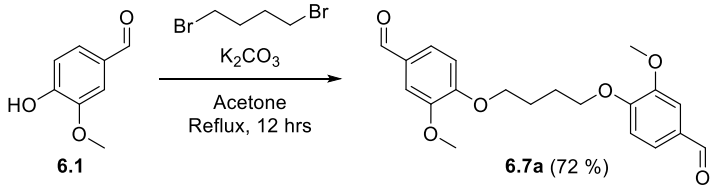

Scheme 6-3: Synthesis of ether linked vanillin **6.7a**

The ester linked dialdehyde **6.7b** was formed in a similar manner although due to the reactivity of succinyl chloride this reaction was done under N_2 and with dry acetone. A precipitate did not form and so after 4 hours the acetone was removed *in vacuo*. The residue was taken into EtOAc and washed with water and brine to leave a crude solid. To purify by column chromatography the solid required dry loading. When this was carried out however the product loaded silica would not wet when placed on the column. The column was still run however it caused the dialdehyde to come out over an extremely long period of time which caused significant overlap with a more polar impurity. Due to the complications during purification a low yield of **6.7b** was recovered as a pure white solid (29 %).

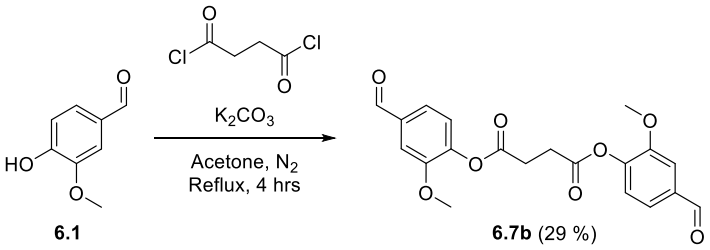

Scheme 6-4: Synthesis of ester linked vanillin **6.7b**

Formation of the oximes was done in the same manner as with previous compounds (sections 2.3.1, 4.3, and 6.3.1). Neither **6.7a** or **6.7b** dissolved in the water : ethanol (1 : 1) solvent mixture at room temperature. The 4-carbon linked **6.7a** could be heated to reflux to increase solubility, it formed a precipitate during the reaction that could be collected by filtration, resulting in a high yield of **6.8a** as a pure white solid (94 %). As in section 6.3 where **6.4h** was not heated in order to preserve the ester linkage **6.7b**. To further protect the ester bond in **6.7b** it was used in a slight excess compared to $NH_2OH.HCl$ and NaOAc, however these precautions were not sufficient and purification by column chromatography resulted in a 7 % yield of pure white **6.8b**.

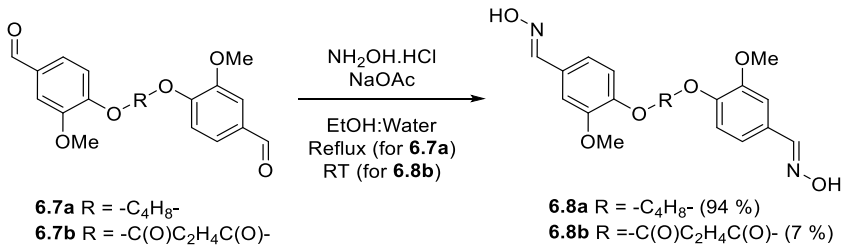

Scheme 6-5: Synthesis of aldoximes **6.8** from linked vanillin molecules **6.7**.

Chlorination to form the oximoyl chloride monomers **6.9a** and **6.9b** was achieved using NCS. When poured into cold water **6.9a** formed a precipitate that was collected

by Büchner filtration. Due to the two strong electron donating substituents on the ring some ring chlorination was to be expected. Some impurities were evident in the 400 MHz ^{1}H NMR spectrum and so the monomer was purified by recrystallisation from acetone, leaving a white solid (63 %). Ester linked **6.9b** did not form a precipitate when introduced into cold water, instead forming an emulsion. It was therefore extracted using EtOAc, then washed with brine and the solvent removed *in vacuo* to leave a white solid (78 %). The monomer (**6.9b**) was not further purified and only 98 mg of monomer was recovered, furthermore the small impurity peaks in the 400 MHz ^{1}H NMR spectrum were determined to be caused by ring chlorination which would be difficult to separate and should not interfere with polymerisation.

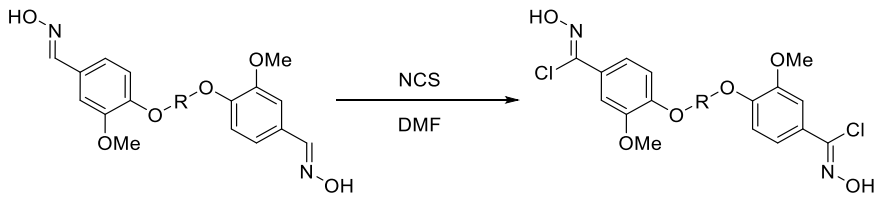

Scheme 6-6: Synthesis of oximoyl chloirdes **6.9** from linked vanillin aldoximes **6.8**.

6.4.2 Thermal analysis of renewably derived oximoyl chlorides

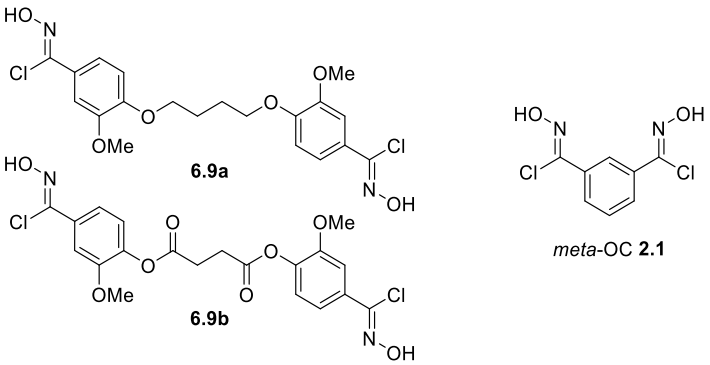

Figure 6-11: Oximoyl chlorides: *meta-OC* **2.1**, **6.4f/h**, **6.9a/b**.

The two renewably derived oximoyl chlorides **6.9a** and **6.9b** were analysed by TGA, heating the compounds under N_2 from 25 ºC to 600 ºC at 10 ºC / min. From the results of section 6.3 it was anticipated that ester linked **6.9b** would be slightly more thermally stable than **6.9a** and have a similar stability to *meta*-OC **2.1**.

As predicted, the ester linked **6.9b** has similar thermal stability to *meta*-OC **2.1** (4b & 4c, Table 6-4, ΔT_5 = 1 ºC, ΔT_E = 4 ºC), however the ether linked monomer **6.9a** (4a, Table 6-4) had a higher thermal stability than expected (higher than both **6.9b** and *meta*-OC **2.1** (4b & 4c, Table 6-4). The temperature at which full elimination of HCl

was reached (T_E) was 9 °C higher for **6.9a** than **6.9b**, the more significant difference however was in the onset of decomposition temperature (T_5) which was 25 °C higher for the ether linked monomer **6.9a**. From the thermal analysis of the vanillin derived monomers, the ether linked oximoyl chloride **6.9a** was now expected to be less reactive than the ester linked monomer **6.9b** and *meta*-OC **2.1** in polymerisations.

Entry	Oximoyl Chloride	T_5	T_{10}	T_{20}	T_E
4a	**6.9a**	189	198	263	218
4b	**6.9b**	164	190	244	209
4c	*Meta*-OC **2.1**	163	171	193	213

Table 6-4: TGA data of *meta-OC* **2.1**, **6.9a/b**.

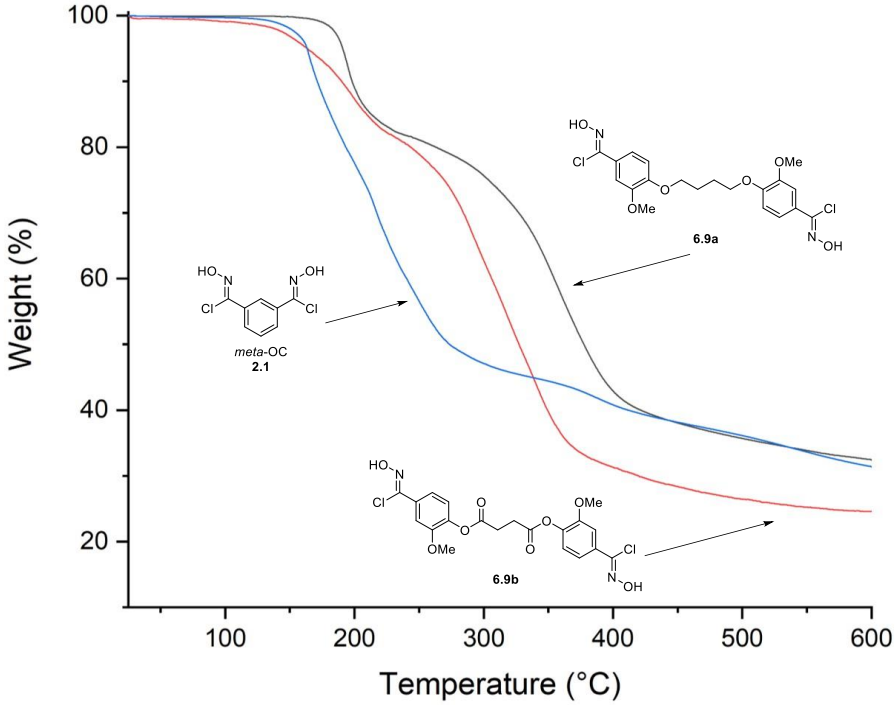

Figure 6-12: TGA plot of *meta*-OC **2.1**, **6.9a**, and **6.9b**

6.4.3 Polymerisation using renewably derived oximoyl chlorides

The two vanillin derived oximoyl chloride monomers **6.9a** and **6.9b** were used for polymerisations with the fatty acid derived dialkyne DEAyS **5.2S** to form completely renewably derived polymers. Polymerisations were performed using the extended thermal conditions (P^{t2}), polymer work up was the same as used in previous chapters (chapters 2 – 5). Polymer nomenclature was also the same as in previous chapters although using a subscript '**6.9a**' or '**6.9b**' in place of 'm' in reference to the oximoyl chloride used.

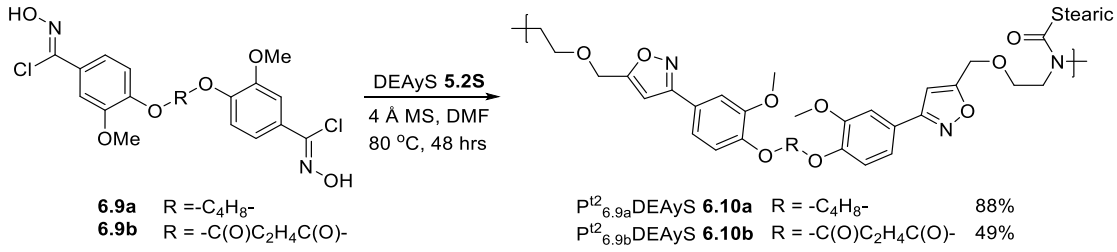

Scheme 6-7: Synthesis of completely renewably derived polymers **6.10a** and **6.10b**.

Both vanillin derived nitrile oxide precursors **6.9a-b** resulted in fully renewably derived polymers **6.10a-b** when reacted with DEAyS **5.2S**. The ether linked oximoyl chloride **6.9a** → **6.10a** (5a, Table 6-5) resulted in a higher yield than the ester linked nitrile oxide precursor **6.9b** → **6.10b** (5b, Table 6-5), both polymers/oligomers were recovered as malleable brown solids. The materials were soluble in $CHCl_3$ and so were analysed by 500 MHz ^{1}H and 125 MHz ^{13}C NMR. Proton NMR indicated that oximoyl chlorides functional groups were still present in the oligomers **6.10a** and **6.10b** with weak resonance peaks around 10 ppm that relate to the hydroxyl group of the oximoyl chloride. End group analysis by 500 MHz ^{1}H NMR estimated $P^{t2}_{6.9a}$DEAyS **6.10a** to contain more repeat units on average than $P^{t2}_{6.9b}$DEAyS **6.10b**. GPC estimations of molecular weight agreed with end group analysis and indicated that $P^{t2}_{6.9a}$DEAyS **6.10a** contained more repeat units on average.

Entry	Polymer	RU MW	Yield / %	RU NMR	M_n / kDa[a]	M_w / kDa[a]	$Đ$	M_n / RU[b]	M_w / RU[b]
5a	$P^{t2}_{6.9a}$DEAyS **6.10a**	831.5	88	5.5	10.3	32.4	3.1	12.3	39.0
5b	$P^{t2}_{6.9b}$DEAyS **6.10b**	859.5	49	3.5	7.7	14.9	1.9	9.0	17.3
5c	P^{t2}_{m}DEAyS **5.11S**	607.4	84	10	4.8	12.7	2.7	7.9	20.9

a-GPC estimates, $CHCl_3$ used as eluent against PS standards, b-Calculated by division of GPC estimates by RU MW

Table 6-5: Yield, repeat unit and GPC estimates for **6.10a** and **6.10b**, **5.11S** shown for comparison.

Oximoyl chloride monomer **6.9b** was expected to have a similar reactivity to *meta*-OC **2.1**, however the 500MHz ^{1}H NMR spectra of both the polymers **6.10a** and **6.10b** showed unreacted monomer and low levels of oligomerisation indicating lesser reactivity. While analysis of both **6.10a** and **6.10b** by GPC led to an indication of a higher degree of polymerisation the work described in previous chapters suggests that this should be treated with caution.

6.4.4 MALDI-TOF analysis of renewable derived polymers

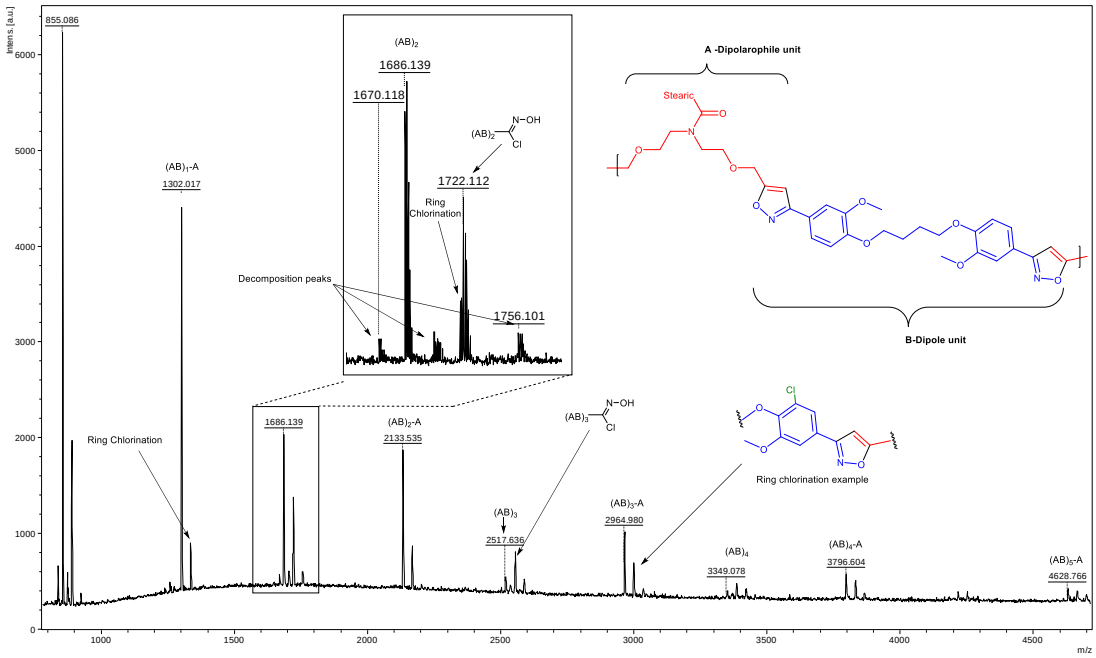

Figure 6-13: MALDI-TOF spectrum of P$^{t2}_{6.9a}$DEAyS **6.10a**.

Analysis of the MALDI-TOF spectrum of both P$^{t2}_{6.9a}$DEAyS **6.10a** and P$^{t2}_{6.9b}$DEAyS **6.10b** between 800 and 4700 Da indicated successful polymerisation with repeat unit numbers of at least 5 and above indicating that the true molecular weights are most likely between those predicted by GPC and NMR. The large molecular weight of the repeat units meant that masses could only be seen up to $(AB)_5$-A for P$^{t2}_{6.9a}$DEAyS **6.10a** (4628 Da, Figure 6-13) and a weak peak relating to $(AB)_5$ for P$^{t2}_{6.9b}$DEAyS **6.10b** (4321 Da). Weak decomposition peaks in the spectra of **6.10a** and **6.10b** relate to decomposition of the compound during MALDI-TOF analysis, in particular a mass loss caused by the decomposition of the isoxazole ring. The spectra of both **6.10a** and **6.10b** include masses that indicate the presence of end group oximoyl chlorides ($(AB)_n$-OC) in the growing oligomers. These masses are 36 Da higher than the $(AB)_n$ masses and are more intense in the spectrum of P$^{t2}_{6.9a}$DEAyS **6.10a** than P$^{t2}_{6.9b}$DEAyS **6.10b**. This reinforces the observation that polymerisation is slower for these monomers. Interestingly the MALDI-TOF spectra of P$^{t2}_{6.9a}$DEAyS **6.10a** and P$^{t2}_{6.9b}$DEAyS **6.10b** also indicated peaks at 34 Da higher than the $(AB)_n$-A and $(AB)_n$ peaks, these were identified as arising from oligomers containing an extra chlorine atom (from ring chlorination during the synthesis of **6.9a** and **6.9b**).

6.4.5 Thermal analysis of renewably derived polymers

Physical properties of $P^{t2}_{6.9a}$DEAyS **6.10a** and $P^{t2}_{6.9b}$DEAyS **6.10b** were determined using TGA and DSC. Glass transition temperatures (T_g) of the vanillin derived polymers **6.10a** and **6.10b** were higher than the corresponding *meta*-OC **2.1** derived polymer **5.11S** (Table 6-6). While the vanillin derived polymers **6.10a** and **6.10b** contain an additional short flexible chain between the isoxazole rings in the polymer backbone compared to **5.11S** the inclusion of a second benzene ring and the accompanying π stacking appears to have counteracted the effect of the flexible chain and increased the T_g of **6.10a** relative to **5.11S** (6a & 6c, Table 6-6, ΔT_g = +7 ºC). Incorporation of the polar ester group in **6.10b** has further increased the T_g of **6.10b** relative to **5.11S** (6b & 6c, Table 6-6, ΔT_g = +16 ºC).

Entry	Polymer	T_g / ºC	T_5 / ºC	T_{20} / ºC
6a	$P^{t2}_{6.9a}$DEAyS **6.10a**	12	286	335
6b	$P^{t2}_{6.9b}$DEAyS **6.10b**	21	271	310
6c	P^{t2}_{m}DEAyS **5.11S**	5	279	327

Table 6-6: Thermal analysis data of **6.10a** and **6.10b**, **5.11S** shown for comparison.

Thermal stability of the polymers was determined using TGA. Both polymers **6.10a** and **6.10b** showed similar thermal stability to P^{t2}_{m}DEAyS **5.11S**. Low concentrations of remaining oximoyl chloride monomer or oximoyl end groups was confirmed by analysing the weight loss of $P^{t2}_{6.9a}$DEAyS **6.10a** at 218 ºC (the T_E of **6.9a**, 4a, Table 6-4, T_E = 218 ºC). At this temperature $P^{t2}_{6.9a}$DEAyS **6.10a** had only lost 1 % weight (W_{218} = 99.0 %) while a similar analysis for $P^{t2}_{6.9b}$DEAyS **6.10b** indicated 0.4 % weightloss (W_{209} = 99.6 %) at 209 ºC (the T_E of **6.9b**, Table 6-4, T_E = 209 ºC).

6.5 Fully vanillin derived polymers

The polyisoxazoles formed in section 6.4 were derived from fatty acids **5.1** and vanillin **6.1** both of which are renewable feedstocks. There are issues surrounding fatty acids and vegetable oils as renewable feedstocks for chemicals, this is most notable in the food vs fuel arguments surrounding bio-fuels. Vanillin **6.1** however can be derived from lignin, a by-product of the paper making industry which is currently burnt to fuel paper manufacturing. As vanillin **6.1** is a non-controversial renewable feedstock it was explored as a source for both a dipole monomer and a dipolarophile monomer. The nomenclature for the vanillin derived dipolarophile monomer will be similar the dipolarophiles used in chapters 3 - 5. DAyV **6.11** therefore refers to a dialkyne derived from vanillin **6.1**.

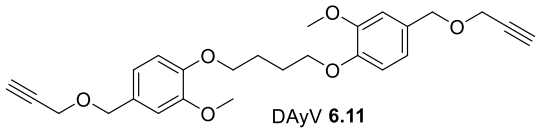

Figure 6-14: Vanillin derived dialkyne dipolarophile monomer.

6.5.1 Synthesis of vanillin derived dialkyne monomer

To form the vanillin derived dialkyne DAyV **6.11** the *bis*-vanillin compound **6.7a** was used as the starting material. Ether linked vanillin **6.7a** was reduced to diol **6.12** using $NaBH_4$ (Scheme 6-9). Dialdehyde **6.7b** was dispersed in MeOH and $NaBH_4$ was introduced in 5 parts over the course of 30 minutes. The reaction was left for a further hour before the precipitate was recovered by Büchner filtration and washed with water and MeOH, resulting in a pure white solid **6.12** (86 %).

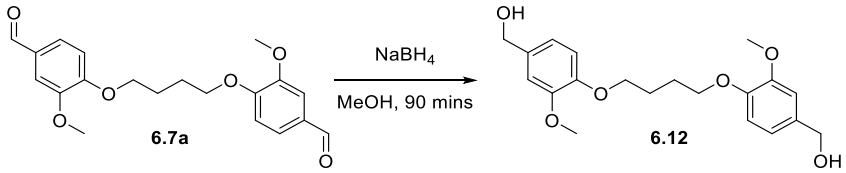

Scheme 6-8: Reduction of dialdehyde **6.7a** to diol **6.12**.

Diol **6.12** was dissolved in DMF along with KOH and placed in an ice bath. After 30 minutes propargyl bromide diluted with DMF was added dropwise to the cooled solution which was warmed to room temperature and left overnight. The following morning the solution was taken into EtOAc and washed extensively with water and brine. The organic layer was dried with $MgSO_4$ and reduced *in vacuo* to leave a crude

brown product. Purification by column chromatography through a silica plug resulted in the dialkyne DAyV **6.11** as a pure white solid (44 %). A mono-alkylated product was also recovered from the column with a 33 % yield, explaining the low yield of **6.11**. Characterisation of **6.11** and **6.12** was achieved using ^{1}H and ^{13}C NMR, infrared and mass spectroscopic analysis, as well as by TGA for **6.11**. Thermal analysis of DAyV **6.11** showed it to have thermal stability above 80 ºC, indicating it could be used in polymerisation reactions using the extended thermal conditions (P^{t2}).

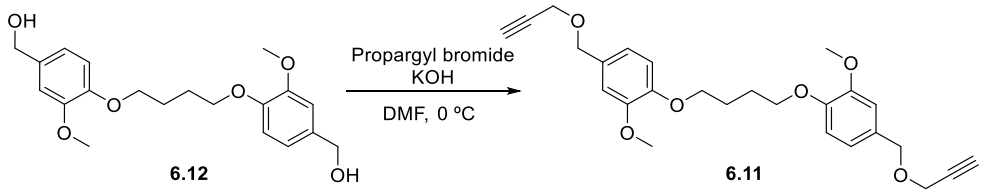

Scheme 6-9: Synthesis of vanillin derived dialkyne **6.11**.

6.5.2 Polyisoxazoles synthesised using vanillin derived dialkyne **6.11**.

Polyisoxazoles were formed from DAyV **6.11** using both *meta*-OC **2.1** and **6.9a** as the nitrile oxide precursors. *Meta*-OC **2.1** was used to allow a comparison between DAyV **6.11** and fatty acid derived monomers, whilst **6.9a** was used to form a polymer completely derived from vanillin $P^{t2}_{6.9a}$DAyV **6.14**.

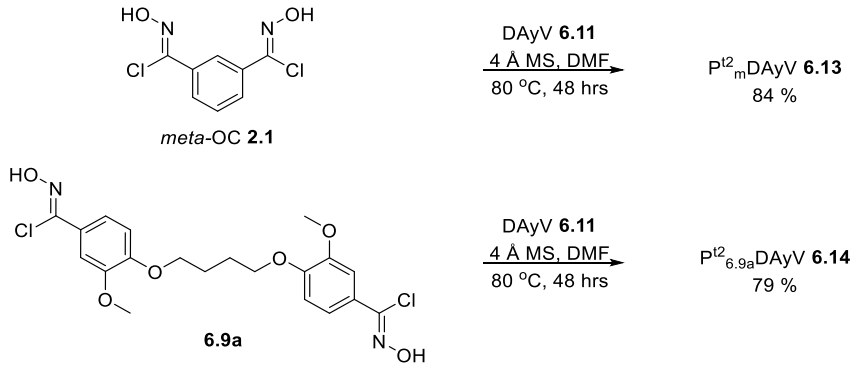

Scheme 6-10: Synthesis of polymers using vanillin derived dialkyne **6.11**

Polymerisation using **6.11** was successful with both nitrile oxide precursors forming P^{t2}_{m}DAyV **6.13** and $P^{t2}_{6.9a}$DAyV **6.14** in similar yields, 84 % and 79 %. P^{t2}_{m} DAyV **6.13** was recovered as a brown solid whilst $P^{t2}_{6.9a}$DAyV **6.14** was a robust brown foam after the final solvent reduction *in vacuo*. The solid polymers **6.13** and **6.14** were soluble in $CHCl_3$ and were analysed by 500 MHz ^{1}H and 125MHz ^{13}C NMR, as with the polymers in section 6.4 weak resonance peaks were evident around 10 ppm in the ^{1}H spectra, indicating residual oximoyl chloride. End group analysis using the 500

MHz ^{1}H NMR spectrum indicated that $P^{t2}{}_{m}$DAyV **6.13** and $P^{t2}{}_{6.9a}$DAyV **6.14** contained a similar average number of repeat units.

Entry	Polymer	RU MW	Yield / %	RU NMR	M_n / kDa	M_w / kDa	$Đ$	M_n / RU	M_w / RU
7a	$P^{t2}{}_{m}$DAyV **6.13**	598.2	84	7.5	6.5	21.9	3.4	10.9	36.6
7b	$P^{t2}{}_{6.9a}$DAyV **6.14**	822.3	79	7	10.5	36.7	3.5	12.8	44.6

a-GPC estimates, $CHCl_3$ used as eluent against PS standards, b-Calculated by division of GPC estimates by RU MW

Table 6-7: Yield, repeat unit and GPC molecular weight estimates for **6.13** and **6.14**.

The average molecular weights of $P^{t2}{}_{m}$DAyV **6.13** and $P^{t2}{}_{6.9a}$DAyV **6.14** were estimated by GPC using $CHCl_3$ as eluent against PS standards. The fully vanillin derived polymer $P^{t2}{}_{6.9a}$DAyV **6.14** (7a, Table 6-7) was estimated to contain more repeat units by both M_n and M_w than $P^{t2}{}_{m}$DAyV **6.13** (7b, Table 6-7). $P^{t2}{}_{m}$DAyV **6.13** and $P^{t2}{}_{6.9a}$DAyV **6.14** were both estimated to have high $Đ$ values.

6.5.3 MALDI-TOF analysis of vanillin derived polyisoxazoles

MALDI-TOF analysis between 800 and 4700 Da indicated polymers chains of $P^{t2}{}_{m}$DAyV **6.13** and $P^{t2}{}_{6.9a}$DAyV **6.14** were formed up to at least 4500 Da, $(AB)_7$-A (4649.75) for **6.13** and $(AB)_5$-A (4573.834) for **6.14** (appendix E). At all molecular weights masses relating to $(AB)_n$-A chains were more intense than their related $(AB)_n$ chains. The MALDI-TOF spectra of $P^{t2}{}_{m}$DAyV **6.13** and $P^{t2}{}_{6.9a}$DAyV **6.14** contain decomposition peaks, the two most prevalent relate to breaking of the isoxazole ring or breaking of an ether bond. Residual oximoyl chloride peaks ($(AB)_n$-OC) can be seen in both spectra, with an extremely weak peak in the spectrum of $P^{t2}{}_{m}$DAyV **6.13**. Intensities of masses relating to $(AB)_n$-OC are much stronger in the spectrum of $P^{t2}{}_{6.9a}$DAyV **6.14**, this was expected as **6.9a** is less reactive than *meta*-OC **2.1**. Like $P^{t2}{}_{6.9a}$DAyS **6.10a** and $P^{t2}{}_{6.9b}$DAyS **6.10b**, there is a repeating mass 34 Da higher than the $(AB)_n$ and $(AB)_n$-A peaks throughout the spectrum of $P^{t2}{}_{6.9a}$DAyV **6.14** that is caused by ring chlorination during **6.9a** during synthesis.

6.5.4 Thermal analysis of vanillin derived polyisoxazoles

Physical characteristic of $P^{t2}{}_{m}$DAyV **6.13** and $P^{t2}{}_{6.9a}$DAyV **6.14** were determined by DSC and TGA. Glass transition temperatures were expected to be higher for $P^{t2}{}_{m}$DAyV **6.13** than the equivalent fatty acid derived polymers due to the lack of the

long aliphatic side chain. This was found to be true with $P^{t2}{}_{m}$DAyV **6.13** (8a, Table 6-8) recording a T_g 30 ºC higher than $P^{t2}{}_{m}$DEAyS **5.11S** (5b, Table 5-5, T_g = 5 ºC). In section 6.4 the vanillin derived oximoyl chlorides led to polymers with higher T_g's than those formed from *meta*-OC **2.1**. The same relationship was seen with here with $P^{t2}{}_{6.9a}$DAyV **6.14** having a T_g 14 ºC higher than $P^{t2}{}_{m}$DAyV **6.13** (Table 6-8).

Entry	Polymer	T_g / ºC	T_5 / ºC	T_{20} / ºC
8a	$P^{t2}{}_{m}$DAyV **6.13**	35	268	405
8b	$P^{t2}{}_{6.9a}$DAyV **6.14**	49	267	392

Table 6-8: Thermal analysis of vanillin derived polymers **6.13** and **6.14**

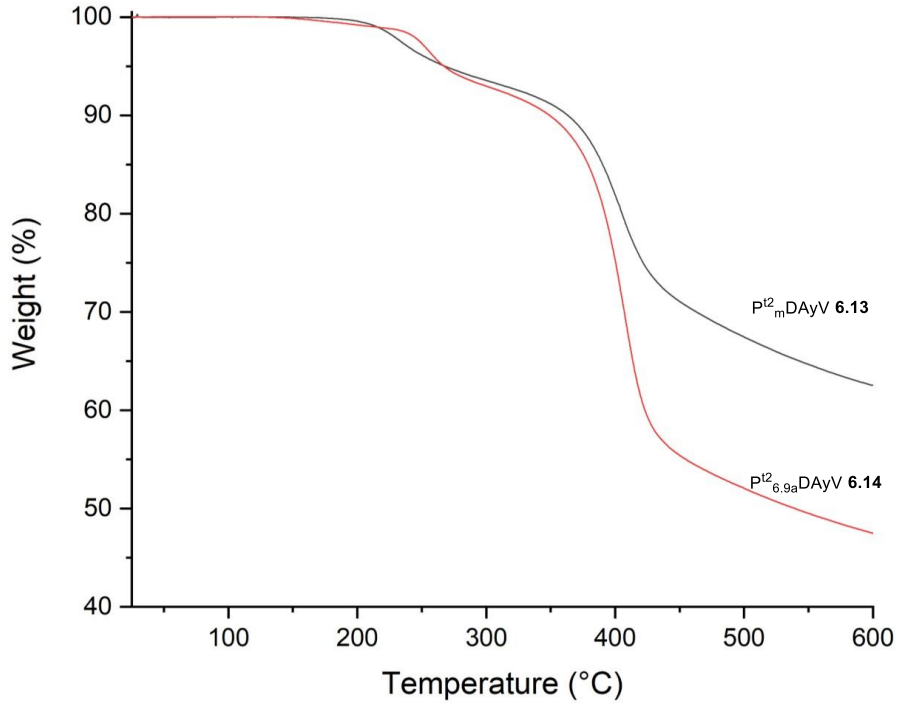

Figure 6-15: TGA plot of $P^{t2}{}_{m}$DAyV **6.13** and $P^{t2}{}_{6.9a}$DAyV **6.14**

The different oximoyl chlorides influenced the T_g but did not cause much difference in thermal stability when $P^{t2}{}_{m}$DAyV **6.13** and $P^{t2}{}_{6.9a}$DAyV **6.14** were analysed by TGA. Analysis by 500 MHz ^{1}H NMR and MALDI-TOF analysis of **6.13** and **6.14** indicated that they contained residual oximoyl chloride. For $P^{t2}{}_{m}$DAyV **6.13** this caused an initial weight loss of 1 % (W_{213} = 99.0 %) by the T_E of *meta*-OC **2.1** (4c, Table 6-4, T_E = 213 ºC) and a 1.2 % weight loss (W_{218} = 98.8 %) in $P^{t2}{}_{6.9a}$DAyV **6.14** by the T_E of **6.9a** (4a, Table 6-4, T_E = 218 ºC).

6.6 A renewably derived dual functional monomer

Step-growth polymerisations require high conversion to achieve high molecular weights. When using two different monomers high conversions can only be accessed when equal ratios of monomers are used. The simplest way of doing this is to use a dual functional monomer that can be activated to polymerise with itself, such as in the production of PEG.[363] In sections 6.4 and 6.5 vanillin was converted into both a nitrile oxide precursor and a dipolarophile monomer, it is therefore a viable feedstock for a dual functionalised monomer that could be used to form a homopolyisoxazole.

6.6.1 Synthesis of an oximoyl chloride / alkyne bifunctional monomer

As the formation of a vanillin based oximoyl chloride was shown to be relatively unstable (**6.4j**, section 6.2), the oximoyl chloride group had to be formed last. The propargyl group was introduced using propargyl bromide and similar reaction conditions to the synthesis of divanillin compounds **6.7a** and **6.7b** (section 6.4.1). Purification by column chromatography gave **6.15** as a white solid in a 55 % yield.

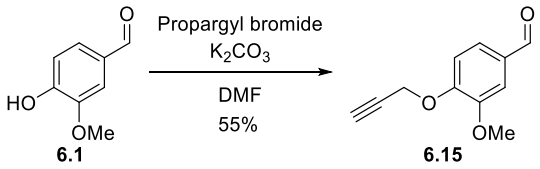

Scheme 6-11: Alkylation of vanillin

Aldehyde **6.15** was converted into an oximoyl chloride *via* an oxime using the same protocol previously described. Formation of oxime **6.16** was achieved at room temperature and resulted in a white solid in 87% yield that did not require further purification, 87 % (Scheme 6-12). In the previous section 6.1 it was observed that electron donating alkoxy groups facilitated chlorination of the benzene ring during oximoyl chloride synthesis, the source of electrophilic chlorine in NCS also posed a risk of reacting with the alkyne to give a halogenated alkene or alkane. As polymerisation would still be possible using dual functional monomers modified with ring chlorination or halogenated alkenes, a small excess of NCS (1.2 eq.) was used to ensure the highest yield of oximoyl chloride. Hence, oxime **6.16** was dissolved in DMF and NCS was added in portions over 1 hour. Once complete the reaction was poured into cold water causing a white precipitate to form which was collected by Büchner

filtration to give crude **6.17** as a white solid, 94 %. The solid was sparingly soluble in $CDCl_3$ and in d_6-acetone, analysis by 500 MHz ^1H and 125 MHz ^{13}C NMR revealed that **6.17** contained small impurities. Purification of **6.17** by recrystallisation did not improve purity whilst column chromatography caused the compound to decompose. Polymerisation reactions were therefore carried out using **6.17** without further purification.

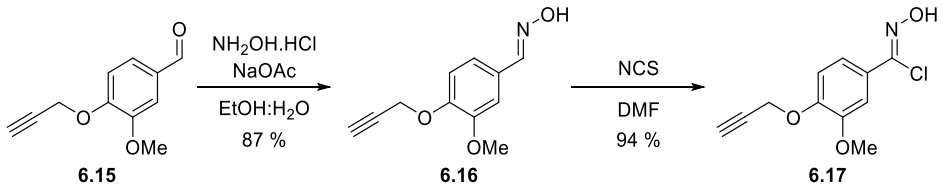

Scheme 6-12: Synthesis of oximoyl chloride to form dual functional monomer

6.6.2 Thermal analysis of the dual functional monomer **6.17**

Using TGA and DSC, homomonomer **6.17** was analysed between 25 ºC and 600 ºC. Oxime **6.16** was also analysed to set a base-line for compound decomposition as the propargyl ether of **6.16** and **6.17** may cause them to perform transformations similar to a Claisen rearrangement at elevated temperatures (Figure 6-16).[363]

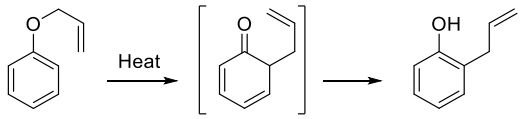

Figure 6-16: Claisen rearrangement mechanism

Entry	Oximoyl Chloride	T_5 / °C	T_{10} / °C	T_{20} / °C	T_E / °C	W_{600} / %
9a	Oxime **6.16**	208	221	241	-	48
9b	Homomonomer **6.17**	153	160	320	289	54

Table 6-9: Thermal analysis of aldoxime **6.16** and homomonomer **6.17**

As expected, the oxime **6.16** had significantly higher thermal stability than the oximoyl chloride **6.17** (9a & 9b, Table 6-9, ΔT_5 = 55 ºC). The initial mass loss (9b, Table 6-9, T_5 = 153 ºC) of **6.17** was therefore caused by the decomposition of oximoyl chloride to form nitrile oxide. If it was assumed that 6.17 was 100% pure then complete degradation of oximoyl chloride (T_E) was not reached until 289 ºC, although in reality the weight loss plateaus much earlier, around 180 ºC (Figure 6-17). DSC analysis of **6.17** shows an exothermic peak between 115 ºC and 180 ºC correlating with the initial mass loss and indicating complete loss of HCl has occurred by 180 ºC (Figure 6-17). Once **6.17** decomposes to a nitrile oxide it should undergo polymerisation. By

integrating the exotherm peaking at 159 ºC, enthalpy of nitrile oxide formation and subsequent polymerisation was determined to be 138 kJ mol^{-1}. There was a second significant exotherm of 245 kJ mol^{-1} that peaked at 320 ºC, this related to the second stage of mass loss which was presumed to be caused by polymer degradation.

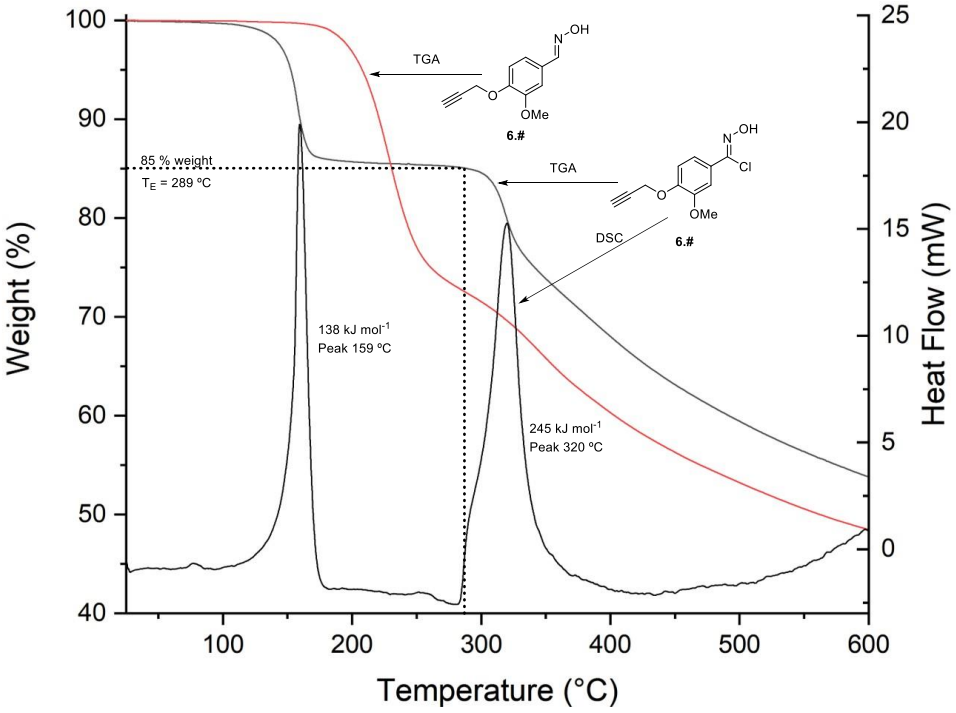

Figure 6-17: TGA plot of dual functionalised monomer **6.17** and aldoxime **6.16**, DSC plot of **6.17**

6.6.3 Homopolymerisation of a renewably derived monomer

Polymer nomenclature followed a similar format as previous polymers, although as only one monomer was used the monomers were replaced with **HOMO** to indicate a homopolymerisation (P^{t2}HOMO **6.18**). Two separate materials were collected during the workup of P^{t2}HOMO **6.18**, one from the filtrate and another insoluble material, these were indicated following the Arabic numeral (**6.18-filtrate** and **6.18-solid**)

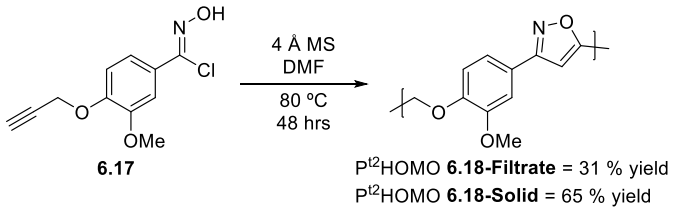

Scheme 6-13: Polymerisation of dual functionalised monomer to form homopolymer **6.18**

A homopolymer was formed from **6.17** using the extended thermal polymerisation conditions (P^{t2}). Unlike previous polymerisations a precipitate formed during the

reaction. After 24 hours the mixture was grainy and by 48 hours the reaction was unable to stir due to the amount of precipitate. Following the workup of previous polymerisations, the mixture was diluted with $CHCl_3$ and filtered to remove molecular sieves, the filtrate was then reduced *in vacuo* to leave a brown solid **6.18-filtrate** (31 %). The majority of the polymer however was not soluble in $CHCl_3$ and was still mixed with the molecular sieves as a hard brown solid. The polymer floated on $CHCl_3$ whilst the sieves did not. This polymeric material was suspended in chloroform and collected by filtration, the process was repeated until no polymeric material could be seen with the molecular sieves. The collected brown solid polymer **6.18-solid** was dried *in vacuo* to give a yield of 65 %.

The polymeric material collected by suspension and filtration P^{t2}HOMO **6.18-solid** was found to be insoluble in all common laboratory solvents, it therefore could not be analysed by NMR or GPC. The polymer collected from the initial filtrate P^{t2}HOMO **6.18-filtrate** could be dissolved in $CDCl_3$ using a sonicator for 300 MHz ^{1}H NMR analysis. P^{t2}HOMO **6.18-filtrate** did however precipitate out of $CHCl_3$ quickly and so could not be used for GPC analysis without risking damage to the instruments.

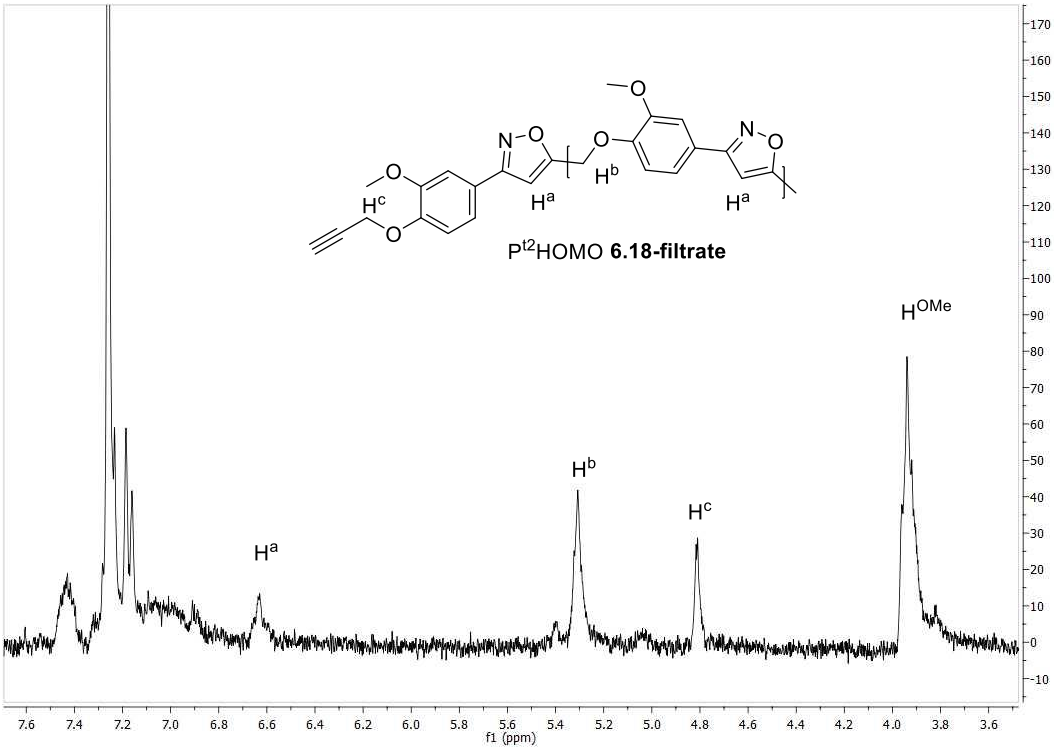

Figure 6-18: ^{1}H NMR spectrum of P^{t2}HOMO **6.18-filtrate**

P^{t2}HOMO **6.18-filtrate** had a weak signal in the 300 MHz ^{1}H NMR and gave a poor spectrum due to it's low solubility. Tentative evidence of polymerisation could be seen in the spectrum with resonances peaks at 6.6 ppm and 5.3 ppm which relate to isoxazole and α-isoxazole environments represented by H^a and H^b respectively (Figure 6-18). End group analysis using the shifts at 5.3 ppm and 4.8 ppm estimates an average of 2.5 repeat units. As P^{t2}HOMO **6.18-filtrate** was still partially soluble in $CHCl_3$ and P^{t2}HOMO **6.18-solid** was not, it was assumed that **6.18-solid** underwent a further degree of polymerisation and contains a higher average number of repeat units.

6.6.4 Analysis of P^{t2}HOMO **6.18** by IR, TGA and DMA

Polymers P^{t2}HOMO **6.18-filtrate** and **6.18-solid** could be analysed by IR, TGA and DMA. IR analysis (appendix E) of P^{t2}HOMO **6.18-filtrate** contained a strong water peak which masked any residual alkyne frequency (≡C-H ~ 3300 cm^{-1}), the spectrum did however contain an adsorption at 2122 cm^{-1} indicating a C≡C bond. There are also weak adsorptions at 1659 cm^{-1} and 1604 cm^{-1} that relate to the isoxazole ring. The IR spectrum of P^{t2}HOMO **6.18-solid** was similar to **6.18-filtrate** although with only a weak water adsorption, no terminal alkyne proton stretch (≡C-H) could be seen as well as no adsorption indicating a C≡C stretch. The presence of isoxazole rings in P^{t2}HOMO **6.18-solid** was indicated by weak adsorptions at 1654 cm^{-1} and 1605 cm^{-1}.

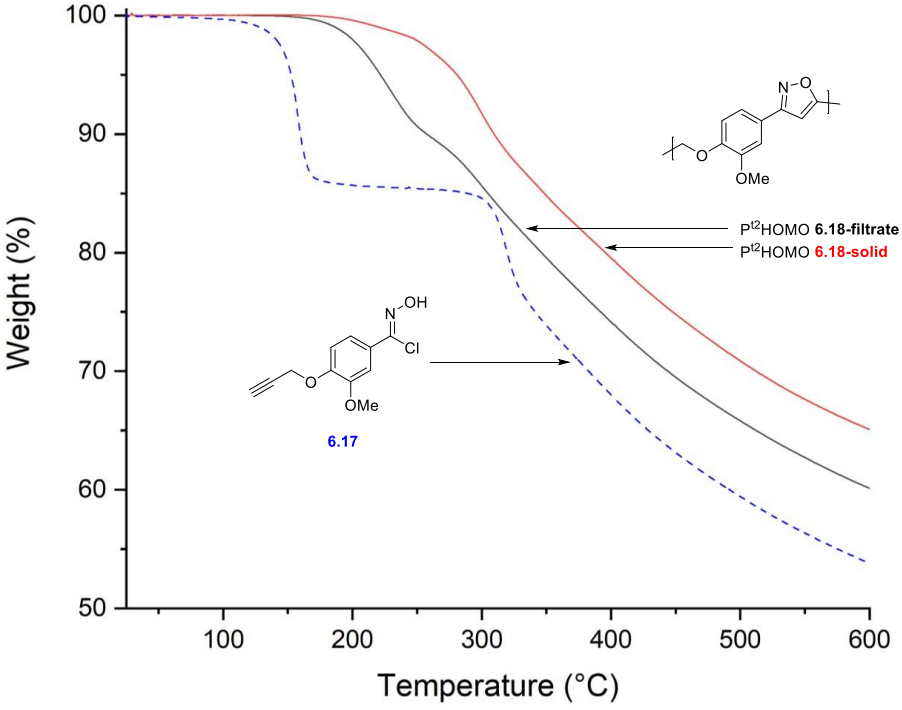

Figure 6-19: TGA plot of monomer **6.17**, and polymers **6.18-filtrate** and **6.18-solid**

Thermal stability analysis of P^{t2}HOMO **6.18-filtrate** and **6.18-solid** was carried out using TGA (Figure 6-19), heating the polymers from 25 ºC to 600 ºC at 10 ºC / min under N_2. The polymer collected from the filtrate P^{t2}HOMO **6.18-filtrate** had lower thermal stability than P^{t2}HOMO **6.18-solid** (10a & 10b, Table 6-10, ΔT_5 = 59 ºC). The initial degradations of **6.18-filtrate** and **6.18-solid** occur at much higher temperatures than in the monomer **6.17**, indicating that oximoyl chloride is no longer present in the polymers. The final and major degradation step of **6.18-filtrate** and **6.18-solid** does occur at a similar temperature to the second step of **6.17** degradation, inferring that monomer **6.17** forms a polymer under thermal conditions with no solvent or additives.

Entry	Compound	T_5 / °C	T_{20} / °C	W_{600} / %
10a	P^{t2}HOMO **6.18**-Filtrate	222	346	60
10b	P^{t2}HOMO **6.18**-solid	281	396	65
10c	Homomonomer **6.17**	153	320	54

Table 6-10: Thermal analysis of **6.18-filtrate** and **6.18-solid**

P^{t2}HOMO **6.18-filtrate** and **6.18-solid** were analysed by DSC to determine glass transition temperatures, they were heated from 25 ºC to 100 ºC, cooled to −100 and heated to 250 ºC, under N_2. TGA had indicated that **6.18-filtrate** and **6.18-solid** were not stable above 250 ºC. No enthalpic changes relating to glass transitions were evident when either **6.18-filtrate** and **6.18-solid** were analysed by DSC.

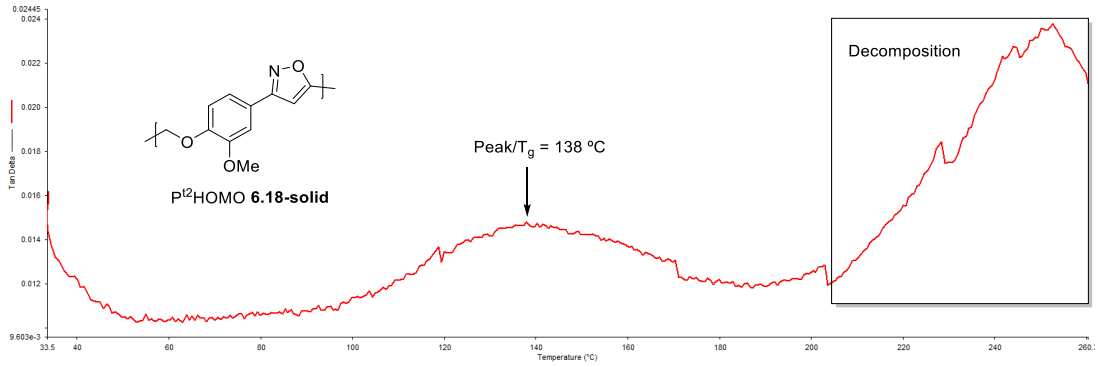

Figure 6-20: Tan Δ plot of taken from DMA of P^{t2}HOMO **6.18-solid**

Dynamic mechanical analysis (DMA) is a more sensitive method of determining glass transition temperatures. DMA applies a mechanical stress to a material whilst measuring the strain in the material, this allows physical properties of the material to be determined by varying the applied stress or by varying the temperature. To determine their T_g's **6.18-filtrate** and **6.18-solid** were analysed using a single cantilever method from 30 ºC to 260 ºC. Glass transition temperature can be

determined by taking the inflection point of the storage modulus plot or the peak of the loss factor tan Δ plot. The signal given by P^{t2}HOMO **6.18-solid** was weak and no inflection point was found in the storage modulus plot, but the plot of tan Δ did give a small peak at 138 ºC before decomposition begins (Figure 6-20). No T_g could be determined using either method for the oligomer recovered from the **6.18-filtrate**.

6.6.5 Thermal analysis of **6.17** for solvent free homopolymerisations

Analysis of the monomer **6.17** by TGA and DSC in section 6.6.2 was achieved using a simultaneous thermal analysis (STA) instrument. Analysis was carried out between 25 ºC and 600 ºC under N_2 and indicated that polymerisation could be achieved in solvent free conditions with no additives. The compound formed during TGA analysis of **6.17** in section 6.6.2 was more stable than the polymers formed using the extended thermal polymerisation (P^{t2}) method. The second degradation step of **6.17** did not begin until 280 ºC which was higher than the initial degradation of the P^{t2} polymers (Figure 6-19). To investigate solvent free polymerisation, **6.17** was polymerised in a more sensitive DSC instrument under N_2.

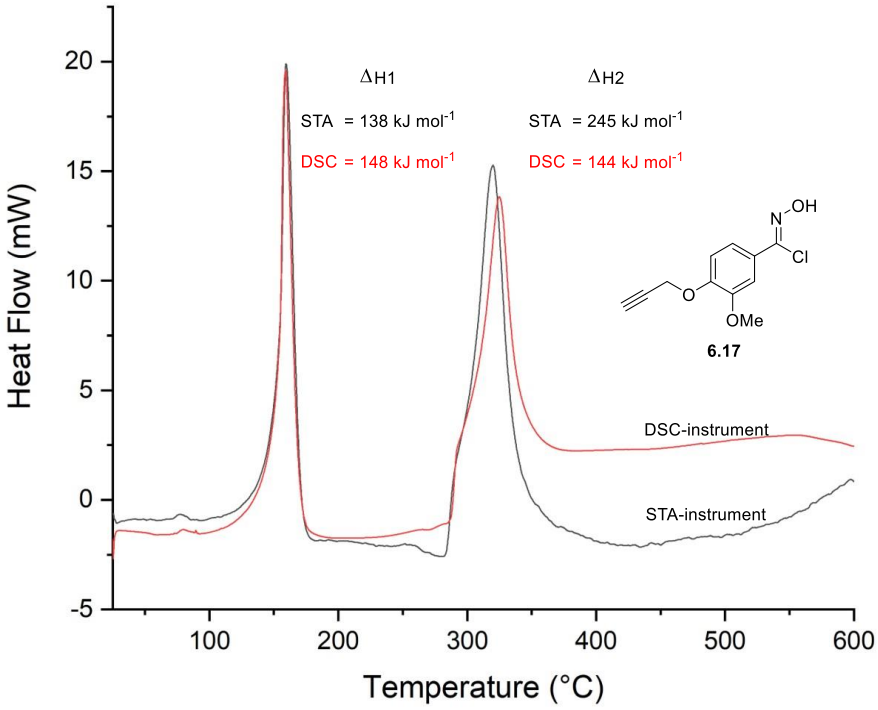

Figure 6-21: Enthalpic change plot of **6.17** measured using a STA instrument and a DSC instrument between 25 ºC and 600 ºC at a heating rate of 10 ºC min^{-1} under N_2.

As a more sensitive DSC instrument was used for these investigations, **6.17** was first heated from 25 ºC to 600 ºC at 10 ºC / min to measure the enthalpy of polymerisation

and decomposition more accurately. The exothermic peak relating to decomposition of oximoyl chloride and subsequent polymerisation began gradually around 100 ºC and ended by 180 ºC. The enthalpy of polymerisation was similar between the two instruments (ΔH1, Figure 6-21), the decomposition enthalpy measurements however were significantly different (ΔH2, Figure 6-21), this may be due to a large step up to the decomposition step when measured by the DSC instrument. As with the initial measurements made during analysis by STA, decomposition began at 280 ºC.

For polymerisations in the DSC instrument and subsequent analysis, **6.17** was heated from 25 ºC to 200 ºC at 10 ºC / min to induce polymerisation, the polymer was then analysed by cooling to −50 ºC then heating to 250 ºC at 20 ºC / min. Cooling to −50 ºC and heating to 250 ºC was repeated, the sample was then cooled to −50 ºC and heated to 600 ºC.

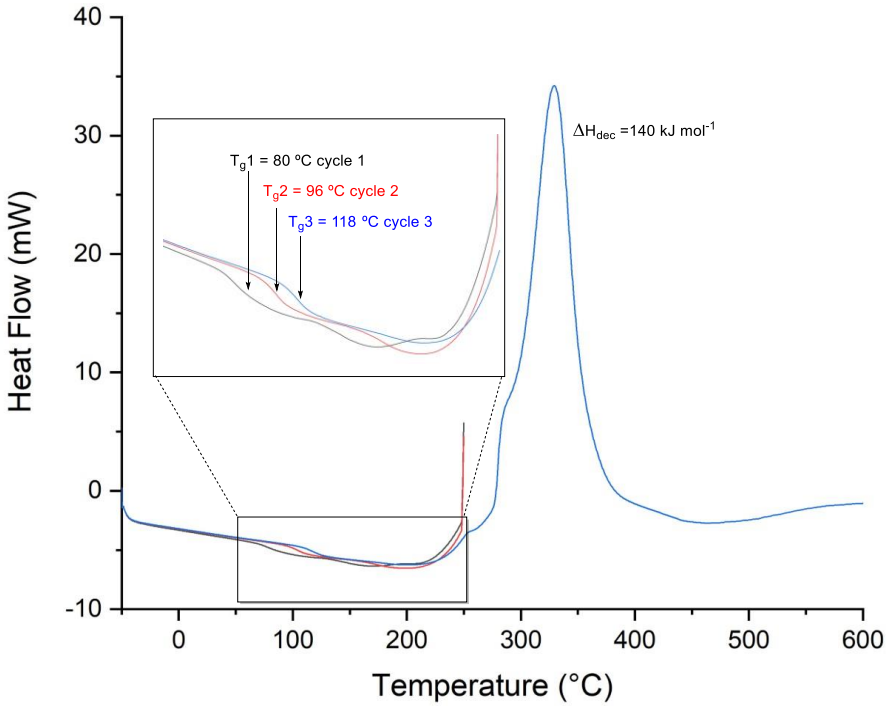

Figure 6-22: Three heating cycles of the polymer formed from **6.17** in the DSC, cycle 1, cycle 2 and cycle 3

Polymerisation of **6.17** in the DSC instrument was successful, the exothermic polymerisation peaked around 100 ºC but did not return to the baseline before 200 ºC and so enthalpy of polymerisation could not be calculated. The polymer was cooled and heated three times to determine the polymers T_g (Figure 6-22). On the first heating cycle a T_g of 80 ºC was recorded, this was much lower than the T_g of P^{t2}HOMO **6.18-solid** recorded by DMA (Figure 6-20, T_g = 138 ºC). The glass transition temperature

increased on each heating cycle by around 20 ºC (Figure 6-22). Before each heating cycle reached 250 ºC a small exothermic rise could be seen, this may have related to further curing of the polymer causing T_g to increase on the subsequent heating cycling. On the final heating cycle the compound was heated through to 600 ºC to determine enthalpy of decomposition, an exothermic peak of 140 kJ mol^{-1} was detected. The enthalpy of decomposition agreed with the value measured previously using the DSC instrument, not the STA instrument (Figure 6-21).

6.6.6 Solvent free homopolymerisations

Thermal analysis of **6.17** by TGA and DSC proved that polymerisation could be achieved without additives or solvent. Previous polymerisations in this work used 4 Å molecular sieves as a mildly basic additive to encourage oximoyl chloride decomposition. To investigate whether the inclusion of molecular sieves would help or hinder solvent free polymerisation they were included over a range of weight percent's (0 wt. % - 50 wt. %).

Polymer nomenclature followed a similar format as previous polymers,

P^{sf} signified solvent free polymers, **P^{SF}**HOMO(0wt%) 6.19

HOMO indicated that it was a homopolymer, P^{sf}**HOMO**(0wt%) 6.19

Weight percent of 4Å MS used in polymerisation was shown P^{sf}HOMO(**0wt%**) 6.19

Each polymer was then assigned an Arabic numeral, P^{sf}HOMO(0wt%) **6.19**

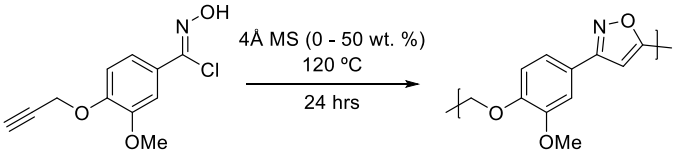

6.17 P^{sf}HOMO(0-50wt%) **6.19-6.24**

Scheme 6-14: Solvent free synthesis of polyisoxazoles P^{sf}HOMO(0-50wt%)

From the DSC analysis of **6.17** above it appeared that polymerisation begins around 100 ºC, consequently the solvent free polymerisation of **6.17** was therefore carried out in an oven at 120 ºC over 24 hours. After 24 hours the polymers were removed from the oven to reveal crumbly light brown solids. These polymers were weighed and all showed the expected mass loss caused by the loss of HCl during nitrile oxide formation (Table 6-11). As with P^{t2}HOMO **6.18-solid**, the polymers P^{SF}HOMO(0-50wt%) **6.19**

- **6.24** were not soluble in any common laboratory solvents, they were therefore only analysed by infrared, DMA and TGA.

Entry	Polymer	Yield / %
11a	P^{t2}HOMO **6.18-solid**	65
11b	P^{sf}HOMO(0wt%) **6.19**	97
11c	P^{sf}HOMO(10wt%) **6.20**	101
11d	P^{sf}HOMO(20wt%) **6.21**	98
11e	P^{sf}HOMO(30wt%) **6.22**	98
11f	P^{sf}HOMO(40wt%) **6.23**	99
11g	P^{sf}HOMO(50wt%) **6.24**	101

Table 6-11: Yield of homopolymers **6.18-Solid** and P^{sf}HOMO(0-50wt%) **6.19-6.24.**

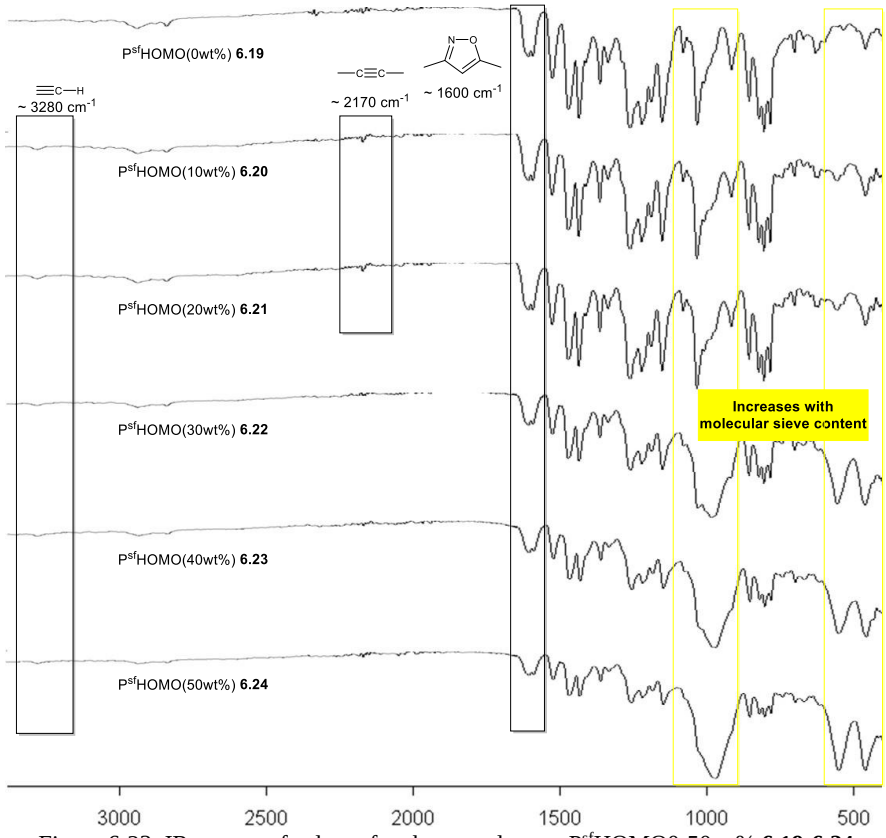

Figure 6-23: IR spectra of solvent free homo polymers P^{sf}HOMO0-50wt% **6.19-6.24**

Solvent free polymers P^{sf}HOMO(10-50%) **6.20-6.24** contained molecular sieves and so would take on atmospheric water, the polymers were therefore immediately analysed by IR to reduce water adsorption and allow the alkyne end group absorption frequency to be observed (Figure 6-23). Only the IR spectra of P^{sf}HOMO(10wt%) **6.20** and P^{sf}HOMO(20wt%) **6.21** showed adsorptions relating to C≡C stretching frequency at 2169 cm^{-1}. Additive free P^{sf}HOMO(0wt%) **6.19** showed no evidence of terminal alkyne whilst all the composites **6.20** – **6.24** did have adsorptions around 3280

cm^{-1} (≡C-H stretch). Polymers **6.19 – 6.24** all showed isoxazoles adsorptions around 1605 cm^{-1} and 1590 cm^{-1}. As molecular sieve composition increased so did the transmittance at 971 cm^{-1}, 553 cm^{-1} and 462 cm^{-1} until they dominated the spectrum of P^{sf}HOMO(50wt%) **6.24**, hiding the ether adsorption at 1033 cm^{-1}.

The polymers were analysed by DMA (appendix E) to determine glass transition temperature, the storage modulus and tan Δ could be used to calculate T_g for all the polymers **6.19 – 6.24**. The values given by the two plots were generally in agreement except for the P^{sf}HOMO(50wt%) **6.24** (12a, Table 6-12). The solvent free polymers had higher T_g's than the polymer formed using the extended thermal conditions in solution (P^{t2}), with the no additive polymer P^{sf}HOMO(0wt%) **6.19** having the highest T_g of all the polymers formed in this work. Polymers formed using powdered molecular sieves all had T_g's around 160 ºC with no trend in T_g as the wt. % of molecular sieves changed.

Entry	Polymer	Tan Δ T_g / ºC	Storage modulus T_g / ºC
12a	P^{t2}HOMO **6.18-solid**	138	-
12b	P^{sf}HOMO(0wt%) **6.19**	176	175
12c	P^{sf}HOMO(10wt%) **6.20**	157	155
12d	P^{sf}HOMO(20wt%) **6.21**	161	160
12e	P^{sf}HOMO(30wt%) **6.22**	155	159
12f	P^{sf}HOMO(40wt%) **6.23**	165	163
12g	P^{sf}HOMO(50wt%) **6.24**	163	176

Table 6-12: Glass transition temperatures of homopolymers measured using DMA.

The polymers thermal stability was analysed by TGA under N_2. As P^{sf}HOMO(10-50%) **6.20-6.24** contained molecular sieves they would have taken on atmospheric water. In order to record accurate thermal stability data water was removed from the polymers by heating them to 120 ºC at 10 ºC / min, the samples were then cooled back to 25 ºC before heating them to 600 ºC at 10 ºC.

Entry	Polymer	T_5 / ºC	T_{20} / ºC	W_{600} / %
13a	P^{t2}HOMO **6.18-solid**	281	396	65
13b	P^{sf}HOMO(0wt%) **6.19**	313	382	61
13c	P^{sf}HOMO(10wt%) **6.20**	311	396	64
13d	P^{sf}HOMO(20wt%) **6.21**	314	408	67
13e	P^{sf}HOMO(30wt%) **6.22**	310	427	70
13f	P^{sf}HOMO(40wt%) **6.23**	314	445	72
13g	P^{sf}HOMO(50wt%) **6.24**	298	483	76

Table 6-13: TGA analysis of P^{t2}HOMO **6.18-solid** and P^{sf}HOMO(0-50wt%) **6.19-6.24**

P^{sf}HOMO(0-50wt%) **6.19-6.24** all showed high thermal stability (T_5 > 295 ºC, Table 6-13), although even with the initial heating step P^{sf}HOMO(0-50%) **6.19-6.24** still contained residual water (Figure 6-24). Major decomposition of **6.19-6.24** did not begin until above 300 ºC with a similar decomposition profile to the second step in TGA plot of **6.17** (Figure 6-17). Solvent free polymers **6.19-6.24** were all more thermally stable than the polymer formed using the solvent based extended thermal conditions P^{t2}HOMO **6.18-solid** (Table 6-13).

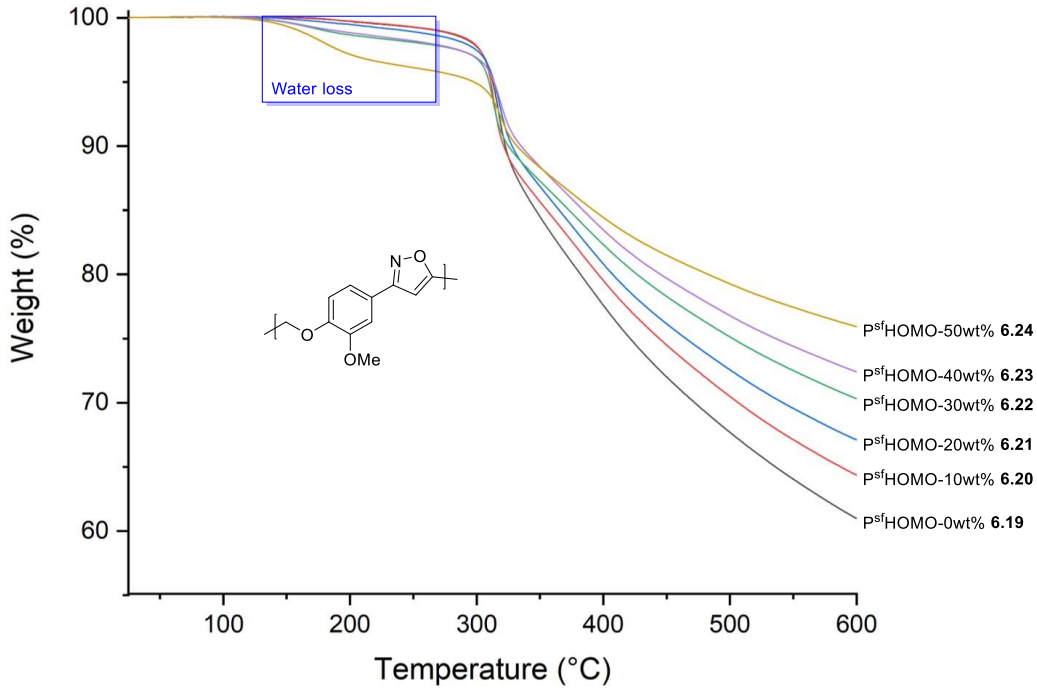

Figure 6-24: TGA plot of solvent free homo polymers P^{sf}HOMO(0-50wt%) **6.19-6.24**

To determine how much atmospheric water each polymer had taken on they were heated from 25 ºC to 600 ºC under N_2 and the initial weight loss step analysed. As polymer degradation was known to begin above 280 ºC, water loss was assessed at 250 ºC. As expected, water content increased with molecular sieve composition of the polymer (Table 6-14). TGA demonstrated that 2 wt % of water was taken on for every 10 wt. % of molecular sieves in the composites P^{sf}HOMO(0-50wt%) **6.19-6.24**.

Entry	Polymer	W_{250} / %	Water content / %
14a	P^{sf}HOMO(0wt%) **6.19**	99	1
14b	P^{sf}HOMO(10wt%) **6.20**	97	3
14c	P^{sf}HOMO(20wt%) **6.21**	95	5
14d	P^{sf}HOMO(30wt%) **6.22**	94	6
14e	P^{sf}HOMO(40wt%) **6.23**	92	8
14f	P^{sf}HOMO(50wt%) **6.24**	90	10

Table 6-14: Weight of P^{sf}HOMO(0-50wt%) **6.19-6.24** at 250ºC.

6.7 Summary and conclusions

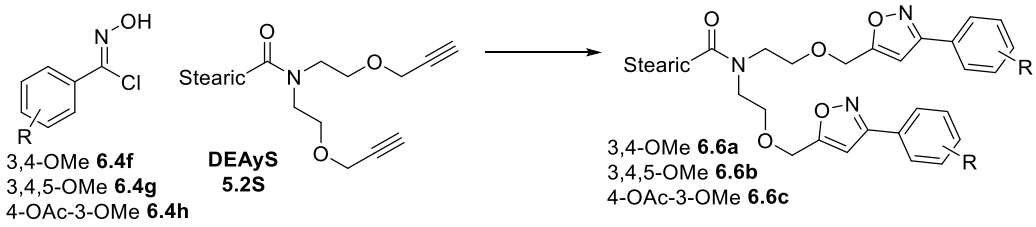

Figure 6-25: Oximoyl chloride reactivity study using **6.4f-h**, **5.2S** to form **6.6a-c**

Aromatic oximoyl chlorides **6.4a-j** were synthesised with a variety of ring substitutions and their thermal stability was assessed by TGA. Electron donating groups *para* to the oximoyl chloride functional group did not alter stability significantly, while electron withdrawing groups *para* to the oximoyl chloride or electron donating groups at the *meta* position increased stability. Compound **6.4a** with a ortho-substituted substituent showed decreased stability forming furoxan readily. Oximoyl chloride reactivity was assessed by reacting **6.4f-h** with the dipolarophile DEAyS **5.2S** (Figure 6-25). The conversion of dipolarophile **5.2S** to isoxazoles **6.6a-c** was measured and results indicated that oximoyl chlorides with higher stabilities led to lower cycloaddition conversions of alkyne to isoxazole.

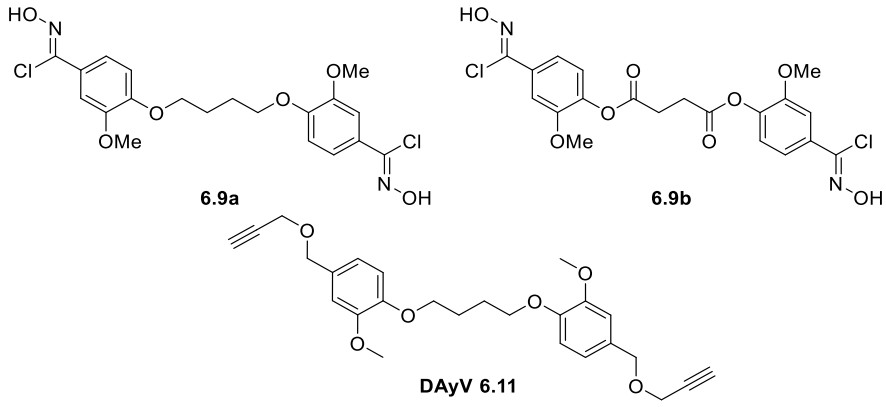

Figure 6-26: Vanillin derived oximoyl chloride pre-monomers **6.9a-b** and dialkyne DAyV **6.11**

Using vanillin **6.1** as a renewable feedstock, di(oximoyl chloride) monomers **6.9a** and **6.9b** were prepared and their reaction with stearic acid derived dialkyne DEAyS **5.2S** studied, resulting in completely renewably derived polyisoxazoles **6.10a** and **6.10b**. The ether linked renewably derived oximoyl chloride monomer **6.9a** resulted in polymers $P^{t2}_{6.9a}$DEAyS **6.10a** containing a higher average number of repeat units than the comparable *meta*-OC polymers P^{t2}_{m}DEAyS **5.11S**. The fully renewably derived polymers also had higher glass transition temperatures than **5.11S**. Vanillin **6.1** was

also used to form a dipolarophilic monomer **6.11** that was used to form a fully vanillin derived polymer **6.14** and showed similar reactivity to DEAyS **5.2S**.

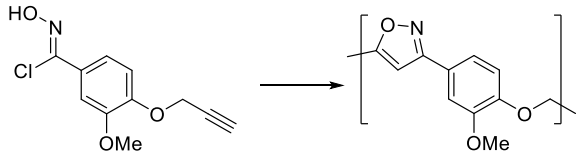

6.17 **6.18 - 6.24**

Figure 6-27: Vanillin derived dual functional monomer **6.17** and homopolyisoxazoles **6.18 – 6.24**.

A dual functionalised monomer **6.17** was derived from vanillin **6.1**, containing an oximoyl chloride and a terminal alkyne. This monomer formed polyisoxazole **6.18** using the solvent based polymerisation conditions used throughout the work (P^{t2}). It was also able to undergo solvent free polymerisations at 120 ºC with and without molecular sieves as additives. The solvent free polymers **6.19** – **6.24** had higher thermal stability and glass transition temperatures than the solvent based polymer **6.18**. The polyisoxazole formed without solvent or additives **6.19** had the highest glass transition temperature of all the polymers formed during this work. Due to a lack of solubility in common laboratory solvents the homopolymers **6.18** – **6.24** were only analysed by IR, TGA and DMA.

7.0 Summary, conclusion, and future work

The aim of this work was to investigate the application of nitrile- oxide/dipolarophile cycloaddition reactions to the synthesis of renewable polymers. These 1,3-dipolar cycloadditions have been thoroughly investigated and exploited for small molecule synthesis and in post-polymerisation modifications of macromolecules.[257,295,342,347] There has however been limited evidence of step-grown polymers formed by nitrile-oxide/dipolarophile cycloadditions[297,298,300,301,312,317,318,364] and no evidence (to my knowledge) of their use in the formation of renewably derived polymers.

7.1 Initial investigation

Takata *et* al.[317,318] published some of the few literature examples of polymerisation by nitrile-oxide/dipolarophile cycloadditions. They described the successful formation of various low molecular weight polymers. The conditions used molecular sieves as a mildly basic additive to form difunctional nitrile-oxides *in situ* from oximoyl chloride precursors. These polymerisation conditions were used as the foundation for the work presented in this thesis.

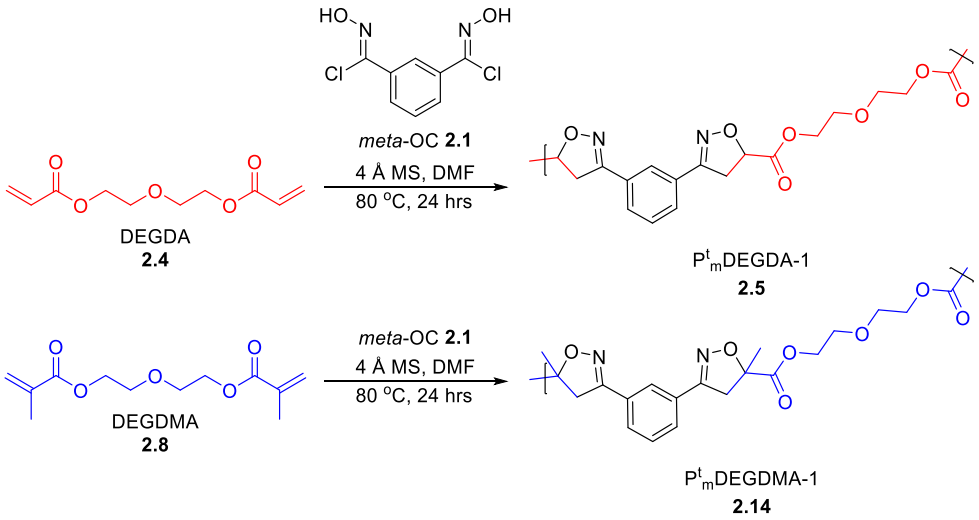

Figure 7-1: Synthesis of P$^{t}_{m}$DEGDA-1 **2.5** and P$^{t}_{m}$DEGDMA-1 **2.14** using Takata's conditions.[317,318]

As the area of research was relatively unexplored it was deemed prudent to initially reproduce polymers reported by Takata *et al.*[317] using their conditions. The conditions successfully formed comparable polymers, (P$^{t}_{m}$DEGDA-1 **2.5** and P$^{t}_{m}$DEGDA-1 **2.14**), to those described by Takata *et al.*[317] although with some variance in molecular

weight and glass transition temperature. The structures of polymers **2.5** and **2.14** were investigated using MALDI-TOF which revealed a propensity for forming $(AB)_n$ chains (cyclical or linear furoxan linked) over $(AB)_n$-A (linear), where A and B relate to the dipolarophile and nitrile oxide monomer respectively.

After the conditions reproducibility was established, diacrylate monomers EGDA **2.9** and PEGDA **2.10** were used to investigate the effect of dipolarophile monomer length on polymerisation and polymer properties. This showed a strong correlation between glass transition temperature and separation of dipolarophilic groups in the monomer.

Figure 7-2: Commercially available diacrylates with a large varience in glycol chain length

The initial study into the polymerisation also explored the effect monomer ratio had on the resulting polymers. The use of excess dipolarophile (monomer A) led to linear $(AB)_n$-A chains preferentially although it also caused lower molecular weights and T_g's. Increasing the ratio of *meta*-OC **2.1** (monomer B) relative to dipolarophile monomers caused the formation of $(AB)_n$ structures exclusively.

7.2 Monomer design

The initial investigation showed that the polymerisation condition reported by Takata[317] was reproducible and gave an insight into how monomers effected the resulting polymers. With this in mind 4 monomer models **3.5-3.8** were produced. The aim was to eventually form the monomers from vegetable oil derivatives, for the model studies however the fatty acid chains were replaced with an acetyl group. The monomers were used along with *meta*-OC **2.1** to form ABA oligomers which allowed their structures to be investigated and characterised.

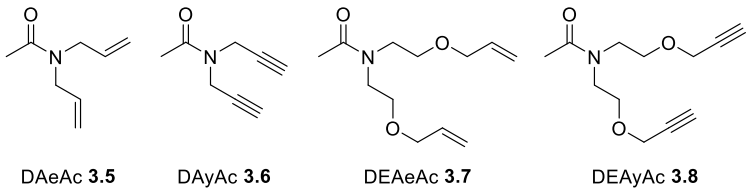

Figure 7-3: Model acetyl amide dipolarophilic monomers

The model monomers were then used to form polyisoxazoles and polyisoxazolines. The smaller non-ether containing monomers **3.5** and **3.6** gave polymers **3.22** and **3.23** with higher glass transition temperature but contained fewer repeat units and gave lower yields than the ether containing monomers **3.7** and **3.8**. The study also indicated that polyisoxazoles **3.23** and **3.25** were more thermally stable but had lower T_g's than their respective polyisoxazolines **3.22** and **3.24.**

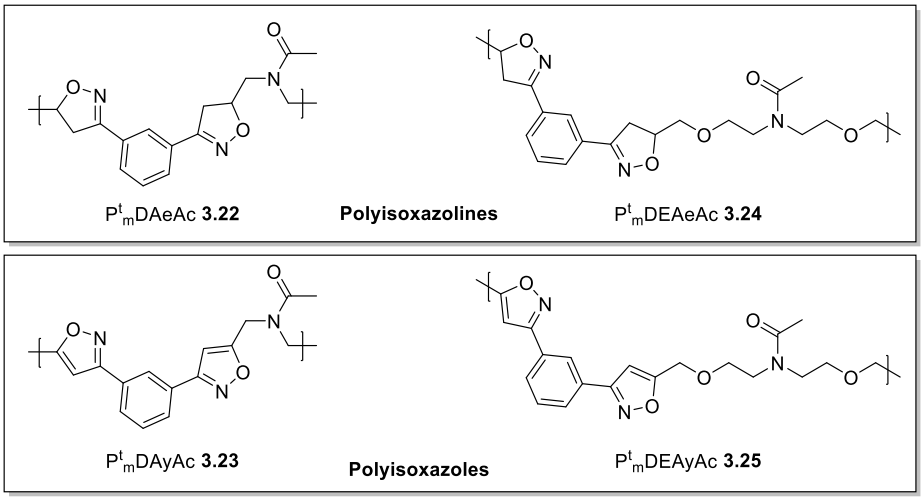

Figure 7-4: Polymers formed using *meta*-OC **2.1** and model dipolarophile monomers **3.5-3.8.**

7.3 Optimisation

In chapters 2 and 3 low molecular weight polymers were formed using the conditions reported by Takata[317] (P^t). Using these conditions as a basis, an optimisation study was performed to improve achievable molecular weight. The study used a monofunctional oximoyl chloride **4.1** along with DEAyAc **3.8** to examine the conversion of alkyne to isoxazole using a variety of conditions. The study concluded that the use of 3 Å MS at 25 ºC in DMF gave the best conversion of alkyne to isoxazole. The study also showed that EtOH, a greener solvent, could be used in place of DMF whilst still achieving high conversion of **3.8** to DIAc **4.7**.

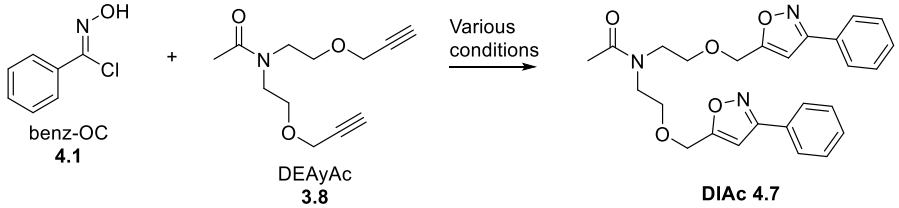

Figure 7-5: Optimisation study used the reaction between oximoyl chloride **4.1** and DEAyAc **3.8**.

Although successful for small molecule synthesis these "optimised" conditions (P^o) were poor when trialled as a polymerisation method. The conditions resulted in a slow polymerisation rate leading to a low yield of low molecular weight polymers after 14 days of reaction. During the trialling of the "optimised" conditions the original conditions used by Takata *et al.*[317] (P^t) were used as baseline. The trial revealed that these conditions did not give complete polymerisation after 24 hours, as had previously been done, but rather after 48 hours. Moving forwards polymerisation were carried out using the original conditions but now over 2 days (P^{t2}) rather than 1.

7.4 Renewable dialkynes

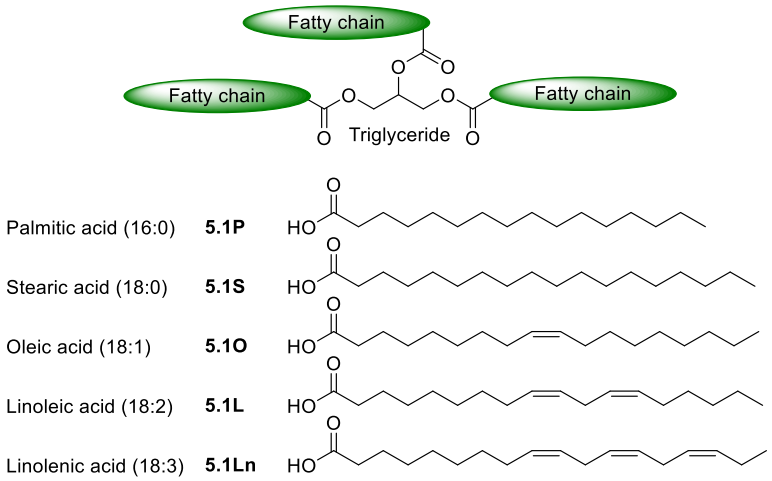

Figure 7-6: Triglyceride structure (above) five most common fatty acids in vegetable oils (below).

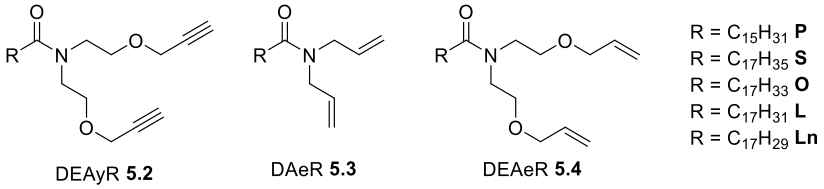

Figure 7-7: Dipolarophilic monomers derived from fatty acids

The five most common fatty acids **5.1P-Ln** found in vegetable oils were used as a feedstock for dipolarophilic monomers **5.2**, **5.3** and **5.4** based on the model monomers from chapter 3. The variety of monomers was chosen as they were predicted to produce polymers with different physical characteristics. These fatty acid derived polymers had lower glass transition temperatures than the related acetyl polymers in chapter 3. Between the fatty acid derived polymers the inclusion of the ether link in the monomer had the greatest effect on decreasing T_g. Cross-linking/branching was also observed in

the polymers derived from unsaturated fatty acids (oleic, linoleic and linolenic acid **5.1O-Ln**), this was more evident in the polyisoxazoles than the polyisoxazolines.

An investigation into reductive cleavage of isoxazoles was attempted for post-polymerisation modification applications. The trials used conditions ($LiAlH_4$ based and iron based) taken from a Takata *et al*.[318] paper. Both methods trialled were unsuccessful.

7.5 Renewably derived nitrile oxide precursors

Prior to forming renewably derived aromatic oximoyl chloride pre-monomers, a study into the effect of ring substituent on oximoyl chloride stability was performed. The stability of 10 oximoyl chlorides was assessed by TGA. The study indicated that electron donating groups *ortho* to the oximoyl chloride reduced stability whilst groups *para* to the oximoyl chloride had limited effect. Electron withdrawing groups in the *para* position however increased stability as did electron donating groups in the *meta* position. The effect of stability on reactivity was assessed using 3 oximoyl chlorides with a range of stabilities and a dialkyne, the results inferred that higher stabilities resulted in lower conversions of alkyne to isoxazole. From this initial work vanillin **6.1** was chosen as a renewable feedstock for aromatic oximoyl chlorides as it was predicted to form compounds with similar thermal stabilities to *meta*-OC **2.1**.

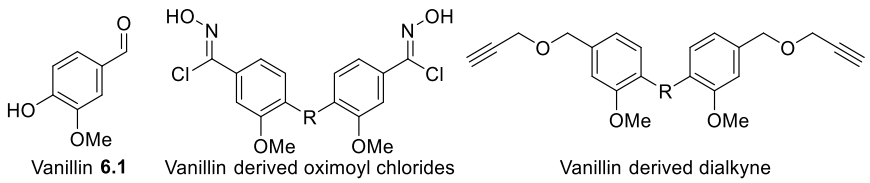

Figure 7-8: Monomer types derived from renewable vanillin **6.1** for use in polyisoxazole synthesis.

Vanillin **6.1** was used to form 2 oximoyl chloride pre-monomers as well as a dialkyne dipolarophilic monomer. The two vanillin derived oximoyl chlorides and DEAyS **5.2S** were used to form the first (to my knowledge) fully renewably derived polyisoxazoles. Whilst the vanillin derived dialkyne was used with the ether linked oximoyl chloride to form a completely vanillin derived polyisoxazole.

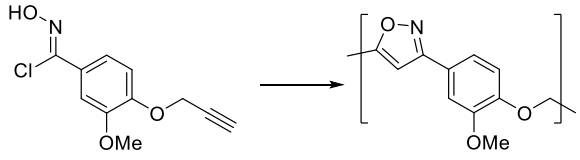

6.17 **6.18 - 6.24**

Figure 7-9: Vanillin derived dual functional monomer 6.17 and homopolyisoxazoles 6.18 – 6.24.

As both oximoyl chlorides and dialkynes could be derived from vanillin **6.1** it could be used to form a dual functionalised monomer **6.17**. This monomer was used to form a homopolymer under the standard polymerisation condition (P^{t2}), the resulting polymer P^{t2}HOMO-solid **6.18** was insoluble with high thermal stability (T_5 = 281 ºC) and a T_g of 138 ºC. Homopolymers could also be formed from **6.17** by solvent free polymerisations at 120 ºC both with and without molecular sieves. The solvent free polymers P^{sf}HOMO **6.19 – 6.24** were also insoluble and had higher thermal stability and glass transition temperatures than P^{t2}HOMO-solid **6.18**.

7.6 Conclusion

The work in this thesis explored whether renewably derived polymers could be formed by nitrile-oxide/dipolarophile cycloadditions and examined the properties and structure of the resulting materials. It was determined that polyisoxazoles and polyisoxazolines with low numbers of repeat units could be achieved by step growth polymerisation using nitrile-oxide/dipolarophile cycloadditions. Monomers for these step-growth polymerisation were successfully derived from renewable sources and applied to form renewably derived polymers, with vegetable oil as a feedstock for dipolarophiles and vanillin as a feedstock for dipolarophiles and nitrile-oxides. Unsaturated vegetable oils allowed the formation of branched polymers, whilst vanillin gave access to dual functional monomers and the resulting homopolymers.

The polymerisation conditions used repeatedly resulted in low numbers of repeat units and cyclical polymer structures. A study into reductive cleavage of isoxazoles for post-polymer modification was also attempted. The conditions reported by Takata *et al.*[313] were trial and resulted in aziridines as opposed to the desired β-amino alcohols or no reaction at all.

7.7 Future work

Low numbers of repeat units was a limitation of the polymers formed by nitrile-oxide/dipolarophile cycloadditions. Use of macromonomers may be a method of achieving polyisoxazolines and polyisoxazoles with higher molecular weights and large numbers of repeat units. During the study into alternative oximoyl chloride feedstocks an ABA oligomer **6.6c** was formed using **6.4h** and DEAyS **5.2S**. The diisoxazole **6.6c** could be deprotected to give a diphenol macromonomer. High molecular weight polyisoxazoles could therefore be attained by using the diphenol macromonomer in well-studied polymerisations such as in the formation of polyesters and polyethers.

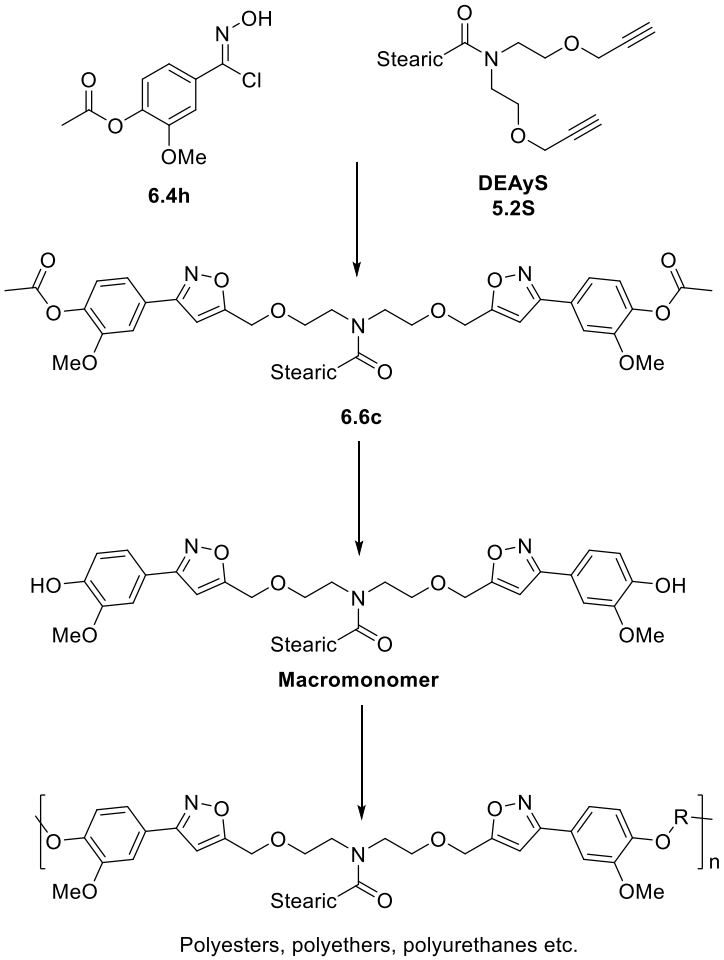

Figure 7-10: Possible formation of a high molecular weight polyisoxazoles *via* a macromonomer.

The limited study into isoxazole reductive cleavage was unsuccessful, either resulting in aziridines or no reaction. There are a multitude of methods reported for isoxazole reductive cleavage in the literature. These methods should be explored using a model

oligomer such as O_mDEAyS-ABA **5.8** to determine how to achieve reductive cleavage and the nature of the resulting functional groups. This study could then be applied to vegetable oil derived polyisoxazoles for post polymer modification, giving access to a range of functional groups and polymer properties.

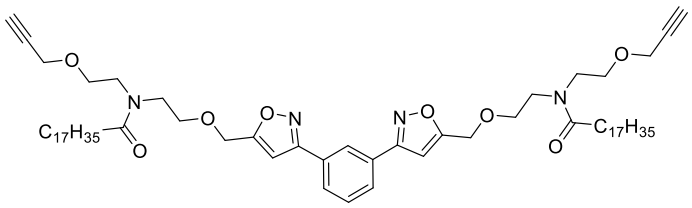

O_mDEAyS-ABA **5.8**

Figure 7-11: Vegetable oil derived isoxazole oligomer O_mDEAyS-ABA **5.8** that could be used to study isoxazole reductive cleavage conditions for applications in post-polymerisation modifications of polyisoxazoles.

8.0 Experimental

8.1 General Information

Solvents and starting materials were used as received without further purification. Reactions were performed under atmospheric conditions unless stated otherwise. Thin layer chromatography was performed using Merck 60 F_{254} silica gel plates. Visualisation was done using UV light (254nm) and permanganate dip. Column purification was achieved using Aldrich Chemistry® silica gel, technical grade, pore size 60 Å, 40 – 63 μm.

^{1}H & ^{13}C NMR spectra were obtained using Bruker Avance 300, 400, 500, and 600 MHz spectrometers. Chemical shifts are given in parts per million (ppm) relative to tetramethylsilane (TMS). Coupling constants (*J*) are expressed in Hertz (Hz). Multiplicites are recorded as: s (singlet), brs (broad singlet), d (doublet), t (triplet), q (quartet), m (multiplet), brm (broad multiplet). Proton environment is indicated by a superscript symbol (H^{x}).

IR spectra were performed on a Bruker ALPHA platinum ATR Fourier Transform spectrometer. Absorptions are given in wavenumbers (cm^{-1}). ES-MS was achieved using an Agilent 6310B single Quad. Melting points were gathered with a Gallenkamp MDP350.

GPC analysis of compounds with $CHCl_3$ as eluent was achieved using an Agilent Infinity II MDS instrument equipped with differential refractive index (DRI), viscometry (VS), dual angle light scatter (LS) and multiple wavelength UV detectors. The system was equipped with 2 x PLgel Mixed C columns (300 x 7.5 mm) and a PLgel 5 μm guard column. The eluent is $CHCl_3$ with 2 % TEA (triethylamine) additive. Samples were run at 1ml/min at 30'C. Poly(methyl methacrylate), and polystyrene standards (Agilent EasyVials) were used for calibration. Ethanol was added as a flow rate marker. Analyte samples were filtered through a GVHP membrane with 0.22 μm pore size before injection. Respectively, experimental molar mass ($M_{n,SEC}$) and dispersity ($Đ$) values of synthesized polymers were determined by conventional calibration using Agilent GPC/SEC software.

GPC analysis of compounds with DMF as eluent was achieved using an Agilent Infinity II MDS instrument equipped with differential refractive index (DRI), viscometry (VS), dual angle light scatter (LS) and variable wavelength UV detectors. The system was equipped with 2 x PLgel Mixed D columns (300 x 7.5 mm) and a PLgel 5 µm guard column. The eluent is DMF with 5 mmol NH_4BF_4 additive. Samples were run at 1ml/min at 50'C. Poly(methyl methacrylate) standards (Agilent EasyVials) were used for calibration between 955,000 – 550 $gmol^{-1}$. Analyte samples were filtered through a nylon membrane with 0.22 μm pore size before injection. Respectively, experimental molar mass ($Mn,_{SEC}$) and dispersity ($Đ$) values of synthesized polymers were determined by conventional calibration and universal calibration using Agilent GPC/SEC software.

MALDI-TOF was performed using a Bruker Autoflex Speed MALDI-TOF. Samples were prepared for MALDI-TOF analysis using DMF doped with NaI (0.1 mg ml^{-1}). Samples were dissolved in the doped DMF (10 mg ml^{-1}). The matrix (DCTB) was also dissolved in separate doped DMF (40 mg ml^{-1}). Equal volumes (10 µl) of the two DMF solutions were mixed, a small amount of the resulting mixture was placed on ground steel plate and dried in a vacuum oven at 25 °C and 0.01 atm for 30 minutes.

DSC was achieved using a Mettler-Toledo DSC1 with autosampler. DSC samples were all heated and cooled under N_2 in 40 µl aluminium pans, specific heating cycles are described in the appropriate sections. T_g's were taken as the midpoint of transitions. TGA was achieved using a Mettler-Toledo TGA with autosampler. TGA samples, under nitrogen, were heated from 25 °C to 600 °C at 10 ºC / min in 40 µl aluminium pans unless stated otherwise. DMA was run using a Perkin Elmer DMA 8000 with liquid nitrogen cooling. Samples were loaded in aluminium envelopes and analysed using the single cantilever method between 30 ºC and 260 ºC at a heating rate of 5 ºC / min.

8.2 General procedures in chapter 2

8.2.1 Oximoyl chloride synthesis for optimised polymerisation trial

(1E,3E)-isophthalaldehyde dioxime (2.12)[317]

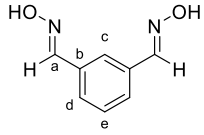

Sodium acetate (13.4 g, 16.3 mmol, 2.2 eq.) and hydroxyamine hydrochloride (11.4 g, 16.3 mmol , 2.2 eq.) were dissolved in water (50 ml) and introduced to isophthaladehyde **2.11** (10.0 g, 7.5 mol, 1 eq.) dispersed in ethanol (50 ml). A white precipitate began to form within 30 minutes. After 4 hours the solid precipitate was recovered by Buchner filtration and washed with cold ethanol, purification of the precipitate by recrystallisation from EtOAc gave a cream powder. (71 %); R_f = 0.3 in 50 % EtOAc, m.p. 186 – 188 °C (lit. 181.2 – 182.0 °C); ν_{max}/cm^{-1} 3203 (OH), 2920 (C-H), 2790 (C-H), 1642 (C=N), 1490 (N-O), 945 (C-H); ^{1}H NMR (400MHz, Acetone) δ 10.46 (s, 2H, H^{OH}), 8.17 (s, 2H, H^a), 7.88 (s, 1H, H^c), 7.62 (dd, *J* = 7.5, 1.5 Hz, 2H, H^d), 7.42 (t, *J* = 7.5 Hz 1H, H^e); ^{13}C (101 MHz, d-Acetone) δ 148.97 (C^a), 134.74 (C^b), 129.86 (C^e), 128.25 (C^d), 125.47 (C^c); *m/z* (ES^+) calcd. ($C_8H_8N_2O_2 + H^+$): 165.0659, found: 165.0655 ($M + H^+$).

(1Z,3Z)-N'1,N'3-dihydroxyisophthalimidoyl dichloride (*Meta*-OC, 2.1)[317]

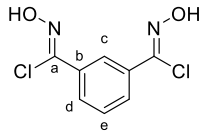

Isophthalaldehyde dioxime (**2.12**) (7.4 g, 45.1 mmol, 1eq.) was dissolved in DMF (50 ml) at RT. *N*-Chlorosuccinimide (13.2 g, 99.2 mmol, 2.2 eq) was introduced in 5 parts over the course of an hour. 2 hours after the last portion was added the reaction mixture was poured into cold water (150 ml) and extracted with ethyl acetate (150 ml). The organic layer was washed with water (5 × 50 ml) and saturated sodium thiosulfate solution (1 × 50 ml), then dried over magnesium sulphate. Solvent removal *in vacuo* gave a crude yellow solid, which was purified by recrystallization from toluene to give a cream solid. (84 %); R_f = 0.7 in 50 % EtOAc; m.p. 159 – 161 °C (lit. 155.7 – 156.0 °C) ν_{max}/cm^{-1} 3265 (OH), 1624 (C=N), 1483 (N-O), 990 (C-H), 802 (C-Cl); ^{1}H NMR (500MHz, Acetone) 11.58 (s, 2H, H^{OH}), 8.35 (s, 1H, H^c), 7.96 (dd, *J* = 8.0, 1.5 Hz, 2H, H^d), 7.57 (t, *J* = 8.0 Hz, 1H, H^e); ^{13}C NMR (126 MHz, Acetone) δ 136.90 (C^a), 134.45 (C^b), 129.93 (C^e), 129.37 (C^d), 125.82 (C^c); *m/z* (ES^+) calcd. ($C_8H_6Cl^{35}{}_2N_2O_2 + H^+$): 232.9879, found:

232.9878 ($M + H^+$); calcd. ($C_8H_6Cl^{35}Cl^{37}N_2O_2 + H^+$): 234.9850, found: 234.9848 ($M + H^+$); calcd. ($C_8H_6Cl^{37}{}_2N_2O_2 + H^+$): 236.9822, found: 236.9821 ($M + H^+$).

8.2.2 General procedure used for synthesis of polyisoxazolines[317]

(1Z,3Z)-N'1,N'3-dihydroxyisophthalimidoyl dichloride (*meta*-OC, **2.1**) and dipolarophile were dissolved in DMF (1 M). 4 Å molecular sieves were added (1600 g / mol of di(oximoyl chloride)) and stirred (50 RPM) at 25 ^oC for 30 minutes. The temperature was then raised to 80 ^oC for 24 hours. The reaction mixture was diluted with $CHCl_3$ (5 ml) and filtered to remove molecular sieves, the sieves were washed further with warm $CHCl_3$ (5ml), the filtrate was then reduced *in vacuo* to leave the polymer in DMF. The polymer was taken back into a small amount of $CHCl_3$ (2 ml) and added dropwise to MeOH (40 ml) causing a ppt to form. The ppt was collected by passing the solution through filter paper on a sintered funnel. The ppt was washed with MeOH (3 x 25 ml), then collected off the filter paper with warm $CHCl_3$ (3 x 25 ml). The $CHCl_3$ was reduced *in vacuo* to leave a polymeric product.

P^t_mDEGDA-1 (2.5)[317]

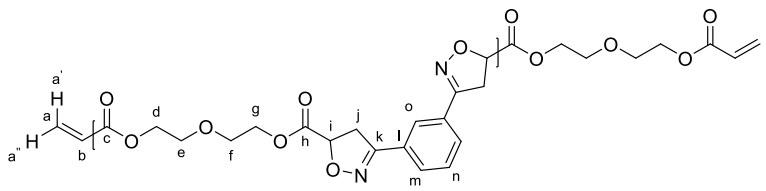

The general procedure for the synthesis of polyisoxazolines was applied using *meta*-OC **2.1** (100 mg, 0.43 mmol, 1eq.) and DEGDA **2.4** (91.9 mg, 0.43 mmol, 1eq.) to give a pale orange solid. (70 %); ν_{max} / cm^{-1}: 2953 (C-H), 2873 (C-H), 1736 (C=O), 1605 ($C=N_{furoxan}$), 1575 ($C=N_{furoxan}$), 1332 (N-O), 1198 (C-O), 1132 (C-O), 895 (C-H). ^1H NMR (400 MHz, $CDCl_3$) δ 7.87 (brs, H^o), 7.69 (brs, H^m), 7.41 (brs, H^n), 6.41 (d, *J* = 17.0 Hz, $H^{a'}$), 6.13 (dd, *J* = 17.5, 10.0 Hz, H^b), 5.83 (d, *J* = 10.5 Hz, $H^{a''}$), 5.21 (brs, H^i), 4.51 – 4.13 (brm, $H^{d/g}$), 3.72 (brs, $H^{e/f}$), 3.64 (brs, H^j); ^{13}C NMR (101 MHz, $CDCl_3$) δ 170.07 ($C^{c/h}$), 155.77 (C^i), 131.33 (C^a), 129.43 (C^{Ar}), 129.35 (C^l), 128.81 (C^{Ar}), 128.28 (C^b), 125.40 (C^{Ar}), 78.30 (C^i), 69.24 ($C^{e/f}$), 68.83 ($C^{e/f}$), 64.91 ($C^{d/g}$) 64.75 ($C^{d/g}$), 63.62 ($C^{d/g}$), 38.85 (C^j).

P$^{t}_{m}$DEGDMA-1 (2.14)[317]

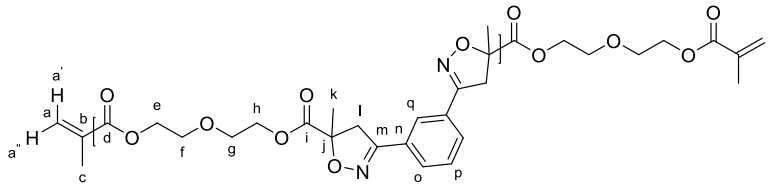

The general procedure for the synthesis of polyisoxazolines was applied using *meta*-OC **2.1** (100 mg, 0.43 mmol, 1eq.) and DEGDMA **2.8** (104.0 mg, 0.43 mmol, 1 eq.) to give a pale orange solid. (84 %); ν_{max} / cm^{-1}: 2932 (C-H), 2871 (C-H), 1732 (C=O), 1606 (C=N$_{furoxan}$), 1571 (C=N$_{furoxan}$), 1338 (N-O), 1182 (C-O), 1135 (C-O), 1104 (C-O), 909 (C-H); ^{1}H NMR (400 MHz, $CDCl_3$) δ 7.87 (brs, H^{q}), 7.69 (brs, H^{o}), 7.42 (brs, H^{p}), 6.10 (s, H$^{a'}$), 5.56 (s, H$^{a''}$), 4.29 (brs, H$^{e/h}$), 3.89 (d, *J* = 16.5 Hz, H^{l}), 3.71 (brs, H$^{f/g}$), 3.24 (d, *J* = 16.5 Hz, H^{l}), 1.92 (s, H^{c}), 1.70 (s, H^{k}); ^{13}C NMR (101 MHz, $CDCl_3$) δ 171.78 (C$^{d/i}$), 155.95 (C^{m}), 131.33 (C^{a}), 129.85 (C^{n}), 129.38 (C^{Ar}), 128.51 (C^{Ar}), 125.07 (C^{Ar}), 86.60 (C^{j}), 68.90 (C$^{f/g}$), 64.99 (C$^{e/h}$), 44.67 (C^{l}), 23.63 (C$^{k/c}$).

Synthesis of P$^{t}_{m}$EGDA-1 (2.27)

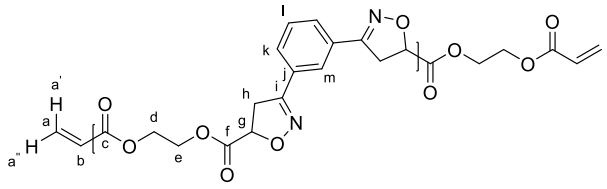

The general procedure for the synthesis of polyisoxazolines was applied using *meta*-OC **2.1** (100 mg, 0.43 mmol, 1eq.) and EGDA **2.9** (73.0 mg, 0.43 mmol, 1eq.) to give a pale orange solid. (48 %), ν_{max} / cm^{-1}: 2957 (C-H), 2926 (C-H), 1738 (C=O), 1672 (C=N), 1331 (N-O), 1184 (C-O), 893 (C-H); ^{1}H NMR (400 MHz, $CDCl_3$) δ 7.83 (brs, H^{m}), 7.72 (brs, H^{k}), 7.39 (brs, H^{l}), 6.37 (d, *J* = 17.5 Hz, H$^{a'}$), 6.08 (dd, *J* = 17.0, 10.5 Hz, H^{b}), 5.82 (d, *J* = 10.0 Hz, H$^{a''}$), 5.15 (br, H^{g}), 4.62 – 4.20 (brm, H$^{d/e}$), 3.63 (brs, H^{h}); ^{13}C NMR (101 MHz, $CDCl_3$) δ 169.97 (C$^{c/f}$), 155.83 (C^{i}), 131.77 (C^{d}), 129.43 (C^{Ar}), 129.19 (C^{j}), 128.87 (C^{Ar}), 127.87 (C^{Ar}), 125.45 (C^{Ar}), 78.15 (C^{g}), 78.11 (C^{g}), 63.64 (C$^{d/e}$), 63.22 (C$^{d/e}$), 63.13 (C$^{d/e}$), 61.93 (C$^{d/e}$), 38.82 (C^{h}).

Synthesis of P$^{t}_{m}$PEGDA-1 (2.28)

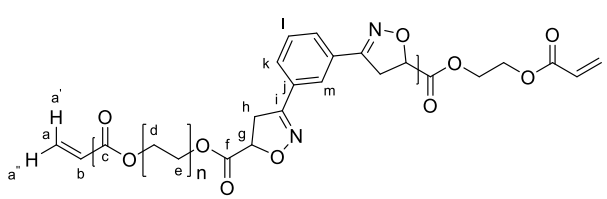

The general procedure for the synthesis of polyisoxazolines was applied using *meta*-OC **2.1** (100 mg, 0.43 mmol, 1eq.) and PEGDA 575

av. MW **2.10** (246.7 mg, 0.43 mmol, 1 eq.) to give a brown viscous oil. (43 %); ν_{max} / cm^{-1}: 2868 (C-H), 1737 (C=O), 1606 (C=$N_{furoxan}$), 1332 (N-O), 1199 (C-O), 897 (C-H); ^{1}H NMR (400 MHz, $CDCl_3$) δ 7.93 (brs, H^{m}), 7.74 (brd, *J* = 7.0 Hz, H^{k}), 7.46 (brt, *J* = 7.0 Hz, H^{l}), 6.42 (d, *J* = 17.0 Hz, $H^{a'}$), 6.15 (dd, *J* = 17.5, 10.0 Hz, H^{b}), 5.83 (d, *J* = 10.5 Hz, $H^{a''}$), 5.23 (t, *J* = 9.0 Hz, H^{g}), 4.36 (brs, $H^{d/e}$), 3.74 (brs, $H^{d/e}$), 3.65 (brs, H^{h}); ^{13}C NMR (101 MHz, $CDCl_3$) δ 170.05 ($C^{c/f}$), 155.63 (C^{i}), 128.86 (C^{Ar}), 125.43 (C^{Ar}), 78.33 (C^{g}), 70.77 – 70.71 ($C^{d/e}$), 68.83 ($C^{d/e}$), 65.07 ($C^{d/e}$), 38.85 (C^{h}).

Synthesis of P^{t}_{m}DEGDA-0.8 (2.29)

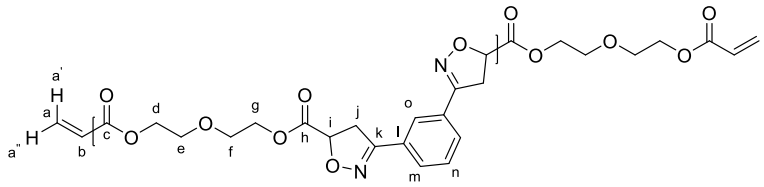

The general procedure for the synthesis of polyisoxazolines was applied using *meta*-OC **2.1** (100 mg, 0.43 mmol, 1eq.) and DEGDA **2.4** (73.5 mg, 0.34 mmol, 0.8 eq.) to give a pale brown solid. (83 %); ν_{max} / cm^{-1}: 2953 (C-H), 2873 (C-H), 1733 (C=O), 1605 (furoxan), 1574 (furoxan), 1332 (N-O), 1195 (C-O), 1131 (C-O), 895 (C-H); ^{1}H NMR (400 MHz, $CDCl_3$) δ 7.87 (brs, H^{o}), 7.68 (brs, H^{m}), 7.39 (brs, H^{n}), 5.20 (brs, H^{i}), 4.32 (brs, $H^{d/g}$), 3.72 (brs, $H^{e/f}$), 3.65 (brs, H^{j}); ^{13}C NMR (101 MHz, $CDCl_3$) δ 170.11 ($C^{c/h}$), 155.80 (C^{k}), 129.44 (C^{Ar}), 129.38 (C^{l}), 128.82 (C^{Ar}), 125.41 (C^{Ar}), 78.32 (C^{i}), 68.86 ($C^{e/f}$), 64.79 ($C^{d/g}$), 38.88 (C^{j}).

Synthesis of P^{t}_{m}DEGDA-1.2 (2.30)

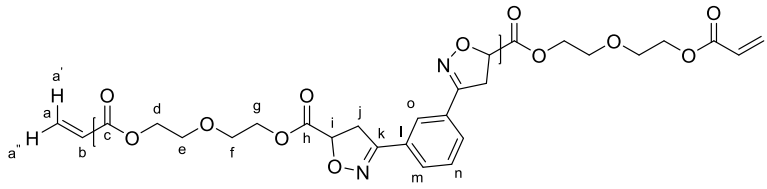

The general procedure for the synthesis of polyisoxazolines was applied using *meta*-OC **2.1** (100 mg, 0.43 mmol, 1eq.) and DEGDA **2.4** (110.3 mg, 0.52 mmol, 1.2 eq.) to give a pale orange solid. (72 %); ν_{max} / cm^{-1}: 2953 (C-H), 2873 (C-H), 1733 (C=O), 1605 (C=$N_{furoxan}$), 1574 (C=$N_{furoxan}$), 1332 (N-O), 1195 (C-O), 1130 (C-O), 893 (C-H); ^{1}H NMR (400 MHz, $CDCl_3$) δ 7.95 (brs, H^{o}), 7.70 (brs, H^{m}), 7.42 (brs, H^{n}), 6.41 (d, *J* = 17.0 Hz, $H^{a'}$), 6.13 (dd, *J* = 17.5, 10.0 Hz, H^{b}), 5.83 (d, *J* = 10.5 Hz, $H^{a''}$), 5.21 (brs, H^{i}), 4.33 (brs, $H^{d/g}$), 3.73 (s, $H^{e/f}$), 3.65 (s, H^{j}); ^{13}C NMR (101 MHz, $CDCl_3$) δ 170.06 ($C^{c/h}$), 155.77 (C^{k}), 131.34 (C^{a}), 129.44 (C^{Ar}), 129.38 (C^{l}), 128.82 (C^{Ar}), 128.29 (C^{b}),

125.41 (C^{Ar}), 78.31 (C^{i}), 69.25 ($C^{e/f}$), 68.85 ($C^{e/f}$), 64.92 ($C^{d/g}$), 64.78($C^{d/g}$), 63.63 ($C^{d/g}$), 38.86 (C^{j}).

Synthesis of P^{t}_{m}EGDA-0.8 (2.31)

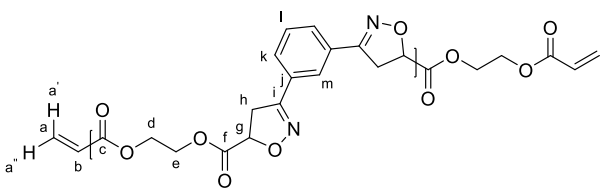

The general procedure for the synthesis of polyisoxazolines was applied using *meta*-OC **2.1** (100 mg, 0.43 mmol, 1eq.) and EGDA **2.9** (58.4 mg, 0.43 mmol, 0.8 eq.) to give a pale orange solid. (60 %); ν_{max} / cm^{-1}: 2940 (C-H), 2929 (C-H), 1740 (C=O), 1689 (C=N), 1608 ($C=N_{furoxan}$), 1570 ($C=N_{furoxan}$), 1332 (N-O), 1186 (C-O), 888 (C-H); ^{1}H NMR (400 MHz, $CDCl_3$) δ 7.95 – 7.55 (brm, $H^{m/k}$), 7.53 – 7.31 (m, H^{l}), 5.16 (brs, H^{g}), 4.64 – 4.22 (brm, $H^{d/e}$), 3.62 (brs, H^{h}); ^{13}C NMR (101 MHz, $CDCl_3$) δ 170.09 ($C^{c/f}$), 155.86 (C^{i}), 129.48 (C^{Ar}), 128.94 (C^{Ar}), 78.15 (C^{g}), 63.25 ($C^{d/e}$), 63.13 ($C^{d/e}$).

Synthesis of P^{t}_{m}EGDA-1.2 (2.32)

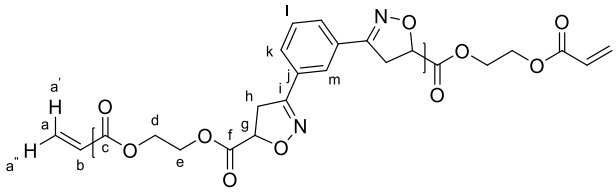

The general procedure for the synthesis of polyisoxazolines was applied using *meta*-OC **2.1** (100 mg, 0.43 mmol, 1eq.) and EGDA **2.9** (87.6 mg, 0.52 mmol, 1.2 eq.) to give a pale orange solid. (56 %); ν_{max} / cm^{-1}: 2959 (C-H), 1737 (C=O), 1671 (C=N), 1616 ($C=N_{furoxan}$), 1573 ($C=N_{furoxan}$), 1331 (N-O), 1182 (C-O), 892 (C-H); ^{1}H NMR (400 MHz, $CDCl_3$) δ 7.83 (brs, H^{m}), 7.70 (brs, H^{k}), 7.40 (brs, H^{l}), 6.37 (d, *J* = 17.0 Hz, $H^{a'}$), 6.22 – 5.97 (m, H^{b}), 5.82 (d, *J* = 10.0 Hz, $H^{a''}$), 5.16 (brs, H^{g}), 4.65 – 4.17 (brm, $H^{d/e}$), 3.64 (brs, H^{h}); ^{13}C NMR (101 MHz, $CDCl_3$) δ 169.93 ($C^{c/f}$), 155.82 (C^{i}), 131.77 (C^{d}), 129.42 (C^{Ar}), 129.19 (C^{j}), 128.87 (C^{Ar}), 127.87 (C^{Ar}), 125.44 (C^{Ar}), 78.17 (C^{g}), 78.11 (C^{g}), 63.63 ($C^{d/e}$), 63.22 ($C^{d/e}$), 63.14 ($C^{d/e}$), 61.92 ($C^{d/e}$), 38.82 (C^{h}).

Synthesis of P^{t}_{m}PEGDA-0.8 (2.33)

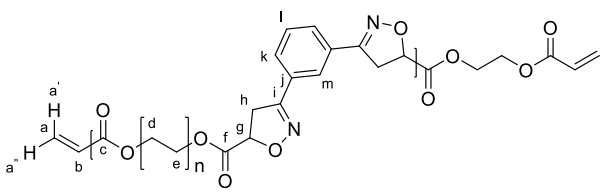

The general procedure for the synthesis of polyisoxazolines was applied using *meta*-OC **2.1** (100 mg, 0.43 mmol, 1eq.) and PEGDA 575

av. MW **2.10** (197.4 mg, 0.34 mmol, 0.8 eq.) to give a brown viscous oil. (79 %); ν_{max} / cm^{-1}: 2866 (C-H), 1735 (C=O), 1605 ($C=N_{furoxan}$), 1332 (N-O), 1198 (C-O), 1090 (C-O), 895 (C-H); ^{1}H NMR (400 MHz, $CDCl_3$) δ 7.93 (brs, H^m), 7.74 (brd, *J* = 7.0 Hz, H^k), 7.50 – 7.42 (brm, H^l), 5.23 (brt, *J* = 9.0 Hz, H^g), 4.35 (brs, $H^{d/e}$), 3.74 (brs, $H^{d/e}$), 3.63 (brs, H^h); ^{13}C NMR (101 MHz, $CDCl_3$) δ 170.04 ($C^{c/f}$), 155.62 (C^i), 129.45 (C^{Ar}), 129.43 (C^j), 128.86 (C^{Ar}), 125.42 (C^{Ar}), 78.33 (C^g), 70.75 – 70.70 ($C^{d/e}$), 68.88 ($C^{d/e}$), 65.06 ($C^{d/e}$), 38.85 (C^h).

Synthesis of P^t_mPEGDA-1.2 (2.34)

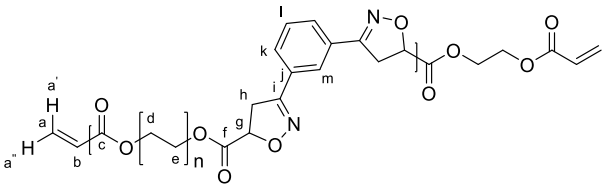

The general procedure for the synthesis of polyisoxazolines was applied using *meta*-OC **2.1** (100 mg, 0.43 mmol, 1eq.) and PEGDA 575 av. MW **2.10** (296.1 mg, 0.52 mmol, 1.2 eq.) to give a brown viscous oil. (30 %); ν_{max} / cm^{-1}: 2868 (C-H), 1737 (C=O), 1606 ($C=N_{furoxan}$), 1332 (N-O), 1198 (C-O), 1093 (C-O), 896 (C-H); ^{1}H NMR (400 MHz, $CDCl_3$) δ 7.94 (brs, H^m), 7.74 (brd, *J* = 7.0 Hz, H^k), 7.46 (brt, *J* = 7.0 Hz, H^l), 6.42 (d, *J* = 17.0 Hz, $H^{a'}$), 6.15 (dd, *J* = 17.5, 10.0 Hz, H^b), 5.83 (d, *J* = 10.5 Hz, $H^{a''}$), 5.23 (brt, *J* = 9.0 Hz, H^g), 4.36 (brs, $H^{d/e}$), 3.74 (brs, $H^{d/e}$), 3.65 (brs, H^h); ^{13}C NMR (101 MHz, $CDCl_3$) δ 170.05 ($C^{c/f}$), 155.63 (C^i), 128.87 (C^{Ar}), 125.43 (C^{Ar}), 78.33 (C^g), 70.77 – 70.71 ($C^{d/e}$), 68.88 ($C^{d/e}$), 65.07 ($C^{d/e}$), 38.86 (C^h).

Synthesis of P^t_mDEGDMA-0.8 (2.35)

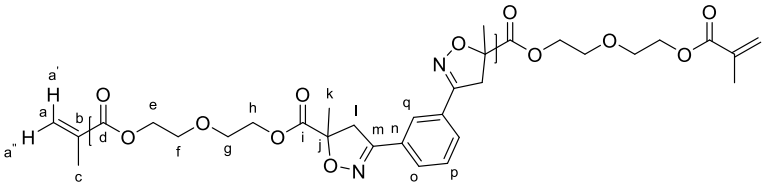

The general procedure for the synthesis of polyisoxazolines was applied using *meta*-OC **2.1** (100 mg, 0.43 mmol, 1 eq.) and DEGDMA **2.8** (83.2 mg, 0.34 mmol, 0.8 eq.) to give a pale orange solid. (72 %); ν_{max} / cm^{-1}: 2933 (C-H), 2872 (C-H), 1734 (C=O), 1604 ($C=N_{furoxan}$), 1573 ($C=N_{furoxan}$), 1338 (N-O), 1183 (C-O), 1106 (C-O), 910 (C-H); ^{1}H NMR (400 MHz, $CDCl_3$) δ 7.87 (brs, H^q), 7.70 (brs, H^o), 7.43 (brs, H^p), 4.29 (brs, $H^{e/h}$), 3.89 (brd, *J* = 16.5 Hz, H^l), 3.71 (brs, $H^{f/g}$), 3.24 (brd, *J* = 17.0 Hz, H^l), 1.70 (brs, H^k); ^{13}C NMR (101 MHz, $CDCl_3$) δ 155.99 (C^m), 129.85 (C^n), 129.41 (C^{Ar}), 128.55 (C^{Ar}), 125.09 (C^{Ar}), 86.63 (C^j), 68.93 ($C^{f/g}$), 65.02 ($C^{e/h}$), 44.70 (C^l), 23.64 (C^k).

Synthesis of P^{t}_{m}DEGDMA-1.2 (2.36)

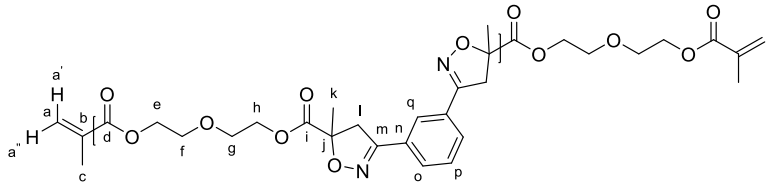

The general procedure for the synthesis of polyisoxazolines was applied using *meta*-OC **2.1** (100 mg, 0.43 mmol, 1eq.) and DEGDMA **2.8** (124.7 mg, 0.51 mmol, 1.2 eq.) to give a pale orange solid. (84 %) ν_{max} / cm^{-1}: 2933 (C-H), 2871 (C-H), 1733 (C=O), 1604 (furoxan), 1338 (N-O), 1182 (C-O), 1104 (C-O), 910 (C-H); ^{1}H NMR (400 MHz, $CDCl_3$) δ 7.87 (brs, H^{q}), 7.69 (brs, H^{o}), 7.42 (brs, H^{p}), 6.10 (s, $H^{a'}$), 5.56 (s, $H^{a''}$), 4.29 (brs, $H^{e/h}$), 3.89 (brd, *J* = 16.5 Hz, H^{l}), 3.71 (brs, $H^{f/g}$), 3.24 (brd, *J* = 17.0 Hz, H^{l}), 1.92 (s, H^{c}), 1.70 (s, H^{k}); ^{13}C NMR (101 MHz, $CDCl_3$) δ 171.78 ($C^{d/i}$), 155.95 (C^{m}), 131.33 (C^{a}), 129.85 (C^{n}), 129.38 (C^{Ar}), 128.51 (C^{Ar}), 125.07 (C^{Ar}), 86.60 (C^{j}), 68.90 ($C^{f/g}$), 64.99 ($C^{e/h}$), 44.67 (C^{l}), 23.63 (C^{k}).

8.3 General Procedures Chapter 3

8.3.1 Procedures for the synthesis of dipolarophile acetamide monomers

***N,N*-diallylacetamide – DAeAc (3.5)**[365]

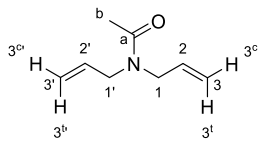

Diallylamine (15.0 g, 150 mmol, 1 eq.) was added dropwise to cooled (0 °C) acetic anhydride (26.8 g, 260 mmol, 1.75 eq) under nitrogen. After addition was complete the reaction was increased to 100 °C for 90 minutes. The reaction was then allowed to cool to room temperature before being distilled under vacuum. The acetic anhydride was distilled off at 100 °C, pure DAeAc **3.5** was collected at 150 °C as a colourless liquid. (89 %); R_f = 0.3 in 33 % EtOAc; ν_{max} / cm^{-1}: 3082 (=C-H), 2982 (C-H), 2922 (C-H), 1639 (C=O), 1410 (C-N), 918 (=C-H); ^{1}H NMR (500 MHz, $CDCl_3$) δ 5.87 – 5.59 (m, 2H, $H^{2/2'}$), 5.30 – 5.02 (m, 2H, $H^{3/3'}$), 3.98 (d, J = 6.0 Hz, 2H, $H^{1/1'}$), 3.85 (d, J = 5.0 Hz, 2H, $H^{1/1'}$), 2.09 (s, 3H, H^{b}); ^{13}C NMR (126 MHz, $CDCl_3$) δ 170.86 (C^{a}), 133.37 ($C^{2/2'}$), 132.74 ($C^{2/2'}$), 117.40 ($C^{3/3'}$), 116.77 ($C^{3/3'}$), 50.09 ($C^{1/1'}$), 47.92 ($C^{1/1}$), 21.45 (C^{b}); *m/z* (ES^{+}) m/z calcd. ($C_8H_{13}NO + Na^{+}$): 162.0889, found: 162.0889 ($M + Na^{+}$).

***N*,*N*-di(prop-2-yn-1-yl)acetamide – DAyAc (3.6)**

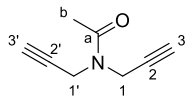

Dipropargylamine (1.0 g, 10.7 mmol, 1 eq.) was added dropwise to cooled (0 °C) acetic anhydride (1.3 g, 12.9 mmol, 1.2 eq) under nitrogen. After addition was complete the reaction was increased to 100 °C for 1 hour. The R_f of the product is similar to dipropargylamine, therefore the reaction was deemed complete using MS. The reaction was allowed to cool to room temperature before being taken into water (30 ml) and extracted with $CHCl_3$ (3 × 25 ml). The first extraction took a long time to separate. The organic extracts were combined and washed with water (50 ml) and brine (50 ml) before drying with $MgSO_4$ and removing the solvent *in vacuo* to leave a crude dark brown liquid. Purification through a silica plug resulted in DAyAc **3.6** as a pale yellow liquid. (93 %); R_f = 0.3 in 50 % EtOAc; ν_{max} / cm^{-1}: 3290 (≡C−H), 3245 (≡C−H), 2978 (C-H), 2119 (C≡C), 1646 (C=O), 1413 (C-N); ^{1}H NMR (500 MHz, $CDCl_3$) δ 4.31 (d, *J* = 2.0 Hz, 2H, $H^{1/1'}$), 4.18 (d, *J* = 2.0 Hz, 2H, $H^{1/1'}$), 2.30 (t, *J* = 2.0, 1H, $H^{3/3'}$), 2.22 (t, *J* = 2.0, 1H, $H^{3/3'}$), 2.18 (s, 3H, H^b); ^{13}C NMR (126 MHz, $CDCl_3$) δ 170.06 (C^a), 78.49 ($C^{2/2'}$), 77.79 ($C^{2/2'}$), 73.09 ($C^{3/3'}$), 72.40 ($C^{3/3'}$), 37.08 ($C^{1/1'}$), 33.90 ($C^{1/1'}$), 21.58 (C^b); *m/z* (ES^+) calcd. ($C_8H_9NO + Na^+$): 158.0576, found: 158.0577 ($M + Na^+$).

8.3.2 Procedure for the synthesis of diethanol acetamide **3.11**

***N*,*N*-bis(2-hydroxyethyl)acetamide - DOAc (3.11)**[338]

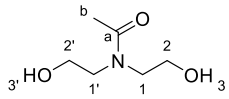

Diethanolamine (20.0 g, 19.0 mmol, 1 eq.) was dissolved in THF (150 ml) and cooled to 0 ºC in an ice bath. Acetic anhydride (23.3 g, 22.8 mmol, 1.2 eq.) was added dropwise (1 drop every two seconds) over the course of 4 hours. The solution was left to come to room temperature overnight. A sample was taken in the morning and analysed with NMR and MS, revealing a mixture of products. The solution was put under vacuum at 65 °C to remove acetic acid and any residual acetic anhydride. MS/NMR continued to show multiple products, particularly twice acetylated impurities. The crude product was taken back into methanol (100 ml) along with K_2CO_3 (7.00 g, 50.6 mmol) and refluxed for 5 hours. Water was then added until the solution was clear, following this it was neutralised with aqueous HCl (2 M, 80 ml). Methanol and water were removed in vacuo, to leave a yellow oil and solid. The oil was taken into acetone and filtered to remove the solid. The filtrate was then

reduced *in vacuo* to leave a yellow oil and some white solid. Under N_2 the yellow oil was taken into dry acetone and dried with 4 Å MS for 1 hour, the solution was then filtered to remove the residual white solid and sieves. The filtrate was once again reduced *in vacuo* to leave a yellow oil. (69 %); ν_{max} / cm^{-1}: 3353 (OH), 2934 (C-H), 1605 (C=O), 1036 (C-O); ^{1}H NMR (400 MHz, $CDCl_3$) δ 4.81 (brs, 2H, H^{OH}), 3.76 – 3.67 (m, 4H, $H^{2/2'}$), 3.51 – 3.38 (m, 4H, $H^{1/1'}$), 2.09 (s, 3H, H^{b}); ^{13}C NMR (101 MHz, $CDCl_3$) δ 173.15 (C^{a}), 60.84 ($C^{1/1'}$), 60.46 ($C^{1/1'}$), 53.15 ($C^{2/2'}$), 50.34 ($C^{2/2'}$), 22.07 (C^{b}); *m/z*: (ES^+) 169.5 $[MNa]^+$.

8.3.3 General procedure for the synthesis of ether containing monomers.

DOAc **3.11** (1 eq.) was dissolved in dry THF (0.5 M) under N_2. In a separate round bottom flask sodium hydride (60% in mineral oil, 2.2 eq.), was washed with pet. under N_2. Using a cannula the dissolved diethanolamide **3.11** was transferred into the vessel with NaH and left to homogenise for 30 mins at -78 °C. Alkyl halide (2.2 eq.) was added dropwise, and the reaction mixture was left to come to room temperature overnight. Water (10 ml) was added dropwise, under nitrogen, followed by aqueous 2M HCl (10 ml) to quench the reaction. Extraction with Et_2O was followed by washing the organic layer with water (2 x 50ml) and brine (50 ml) before drying with $MgSO_4$. Solvent was removed *in vacuo* to leave a crude product. Column purification through a silica plug resulted in an oil.

***N,N*-bis(2-(allyloxy)ethyl)acetamide – DEAeAc (3.7)**

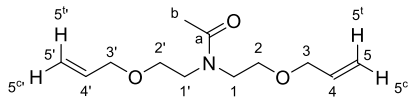

General procedure for the synthesis of an ether containing monomer was followed using DOAc (5.00 g, 34.0 mmol, 1 eq.), NaH (60% in mineral oil, 2.99 g, 74.7 mmol, 2.2 eq.), and allyl bromide (9.05 g, 74.7 mmol, 2.2 eq.). Column purification through a silica plug resulted in DEAeAc **3.7** a pure very pale yellow oil. (59 %); R_f = 0.3 in 25 % EtOAc; ν_{max} / cm^{-1}: 3080 (=C-H), 2980 (C-H), 2935 (C-H), 2858 (C-H), 1639 (C=O), 1417 (C-N), 1098 (C-O), 993 (=C-H), 921 (=C-H); ^{1}H NMR (500 MHz, $CDCl_3$) δ 5.94 – 5.72 (m, 2H, $H^{4/4'}$), 5.27 – 5.20 (m, 2H, $H^{5t/5t'}$), 5.19 – 5.11 (m, 2H, $H^{5c/5c'}$), 3.97 – 3.91 (m, 4H, $H^{3/3'}$), 3.60 – 3.51 (m, 8H, $H^{1/1'/2/2'}$), 2.12 (s, 3H, $H^{b'}$); ^{13}C NMR (126 MHz, CDCl3) δ 171.33 (C^{a}), 134.75 ($C^{4/4'}$), 134.47 ($C^{4/4'}$), 117.12 ($C^{5/5'}$), 116.90 ($C^{5/5'}$), 72.27 ($C^{3/3'}$), 72.05 ($C^{3/3'}$), 68.90 ($C^{2/2'}$), 68.21 ($C^{2/2'}$), 50.00 ($C^{1/1'}$), 46.42

($C^{1/1'}$), 21.83 (C^{b}); *m/z*: (ES^+) calcd. ($C_8H_{21}NO_3 + Na^+$): 250.1414, found: 250.1412 ($M + Na^+$).

***N,N*-bis(2-(prop-2-yn-1-yloxy)ethyl)acetamide – DEAyAc (3.8)**

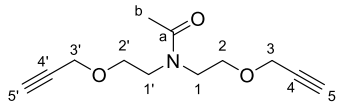

General procedure for the synthesis of an ether containing monomer was followed using DOAc (7.08, 48.1 mmol), NaH (60% in mineral oil, 4.24 g, 105.9 mmol, 2.2 eq.), and propargyl bromide (80 % in tolunene, 15.75 g, 105.9 mmol, 2.2 eq.). Column purification through a silica plug resulted in a pure pale yellow oil. (44 %); R_f = 0.3 in 14 % EtOAc; ν_{max} / cm^{-1}: 3283 (C≡C−H), 2941 (C-H), 2869 (C-H), 2114 (C≡C), 1625 (C=O), 1419 (C-N), 1098 (C-O); ^{1}H NMR (500 MHz, $CDCl_3$) δ 4.10 (d, J = 2.5 Hz, 2H, $H_{3/3'}$), 4.08 (d, J = 2.5 Hz, 2H, $H^{3/3'}$), 3.66 – 3.58 (m, 4H, $H^{2/2'}$), 3.58 – 3.47 (m, 4H, $H^{1/1'}$), 2.42 (t, J = 2.5 Hz, 1H, $H^{5/5'}$), 2.39 (t, J = 2.5 Hz, 1H, $H^{5/5'}$), 2.08 (s, 3H, H^{b}); ^{13}C NMR (126 MHz, $CDCl_3$) δ 171.33 (C^{a}), 79.63 ($C^{4/4'}$), 79.32 ($C^{4/4'}$), 74.88 ($C^{5/5'}$), 74.56 ($C^{5/5'}$), 68.65 ($C^{2/2'}$), 67.88 ($C^{2/2'}$), 58.49 ($C^{3/3'}$), 58.29 ($C^{3/3'}$), 49.70 ($C^{1/1}$), 46.16 ($C^{1/1'}$), 21.79 (C^{b}); ^{1}H NMR (600 MHz, DMSO) δ 4.15 (d, J = 2.5 Hz, 2H, $H^{3/3'}$), 4.12 (d, J = 2.5 Hz, 2H, $H^{3/3'}$), 3.57 (t, J = 5.5 Hz, 2H, $H^{2/2'}$), 3.53 – 3.48 (m, 4H, $H^{1/1'/2/2'}$), 3.45 (t, J = 2.0 Hz, 1H, $H^{5/5'}$) 3.47 – 3.39 (m, 3H, $H^{1/1'/5/5'}$), 2.00 (s, 2H, H^{b}); ^{13}C NMR (151 MHz, DMSO) δ 170.05 (C^{a}), 80.26 ($C^{4/4'}$), 80.13 ($C^{4/4'}$), 77.32 ($C^{5/5}$), 77.19 ($C^{5/5'}$), 67.56 ($C^{2/2'}$), 67.15 ($C^{2/2'}$), 57.74 ($C^{3/3'}$), 57.46 ($C^{3/3'}$), 48.43 ($C^{1/1'}$), 44.78 ($C^{1/1'}$), 21.54 (C^{b}); *m/z*: (ES^+) calcd. ($C_{12}H_{17}NO_3 + Na^+$): 246.1101, found: 246.1102 ($M + Na^+$).

8.3.4 General procedure for the synthesis of acetamide derived oligomers

Meta-OC **2.1** (1 eq.) was dissolved in DMF (0.5 M) followed by dipolarophile (8 eq.) and 4 Å MS (1600 g / mol of *meta*-OC **2.1**), the mixture was then raised to 80 °C for 24 hours. The solution was diluted with $CHCl_3$ (100 ml) and the sieves were removed by filtration. The organic filtrate was washed with water (6 × 100 ml) and brine (100 ml), then dried with $MgSO_4$ and solvent removed *in vacuo*, to leave a crude mixture of repeat units and dipolarophile. The crude product was separated by column chromatography, initially running in 100 % EtOAc to recover residual dipolarophile followed by 20 % Acetone in EtOAc then 50 % Acetone in EtOAc to recover the oligomers seperately.

***N,N'*-((1,3-phenylenebis(4,5-dihydroisoxazole-3,5-diyl))bis(methylene))bis(*N*-allylacetamide) – O_mDAeAc –ABA (3.14)**

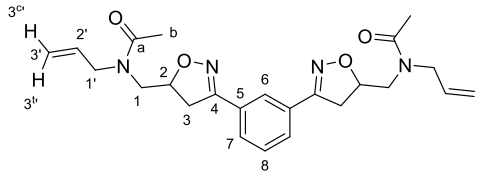

General procedure was followed using DAeAc **3.5** (1.2 g, 8.58 mmol, 8 eq.) and *meta*-OC **2.1** (0.25 g, 1.07 mmol, 1 eq.) resulting in a thick pale yellow oil, O_mDAeAc –ABA **3.14**. (44 %); Rf 0.15 in 100 % EtOAc; ν_{max} / cm^{-1}: 3075 (C=C-H), 2980 (C-H), 2929 (C-H), 2628 (C=O), 1411 (C-N), 1035 (C-O), 906 (C-H); ^{1}H NMR (500 MHz, $CDCl_3$) δ 7.91 (s, 1H, H^6), 7.74 (d, *J* = 7.5 Hz, 2H, H^7), 7.45 (t, *J* = 8.0 Hz, 1H, H^8), 5.91 – 5.74 (m, 2H, $H^{2'}$), 5.22 (d, J = 10.5 Hz, 2H, $H^{3c'}$), 5.14 (d, J = 17.0 Hz, 2H, $H^{3t'}$), 5.07 – 4.96 (m, 2H, H^2), 4.24 – 4.02 (m, 4H, H^1), 3.90 – 3.83 (m, 4H, $H^{1'}$), 3.46 – 3.38 (m, 2H, H^3), 3.38 – 3.30 (m, 4H, H^1), 3.18 – 3.10 (m, 2H, H^3), 2.18 (s, 3H, H^2-min), 2.10 (s, 3H, $H^{2'}$-maj); ^{13}C NMR (126 MHz, $CDCl_3$) δ 171.99 (C^a-maj), 171.97 (C^a-maj), 170.88 (C^a-min), 156.67 (C^4-maj), 156.19 (C^4-min), 133.35 ($C^{2'}$-min), 132.74 ($C^{2'}$-maj), 130.22 (C^5-min), 130.13 (C^5-maj), 129.82 (C^5-min), 129.45 (C^8-min), 129.33 (C^8-maj), 128.65 (C^7-min), 128.36 (C^7-maj), 128.27 (C^7-min), 124.97 (C^6-equal), 124.95 (C^6-equal), 117.52 ($C^{3'}$-min), 116.67 ($C^{3'}$-min), 116.62 ($C^{3'}$-maj), 80.91 (C^2-min), 80.83 (C^2-maj), 79.37 (C^2-min), 79.35 (C^2-min), 53.92 ($C^{1'}$-min), 52.74 – 52.55 ($C^{1'}$-maj), 51.42 ($C^{1'}$-min), 51.37 ($C^{1'}$-min), 49.12 (C^1-maj), 49.05 (C^1-maj), 48.62 (C^1-min), 38.17 (C^3-min), 38.11 (C^3-maj), 38.08(C^3-min) 31.06 (C^b-min), 29.40 (C^b-min) 21.97 (C^b-min), 21.49 (C^b-maj); *m/z*: (ES^+) calcd. ($C_{24}H_{30}N_4O_4$ + Na^+): 461.2159, found: 461.2156 (M + Na^+).

***N,N'*-((1,3-phenylenebis(isoxazole-3,5-diyl))bis(methylene))bis(*N*-(prop-2-yn-1-yl)acetamide) – O_mDAyAc-ABA (3.15)**

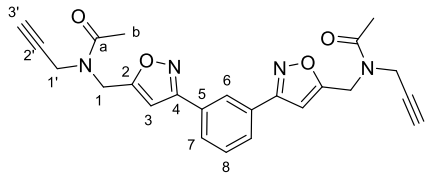

General procedure was followed using DAyAc **3.6** (0.6577 g, 4.87 mmol, 8 eq.) and *meta*-OC **2.1** (0.1417 g, 0.61 mmol, 1 eq.) resulting in an orange waxy oil, pure O_mDAyAc-ABA **3.15**. (53 %); Rf = 0.55 in 100 % EtOAc; ν_{max} / cm^{-1}: 3289 (C≡C−H), 3241 (C≡C−H), 2925 (C-H), 2854 (C-H), 2118 (C≡C), 1647 (C=O), 1407 (C-N), 912 (C-H); ^{1}H NMR (500 MHz, $CDCl_3$) δ 8.14 (m, 1H, H^6), 7.91 – 7.86 (m, 2H, H^7), 7.59 – 7.50 (m, 1H, H^8), 6.61 (s, 2H, H^3-

min), 6.60 (s, 2H, H^3-maj), 4.82 (s, 4H, H^1), 4.35 (d, *J* = 2.0 Hz, 4H, $H^{1'}$-min), 4.18 (s, 4H, $H^{1'}$-maj), 2.36 (t, *J* = 2.0 Hz, 2H, $H^{3'}$-maj), 2.29 (t, *J* = 2.0 Hz, 2H, $H^{3'}$-maj), 2.27 (s, 6H, H^b-min), 2.25 (s, 6H, H^b-maj); ^{13}C NMR (126 MHz, $CDCl_3$) δ 170.62 (C^a-maj), 170.22 (C^a-min), 169.31 (C^2-min), 169.22 (C^2-maj), 168.59 (C^2-min), 168.47 (C^2-maj), 162.19 (C^4-maj), 162.11 (C^4-min), 129.93 (C^5-min), 129.87 (C^8-maj), 129.79 (C^5-maj), 129.76 (C^8-min), 129.54 (C^5-min), 129.40 (C^5-maj), 128.70 (C^7-min), 128.41 (C^7-maj), 125.36 (C^6-min), 125.33 (C^6-maj), 101.47 (C^3-maj), 101.17 (C^3-min), 101.14 (C^3-min), 78.25 ($C^{2'}$-min), 77.54 ($C^{2'}$-min), 73.70 ($C^{3'}$-maj), 73.25 ($C^{3'}$-min), 43.37 (C^1-min), 40.80 (C^1-maj), 38.85 ($C^{1'}$-maj), 38.81 ($C^{1'}$-maj), 34.62 ($C^{1'}$-min), 21.72 (C^b-min), 21.59 (C^b-maj); *m/z*: (ES^+) calcd. ($C_{24}H_{22}N_4O_4$ + Na^+): 453.1533, found: 453.1531 (M + Na^+).

_N,N'_-((((1,3-phenylenebis(4,5-dihydroisoxazole-3,5-diyl))bis(methylene))bis(oxy))bis(ethane-2,1-diyl))bis(_N_-(2-(allyloxy)ethyl)acetamide)–O_mDEAeAc-ABA (3.16)

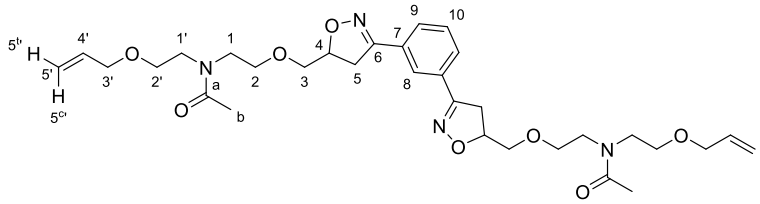

General procedure was followed using DEAeAc **3.6** (1.95 g, 8.6 mmol, 8 eq.) and *meta*-OC **2.1** (0.25 g, 1.1 mmol, 1 eq.) resulting in pure O_mDEAeAc –ABA **3.16**. (31 %); Rf = 0.05 in 100 % EtOAc; ν_{max} / cm^{-1}: 3079 (C=C-H), 2928 (C-H), 2860 (C-H), 1633 (C=O), 1418 (C-N), 1122 (C-O), 1100 (C-O), 913 (C-H); ^{1}H NMR (500 MHz, $CDCl_3$) δ 7.94 – 7.88 (m, 1H, H^8), 7.75 – 7.68 (m, 2H, H^9), 7.44 (t, *J* = 8.0 Hz, 1H, H^{10}), 5.90 – 5.76 (m, 2H, $H^{4'}$), 5.22 (brd, *J* = 17.0 Hz, 2H, $H^{5t'}$), 5.14 (dd, *J* = 10.5, 4.5 Hz, 2H, $H^{5c'}$), 4.93 – 4.86 (m, 2H, H^4), 3.93 – 3.88 (m, 4H, $H^{3'}$), 3.69 – 3.64 (m, 4H, H^2), 3.63 (d, *J* = 4.5 Hz, 4H, H^3-min), 3.61 (d, *J* = 4.5 Hz, 4H, H^3-maj), 3.59 – 3.51 (m, 8H, $H^{1'/2'}$), 3.51 – 3.44 (m, 4H, H^1), 3.43 – 3.33 (m, 4H, H^5), 3.27 – 3.18 (m, 4H, H^5), 2.09 (d, *J* = 2.5 Hz, 6H, H^b-maj), 2.05 (d, *J* = 2.0 Hz, 6H, H^b-min); ^{13}C NMR (126 MHz, $CDCl_3$) δ 171.38 (C^a-maj), 171.27 (C^a-min), 156.04 – 155.88 (C^6), 134.74 ($C^{4'}$-maj), 134.47 ($C^{4'}$-min), 130.29 (C^7-maj), 130.14 (C^7-min), 129.29 (C^{10}-min), 129.27 (C^{10}-maj), 129.25 (C^{10}-min), 128.26 (C^9-min), 128.21 (C^9-maj), 128.15 (C^9-min), 124.90 (C^8), 124.89 (C^8), 117.11 ($C^{5'}$) 117.10 ($C^{5'}$), 116.95 ($C^{5'}$), 116.94 ($C^{5'}$), 80.19 (C^4), 72.40 – 72.29 (C^2), 72.23 ($C^{3'}$), 72.21 – 72.10 (C^2), 72.05 ($C^{3'}$), 70.25 (C^3), 70.23 (C^3), 70.21

(C^3), 70.19 (C^3), 69.96 (C^3), 69.93 (C^3), 68.93 ($C^{2'}$), 68.21 ($C^{2'}$), 68.20 ($C^{2'}$), 49.93 ($C^{1'}$), 49.85 (C^1), 46.42 ($C^{1'}$), 46.40 ($C^{1'}$), 46.02 (C^1), 36.92 (C^5), 36.91 (C^5), 36.89 (C^5), 21.84 (C^b); *m/z*: (ES^+) calcd. ($C_{32}H_{46}N_4O_8$ + Na^+): 637.3208, found: 637.3203 (M + Na^+).

_N_,_N'_-((((1,3-phenylenebis(isoxazole-3,5-diyl))bis(methylene))bis(oxy))bis(ethane-2,1-diyl))bis(_N_-(2-(prop-2-yn-1-yloxy)ethyl)acetamide) –O_mDEAyAc–ABA (3.17)

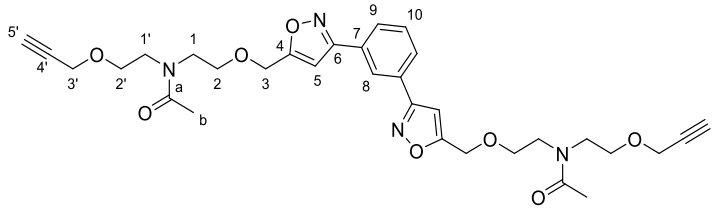

General procedure was followed using DEAyAc **3.7** (1.92 g, 8.60 mmol, 8 eq.) and *meta*-OC **2.1** (0.25 g, 1.07 mmol, 1 eq.) resulting in pure O_mDEAyAc –ABA **3.17** (75 %); Rf = 0.20 in 100 % EtOAc; ν_{max} / cm^{-1}: 3286 (C≡C−H), 2922 (C-H), 2854 (C-H), 2114 (C≡C), 1630 (C=O), 1435 (C-N), 1098 (C-O), 910 (C-H); ^{1}H NMR (500 MHz, $CDCl_3$) δ 8.49 (d, *J* = 3.5 Hz, $H_{4,5\text{-isoxazoline}}$), 8.22 (s, 1H, H_8), 7.93 – 7.87 (m, 2H, H_9), 7.59 – 7.53 (m, 1H, H_{10}), 6.64 (s, 2H, H_5), 6.63 (s, 2H, H_5), 6.62 (s, 2H, H_5), 6.61 (s, 2H, H_5), 4.67 (s, 4H, H_3-min), 4.64 (s, 4H, H_3-maj), 4.14 (d, *J* = 2.5 Hz, 4H, $H_{3'}$-maj), 4.12 (d, *J* = 2.5 Hz, 4H, $H_{3'}$-min), 3.74 (dt, *J* = 10.5, 5.5 Hz, 4H, H_2), 3.67 (dt, *J* = 14.5, 4.5 Hz, 8H, $H_{2'}$), 3.64 – 3.56 (m, 8H, $H_{1/1'}$), 2.43 (t, *J* = 2.5 Hz, $H_{5'}$-maj), 2.41 (t, *J* = 2.5 Hz, $H_{5'}$-min), 2.16 (s, H_b-min), 2.13 (s, H_b-maj); ^{13}C NMR (126 MHz, $CDCl_3$) δ 171.47 (C_a-maj), 171.43 (C_a), 170.02 (C_3-maj), 169.92 (C_3), 162.04 (C_6), 161.95 (C_6-maj), 129.88 (C_7), 129.85 (C_7), 129.84 (C_{10}-min), 129.81 (C_{10}-maj), 129.77 (C_{10}-min), 129.75 (C_7), 128.49 (C_9), 128.45 (C_9), 125.37 (C_8), 101.33 (C_5), 101.30 (C_5), 101.23 (C_5), 101.21 (C_5), 79.69 ($C_{4'}$-min), 79.37 ($C_{4'}$-maj), 75.01 ($C_{5'}$-maj), 74.68 ($C_{5'}$-min), 69.87 (C_2-maj), 69.44 (C_2-min), 68.90 ($C_{2'}$-min), 68.07 ($C_{2'}$-maj), 64.30 (C_3-min), 64.00 (C_3-maj), 58.63 ($C_{3'}$-maj), 58.44 ($C_{3'}$-min), 49.95 ($C_{1/1'}$-maj), 49.91 ($C_{1/1'}$-min), 46.45 ($C_{1/1'}$-min), 46.43 ($C_{1/1'}$-maj), 21.98 (C_b-min), 21.93 (C_b-maj); *m/z*: (ES^+) calcd. ($C_{32}H_{38}N_4O_8$ + Na^+): 629.2582, found: 629.2578 (M + Na^+).

***N*-allyl-*N*-((3-(3-(5-((*N*-((3-(3-(5-((*N*-allylacetamido)methyl)-4,5-dihydroisoxazol-3-yl)phenyl)-4,5-dihydroisoxazol-5-yl)methyl)acetamido)methyl)-4,5-dihydroisoxazol-3-yl)phenyl)-4,5-dihydroisoxazol-5-yl)methyl)acetamide– O_mDAeAc-ABABA (3.18)**

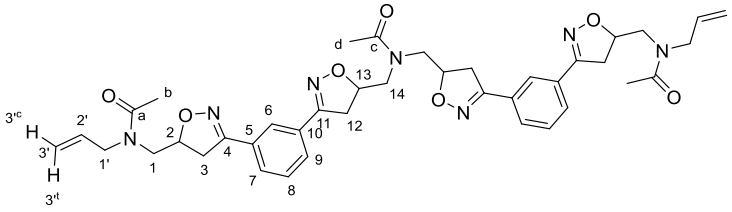

General oligomer synthesis procedure was followed using DAeAc **3.5** (1.2 g, 8.58 mmol, 8 eq.) and *meta*-OC **2.1** (0.25 g, 1.07 mmol, 1 eq.) resulting in a pale yellow solid, O_mDAeAc –ABABA **3.18**. (6 %); Rf = 0.1 in 20 % acetone in EtOAc; ^{1}H NMR (500 MHz, $CDCl_3$) δ 7.95 – 7.88 (m, H^6), 7.77 – 7.65 (m, $H^{7/9}$), 7.50 – 7.40 (m, H^8), 5.84 – 5.74 (m, $H^{2'}$), 5.21 (d, *J* = 10.5 Hz, $H^{3'c}$), 5.13 (d, *J* = 17.5 Hz, $H^{3't}$), 5.09 – 5.04 (m, $H^{2/13}$), 5.04 – 4.93 (m, $H^{2/13}$), 4.22 – 4.02 (m, H^{CH_2}), 4.02 – 3.95 (m, H^{CH_2}), 3.89 – 3.81 (m, H^{CH_2}), 3.81 – 3.72 (m, H^{CH_2}), 3.68 – 3.60 (m, H^{CH_2}), 3.59 – 3.29 (m, H^{CH_2}), 3.20 – 3.08 (m, H^3), 3.07 – 2.94 (m, H^{CH_2}), 2.19 (s, $H^{b/d}$), 2.17 (s, $H^{b/d}$), 2.09 (s, $H^{b/d}$); ^{13}C NMR (126 MHz, $CDCl_3$) δ 172.23 – 171.68 $C^{a/c}$), 157.02 – 156.18 ($C^{4/11}$), 132.73 ($C^{2'}$), 130.30 – 129.72 ($C^{5/10}$), 129.58 – 129.28 (C^8), 128.72 – 128.29 ($C^{7/9}$), 125.07 – 124.86 (C^6), 116.71 – 116.59 ($C^{3'}$), 81.09 – 80.50 ($C^{2/13}$), 54.16 – 53.23 (C^{CH_2}), 52.65 (C^{CH_2}), 49.06 (C^{CH_2}), 38.63 – 37.92 (C^{CH_2}), 22.03 ($C^{b/d}$), 21.96 ($C^{b/d}$), 21.50 ($C^{b/d}$); *m/z*: (ES^+) calcd. ($C_{40}H_{47}N_7O_7$ + Na^+): 760.3429, found: 760.3429 (M + Na^+).

***N*-(prop-2-yn-1-yl)-*N*-((3-(3-(5-((*N*-((3-(3-(5-((*N*-(prop-2-yn-1-yl)acetamido)methyl)isoxazol-3-yl)phenyl)isoxazol-5-yl)methyl)acetamido)methyl)isoxazol-3-yl)phenyl)isoxazol-5-yl)methyl)acetamide – O_mDAyAc-ABABA (3.19)**

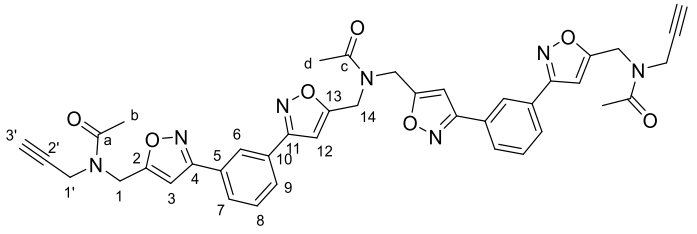

General oligomer synthesis procedure was followed using DAyAc **3.6** (0.6577 g, 4.87 mmol, 8 eq.) and *meta*-OC **2.1** (0.1417 g, 0.61 mmol, 1 eq.) resulting in an orange solid, O_mDAyAc-ABABA **3.19**, (4 %); Rf = 0.25 in 100 % EtOAc; ^{1}H NMR (500

MHz, $CDCl_3$) δ 8.18 – 8.04 (m, H^6), 7.90 – 7.75 (m, $H^{7/9}$), 7.63 – 7.40 (m, H^8), 6.69 – 6.45 (m, $H^{3/12}$), 4.88 – 4.73 (m, $H^{1/14}$), 4.38 – 4.31 (m, $H^{1'}$-min), 4.22 – 4.14 (m, $H^{1'}$-maj), 2.37 (t, *J* = 2.5 Hz, $H^{3'}$-maj), 2.35 (s, $H^{b/d}$), 2.30 (t, *J* = 2.5 Hz, $H^{3'}$-min), 2.28 – 2.24 (m, $H^{b/d}$); ^{13}C NMR (126 MHz, $CDCl_3$) δ 170.76 ($C^{a/c}$), 170.67 ($C^{a/c}$), 170.27 ($C^{a/c}$), 169.25 ($C^{2/13}$), 169.18 ($C^{2/13}$), 168.96 ($C^{2/13}$), 168.88 ($C^{2/13}$), 168.56 ($C^{2/13}$), 168.54 ($C^{2/13}$), 168.45 ($C^{2/13}$), 168.02 ($C^{2/13}$), 167.93 ($C^{2/13}$), 162.32 ($C^{4/11}$), 162.20 ($C^{4/11}$), 162.12 ($C^{4/11}$), 162.09 ($C^{4/11}$), 162.02 ($C^{4/11}$), 129.92 (C^8), 129.81 (C^8), 129.72 (C^8), 129.52 ($C^{5/10}$), 129.37 ($C^{5/10}$), 129.30 ($C^{5/10}$), 129.17 ($C^{5/10}$), 128.66 ($C^{7/9}$), 128.42 ($C^{7/9}$), 128.38 ($C^{7/9}$), 125.27 (C^6), 124.90 (C^6), 101.72 ($C^{3/12}$), 101.44 ($C^{3/12}$), 101.15 ($C^{3/12}$), 78.25 ($C^{2'}$), 77.54 ($C^{2'}$), 73.78 ($C^{3'}$), 73.72 ($C^{3'}$), 73.25 ($C^{3'}$), 44.85 ($C^{1/14}$), 43.37 ($C^{1/14}$), 41.09 ($C^{1/14}$), 40.82 ($C^{1/14}$), 38.84 ($C^{1'}$), 38.81 ($C^{1'}$), 34.63 ($C^{1'}$), 21.72 ($C^{b/d}$), 21.67 ($C^{b/d}$), 21.59 ($C^{b/d}$); MS (ESI) m/z calcd. ($C_{40}H_{35}N_7O_7$ + Na^+): 748.2490, found: 748.2482 (M + Na^+).

_N_-(2-(prop-2-yn-1-yloxy)ethyl)-_N_-(2-((3-(3-(5-((2-(_N_-(2-((3-(3-(5-((2-(_N_-(2-(prop-2-yn-1-yloxy)ethyl)acetamido)ethoxy)methyl)isoxazol-3-yl)phenyl)isoxazol-5-yl)methoxy)ethyl)acetamido)ethoxy)methyl)isoxazol-3-yl)phenyl)isoxazol-5-yl)methoxy)ethyl)acetamide - O_mDEAyAc-ABABA (3.20)

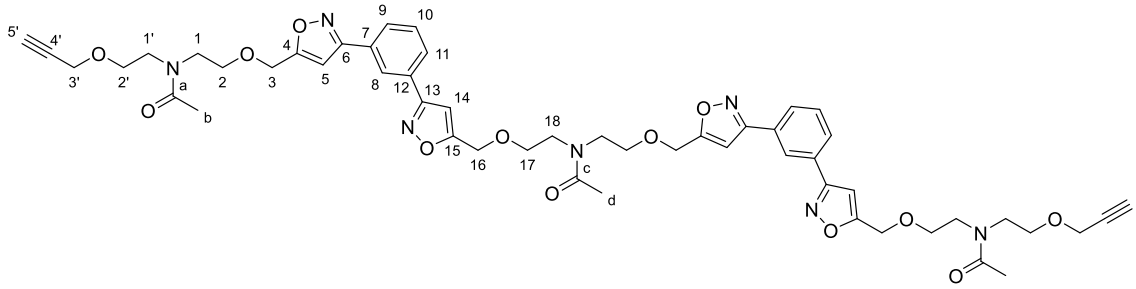

General oligomer synthesis procedure was followed using DEAyAc **3.8** (1.92 g, 8.60 mmol, 8 eq.) and *meta*-OC **2.1** (0.25 g, 1.07 mmol, 1 eq.) resulting in a cream solid, O_mDEAyAc-ABABA **3.20** (3 %); Rf = 0.1 in 20 % Ac in EtOAc; ^{1}H NMR (500 MHz, $CDCl_3$) δ 8.49 (d, *J* = 3.5 Hz, $H_{4,5\text{-isoxazoline}}$), 8.21 (s, 2H, H^8), 7.93 – 7.84 (m, 4H, $H^{9/11}$), 7.54 (t, *J* = 7.5 Hz, 2H, H^{10}), 6.66 – 6.58 (m, 4H, $H^{5/14}$), 4.72 – 4.58 (m, 8H, $H^{3/16}$), 4.14 (d, *J* = 2.5 Hz, 4H, $H^{3'}$-maj), 4.11 (d, *J* = 2.5 Hz, 4H, $H^{3'}$-min), 3.79 – 3.70 (m, 8H, $H^{2/17}$), 3.70 – 3.55 (m, 16H, $H^{1/18/1'/2'}$), 2.43 (t, *J* = 2.5 Hz, 2H, $H^{5'}$-maj), 2.41 (t, *J* = 2.5 Hz, 2H, $H^{5'}$-min), 2.16 (s, 9H, $H^{b/d}$-maj), 2.12 (s, 9H, $H^{b/d}$-min); ^{13}C NMR (126 MHz, $CDCl_3$) δ 171.52 ($C^{a/c}$), 171.49 ($C^{a/c}$), 171.45 ($C^{a/c}$), 170.02 ($C^{5/14}$), 169.92

($C^{5/14}$), 169.89 ($C^{5/14}$), 169.82 ($C^{5/14}$), 162.01 ($C^{6/13}$), 161.95 ($C^{6/13}$), 161.93 ($C^{6/13}$), 129.87 ($C^{7/12}$), 129.85 ($C^{7/12}$), 129.83 (C^{10}), 129.80 (C^{10}), 129.75 ($C^{7/12}$), 129.72 ($C^{7/12}$), 128.47 ($C^{9/11}$), 128.43 ($C^{9/11}$), 128.34 ($C^{9/11}$), 125.34 (C^{8}), 101.41 ($C^{5/14}$), 101.39 ($C^{5/14}$), 101.33 ($C^{5/14}$), 101.31 ($C^{5/14}$), 101.23 ($C^{5/14}$), 101.20 ($C^{5/14}$), 79.70 ($C^{4'}$), 79.38 ($C^{4'}$), 75.02 ($C^{5'}$-maj), 74.69 ($C^{5'}$-min), 69.95 ($C^{2/17/2'}$), 69.86 ($C^{2/17/2'}$), 69.46 ($C^{2/17/2'}$), 68.88 ($C^{2/17/2'}$), 68.06 ($C^{2/17/2'}$), 64.29 ($C^{3/16}$), 64.23 ($C^{3/16}$), 63.99 ($C^{3/16}$), 63.95 ($C^{3/16}$), 58.63 ($C^{3'}$), 58.44 ($C^{3'}$), 50.06 ($C^{1/18/1'}$), 49.95 ($C^{1/18/1'}$), 49.91 ($C^{1/18/1'}$), 46.65 ($C^{1/18/1'}$), 46.44 ($C^{1/18/1'}$), 46.42 ($C^{1/18/1'}$), 21.98 ($C^{b/d}$-maj), 21.93 ($C^{b/d}$-maj) ; MS (ESI) m/z calcd. ($C_{52}H_{59}N_7O_{13} + Na^+$): 1012.4063, found: 1012.4067 ($M + Na^+$).

(Z)-3-(5-((N-allylacetamido)methyl)-4,5-dihydroisoxazol-3-yl)-N-((N-methylformamido)methoxy)benzimidoyl chloride (3.21)

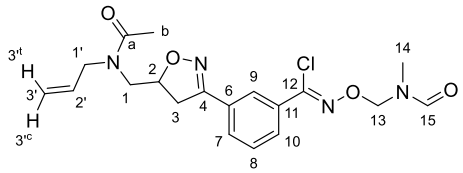

General oligomer synthesis procedure was followed using DAeAc **3.5** (1.2 g, 8.58 mmol, 8 eq.) and *meta*-OC **2.1** (0.25 g, 1.07 mmol, 1 eq.) resulting in a white oil, **3.21**. (6 %); Rf = 0.4 in 20 % acetone in EtOAc; ^{1}H NMR (500 MHz, $CDCl_3$) δ 8.37 (s, 1H, H^{15}), 8.09 (s, 1H, H^9), 7.85 (d, *J* = 8.0 Hz, 1H, H^{10}), 7.74 (d, *J* = 8.0 Hz, 1H, H^7), 7.44 (t, *J* = 8.0 Hz, 1H, H^8), 5.79 (ddt, *J* = 17.0, 11.0, 5.0 Hz, 1H, $H^{2'}$), 5.36 (s, 2H, H^{13}), 5.22 (brd, J = 10.0 Hz, 1H, $H^{3'c}$) 5.13 (brd, *J* = 17.0 Hz, 1H, $H^{3't}$), 5.07 – 4.97 (m, 1H, H^2), 4.24 – 4.02 (m, 2H, $H^{1'}$), 3.89 – 3.83 (m, 2H, H^1), 3.46 – 3.35 (m, 2H, H^3), 3.19 – 3.13 (m, 2H, H^3), 3.01 (s, 3H, H^{14}), 2.10 (s, 3H, H_b); ^{13}C NMR (126 MHz, $CDCl_3$) δ 172.07 (C^a), 163.98 (C^{15}), 156.51 (C^4), 140.01 (C^{12}), 132.79 (C^{11}), 132.73 ($C^{2'}$), 130.07 (C^6), 129.24 (C^7), 129.17 (C^8), 128.85 (C^{10}), 125.61 (C^9), 116.65 ($C^{3'}$), 83.76 (C^{13}), 81.02 (C^2), 52.66 ($C^{1'}$), 49.05 (C^1), 38.04 (C^3), 29.80 (C^{14}), 21.50 (C^b); MS (ESI) m/z calcd. ($C_{19}H_{23}ClN_4O_4 + Na^+$): 429.1300, found: 429.1299 ($M + Na^+$).

8.3.5 General synthesis for the synthesis of acetamide based polymers

Meta-OC **2.1** (1 eq.) and dipolarophile (1 eq.) were dissolved in DMF (1 M). Molecular sieves (4 Å) were added (1600 g / mol of *meta*-OC **2.1**) and the mixture was stirred (50 RPM) at 25 ^{o}C for 30 minutes. The temperature was then raised to 80 ^{o}C for 24 hours. The reaction mixture was diluted with $CHCl_3$ (5 ml) and filtered to remove molecular sieves, the sieves were washed further with warm $CHCl_3$ (5ml), the

filtrate was then reduced *in vacuo* to leave the polymer in DMF. The polymer was taken back into a small amount of $CHCl_3$ (2 ml) and added dropwise to MeOH (40 ml) causing a precipitate to form. The precipitate was collected by passing the solution through filter paper on a sintered funnel. The precipitate was then washed with MeOH (3 x 25 ml), it was collected off the filter paper with warm $CHCl_3$ (3 x 25 ml). The $CHCl_3$ was combined and reduced *in vacuo* to leave a polymeric product.

P^t_mDAeAc (3.24)

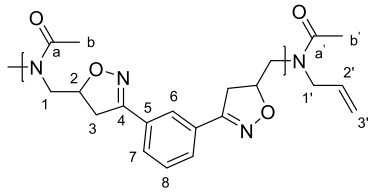

The general procedure for the synthesis of polyisoxazolines was applied using *meta*-OC **2.1** (500.0 mg, 2.15 mmol, 1 eq.) and DAeAc **3.5** (298.6 mg, 2.15 mmol, 1 eq.) to give a pale orange/brown brittle solid. (62 %); ν_{max} / cm^{-1}: 2984 (C-H), 2928 (C-H), 2851 (C-H), 1631 (C=O), 1034 (C-O), 1413 (C-N), 1034 (C-O), 905 (C-H); ^{1}H NMR (500 MHz, $CDCl_3$) δ 7.89 (s, H^6), 7.70 (s, H^7), 7.44 (s, H^8), 5.79 (s, $H^{2'}$), 5.26 – 5.13 (m, $H^{3'}$), 5.10 – 4.89 (brm, H^2), 4.22 – 3.92 (m, $H^{1'}$), 3.92 – 3.72 (m, $H^{1/3}$), 3.72 – 3.58 (m, $H^{1/3}$), 3.58 – 3.23 (m, $H^{1/3}$), 3.24 – 2.98 (m, $H^{1/3}$), 2.19 (s, H^b), 2.10 (s, $H^{b'}$); ^{13}C NMR (126 MHz, $CDCl_3$) δ 172.09 (C^a), 156.88 (C^4), 156.68 (C^4), 156.40(C^4), 132.71 ($C^{2'}$), 130.01 (C^5), 129.92 (C^5), 129.46 (C^8), 128.66 (C^7), 128.41 (C^7), 124.95 (C^6), 116.70 ($C^{3'}$), 80.83 (C^2), 80.72 (C^2), 79.89 (C^2), 78.91 (C^2), 54.00 ($C^{1'}$), 53.43 ($C^{1'}$), 52.67 ($C^{1'}$), 50.59 (C^1), 49.70 (C^1), 49.12 (C^1), 38.33 (C^3), 38.12 (C^3), 22.04 (C^b), 21.97 (C^b), 21.50 ($C^{b'}$)

P^t_mDAyAc (3.25)

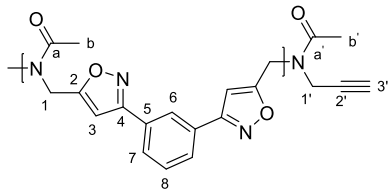

The general procedure for the synthesis of polyisoxazolines was applied using *meta*-OC **2.1** (500.0 mg, 2.15 mmol, 1 eq.) and DAyAc **3.6** (290.0 mg, 2.15 mmol, 1 eq.) to give a pale orange/brown brittle solid. (64 %); ν_{max} / cm^{-1}: 3115 (C≡C−H), 2961 (C-H), 1651 (C=O),1603 (C=O), 1406 (C-N), 901 (C-H); ^{1}H NMR (500 MHz, $CDCl_3$) δ 8.04 (brs, H^6), 7.77 (brs, H^7), 7.50 (brs, H^8), 6.67 – 6.39 (brm, H^3), 4.91 – 4.70 (brm, H^1), 4.34 (brs, $H^{1'}$-min), 4.18 (brs, $H^{1'}$-maj), 2.33 (brs, H^2), 2.25 (s, $H^{2'}$); ^{13}C NMR (126 MHz, $CDCl_3$) δ 170.89 (C^a), 168.98 (C^2), 168.06 (C^2), 162.11 (C^4), 129.78 (C^8), 129.48 (C^5), 129.17 (C^5), 128.67 (C^7), 128.38 (C^7), 125.25 (C^6), 125.21 (C^6), 101.67 (C^3), 101.46 (C^3),

101.18 (C^3), 100.93 (C^3), 73.74 ($C^{3'}$), 73.26 ($C^{3'}$), 44.89 (C^1), 43.39 (C^1), 41.15 (C^1), 40.83 (C^1), 38.85 ($C^{1'}$), 38.81 ($C^{1'}$), 34.66 ($C^{1'}$), 21.69 (C^2), 21.59 (C^2).

P^t_mDEAeAc (3.26)

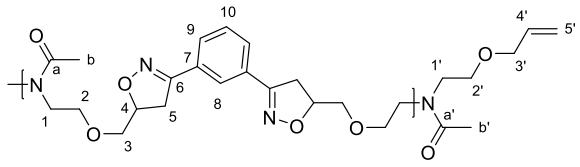

The general procedure for the synthesis of polyisoxazolines was applied using *meta*-OC **2.1** (500.0 mg, 2.15 mmol, 1 eq.) and DEAeAc **3.7** (487.7 mg, 2.15 mmol, 1 eq.) to give a pale orange/brown brittle solid. (76 %); ν_{max} / cm^{-1}: 2881 (C-H), 1633 (C=O), 1423 (C-N), 1122 (C-O), 1033 (C-O), 910 (C-H); ^{1}H NMR (500 MHz, $CDCl_3$) δ 8.50 – 8.05 (m, H^{Ar}-min) 7.89 (brs, H^8), 7.67 (brs, H^9), 7.42 (brs, H^{10}), 5.90 – 5.75 (m, $H^{4'}$), 5.20 (d, *J* = 17.5 Hz, $H^{5't}$), 5.14 (d, *J* = 10.0 $H^{5'c}$), 4.86 (brs, H^4), 4.52 – 4.37 (brm, $H^{CH/CH2}$-min), 4.37 (brm, $H^{CH/CH2}$-min), 3.94 – 3.87 (m, $H^{3'}$) 3.58 (brs, $H^{1/2/3}$), 3.53 – 3.40 (brm, $H^{1/2/3}$), 3.39 – 3.20 (m, H^5), 3.20 – 3.03 (m, H^5), 2.09 (brs, $C^{b'}$), 2.07 – 1.96 (brm, C^b); ^{13}C NMR (126 MHz, $CDCl_3$) δ 171.47 (C^a), 155.98 (C^6), 134.68 ($C^{4'}$), 134.42 ($C^{4'}$), 130.19 (C^7), 130.08 (C^7), 129.27 (C^9), 128.20 (C^8), 124.80 (C^{10}), 117.07 ($C^{5'}$), 116.93 ($C^{5'}$), 80.20 (C^4), 72.34 (C^2), 72.18 (C^2), 72.00 ($C^{3'}$), 70.16 ($C^{3'}$), 69.85 (C^3), 68.92 ($C^{2'}$), 68.13 ($C^{2'}$), 49.89 ($C^{1'}$), 49.78 (C^1), 46.35 ($C^{1'}$), 46.07 (C^1), 36.83 (C^5), 21.78 (C^b).

P^t_mDEAyAc (3.27)

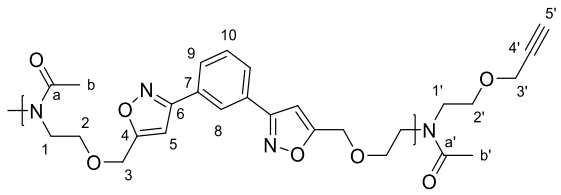

The general procedure for the synthesis of polyisoxazolines was applied using *meta*-OC **2.1** (500.0 mg, 2.15 mmol, 1 eq.) and DEAyAc **3.8** (479.0 mg, 2.15 mmol, 1 eq.) to give a pale orange/brown brittle solid. (78 %); ν_{max} / cm^{-1}: 2932 (C-H), 2870 (C-H), 1631 (C=O), 1613 (C=O), 1433 (C-N), 1099 (C-O), 908 (C-H); ^{1}H NMR (500 MHz, $CDCl_3$) δ 8.48 (s, $H^{3,4\text{-isoxazole}}$), 8.18 (brs, H^7), 7.84 (brs, H^9), 7.45 (brs, H^{10}), 6.60 (brs, H^5), 4.62 (brs, H^3), 4.13 (d, *J* = 2.0 Hz, $H^{3'}$), 4.11 (d, *J* = 2.0 Hz, $H^{3'}$), 3.72 (brs, H^2), 3.61 (brs, $H^{1/1'/2'}$), 2.43 (t, *J* = 2.0 Hz, $H^{5'}$), 2.41 (t, *J* = 2.0 Hz, $H^{5'}$), 2.15 (brs, H^b); ^{13}C NMR (126 MHz, $CDCl_3$) δ 171.97 – 171.45 (C^a), 169.89 (C^4), 169.82 (C^4), 161.96 (C^6), 161.91 (C^6), 129.80 (C^9), 129.69 (C^7), 128.45 (C^8), 125.30 (C^{10}), 101.45 (C^5), 101.35 (C^5), 75.05 ($C^{5'}$), 74.72 ($C^{5'}$), 69.88 (C^2), 69.46 (C^2), 68.85

($C^{2'}$), 68.05 ($C^{2'}$), 64.21 (C^{3}), 63.92 (C^{3}), 58.62 ($C^{3'}$), 58.44 ($C^{3'}$), 50.34 – 49.82 ($C^{1/1'}$), 46.62 ($C^{1/1'}$), 46.43 ($C^{1/1'}$), 21.97 (C^{b}).

8.4 General procedures Chapter 4

Benzaldehyde oxime (*benz*-O, 4.3)[366]

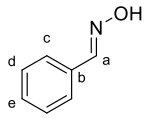

Sodium acetate (9.27 g, 113 mmol, 1.2 eq.) and hydroxyamine hydrochloride (7.86 g, 113 mmol , 1.2 eq.) in water (50 ml) was introduced to benzaldehyde (10.0 g, 94 mmol, 1eq.) dispersed in ethanol (50 ml). After 30 minutes the solution was poured into cold water and extracted with EtOAc (3 × 50 ml). The organic layers were combined and washed with water (2 x 50 ml) and brine (50 ml), dried with $MgSO_4$ and solvent removed *in vacuo* to give a clear crude oil product. Column purification gave a pure white solid. (60 %); R_f = 0.31 in 20 % EtOAc; ν_{max} / cm^{-1}: 3234 (OH), 3062 (C-H), 1620 (C=N); ^{1}H NMR (400 MHz, $CDCl_3$) δ 9.69 (s, br, 1H, H^{OH}), 8.21 (s, 1H, H^{a}), 7.62 – 7.54 (m, 2H, H^{c}), 7.45 -7.36 (m, 3H, $H^{d/e}$); ^{13}C NMR (101 MHz, $CDCl_3$) 150.53 (C^{a}), 132.08 (C^{b}), 130.21 (C^{d}), 128.86 (C^{e}), 127.23 (C^{c}); *m/z*: (ES^+) calcd. ($C_7H_7NO + Na^+$): 144.0420, found: 144.0420 ($M + Na^+$).

(Z)-N-hydroxybenzimidoyl chloride (*benz*-OC, 4.1)[366]

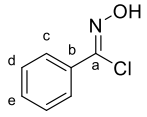

Benz-O **4.1** (6.00 g, 49.5 mmol, 1 eq.) was dissolved in DMF (50 ml). *N*-Chlorosuccinimide (7.28 g, 54.5 mmol, 1.1 eq) was introduced in 5 parts over the course of an hour. 2 hours after the last addition of NCS the reaction mixture was poured into cold water (150 ml) and extracted with ethyl acetate (3 × 50 ml). The organic layers were combined and washed with water (5 × 50 ml) and saturated sodium thiosulfate solution (1 × 50 ml), then dried over $MgSO_4$. Solvent removed *in vacuo* gave a crude yellow solid. Column purification resulted in a cream solid. (73 %); R_f = 0.6 in 20 % EtOAc; m.p. 44 – 46 °C; ν_{max}/cm^{-1} 3264 (OH), 3027 (C-H), 1623 (C=N); ^{1}H NMR (500 MHz, CDCl3) δ 8.18 (s, 1H, H^{OH}), 7.85 (d, J = 7.0 Hz, 1H, H^{c}), 7.50 – 7.37 (m, 4H, $H^{d/e}$); ^{13}C NMR (126 MHz, $CDCl_3$) δ 140.42 (C^{a}), 132.52 (C^{b}), 130.92 (C^{d}), 128.67 (C^{c}), 127.35 (C^{e}); *m/z*: (ES^+) calcd. ($C_7H_7ClNO + H^+$): 156.0211, found: 156.0208 ($M + H^+$).

8.4.1 Optimisation products and procedures

7.4.1.1 Baseline reaction and characterisation of products

DEAyAc **3.8** (0.50 g, 2.2 mmol, 1 eq.) and *benz*-OC **4.1** (0.70 g 4.5 mmol, 2 eq.) were dissolved in DMF (5 ml) at RT along with 4 Å MS (800 g / mol of *benz*-oc). The solution was stirred at 25 °C for 1 hour after which a sample was taken. The temperature was then raised to 80 °C for 24 hours, samples were taken once an hour for the first 6 hours. After 24 hours the reaction mixture was diluted with $CHCl_3$ (50 ml) and filtered. The filtrate was washed with water (50 ml), then removed. The aqueous layer was then extracted with $CHCl_3$ (3 x 20 ml). The 4 chloroform layers were combined and washed with water (4 x 50 ml) and brine (50 ml), followed by drying with $MgSO_4$ and the solvent removed *in vacuo* to leave a crude product. The same work up process was carried out on the samples but on a smaller scale.

The crude product was separated by column chromatography (12.5 % EtOAc followed by 70 % EtOAc) to isolate three major products, diphenyl furoxan **2.18** (12.5 % EtOAc R_f 0.4), OCAc **4.6** (70 % EtOAc R_f 0.21), and DIAc **4.7** (70 % EtOAc R_f 0.12).

3,4-diphenyl-1,2,5-oxadiazole 2-oxide (Diphenylfuroxan 2.18)[367]

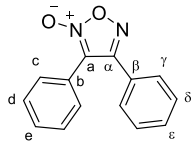

White needles; m.p. 110 – 112 ºC; ν_{max} / cm^{-1}: 1591 (C=N), 1572 (C=N), 1504, 1441, 1419, 1327; ^{1}H NMR (500 MHz, $CDCl_3$) δ 7.58 – 7.51 (m, 5H, $H^{c\gamma\varepsilon}$), 7.47 – 7.42 (m, 5H, $H^{d\delta e}$); ^{13}C NMR (126 MHz, $CDCl_3$) δ 156.34 (C^{α}), 131.10 (C^{ε}), 130.66 (C^{e}), 129.13 ($C^{d/\delta}$), 129.05 ($C^{d/\delta}$), 128.78 (C^{c}), 128.39 (C^{γ}), 126.75 (C^{β}), 122.96 (C^{b}), 114.38(C^{a}); *m/z*: (ES^+) calcd. ($C_{14}H_{10}N_2O_2$ + Na^+): 261.0634, found: 261.0636 (M + Na^+).

***N*-(2-((3-phenylisoxazol-5-yl)methoxy)ethyl)-*N*-(2-(prop-2-yn-1-yloxy)ethyl)acetamide – OCAc (4.6)**

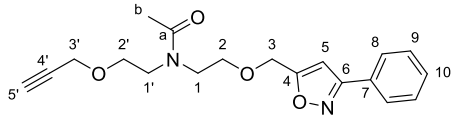

Cream wax; ^{1}H NMR (400 MHz, $CDCl_3$) δ 8.46 (s, 1H, very low intensity relating to 3,4 isoxazole), 7.79 (brs, 2H, H^{8}), 7.45 (brs, 3H, $H^{9/10}$), 6.54 (brs, 1H, H^{5}), 4.65 (s, 2H, H^{3}-min), 4.63 (s, 2H, H^{3}-maj) 4.13 (s, 2H, $H^{3'}$-maj) 4.11 (s, 2H, $H^{3'}$-min), 3.80 – 3.53 (m, 8H, $H^{2/2'/1/1'}$), 2.42 (s, 1H, $H^{5'}$-maj), 2.40 (s, 1H, $H^{5'}$-min), 2.15 (s, 3H, H^{b}-min) 2.13 (s, 3H, H^{b}-maj); ^{13}C NMR (101 MHz,

$CDCl_3$) δ 171.46 (C^a-maj), 171.44 (C^a-min), 169.63 (C^4-maj), 169.56 (C^4-min), 162.59 (C^6-min), 162.51 (C^6-maj), 130.25 (C^{10}-min), 130.19 (C^{10}-maj), 129.09 (C^9-min), 129.06 (C^9-maj), 129.00 (C^7), 128.91 (C^7), 126.95 (C^8), 101.29 (C^5-maj), 101.14 (C^5-min), 79.69 ($C^{4'}$), 79.36 ($C^{4'}$), 74.97 ($C^{5'}$-maj), 74.64 ($C^{5'}$-min), 69.83 (C^2-maj), 69.36 (C^2-min), 68.89 ($C^{2'}$-min), 68.05 ($C^{2'}$-maj), 64.30 (C^3-min), 63.98 (C^3-maj), 58.61 ($C^{3'}$-maj), 58.43 ($C^{3'}$-min), 49.93 ($C^{1/1'}$-maj), 49.91 ($C^{1/1'}$-min), 46.43 ($C^{1/1'}$), 21.94 (C^b-min), 21.90 (C^b-maj); *m/z*: (ES^+) calcd. ($C_{19}H_{22}N_2O_4$ + Na^+): 365.1472, found: 365.1474 (M + Na^+).

***N*,*N*-bis(2-((3-phenylisoxazol-5-yl)methoxy)ethyl)acetamide – DIAc (4.7)**

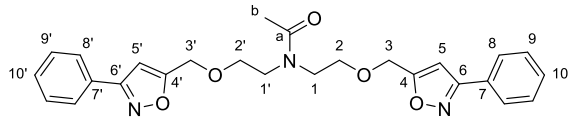

Cream wax; ν_{max} / cm^{-1}: 2963 (C-H), 2922 (C-H), 2864 (C-H), 1620 (C=O), 1583 (C=N), 1031 (C-O), 766 (C-H), 685 (C-H); ^{1}H NMR (500 MHz, $CDCl_3$) δ 8.43 (s, 1H, $H^{3,4\text{-isoxazole}}$-min), 7.80 – 7.74 (m, 4H, $H^{8/8'}$), 7.46 – 7.36 (m, 6H, $H^{9/9'/10/10'}$), 6.53 – 6.50 (m, 2H, $H^{5/5'}$), 4.59 (s, 4H, $H^{3/3'}$), 4.57 (s, 4H, $H^{3/3'}$), 3.70 (t, *J* = 5.0, 2H, $H^{2/2'}$), 3.67 (t, *J* = 5.0, 2H, $H^{2/2'}$), 3.61 – 3.54 (m, 4H, $H^{1/1'}$), 2.15 (s, 3H, H^b); ^{13}C NMR (126 MHz, $CDCl_3$) δ 171.37 (C^a), 169.41 ($C^{4/4'}$), 169.36 ($C^{4/4'}$), 162.41 ($C^{6/6'}$), 162.36 ($C^{6/6'}$), 130.12 ($C^{10/10'}$), 130.09 ($C^{10/10'}$), 128.96 ($C^{9/9'}$), 128.80 ($C^{7/7'}$), 128.75 ($C^{7/7'}$), 126.79 ($C^{8/8'}$), 126.79 ($C^{8/8'}$), 101.25 ($C^{5/5'}$), 101.13 ($C^{5/5'}$), 69.71 ($C^{2/2'}$), 69.23 ($C^{2/2'}$), 64.04 ($C^{3/3'}$), 63.75 ($C^{3/3'}$), 49.86 ($C^{1/1'}$), 46.43 ($C^{1/1'}$), 21.80 (C^b); *m/z*: (ES^+) calcd. ($C_{26}H_{27}N_3O_5$ + Na^+): 484.1843, found: 484.1845 (M + Na^+).

7.4.1.2 Cycloaddition method trial and optimisation general method

DEAyAc **3.8** (1 eq.) was dispersed in solvent (0.5 M) along with *benz*-OC **4.1** (2 eq.) and an additive. The reaction mixture was set to the designated temperature and left for 24 hours. After 24 hours the reaction mixture was diluted with $CHCl_3$ (25 ml) and filtered to remove any additives. The organic filtrate was washed with water (3 × 25 ml) then set to one side, the aqueous washes were combined and extracted with $CHCl_3$ (3 × 25 ml). The 4 $CHCl_3$ layers were combined and washed with brine, then dried with $MgSO_4$. Solvent was removed *in vacuo* to leave a crude product that was analysed with ^{1}H NMR to determine conversion.

The variants of this reaction are given in the tables in sections 4.4 and 4.5, the only exception to this work up was the solvent and additive free method (1b, Table 4-1, section 4.5) which required no work up.

8.4.2 Optimised polymerisation trial

Sampled optimised method polymerisation (P^{o}_{m}DEAyAc)

DEAyAc **3.8** (0.1925 g, 0.86 mmol, 1 eq.) was dispersed in DMF (4 ml) along with *meta*-OC **2.1** (0.2000 g, 0.86 mmol, 1 eq.) and 3 Å MS (1.4 g) at 25 °C. The reaction was sampled every 24 hours for 14 days and analysed by GPC. The reaction stopped after 14 days when polymer growth was obviously limited.

Sampled Takata's method polymerisation (P^{t}_{m}DEAyAc)

DEAyAc **3.8** (0.1925 g, 0.86 mmol, 1 eq.) was dispersed in DMF (4 ml) along with *meta*-OC **2.1** (0.2000 g, 0.86 mmol, 1 eq.) and 4 Å MS (1.4 g) at room temperature for half an hour before the temperature was raised to 80 °C. The reaction was sampled every 24 hours for 3 days and analysed by GPC. The reaction was stopped after 3 days as GPC analysis showed no increase in molecular weight between day 2 and 3.

Optimised method polymerisation – P^{o14}_{m}DEAyAc (4.8)

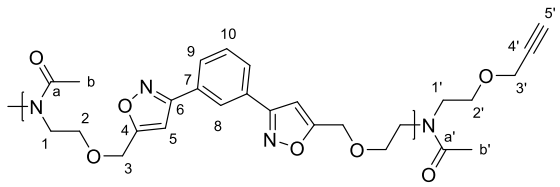

Meta-OC, **2.1** (250 mg, 1.07 mmol, 1 eq.) and DEAyAc **3.8** (239.5 mg, 1.07 mmol, 1 eq.) were dissolved in DMF (1 M). 3 Å molecular sieves were added (1600 g / mol of *meta*-OC **2.1**) and stirred (50 RPM) at 25 ^{o}C for 14 days. After 14 days the reaction mixture was taken into $CHCl_3$ (5 ml) and filtered to remove molecular sieves, the sieves were washed further with warm $CHCl_3$ (5ml), the filtrate was then reduced *in vacuo* to leave the polymer in DMF. The polymer was taken back into a small amount of $CHCl_3$ (2 ml) and added dropwise to MeOH (40 ml) causing a ppt to form. The ppt was collected by passing the mixture through filter paper on a sintered funnel. The ppt was washed with MeOH (3 x 25 ml) then collected from the filter paper with warm $CHCl_3$ (3 x 25 ml) which was reduced *in vacuo* to leave a pale orange solid. (9 %); ν_{max} / cm^{-1}: 2924 (C-H), 2893 (C-H), 1634 (C=O), 1622 (C=O), 1433 (C-N), 1066 (C-O), 900 (C-H); ^{1}H NMR (300 MHz, $CDCl_3$) δ 11.54 (s, H^{OH-}

oximoyl chloride), 8.48 (brs, $H^{3,4\text{-isoxazole}}$-min), 8.18 (brs, H^{8}), 7.82 (s, H^{9}), 7.49 (brs, H^{10}), 6.59 (s, H^{5}), 4.61 (brs, H^{3}), 4.17 – 4.05 (m, $H^{3'}$), 3.71 (brs, $H^{2/2'}$), 3.60 (brs, $H^{1/1'}$), 2.47 – 2.37 (m, $H^{5'}$), 2.14 (s, H^{b}).

Takata's method 2 day polymerisation – P^{t2}_{m}DEAyAc (4.9)

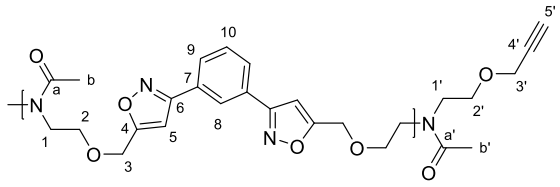

Meta-OC, **2.1** (250 mg, 1.07 mmol, 1 eq.) and DEAyAc **3.8** (239.5 mg, 1.07 mmol, 1 eq.) were dissolved in DMF (1 M). 4 Å molecular sieves were added (1600 g / mol of *meta*-OC **2.1**) and stirred (50 RPM) at 25 ^{o}C for for 30 minutes. The temperature was then raised to 80 ^{o}C for 48 hours. After 2 days the reaction mixture was taken into $CHCl_3$ (5 ml) and filtered to remove molecular sieves, the sieves were washed further with warm $CHCl_3$ (5ml), the filtrate was then reduced *in vacuo* to leave the polymer in DMF. The polymer was taken back into a small amount of $CHCl_3$ (2 ml) and added dropwise to MeOH (40 ml) causing a ppt to form. The ppt was collected by passing the solution through filter paper on a sintered funnel. The ppt was washed with MeOH (3 x 25 ml) then collected from the filter paper with warm $CHCl_3$ (3 x 25 ml) which was reduced *in vacuo* to leave a pale brown solid. (86 %); ν_{max} / cm^{-1}: 2920 (C-H), 2868 (C-H), 1629 (C=O), 1434 (C-N), 1100 (C-O), 911 (C-H); ^{1}H NMR (300 MHz, $CDCl_3$) δ 8.49 (s, $H^{3,4\text{-isoxazole}}$), 8.19 (brs, H^{7}), 7.85 (brs, H^{9}), 7.51 (brs, H^{10}), 6.61 (brs, H^{5}), 4.63 (brs, H^{3}), 4.13 (d, $H^{3'}$), 4.17 – 4.08 (m, $H^{3'}$), 3.73 (brs, H^{2}), 3.62 (brs, $H^{1/1'/2'}$), 2.46 – 2.39 (m, $H^{5'}$), 2.15 (brs, H^{b}).

8.5 General procedures Chapter 5

8.5.1 Fatty dipolarophile monomer synthesis

8.5.2 General procedure for the synthesis of diallyl fatty amides – **5.3**

A three-necked RBF equipped with a magnetic stirrer and reflux condenser, was charged with fatty acid (1 eq.) and placed under N_2 before adding dry toluene (70 ml). The mixture was heated to reflux. Oxalyl chloride (1.2 eq.) was added dropwise over the course of 30 minutes. The mixture was stirred at reflux for an additional 3 hours and ambient temperature overnight. For saturated fatty acids the solution was filtered

to remove residual fatty acid. The filtrate was reduced *in vacuo* to remove solvent and HCl, resulting in saturated fatty acid chloride as yellow liquids that solidified to an off white solid when placed in ice water and slowly melted at room temperature. The unsaturated fatty acids were not filtered to remove starting material, solvent and HCl were removed *in vacuo* to give the unsaturated acid chlorides as yellow liquids.

The acid chloride was then taken into dry toluene (20 ml) and added dropwise to a stirred solution of diallylamine (1.2 eq.) and TEA (1.2 eq.) in dry toluene (60 ml) at RT under N_2. The reaction reached completion 2 hours after the end of dropwise addition. The reaction was quenched with 2 M HCl (20 ml) then diluted with Et_2O (150 ml). The organic layer was washed with water (3 × 100 ml) and brine (100 ml), dried with $MgSO_4$ and reduced *in vacuo.* Saturated fatty acids resulted white solids that did not require further purification. Unsaturated fatty acids gave a crude yellow liquid that was purified by column chromatography through a silica plug (10 % EtOAc) to give a pure colourless liquid.

***N,N*-diallylpalmitamide – DAeP (5.3P)**

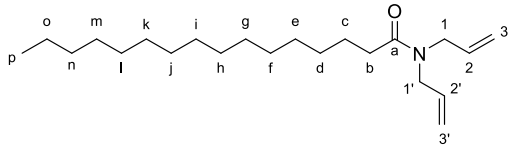

General Procedure for the synthesis of diallyl fatty amides was followed using palmitic acid (10.0 g, 39.0 mmol 1 eq.), oxalyl chloride (5.9 g, 46.8 mmol, 1.2 eq.), diallylamine (4.5 g, 46.8 mmol, 1.2 eq.), and TEA (4.7 g, 46.8 mmol, 1.2 eq.) to give a white solid. (91 %); R_f = 0.5 in 20 % EtOAc; m.p. 39 – 41 ° C; ν_{max} / cm^{-1}: 3081 (=C-H), 2922 (C-H), 2852 (C-H), 1650 (C=O), 1463 (C-H), 1411 (C-N), 919 (=C-H); ^{1}H NMR (500 MHz, $CDCl_3$) δ 5.83 – 5.71 (m, $H^{2/2'}$), 5.22 – 5.07 (m, $H^{3/3'}$), 3.98 (d, *J* = 6.0 Hz, $H^{1/1'}$), 3.86 (d, *J* = 5.0 Hz, $H^{1/1'}$), 2.29 (t, *J* = 7.5 Hz, H^b), 1.69 – 1.59 (m, H^c), 1.35 – 1.19 (m, H^{d-o}), 0.87 (t, *J* = 7.0 Hz, H^p); ^{13}C NMR (126 MHz, $CDCl_3$) δ 173.34 (C^a), 133.65 ($C^{2/2'}$), 133.18 ($C^{2/2'}$), 117.18 ($C^{3/3'}$), 116.64 ($C^{3/3'}$), 49.29 ($C^{1/1'}$), 47.93 ($C^{1/1'}$), 33.21 (C^b), 32.06 (C^n), 29.99 – 29.28 (C^{d-m}), 25.51 (C^c), 22.83 (C^o), 14.26 (C^p); *m/z*: (ES^+) calcd. ($C_{22}H_{41}NO + Na^+$): 358.3080, found: 358.3079 ($M + Na^+$).

***N,N*-diallylstearamide – DAeS (5.3S)**

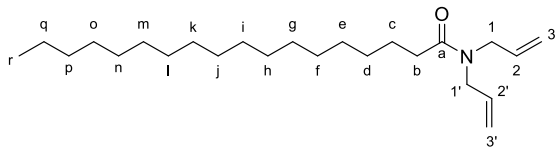

General Procedure for the synthesis of diallyl fatty amides was followed using stearic acid (10.0 g, 35.2 mmol 1 eq.), oxalyl chloride (5.4 g, 42.2 mmol, 1.2 eq.), diallylamine (4.1 g, 42.2 mmol, 1.2 eq.), and TEA (4.3 g, 42.2 mmol, 1.2 eq.) to give a white solid. (94 %); R_f = 0.5 in 20 % EtOAc; m.p. 43 – 45 °C; ν_{max} / cm^{-1}: 3083 (=C-H), 2912 (C-H), 2848 (C-H), 1632 (C=O), 1468 (C-H), 1413 (C-N), 920 (=C-H); ^{1}H NMR (500 MHz, $CDCl_3$) δ 5.86 – 5.67 (m, 2H, $H^{2/2'}$), 5.28 – 5.01 (m, 4H, $H^{3/3'}$), 3.98 (d, *J* = 6.0 Hz, 2H, $H^{1/1'}$), 3.86 (d, *J* = 5.0 Hz, 2H, $H^{1/1,}$), 2.29 (t, *J* = 7.5 Hz, 2H, H^{b}), 1.70 – 1.54 (m, 2H, H^{c}), 1.39 – 1.12 (m, 28H, H^{d-q}), 0.87 (t, *J* = 7.0 Hz, 3H, H^{r}); ^{13}C NMR (126 MHz, $CDCl_3$) δ 173.33 (C^{a}), 133.65 ($C^{2/2'}$), 133.18 ($C^{2/2'}$), 117.17 ($C^{3/3'}$), 116.63 ($C^{3/3'}$), 49.29 ($C^{1/1'}$), 47.93 ($C^{1/1'}$), 33.20 (C^{b}), 32.06 (C^{p}), 30.03 – 29.34 (C^{d-o}), 25.50 (C^{c}), 22.83 (C^{q}), 14.26 (C^{r}); *m/z*: (ES^+) calcd. ($C_{24}H_{45}NO + Na^+$): 386.3393, found: 386.3395 ($M + Na^+$).

***N,N*-diallyloleamide – DAeO (5.3O)**

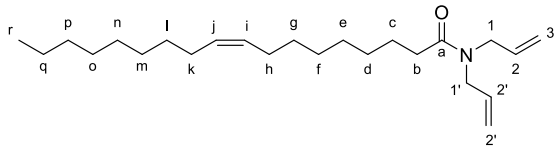

General Procedure for the synthesis of diallyl fatty amides was followed using oleic acid (10.0 g, 35.4 mmol 1 eq.), oxalyl chloride (5.4 g, 42.5 mmol, 1.2 eq.), diallylamine (4.1 g, 42.5 mmol, 1.2 eq.), and TEA (4.3 g, 42.5 mmol, 1.2 eq.) to give a pure clear liquid. (88 %); R_f = 0.5 in 20 % EtOAc; ν_{max} / cm^{-1}: 3082 (=C-H), 3005 (=C-H) 2923 (C-H), 2853 (C-H), 1640 (C=O), 1462 (C-H), 1438 (C-N), 921 (=C-H), 752 (=C-H); ^{1}H NMR (500 MHz, $CDCl_3$) δ 5.81 – 5.69 (m, 2H, $H^{2/2'}$), 5.43 – 5.27 (m, 2H, $H^{i/j}$), 5.23 – 5.02 (m, 4H, $H^{3/3'}$), 3.98 (d, *J* = 6.0 Hz, 2H, $H^{1/1'}$), 3.86 (d, *J* = 5.0 Hz, 2H, $H^{1/1'}$), 2.29 (t, *J* = 7.5 Hz, 2H, H^{b}), 2.07 – 1.95 (m, 4H, H^{hk}), 1.68 – 1.57 (m, 2H, H^{c}), 1.40 – 1.17 (m, 20H, $^{Hd-g,l-q}$), 0.87 (t, *J* = 7.0 Hz, 3H, H^{r}); ^{13}C NMR (126 MHz, $CDCl_3$) δ 173.26 (C^{a}), 133.63 ($C^{2/2'}$), 133.16 ($C^{2/2'}$), 130.08 (C^{j}), 129.92 (C^{i}), 117.18 ($C^{3/3'}$), 116.63 ($C^{3/3'}$), 49.27 ($C^{1/1'}$), 47.93 ($C^{1/1'}$), 33.18 (C^{b}), 32.03 (C^{p}), 30.20 – 28.95 ($C^{d-g/l-o}$), 27.34 (C^{h}), 27.32 (C^{k}) 25.48 (C^{c}), 22.81 (C^{q}), 14.24 (C^{r}); *m/z*: (ES^+) calcd. ($C_{24}H_{43}NO + H^+$): 362.3412, found: 362.3412 ($M + H^+$).

***N,N*-diallyllinileamide – DAeL (5.3L)**

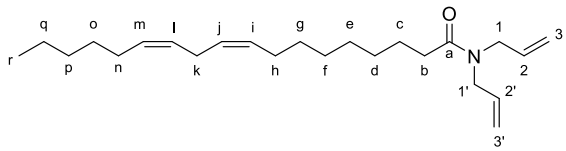

General Procedure for the synthesis of diallyl fatty amides was followed using linoleic acid (10.0 g, 35.7 mmol 1 eq.), oxalyl chloride (5.4 g, 42.8 mmol, 1.2 eq.), diallylamine (4.2 g, 42.8 mmol, 1.2 eq.), and TEA (4.3 g, 42.8 mmol, 1.2 eq.) to give a pure clear liquid. (71 %); R_f = 0.5 in 20 % EtOAc; ν_{max} / cm^{-1}: 3081 (=C-H), 3009 (=C-H) 2924 (C-H), 2854 (C-H), 1651 (C=O), 1460 (C-H), 1411 (C-N), 919 (=C-H), 753 (=C-H); ^{1}H NMR (500 MHz, $CDCl_3$) δ 5.88 – 5.65 (m, 2H, $H^{2/2'}$), 5.46 – 5.25 (m, 4H, $H^{ij,lm}$), 5.25 – 5.02 (m, 4H, $H^{3/3'}$), 3.97 (d, *J* = 6.0 Hz, 2H, $H^{1/1'}$), 3.86 (d, *J* = 4.5 Hz, 2H, $H^{1/1'}$), 2.76 (t, *J* = 6.5 Hz, 2H, H^{k}), 2.29 (t, *J* = 6.5 Hz, 2H, H^{b}), 2.09 – 19.6 (m, 4H, H^{hn}), 1.69 -1.57 (m, 2H, H^{c}), 1.42 – 1.19 (m, 14H, $H^{d-g/o-q}$), 0.88 (t, *J* = 7.0 Hz, H^{r}); ^{13}C NMR (126 MHz, $CDCl_3$) δ 173.25 (C^{a}), 133.60 ($C^{2/2'}$), 133.14 ($C^{2/2'}$), 130.31 (C^{m}), 130.20 (C^{i}), 128.11 (C^{j}), 128.03 (C^{l}), 117.17 ($C^{3/3'}$), 116.61 ($C^{3/3'}$), 49.26 ($C^{1/1'}$), 47.92 ($C^{1/1'}$), 33.15 (C^{b}), 31.63 (C^{p}), 29.74 (C^{g}), 29.54 (C^{o}), 29.47 (C^{d}), 29.46 (C^{e}), 29.28 (C^{f}), 27.32 (C^{n}), 27.31 (C^{h}), 25.74 (C^{k}), 25.46 (C^{c}), 22.69 (C^{q}), 14.19 (C^{r}); *m/z*: (ES^+) calcd. ($C_{24}H_{41}NO + H^+$): 360.3261, found: 360.3256 ($M + H^+$).

***N,N*-diallyllinilenamide – DAeLn (5.3Ln)**

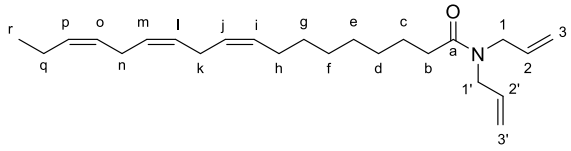

General Procedure for the synthesis of diallyl fatty amides was followed using half the volume of solvents, linoleneic acid (5.0 g, 17.9 mmol, 1 eq.), oxalyl chloride (2.7 g, 21.5 mmol, 1.2 eq.), diallylamine (2.1 g, 21.5 mmol, 1.2 eq.), and TEA (2.2 g, 21.5 mmol, 1.2 eq.) to give a pure clear liquid. (97 %); R_f = 0.5 in 20 % EtOAc; ν_{max} / cm^{-1}: 3082 (=C-H), 3010 (=C-H) 2925 (C-H), 2854 (C-H), 1651 (C=O), 1461 (C-H), 1411 (C-N), 920 (=C-H), 719 (=C-H), 691 (=C-H); ^{1}H NMR (500 MHz, $CDCl_3$) δ 5.85 – 5.67 (m, 2H, $H^{2/2'}$), 5.45 – 5.25 (m, 6H, $H^{i/j/l/m/o/p}$), 5.23 – 5.07 (m, 4H, $H^{3/3'}$), 3.98 (d, *J* = 6.0 Hz, 2H, $H^{1/1'}$), 3.87 (d, *J* = 4.5 Hz, 2H, $H^{1/1'}$), 2.84 – 2.78 (m, 4H, H^{kn}), 2.77 (t, *J* = 7.0 Hz, $H^{linoleic}$), 2.30 (t, *J* = 7.0 Hz, 2H, H^{b}), 2.12 – 2.06 (m, 4H, H^{hq}), 1.69 – 1.56 (m, 2H, H^{c}), 1.42 – 1.19 (m, 8H, H^{d-g}), 0.97 (t, *J* = 7.5 Hz, 3H, H^{r}), 0.89 (t, *J* = 7.0 Hz, $H^{linoleic}$); ^{13}C NMR (126 MHz, $CDCl_3$) δ 173.30 (C^{a}), 133.65 ($C^{2/2'}$), 133.18 ($C^{2/2'}$), 132.11 ($C^{i/j/l/m/o/p}$), 130.47 ($C^{i/j/l/m/o/p}$), 130.36 ($C^{linoleic-m}$), 130.25 ($C^{linoleic-i}$), 128.42 ($C^{i/j/l/m/o/p}$) 128.15 ($C^{linoleic-j}$),

128.07 ($C^{linoleic\text{-}l}$), 127.83 ($C^{i/j/l/m/o/p}$), 127.27 ($C^{i/j/l/m/o/p}$), 117.21 ($C^{3/3'}$), 116.66 ($C^{3/3'}$), 49.29 ($C^{1/1'}$), 47.95 ($C^{1/1'}$), 33.19 (C^{b}), 31.67 (C^{p}), 29.76 (C^{g}), 29.58 (C^{d}), 29.50 (C^{e}), 29.31 (C^{f}), 27.37 (C^{h}), 25.76 (C^{k}), 25.67 (C^{n}), 25.46 (C^{c}), 22.72 ($C^{linoleic}$), 20.69 (C^{q}), 14.42 (C^{r}) 14.22($C^{linoleic}$); *m/z*: (ES^+) calcd. ($C_{24}H_{39}NO + H^+$): 358.3100, found: 358.3101 ($M + H^+$).

8.5.3 General procedure for the synthesis of diol fatty amides – **5.6**

The desired fatty acid (1 eq.) was dissolved in solvent (0.5 M), (Et_2O for saturated fatty acids, THF for unsaturated fatty acid), with NMM (1.1 eq.) and left to homogenise at 0 ºC for 5 minutes. Ethyl chloroformate (1.1 eq.) was added dropwise and the reaction was stirred for 30 minutes. NMM hydrochloride was filtered off and the filtrate was added dropwise to diethanolamine (1.1 eq.) and TEA (1.1 eq.) in dry DMF (0.5) at RT under N_2. (The saturated fatty anhydrides partly crashed out of solution after filtration, to improve yield the solution was reduced *in vacuo* and the anhydride was taken into $CHCl_3$ (20 ml) for dropwise addition). The reaction was monitored by TLC and concluded between 2 – 3 hours. On completion the reaction was quenched with 2 M HCl (20 ml). After extraction with Et_2O (200 ml) the organic layer was washed with water (2 x 50 ml) and brine (50 ml), before drying with $MgSO_4$. Solvent was removed *in vacuo* to leave a crude product. Unsaturated fatty diol amides were purified by column chromatography through a silica plug (EtOAc, R_f = 0.2). Saturated fatty diol amides were purified by recrystallisation from Et_2O.

***N,N*-bis(2-hydroxyethyl)palmitamide – DOP (5.6P)**

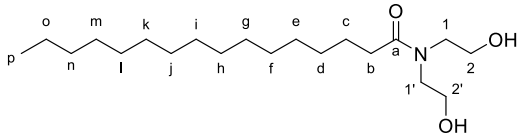

General procedure for the synthesis of diethanol fatty amides was followed using palmitic acid (12.8 g, 49.9 mmol, 1 eq.), NMM (5.55 g, 54.9 mmol, 1.1 eq.), ethyl chloroformate (5.96 g, 54.9 mmol, 1.1 eq.), diethanolamine (5.8 g, 54.9 mmol, 1.1 eq.), and TEA (5.6 g, 54.9 mmol, 1.1 eq.) to give a white solid. (55%); R_f = 0.2 in 100 % EtOAc; m.p. 60 – 62 °C; ν_{max}/cm^{-1} 3317 (O-H), 2916 (C-H), 2849 (C-H), 1611 (C=O); ^1H NMR (400 MHz, $CDCl_3$) δ 3.90 (t, J = 5.0 Hz, 2H, $H^{1/1'}$), 3.79 (t, J = 5.0 Hz, 2H, $H^{1/1'}$), 3.57 (t, J = 5.0 Hz, 2H, $H^{2/2'}$), 3.49 (t, J = 5.0 Hz, 2H, $H^{2/2'}$), 3.24 (brs, 2H, H^{OH}), 2.39 (t, J = 7.5 Hz, 2H, H^{b}), 1.73 – 1.50 (m, 2H, H^{c}) 1.37 – 1.15 (m, 24H, $H^{d\text{-}o}$), 0.88 (t, J = 7.0 Hz, 3H, H^{p}); ^{13}C NMR (101

MHz, $CDCl_3$) δ 175.85 (C^a), 61.52 ($C^{2/2'}$), 61.12 ($C^{2/2'}$), 52.42 ($C^{1/1'}$), 50.77 ($C^{1/1'}$), 33.89 (C^b), 31.98 (C^n), 29.87 – 29.23 (C^{d-m}), 25.14 (C^c), 22.74 (C^o), 14.13 (C^p); *m/z*: (ES^+) calcd. ($C_{20}H_{41}NO_3 + Na^+$): 366.3, found: 366.1 ($M + Na^+$).

***N,N*-bis(2-hydroxyethyl)stearamide – DOS (5.6S)**[203]

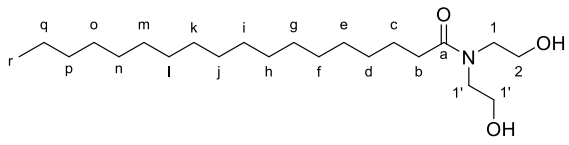

General procedure for the synthesis of diethanol fatty amides was followed using stearic acid (30.0 g, 105.4 mmol, 1 eq.), NMM (11.7 g, 116.0 mmol, 1.1 eq.), ethyl chloroformate (12.6 g, 116.0 mmol, 1.1 eq.), diethanolamine (12.2 g, 116.0 mmol, 1.1 eq.), and TEA (11.7 g, 116.0 mmol, 1.1 eq.) to give a white solid. (64 %); R_f = 0.2 in 100 % EtOAc; m.p. 72 – 75 °C; ν_{max}/cm^{-1} 3409 (O-H) 2918 (C-H), 2849 (C-H), 1616 (C=O); ^1H NMR (400 MHz, $CDCl_3$) δ 3.86 (t, J = 5.0 Hz, 2H, $H^{2/2'}$), 3.80 (t, J = 5.0 Hz, 2H, $H^{2/2'}$), 3.57 (t, J = 5.0, 2H, $H^{1/1'}$), 3.52 (t, J = 5.0 Hz, 2H, $H^{1/1'}$), 2.40 (t, J = 7.5 Hz, 2H, H^b), 1.71 – 1.58 (m, 2H, H^c), 1.40 – 1.19 (m, 28H, H^{d-q}), 0.90 (t, J = 7.0 Hz, 3H, H^r); ^{13}C NMR (101 MHz, $CDCl_3$) δ 175.92 (C^a), 61.87 ($C^{2/2'}$), 61.04 ($C^{2/2'}$), 52.35 ($C^{1/1'}$), 50.68 ($C^{1/1}$), 33.78 (C^b), 32.06 (C^p), 20.95 – 29.40 (C^{d-q}), 25.43 (C^c), 22.83 (C^q), 14.13 (C^r); *m/z*: (ES^+) calcd. ($C_{22}H_{45}NO_3 + Na^+$): 394.3, found: 394.1 ($M + Na^+$).

***N,N*-bis(2-hydroxyethyl)oleamide – DOO (5.6O)**[368]

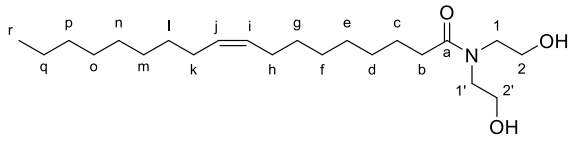

General procedure for the synthesis of diethanol fatty amides was followed using oleic acid (30 g, 106.2 mmol, 1 eq.), NMM (11.8 g, 116.8 mmol, 1.1 eq.), ethyl chloroformate (12.7 g, 116.8 mmol, 1.1 eq.), diethanolamine (12.3 g, 116.8 mmol, 1.1 eq.), and TEA (11.4 g, 116.8 mmol, 1.1 eq.) to give a pale yellow oil. (86 %); R_f = 0.2 in 100 % EtOAc; ν_{max}/cm^{-1} 3309 (O-H), 3005(=C-H), 2922 (C-H), 2853 (C-H), 1610 (C=O), 1463 (C-H), 1419 (C-N), 756 (=C-H); ^1H NMR (400 MHz, $CDCl_3$) δ 5.42 – 5.24 (m, 2H, $H^{i/j}$), 4.51 (brs, 2H, H^{OH}), 3.79 (t, J = 5.0 Hz, 2H, $H^{2/2'}$), 3.75 (t, J = 5.0 Hz, 2H, $H^{2/2'}$), 3.52 (t, J = 5.0 Hz, 2H, $H^{1/1'}$), 3.48 (t, J = 5.0 Hz, 2H, $H^{1/1'}$), 2.77 (t, J = 6.5 Hz, $H^{linoleic}$), 2.48 (t, *J* = 7.5 Hz, 2H, H^b), 2.07 – 1.94 (m, 4H, $H^{h/k}$), 1.67 – 1.54 (m, 2H, H^c), 1.38 – 1.21 (m, 20H, $H^{d-g/l-q}$), 0.88 (t, J = 7.0 Hz, 3H, H^r); ^{13}C NMR (101 MHz, $CDCl_3$) δ 175.63 (C^a), 130.21 ($C^{linoleic}$), 130.02 (C^i), 129.78 (C^j), 127.92 ($C^{linoleic}$), 61.22 ($C^{2/2'}$), 60.73 ($C^{2/2'}$), 52.31 ($C^{1/1'}$), 50.63 ($C^{1/1'}$), 33.66 (C^b), 31.95 (C^p), 30.87 – 29.20 ($C^{d-g/l-o}$), 27.27 (C^h), 27.25

(C^{k}), 25.63 ($C^{linoleic}$), 25.37 (C^{c}), 22.72 (C^{q}), 14.16 (C^{r}); *m/z*: (ES^{+}) calcd. ($C_{22}H_{43}NO_3$ + Na^{+}): 392.3, found: 392.4 (M + Na^{+}).

(9Z,12Z)-*N*,*N*-bis(2-hydroxyethyl)octadeca-9,12-dienamide – DOL (5.6L)[368]

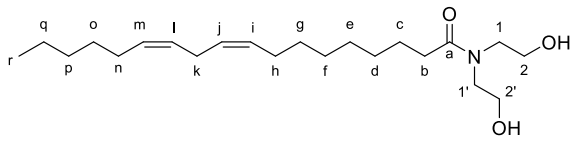

General procedure for the synthesis of diethanol fatty amides was followed using linoleic acid (30 g, 107.0 mmol, 1 eq.), NMM (11.9 g, 117.7 mmol, 1.1 eq.), ethyl chloroformate (12.8 g, 117.7 mmol, 1.1 eq.), diethanolamine (12.4 g, 117.7 mmol, 1.1 eq.), TEA (11.9 g, 117.7 mmol, 1.1 eq.). to give a pale yellow oil, (78 %, R_f = 0.2 in 100% EtOAc). ν_{max}/cm^{-1}: 3339 (O-H), 3008 (=C-H), 2922 (C-H), 2853 (C-H), 1616 (C=O), 1464 (C-H), 1420 (C-N), 1050 (C-OH), 723 (=C-H); ^{1}H NMR (400 MHz, $CDCl_3$) δ 5.55 – 5.17 (m, 4H, $H^{i/j/l/m}$), 4.87 (brs, 2H, H^{OH}), 3.79 (t, J = 5.0 Hz, 2H, $H^{2/2'}$), 3.76 (t, J = 5.0 Hz, 2H, $H^{2/2'}$), 3.53 (t, J = 4.5 Hz, 2H, $H^{1/1'}$), 3.49 (t, J = 5.0 Hz, 2H, $H^{1/1'}$), 2.77 (t, J = 6.5 Hz, 2H, H^{k}), 2.39 (t, J = 7.5 Hz, 2H, H^{b}), 2.07 – 2.02 (m, 4H, $H^{h/n}$), 1.70 – 1.53 (m, 2H, H^{d}), 1.41 – 1.21 (m, 14H, $H^{c\text{-}g/o\text{-}q}$), 0.89 (t, J = 7.0 Hz, 3H, H^{r}); ^{13}C NMR (101 MHz, $CDCl_3$) δ 175.79 (C^{a}), 130.20 (C^{m}), 130.01 (C^{i}), 128.02 (C^{j}), 127.90 (C^{l}), 61.05 ($C^{2/2'}$), 60.63 ($C^{2/2'}$), 52.31 ($C^{1/1'}$), 50.54 ($C^{1/1'}$), 33.61 (C^{b}), 31.52 (C^{p}), 29.66 (C^{g}), 29.50 (C^{o}), 29.45 (C^{d}), 29.43 (C^{e}), 29.24 (C^{f}), 27.23 (C^{n}), 27.19 (C^{h}), 25.63 (C^{k}), 25.33 (C^{c}), 22.57 (C^{q}), 14.08 (C^{r}); *m/z*: (ES^{+}) calcd. ($C_{22}H_{41}NO_3$ + Na^{+}): 390.3, found: 390.4 (M + Na^{+}).

(9Z,12Z,15Z)-*N*,*N*-bis(2-hydroxyethyl)octadeca-9,12,15-trienamide – DOLn (5.6Ln)[368]

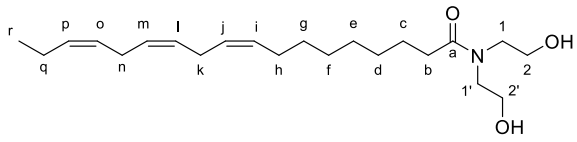

General procedure for the synthesis of diethanol fatty amides was followed using linolenic acid, 70 % (9 g, 32.3 mmol, 1.1 eq.), NMM (3.6 g, 35.6 mmol, 1.1 eq.), ethyl chloroformate (3.9 g, 35.6 mmol, 1.1 eq.), diethanolamine (3.7 g, 35.6 mmol, 1.1 eq.) and TEA (3.6 g, 35.6 mmol, 1.1 eq.) to give a pale yellow oil. (59 %); R_f = 0.2 in 100 % EtOAc; ν_{max}/cm^{-1} 3345(O-H) 2920 (C-H), 2857 (C-H), 1624 (C=O); ^{1}H NMR (400 MHz, $CDCl_3$) δ 5.54 – 5.17 (m, 6H, $H^{i/j/l/m/o/p}$), 4.13 (brs, 2H, H^{OH}), 3.79 (t, J = 5.0 Hz, 2H, $H^{2/2'}$), 3.74 (t, J = 5.0 Hz, 2H, $H^{2/2'}$), 3.51 (t, J = 5.0 Hz, 2H, $H^{1/1'}$), 3.47 (t, J = 5.0 Hz, 2H, $H^{1/1'}$), 2.87 – 2.71 (m, 4H, H^{kn}), 2.36 (t, J = 7.5 Hz, 2H, H^{b}), 2.14 – 1.94 (m, 4H, H^{hq}), 1.75 – 1.49 (m, 2H, H^{c}), 1.37 – 1.22 (m, 8H, $H^{d\text{-}g}$), 0.95 (t, J = 7.5 Hz, 3H, H^{r}), 0.87 (t, J = 7 Hz, 3H,

$H^{r(linoleic)}$); ^{13}C NMR (101 MHz, $CDCl_3$) δ 175.74 (C^{a}), 132.04 ($C^{i/j/l/m/o/p}$), 130.35 ($C^{i/j/l/m/o/p}$), 130.31 ($C^{linoleic\text{-}m}$), 130.13 ($C^{linoleic\text{-}i}$), 128.37 ($C^{i/j/l/m/o/p}$), 128.33 ($C^{i/j/l/m/o/p}$), 128.12 ($C^{linoleic\text{-}j}$), 127.99 ($C^{linoleic\text{-}l}$), 127.80 ($C^{i/j/l/m/o/p}$), 127.20 ($C^{i/j/l/m/o/p}$), 61.46 ($C^{2/2'}$), 60.84 ($C^{2/2'}$), 52.35 ($C^{1/1'}$), 50.68 ($C^{1/1'}$), 33.70 (C^{b}), 31.67 ($C^{linoleic}$), 29.70 (C^{g}), 29.51 (C^{d}), 29.48 (C^{e}), 29.42($C^{linoleic}$), 29.28 (C^{f}), 27.31 (C^{h}), 27.28($C^{linoleic}$), 25.70 (C^{k}), 25.61 (C^{n}), 25.38 (C^{c}), 22.65 ($C^{linoleic}$), 20.63 (C^{q}), 14.36 (C^{r}), 14.16 ($C^{linoleic}$); *m/z*: (ES^+) calcd. ($C_{22}H_{39}NO_3 + Na^+$): 388.3, found: 388.1 ($M + Na^+$).

8.5.4 General procedure for di(dipolarophilic) fatty amide synthesis – **5.2** & **5.4**

The desired fatty amide (1 eq.) was dissolved in Dry THF (0.5 M) under N_2. In a separate round bottom flask under N_2 sodium hydride (60% in mineral oil, 2.2 eq.), was washed with pet. Using a cannula the fatty amide solution was transferred into the vessel with washed NaH and left to homogenise for 30 mins. For unsaturated fatty acid based compounds the reactions were carried out at -78 °C, saturated compounds were reacted at 0 °C with slower addition at each step. Alkyl halide (2.2 eq.) was added dropwise, and the reaction mixture was left to come to room temperature overnight. To quench the reaction water (10 ml) was added dropwise, under nitrogen, followed by 2 M HCl (10 ml). THF was then removed *in vacuo*. The residue was taken into Et_2O (150 ml) and washed with water (2 x 50 ml) and brine (50 ml) before drying with $MgSO_4$. Solvent was removed *in vacuo* to leave a crude product. Column purification through a silica plug (20 % EtOAc) resulted in a pure product.

***N*,*N*-bis(2-(prop-2-yn-1-yloxy)ethyl)palmitamide – DEAyP (5.2P)**

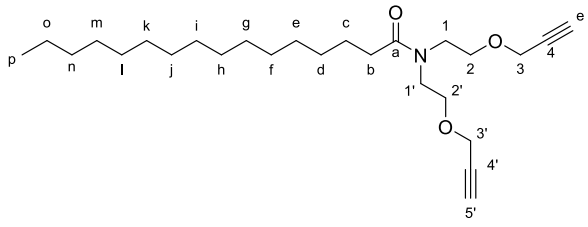

General procedure for the synthesis of dialkyne fatty amides was followed using DOP **5.6P** (9.4 g, 27.3 mmol, 1 eq.), NaH 60 % (2.4 g, 60.2 mmol, 2.2 eq.), propargyl bromide (80 % in toluene, 9.0 g, 60.2 mmol, 2.2 eq.) to give a white solid. (83 %); R_f = 0.3 in 25% EtOAc; m.p. 38 – 40 °C; ν_{max}/cm^{-1} 3306 (≡C-H), 2916 (C-H), 2849 (C-H), 2114 (C≡C), 1611 (C=O); 1466 (C-H), 1412 (C-N), 1098 (C-O), 1037 (C-O); ^1H NMR (500 MHz, $CDCl_3$) δ 4.14 (d, *J* = 2.0 Hz, 2H, $H^{3/3'}$), 4.12 (d, *J* = 2.0Hz, 2H, $H^{3/3'}$), 3.70 –

3.62 (m, 4H, $H^{2/2'}$), 3.62 – 3.54 (m, 4H, $H^{1/1'}$), 2.43 (t, *J* = 2.0 Hz, 1H, $H^{5/5'}$), 2.41 (t, *J* = 2.0 Hz, 1H, $H^{5/5'}$), 2.38 – 2.33 (t, *J* = 7.5 Hz, 2H, H^{b}), 1.70 – 1.57 (m, 2H, H^{c}), 1.36 – 1.21 (m, 24H, H^{d-o}), 0.87 (t, *J* = 7.0 Hz, 3H, H^{p}); ^{13}C NMR (126 MHz, $CDCl_3$) δ 173.94 (C^{a}), 79.80 ($C^{4/4'}$), 79.45 ($C^{4/4'}$), 74.90 ($C^{5/5'}$), 74.54 ($C^{5/5'}$), 68.87 ($C^{2/2'}$), 68.17 ($C^{2/2'}$), 58.63 ($C^{3/3'}$), 58.41 ($C^{3/3'}$), 48.91 ($C^{1/1'}$) , 46.52 ($C^{1/1'}$), 33.25 (C^{b}), 32.06 (C^{n}), 29.91 – 29.40 (C^{d-m}), 25.47 (C^{c}), 22.83 (C^{o}), 14.27 (C^{p}); *m/z:* (ES^+) calcd. ($C_{26}H_{45}NO_3$ + Na^+): 442.3292, found: 442.3283 (M + Na^+).

***N*,*N*-bis(2-(prop-2-yn-1-yloxy)ethyl)stearamide – DEAyS (5.2S)**

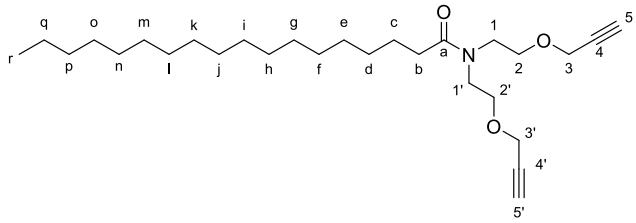

General procedure for the synthesis of dialkyne fatty amides was followed using DOS **5.6S** (13.0 g, 1 eq.), NaH (3.1 g, 2.2 eq.), and propargyl bromide (80 % in toluene, 11.5 g, 2.2 eq.) to give a white solid. (58 %); R_f = 0.3 in 25% EtOAc; m.p. 41 – 43 °C; ν_{max}/cm^{-1} 3307 (≡C-H), 2915 (C-H), 2848 (C-H), 2114 (C≡C), 1612 (C=O), 1466 (C-H), 1414 (C-N), 1099 (C-O), 1037 (C-O); ^{1}H NMR (500 MHz, $CDCl_3$) δ 4.15 (d, J = 2.0 Hz, 2H, $H^{3/3'}$), 4.12 (d, J = 2.0 Hz, 2H, $H^{3/3'}$), 3.67 (t, J = 5.0 Hz, 2H, $H^{2/2'}$), 3.64 (t, J = 5.0 Hz, 2H, $H^{2/2'}$), 3.61 – 3.57 (m, 4H, $H^{1/1'}$), 2.43 (t, J = 2.0 Hz, 1H, $H^{5/5'}$), 2.41 (t, J = 2.0 Hz, 1H, $H^{5/5'}$), 2.36 (t, J = 7.5 Hz 2H, H^{b}), 1.65 – 1.59 (m, 2H, H^{c}), 1.32 – 1.24 (m, 28H, H^{d-q}), 0.88 (t, J = 7.0 Hz, 3H, H^{r}); ^{13}C NMR (126 MHz, $CDCl_3$) δ 173.93 (C^{a}), 79.81 ($C^{4/4'}$), 79.45 ($C^{4/4'}$), 74.90 ($C^{5/5'}$), 74.54 ($C^{5/5'}$), 68.88 ($C^{2/2'}$), 68.18 ($C^{2/2'}$), 58.63 ($C^{3/3'}$), 58.41 ($C^{3/3'}$), 48.91 ($C^{1/1'}$), 46.52 ($C^{1/1'}$), 33.25 (C^{b}), 32.07 (C^{p}), 29.93 – 29.40 (C^{d-o}), 25.47 (C^{c}), 22.84 (C^{q}), 14.27 (C^{r}); *m/z:* (ES^+) calcd. ($C_{28}H_{49}NO_3$ + Na^+): 470.3605, found: 470.3606 (M + Na^+).

***N*,*N*-bis(2-(prop-2-yn-1-yloxy)ethyl)oleamide – DEAyO (5.2O)**

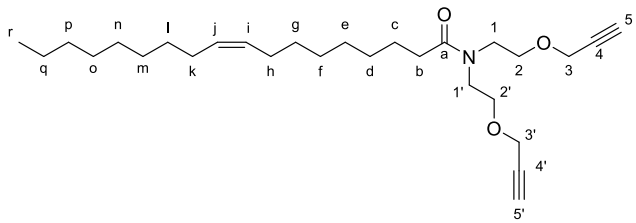

General procedure for the synthesis of dialkyne fatty amides was followed using DOO **5.6O** (15.4 g, 41.7 mmol, 1 eq.), NaH 60 % (3.67 g, 91.7 mmol 2.2 eq.), propargyl bromide (80 % in toluene, 13.6 g, 91.7 2.2 eq.) to give a yellow oil. (76 %); R_f = 0.3 in 25% EtOAc; ν_{max}/cm^{-1} 3308 (≡C-H), 3003 (=C-H), 2922 (C-H), 2852 (C-

H), 2115 (C≡C), 1639 (C=O), 1463 (C-H), 1442 (C-N), 1102 (C-O), 1031 (C-O), 755 (=C-H); ^{1}H NMR (500 MHz, $CDCl_3$) δ 5.47 – 5.27 (m, 2H, $H^{i/j}$), 4.14 (d, J = 2.0 Hz, 2H, $H^{3/3'}$), 4.12 (d, J = 2.0 Hz, 2H, $H^{3/3'}$), 3.72 – 3.63 (m, 4H, $H^{2/2'}$), 3.63 – 3.53 (m, 4H, $H^{1/1'}$), 2.45 (t, J = 2.0 Hz, 1H, $H^{5/5'}$), 2.42 (t, J = 2.0 Hz, 1H, $H^{5/5'}$), 2.36 (t, J = 7.5 Hz 2H, H^{b}), 2.02 – 1.99 (m, 4H, H^{hk}), 1.67 – 1.58 (m, 2H, H^{c}), 1.31 – 1.27 (m, 20H, $H^{d\text{-}g/l\text{-}q}$), 0.88 (t, J = 7.0 Hz, 3H, H^{r}); ^{13}C NMR (126 MHz, $CDCl_3$) δ 173.74 (C^{a}), 129.95 (C^{j}), 129.82 (C^{i}), 79.67 ($C^{4/4'}$), 79.32 ($C^{4/4'}$), 74.83 ($C^{5/5'}$), 74.47 ($C^{5/5'}$), 68.72 ($C^{2/2'}$), 68.04 ($C^{2/2'}$), 58.49 ($C^{3/3'}$), 58.27 ($C^{3/3'}$), 48.79 ($C^{1/1'}$), 46.39 ($C^{1/1'}$), 33.09 (C^{b}), 31.92 (C^{p}), 29.86 – 29.02 ($C^{d\text{-}g/l\text{-}o}$), 27.23 ($C^{h/k}$), 25.29 ($C^{c}$), 22.70 ($C^{q}$), 14.14 ($C^{r}$); *m/z:* ($ES^{+}$) calcd. ($C_{28}H_{47}NO_3 + Na^{+}$): 468.3448, found: 468.3454 ($M + Na^{+}$).

(9Z,12Z)-*N*,*N*-bis(2-(prop-2-yn-1-yloxy)ethyl)octadeca-9,12-dienamide – DEAyL (5.2L)

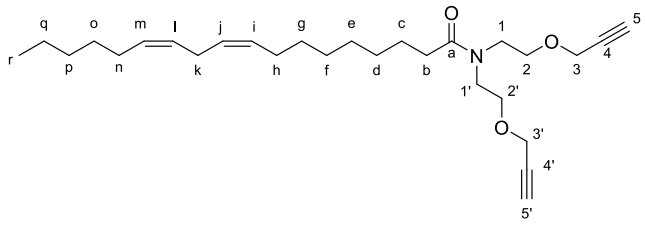

General procedure for the synthesis of dialkyne fatty amides was followed using DOL **5.6L** (22.4 g, 60.9 mmol, 1 eq.), NaH 60 % (5.4 g, 134.1 mmol, 2.2 eq.), propargyl bromide (80 % in toluene, 19.9 g, 134.1 mmol, 2.2 eq.) to give a yellow oil. (57 %); R_f = 0.3 in 25% EtOAc; ν_{max}/cm^{-1} 3305 (≡C-H), 3008 (=C-H), 2924 (C-H), 2853 (C-H), 1638 (C=O), 1464 (C-H), 1444 (C-N), 1102 (C-O), 1031 (C-O), 755 (=C-H); ^{1}H NMR (500 MHz, $CDCl_3$) δ 5.37 – 5.21 (m, 4H, $H^{i/j/l/m}$), 4.09 (d, J = 2.0 Hz, 2H, $H^{3/3'}$), 4.06 (d, J = 2.0 Hz, 2H, $H^{3/3'}$), 3.65 – 3.57 (m, 4H, $H^{2/2'}$), 3.55 – 3.51 (m, 4H, $H^{1/1'}$), 2.71 (t, J = 7.0 Hz, 2H, H^{k}), 2.40 (t, J = 2.0 Hz, 1H, $H^{5/5'}$), 2.37 (t, J = 2.0 Hz, 1H, $H^{5/5'}$), 2.31 (t, J = 7.5 Hz, 2H, H^{b}), 2.01 – 1.97 (m, 4H, $H^{h/n}$), 1.60 – 1.54 (m, 2H, H^{c}), 1.34 – 1.18 (m, 14H, $H^{d\text{-}g/o\text{-}q}$), 0.83 (t, J = 7.0 Hz, 3H, H^{r}); ^{13}C NMR (126 MHz, $CDCl_3$) δ 173.71 (C^{a}), 130.15 (C^{m}), 130.05 (C^{i}), 127.97 (C^{j}), 127.90 (C^{l}), 79.64 ($C^{4/4'}$), 79.29 ($C^{4/4'}$), 74.81 ($C^{5/5'}$), 74.46 ($C^{5/5'}$), 68.66 ($C^{2/2'}$), 67.99 ($C^{2/2'}$), 58.44 ($C^{3/3'}$), 58.22 ($C^{3/3'}$), 48.75 ($C^{1/1'}$), 46.35 ($C^{1/1'}$), 33.05 (C^{b}), 31.51 (C^{p}), 29.64 (C^{g}), 29.40 ($C^{o/d}$), 29.33 (C^{e}), 29.19(C^{f}), 27.22 (C^{n}), 27.19 (C^{h}), 25.62 (C^{k}), 25.28 (C^{c}), 22.57 (C^{q}), 14.08 (C^{r}); *m/z:* (ES^{+}) calcd. ($C_{28}H_{45}NO_3 + Na^{+}$): 466.3292, found: 466.3299 ($M + Na^{+}$).

(9Z,12Z,15Z)-*N*,*N*-bis(2-(prop-2-yn-1-yloxy)ethyl)octadeca-9,12,15-trienamide – DEAyLn (5.2Ln)

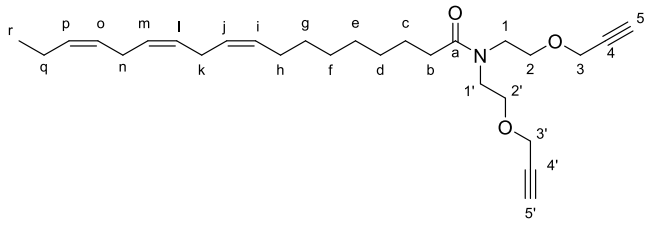

General procedure for the synthesis of dialkyne fatty amides was followed using DOLn **5.6Ln** (5.5 g, 15.0 mmol, 1 eq.), NaH (1.3 g, 33.1 mmol, 2.2 eq.), propargyl bromide (80 % in toluene, 4.9 g, 33.1 mmol, 2.2 eq.) to give a pale yellow oil. (84 %); R_f = 0.3 in 25% EtOAc; ν_{max} /cm^{-1} 3296 (≡C-H), 3009 (=C-H), 2926 (C-H), 2854 (C-H), 2115 (C≡C), 1639 (C=O), 1463 (C-H), 1443 (C-N), 1100 (C-O), 1031 (C-O), 666 (=C-H); ^{1}H NMR (500 MHz, $CDCl_3$) δ 5.47 – 5.26 (m, 6H, $H^{i/j/l/m/o/p}$), 4.13 (d, J = 2.0 Hz, 2H, $H^{3/3'}$), 4.11 (d, J = 2.0 Hz, 2H, $H^{3/3'}$), 3.67 (t, J = 5.5 Hz, 2H, $H^{2/2'}$), 3.63 (t, J = 5.5 Hz, 2H, $H^{2/2'}$), 3.60 – 3.56 (m, 4H, $H^{1/1'}$), 2.87 – 2.74 (m, 4H, $H^{k/n}$), 2.43 (t, J = 2.0 Hz, 1H, $H^{5/5'}$), 2.40 (t, J = 2.0 Hz, 1H, $H^{5/5'}$), 2.36 (t, J = 7.5 Hz, 2H, H^{b}), 2.08 – 2.02 (m, 4H, $H^{h/q}$), 1.76 – 1.45 (m, 2H, H^{c}), 1.39 – 1.22 (m, 8H, H^{d-g}), 0.96 (t, J = 7.5 Hz, 3H, H^{r}), 0.88 (t, J = 7.0 Hz, 3H, $H^{linoleic}$); ^{13}C NMR (101 MHz, $CDCl_3$) δ 175.85 (C^{a}), 132.07 ($C^{i/j/l/m/o/p}$), 130.44 ($C^{i/j/l/m/o/p}$), 130.33 ($C^{linoleic-m}$), 130.22 ($C^{linoleic-i}$), 128.39 ($C^{i/j/l/m/o/p}$), 128.38 ($C^{i/j/l/m/o/p}$), 128.11 ($C^{linoleic-j}$), 128.04 ($C^{linoleic-l}$), 127.80 ($C^{i/j/l/m/o/p}$), 127.24 ($C^{i/j/l/m/o/p}$), 79.77 ($C^{4/4'}$), 79.42 ($C^{4/4'}$), 74.89 ($C^{5/5'}$), 74.53 ($C^{5/5'}$), 68.83 ($C^{2/2'}$), 68.13 ($C^{2/2'}$), 58.60 ($C^{3/3'}$), 58.38 ($C^{3/3'}$), 48.88 ($C^{1/1'}$), 46.48 ($C^{1/1'}$), 33.20 (C^{b}), 31.63 ($C^{linoleic}$), 29.77 ($C^{linoleic}$), 29.75 (C^{g}), 29.53 ($C^{d/e}$), 29.46($C^{linoleic}$), 29.32 (C^{f}), 27.35 (C^{h}), 27.31($C^{linoleic}$), 25.73 (C^{k}), 25.64 (C^{n}), 25.41 (C^{c}), 22.69 ($C^{linoleic}$), 20.66 (C^{q}), 14.40 (C^{r}), 14.19 ($C^{linoleic}$); *m/z:* (ES$^+$) calcd. ($C_{28}H_{43}NO_3$ + Na$^+$): 464.3135, found: 464.3145 (M + Na$^+$).

***N*,*N*-bis(2-(allyloxy)ethyl)stearamide – DEAeS (5.4)**

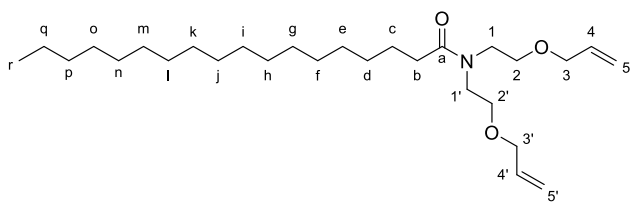

General Procedure for the synthesis of dialkyne fatty amides was followed using DOS **5.6S** (3.3 g, 8.8 mmol, 1 eq.), NaH 60 % (0.7 g, 17.8 mmol, 2.2 eq.), and allyl bromide (2.14 g, 17.8 mmol, 2.2 eq.) to give a colourless oil. (98 %); R_f = 0.3 in 20 % EtOAc; ν_{max}/cm^{-1} 3081 (=C-H), 2922 (C-H), 2852 (C-H), 1639 (C=O), 1465 (C-H), 1417 (C-N), 1103 (C-O) 923 (=C-H); ^{1}H NMR

(500 MHz, $CDCl_3$) δ 5.94 – 5.81 (m, 2H, $H^{4/4'}$), 5.25 (brd, *J* = 17.0 Hz, 2H, $H^{5t/5t'}$), 5.20 – 5.12 (m, 2H, $H^{5c/5c'}$), 3.98 – 3.94 (m, 4H, $H^{3/3'}$), 3.63 – 3.52 (m, 8H, $H^{1/1'/2/2'}$), 2.37 (t, *J* = 8.6 Hz, 2H, H^{b}), 1.67 – 1.56 (m, 2H, H^{c}), 1.42 – 1.14 (m, 28H, H^{d-q}), 0.88 (t, *J* = 7.0 Hz, 3H, H^{r}); ^{13}C NMR (126 MHz, $CDCl_3$) δ 173.91 (C^{a}), 134.84 ($C^{4/4'}$), 134.53 ($C^{4/4'}$), 117.21 ($C^{5/5'}$), 116.92 ($C^{5/5'}$), 72.34 ($C^{3/3'}$), 72.10 ($C^{3/3'}$), 68.97 ($C^{2/2'}$), 68.40 ($C^{2/2'}$), 49.13 ($C^{1/1'}$), 46.69 ($C^{1/1'}$), 33.24 (C^{b}), 32.07 (C^{p}), 29.95 – 29.44 (C^{d-o}), 25.50 (C^{c}), 22.84 (C^{q}), 14.26 (C^{r}); *m/z:* (ES^+) calcd. ($C_{28}H_{53}NO_3$ + Na^+): 474.3918, found: 474.3917 (M + Na^+).

***N*,*N*-bis(2-(allyloxy)ethyl)oleamide – DEAeO (5.6O)**

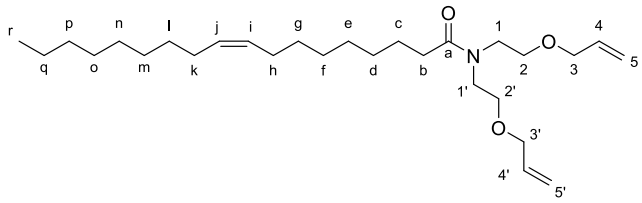

General procedure for the synthesis of dialkyne fatty amides was followed using DOO **5.6O** (3.0 g, 8.1 mmol, 1 eq.), NaH 60% (0.7 g, 17.9 mmol, 2.2 eq.), allyl bromide (2.2 g, 17.9 mmol, 2.2 eq.) to give a yellow oil. (76 %); R_f = 0.3 in 20 % EtOAc; ν_{max}/cm^{-1} 3080 (=C-H), 2923 (C-H), 2853 (C-H), 1646 (C=O), 1464 (C-H), 1418 (C-N), 1104 (C-O) 921 (=C-H); 722 (=C-H); ^{1}H NMR (500 MHz, $CDCl_3$) δ 5.96 – 5.79 (m, $H^{4/4'}$), 5.44 – 5.29 (m, $H^{i/j}$) 5.25 (brd, *J* = 17.0 Hz, 2H, $H^{5t/5t'}$), 5.20 – 5.13 (m, 2H, $H^{5c/5c'}$), 3.98 – 3.93 (m, 4H, $H^{3/3'}$), 3.64 – 3.48 (m, 8H, $H^{1/1'/2/2'}$), 2.37 (t, *J* = 7.0 Hz, 2H, H^{b}), 2.05 – 1.95 (m, 4H, $H^{h/k}$), 1.67 – 1.57 (m, 2H, H^{c}), 1.40 – 1.19 (m, 20H, $H^{d-g/l-q}$), 0.88 (t, *J* = 7.0 Hz, 3H, H^{r}); ^{13}C NMR (126 MHz, $CDCl_3$) δ 173.87 (C^{a}), 134.84 ($C^{4/4'}$), 134.52 ($C^{4/4'}$), 130.09 (C^{j}), 129.96 (C^{i}) 117.21 ($C^{5/5'}$), 116.92 ($C^{5/5'}$), 72.34 ($C^{3/3'}$), 72.10 ($C^{3/3'}$), 68.97 ($C^{2/2'}$), 68.39 ($C^{2/2'}$), 49.12 ($C^{1/1'}$), 46.69 ($C^{1/1'}$), 33.22 (C^{b}), 32.05 (C^{p}), 30.02 – 29.00 ($C^{d-g/l-o}$), 27.36 ($C^{h/k}$) 25.48 (C^{c}), 22.83 (C^{q}), 14.26 (C^{r}); *m/z:* (ES^+) calcd. ($C_{28}H_{51}NO_3$ + Na^+): 472.3761, found: 472.3762 (M + Na^+).

8.5.5 Model isoxazole and isoxazoline synthesis from fatty acid derivatives

_N,N'_-((((1,3-phenylenebis(isoxazole-3,5-diyl))bis(methylene))bis(oxy))bis(ethane-2,1-diyl))bis(N-(2-(prop-2-yn-1-yloxy)ethyl)oleamide) – O_mDEAyS-ABA (5.8)

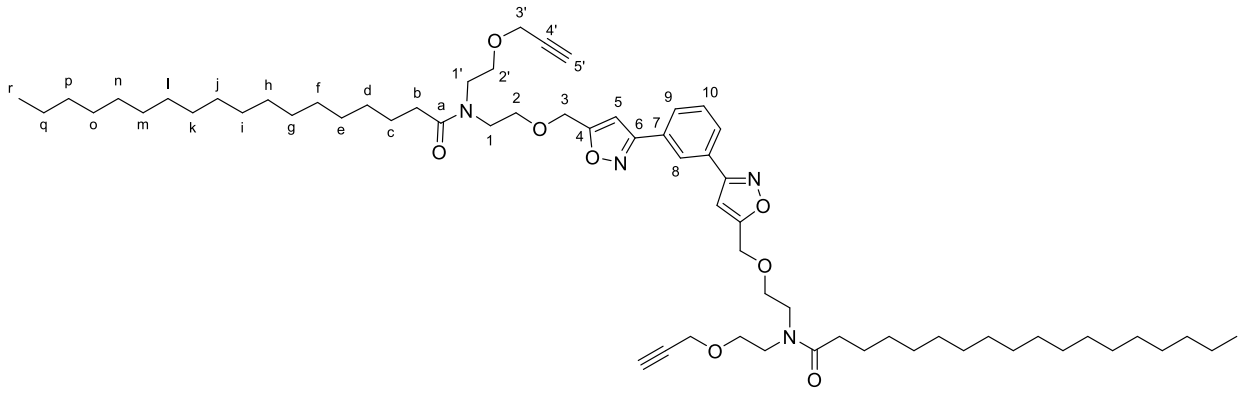

DEAyS **5.2S** (3.3 g, 7.2 mmol, 8 eq.) and *meta*-OC **2.1** (0.2 g, 0.9 mmol, 1 eq.) were dissolved in DMF (0.5 M) at RT, 4Å MS (1800 g / mol *meta*-OC **2.1**) were added and the mixture was stirred for 30 minutes. It was then heated to 80 °C for 24 hours. The solution was diluted with $CHCl_3$ (100 ml) and the sieves were removed by filtration. The organic filtrate was washed with water (6 × 100 ml) and brine (100 ml), then dried with $MgSO_4$ and filtered. Solvent was removed *in vacuo* to leave a crude product Purified by column chromatography through a silica plug resulted in a white waxy residue. (48 %); Rf 0.1 in 50 % EtOAc; ^{1}H NMR (500 MHz, $CDCl_3$) δ 8.49 (s, $H^{3,4\text{-isoxazole}}$), 8.25 – 8.21 (m, 1H, H^8), 7.92 – 7.88 (m, 2H, H^9), 7.59 – 7.53 (m, 1H, H^{10}), 6.64 (s, 2H, H^5), 6.63 (s, 2H, H^5) 6.62 (s, 2H, H^5), 6.62 (s, 2H, H^5) 4.67 (s, 2H, H^3-min), 4.64 (s, 2H, H^3-maj), 4.14 (d, *J* = 2.5 Hz, 2H, $H^{3'}$-maj), 4.12 (d, *J* = 2.5 Hz, 2H, $H^{3'}$-min), 3.77 – 3.57 (m, 8H, $H^{1/1'/2/2'}$), 2.43 (t, *J* = 2.5 Hz, 2H, $H^{5'}$), 2.41 (t, *J* = 2.5 Hz, 2H, $H^{5'}$), 2.40 – 2.33 (m, 2H, H^b), 1.66 – 1.57 (m, 2H, H^c), 1.34 – 1.18 (m, 56H, $H^{d\text{-}q}$), 0.88 (t, *J* = 6.9 Hz, 6H, H^r); ^{13}C NMR (126 MHz, $CDCl_3$) δ 173.98 (C^a-maj), 173.93 (C^a-min) 170.10 (C^4-maj), 169.94 (C^4-min), 162.02 (C^6), 161.94 (C^6), 129.93 (C^7), 129.89 (C^7), 129.83 (C^{10}), 129.79 ($C^{10)}$, 129.76 (C^{10}), 128.49 (C^9), 128.45 (C^9), 125.35 (C^8), 101.27 (C^5), 101.25 (C^5), 101.23 (C^5), 79.76 ($C^{4'}$-maj), 79.40 ($C^{4'}$-min), 75.00 ($C^{5'}$-maj), 74.62 ($C^{5'}$-min), 69.94 (C^2-maj), 69.62 (C^2-min), 68.97 ($C^{2'}$-min), 68.24 ($C^{2'}$-maj), 64.32 (C^3-min), 64.02 (C^3-maj), 58.64 ($C^{3'}$-maj), 58.44 ($C^{3'}$-min),

49.02 ($C^{1/1'}$-maj), 48.99 ($C^{1/1'}$-min), 46.69 ($C^{1/1'}$-min), 46.44 ($C^{1/1'}$-maj), 33.32 (C^{b}), 33.28 (C^{b}), 32.07 (C^{p}), 29.89 – 29.51 ($C^{d\text{-}o}$), 25.49 (C^{c}), 25.44 (C^{c}), 22.84 (C^{q}), 14.27 (C^{r}); *m/z:* (ES^+) calcd. ($C_{64}H_{102}N_4O_8 + Na^+$): 1077.7590, found: 1077.7590 ($M + Na^+$).

methyl 8-(4-octyl-3-phenyl-4,5-dihydroisoxazol-5-yl)octanoate (5.10)

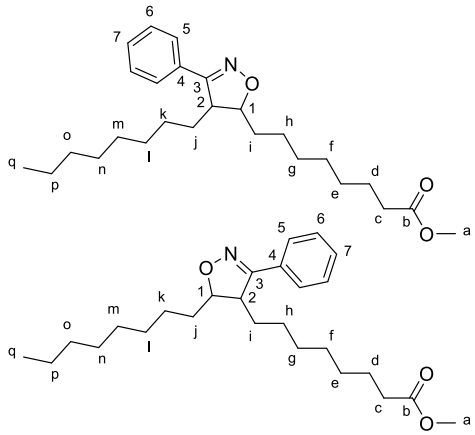

Methyl oleate (0.38 g, 1.3 mmol, 1 eq.) and benz-OC **4.1** (0.20 g, 1.3 mmol, 1 eq.) were dissolved in DMF (0.5 M) at RT, 4Å MS (1800 g / mol *meta*-OC **2.1**) were added and the mixture was stirred for 30 minutes. It was then heated to 80 °C for 24 hours. The solution was diluted with $CHCl_3$ (100 ml) and the sieves were removed by filtration. The organic filtrate was washed with water (6 × 100 ml) and brine (100 ml), then dried with $MgSO_4$ and filtered. Solvent was removed *in vacuo* to leave a crude product. Purification by column chromatography through a silica plug resulted in a clear oil. (8 %); R_f = 0.2 in 20 % EtOAc; ν_{max}/cm^{-1} 2925 (C-H), 2854 (C-H), 1737 (C=O), 1196 (C-O), 1108 (C-O), 765, 692; ^1H NMR (600 MHz, $CDCl_3$) δ 7.70 – 7.65 (m, 2H, H^5), 7.60 – 7.36 (m, 3H, $H^{6/7}$), 4.50 – 4.45 (m, 1H, H^1), 4.45 – 4.40 (m, 1H, H^1), 3.69 – 3.63 (m, 3H, H^a), 3.43 – 3.38 (m, 1H, H^2), 3.27 – 3.23 (m, 1H, H^2), 2.35 – 2.21 (m, 2H, H^c), 1.89 – 1.59 (m, 2H, H^d), 1.58 – 1.10 (m, 24H, $H^{e\text{-}i,j\text{-}p}$), 0.98 – 0.72 (m, 3H, H^q); ^{13}C NMR (151 MHz, $CDCl_3$) δ 174.45 (C^b), 174.38 (C^b), 162.29 (C^3), 162.23 (C^3), 159.36 (C^3), 159.28 (C^3), 130.04 (C^4), 129.95 (C^7), 129.84 (C^7), 129.52 (C^4), 128.89 (C^6), 128.86 (C^6), 127.12 (C^5), 127.02 (C^5), 86.65 (C^1), 86.60 (C^1), 85.52 (C^1), 85.46 (C^1), 52.69 (C^2), 52.63 (C^2), 51.61 (C^a), 48.47 (C^2), 48.39 (C^2), 35.55 (C^c), 34.29 – 22.57 ($C^{d\text{-}i/j\text{-}o}$), 14.28 – 14.21 ($C^q$); *m/z:* ($ES^+$) calcd. ($C_{26}H_{41}NO_3 + Na^+$): 438.2979, found: 438.2977 ($M + Na^+$).

8.5.6 General procedure for polyisoxazoles and polyisxazoline synthesis

Meta-oc, **2.1** (1 eq.) and dipolarophile monomer (1 eq.) were dissolved in DMF (1 M). 4 Å molecular sieves were added (1600 g / mol of *meta*-OC **2.1**) and stirred (50 RPM) at 25 °C for 30 minutes. The temperature was then raised to 80 °C for 48 hours. After 2 days the reaction mixture was taken into $CHCl_3$ (5 ml) and filtered to remove

molecular sieves, the sieves were washed further with warm $CHCl_3$ (5ml), the filtrate was then reduced *in vacuo* to leave the polymer in DMF. The polymer was taken back into a small amount of $CHCl_3$ (2 ml) and added dropwise to MeOH (40 ml) causing a ppt to form. The ppt was collected by passing the solution through filter paper on a sintered funnel. The ppt was washed with MeOH (3 x 25 ml) then collected from the filter paper with warm $CHCl_3$ (3 x 25 ml) which was reduced *in vacuo* to leave polymeric material.

$P^{t2}{}_m$DAeP (5.12P)

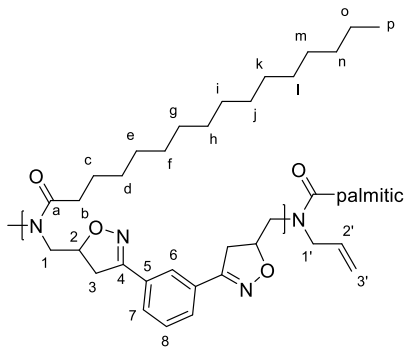

General procedure for polymerisation using vegetable oil derived monomers was followed with *meta*-OC **2.1** (500 mg, 2.15 mmol, 1 eq.) and DAeP **5.3P** (720 mg, 2.15 mmol, 1 eq.) to give a brittle yellow solid. (83 %); ν_{max} / cm^{-1}: 2921 (C-H), 2851 (C-H), 1641 (C=O), 1464 (C-H), 1436 (C-N), 1166 (C-O), 909 (C-H); ^{1}H NMR (500 MHz, $CDCl_3$) δ 8.51 – 8.02 (brm, H^{Ar}-min), 7.89 (brs, H^6), 7.69 (brs, H^7), 7.44 (brs, H^8), 5.84 – 5.72 (brm, $H^{2'}$), 5.19 (brd, *J* = 10.0 Hz, $H^{3'}$), 5.14 – 5.09 (brm, $H^{3'}$), 5.08 – 4.85 (brm, H^2), 4.55 – 4.24 (brm, H^{CH}-min), 4.21 – 4.12 (brm, $H^{1'}$), 4.12 – 3.92 (brm, $H^{1/1'}$), 3.91 – 3.72 (brm, $H^{1/3}$), 3.66 (brs, $H^{1/3}$), 3.59 – 3.28 (brm, $H^{1/3}$), 3.14 (brs, $H^{1/3}$) 3.03 (brs, $H^{1/3}$), 2.44 (brs, H^b), 2.39 – 2.22 (brm, H^b), 2.18 (s, H^b-min), 1.60 (brs, H^c), 1.23 (brs, H^{d-o}), 0.86 (brs, H^p); ^{13}C NMR (126 MHz, $CDCl_3$) δ 174.70 – 174.29 (C^a), 156.95 – 156.52 (C^4), 156.37 – 156.06 (C^4), 133.06 ($C^{2'}$), 130.26 – 129.99 (C^5), 129.99 – 129.77 (C^5), 129.63 – 129.20 (C^8), 128.73 – 128.46 (C^7), 128.46 – 128.12 (C^7), 124.93 (C^6), 116.61 – 116.43 ($C^{3'}$), 81.09 – 80.76 (C^2), 80.40 – 80.09 (C^2), 79.38 – 79.14 (C^2), 53.28 – 52.99 (C^1), 52.57 – 52.34 (C^1), 51.80 (C^1), 51.03 – 50.72 (C^1-min), 49.99 – 49.80 (C^1), 49.33 – 49.15 (C^1), 38.60 – 37.94 (C^3), 33.54 – 33.24 (C_b), 33.08 (C^b), 32.03 (C^n), 29.89 – 29.26 (C^{d-m}), 25.41 (C^c), 25.36 (C^c), 22.80 (C^o) 14.24 (C^p).

P^{t2}_{m}DAeS (5.12S)

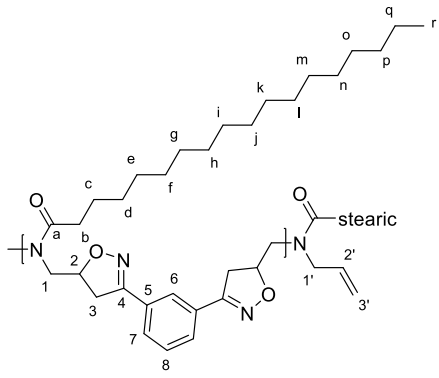

General procedure for polymerisation using vegetable oil derived monomers was followed with *meta*-OC **2.1** (500 mg, 2.15 mmol, 1 eq.) and DAeS **5.3S** (780 mg, 2.15 mmol, 1 eq.) to give a brittle yellow solid. (87 %); ν_{max} / cm^{-1}: 2920 (C-H), 2851 (C-H), 1642 (C=O), 1464 (C-H), 1437 (C-N), 1167 (C-O), 909 (C-H); ^{1}H NMR (500 MHz, $CDCl_3$) δ 8.53 – 8.02 (brm, H^{Ar}-min), 7.89 (brs, H^{6}), 7.68 (brs, H^{7}), 7.43 (brs, H^{8}), 5.84 – 5.73 (brm, $H^{2'}$), 5.19 (brd, *J* = 10.0 Hz, $H^{3'}$), 5.14 – 5.08 (brm, $H^{3'}$), 5.07 – 4.82 (brm, H^{2}), 4.54 – 4.24 (brm, H^{CH}-min), 4.25 – 4.12 (brm, $H^{1'}$), 4.11 – 3.93 (brm, $H^{1/1'}$), 3.90 – 3.73 (brm, $H^{1/3}$), 3.66 (brs, $H^{1/3}$), 3.58 – 3.26 (brm, $H^{1/3}$), 3.14 (brs, $H^{1/3}$) 3.03 (brs, $H^{1/3}$), 2.44 (brs, H^{b}), 2.39 – 2.21 (brm, H^{b}), 2.18 (s, H^{b}-min), 1.60 (brs, H^{c}), 1.24 (brs, H^{d-q}), 0.86 (brt, *J* = 6.5, H^{r}); ^{13}C NMR (126 MHz, $CDCl_3$) δ 174.79 – 174.29 (C^{a}), 156.97 – 156.45 (C^{4}), 156.33 – 156.08 (C^{4}), 133.04 ($C^{2'}$), 130.31 – 129.72 (C^{5}), 129.57 – 129.20 (C^{8}), 128.70 – 128.47 (C^{7}), 128.47 – 128.20 (C^{7}), 124.92 (C^{6}), 116.61 – 116.41 ($C^{3'}$), 81.12 – 80.77 (C^{2}), 80.36 – 80.07 (C^{2}), 79.36 – 79.09 (C^{2}), 53.33 – 52.96 (C^{1}), 52.60 – 52.32 (C^{1}), 51.79 (C^{1}), 51.09 – 50.66 (C^{1}-min), 50.01 – 49.77 (C^{1}), 49.34 – 49.13 (C^{1}), 38.62 – 37.86 (C^{3}), 33.50 – 33.23 (C^{b}), 33.07 (C^{b}), 32.02 (C^{p}), 29.91 – 29.22 (C^{d-o}), 25.40 (C^{c}), 25.35 (C^{c}), 22.78 (C^{q}) 14.23 (C^{r}).

P^{t2}_{m}DAeO (5.12O)

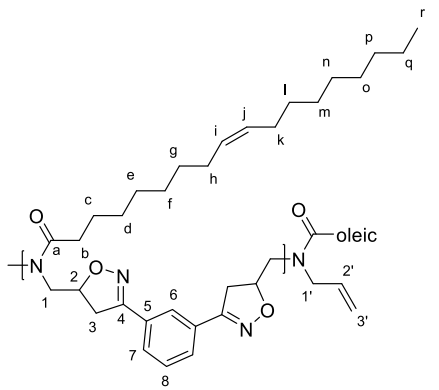

General procedure for polymerisation using vegetable oil derived monomers was followed with *meta*-OC **2.1** (500 mg, 2.15 mmol, 1 eq.) and DAeO **5.3O** (776 mg, 2.15 mmol, 1 eq.) to give a yellow brittle solid. (77 %); ν_{max} / cm^{-1}: 3002 (=C-H), 2922 (C-H), 2852 (C-H), 1643 (C=O), 1459 (C-H), 1436 (C-N), 1166 (C-O), 907 (C-H); ^{1}H NMR (500 MHz, $CDCl_3$) δ 8.54 – 8.00 (brm, H^{Ar}-min), 7.88 (brs, H^{6}), 7.69 (brs, H^{7}), 7.43 (brs, H^{8}), 5.84 – 5.72 (brm, $H^{2'}$), 5.31 (brs, $H^{i/j}$), 5.19 (brd, *J* = 10.0 Hz, $H^{3'}$), 5.15 – 5.08 (brm, $H^{3'}$), 5.08 – 4.83 (brm, H^{2}), 4.55 – 4.24 (brm, $H^{CH/CH2}$-min) 4.23 – 4.12 (brm, $H^{1'}$), 4.12 – 3.92 (brm, $H^{1/1'}$), 3.88 – 3.71 (brm, $H^{1/3}$), 3.64 (brs, $H^{1/3}$), 3.57 –

3.23 (brm, $H^{1/3}$), 3.11 (brs, $H^{1/3}$) 3.02 (brs, $H^{1/3}$), 2.73 (brs, $H^{linoleic}$) 2.44 (brs, H^{b}), 2.38 – 2.22 (brm, H^{b}), 2.18 (s, H^{b}-min), 1.98 (brs, H^{hk}), 1.61 (brs, H^{c}), 1.25 (brs, H^{d-q}), 0.86 (brs, H^{r}); ^{13}C NMR (126 MHz, $CDCl_3$) δ 174.97 – 174.20 (C^{a}), 157.08 – 156.54 (C^{4}), 156.52 – 156.03 (C^{4}), 133.01 ($C^{2'}$), 130.31 ($C^{linoleic}$) 130.06 (C^{j}), 129.86 (C^{i}), 129.63 – 129.17 (C^{8}), 128.66 – 128.46 (C^{7}), 128.46 – 128.23 (C^{7}), 128.11 ($C^{linoleic}$), 127.99 ($C^{linoleic}$), 124.91 (C^{6}), 116.63 – 116.40 ($C^{3'}$), 81.20 – 80.56 (C^{2}), 80.40 – 80.01 (C^{2}), 79.41 – 78.93 (C^{2}), 53.38 – 52.93 (C^{1}), 52.66 – 52.29 (C^{1}), 51.79 (C^{1}), 51.15 – 50.75 (C^{1}-min), 50.23 – 49.67 (C^{1}), 49.39 – 49.14 (C^{1}), 38.67 – 37.84 (C^{3}), 33.46 – 33.19 (C^{b}), 33.05 (C^{b}), 31.98 (C^{p}), 30.11 – 28.99 ($C^{d-g/l-o}$), 27.31 ($C^{h/k}$), 25.49 – 25.10 (C^{c}), 22.71 (C^{q}) 14.22 (C^{r}).

$P^{t2}{}_{m}$DAeL (5.12L)

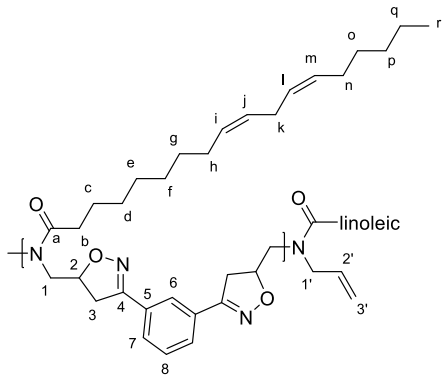

General procedure for polymerisation using vegetable oil derived monomers was followed with *meta*-OC **2.1** (500 mg, 2.15 mmol, 1 eq.) and DAeL **5.3L** (772 mg, 2.15 mmol, 1 eq.) to give a yellow brittle solid. (74 %); ν_{max} / cm^{-1}: 3004 (=C-H), 2921 (C-H), 2852 (C-H), 1645 (C=O), 1462 (C-H), 1438 (C-N), 1166 (C-O), 904 (C-H); ^{1}H NMR (500 MHz, $CDCl_3$) δ 8.58 – 8.06 (brm, H^{Ar}-min), 7.90 (brs, H^{6}), 7.70 (brs, H^{7}), 7.44 (brs, H^{8}), 5.86 – 5.73 (brm, $H^{2'}$), 5.33 (brs, $H^{i/j/l/m}$), 5.19 (brd, *J* = 10.0 Hz, $H^{3'}$), 5.14 – 5.07 (brm, $H^{3'}$), 5.07 – 4.85 (brm, H^{2}), 4.57 – 4.28 (brm, $H^{CH/CH2}$-min), 4.22 – 4.12 (brm, $H^{1'}$), 4.12 – 3.91 (brm, $H^{1/1'}$), 3.90 – 3.71 (brm, $H^{1/3}$), 3.70 – 3.58 (brs, $H^{1/3}$), 3.57 – 3.27 (brm, $H^{1/3}$), 3.12 (brs, $H^{1/3}$) 3.03 (brs, $H^{1/3}$), 2.75 (brs, H^{k}) 2.45 (brs, H^{b}), 2.39 – 2.20 (brm, H^{b}), 2.16 (brs, H^{b}-min), 2.02 (brs, H^{hn}), 1.60 (brs, H^{c}), 1.27 (brs, H^{d-q}), 0.87 (brs, H^{r}); ^{13}C NMR (126 MHz, $CDCl_3$) δ 174.83 – 174.15 (C^{a}), 157.09 – 156.57 (C^{4}), 156.45 – 156.08 (C^{4}), 133.07 ($C^{2'}$), 130.35 (C^{m}) 130.20 (C^{i}), 130.15 – 129.85 (C^{5}), 129.59 – 129.19 (C^{8}), 128.75 – 128.50 (C^{7}), 128.48 – 128.32 (C^{7}), 128.15 (C^{j}), 128.03 (C^{l}), 124.93 (C^{6}), 116.61 – 116.46 ($C^{3'}$), 81.15 – 80.75 (C^{2}), 80.40 – 80.01 (C^{2}), 79.33 – 79.13 (C^{2}), 53.37 – 52.96 (C^{1}), 52.64 – 52.34 (C^{1}), 51.81 (C^{1}), 50.00 – 49.80 (C^{1}), 49.44 – 49.15 (C^{1}), 38.51 – 38.28 (C^{3}), 38.28 – 37.97 (C^{3}), 33.52 – 33.16 (C^{b}), 33.07 (C^{b}), 31.63 (C^{p}), 29.88 – 29.05 ($C^{d-g/o}$), 27.32 ($C^{h/n}$), 25.76 (C^{k}), 5.47 – 25.12 (C^{c}), 22.70 (C^{q}) 14.22 (C^{r}).

P^{t2}_{m}DAeLn (5.12Ln)

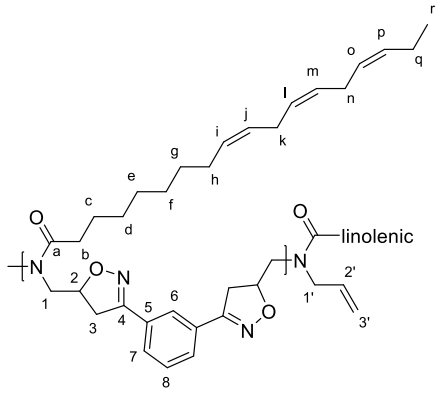

General procedure for polymerisation using vegetable oil derived monomers was followed with *meta*-OC **2.1** (500 mg, 2.15 mmol, 1 eq.) and DAeLn **5.3Ln** (767 mg, 2.15 mmol, 1 eq.) to give a yellow brittle solid. (72 %); ν_{max} / cm^{-1}: 3007 (=C-H), 2925 (C-H), 2853 (C-H), 1637 (C=O), 1461 (C-H), 1434 (C-N), 1165 (C-O), 906 (C-H); ^{1}H NMR (500 MHz, $CDCl_3$) δ 8.51 – 8.05 (brm, H^{Ar}-min), 7.90 (brs, H^{6}), 7.69 (brs, H^{7}), 7.44 (brs, H^{8}), 5.85 – 5.69 (brm, $H^{2'}$), 5.34 (brs, $H^{i/j/l/m/o/p}$), 5.19 (brd, *J* = 10.0 Hz, $H^{3'}$), 5.13 – 5.08 (brm, $H^{3'}$), 5.08 – 4.88 (brm, H^{2}), 4.57 – 4.23 (brm, $H^{CH/CH2}$-min), 4.20 – 4.11 (brm, $H^{1'}$), 4.11 – 3.91 (brm, $H^{1/1'}$), 3.89 – 3.71 (brm, $H^{1/3}$), 3.70 – 3.58 (brm, $H^{1/3}$), 3.57 – 3.22 (brm, $H^{1/3}$), 3.12 (brs, $H^{1/3}$) 3.03 (brs, $H^{1/3}$), 2.79 (brs, $H^{k/n}$), 2.45 (brs, H^{b}), 2.38 – 2.12 (brm, H^{b}), 2.04 (br, $H^{h/q}$), 1.60 (brs, H^{c}), 1.27 (brs, H^{d-g}), 0.96 (brs, H^{r}), 0.87 ($H^{linoleic}$); ^{13}C NMR (126 MHz, $CDCl_3$) δ 174.83 – 174.20 (C^{a}), 157.01 – 156.50 (C^{4}), 156.48 – 156.06 (C^{4}), 133.06 ($C^{2'}$), 132.07 ($C^{i/j/l/m/o/p}$), 130.41 ($C^{i/j/l/m/o/p}$), 130.34 ($C^{linoleic-m}$), 130.19 ($C^{linoleic--i}$), 130.15 – 129.78 (C^{5}), 129.57 – 129.23 (C^{8}), 128.71 – 128.49 (C^{7}), 128.40 ($C^{i/j/l/m/o/p}$), 128.37 ($C^{i/j/l/m/o/p}$), 128.15 ($C^{linoleic-j}$), 128.03 ($C^{linoleic-l}$), 127.82 ($C^{i/j/l/m/o/p}$), 127.23 ($C^{i/j/l/m/o/p}$), 124.92 (C^{6}), 116.78 – 116.35 ($C^{3'}$), 85.36 ($C^{cross-link}$) 81.10 – 80.79 (C^{2}), 80.28 – 80.12 (C^{2}), 79.31 – 79.12 (C^{2}), 53.28 – 52.98 (C^{1}), 52.57 – 52.35 (C^{1}), 51.80 (C^{1}), 50.03 – 49.77 (C^{1}), 49.42 – 49.11 (C^{1}), 38.53 – 38.29 (C^{3}), 38.29 – 38.02 (C^{3}), 33.43 – 33.20 (C^{b}), 33.06 (C^{b}), 31.62 ($C^{linoleic}$), 29.97 – 29.05 (C^{d-g}), 27.38 – 27.26 (C^{h}), 25.73 (C^{k}), 25.64 (C^{n}), 25.38 (C^{c}), 22.68 ($C^{linoleic}$), 20.67 (C^{q}), 14.41 (C^{r}), 14.21 ($C^{linoleic}$).

P^{t2}_{m}DEAyP (5.11P)

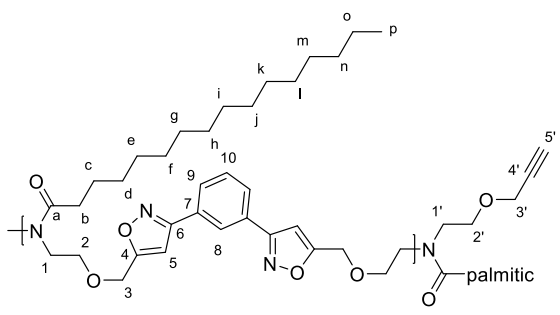

General procedure for polymerisation using vegetable oil derived monomers was followed with *meta*-OC **2.1** (500 mg, 2.15 mmol, 1 eq.) and DEAyP **5.2P** (900 mg, 2.15 mmol, 1 eq.) to give a malleable brown solid. (87 %); ν_{max} / cm^{-}

[1] 2921 (C-H), 2852 (C-H), 1636 (C=O), 1464 (C-H), 1437 (C-N), 1157 (C-O), 1102 (C-O), 912 (C-H); ^{1}H NMR (500 MHz, $CDCl_3$) δ 8.48 (s, H^{CH}-min), 8.19 (brs, H^{8}), 7.85 (brs, H^{9}), 7.60 – 7.45 (m, H^{10}), 6.65 – 6.54 (brm, H^{5}), 4.76 – 4.52 (brm, H^{3}), 4.49 – 4.45 (m, H^{CH_2}-min), 4.13 (d, *J* = 2.0 Hz, $H^{3'}$), 4.11 (d, J = 2.0 Hz, $H^{3'}$), 3.78 – 3.67 (m, H^{2}), 3.67 – 3.54 (m, H^{1}), 2.43 (t, *J* = 2.0, $H^{5'}$), 2.40 (t, *J* = 2.0, $H^{5'}$), 2.39 – 2.30 (m, H^{b}), 1.65 – 1.51 (m, H^{c}), 1.33 – 1.13 (brm, H^{d-o}), 0.86 (brt, *J* = 6.5 Hz, H^{p}); ^{13}C NMR (126 MHz, $CDCl_3$) δ 173.97 (C^{a}), 169.93 (C^{4}), 169.81 (C^{4}), 161.93 (C^{6}), 161.87 (C^{6}), 129.82 (C^{7}), 129.80 – 129.73 (C^{10}), 129.71 (C^{7}), 128.43 (C^{9}), 125.32 – 125.18 (C^{8}), 101.39 – 101.23 (C^{5}), 79.74 ($C^{4'}$), 79.38 ($C^{4'}$), 74.99 ($C^{5'}$), 74.62 ($C^{5'}$), 70.04 – 69.83 (C^{2}), 69.69 – 69.54 (C^{2}), 68.91 ($C^{2'}$), 68.21 ($C^{2'}$), 64.35 – 64.14 (C^{3}), 64.04 – 63.81 (C^{3}), 58.60 ($C^{3'}$), 58.41 ($C^{3'}$), 49.23 – 48.81 ($C^{1/1'}$), 46.92 – 46.50 ($C^{1/1'}$), 33.44 – 33.19 (C^{b}), 32.03 (C^{n}), 29.99 – 29.17 (C^{d-m}), 25.42 (C^{c}), 22.80 (C^{o}), 14.24 (C^{p}).

P^{t2}_{m}DEAyS (5.11S)

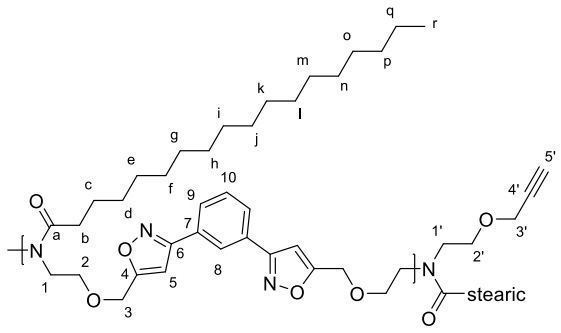

General procedure for polymerisation using vegetable oil derived monomers was followed with *meta*-OC **2.1** (500 mg, 2.15 mmol, 1 eq.) and DEAyS **5.2S** (961 mg, 2.15 mmol, 1 eq.) to give a malleable brown solid. (88 %); ν_{max} / cm^{-1}: 2921 (C-H), 2851 (C-H), 1637 (C=O), 1464 (C-H), 1438 (C-N), 1157 (C-O), 1102 (C-O), 913 (C-H); ^{1}H NMR (500 MHz, $CDCl_3$) δ 8.48 (s, H^{CH}-min), 8.21 (brs, H^{8}), 7.85 (brs, H^{9}), 7.58 – 7.43 (m, H^{10}), 6.66 – 6.54 (brm, H^{5}), 4.67 – 4.56 (brm, H^{3}), 4.49 – 4.43 (m, H^{CH_2}-min), 4.13 (d, *J* = 2.0 Hz, $H^{3'}$), 4.11 (d, J = 2.0 Hz, $H^{3'}$), 3.77 – 3.68 (m, H^{2}), 3.66 – 3.56 (m, H^{1}), 2.43 (t, *J* = 2.0, $H^{5'}$), 2.40 (t, *J* = 2.0, $H^{5'}$), 2.39 – 2.32 (m, H^{b}), 1.66 – 1.54 (m, H^{c}), 1.36 – 1.08 (brm, H^{d-q}), 0.86 (brt, *J* = 6.5 Hz, H^{r}); ^{13}C NMR (126 MHz, $CDCl_3$) δ 173.98 (C^{a}), 169.94 (C^{4}), 169.81 (C^{4}), 161.93 (C^{6}), 161.87 (C^{6}), 129.82 (C^{7}), 129.81 – 129.73 (C^{10}), 129.72 (C^{7}), 128.43 (C^{9}), 125.34 – 125.19 (C^{8}), 101.43 – 101.20 (C^{5}), 79.74 ($C^{4'}$), 79.39 ($C^{4'}$), 74.99 ($C^{5'}$), 74.62 ($C^{5'}$), 70.04 – 69.86 (C^{2}), 69.71 – 69.52 (C^{2}), 68.92 ($C^{2'}$), 68.21 ($C^{2'}$), 64.32 – 64.14 (C^{3}), 64.02 – 63.81 (C^{3}), 58.61 ($C^{3'}$), 58.41 ($C^{3'}$), 49.19 – 48.90 ($C^{1/1'}$), 46.88 – 46.55 ($C^{1/1'}$), 33.42 – 33.18 (C^{b}), 32.04 (C^{p}), 29.92 – 29.32 (C^{d-o}), 25.42 (C^{c}), 22.81 (C^{q}), 14.25 (C^{r}).

P$^{t2}_{m}$DEAyO (5.11O)

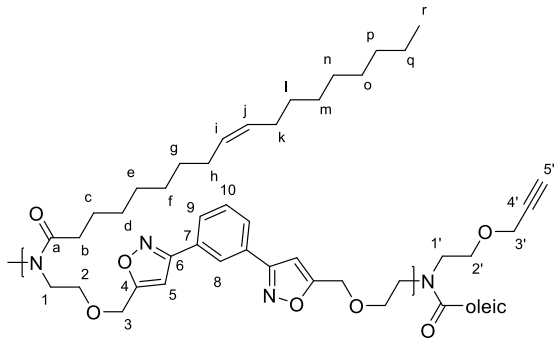

General procedure for polymerisation using vegetable oil derived monomers was followed with *meta*-OC **2.1** (500 mg, 2.15 mmol, 1 eq.) and DEAyO **5.2O** (956 mg, 2.15 mmol, 1 eq.) to give a malleable brown solid. (80 %); ν_{max} / cm^{-1}: 3002 (=C-H), 2923 (C-H), 2853 (C-H), 1637 (C=O), 1462 (C-H), 1438 (C-N), 1159 (C-O), 1102 (C-O), 912 (C-H); ^{1}H NMR (500 MHz, $CDCl_3$) δ 8.48 (s, H^{CH}-min), 8.21 (brs, H^{8}), 7.85 (brs, H^{9}), 7.58 – 7.44 (brm, H^{10}), 6.65 – 6.55 (brm, H^{5}), 5.30 (brs, H$^{i/j}$), 4.71 – 4.52 (brm, H^{3}), 4.49 – 4.44 (m, H^{CH_2}-min/crosslinked), 4.14 (brs, H$^{3'}$), 4.10 (brs, H$^{3'}$), 3.78 – 3.67 (m, H^{2}), 3.66 – 3.54 (m, H^{1}), 2.43 (brs, H$^{5'}$), 2.40 (br, H$^{5'}$), 2.39 – 2.30 (m, H^{b}), 2.03 – 1.90 (brm, H^{hk}), 1.60 (brs, H^{c}), 1.25 (brs, H$^{d\text{-}g/l\text{-}q}$), 0.86 (brs, H^{r}); ^{13}C NMR (126 MHz, $CDCl_3$) δ 173.97 (C^{a}), 169.94 (C^{4}), 169.81 (C^{4}), 161.94 (C^{6}), 161.88 (C^{6}), 130.05 (C^{j}), 129.90 (C^{i}), 129.72 (C^{7}), 129.83 – 129.74 (C^{10}), 129.72 (C^{7}), 128.45 (C^{9}), 125.35 – 125.16 (C^{8}), 101.35 (C^{5}), 75.02 (C$^{5'}$), 74.66 (C$^{5'}$), 70.06 – 69.81 (C^{2}), 69.71 – 69.48 (C^{2}), 68.91 (C$^{2'}$), 68.20 (C$^{2'}$), 64.32 – 64.08(C^{3}), 63.98 – 63.81 (C^{3}), 58.61 (C$^{3'}$), 58.42 (C$^{3'}$), 49.19 – 48.87 (C$^{1/1'}$), 46.88 – 46.55 (C$^{1/1'}$), 33.37 – 33.19 (C^{b}), 32.02 (C^{p}), 29.96 – 29.12 (C$^{d\text{-}g/l\text{-}o}$), 27.39 – 27.27 (C^{k}), 25.41 (C^{c}), 22.80 (C^{q}), 14.25 (C^{r}).

P$^{t2}_{m}$DEAyL (5.11L)

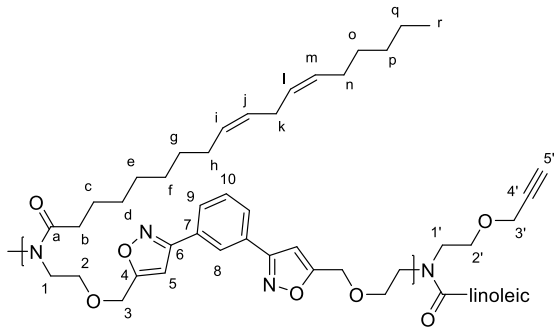

General procedure for polymerisation using vegetable oil derived monomers was followed with *meta*-OC **2.1** (500 mg, 2.15 mmol, 1 eq.) and DEAyL **5.2L** (952 mg, 2.15 mmol, 1 eq.) to give a malleable brown solid. (76 %); ν_{max} / cm^{-1}: 3276 (C≡C), 3007 (=C-H), 2925 (C-H), 2853 (C-H), 1636 (C=O), 1463 (C-H), 1437 (C-N), 1158 (C-O), 1101 (C-O), 912 (C-H); ^{1}H NMR (500 MHz, $CDCl_3$) δ 8.48 (s, H^{CH}-min), 8.21 (brs, H^{8}), 7.85 (brs, H^{9}), 7.59 – 7.41 (brm, H^{10}), 6.64 – 6.51 (brm, H^{5}), 5.40 – 5.20 (brm, H$^{i/j/l/m}$), 4.68 – 4.56 (brm, H^{3}), 4.49 – 4.44 (m, H^{CH_2}-min/crosslinked), 4.13 (brs, H$^{3'}$), 4.11 (brs, H$^{3'}$), 3.78 – 3.66 (m, H^{2}), 3.66 – 3.53 (m, H^{1}), 2.79 – 2.69

(brm, H^{k}), 2.51 (brs, $H^{cross\text{-}linked}$), 2.43 (brs, $H^{5'}$), 2.40 (br, $H^{5'}$), 2.39 – 2.29 (m, H^{b}), 2.07 – 1.95 (brm, H^{hn}), 1.60 (brs, H^{c}), 1.27 (brs, $H^{d\text{-}g/o\text{-}q}$), 0.87 (brs, H^{r}); ^{13}C NMR (126 MHz, $CDCl_3$) δ 173.93 (C^{a}), 170.37 – 169.69 (C^{4}), 162.04 – 161.84 (C^{6}), 130 .33 (C^{m}), 130.20 (C^{i}), 129.84 – 129.74 (C^{10}), 129.71 (C^{7}), 128.44 (C^{9}), 128.09 (C^{j}), 128.02 (C^{l}), 125.32 – 125.18 (C^{8}), 101.33 (C^{5}), 85.47 ($C^{cross\text{-}linked}$), 79.73 ($C^{4'}$), 79.37 ($C^{4'}$), 74.99 ($C^{5'}$), 74.63 ($C^{5'}$), 70.04 – 69.78 (C^{2}), 69.73 – 69.49 (C^{2}), 68.90 ($C^{2'}$), 68.19 ($C^{2'}$), 64.35 – 64.10 (C^{3}), 64.02 – 63.80 (C^{3}), 58.60 ($C^{3'}$), 58.40 ($C^{3'}$), 49.15 – 48.82 ($C^{1/1'}$), 46.86 – 46.48 ($C^{1/1'}$), 33.37 – 33.09 (C^{b}), 31.61 (C^{p}), 29.88 – 29.18 ($C^{d\text{-}g/o}$), 27.35 – 27.27 ($C^{h/n}$), 25.73 (C^{k}), 25.38 (C^{c}), 22.68 (C^{q}), 14.19 (C^{r}).

$P^{t2}{}_{m}$DEAyLn (5.11Ln)

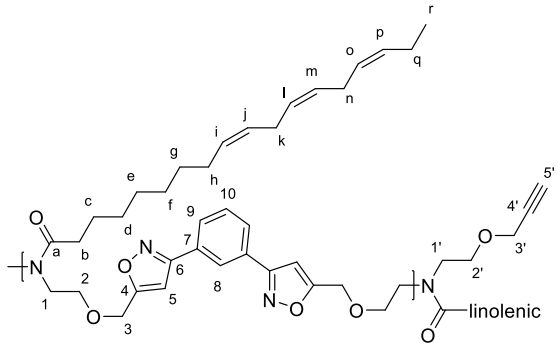

General procedure for polymerisation using vegetable oil derived monomers was followed with *meta*-OC **2.1** (500 mg, 2.15 mmol, 1 eq.) and DEAyLn **5.2Ln** (948 mg, 2.15 mmol, 1 eq.) to give a malleable brown solid. (71 %); ν_{max} / cm^{-1}: 3269 (C≡C), 3008 (=C-H), 2925 (C-H), 2854 (C-H), 1635 (C=O), 1461 (C-H), 1438 (C-N), 1159 (C-O), 1101 (C-O), 912 (C-H); ^{1}H NMR (500 MHz, $CDCl_3$) δ 8.48 (s, H^{CH}-min), 8.21 (brs, H^{8}), 7.85 (brs, H^{9}), 7.58 – 7.42 (brm, H^{10}), 6.67 – 6.53 (brm, H^{5}), 5.43 – 5.23 (brm, $H^{i/j/l/m/o/p}$), 4.73 – 4.50 (brm, H^{3}), 4.50 – 4.45 (m, H^{CH_2}-min/cross-linked), 4.13 (brs, $H^{3'}$), 4.11 (brs, $H^{3'}$), 3.72 (brs, H^{2}), 3.68 – 3.52 (brm, H^{1}), 2.78 (brs, H^{kn}), 2.57 (brs, $H^{cross\text{-}linked}$), 2.43 (brs, $H^{5'}$), 2.40 (br, $H^{5'}$), 2.39 – 2.25 (m, H^{b}), 2.08 – 1.95 (brm, H^{hq}), 1.60 (brs, H^{c}), 1.37 – 1.16 (brm, $H^{d\text{-}g}$), 0.96 (brs, H^{r}), 0.87 ($H^{linoleic}$); ^{13}C NMR (126 MHz, $CDCl_3$) δ 173.95 (C^{a}), 170.27 – 169.70 (C^{4}), 162.09 – 161.76 (C^{6}), 132.09 ($C^{i/j/l/m/o/p}$), 130.44 ($C^{i/j/l/m/o/p}$), 130.35 ($C^{linoleic\text{-}m}$), 130.22 ($C^{linoleic\text{-}i}$), 129.85 – 129.75 (C^{10}), 128.55 – 128.43 (C^{9}), 128.41 ($C^{i/j/l/m/o/p}$), 128.39 ($C^{i/j/l/m/o/p}$), 128.11 ($C^{linoleic\text{-}j}$), 128.04 ($C^{linoleic\text{-}l}$), 127.83 – 127.75 ($C^{i/j/l/m/o/p}$), 127.24 ($C^{i/j/l/m/o/p}$), 125.33 – 125.17 (C^{8}), 101.34 (C^{5}), 85.39 ($C^{cross\text{-}linked}$), 79.74 ($C^{4'}$), 79.39 ($C^{4'}$), 75.04 ($C^{5'}$), 74.66 ($C^{5'}$), 70.04 – 69.79 (C^{2}), 69.66 – 69.47 (C^{2}), 68.91 ($C^{2'}$), 68.21 ($C^{2'}$), 64.34 – 64.13 (C^{3}), 64.02 – 63.80 (C^{3}), 58.62 ($C^{3'}$), 58.42 ($C^{3'}$), 49.18 – 48.83 ($C^{1/1'}$), 46.90 – 46.54 ($C^{1/1'}$), 33.38 – 33.17 (C^{b}),

31.64 ($C^{linoleic}$), 29.87 – 29.20 (C^{d-g}), 27.35 (C^{h}), 25.74 (C^{k}), 25.65 (C^{n}), 25.40 (C^{c}), 22.70 ($C^{linoleic}$), 20.68 (C^{q}), 14.42 (C^{r}), 14.22 ($C^{linoleic}$).

P^{t2}_{m}DEAeS (5.13S)

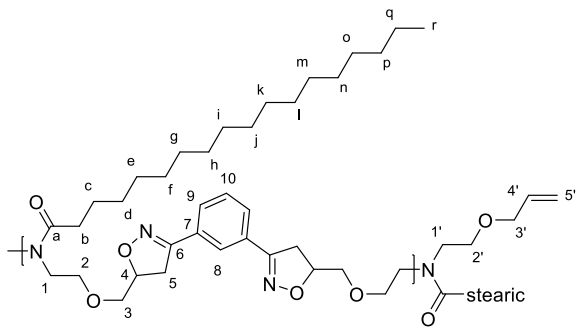

General procedure for polymerisation using vegetable oil derived monomers was followed with *meta*-OC **2.1** (500 mg, 2.15 mmol, 1 eq.) and DEAeS **5.4S** (969 mg, 2.15 mmol, 1 eq.) to give a malleable brown solid. (87 %); 3069 (=CH_2), 2921 (C-H), 2851 (C-H), 1639 (C=O), 1465 (C-H), 1440 (C-N), 1173 (C-O), 1123 (C-O), 912 (C-H); ^{1}H NMR (500 MHz, $CDCl_3$) δ 8.53 – 7.99 (brm, H^{Ar}-min), 7.90 (brs, H^{8}), 7.68 (brs, H^{9}), 7.41 (brs, H^{10}), 5.89 – 5.77 (brm, $H^{4'}$), 5.19 (brd, *J* = 18.0 Hz, $H^{5'}$), 5.18 – 5.10 (brm, $H^{5'}$), 4.86 (brs, H^{4}), 4.52 – 4.40 (m, H^{CH/CH_2}-min), 4.29 – 4.19 (m, H^{CH/CH_2}-min), 3.92 (brs, $H^{3'}$), 3.72 – 3.42 (brm, $H^{1/2/3}$), 3.36 (brs, H^{5}), 3.19 (brs, H^{5}), 2.27 (brs, H^{b}), 1.53 (brs, H^{c}), 1.24 (brs, H^{d-q}), 0.87 (brt, *J* = 6.5 Hz, H_r). ^{13}C NMR (126 MHz, $CDCl_3$) δ 173.83 (C^{a}), 155.97 (C^{6}), 134.79 ($C^{4'}$), 134.49 ($C^{4'}$), 130.29 (C^{7}), 130.18 (C^{7}), 129.28 (C^{10}), 128.21 (C^{9}), 124.86 (C^{8}), 117.13 ($C^{5'}$), 116.91 ($C^{5'}$), 80.26 (C^{4}), 72.66 – 71.94 ($C^{2/3'}$), 70.54 – 69.93 (C^{3}), 68.92 ($C^{2'}$), 68.37 ($C^{2'}$), 48.87 ($C^{1/1'}$), 46.34 ($C^{1/1'}$), 36.94 (C^{5}), 33.40 – 33.17 (C^{b}), 32.04 (C^{p}), 29.99 – 29.10 (C^{d-o}), 25.44 (C^{c}), 22.81 (C^{q}), 14.25 (C^{r}).

P^{t2}_{m}DEAeO (5.13O)

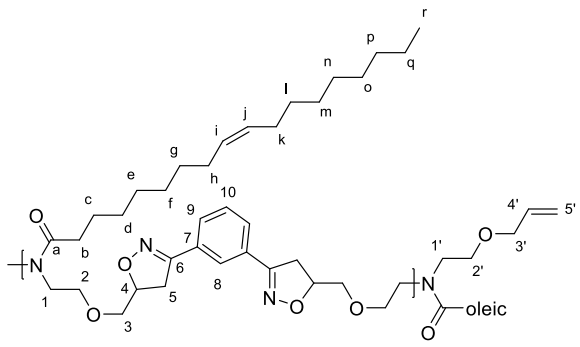

General procedure for polymerisation using vegetable oil derived monomers was followed with *meta*-OC **2.1** (500 mg, 2.15 mmol, 1 eq.) and DEAeO **5.4O** (965 mg, 2.15 mmol, 1 eq.) to give a malleable brown solid. (83 %); 3079 (=CH_2), 3002 (=C-H), 2923 (C-H), 2853 (C-H), 1646 (C=O), 1464 (C-H), 1104 (C-O), 921 (C-H); ^{1}H NMR (500 MHz, $CDCl_3$) δ 8.44 – 8.04 (brm, H^{Ar}-min), 7.89 (brs, H^{8}), 7.67 (brs, H^{9}), 7.41 (brs, H^{10}), 5.92 – 5.76 (brm, $H^{4'}$), 5.32 (brs, H^{ij}), 5.21 (brd, *J* = 17.5 Hz, $H^{5'}$), 5.17 – 5.08 (brm, $H^{5'}$), 4.86 (brs, H^{4}), 4.53 – 4.39 (m, H^{CH/CH_2}-min/cross-linked), 4.32 – 4.16 (m,

H^{CH/CH_2}-min/cross-linked), 3.92 (brs, $H^{3'}$), 3.71 – 3.43 (brm, $H^{1/2/3}$), 3.35 (brs, H^5), 3.20 (brs, H^5), 2.75 (brs, $H^{linoleic}$), 2.41 – 2.16 (brs, H^b), 1.98 (brs, $H^{h/k}$), 1.54 (brs, H^c), 1.25 (brs, $H^{d\text{-}g/l\text{-}q}$), 0.86 (brt, J = 6.5 Hz, H_r). ^{13}C NMR (126 MHz, $CDCl_3$) δ 174.22 – 173.59 (C^a), 155.95 (C^6), 134.77 ($C^{4'}$), 134.47 ($C^{4'}$), 130.27 (C^7), 130.16 (C^7), 130.06 (C^j), 130.06 (C^i), 129.26 (C^{10}), 128.99 (C^{10}), 128.34 – 128.08 (C^9), 124.86 (C^8), 117.13 ($C^{5'}$), 116.91 ($C^{5'}$), 85.78 ($C^{cross\text{-}linked}$), 80.24 (C^4), 72.74 – 71.87 ($C^{2/3'}$), 70.74 – 69.68 (C^3), 68.90 ($C^{2'}$), 68.32 ($C^{2'}$), 49.29 – 48.32 ($C^{1/1'}$), 46.77 – 45.78 ($C^{1/1'}$), 37.11 – 36.58 (C^5), 33.45 – 33.10 (C^b), 32.00 (C^p), 30.13 – 28.90 ($C^{d\text{-}g/l\text{-}o}$), 27.33 ($C^{h/k}$), 25.40 ($C^c$), 22.79 ($C^q$), 14.24 ($C^r$).

$P^{t2}{}_m$DAeS – 0.8 (5.14S)

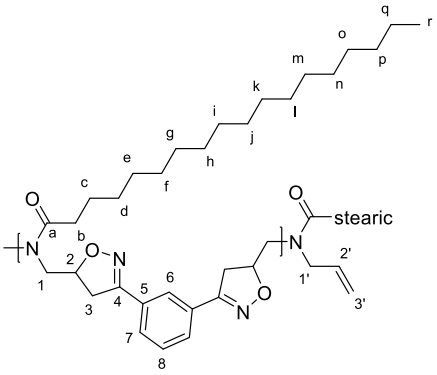

General procedure for polymerisation using vegetable oil derived monomers was followed with *meta*-OC **2.1** (600 mg, 2.57 mmol, 1 eq.) and DAeS **5.3S** (780 mg, 2.15 mmol, 0.8 eq.) to give a brittle yellow solid. (88 %); 2920 (C-H), 2851 (C-H), 1642 (C=O), 1463 (C-H), 1436 (C-N), 1166 (C-O), 909 (C-H); ^{1}H NMR (500 MHz, $CDCl_3$) δ 8.51 – 8.02 (brm, H^{Ar}-min), 7.89 (brs, H^6), 7.69 (brs, H^7), 7.43 (brs, H^8), 5.84 – 5.71 (brm, $H^{2'}$), 5.19 (brd, J = 10.0 Hz, $H^{3'}$), 5.16 – 4.82 (brm, $H^{2/3'}$), 4.53 – 4.32 (brm, H H^{CH/CH_2}-min), 4.25 – 4.12 (brm, $H^{1'}$), 4.11 – 3.91 (brm, $H^{1/1'}$), 3.90 – 3.72 (brm, $H^{1/3}$), 3.65 (brs, $H^{1/3}$), 3.57 – 3.26 (brm, $H^{1/3}$), 3.2 – 2.82 (brm, $H^{1/3}$), 2.44 (brs, H^b), 2.38 – 2.21 (brm, H^b), 2.18 (brs, H^b-min), 1.61 (brs, H^c), 1.23 (brs, $H^{d\text{-}q}$), 0.86 (brt, J = 6.5, H^r); ^{13}C NMR (126 MHz, $CDCl_3$) δ 174.76 – 174.32 (C^a), 156.94 – 156.45 (C^4), 156.33 – 156.12 (C^4), 133.02 ($C^{2'}$), 130.29 – 129.71 (C^5), 129.59 – 129.19 (C^8), 128.69 – 128.45 (C^7), 128.45 – 128.16 (C^7), 124.91 (C^6), 116.59 – 116.43 ($C^{3'}$), 81.10 – 80.76 (C^2), 80.40 – 80.09 (C^2), 79.33 – 79.10 (C^2), 53.36 – 52.89 (C^1), 52.71 – 52.32 (C^1), 51.79 (C^1), 51.16 – 50.64 (C^1-min), 50.06 – 49.80 (C^1), 49.40 – 49.12 (C^1), 38.58 – 37.74 (C^3), 33.50 – 33.23 (C^b), 33.07 (C^b), 32.01 (C^p), 3.00 – 29.13 ($C^{d\text{-}o}$), 25.54 – 25.19 (C^c), 22.78 (C^q) 14.23 (C^r).

P^{t2}_{m}DAeO – 0.8 (5.14O)

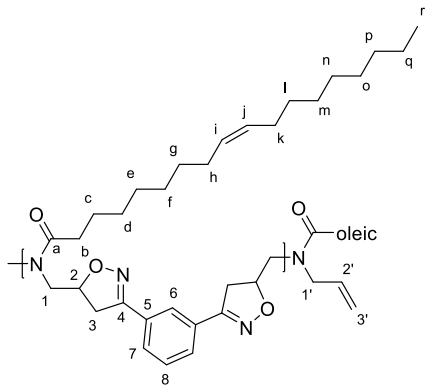

General procedure for polymerisation using vegetable oil derived monomers was followed with *meta*-OC **2.1** (600 mg, 2.57 mmol, 1 eq.) and DAeO **5.3O** (776 mg, 2.15 mmol, 0.8 eq.) to give a brittle yellow solid. (68 %); 3003 (=C-H), 2922 (C-H), 2851 (C-H), 1641 (C=O), 1462 (C-H), 1435 (C-N), 1166 (C-O), 906 (C-H); ν_{max} / cm^{-1}: 3002 (=C-H), 2922 (C-H), 2852 (C-H), 1643 (C=O), 1459 (C-H), 1436 (C-N), 1166 (C-O), 907 (C-H); ^{1}H NMR (500 MHz, $CDCl_3$) δ 8.48 – 8.01 (brm, H^{Ar}-min), 7.88 (brs, H^{6}), 7.68 (brs, H^{7}), 7.42 (brs, H^{8}), 5.82 – 5.73 (brm, $H^{2'}$), 5.31 (brs, $H^{i/j}$), 5.19 (brd, *J* = 10.0 Hz, $H^{3'}$), 5.14 – 5.88 (brm, $H^{2/3'}$), 4.53 – 4.32 (brm, H^{CH/CH_2}-min/cross-linked), 4.21 – 4.13 (brm, $H^{1'}$), 4.10 – 3.94 (brm, $H^{1/1'}$), 3.88 – 3.72 (brm, $H^{1/3}$), 3.64 (brs, $H^{1/3}$), 3.58 – 3.23 (brm, $H^{1/3}$), 3.20 – 2.97 (brm, $H^{1/3}$), 2.75 (brs, $H^{linoleic}$) 2.45 (brs, H^{b}), 2.33 (brs, H^{b}), 2.18 (brs, H^{b}-min), 1.98 (brs, H^{hk}), 1.61 (brs, H^{c}), 1.25 (brs, H^{d-q}), 0.86 (brs, H^{r}); ^{13}C NMR (126 MHz, $CDCl_3$) δ 174.86 – 174.32 (C^{a}), 157.12 – 156.57 (C^{4}), 156.57 – 155.94 (C^{4}), 133.03 ($C^{2'}$), 130.34 ($C^{linoleic}$) 130.08 (C^{j}), 129.88 (C^{i}), 129.57 – 129.27 (C^{8}), 128.73 – 128.23 (C^{7}), 128.01 ($C^{linoleic}$), 124.93 (C^{6}), 116.54 ($C^{3'}$), 85.78 ($C^{cross-linked}$), 81.21 – 80.70 (C^{2}), 80.46 – 80.05 (C^{2}), 79.48 – 79.00 (C^{2}), 53.29 – 53.03 (C^{1}), 52.66 – 52.32 (C^{1}), 50.05 – 49.83 (C^{1}), 38.67 – 37.85 (C^{3}), 33.57 – 33.19 (C^{b}), 32.01 (C^{p}), 30.11 – 28.88 ($C^{d-g/l-o}$), 27.33 ($C^{h/k}$), 25.53 – 25.19 (C^{c}), 22.79 (C^{q}) 14.24 (C^{r}).

P^{t2}_{m}DEAeS – 0.8 (5.15S)

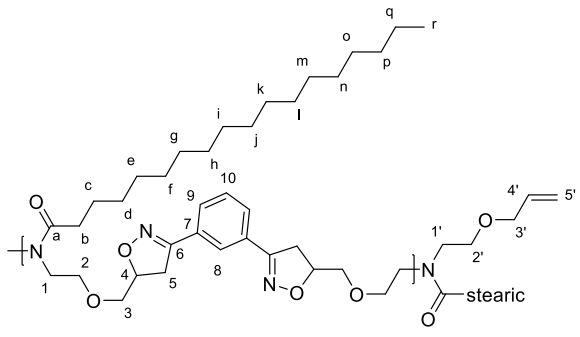

General procedure for polymerisation using vegetable oil derived monomers was followed with *meta*-OC **2.1** (600 mg, 2.57 mmol, 1 eq.) and DEAeS **5.4S** (969 mg, 2.15 mmol, 0.8 eq.) to give a malleable brown solid. (83 %); ν_{max} / cm^{-1}: 2921 (C-H), 2851 (C-H), 1638 (C=O), 1465 (C-H), 1439 (C-N), 1174 (C-O), 1124 (C-O), 911 (C-H); ^{1}H NMR (500 MHz, $CDCl_3$) δ 8.48 – 8.03 (brm, H^{Ar}-min), 7.93 – 7.78 (brm, H^{8}), 7.78 (brs, H^{9}), 7.40 (brs, H^{10}), 5.89 – 5.77 (brm, $H^{4'}$), 5.22 (brd, *J* = 18.0 Hz, $H^{5'}$), 5.17 – 5.11 (brm, $H^{5'}$), 4.85 (brs, H^{4}), 4.54 – 4.40 (m, H^{CH/CH_2}-min),

4.31 – 4.20 (m, H^{CH/CH_2}-min), 3.92 (brs, $H^{3'}$), 3.72 – 3.43 (brm, $H^{1/2/3}$), 3.34 (brs, H^5), 3.19 (brs, H^5), 2.28 (brs, H^b), 1.54 (brs, H^c), 1.25 (brs, H^{d-q}), 0.87 (brt, J = 6.5 Hz, H_r). ^{13}C NMR (126 MHz, $CDCl_3$) δ 174.68 – 173.71(C^a), 156.00(C^6), 134.74 ($C^{4'}$), 134.49 ($C^{4'}$), 130.28 (C^7), 130.17 (C^7), 129.30 (C^{10}), 129.03 (C^{10}) 128.40 – 127.90 (C^9), 125.27 – 125.05 (C^8), 124.98 – 124.72 (C^8), 117.16 ($C^{5'}$), 116.96 ($C^{5'}$), 80.25 – 80.12 (C^4), 72.56 – 71.98 ($C^{2/3'}$), 70.51 – 69.89 (C^3), 49.24 – 48.67 ($C^{1/1'}$), 46.91 – 46.21 ($C^{1/1'}$), 37.15 – 36.49 (C^5), 33.48 – 33.15 (C^b), 32.05 (C^p), 29.95 – 29.20 (C^{d-o}), 25.48 (C^c), 22.82 (C^q), 14.26 (C^r).

$P^{t2}{}_m$DEAeO – 0.8 (5.15O)

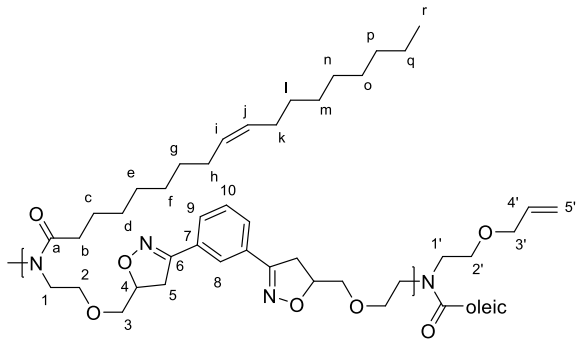

General procedure for polymerisation using vegetable oil derived monomers was followed with *meta*-OC **2.1** (600 mg, 2.57 mmol, 1 eq.) and DEAeO **5.4O** (965 mg, 2.15 mmol, 0.8 eq.) to give a malleable brown solid. (74 %); ν_{max} / cm^{-1}: 3004 (=C-H), 2922 (C-H), 2852 (C-H), 1639 (C=O), 1464 (C-H), 1439 (C-N), 1173 (C-O), 1123 (C-O), 912 (C-H); ^{1}H NMR (500 MHz, $CDCl_3$) δ 8.46 – 8.02 (brm, H^{Ar}-min), 7.90 (brs, H^8), 7.68 (brs, H^9), 7.41 (brs, H^{10}), 5.89 – 5.75 (brm, $H^{4'}$), 5.32 (brs, H^{ij}), 5.22 (brd, J = 17.5 Hz, $H^{5'}$), 5.17 – 5.11 (brm, $H^{5'}$), 4.86 (brs, H^4), 4.47 (brs, H^{CH/CH_2}-min/cross-linked), 4.29 – 4.19 (m, H^{CH/CH_2}-min/cross-linked), 3.92 (brs, $H^{3'}$), 3.71 – 3.42 (brm, $H^{1/2/3}$), 3.36 (brs, H^5), 3.19 (brs, H^5), 2.75 (brs, $H^{linoleic}$), 2.38 – 2.19 (brm, H^b), 1.98 (brs, $H^{h/k}$), 1.54 (brs, H^c), 1.25 (brs, $H^{d-g/l-q}$), 0.87 (brt, J = 6.5 Hz, H_r). ^{13}C NMR (126 MHz, $CDCl_3$) δ 174.28 – 173.0 (C^a), 155.99 (C^6), 134.78 ($C^{4'}$), 134.49 ($C^{4'}$), 130.30 (C^7), 130.19 (C^7), 130.10 (C^j), 129.92 (C^i), 129.39 – 129.22 (C^{10}), 129.13 – 129.00 (C^{10}), 128.37 – 128.10 (C^9), 124.99 – 124.79 (C^8), 117.15 ($C^{5'}$), 116.93 ($C^{5'}$), 80.27 (C^4), 72.59 – 71.91 ($C^{2/3'}$), 70.63 – 69.90 (C^3), 68.94 ($C^{2'}$), 68.36 ($C^{2'}$), 49.12 – 48.76 ($C^{1/1'}$), 46.89 – 46.18 ($C^{1/1'}$), 37.05 – 36.47 (C^5), 33.40 – 33.01 (C^b), 32.04 (C^p), 29.99 – 29.14 ($C^{d-g/l-o}$), 27.36 ($C^{h/k}$), 25.44 (C^c), 22.82 (C^q), 14.27 (C^r).

P$^{t2}_{m}$DEAyS – 0.8 (5.16S)

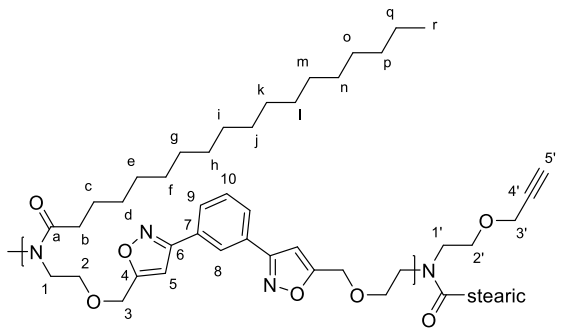

General procedure for polymerisation using vegetable oil derived monomers was followed with *meta*-OC **2.1** (600 mg, 2.57 mmol, 1 eq.) and DEAyS **5.4S** (961 mg, 2.15 mmol, 0.8 eq.) to give a malleable brown solid. (88 %); ν_{max} / cm^{-1}: 2921 (C-H), 2852 (C-H), 1638 (C=O), 1464 (C-H), 1438 (C-N), 1158 (C-O), 1103 (C-O), 912 (C-H); ^{1}H NMR (500 MHz, $CDCl_3$) δ 8.48 (s, H^{CH}-min), 8.21 (brs, H^{8}), 7.85 (brs, H^{9}), 7.57 – 7.43 (m, H^{10}), 6.68 – 6.50 (brm, H^{5}), 4.73 – 4.50 (brm, H^{3}), 4.49 – 4.44 (m, H^{CH_2}-min), 4.13 (brs, H$^{3'}$), 4.11 (brs, H$^{3'}$), 3.78 – 3.68 (m, H^{2}), 3.67 – 3.55 (m, H^{1}), 2.43 (brs, H$^{5'}$), 2.41 – 2.30 (brm, H$^{b/5'}$), 1.60 (brs, H^{c}), 1.33 – 1.14 (brm, H^{d-q}), 0.86 (brt, *J* = 6.5 Hz, H^{r}); ^{13}C NMR (126 MHz, $CDCl_3$) δ 174.03 (C^{a}), 169.93 (C^{4}), 169.81 (C^{4}), 161.93 (C^{6}), 161.87 (C^{6}), 129.82 (C^{7}), 129.80 – 129.76 (C^{10}), 129.71 (C^{7}), 128.44 (C^{9}), 125.40 – 125.19 (C^{8}), 101.40 – 101.19 (C^{5}), 75.00 (C$^{5'}$), 74.63 (C$^{5'}$), 70.09 – 69.83 (C^{2}), 69.73 – 69.51 (C^{2}), 68.92 (C$^{2'}$), 68.21 (C$^{2'}$), 64.35 – 64.10 (C^{3}), 64.03 – 63.79 (C^{3}), 58.62 (C$^{3'}$), 58.42 (C$^{3'}$), 49.34 – 48.88 (C$^{1/1'}$), 46.93 – 46.48 (C$^{1/1'}$), 33.49 – 33.19 (C^{b}), 32.04 (C^{p}), 29.92 – 29.36 (C^{d-o}), 25.43 (C^{c}), 22.81 (C^{q}), 14.25 (C^{r}).

P$^{t2}_{m}$DEAyO – 0.8 (5.16O)

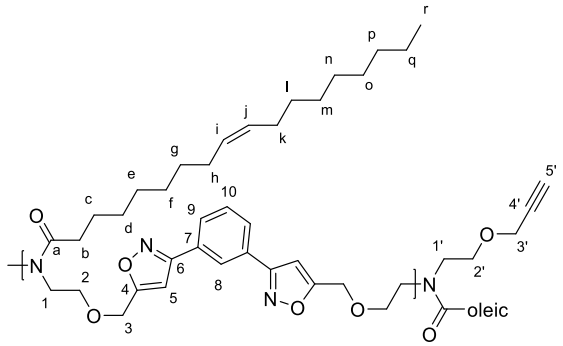

General procedure for polymerisation using vegetable oil derived monomers was followed with *meta*-OC **2.1** (600 mg, 2.57 mmol, 1 eq.) and DEAyO **5.2O** (956 mg, 2.15 mmol, 0.8 eq.) to give a malleable brown solid. (70 %); ν_{max} / cm^{-1}: 3003 (=C-H), 2923 (C-H), 2853 (C-H), 1638 (C=O), 1462 (C-H), 1439 (C-N), 1159 (C-O), 1103 (C-O), 912 (C-H); ^{1}H NMR (500 MHz, $CDCl_3$) δ 8.48 (s, H^{CH}-min), 8.21 (brs, H^{8}), 7.85 (brs, H^{9}), 7.51 (brs, H^{10}), 6.73 – 6.50 (brm, H^{5}), 5.30 (brs, H$^{i/j}$), 4.71 – 4.53 (brm, H^{3}), 4.50 – 4.44 (m, H^{CH_2}-min), 4.13 (brs, H$^{3'}$), 4.10 (brs, H$^{3'}$), 3.72 (brs, H^{2}), 3.62 (brs, H^{1}), 2.75 (H^{linoleic}), 2.43 (brs, H$^{5'}$), 2.37 (brs, H$^{b/5'}$), 1.96 (brs, H^{hk}), 1.60 (brs, H^{c}), 1.24 (brs, H$^{d-g/l-q}$), 0.86 (brs, H^{r}); ^{13}C NMR (126 MHz, $CDCl_3$) δ 173.99 (C^{a}), 169.91 (C^{4}), 169.79 (C^{4}), 161.91

(C^{6}), 161.85 (C^{6}), 130.05 (C^{j}), 129.88 (C^{i}), 129.84 – 129.74 (C^{10}), 129.69 (C^{7}), 128.42 (C^{9}), 125.38 – 125.15 (C^{8}), 101.35 (C^{5}), 85.74 ($C^{\text{cross-linked}}$), 74.99 ($C^{5'}$), 74.64 ($C^{5'}$), 70.01 – 69.80 (C^{2}), 69.67 – 69.52 (C^{2}), 68.88 ($C^{2'}$), 68.18 ($C^{2'}$), 64.30 – 64.09 (C^{3}), 64.02 – 63.80 (C^{3}), 58.60 ($C^{3'}$), 58.40 ($C^{3'}$), 49.26 – 48.89 ($C^{1/1'}$), 48.17 ($C^{\text{cross-linked}}$), 46.93 – 46.52 ($C^{1/1'}$), 33.28 (C^{b}), 32.00 (C^{p}), 29.95 – 29.16 ($C^{\text{d-g/l-o}}$), 27.33 – 27.26 (C^{k}), 25.40 (C^{c}), 22.78 (C^{q}), 14.23 (C^{r}).

8.5.7 Reductive cleavage ring opening studies

Attmepted reductive cleavage of DIAc 4.7 with $LiAlH_4$ resulting in a mixture of N-ethyl-2-(2-(3-phenylaziridin-2-yl)ethoxy)-N-(2-(2-(3-phenylaziridin-2-yl)ethoxy)ethyl)ethan-1-amine (5.17) and 2-(2-(ethyl(2-(2-(3-phenylaziridin-2-yl)ethoxy)ethyl)amino)ethoxy)-1-(3-phenylaziridin-2-yl)ethan-1-ol (5.18)

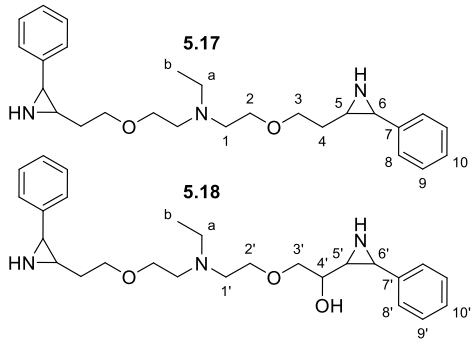

DIAc **4.7** (50 mg, 0.11 mmol, 1 eq.) was weighed into a 2-neck RBF and flushed with N_2. Dry THF (1 ml) was added and the solution was cooled in an ice bath. 4 M $LiAlH_4$ solution (0.4 ml, 62 mg, 1.63 mmol, 15 eq.) was slowly introduced, the temperature was then increased to 75 °C and left to reflux. After 24 hours the solution was cooled in an ice bath and quenched with sat. $NaSO_4$ solution (5 ml). The aqueous layer was extracted with DCM (4 × 10 ml), the organic layers were combined, dried with $MgSO_4$ and reduced *in vacuo* to leave a crude red oil, (13.8 mg). ^{1}H NMR (500 MHz, $CDCl_3$) δ 7.51 – 7.09 (m, H^{Ar}), 3.74 – 3.21 (m, $H^{2/2'/3/3'/4'}$), 2.79 – 2.34 (m, $H^{a/1/1}$), 1.48 – 1.19 (m, $H^{4/5/5'/6/6'}$), 1.07 – 0.98 (m, H_b); ^{13}C NMR (126 MHz, $CDCl_3$) δ 140.48 ($C^{7/7'}$), 137.71 ($C^{7/7'}$), 137.11 ($C^{7/7'}$), 128.99 – 127.71 ($C^{\text{Ar-H}}$), 127.59 – 126.41 ($C^{\text{Ar-H}}$), 126.06 – 123.43 ($C^{\text{Ar-H}}$), 74.56 ($C^{3'}$), 69.88 – 68.92 ($C^{2/2'/3}$), 68.65 ($C^{4'}$), 54.30 – 54.07 ($C^{1/1'}$), 53.66 – 53.38 ($C^{1/1'}$), 53.04 ($C^{1/1'}$), 52.80 ($C^{1/1'}$), 49.14 (C^{a}), 48.89 (C^{a}), 48.74 (C^{a}), 38.42 – 38.14 ($C^{5/5'/6/6'}$), 36.93 – 36.81 ($C^{5/5'/6/6'}$), 36.43 – 36.33 ($C^{5/5'/6/6'}$), 34.79 ($C^{5/5'/6/6'}$), 30.46 ($C^{5/5'/6/6'}$), 29.88 – 29.67 (C^{4}), 28.85 – 28.59 (C^{4}), 11.92 (C^{b}), 11.41 (C^{b}); MS (ESI) m/z calcd. ($C_{26}H_{37}N_3O_2 + H^+$): 424.3, found: 424.4 ($M_a + H^+$); MS (ESI) m/z calcd. ($C_{26}H_{37}N_3O_3 + H^+$): 440.3, found: 440.4 ($M_b + H^+$).

Attmepted reductive cleavage of O_mDEAyS–ABA 5.10 with iron – (Aerobic)

O_mDEAyS–ABA **5.10** (100 mg, 0.09 mmol, 1 eq.) and NH_4Cl (52 mg, 0.9 mmol, 10 eq.) were stirred in MeOH (3 ml) and DMF (3 ml) at 80 °C. The mixture was initially colourless and opaque, after 1 hour it had acquired an orange tint after 2 hours it was opaque with a deep orange colour. Monitoring by TLC and NMR showed no change after 24, 48, and 72 hrs. After 72 hours the reaction was allowed to cool to RT then diluted with DCM (20 ml) and filtered through a celite pad topped with silica. The organic filtrate was washed with 1M $HCl_{(aq)}$ (20 ml) followed by water (3 × 50 ml) and brine (50 ml). The organic layer was dried with $MgSO_4$ and reduced *in vacuo* to give the starting material. MS and NMR analysis showed no evidence of ring opening.

Attmepted reductive cleavage of O_mDEAyS–ABA 5.10 with iron – (Anaerobic)

O_mDEAyS–ABA **5.10** (100 mg, 0.09 mmol, 1 eq.) and NH_4Cl (52 mg, 0.9 mmol, 10 eq.) were placed in a 2 neck RBF and flushed with N_2. Dry MeOH (3 ml) and dry DMF (3 ml) were introduced and the solution was stirred at 80 °C. After 24 hrs the solution was opaque with a slight orange tint, TLC monitoring appeared to show consumption of the starting material. Water (0.5 ml) was added causing the reaction to gradually become green. After 4 hours the reaction was allowed to cool to RT then diluted with DCM (20 ml) and filtered through a celite pad topped with silica. The organic filtrate was washed with 1M $HCl_{(aq)}$ (20 ml) followed by water (3 × 50 ml) and brine (50 ml). The organic layer was dried with $MgSO_4$ and reduced *in vacuo* to give the starting material which now reappeared when analysed by TLC. MS and NMR analysis showed no evidence of ring opening.

8.6 General procedures Chapter 6

8.6.1 Aromatic oximoyl chloride Alternative

7.6.1.1 General procedure – Oxime synthesis

The aromatic aldehydes (1 eq.) were dissolved/suspended in ethanol (1.5 M) at room temperature. Sodium acetate and hydroxylamine hydrochloride were dissolved in water (1.5 M) and introduced to the ethanol solution. The reactions were all complete within 2 hours. Once complete the reaction mixture was poured into cold water to

encourage ppt to form, which could be collected by Büchner filtration. Most compounds did not form a ppt or the ppt passed through the filter paper and so were extracted from water using EtOAc (3 × 50 ml), organic layers were combined and washed with water (50 ml) and brine (50 ml), then dried with $MgSO_4$ and reduced *in vacuo* to leave a crude product, these were purified by recrystallisation or column chromatography.

(E)-2-methoxybenzaldehyde oxime 6.2a[272]

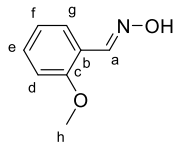

General synthesis procedure for the synthesis of oximes was followed using *o*-anisaldehyde (5.00 g, 36.7 mmol), sodium acetate (3.61 g, 44.1 mmol, 1.2 eq.), and hydroxylamine hydrochloride (3.06 g, 44.1 mmol, 1.2 eq.). A white ppt formed during the reaction which was collected by Büchner filtration, the ppt was washed with water and cold ethanol then dried in a desiccator to give a pure white solid. (92 %); m.p. 93 – 95 °C; ν_{max} / cm^{-1}: 3150 (O-H), 3059 (C-H), 3001 (C-H), 2840 (C-H), 2741 (CHN), 1598 (C=N), 1157 (C-O), 745 (C-H); ^{1}H NMR (400 MHz, $CDCl_3$) δ 8.63 (s, 1H, H_{OH}), 8.48 (s, 1H, H_a), 7.67 (d, *J* = 7.5 Hz, 1H, H_e), 7.36 (t, *J* = 7.5 Hz, 1H, H_d), 6.97 (t, *J* = 7.5 Hz, 1H, H_f), 6.92 (d, *J* = 8.5 Hz, 1H, H_g), 3.87 (s, 3H, H_h); ^{13}C NMR (101 MHz, $CDCl_3$) δ 157.77 (C_c), 146.91 (C_a), 131.31 (C_d), 127.42 (C_e), 120.92 (C_f), 120.75 (C_b), 111.29 (C_g), 55.69 (C_h); MS (ESI) m/z calcd. ($C_8H_9NO_2$ + Na^+): 174.0525, found: 174.0524 (M + Na^+).

(E)-3-methoxybenzaldehyde oxime 6.2b[369]

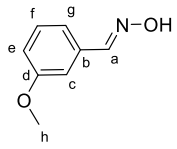

General synthesis procedure for the synthesis of oximes was followed using *m*-anisaldehyde (5.00 g, 36.7 mmol), sodium acetate (3.61 g, 44.1 mmol, 1.2 eq.), and hydroxylamine hydrochloride (3.06 g, 44.1 mmol, 1.2 eq.). A ppt did not form during the reaction, to encourage precipitation the reaction was poured into cold water, a ppt still did not form. Extraction and washing resulted in a crude oil. Purification through a silica plug (20 % EtOAc, R_f 0.24) gave a pure clear oil. (57 %); ν_{max} / cm^{-1}: 3284 (O-H), 2962 (C-H), 2836 (C-H), 1599 (C=N), 1156 (C-O), 765 (C-H); ^{1}H NMR (400 MHz, CDCl3) δ 9.13 (s, 1H, H_{OH}), 8.13 (s, 1H, H_a), 7.28 (t, J = 8.0 Hz, 1H, H_f), 7.16 (s, 1H, H_c), 7.12 (d, J = 7.5 Hz, 1H, H_g), 6.93 (d, J = 8.0 Hz, 1H, H_e), 3.81 (s, 3H, H_h); ^{13}C NMR (101 MHz, $CDCl_3$) δ 159.92 (C_d), 150.50 (C_a), 133.29 (C_b), 129.92 (C_f), 120.27 (C_g), 116.57 (C_e), 111.37 (C_c),

55.41 (C_h); MS (ESI) m/z calcd. ($C_8H_9NO_2$ + Na^+): 174.0525, found: 174.0525 (M + Na^+).

(E)-4-methoxybenzaldehyde oxime 6.2c[370]

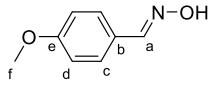

General synthesis procedure for the synthesis of oximes was followed using *p*-anisaldehyde (5.00 g, 36.7 mmol), sodium acetate (3.61 g, 44.1 mmol, 1.2 eq.), and hydroxylamine hydrochloride (3.06 g, 44.1 mmol, 1.2 eq.). A ppt formed when the reaction was poured into cold water. The ppt was collected by Büchner filtration and washed with water and cold ethanol to leave a crude brown solid. Recrystallisation from hexane resulted in a pure white solid. (57 %); m.p. 64 – 66 °C; ν_{max} / cm^{-1}: 3298 (O-H), 3006 (C-H), 2962 (C-H), 2836 (CHO), 1606 (C=N), 1167 (C-O), 822 (C-H); 1H NMR (400 MHz, CDCl3) δ 8.09 (s, 1H, H_a), 7.58 (br, 1H, H_{OH}), 7.52 (d, J = 8.0 Hz, 2H, H_c), 6.91 (d, J = 8.0 Hz, 2H, H_d), 3.84 (s, 3H, H_f); 13C NMR (101 MHz, CDCl3) δ 161.20 (C_e), 150.16 (C_a), 128.64 (C_c), 124.80 (C_b), 114.38 (C_d), 55.49 (C_f); MS (ESI) m/z calcd. ($C_8H_9NO_2$ + Na^+): 174.0525, found: 174.0525 (M + Na^+).

(E)-4-fluorobenzaldehyde oxime 6.2d[370]

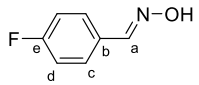

General synthesis procedure for the synthesis of oximes was followed using *m*-anisaldehyde (5.00 g, 40.3 mmol), sodium acetate (3.97 g, 48.3 mmol, 1.2 eq.), and hydroxylamine hydrochloride (3.34 g, 48.3 mol, 1.2 eq.). A ppt did not form during the reaction, to encourage precipitation the reaction was poured into cold water, a ppt still did not form. Extraction and washing resulted in a light brown solid. Recrystallisation from petrol resulted in a pure white solid. (89 %); m.p. 86 – 88 °C; ν_{max} / cm^{-1}: 3204 (O-H), 3008 (C-H), 2968 (C-H), 1604 (C=N), 824 (C-H); ^{1}H NMR (400 MHz, $CDCl_3$) δ 8.12 (s, Ha), 7.70 (s, H_{OH}), 7.62 – 7.51 (m, 2H, H_c), 7.08 (t, *J* = 8.2 Hz, 2H, H_d); ^{13}C NMR (101 MHz, $CDCl_3$) δ 163.92 (d, *J* = 250.5 Hz, C_e), 149.42 (C_a), 129.00 (d, *J* = 8.5 Hz, C_c), 128.39 (C_b), 116.08 (d, *J* = 22.0 Hz, C_d); MS (ESI) m/z calcd. (C_7H_6FNO + Na^+): 162.0326, found: 162.0324 (M + Na^+).

(E)-4-(trifluoromethyl)benzaldehyde oxime 6.2e[370]

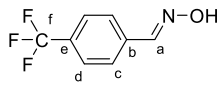

General synthesis procedure for the synthesis of oximes was followed using 4-(trifluormethyl) benzaldehyde (1.00 g, 5.74

mmol, 1eq.), sodium acetate (0.52 g, 6.32 mmol, 1.1 eq.), and hydroxylamine hydrochloride (0.44 g, 6.32 mmol, 1.1 eq). A ppt did not form during the reaction, to encourage precipitation the reaction was poured into cold water, a ppt still did not form. Extraction and washing resulted in a pure white solid. (91 %), m.p. 101 – 103 °C; ν_{max} / cm^{-1}: 3266 (O-H), 3008 (C-H), 2924 (C-H), 2854 (CHO), 1581 (C=N), 1320 (C-F), 833 (C-H); ^{1}H NMR (500 MHz, $CDCl_3$) δ 10.11 (s, H_{OH}), 8.17 (s, H_a), 7.70 (d, *J* = 8.0 Hz, H_c), 7.64 (d, *J* = 8.0 Hz, H_d); ^{13}C NMR (126 MHz, $CDCl_3$) δ 149.26 (C_a), 135.63 (C_b), 131.93 (C_f), 131.67 (C_f), 131.22 (C_f), 130.09 (C_f), 127.37 (C_c), 125.87 (q, *J* = 3.8 Hz, C_d), 125.10 (C_e), 122.93 (C_e); ^{19}F NMR (376 MHz, $CDCl_3$) δ -62.87 (s); MS (ESI) m/z calcd. ($C_8H_6F_3NO + H^+$): 190.0474, found: 190.0472 ($M + H^+$).

(E)-3,4-dimethoxybenzaldehyde oxime 6.2f[371]

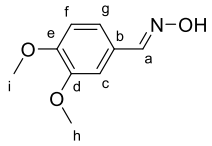

General synthesis procedure for the synthesis of oximes was followed using 3,4-dimethoxy benzaldehyde (5.00 g, 30.0 mol), sodium acetate (2.71 g, 33.1 mmol, 1.1 eq.), and hydroxylamine hydrochloride (2.30 g, 33.1 mmol). A ppt did not form during the reaction, to encourage precipitation the reaction was poured into cold water, a ppt still did not form. Extraction and washing resulted in a pure white solid. (96 %); m.p. 89 – 92 °C; ν_{max} / cm^{-1}: 3445 (O-H), 3013 (C-H), 2973 (C-H), 2839 (CHO), 1602 (C=N), 1154 (C-O), 1135 (C-O); ^{1}H NMR (400 MHz, $CDCl_3$) δ 8.08 (s, 1H), 7.56 (s, 1H, H_{OH}), 7.22 (d, *J* = 2.0 Hz, 1H, H_c), 7.03 (dd, *J* = 8.0, 2.0 Hz, 1H, H_g), 6.86 (d, *J* = 8.0 Hz, 1H, H_f), 3.91 (d, *J* = 1.5 Hz, 6H, $H_{h/h'}$); ^{13}C NMR (101 MHz, $CDCl_3$) δ 150.96 (C_d), 150.39 (C_a), 149.47 (C_e), 125.05 (C_b), 121.81 (C_g), 110.91 (C_f), 108.11 (C_c), 56.07 (C_h), 56.03 (C_h); MS (ESI) m/z calcd. ($C_9H_{11}NO_3 + Na^+$): 204.0631, found: 204.0631 ($M + Na^+$).

(**E)-3,4,5-trimethoxybenzaldehyde oxime 6.2g**

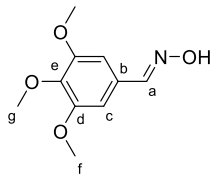

General synthesis procedure for the synthesis of oximes was followed using 3,4,5- trimethoxy benzaldehyde (5.00 g, 25.5 mmol, 1 eq.), sodium acetate (3.13 g, 38.2 mmol, 1.5 eq.), and hydroxylamine hydrochloride (2.66 g, 39.0 mol). The aldehyde did not dissolve in the solvent mixture and so the reaction was heated to reflux. A white ppt formed during the reaction which was collected by Büchner filtration, the ppt was washed with water and cold ethanol then dried in a desiccator to give a pure white

solid. (93 %); m.p. 88 – 90 °C; ν_{max} / cm^{-1}: 3464 (O-H), 3063 (C-H), 2985 (C-H), 2839 (CHO), 2768 (CHO), 1628 (C=N), 1154 (C-O), 1122 (C-O); ^{1}H NMR (400 MHz, Acetone) δ 10.21 (s, 1H, H_{OH}), 8.06 (s, 1H, H_a), 6.93 (s, 2H, H_c), 3.84 (s, 6H, H_f), 3.74 (s, 3H, H_g); ^{13}C NMR (101 MHz, Acetone) δ 154.58 (C_d), 149.30 (C_a), 140.40 (C_e), 129.64 (C_b), 104.90 (C_c), 60.58 (C_g), 56.39 (C_f); MS (ESI) m/z calcd. ($C_{10}H_{13}NO_4$ + Na^+): 234.0737, found: 234.0738 (M + Na^+).

(E)-4-((hydroxyimino)methyl)-2-methoxyphenyl acetate 6.2h

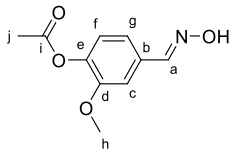

General synthesis procedure for the synthesis of oximes was followed using 4-acetoxy-3-methoxy benzaldehyde (5.00 g, 25.7 mmol, 1 eq.), sodium acetate (2.11 g, 25.7 mmol, 1 eq.), and hydroxylamine hydrochloride (1.79 g, 25.7 mmol, 1 eq.). The aldehyde did not dissolve in the solvent mixture but was not heated to protect the acetyl ester, the reaction was left overnight to allow for the poor solubility. The reaction was poured into cold water then extracted, washed, and reduced *in vacuo* to give a crude yellow solid. Purification by column chromatography afforded a white solid. (30 %, Rf = 0.3 in 33 % EtOAc), m.p. 79 – 82 °C; ν_{max} / cm^{-1}: 3222 (O-H), 3011 (C-H), 2966 (C-H), 2849 (CHO), 1644 (C=O), 1117 (C-O); ^{1}H NMR (500 MHz, $CDCl_3$) δ 8.10 (s, H_a), 7.28 (s, H_c), 7.10 – 7.04 (m, H_{fg}), 3.86 (s, H_h), 2.32 (s, H_j); ^{13}C NMR (126 MHz, $CDCl_3$) δ 168.99 (C_i), 151.58 (C_d), 149.86 (C_a), 141.42 (C_e), 130.99 (C_b), 123.22 (C_f), 120.90 (C_g), 109.66 (C_c), 56.08 (C_h), 20.80 (C_j); MS (ESI) m/z calcd. ($C_{10}H_{11}NO_4$ + Na^+): 232.0580, found: 232.0583 (M + Na^+).

(1E,4E)-terephthalaldehyde dioxime 6.2i[317]

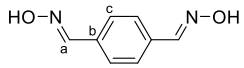

General synthesis procedure for the synthesis of oximes was followed using terephthaldehyde (10 g, 74.6 mmol, 1 eq.), sodium acetate (13.4 g, 164.1 mmol, 2.2 eq.), and hydroxylamine hydrochloride (11.4 g, 164.1 mmol, 2.2 eq.). A white ppt formed during the reaction which was collected by Büchner filtration, the ppt was washed with water and cold ethanol then recrystallised from EtOAc to give a pure white solid. (76 %), m.p. 176 -178 °C; ν_{max} / cm^{-1}: 3137 (O-H), 2983 (C-H), 1624 (C=N); ^{1}H NMR (400MHz, d-Acetone) δ 10.44 (s, 2H, H_{OH}), 8.15 (s, 2H, H_a), 7.65 (s, 4H, H_c); ^{13}C NMR (101 MHz, d-Acetone) 148.98 (C_a), 135.14 (C_b), 127.71 (C_c).

(E)-4-hydroxy-3-methoxybenzaldehyde oxime 6.2j

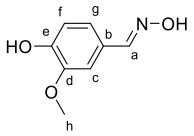

General synthesis procedure for the synthesis of oximes was followed using vanillin (5.0 g, 32.9 mmol, 1 eq.), sodium acetate (3.2 g, 39.4 mmol, 1.2 eq.), and hydroxylamine hydrochloride (2.7 g, 39.4 mmol, 1.2 eq.). After 1 hour the was complete but no ppt had formed, the reaction mixture poured into cold water (200 ml) and extracted with EtOAc (3 × 50 ml). The organic layers were combined, washed with brine (50 ml) then dried with $MgSO_4$. Reduction *in vacuo* left a white solid that need no further purification. (86 %, Rf = 0.6 in 66 % EtOAc), °C; ν_{max} / cm^{-1}: 3222 (O-H), 3011 (C-H), 2966 (C-H), 2849 (CHO), 1644 (C=O), 1117 (C-O); ^{1}H NMR (500 MHz, $CDCl_3$) δ 8.06 (s, 1H, H_a), 7.22 (d, *J* = 1.5 Hz, 1H, H_c), 7.00 (dd, *J* = 8.0, 1.5 Hz, 1H, H_g), 6.92 (d, *J* = 8.0 Hz, 1H, H_g), 3.93 (s, 3H H_h); ^{13}C NMR (126 MHz, $CDCl_3$) δ 150.55 (C_a), 147.82 (C_{Ar-O}), 147.04 (C_{Ar-O}), 124.44 (C_{Ar-C}), 122.58 (C_{Ar-H}), 114.53 (C_{Ar-H}), 107.71 (C_{Ar-H}), 56.13 (C_h).

7.6.1.2 General procedure – Oximoyl chloride synthesis

The oximes (1eq.) were dissolved in DMF (3.0 M) and cooled using an ice bath. *N*-Chlorosuccinimide (1.2 eq) was introduced in 5 parts over the course of an hour. 2 hours after the last addition of NCS the reaction mixture was poured into cold water (150 ml) and extracted with ethyl acetate (150 ml). The organic layer was washed with water (5 × 50 ml) and saturated sodium thiosulfate solution (1 × 50 ml), then dried over magnesium sulphate and solvent removed *in vacuo* to leave a crude solid. Some compounds could be purified others degraded during purification and so were examined by thermal analysis without further purification.

(Z)-N-hydroxy-2-methoxybenzimidoyl chloride (6.3a)[272]

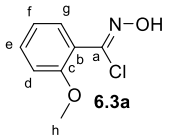

6.3a

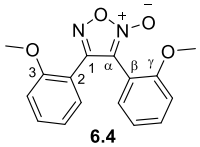

6.4

The desired compound was more unstable than other oximoyl chlorides there addition of NCS was slower (10 parts over 2 hours) and the temperature wasn't raised above 35 °C throughout the reaction and work up. Previous attempts to purify **6.3a** resulted in the formation of furoxan **6.4**. With these slight alterations general synthesis procedure for the synthesis of oximoyl chlorides was followed using (E)-2-methoxybenzaldehyde oxime **6.2a** (0.50 g, 3.3 mmmol, 1 eq.), and NCS (0.44 g, 3.3 mmol, 1 eq.) to give a crude white solid. (0.48 g, 13 % furoxan

impurity); m.p. 98 – 100 °C; ν_{max} / cm^{-1}: 3312 (O-H), 3018 (C-H), 2983 (C-H), 1625 (C=N), 1177 (C-O), 752 (C-Cl); ^{1}H NMR (400 MHz, $CDCl_3$) δ 9.54 (s, 1H, H_{OH}), 7.59 (dd, *J* = 7.5, 1.5 Hz, 1H, H_d), 7.44 – 7.38 (m, 1H, H_e), 7.04 – 6.96 (m, 2H, H_{fg}), 3.91 (s, *J* = 8.5 Hz, 3H, H_h); ^{13}C NMR (101 MHz, $CDCl_3$) δ 157.32 (C_c), 137.01 (C_b), 131.87 (C_e), 131.09 (C_d), 122.13 (C_b), 120.68 (C_f), 111.75 (C_g), 56.00 (C_h). (13 % furoxan impurity **6.4** ^{1}H NMR (500 MHz, $CDCl_3$) δ 7.55 (dd, *J* = 7.5, 1.5 Hz, 1H, H_{Ar}), 7.44 – 7.34 (m, 3H, H_{Ar}), 7.05 (t, *J* = 7.5 Hz, 1H, H_{Ar}), 7.01 (t, *J* = 7.5 Hz, 1H, H_{Ar}), 6.85 (d, *J* = 8.5 Hz, 1H, H_{Ar}), 6.81 (d, *J* = 8.5 Hz, 1H, H_{Ar}), 3.42 (s, 3H, H_{OMe}), 3.27 (s, 3H, H_{OMe}); ^{13}C NMR (126 MHz, $CDCl_3$) δ 157.20 ($C_{Ar\text{-}O}$), 157.01 ($C_{Ar\text{-}O}$), 156.36 (C_1), 132.08 ($C_{Ar\text{-}H}$), 131.74 ($C_{Ar\text{-}H}$), 130.17 ($C_{Ar\text{-}H}$), 129.86 ($C_{Ar\text{-}H}$), 120.94 ($C_{Ar\text{-}H}$), 120.77 ($C_{Ar\text{-}H}$), 117.47 ($C_β$), 114.46 ($C_α$), 113.89 (C_2), 111.21 ($C_{Ar\text{-}H}$), 111.15 ($C_{Ar\text{-}H}$), 55.14 (C_{OMe}), 54.87 (C_{OMe}); MS (ESI) m/z calcd. ($C_8H_8ClNO_2 + H^+$): 186.0316, found: 186.0320 ($M + H^+$).

(Z)-N-hydroxy-3-methoxybenzimidoyl chloride (6.3b)

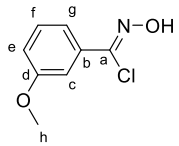

General synthesis procedure for the synthesis of oximoyl chlorides was followed using (E)-3-methoxybenzaldehyde oxime **6.2b** (1.00 g, 6.6 mmol, 1 eq.), and NCS (1.06 mg, 7.9 mmol, 1.2 eq.) to give an impure soft red solid, (0.8959 g); m.p 28 – 30 °C; ν_{max} / cm^{-1}: 3306 (O-H), 30333 (C-H), 2979 (C-H), 2845 (C-H), 1601 (C=N), 1167 (C-O), 797 (C-H), 777 (C-Cl); ^{1}H NMR (500 MHz, $CDCl_3$) δ 8.19 (brs, 1H, H_{OH}), 7.44 (d, *J* = 8.0 Hz, 1H, H_g), 7.40 – 7.37 (m, 1H, H_c), 7.35 – 7.30 (m, 1H, H_f), 7.00 (dd, *J* = 8.0, 2.5 Hz, 1H, H_e), 3.85 (s, 3H, H_h); ^{13}C NMR (126 MHz, $CDCl_3$) δ 159.65 (C_d), 140.09 (C_a), 133.84 (C_b), 129.63 (C_f), 119.88 (C_g), 116.85 (C_e), 112.49 (C_c), 55.57 (C_h); MS (ESI) m/z calcd. ($C_8H_8Cl^{35}NO_2 + H^+$): 186.0316, found: 186.0317 ($M + H^+$); calcd. ($C_8H_8Cl^{37}NO_2 + H^+$): 188.0287, found: 188.0294 ($M + H^+$).

(Z)-N-hydroxy-4-methoxybenzimidoyl chloride (6.3c)[370]

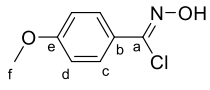

General synthesis procedure for the synthesis of oximoyl chlorides was followed using (E)-4-methoxybenzaldehyde oxime **6.2c** (2.50 g, 16.5 mmol), and NCS (2.65 g, 19.8 mmol, 1.2 eq.) to give a impure yellow solid, recrystallisation from petrol improved the purity, this resulted in a very pale yellow solid (73 %); m.p 74 – 76 °C; ν_{max} / cm^{-1}: 3332 (O-H), 2984 (C-H), 2839 (C-H), 1652

(C=N), 1171 (C-O), 831 (C-H), 788 (C-Cl); ^{1}H NMR (400 MHz, $CDCl_3$) δ 8.55 (s, 1H, H_{OH}), 7.78 (d, *J* = 8.0 Hz, 2H, H_c), 6.91 (d, *J* = 8.0 Hz, 2H, H_d), 3.84 (s, 3H, H_f); ^{13}C NMR (101 MHz, $CDCl_3$) δ 162.00 (C_e), 140.20 (C_a), 129.20 (C_c), 127.38 (C_b), 114.33 (C_d), 55.88 (C_f); MS (ESI) m/z calcd. ($C_8H_8Cl^{35}NO_2 + H^+$): 186.0316, found: 186.0316 ($M + H^+$); calcd. ($C_8H_8Cl^{37}NO_2 + H^+$): 188.0287, found: 188.0290 ($M + H^+$)

(Z)-N-hydroxy-4-fluorobenzimidoyl chloride (6.3d)[370]

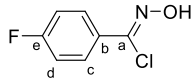

General synthesis procedure for the synthesis of oximoyl chlorides was followed using (E)-4-fluorobenzaldehyde oxime **6.2d** (2.50 g, 18.0 mmol, 1 eq.), and NCS (2.88 g, 21.6 mmol, 1.2 eq.) to give a white solid. (96 %); m.p. 71 – 73 °C; ν_{max} / cm^{-1}: 3369 (O-H), 3073 (C-H), 2851 (C-H), 1598 (C=N), 831 (C-H), 754 (C-Cl); ^{1}H NMR (400 MHz, $CDCl_3$) δ 7.99 – 7.79 (m, 2H, H_c), 7.72 (s, 1H, H_{OH}), 7.10 (t, *J* = 8.5 Hz, 2H, H_d); ^{13}C NMR (101 MHz, $CDCl_3$) δ 164.31 (d, *J* = 251.7 Hz, C_e), 139.03 (C_a), 129.34 (d, *J* = 8.5 Hz, C_c), 128.77 (d, *J* = 3.5 Hz, C_b), 115.74 (d, *J* = 22.0 Hz, C_d); MS (ESI) m/z calcd. ($C_7H_5ClFNO + H^+$): 174.0116, found: 174.0116 ($M + H^+$); calcd. ($C_7H_5ClFNO + H^+$): 176.0087, found: 176.0085 ($M + H^+$)

(Z)-N-hydroxy-4-(trifluoromethyl)benzimidoyl chloride (6.3e)[370]

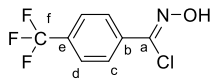

General synthesis procedure for the synthesis of oximoyl chlorides was followed using (E)-4-(trifluoromethyl)benzaldehyde oxime **6.2e** (0.60 mg, 3.2 mmol, 1 eq.) and NCS (0.51 mg, 3.8 mmol, 1.2 eq.) initially. The reaction was not complete after 16 hrs so a further 0.2 eq. of NCS (0.09 mg, 0.64 mmol) was added. After a further 2 hours the TLC indicicated the reaction had reached completion. It was worked up to give a white solid (89 %; R_f = 0.8 in 20 % EtOAc); m.p. 86-88 °C. ^{1}H NMR (400 MHz, $CDCl_3$) δ 8.20 (s, 1H, H_{OH}), 7.97 (d, *J* = 8.5 Hz, 2H, H_d), 7.67 (d, *J* = 8.5 Hz, 2H, H_d); MS (ESI) m/z calcd. ($C_8H_4ClF_3NO - H^+$): 221.9939, found: 221.9937 ($M - H^+$).

(Z)-N-hydroxy-3,4-dimethoxybenzimidoyl chloride (6.3f)[371]

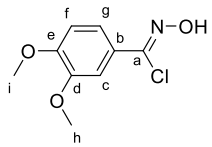

General synthesis procedure for the synthesis of oximoyl chlorides was followed using (E)-3,4-dimethoxybenzaldehyde oxime **6.2f** (1.00 g, 5.5 mmol), and NCS (0.81 g, 6.1 mmol, 1.1 eq.) to give a impure brown solid, recrystallisation from DCM resulted in a pure white solid. (94 %);

m.p. 156 -158 °C; ν_{max} / cm^{-1}: 3375 (O-H), 3016 (C-H), 2976 (C-H), 2841 (CHO), 1599 (C=N), 1164 (C-O), 1140 (C-O), 767 (C-Cl); ^{1}H NMR (400 MHz, $CDCl_3$) δ 7.88 (s, 1H, H_{OH}), 7.44 (dd, *J* = 8.5, 2.0 Hz, 1H, H_g), 7.37 (d, *J* = 2.0 Hz, 1H, H_c), 6.88 (d, *J* = 8.5 Hz, 1H, H_f), 3.92 (s, 6H, $H_{h/i}$); ^{13}C NMR (101 MHz, $CDCl_3$) δ 151.43 (C_e), 148.90 (C_d), 139.97 (C_a), 125.15 (C_b), 121.05 (C_g), 110.66 (C_f), 109.62 (C_d), 56.14 ($C_{h/i}$), 56.12 ($C_{h/i}$); MS (ESI) m/z calcd. ($C_9H_{10}Cl^{35}NO_3$ + Na^+): 238.0241, found: 238.0240 (M + Na^+); ($C_9H_{10}Cl^{37}NO_3$ + Na^+): 240.0212, found: 240.0211 (M + Na^+).

(Z)-N-hydroxy-3,4,5-trimethoxybenzimidoyl chloride (6.3g)

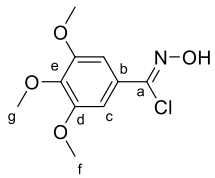

General synthesis procedure for the synthesis of oximoyl chlorides was followed using (E)-3,4,5-methoxybenzaldehyde oxime **6.2g** (3.40 g, 16.1 mmol), and NCS (2.57 g, 19.2 mmol, 1.2 eq.) to give a impure red solid, recrystallisation from petrol improved the purity marginally, this resulted in a pale red solid, NMR analysis suggest the impurity was caused by ring chlorination. (3.73 g, 80 %); m.p. 109 – 111 °C; ν_{max} / cm^{-1}: ^{1}H NMR (400 MHz, Acetone) δ 10.59 (s, 1H, H_{OH}), 8.41 (s, 1H, H_a), 7.28 (s, 1H, H_c), 7.23 (s, 1H, H_c), 4.02 – 3.75 (m, 9H, $H_{f/g}$); ^{13}C NMR (101 MHz, Acetone) δ 153.70 (C_d), 151.00 (C_e), 146.04 (C_a), 127.01 (C_b), 120.67 (C_b), 113.44 (C_c), 105.53 (C_c), 61.50 ($C_{f/g}$), 57.06 ($C_{f/g}$), 56.52 ($C_{f/g}$); MS (ESI) m/z calcd. ($C_{10}H_{12}Cl^{35}NO_4$ + Na^+): 268.0347, found: 268.0349 (M + Na^+); calcd. ($C_{10}H_{12}Cl^{37}NO_4$ + Na^+): 270.0318, found: 270.0321 (M + Na^+).

(Z)-4-(chloro(hydroxyimino)methyl)-2-methoxyphenyl acetate (6.3h)

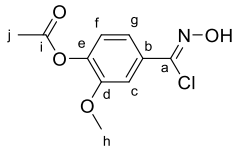

General synthesis procedure for the synthesis of oximoyl chlorides was followed using (E)-4-acetoxy-3-methoxy benzaldehyde oxime **6.2h** (3.00 g, 14.3 mmol), and NCS (2.30 g, 17.2 mmol, 1.2 eq.) to give a white solid. (92 %); m.p. 102 – 104 °C; ν_{max} / cm^{-1}: 3336 (O-H), 2981 (C-H), 2842 (C-H), 1741 (C=O), 1589 (C=N), 1123 (C-O), 782 (C-Cl); ^{1}H NMR (400 MHz, $CDCl_3$) δ 7.88 (brs, 1H, H_{OH}), 7.47 – 7.43 (m, H_{cg}), 7.08 (d, *J* = 8.5 Hz, 1H, H_f), 3.88 (s, 3H, H_h), 2.33 (s, 3H, H_j); ^{13}C NMR (101 MHz, $CDCl_3$) δ 168.96 (C_i), 151.14 (C_d), 141.93 (C_a), 131.27 (C_b), 122.95 (C_f), 120.33 (C_g), 111.04 (C_c), 56.16 (C_h), 20.80 (C_j); MS (ESI) m/z calcd. ($C_{10}H_{10}ClNO_4$ + Na^+): 266.0191, found: 266.0189 (M + Na^+).

(1Z,4Z)-N'1,N'4-dihydroxyterephthalimidoyl dichloride 6.3i[317]

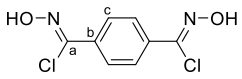

General synthesis procedure for the synthesis of oximoyl chlorides was followed using terephthalaldehyde dioxime **6.2i** (8.7 g, 53.0 mmol), and NCS (14.2 g, 106.0 mmol, 2.2 eq.) to give a white solid, (74 %); m.p. 206 – 208 °C; ν_{max}/cm^{-1} 3260 (O-H), 3053 (C-H), 1675 (C=N), 802 (C-Cl); ^{1}H NMR (500 MHz, Acetone) δ 11.62 (s, 2H, H_{OH}), 7.94 (s, 4H, H_c);^{13}C NMR (126 MHz, Acetone) δ 136.99 (C_a), 135.61 (C_b), 127.83 (C_c); MS (ESI) m/z calcd. ($C_8H_6Cl_2N_2O_2 + H^+$): 232.9879, found: 232.9880 ($M + H^+$).

(Z)-N,4-dihydroxy-3-methoxybenzimidoyl chloride 6.3j

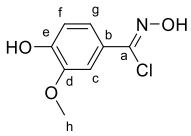

General synthesis procedure for the synthesis of oximoyl chlorides was followed using **6.2j** (3 g, 18.0 mmol), and NCS (2.4 g, 18.0 mmol,) to give a crude solid that could not be purified.

8.6.2 Conversion study

DEAyS **5.2S** (0.25 g, 0.56 mmol, 1 eq.) and oximoyl chloride (2 eq.) were dissolved in DMF (1.6 ml ≈ 0.5 M) at RT along with 4Å MS (0.90 g) and stirred for 30 minutes. The solution was heated to 80 °C and stirred for 24 hours. After 24 hours the reaction mixture was diluted with $CHCl_3$ (25 ml) and filtered to remove the molecular sieves. The organic filtrate was washed with water (3 × 25 ml) then set to one side, the aqueous washes were combined and extracted with $CHCl_3$ (3 × 25 ml). The 4 $CHCl_3$ layers were combined and washed with brine, then dried with $MgSO_4$. Solvent was removed *in vacuo* to leave a crude product that was analysed with ^{1}H NMR to determine conversion.

***N*,*N*-bis(2-((3-(3,4-dimethoxyphenyl)isoxazol-5-yl)methoxy)ethyl)stearamide (6.6a)**

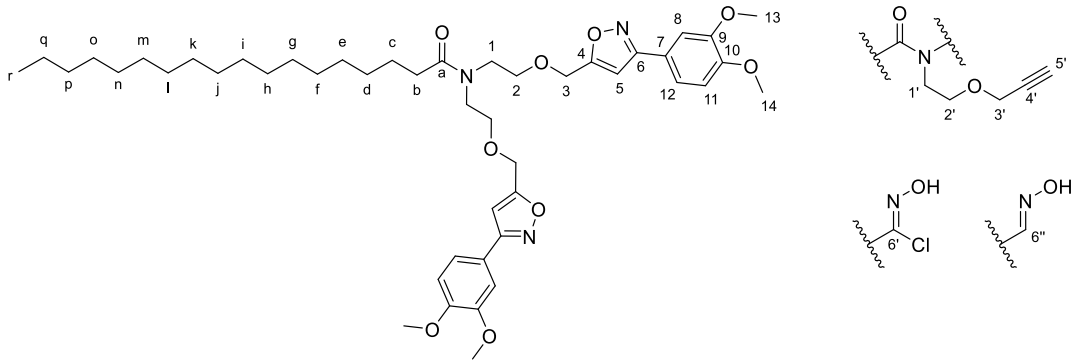

The general procedure was performed using DEAyS **5.2S** (0.25 g, 0.56 mmol, 1 eq.) and (Z)-*N*-hydroxy-3,4-dimethoxybenzimidoyl chloride **6.3f** (0.2408 g, 1.12 mmol, 2 eq.) to give a crude dark brown waxy oil, 0.4389 g, 85 % conversion. ^{1}H NMR (400 MHz, $CDCl_3$) δ 8.48 (s, $H^{3,4\text{-isoxazole}}$), 8.43 (s, $H^{3,4\text{-isoxazole}}$), 7.44 – 7.40 (m, *J* = 1.8 Hz, $H^{8/11/12}$), 7.30 – 7.24 (m, $H^{8/11/12}$), 6.96 – 6.87 (m, $H^{8/11/12}$), 6.52 – 6.47 (m, H^{5}), 4.66 – 4.55 (m, H^{3}), 4.14 (d, *J* = 2.5 Hz, $H^{3'}$), 4.12 (d, *J* = 2.5 Hz, 3H, $H^{3'}$), 3.98 – 3.87 (m, $H^{13/14}$), 3.77 – 3.67 (m, $H^{1/1'/2/2'}$), 3.67 – 3.57 (m, $H^{1/1'/2/2'}$), 2.43 (t, *J* = 2.5 Hz, $H^{5'}$), 2.41 – 2.32 (m, $H^{5'/b}$), 1.67 – 1.55 (m, H^{c}), 1.35 – 1.17 (m, $H^{d\text{-}q}$), 0.88 (t, *J* = 7.0 Hz, H^{r}); MS (ESI) m/z calcd. ($C_{46}H_{67}N_3O_9 + Na^+$): 828.4770, found: 828.4756 ($M + Na^+$); MS (ESI) m/z calcd. ($C_{37}H_{58}N_2O_6 + Na^+$): 649.4187, found: 649.4180 ($M + Na^+$).

(((((stearoylazanediyl)bis(ethane-2,1-diyl))bis(oxy))bis(methylene))bis(isoxazole-5,3-diyl))bis(2-methoxy-4,1-phenylene) diacetate (6.6b)

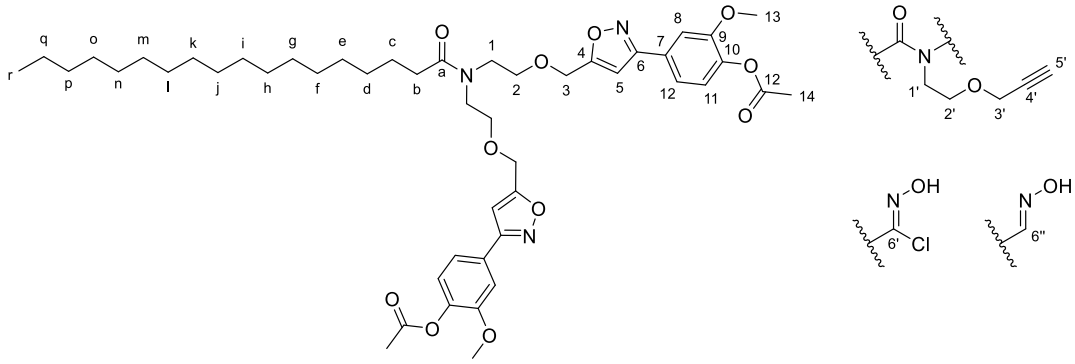

The general procedure was performed using DEAyS **5.2S** (0.25 g, 0.56 mmol, 1 eq.) and ((Z)-4-(chloro(hydroxyimino)methyl)-2-methoxyphenyl acetate **6.3h** (0.2721 g, 1.12 mmol, 2 eq.) to give a crude dark brown waxy oil, 0.4648 g, 67 % conversion. ^{1}H NMR (400 MHz, $CDCl_3$) δ 7.51 – 7.46 (m, H^{Ar}), 7.33 – 7.25 (m, H^{Ar}), 7.14 – 7.08 (m, H^{Ar}), 6.54 – 6.49 (m, H^{5}), 4.67 – 4.59 (m, H^{3}), 4.16 – 4.10 (m, $H^{3'}$), 3.92 – 3.86 (m, H^{13}), 3.76 – 3.66 (m, $H^{1/1'/2/2'}$), 3.65 – 3.55 (m, $H^{1/1'/2/2'}$), 2.46 – 2.30 (m, $H^{5'/14/b}$), 1.68 – 1.55 (m, H^{c}), 1.32 – 1.19 (m, H^{d-q}), 0.88 (t, *J* = 6.5 Hz, H^{r}); MS (ESI) m/z calcd. ($C_{48}H_{67}N_3O_{11}$ + Na^+): 884.4668, found: 884.4658 (M + Na^+); MS (ESI) m/z calcd. ($C_{38}H_{58}N_2O_7$ + Na^+): 677.4136, found: 677.4131 (M + Na^+).

_N_,_N_-bis(2-((3-(3,4,5-trimethoxyphenyl)isoxazol-5-yl)methoxy)ethyl)stearamide 6.6c

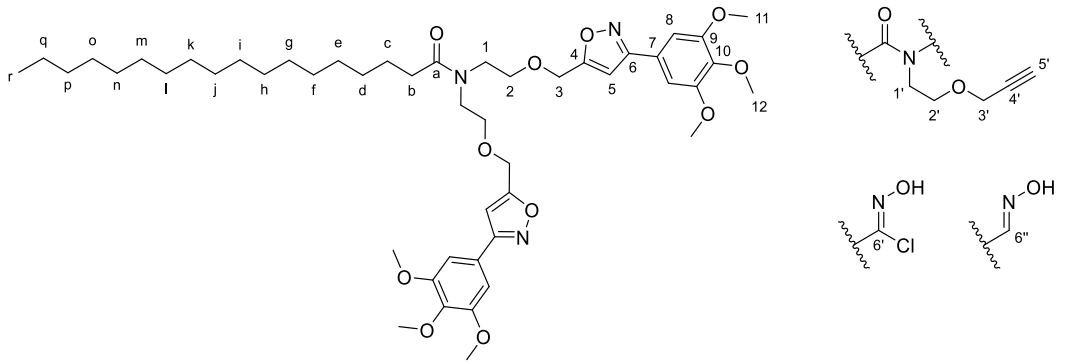

The general procedure was performed using DEAyS **5.2S** (0.25 g, 0.56 mmol, 1 eq.) and (Z)-*N*-hydroxy-3,4,5-trimethoxybenzimidoyl chloride **6.3g** (0.2744 g, 1.12 mmol, 2 eq.) to give a crude pale orange waxy solid, 0.4839 g, 15 % conversion. ^{1}H NMR (400 MHz, $CDCl_3$) δ 8.54 (s, H^{OH}), 7.72 (s, $H^{OH)}$, 7.28 (s, H^{Ar}), 7.20 (s, H^{Ar}), 6.76 – 6.72 (m, H^{5}), 4.68 (s, H^{3}), 4.66 (s, H^{3}), 4.17 (d, *J* = 2.5 Hz, $H^{3'}$), 4.15 (d, *J* = 2.5 Hz, $H^{2'}$), 3.98 – 3.87 (m, $H^{11/12}$), 3.72 – 3.58 (m, $H^{1/1'/2/2'}$), 2.46 (t, *J* = 2.5 Hz, $H^{5'}$), 2.43 (t,

J = 2.5 Hz, $H^{5'}$), 2.39 (t, *J* = 7.5 Hz, H^{b}), 1.69 – 1.59 (m, H^{c}), 1.37 – 1.21 (m, H^{d-q}), 0.90 (t, *J* = 7.0 Hz, H^{r}); *m/z:* (ES^+) calcd. ($C_{28}H_{49}NO_3$ + Na^+): 470.3605, found: 470.3608 ($M + Na^+$).

8.6.3 Synthesis of vanillin derived di(oximoyl chloride) premonomers – **6.9**

4,4'-(butane-1,4-diylbis(oxy))bis(3-methoxybenzaldehyde) (6.7a)[372]

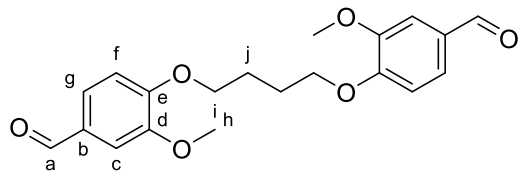

Vanillin (10.00 g, 65.7 mmol, 2.1 eq.) was dispersed in acetone (200 ml) at RT. 2,6-Dibromobutane (6.76 g, 31.3 mmol, 1 eq.) and potassium carbonate (9.12 g, 65.7 mmol, 2.1 eq.) were introduced to the reaction and temperature was increased to reflux for 48 hours. The product was present as a white ppt. After 48 hrs the reaction was cooled to RT and the ppt collected by Büchner filtration. The precipitate was washed with water (3 x 100 ml) and cold acetone (50 ml) then dried in a desiccator overnight to give a pure white product. (72 %); R_f 0.8 in 66 % EtOAc; m.p. 164 – 166 °C; ν_{max} / cm^{-1}: 2957 (C-H), 2936 (C-H), 2838 (C-H), 2736 (CHO), 1674 (C=O), 1262 (C-O), 1237 (C-O), 1131 (C-O); ^{1}H NMR (500 MHz, $CDCl_3$) δ 9.85 (s, 2H, H^a), 7.43 (d, *J* = 8.0 Hz, 2H, H^g), 7.40 (s, 2H, H^c), 6.98 (d, *J* = 8.0 Hz, 2H, H^f), 4.22 (t, *J* = 5.5 Hz, 4H, H^i), 3.90 (s, 6H, H^h), 2.11 (t, *J* = 5.5 Hz, 4H, H^j); ^{13}C NMR (126 MHz, $CDCl_3$) δ 191.06 (C^a), 154.08 (C^e), 149.95 (C^d), 130.18 (C^b), 126.86 (C^g), 111.51 (C^f), 109.37 (C^c), 68.80 (C^i), 56.11 (C^h), 25.91 (C^j); ^{1}H NMR (300 MHz, Acetone) δ 9.86 (s, H^a), 7.53 (dd, *J* = 8.0, 2.0 Hz, H^g), 7.42 (d, *J* = 2.0 Hz, H^c), 7.17 (d, *J* = 8.0 Hz, H^f), 4.26 (t, *J* = 6.0 Hz, H^i), 3.89 (s, H^h), 2.08 (s, H^j); MS (ESI) m/z calcd. ($C_{20}H_{22}O_6$ + Na^+): 381.1309, found: 381.1305 ($M + Na^+$).

bis(4-formyl-2-methoxyphenyl) succinate (6.7b)[373]

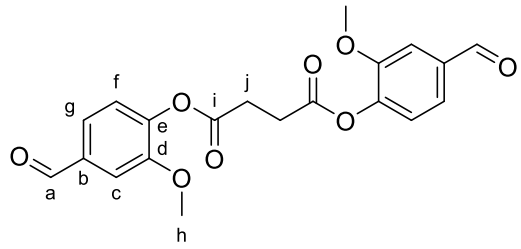

Vanillin (5.00 g, 32.9 mmol, 2.2 eq.) was dissolved in dry acetone (90 ml) at room temperature along with K_2CO_3 (4.50 g, 32.9 mmol, 2.2 eq.) and left to homogenise for 30 minutes under N_2. Succinyl dichloride (2.32 g, 14.9 mmol, 1 eq.) was dissolved in dry acetone (10 ml) and added dropwise to the stirred solution. The mixture was heated to reflux for 4 hours then cooled and reduced *in vacuo* to remove the majority of the acetone, the residue was taken into EtOAc (150 ml) and washed with H_2O (3 × 100 ml) and brine (100 ml). The organic layer was dried with $MgSO_4$ and reduced *in vacuo* to give a solid crude (3.58 g). The solid was purified by column chromatography (40 % EtOAc), whilst dry loading the "product silica" wouldn't wet in the eluent, this led to a very slow column where pure dialdehyde was recovered. The yield of pure dialdehyde was low as many dialdehyde fractions overlapped with a more polar fraction. The pure dialdehyde was a white solid (29 %, R_f = 0.3 in 40% EtOAc); m.p. 134 – 136 °C; ν_{max} / cm^{-1}: 3072 (C-H), 2928 (C-H), 2825 (C-H), 2733 (CHO), 1749 (C=O), 1674 (C=O), 1264 (C-O), 1114 (C-O); ^{1}H NMR (500 MHz, Acetone) δ 10.00 (s, 2H, H^a), 7.61 (d, *J* = 1.5 Hz, 2H, H^c), 7.59 (dd, *J* = 8.0, 1.5 Hz, 2H, H^g), 7.33 (d, *J* = 8.0 Hz, 2H, H^f), 3.92 (s, 6H, H^h), 3.07 (s, 4H, H^j); ^{13}C NMR (126 MHz, Acetone) δ 191.88 (C^a), 170.38 (C^i), 153.05 (C^d), 145.76 (C^b), 136.59 (C^e), 124.46 (brs, C^{fg}), 112.45 (C^c), 56.56 (C^h), 29.50 (C^j); MS (ESI) m/z calcd. ($C_{20}H_{18}O_8$ + Na^+): 409.0894, found: 409.0897 (M + Na^+).

(1E,1'E)-4,4'-(butane-1,4-diylbis(oxy))bis(3-methoxybenzaldehyde) dioxime (6.8a)

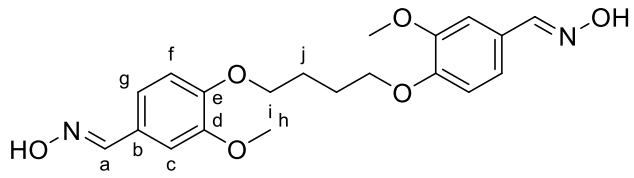

4,4'-(butane-1,4-diylbis(oxy))bis(3-methoxybenzaldehyde) **6.7a** (2.00 g, 5.58 mmol, 1 eq.) was dispersed in EtOH (50 ml). Hydroxylamine hydrochloride (0.85, 12.3 mmol, 2.2 eq.) and sodium acetate (1.01, 12.3 mmol, 2.2 eq.) were dissolved in water (10 ml) and added to the ethanol mixture. The mixture was then heated to reflux to encourage the dialdehyde to dissolve. After 2 hours the reaction was allowed to cool to room temperature and the majority of the ethanol was removed *in vac*uo, resulting in a white ppt suspended in water. This was

poured into cold water to encourage further ppt, the ppt was collected by Büchner filtration, washed with water followed by minimal cold ethanol then dried overnight in a desiccator to give a pure white solid (94 %, Rf 0.8 in 66 % EtOAc); m.p. 188 – 190 °C; ν_{max} / cm^{-1}: 33444 (OH), 3007 (C-H), 2942 (C-H), 2881 (C-H), 2840 (C-H), 1598 (C=N), 1258 (C-O), 1124 (C-O); ^{1}H NMR (500 MHz, Acetone) δ 10.04 (s, 2H, H^{OH}), 8.04 (s, 2H, H^{a}), 7.26 (d, *J* = 2.0 Hz, 2H, H^{c}), 7.08 (dd, *J* = 8.0, 2.0 Hz, 2H, H^{g}), 6.99 (d, *J* = 8.0 Hz, 2H, H^{f}), 4.14 (t, *J* = 6.0 Hz, 4H, H^{i}), 3.82 (s, 6H, H^{h}), 2.01 (t, *J* = 6.0 Hz, 4H, H^{j}); ^{13}C NMR (126 MHz, Acetone) δ 151.04 ($C^{d/e}$), 150.73 ($C^{d/e}$), 149.17 (C^{a}), 127.07 (C^{b}), 121.52 (C^{g}), 113.62 (C^{f}), 109.76 (C^{c}), 69.23 (C^{i}), 56.05 (C^{h}), 26.84 (C^{j}); MS (ESI) m/z calcd. ($C_{20}H_{24}N_2O_6$ + Na^+): 411.1527, found: 411.1529 (M + Na^+).

bis(4-((E)-(hydroxyimino)methyl)-2-methoxyphenyl) succinate (6.8b)

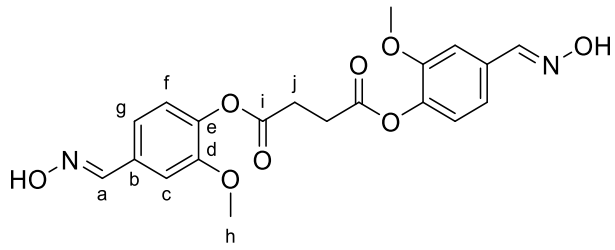

bis(4-formyl-2-methoxyphenyl) succinate **6.7b** (1.44 g, 3.73 mmol, 1 eq.) was dispersed in EtOH (50 ml). Hydroxylamine hydrochloride (0.52 g, 7.45 mmol, 2 eq.) and sodium acetate (0.61, 12.3 mmol, 2 eq.) were dissolved in water (10 ml) and added to the ethanol mixture. To reduce the risk of ester hydrolysis the reaction wasn't heated to encourage the dialdehyde to dissolve, it was instead left to react for 24 hours. The ppt was collected by Büchner filtration and washed with water and cold ethanol to leave a crude brown solid. Purification by column chromatagrophy through a silica plug resulted in a white solid. (7 %, R_f = 0.2 in 50 % EtOAc); m.p. 142 – 144 °C; ν_{max} / cm^{-1}: 3500 (OH), 3085 (C-H), 2925 (C-H), 2842 (C-H), 1747 (C=O), 1591 (C=N), 1263(C-O), 1109 (C-O); ^{1}H NMR (500 MHz, Acetone) δ 10.37 (s, 2H, H^{OH}), 8.13 (s, 2H, H^{a}), 7.38 (d, *J* = 1.0 Hz, 2H, H^{c}), 7.19 (dd, *J* = 8.0, 1.0 Hz, 2H, H^{g}), 7.10 (d, *J* = 8.0 Hz, 2H, H^{f}), 3.83 (s, 6H, H^{h}), 3.01 (s, 2H, H^{j}); ^{13}C NMR (126 MHz, Acetone) δ 170.66 (C^{i}), 152.44 (C^{d}), 148.79 (C^{a}), 141.78 (C^{e}), 133.08 (C^{b}), 123.90 (C^{f}), 120.41 (C^{g}), 110.72 (C^{c}), 56.26 (C^{h}), 29.50 (C^{j}); MS (ESI) m/z calcd. ($C_{20}H_{20}N_2O_8$ + Na^+): 439.1112, found: 439.1112 (M + H^+).

(1Z,1'Z)-4,4'-(butane-1,4-diylbis(oxy))bis(*N*-hydroxy-3-methoxybenzimidoyl chloride) (6.9a)

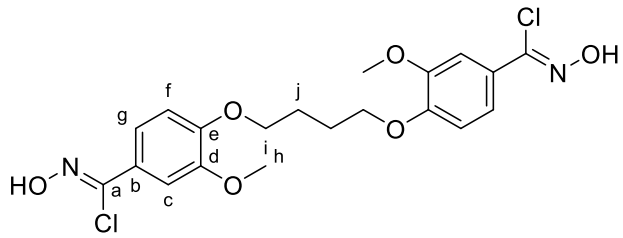

(1E,1'E)-4,4'-(butane-1,4-diylbis(oxy))bis(3-methoxybenzaldehyde) dioxime **6.8a** (1.00 g, 2.57 mmol, 1 eq.) was dissolved in DMF (10 ml). NCS (0.76 g, 5.66 mmol, 2.2 eq.) was introduced in 5 parts over 1 hour. 2 hours after the last addition of NCS the solution was poured into cold water causing a white ppt to form. The ppt was collected by Büchner filtration and washed with water followed by cold ethanol then dried in a desiccator to leave a slightly impure white solid. Recrystallisation from acetone gave a pure white solid. (63 %, Rf = 0.8 in 66 % EtOAc); m.p. 197 – 199 °C; ν_{max} / cm^{-1}: 3328 (OH), 2977 (C-H), 2936 (CH_2), 2877 (CH_2), 1600 (C=N), 1268 (C-O), 1132 (C-O); ^{1}H NMR (500 MHz, Acetone) δ 11.16 (s, 2H, H^{OH}), 7.43 – 7.38 (m, 4H, $H^{c/g}$), 7.04 (d, *J* = 8.0, 2H, H^f), 4.18 (t, *J* = 5.5 Hz, 4H, H^i), 3.87 – 3.81 (m, 6H, H^h), 2.08 (brs, 4H, H^j); ^{13}C NMR (126 MHz, Acetone) δ 151.87 ($C^{d/e}$), 150.32 ($C^{d/e}$), 137.52 (C^a), 126.50 (C^b), 121.27 (C^g), 113.25 (C^f), 110.91 (C^c), 69.33 (C^i), 56.28 (C^h), 26.83 (C^j); MS (ESI) m/z calcd. ($C_{20}H_{22}Cl^{35}{}_2N_2O_6$ + Na^+): 479.0747, found: 479.0742 (M + Na^+); calcd. ($C_{20}H_{22}Cl^{35}Cl^{37}N_2O_6$ + Na^+): 481.0722, found: 481.0717 (M + Na^+).

bis(4-((Z)-chloro(hydroxyimino)methyl)-2-methoxyphenyl) succinate (6.9b)

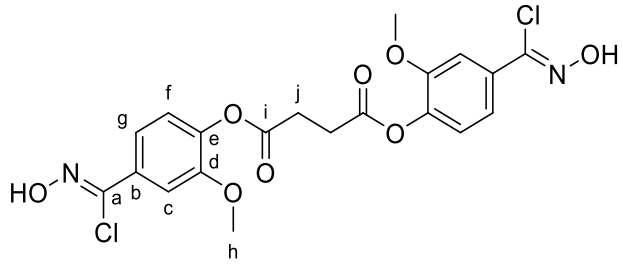

bis(4-((E)-(hydroxyamino)methyl)-2-methoxyphenyl) succinate **6.8b** (0.11 g, 0.2 mmol, 1 eq.) was dissolved in DMF (10 ml). NCS (0.08 g, 0.6 mmol, 2.2 eq.) was introduced in 5 parts over 1 hour. 2 hours after the last addition of NCS the solution was poured into cold water causing a ppt to form. The ppt was collected by Büchner filtration and washed with water followed by cold ethanol then dried in a desiccator to leave a cream solid. (78 %, R_f = 0.2 in 50 % EtOAc); ^{1}H NMR (500 MHz, Acetone) δ 11.53 (s, 2H, H^{OH}), 7.53 (d, *J* = 2.0 Hz, 2H, H^c), 7.46 (dd, *J* = 8.5, 2.0 Hz, 2H, H^g), 7.17 (d, *J* = 8.5 Hz, 2H, H^f), 3.87 (s, 6H, H^h), 3.03 (s, 4H, H^j); ^{13}C NMR (126 MHz, Acetone) δ 170.56 (C^i), 152.19 (C^d), 142.62 (C^{Ar}), 136.89 (C^{Ar}), 132.69 (C^{Ar}), 123.82 (C^f), 120.40 (C^g), 111.58 (C^c), 56.42 (C^h), 29.48 (C^j); MS (ESI) m/z calcd.

($C_{20}H_{18}Cl^{35}{}_2N_2O_8$ + Na^+): 507.0332, found: 507.0330 (M + Na^+); calcd. ($C_{20}H_{18}Cl^{35}Cl^{37}N_2O_8$ + Na^+): 509.0308, found: 509.0306 (M + Na^+).

8.6.4 Synthesis of vanillinin derived dialkyne monomer – **6.11**

((butane-1,4-diylbis(oxy))bis(3-methoxy-4,1-phenylene))dimethanol (6.12)

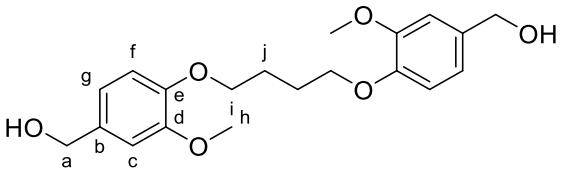

4,4'-(butane-1,4-diylbis(oxy))bis(3-methoxybenzaldehyde) **6.7a** (2.00 g, 5.6 mmol, 1 eq.) was dispersed in MeOH (20 ml). Sodium borohydride (0.53 g, 14.0 mmol, 2.5 eq.) was added in five parts over the course of 30 minutes. The reaction was left for a further hour before the ppt was recovered by Buchner filtration and washed with water followed by methanol then dried in a desiccator overnight, resulting in a pure white solid. (86 %, R_f 0.6 - 66 % EtOAc); m.p. 143 – 145 °C; ν_{max} / cm^{-1}: 3357 (OH), 3072 (C-H), 2963 (C-H), 2944 (C-H), 2865 (C-H), 1266 (C-O), 1112 (C-O), 1057 (C-OH); ^{1}H NMR (500 MHz, $CDCl_3$) δ 6.91 (brs, 2H, H^c), 6.86 (brs, 4H, $H^{g/f}$), 4.62 (d, *J* = 5.0 Hz, 4H, H^a), 4.13 – 4.08 (m, 4H, H^i), 3.86 (s, 6H, H^h), 2.07 – 2.01 (m, 4H, H^j), 1.61 (t, *J* = 5.5 Hz, 2H, H^{OH}); ^{13}C NMR (126 MHz, $CDCl_3$) δ 149.70 (C^d), 148.17 (C^e), 133.79 (C^b), 119.56 (C^g), 113.04 (C^f), 111.06 (C^c), 68.85 (C^i), 65.53 (C^a), 56.05 (C^h), 26.08 (C^j); MS (ESI) m/z calcd. ($C_{20}H_{26}O_6$ + Na^+): 385.2, found: 385.1 (M + Na^+).

1,4-bis(2-methoxy-4-((prop-2-yn-1-yloxy)methyl)phenoxy)butane – DAyV (6.11)

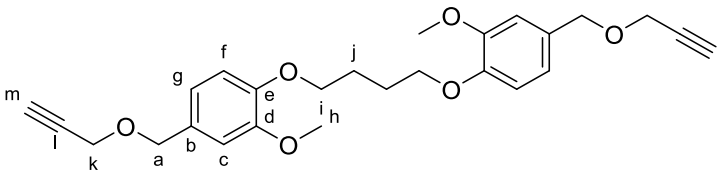

((butane-1,4-diylbis(oxy)) bis(3-methoxy-4,1-phenyl ene))dimethanol **6.12** (1.00 g, 2.76 mmol, 1 eq.) was dissolved in DMF (20 ml) along with KOH (0.93, 16.6 mmol, 6 eq.) and placed in an ice bath. After 30 minutes propargyl bromide (80 % in toluene, 1.64 g, 11.0 mmol, 4 eq.) was diluted with DMF (1 ml) and added dropwise to the cooled solution. The reaction was left to come to room temperature overnight. In the morning the solution was taken into EtOAc (150 ml) and transferred to a separating funnel where it was washed with water (3 × 100 ml) and brine (4 × 100 ml). The organic layer was dried

with $MgSO_4$ and solvent was removed *in vacuo* to leave a crude brown product. After purification through a silica plug pure dialkyne was recovered as a white solid. (44 %, Rf 0.6 in 50 % EtOAc); 102 – 104 °C; ν_{max} / cm^{-1}: 3258 (≡C-H), 2956 (C-H), 2879 (C-H), 2113 (C≡C), 1260 (C-O), 1134 (C-O), 1033 (C-O); ^{1}H NMR (500 MHz, $CDCl_3$) δ 6.90 (s, H^c), 6.89 – 6.81 (m, H^{gf}), 4.54 (s, H^a), 4.15 (d, *J* = 2.5 Hz, H^k), 4.10 (t, *J* = 5.5 Hz, H^i), 3.86 (s, H^h), 2.47 (t, *J* = 2.5 Hz, H^m), 2.03 (t, *J* = 5.5 Hz, H^j); ^{13}C NMR (126 MHz, $CDCl_3$) δ 149.63 (C^d), 148.41 (C^e), 129.96 (C^b), 120.98 (C^g), 112.84 (C^f), 111.96 (C^c), 79.89 (C^l), 74.69 (C^m), 71.63 (C^a), 68.80 (C^i), 56.90 (C^k), 56.05 (C^h), 26.08 (C^j); MS (ESI) m/z calcd. ($C_{26}H_{30}O_6$ + Na^+): 461.1935, found: 461.1935 (M + Na^+).

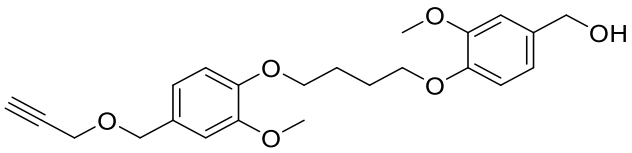

Once alkynated product (3-methoxy -4-(4-(2-methoxy-4-((prop-2-yn-1-yloxy)methyl)phenoxy)butoxy)phenyl)methanol) was also recovered from the column (0.37 g, 0.92 mmol, 33 %, Rf 0.2); MS (ESI) m/z calcd. ($C_{26}H_{28}O_6$ + Na^+): 423.1778, found: 423.1777 (M + Na^+).

8.6.5 Vannilin derived polymers **6.10**, **6.13**, and **6.14**

Dioximoyl chloride (1 eq.) and dipolarophile monomer (1 eq.) were dissolved in DMF (1 M) at 80 °C. 4 Å molecular sieves were added (1600 g / mol of di(oximoyl chloride) and stirred (50 RPM) at 80 °C for 48 hours. After 2 days the reaction mixture was taken into $CHCl_3$ (5 ml) and filtered to remove molecular sieves, the sieves were washed further with warm $CHCl_3$ (5ml), the filtrate was then reduced *in vacuo* to leave the polymer in DMF. The polymer was taken back into a small amount of $CHCl_3$ (2 ml) and added dropwise to MeOH (40 ml) causing a ppt to form. The ppt was collected by passing the solution through filter paper on a sintered funnel and was washed with MeOH (3 x 25 ml). The ppt was collected off the filter paper with warm $CHCl_3$ (3 x 25 ml) which was reduced *in vacuo* to leave polymeric material.

$P^{t2}_{6.9a}$DEAyS (6.10a)

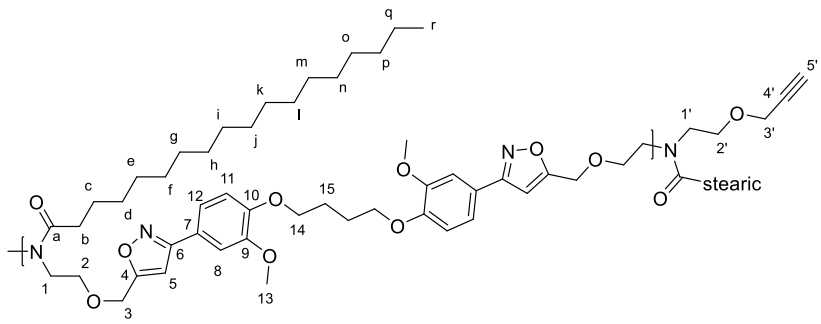

General procedure for vanillin derived polymers was followed using **6.9a** (251 mg, 0.55 mmol, 1 eq.) and DEAyS **5.2S** (246 mg, 0.55 mmol, 1 eq.) to give a malleable brown solid. (88 %); ν_{max} / cm^{-1}: 2918 (C-H), 2850 (C-H), 1639 (C=O) 1585 (C=N), 1257 (C-O), 1101 (C-O), 1032 (C-O); ^{1}H NMR (400 MHz, $CDCl_3$) δ 8.45 (s, H^{CH}-min), 7.39 (brs, H^{8}), 7.25 – 7.20 (brm, H^{12}), 6.97 – 6.87 (brm, H^{11}), 6.76 – 6.72 (m, H^{Ar}-min), 6.48 (brs, H^{5}), 4.67 – 4.54 (m, H^{3}), 4.23 – 4.06 (brm, $H^{3'/14}$), 3.97 – 3.88 (brm, H^{13}), 3.75 – 3.66 (brm, $H^{2/2'}$), 3.66 – 3.52 (m, $H^{1/1'}$), 2.42 (t, J = 2.5 Hz, $H^{5'}$), 2.40 – 2.30 (brm, H^{b}), 2.08 (brs, H^{15}), 1.71 – 1.51 (brm, H^{c}), 1.24 (brs, H^{d-q}), 0.87 (brt, J = 6.5 Hz, H^{r}); ^{13}C NMR (101 MHz, $CDCl_3$) δ 174.01 (C^{a}), 169.37 -169.21 (C^{4}), 169.29 (C^{4}), 162.31 (C^{6}), 162.24 (C^{6}), 150.46 – 150.17 ($C^{9/10}$), 149.80 ($C^{9/10}$), 121.78 – 121.51 (C^{7}), 120.04 (C^{12}), 112.65 (C^{11}), 109.82 – 109.69 (m, C^{8}), 101.36 – 101.00 (C^{5}), 69.89 (C^{2}), 69.53 (C^{2}), 68.70 (C^{14}), 68.22 ($C^{2'}$), 64.27 ($C^{3'}$), 63.93 ($C^{3'}$), 58.62 ($C^{3'}$), 56.17 (C^{13}), 49.24 – 48.95 ($C^{1/1'}$), 46.77 – 46.54 ($C^{1/1'}$), 33.31 (C^{b}), 32.05 (C^{p}), 29.94 – 29.34 (C^{d-o}), 26.06 (C^{15}), 25.43 (C^{c}), 22.82 (C^{q}), 14.26 (C^{r}).

$P^{t2}_{6.9b}$DEAyS (6.10b)

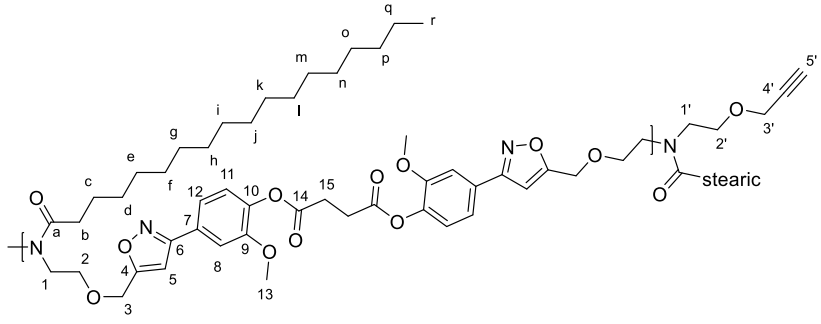

General procedure for vanillin derived polymers was followed using **6.9b** (66 mg, 0.14 mmol, 1 eq.) and DEAyS **5.2S** (61 mg, 0.14 mmol, 1 eq.) to give a brown solid. (49 %); ν_{max} / cm^{-1}: 2921 (C-H), 2852 (C-H), 1760 (C=O), 1639 (C=O) 1607 (C=N), 1261 (C-O), 1115 (C-O), 1030 (C-O); ^{1}H NMR (400 MHz, $CDCl_3$) δ 7.49 (brs, H^{8}), 7.31 – 7.23 (brm, H^{12}), 7.16 – 7.05 (brm, H^{11}), 6.51 (s, H^{5}), 4.67 – 4.56 (brm, H^{3}), 4.16 – 4.07 (brm, $H^{3'}$), 3.87 (brs, H^{13}), 3.77 – 3.66 (brs, $H^{2/2'}$), 3.61 (brs, $H^{1/1'}$), 3.07 (brs, H^{15}), 2.42 (brs, $H^{5'}$), 2.37 (brs, H^{b}), 1.61 (brs, H^{c}), 1.24 (brs, H^{d-q}), 0.87 (brs, H^{r}); ^{13}C NMR

(101 MHz, $CDCl_3$) δ 174.29 – 173.86 (C^a), 170.09 (C^{14}), 169.82 – 169.65 (C^4), 161.97 (C^6), 161.91 (C^6), 151.63 (C^9), 141.49 – 141.07 (C^{10}), 127.97 – 127.77 (C^7), 123.37 (C^{11}), 119.70 (C^{12}), 110.66 (C^8), 101.38 (C^5), 101.25 (C^5), 75.04 – 74.78 ($C^{5'}$), 74.78 – 74.48 ($C^{5'}$), 70.00 – 69.84 (C^2), 69.58 (C^2), 68.94 ($C^{2'}$), 68.21 ($C^{2'}$), 64.38 – 63.96 (H^3), 63.96 – 63.69 (H^3), 58.61 (H^{13}), 58.41 ($H^{3'}$), 56.20 ($C^{3'}$), 49.21 – 48.93 (C^1), 46.71 – 46.44 (C^1), 33.51 – 33.19 (C^b), 32.04 (C^p), 29.98 – 29.33 ($C^{d\text{-}o}$), 29.14 (C^{15}), 25.42 (C^c), 22.81 (C^q), 14.24 (C^r).

P^{t2}_mDAyV (6.13)

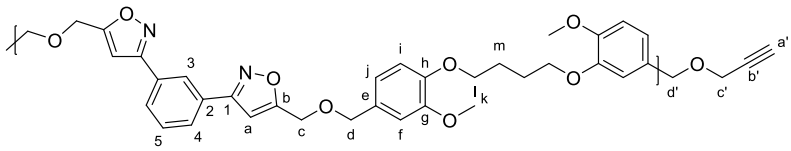

General procedure for vanillin derived polymers was followed using *meta*-OC **2.1** (128 mg, 0.55 mmol, 1 eq.) and DAyV **6.11** (240 mg, 0.55 mmol, 1 eq.) to give a brown solid. (84 %); ν_{max} / cm^{-1}: 2922 (C-H), 2883 (C-H), 1592 (C=N), 1260 (C-O), 1116 (C-O), 1031 (C-O); ^{1}H NMR (400 MHz, $CDCl_3$) δ 8.23 (brs, H^3), 7.88 (brs, H^4), 7.54 (brs, H^5), 6.87 (brm, $H^{f/i/j}$), 6.64 (brs, H^a), 4.65 (brs, H^c), 4.58 (brs, $H^{d/d'}$) 4.20 – 3.98 (brm, $H^{c'/l}$), 3.87 (brs, H^k), 2.46 (brs, $H^{a'}$), 2.03 (brs, H^m); ^{13}C NMR (101 MHz, $CDCl_3$) δ 170.44 (C^b), 161.99 (C^1), 149.74 ($C^{h/g}$), 148.57 ($C^{h/g}$), 129.91 ($C^{2/e}$), 129.77 (C^4), 129.75 ($C^{2/e}$), 128.42 (C^3), 125.33 (C^5), 120.88 (C^j), 112.90 (C^i), 111.98 (C^f), 111.82 (C^f), 101.30 (C^a), 73.12 (C^d), 71.62 ($C^{d'}$), 68.81 (C^l), 62.57 (C^c), 56.91 ($C^{c'}$), 56.11 (C^k), 26.08 (C^m).

$P^{t2}_{6.9a}$DAyV (6.14)

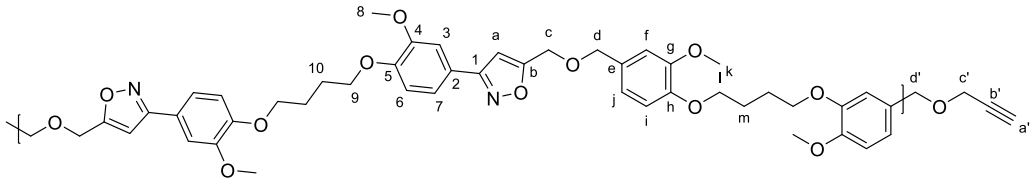

General procedure for vanillin derived polymers was followed using **6.9a** (250 mg, 0.55 mmol, 1 eq.) and DAyV **6.11** (240 mg, 0.55 mmol, 1 eq.) to give a pale brown robust foam. (79 %); ν_{max} / cm^{-1}: 2943 (C-H), 2873 (C-H), 1606 (C=N), 1256 (C-O), 1136 (C-O), 1031 (C-O); ^{1}H NMR (400 MHz, $CDCl_3$) δ 8.47 – 8.41 (m, H^{CH}-min), 7.40 (s, $H^{3/6/7}$), 7.26 (brs, $H^{3/6/7}$ covered by $CHCl_3$ peak), 6.98 – 6.89 (m, J = 11.0 Hz, $H^{3/6/7/f/i/j}$), 6.87 (s, $H^{f/i/j}$), 6.53 (s, H^a), 4.62 (brs, H^c), 4.59 – 4.50 (brm, $H^{d/d'}$), 4.15 (brs,

$H^{9/l}$), 4.09 (brs, $H^{9/l}$), 3.90 (brs, $H^{8/k}$), 3.86 (brs, $H^{8/k}$), 2.47 (brs, $H^{a'}$), 2.08 (brs, H^{10}), 2.03 (brs, H^{m}); ^{13}C NMR (101 MHz, $CDCl_3$) δ 169.75 (C^{b}), 162.17 (C^{1}), 150.10 (C^{Ar}), 149.66 (C^{Ar}), 149.60 (C^{Ar}), 148.43 (C^{Ar}), 129.71 (C^{Ar}), 121.66 (C^{Ar}), 120.85 ($C^{Ar\text{-}H}$), 120.75 ($C^{Ar\text{-}H}$), 119.91 ($C^{Ar\text{-}H}$), 114.29 ($C^{Ar\text{-}H}$), 112.91 ($C^{Ar\text{-}H}$), 112.78 ($C^{Ar\text{-}H}$), 112.57 ($C^{Ar\text{-}H}$), 111.86 ($C^{Ar\text{-}H}$), 111.73 ($C^{Ar\text{-}H}$), 109.68 ($C^{Ar\text{-}H}$), 104.45 (s), 100.99 (C^{a}), 74.61 ($C^{a'}$), 72.93 (C^{d}), 71.50 ($C^{d'}$), 68.69 ($C^{9/l}$), 68.59 ($C^{9/l}$), 62.49 (C^{c}), 56.80 ($C^{c'}$), 56.26 – 55.90 ($C^{8/5}$), 26.12 – 25.77 ($C^{10/m}$).

8.6.6 Vanillin derived monomers for homopolymerisation

3-methoxy-4-(prop-2-yn-1-yloxy)benzaldehyde (6.15)[374]

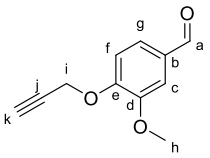

Vanillin (10.0 g, 0.066 mol, 1 eq.) was dissolved in acetone (200 ml) along with potassium carbonate (10.9 g, 0.071 mol, 1.2 eq.). After 15 minutes propargyl bromide (80 % in toluene, 11.7 g, 0.079 mol, 1.2 eq.) was introduced and the temperature increased to reflux. After 1 hour precipitate had stopped the reaction from stirring, more acetone (100 ml) was introduced to allow stirring to continue. After a further 2 hours the reaction was complete. Acetone was removed *in vacuo* and the solid was taken into a Et_2O:DCM (4:1) solution. The organic layer was washed with water (3 × 50 ml) and brine (50 ml). The organic layer was dried with $MgSO_4$ and filtered. Solvent was removed *in vacuo* to leave a crude white solid. Purification through a silica plug (20 % EtOAc, R_f 0.18) resulted in a pure white solid. (55 %); m.p. 196 – 199 °C; ν_{max} / cm^{-1}: 3247, 2985, 2113, 1689, 1587, 1510, 1268, 1199, 938; ^{1}H NMR (500 MHz, $CDCl_3$) δ 9.88 (s, H^{a}), 7.47 (dd, *J* = 8.0, 2.0 Hz, H^{g}), 7.44 (d, *J* = 1.5 Hz, H^{c}), 7.15 (d, *J* = 8.0 Hz, H^{f}), 4.86 (d, *J* = 2.5 Hz, H^{i}), 3.95 (s, H^{h}), 2.56 (t, *J* = 2.5 Hz, H^{k}); ^{13}C NMR (126 MHz, $CDCl_3$) δ 191.06 (C^{a}), 152.26 (C^{e}), 150.19 (C^{d}), 131.09 (C^{b}), 126.44 (C^{g}), 112.72 (C^{f}), 109.59 (C^{c}), 77.58 (C^{j}), 76.82 (C^{k}), 56.75 (C^{i}), 56.20 (C^{h}); m/z: (ES+) 213.1 $[MNa]^+$

(E)-3-methoxy-4-(prop-2-yn-1-yloxy)benzaldehyde oxime (6.16)

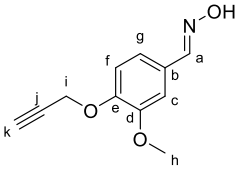

Methoxy-4-(prop-2-yn-1-yloxy)benzaldehyde **6.15** (6.34 g, 0.033 mol, 1 eq.) was dissolved in ethanol (1.5 M). Sodium acetate (4.08 g, 0.050 mol, 1.5 eq.) and hydroxylamine hydrochloride (3.45 g, 0.050 mol, 1.5 eq.) were dissolved in water (1.5 M) and introduced to the ethanol solution. A white precipitate formed within the first half

hour, the reaction was left for 1 hr to ensure completion. Once complete the reaction mixture was cooled in ice, then filtered and washed with cold water followed by cold ethanol, the compound was then dried in a desiccator overnight to leave a pure white solid. (87 %); m.p. 116 – 119 °C ν_{max} / cm^{-1}: 3458, 3436, 3262, 3231, 2117, 1604, 1585, 1507, 1293, 1994, 1135; ^{1}H NMR (500 MHz, $CDCl_3$) δ 8.08 (s, H^{a}), 7.38 (s, $H^{OH)}$, 7.24 (s, H^{C}), 7.06 – 7.00 (m, H^{gf}), 4.80 (d, *J* = 2.5 Hz, H^{i}), 3.91 (s, H^{h}), 2.53 (t, *J* = 2.5 Hz, H^{k}); ^{13}C NMR (126 MHz, $CDCl_3$) δ 150.25 (H^{a}), 150.01 (C^{d}), 148.60 (C^{e}), 126.26 (C^{b}), 121.42 (C^{g}), 113.66 (C^{f}), 108.63 (C^{c}), 78.22 (C^{i}), 76.30 (C^{k}), 56.76 (C^{i}), 56.05 (C^{h}); MS (ESI) m/z calcd. ($C_{11}H_{11}NO_3 + Na^+$): 228.0631, found: 228.0630 (M + Na^+).

(Z)-N-hydroxy-3-methoxy-4-(prop-2-yn-1-yloxy)benzimidoyl chloride (6.17)

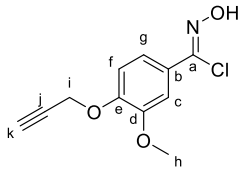

(E)-3-methoxy-4-(prop-2-yn-1-yloxy)benzaldehyde oxime **6.16** (2.00 g, 9.75 mmol, 1 eq.) was dissolved in DMF (3.0 M). *N*-Chlorosuccinimide (1.56 g, 11.7 mmol, 1.2 eq) was introduced in 5 parts over the course of an hour. Once the last portion was introduced to the reaction it was allowed to stir at room temperature for 2 hours. After 2 hours the reaction mixture was poured into cold water (150 ml) causing a white ppt to form. The ppt was collected by Buchner filtration and washed with water and cold ethanol, after which it was transferred to a desiccator and dried overnight to leave a white solid (94 %). Previous attempts to purify **6.17** by recrystallisation failed, purification by column chromatography caused decomposition. m.p. 163 – 165 °C ν_{max} / cm^{-1}: 3357, 3262, 2120, 1602, 1584, 1511, 1269, 1135, 995, 926, 930; ^{1}H NMR (500 MHz, $CDCl_3$) δ 7.63 (s, H^{OH}), 7.45 (dd, *J* = 8.5, 2.0 Hz, H^{g}), 7.40 (d, *J* = 2.0 Hz, H^{c}), 7.05 (d, *J* = 8.5 Hz, H^{f}), 4.81 (d, *J* = 2.5 Hz, H^{i}), 3.92 (s, H^{h}), 2.53 (t, *J* = 2.5 Hz, H^{k}); ^{13}C NMR (126 MHz, $CDCl_3$) δ 149.45 (C^{d}), 149.11 (C^{e}), 139.79 (C^{a}), 126.32 (C^{b}), 120.72 (C^{g}), 113.27 (C^{f}), 110.11 (C^{c}), 78.05 (C^{j}), 76.44 (C^{k}), 56.75 (C^{i}), 56.15 (C^{h}); ^{1}H NMR (300 MHz, Acetone) δ 11.07 (s, 1H, H^{OH}), 7.34 – 7.25 (m, 2H, H^{Ar}), 7.00 (d, *J* = 9.0 Hz, 1H, H^{Ar}), 4.72 (d, *J* = 2.5 Hz, 2H, H^{i}), 3.73 (s, 3H, H^{h}), 2.97 (t, *J* = 2.5 Hz, 1H, H^{k}); MS (ESI) m/z calcd. ($C_{11}H_{11}ClNO_3 + Na^+$): 262.0241, found: 262.0245 (M + Na^+); ($C_{11}H_{11}ClNO_3 + Na^+$): 264.0212, found: 264.0217 (M + Na^+)

8.6.7 Vanillin derived homopolymer – P^{t2}HOMO (**6.18**)

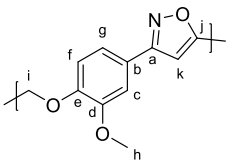

(Z)-N-hydroxy-3-methoxy-4-(prop-2-yn-1-yloxy)benzimidoyl chloride **6.17** (0.50 g, 2.1 mmol, 1 eq.) was dissolved in DMF (1 M) at RT, 4 Å molecular sieves were then added (1600 g / mol of **6.17**) and the mixture was stirred (50 RPM) for 30 minutes. The temperature was then increased to 80 °C and the mixture was stirred (50 RPM) at 80 °C for 48 hours. During the reaction a ppt became evident and after 2 days the reaction mixture had become too thick to stir. The mixture was taken into $CHCl_3$ (5 ml) and filtered to remove molecular sieves, the sieves were washed further with warm $CHCl_3$ (5ml), the filtrate was then reduced *in vacuo* and azeotroped with toluene to remove DMF resulting in a brown solid (**6.18-filtrate** 0.13 g, 31 %). The ppt was not soluble in $CHCl_3$ it was however buoyant and so could be separated from the molecular sieves by floating it in $CHCl_3$ and collecting the ppt from the surface. This was repeated until no ppt could be seen mixed with the molecular sieves. The solid ppt was transferred to a dish and dried *in vacuo* to leave a grey/brown solid. (**6.18-solid** 0.274 g, 65 %).

P^{t2}HOMO **6.18-filtrate** ν_{max} / cm^{-1}: 2935, 2879, 2122, 1659, 1602, 1254, 1007, 803

P^{t2}HOMO **6.18-filtrate** ν_{max} / cm^{-1}: 2930, 2878, 1654, 1605, 1256, 1007, 804

8.6.8 Solvent free Vanillin derived homopolymer – P^{sf}HOMO(0-50wt%)

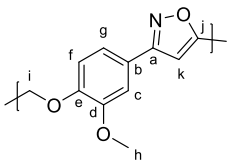

(Z)-N-hydroxy-3-methoxy-4-(prop-2-yn-1-yloxy)benzimidoyl chloride **6.17** (100 – 50 wt %) and powdered 4 Å MS (0 – 50 wt. %) were mixed in a vial for 1 minute using a rotamixer de luxe. To facilitate greater homogenisation a small glass magnetic follower was placed in the vial but removed before polymerisation. Vials were placed in an oven at 120 °C for 24 hours. After 24 hours the vials were removed from the oven and weighed, they showed the expected mass reduction for the loss of HCl.

Vanilin derived homopolymer (0 wt % MS) – P^{sf}HOMO(0wt%) (6.19)

General procedure for solvent free vanillin derived homopolymers was followed using (Z)-N-hydroxy-3-methoxy-4-(prop-2-yn-1-yloxy)benzimidoyl chloride **6.17** (200 mg, 0.83 mmol, 100 wt %) to give a very pale orange clumpy powder. (168.5 mg, 97 %); ν_{max} / cm^{-1}: 2937, 2838, 1606, 1261, 1221, 1032, 805.

Vanilin derived homopolymer (10 wt % MS) – P^{sf}HOMO(10wt%) (6.20)

General procedure for solvent free vanillin derived homopolymers was followed using (Z)-N-hydroxy-3-methoxy-4-(prop-2-yn-1-yloxy)benzimidoyl chloride **6.17** (180 mg, 0.75 mmol, 90 wt %) and powdered 4 Å MS (20 mg, 10 wt %)to give a very pale orange clumpy powder. (175.1 mg, 101 %); ν_{max} / cm^{-1}: 3277, 2936, 2838, 1607, 1261, 1221, 1033, 805.

Vanilin derived homopolymer (20 wt % MS) – P^{sf}HOMO(20wt%) (6.21)

General procedure for solvent free vanillin derived homopolymers was followed using (Z)-N-hydroxy-3-methoxy-4-(prop-2-yn-1-yloxy)benzimidoyl chloride **6.17** (160 mg, 0.67 mmol, 80 wt %) and powdered 4 Å MS (40 mg, 20 wt %)to give a very pale orange clumpy powder. (176.5 mg, 98 %); ν_{max} / cm^{-1}: 3285, 2935, 2838, 1607, 1259, 1221, 1033, 805.

Vanilin derived homopolymer (30 wt % MS) – P^{sf}HOMO(30wt%) (6.22)

General procedure for solvent free vanillin derived homopolymers was followed using (Z)-N-hydroxy-3-methoxy-4-(prop-2-yn-1-yloxy)benzimidoyl chloride **6.17** (140 mg, 0.58 mmol, 70 wt %) and powdered 4 Å MS (60 mg, 30 wt %)to give a very pale orange clumpy powder. (176.5 mg, 98 %); ν_{max} / cm^{-1}: 3277, 2936, 2838, 1607, 1258, 1221, 1031, 938(strong), 805.

Vanilin derived homopolymer (40 wt % MS) – P^{sf}HOMO(40wt%) (6.23)

General procedure for solvent free vanillin derived homopolymers was followed using (Z)-N-hydroxy-3-methoxy-4-(prop-2-yn-1-yloxy)benzimidoyl chloride **6.17** (120 mg, 0.50 mmol, 60 wt %) and powdered 4 Å MS (80 mg, 40 wt %)to give a very pale orange clumpy powder. (180.4 mg, 99 %); ν_{max} / cm^{-1}: 3277, 2936, 2838, 1607, 1257, 1221, 972(v.strong), 805.

Vanilin derived homopolymer (50 wt % MS) – P^{sf}HOMO(50wt%) (6.24)

General procedure for solvent free vanillin derived homopolymers was followed using (Z)-N-hydroxy-3-methoxy-4-(prop-2-yn-1-yloxy)benzimidoyl chloride **6.17** (100 mg, 0.42 mmol, 50 wt %) and powdered 4 Å MS (100 mg, 50 wt %)to give a very pale orange clumpy powder. (187.4 mg, 101 %); ν_{max} / cm^{-1}: 3277, 2936, 2839, 1607, 1257, 1221, 971(v.v.strong), 805.

9.0 Bibliography

(1) Abas, N.; Kalair, A.; Khan, N. Review of Fossil Fuels and Future Energy Technologies. *Futures* **2015**, *69*, 31–49.

(2) Moniz, E.; Deutch, J.; Forsbery, C.; Kadak, A.; Kazimi, M.; Parsons, J. *Update of the MIT 2003 Future of Nuclear Power Study: An Interdisciplinary Study*; Massachusetts Institute of Technology, Cambridge, MA: Cambridge, MA, 2009.

(3) Moniz, E.; Deutch, J.; Asolabelene, S.; Driscol, M.; Gray, P.; Hodren, J.; Joskow, P.; Lester, R.; Todreas, N. *The Future of Nuclear Power: An Interdisciplinary Study*; Massachusetts Institute of Technology, Cambridge, MA: Cambridge, MA, 2003.

(4) Faaij, A. P. C. Bio-Energy in Europe: Changing Technology Choices. *Energy Policy* **2006**, *34* (3), 322–342.

(5) Nocera, D. G.; Nash, M. P. Powering the Planet: Chemical Challenges in Solar Energy Utilization. *Proc. Natl. Acad. Sci. U. S. A.* **2007**, *104* (42), 15729–15735.

(6) Clark, J. H.; Budarin, V.; Deswarte, F. E. I.; Hardy, J. J. E.; Kerton, F. M.; Hunt, A. J.; Luque, R.; Macquarrie, D. J.; Milkowski, K.; Rodriguez, A.; et al. Green Chemistry and the Biorefinery: A Partnership for a Sustainable Future. *Green Chem.* **2006**, *8* (10), 853–860.

(7) Davis, T. L. Paul Schützenberger. *J. Chem. Educ.* **1929**, *6* (9), 1403–1414.

(8) Braconnot, H. No Title. *Ann. Chim. Phys.* **1833**, *52*, 290–294.

(9) Pelouze, J. No Title. *Comptes Rendus Chim.* **1838**, *7*, 713–715.

(10) Dumas, J. B. No Title. *Trait. Chim. Appl. aux Arts* **1843**, *6*, 90.

(11) Kohjiya, S.; Ikeda, Y. *Chemistry, Manufacture & Applications of Rubber*; Woodhead Publ.: Cambridge, UK, 2014.

(12) Goldman, A. S. Catalytic Alkane Metathesis by Tandem Alkane Dehydrogenation-Olefin Metathesis. *Science (80-.).* **2006**, *312* (5771), 257–261.

(13) Clark, J.; Deswarte, F.; Arshadi, M.; Du, C.; Kerton, F.; Koutinas, A.; Sellstedt, A.; Turley, D.; Garcia, C.; Wang, R. H.; et al. *Introduction to Chemicals from Biomass*; Clark, J., Deswarte, F., Eds.; Wiley: Chichester, 2008.

(14) Riduan, S. N.; Zhang, Y. Recent Developments in Carbon Dioxide Utilization under Mild Conditions. *Dalt. Trans.* **2010**, *39* (14), 3347–3357.

(15) Liu, Q.; Wu, L.; Jackstell, R.; Beller, M. Using Carbon Dioxide as a Building Block in Organic Synthesis. *Nat. Commun.* **2015**, *6*, 5933.

(16) Sakakura, T.; Choi, J. C.; Yasuda, H. Transformation of Carbon Dioxide. *Chem. Rev.* **2007**, *107* (6), 2365–2387.

(17) Aresta, M.; Dibenedetto, A.; Angelini, A. Catalysis for the Valorization of Exhaust Carbon: From CO2 to Chemicals, Materials, and Fuels. Technological Use of CO2. *Chem. Rev.* **2014**, *114* (3), 1709–1742.

(18) Grignard, B.; Gennen, S.; Jérôme, C.; Kleij, A. W.; Detrembleur, C. Advances in the Use of CO2 as a Renewable Feedstock for the Synthesis of Polymers. *Chem. Soc. Rev.* **2019**, *48* (16), 4466–4514.

(19) Zhu, Y.; Romain, C.; Williams, C. K. Sustainable Polymers from Renewable Resources. *Nature* **2016**, *540* (7633), 354–362.

(20) Li, C.; Sablong, R. J.; Koning, C. E. Synthesis and Characterization of Fully-Biobased α,ω-Dihydroxyl Poly(Limonene Carbonate)s and Their Initial Evaluation in Coating Applications. *Eur. Polym. J.* **2015**, *67*, 449–458.

(21) Winkler, M.; Romain, C.; Meier, M. A. R.; Williams, C. K. Renewable Polycarbonates and Polyesters from 1,4-Cyclohexadiene. *Green Chem.* **2015**, *17* (1), 300–306.

(22) Byrne, C. M.; Allen, S. D.; Lobkovsky, E. B.; Coates, G. W. Alternating Copolymerization of Limonene Oxide and Carbon Dioxide. *J. Am. Chem. Soc.* **2004**, *126* (37), 11404–11405.

(23) Simpson, W. S.; Crawshaw, G. H. *Wool: Science and Technology*; Woodhead Publ.: Cambridge, UK, 2002.

(24) Schiebel, T. Silk (Speacial Issue). *Appl. Phys. A Mater. Sci. Process.* **2006**, *82*, 191–273.

(25) Birenkiewicz, K. J. *Physical Chemistry of Leather Making*; Krieger: Melbourne, Fl, 1983.

(26) Schreiber, R.; Gareis, H. *Gelatine Handbook*; WILEY-VCH: Weinheim, Du, 2007.

(27) Donnet, J. B.; Bansai, R. C.; Wang, M. J. *Carbon Black: Science and Technology*, 2nd ed.; Marcel Dekker: New York, 1993.

(28) Hicks, E. *Shellac: Its Origins and Applications*; MacDonald: London, 1962.

(29) Hamilton, R. J. *Waxes: Chemistry, Molecular Biology and Functions*; The Oily Press: Dundee, UK, 1995.

(30) Usman, A.; Zia, K. M.; Zuber, M.; Tabasum, S.; Rehman, S.; Zia, F. Chitin and Chitosan Based Polyurethanes: A Review of Recent Advances and Prospective Biomedical Applications. *Int. J. Biol. Macromol.* **2016**, *86*, 630–645.

(31) Ramamoorthy, S. K.; Skrifvars, M.; Persson, A. A Review of Natural Fibers Used in Biocomposites: Plant, Animal and Regenerated Cellulose Fibers. *Polym. Rev.* **2015**, *55* (1), 107–162.

(32) Gandini, A.; Belgacem, M. The State of the Art. In *Monomers, Polymers and Composites from Renewable Resources*; Gandini, A., Belgacem, M., Eds.; Elsevier: Oxford, UK, 2008; pp 1–16.

(33) Tiwari, A.; Marella, T. K. Algal Biomass: Potential Renewable Feedstock for Biofuel Production. In *Substrate Analysis for Effective Biofuels Production*; Springer: Singapore, 2020; pp 1–32.

(34) Rinaudo, M.; Auzely, R.; Mazeau, K. *Encyclopedia of Polymer Science and Technology*; John Wiley & Sons: New York, 2004.

(35) McKeen, L. W. Film Properties of Plastics and Elastomers. In *Film Properties of Plastics and Elastomers*; William Andrew: Oxford, UK, 2017; pp 449–479.

(36) Heinze, T.; Petzold, K. Cellulose Chemistry: Novel Products and Synthesis Paths. In *Monomers, Polymers and Composites from Renewable Resources*; Gandini, A., Belgacem, M., Eds.; Elsevier: Oxford, UK, 2008; pp 343–368.

(37) Gandini, A.; Belgacem, M. Surface Modification of Cellulose Fibres. In

Monomers, Polymers and Composites from Renewable Resources; Gandini, A., Belgacem, M., Eds.; Elsevier: Oxford, UK, 2008; pp 385–400.

(38) Dufresne, A. Cellulose-Based Composites and Nanocomposites. In *Monomers, Polymers and Composites from Renewable Resources*; Gandini, A., Belgacem, M., Eds.; Elsevier: Oxford, UK, 2008; pp 401–418.

(39) Pecoraro, E.; Manzani, D.; Messaddeq, Y.; Ribeiro, S. J. L. Bacterial Cellulose from Glucanacetobacter Xylinus: Preparation, Properties and Applications. In *Monomers, Polymers and Composites from Renewable Resources*; Gandini, A., Belgacem, M., Eds.; Elsevier: Oxford, UK, 2008; pp 369–383.

(40) Rinaudo, M. Main Properties and Current Applications of Some Polysaccharides as Biomaterials. *Polym Int* **2006**, *57* (April 2007), 397–430.

(41) Raabe, D.; Al-Sawalmih, A.; Yi, S. B.; Fabritius, H. Preferred Crystallographic Texture of α-Chitin as a Microscopic and Macroscopic Design Principle of the Exoskeleton of the Lobster Homarus Americanus. *Acta Biomater.* **2007**, *3* (6), 882–895.

(42) Zargar, V.; Asghari, M.; Dashti, A. A Review on Chitin and Chitosan Polymers: Structure, Chemistry, Solubility, Derivatives, and Applications. *ChemBioEng Rev.* **2015**, *2* (3), 204–226.

(43) Tang, W. J.; Fernandez, J. G.; Sohn, J. J.; Amemiya, C. T. Chitin Is Endogenously Produced in Vertebrates. *Curr. Biol.* **2015**, *25* (7), 897–900.

(44) Yu, L.; Christie, G. Microstructure and Mechanical Properties of Orientated Thermoplastic Starches. *J. Mater. Sci.* **2005**, *40* (1), 111–116.

(45) Jiang, T.; Duan, Q.; Zhu, J.; Liu, H.; Yu, L. Starch-Based Biodegradable Materials: Challenges and Opportunities. *Adv. Ind. Eng. Polym. Res.* **2020**, *3* (1), 8–18.

(46) Jiménez, A.; Fabra, M. J.; Talens, P.; Chiralt, A. Edible and Biodegradable Starch Films: A Review. *Food Bioprocess Technol.* **2012**, *5* (6), 2058–2076.

(47) Xie, F.; Yu, L.; Chen, L.; Li, L. A New Study of Starch Gelatinization under Shear Stress Using Dynamic Mechanical Analysis. *Carbohydr. Polym.* **2008**, *72* (2), 229–234.

(48) Xue, T.; Yu, L.; Xie, F.; Chen, L.; Li, L. Rheological Properties and Phase Transition of Starch under Shear Stress. *Food Hydrocoll.* **2008**, *22* (6), 973–978.

(49) Li, M.; Liu, P.; Zou, W.; Yu, L.; Xie, F.; Pu, H.; Liu, H.; Chen, L. Extrusion Processing and Characterization of Edible Starch Films with Different Amylose Contents. *J. Food Eng.* **2011**, *106* (1), 95–101.

(50) Baltá Calleja, F. J.; Rueda, D. R.; Secall, T.; Bayer, R. K.; Schlimmer, M. Influence of Processing Methods on Starch Properties. *J. Macromol. Sci. Part B* **1999**, *38* (4), 461–469.

(51) Wollerdorfer, M.; Bader, H. Influence of Natural Fibres on the Mechanical Properties of Biodegradable Polymers. *Ind. Crops Prod.* **1998**, *8* (2), 105–112.

(52) Arvanitoyannis, I.; Kalichevsky, M.; Blanshard, J. M. V.; Psomiadou, E. Study of Diffusion and Permeation of Gases in Undrawn and Uniaxially Drawn Films Made from Potato and Rice Starch Conditioned at Different Relative Humidities. *Carbohydr. Polym.* **1994**, *24* (1), 1–15.

(53) Zhang, N.; Liu, H.; Yu, L.; Liu, X.; Zhang, L.; Chen, L.; Shanks, R. Developing Gelatin-Starch Blends for Use as Capsule Materials. *Carbohydr. Polym.* **2013**, *92* (1), 455–461.

(54) Zhang, N.; Liu, X.; Yu, L.; Shanks, R.; Petinaks, E.; Liu, H. Phase Composition and Interface of Starch-Gelatin Blends Studied by Synchrotron FTIR Micro-Spectroscopy. *Carbohydr. Polym.* **2013**, *95* (2), 649–653.

(55) Arvanitoyannis, I.; Psomiadou, E.; Nakayama, A.; Aibab, S.; Yamamotob, N. Edible Films Made from Gelatin, Soluble Starch and ....Pdf. *Food Chem.* **1997**, *60* (4), 593–604.

(56) Zhang, N. Z.; Shanks, R.; Liu, X. X.; Yu, L. Phase Composition of Starch-Gelatin Blends Studied by FTIR. *Adv. Mater. Res.* **2014**, *875–877*, 106–109.

(57) Arvanitoyannis, I.; Nakayama, A.; Aiba, S. I. Edible Films Made from Hydroxypropyl Starch and Gelatin and Plasticized by Polyols and Water. *Carbohydr. Polym.* **1998**, *36* (2–3), 105–119.

(58) Khalid, S.; Yu, L.; Feng, M.; Meng, L.; Bai, Y.; Ali, A.; Liu, H.; Chen, L.

Development and Characterization of Biodegradable Antimicrobial Packaging Films Based on Polycaprolactone, Starch and Pomegranate Rind Hybrids. *Food Packag. Shelf Life* **2018**, *18* (September), 71–79.

(59) Ali, A.; Chen, Y.; Liu, H.; Yu, L.; Baloch, Z.; Khalid, S.; Zhu, J.; Chen, L. Starch-Based Antimicrobial Films Functionalized by Pomegranate Peel. *Int. J. Biol. Macromol.* **2019**, *129*, 1120–1126.

(60) Hayrapetyan, H.; Hazeleger, W. C.; Beumer, R. R. Inhibition of Listeria Monocytogenes by Pomegranate (Punica Granatum) Peel Extract in Meat Paté at Different Temperatures. *Food Control* **2012**, *23* (1), 66–72.

(61) Meng, L.; Liu, H.; Yu, L.; Duan, Q.; Chen, L.; Liu, F.; Shao, Z.; Shi, K.; Lin, X. How Water Acting as Both Blowing Agent and Plasticizer Affect on Starch-Based Foam. *Ind. Crops Prod.* **2019**, *134* (February), 43–49.

(62) Masina, N.; Choonara, Y. E.; Kumar, P.; du Toit, L. C.; Govender, M.; Indermun, S.; Pillay, V. A Review of the Chemical Modification Techniques of Starch. *Carbohydr. Polym.* **2017**, *157*, 1226–1236.

(63) Volanti, M.; Cespi, D.; Passarini, F.; Neri, E.; Cavani, F.; Mizsey, P.; Fozer, D. Terephthalic Acid from Renewable Sources: Early-Stage Sustainability Analysis of a Bio-PET Precursor. *Green Chem.* **2019**, *21* (4), 885–896.

(64) Pang, J.; Zheng, M.; Sun, R.; Wang, A.; Wang, X.; Zhang, T. Synthesis of Ethylene Glycol and Terephthalic Acid from Biomass for Producing PET. *Green Chem.* **2016**, *18* (2), 342–359.

(65) Hansen, N. M. L.; Plackett, D. Sustainable Films and Coatings from Hemicelluloses: A Review. *Biomacromolecules* **2008**, *9* (6), 1493–1505.

(66) Flórez-Pardo, L. M.; González-Córdoba, A.; López-Galán, J. E. Evaluation of Different Methods for Efficient Extraction of Hemicelluloses Leaves and Tops of Sugarcane. *DYNA* **2018**, *85* (204), 18–27.

(67) Buranov, A. U.; Mazza, G. Extraction and Characterization of Hemicelluloses from Flax Shives by Different Methods. *Carbohydr. Polym.* **2010**, *79* (1), 17–25.

(68) Nishita, R.; Kuroda, K.; Ota, S.; Endo, T.; Suzuki, S.; Ninomiya, K.; Takahashi,

K. Flame-Retardant Thermoplastics Derived from Plant Cell Wall Polymers by Single Ionic Liquid Substitution. *New J. Chem.* **2019**, *43* (5), 2057–2064.

(69) Smart, C. L.; Whistler, R. L. Films from Hemicellulose Acetates. *Science (80-.).* **1949**, *110* (2870), 713–714.

(70) Ebringerová, A. Structural Diversity and Application Potential of Hemicelluloses. *Macromol. Symp.* **2005**, *232* (333), 1–12.

(71) Lee, Y.; Kwon, E. E.; Lee, J. Polymers Derived from Hemicellulosic Parts of Lignocellulosic Biomass. *Rev. Environ. Sci. Biotechnol.* **2019**, *18* (2), 317–334.

(72) Sjostrom, E. *Wood Chemistry, Fundamentals and Applications*; Academic Press: New York, 1993.

(73) Boerjan, W.; Ralph, J.; Baucher, M. Lignin Biosynthesis. *Annu. Rev. Plant Biol.* **2003**, *54*, 519–546.

(74) Ragauskas, A. J. The Path Forward for Biofuels and Biomaterials. *Science (80-.).* **2006**, *311* (5760), 484–489.

(75) Boerjan, W.; Ralph, J.; Baucher, M. Lignin Biosynthesis. *Annu. Rev. Plant Biol.* **2003**, *54* (1), 519–546.

(76) Gierer, J. No Title. *Wood Sci. Tech.* **1985**, *19* (4), 289–312.

(77) Tomani, P. The Lignoboost Process. *Cellul. Chem. Technol.* **2010**, *44* (1–3), 53–58.

(78) Berlin, A.; Balakshin, M.; Gilkes, N.; Kadla, J.; Maximenko, V.; Kubo, S.; Saddler, J. Inhibition of Cellulase, Xylanase and β-Glucosidase Activities by Softwood Lignin Preparations. *J. Biotechnol.* **2006**, *125* (2), 198–209.

(79) Macfarlane, A. L.; Prestidge, R.; Farid, M. M.; Chen, J. J. J. Dissolved Air Flotation: A Novel Approach to Recovery of Organosolv Lignin. *Chem. Eng. J.* **2009**, *148* (1), 15–19.

(80) Zhao, X.; Cheng, K.; Liu, D. Organosolv Pretreatment of Lignocellulosic Biomass for Enzymatic Hydrolysis. *Appl. Microbiol. Biotechnol.* **2009**, *82* (5), 815–827.

(81) Sameni, J.; Krigstin, S.; Rosa, D. dos S.; Leao, A.; Sain, M. Thermal

Characteristics of Lignin Residue from Industrial Processes. *BioResources* **2014**, *9* (1), 725–737.

(82) Rodrigues Pinto, P. C.; Borges da Silva, E. a.; Rodrigues, A. E. Insights into Oxidative Conversion of Lignin to High-Added-Value Phenolic Aldehydes. *Ind. Eng. Chem. Res.* **2011**, *50* (2), 741–748.

(83) Gargulak, J. D.; Lebo, S. E. *Lignin: Historical, Biological and Materials Perspective*; American Chemical Society: Washington, D.C., 1999.

(84) Gargulak, J. D.; Lebo, E. S. Commercial Use of Lignin-Based Materials. In *Lignin: Historical, Biological, and Materials Perspectives*; ACS Symposium Series; American Chemical Society, 1999; Vol. 742, pp 304–320.

(85) Hu, T. Q. *Chemical Modification, Properties and Usage of Lignin*; Springer US: New York, 2002.

(86) Ragauskas, A. J.; Beckham, G. T.; Biddy, M. J.; Chandra, R.; Chen, F.; Davis, M. F.; Davison, B. H.; Dixon, R. A.; Gilna, P.; Keller, M.; et al. Lignin Valorization: Improving Lignin Processing in the Biorefinery. *Science (80-.).* **2014**, *344* (6185), 1246843–1246843.

(87) Schorr, D.; Diouf, P. N.; Stevanovic, T. Evaluation of Industrial Lignins for Biocomposites Production. *Ind. Crops Prod.* **2014**, *52*, 65–73.

(88) Inside, L.; Access, G.; April, E. A Literature Review of Poly (Lactic Acid). *J. Polym. Environ.* **2001**, *9* (2), 63–84.

(89) Chung, Y. L.; Olsson, J. V.; Li, R. J.; Frank, C. W.; Waymouth, R. M.; Billington, S. L.; Sattely, E. S. A Renewable Lignin-Lactide Copolymer and Application in Biobased Composites. *ACS Sustain. Chem. Eng.* **2013**, *1* (10), 1231–1238.

(90) Spiridon, I.; Leluk, K.; Resmerita, A. M.; Darie, R. N. Evaluation of PLA-Lignin Bioplastics Properties before and after Accelerated Weathering. *Compos. Part B Eng.* **2015**, *69*, 342–349.

(91) Yuan, Y.; Guo, M.; Liu, F. Preparation and Evaluation of Green Composites Using Modified Ammonium Lignosulfonate and Polyethylenimine as a Binder. *BioResources* **2014**, *9* (1), 836–848.

(92) Effendi, A.; Gerhauser, H.; Bridgwater, A. V. Production of Renewable Phenolic Resins by Thermochemical Conversion of Biomass: A Review. *Renew. Sustain. Energy Rev.* **2008**, *12* (8), 2092–2116.

(93) Rong, H.; Gao, B.; Zhao, Y.; Sun, S.; Yang, Z.; Wang, Y.; Yue, Q.; Li, Q. Advanced Lignin-Acrylamide Water Treatment Agent by Pulp and Paper Industrial Sludge: Synthesis, Properties and Application. *J. Environ. Sci. (China)* **2013**, *25* (12), 2367–2377.

(94) Fu, K.; Yue, Q.; Gao, B.; Sun, Y.; Zhu, L. Preparation, Characterization and Application of Lignin-Based Activated Carbon from Black Liquor Lignin by Steam Activation. *Chem. Eng. J.* **2013**, *228*, 1074–1082.

(95) Nowacka, M.; Klapiszewski, Ł.; Norman, M.; Jesionowski, T. Dispersive Evaluation and Surface Chemistry of Advanced, Multifunctional Silica/Lignin Hybrid Biomaterials. *Cent. Eur. J. Chem.* **2013**, *11* (11), 1860–1873.

(96) Ciesielczyk, F.; Klapiszewski, Ł.; Szwarc-Rzepka, K.; Jesionowski, T. A Novel Method of Combination of Kraft Lignin with Synthetic Mineral Support. *Adv. Powder Technol.* **2014**, *25* (2), 695–703.

(97) Ten, E.; Vermerris, W. Recent Developments in Polymers Derived from Industrial Lignin. *J. Appl. Polym. Sci.* **2015**, *132* (24), 1–13.

(98) Llevot, A.; Grau, E.; Carlotti, S.; Grelier, S.; Cramail, H. From Lignin-Derived Aromatic Compounds to Novel Biobased Polymers. *Macromol. Rapid Commun.* **2016**, *37* (1), 9–28.

(99) Tuck, C. O.; Perez, E.; Horvath, I.; Sheldon, R.; Poliakoff, M. Corrections and Clarifications. *Science (80-.).* **2012**, *338* (6107), 604–604.

(100) Pandey, M. P.; Kim, C. S. Lignin Depolymerization and Conversion: A Review of Thermochemical Methods. *Chem. Eng. Technol.* **2011**, *34* (1), 29–41.

(101) Pearl, I. A. Vanillin from Lignin Materials. *J. Am. Chem. Soc.* **1942**, *64* (6), 1429–1431.

(102) Walton, N. J.; Mayer, M. J.; Narbad, A. Vanillin. *Phytochemistry* **2003**, *63* (5), 505–515.

(103) Baskar, C.; Baskar, S.; Dhillon, R. S. *Biomass Conversion*; Springer US: New

York, 2012.

(104) Hocking, M. B. Vanillin: Synthetic Flavoring from Spent Sulfite Liquor. *J. Chem. Educ.* **1997**, *74* (9), 1055–1059.

(105) Fache, M.; Boutevin, B.; Caillol, S. Vanillin, a Key-Intermediate of Biobased Polymers. *Eur. Polym. J.* **2015**, *68*, 488–502.

(106) Voitl, T.; Von Rohr, P. R. Demonstration of a Process for the Conversion of Kraft Lignin into Vanillin and Methyl Vanillate by Acidic Oxidation in Aqueous Methanol. *Ind. Eng. Chem. Res.* **2010**, *49* (2), 520–525.

(107) Fargues, C.; Mathias, Á.; Rodrigues, A. Kinetics of Vanillin Production from Kraft Lignin Oxidation. *Ind. Eng. Chem. Res.* **1996**, *35* (1), 28–36.

(108) Bjørsvik, H. R.; Minisci, F. Fine Chemicals from Lignosulfonates. 1. Synthesis of Vanillin by Oxidation of Lignosulfonates. *Org. Process Res. Dev.* **1999**, *3* (5), 330–340.

(109) Araújo, J. D. P.; Grande, C. A.; Rodrigues, A. E. Vanillin Production from Lignin Oxidation in a Batch Reactor. *Chem. Eng. Res. Des.* **2010**, *88* (8), 1024–1032.

(110) Zabkova, M.; Borges da Silva, E. A.; Rodrigues, A. E. Recovery of Vanillin from Kraft Lignin Oxidation by Ion-Exchange with Neutralization. *Sep. Purif. Technol.* **2007**, *55* (1), 56–68.

(111) Žabková, M.; da Silva, E. A. B.; Rodrigues, A. E. Recovery of Vanillin from Lignin/Vanillin Mixture by Using Tubular Ceramic Ultrafiltration Membranes. *J. Memb. Sci.* **2007**, *301* (1–2), 221–237.

(112) Chu, S.; Subrahmanyam, A. V.; Huber, G. W. The Pyrolysis Chemistry of a β-O-4 Type Oligomeric Lignin Model Compound. *Green Chem.* **2013**, *15* (1), 125–136.

(113) Tarabanko, V. E.; Petukhov, D. V. Study of Mechanism and Improvement of the Process of Oxidative Cleavage of Lignins into the Aromatic Aldehydes. *Chem. Sustain. Dev.* **2003**, *11*, 655–667.

(114) Fargues, C.; Mathias, Á.; Rodrigues, A. Kinetics of Vanillin Production from Kraft Lignin Oxidation. *Ind. Eng. Chem. Res.* **1996**, *35* (1), 28–36.

(115) Voitl, T.; Rohr, P. R. Von. Demonstration of a Process for the Conversion of Kraft Lignin into Vanillin and Methyl Vanillate by Acidic Oxidation in Aqueous Methanol. *Ind. Eng. Chem. Res.* **2010**, *49* (2), 520–525.

(116) Zakzeski, J.; Jongerius, A. L.; Weckhuysen, B. M. Transition Metal Catalyzed Oxidation of Alcell Lignin, Soda Lignin, and Lignin Model Compounds in Ionic Liquids. *Green Chem.* **2010**, *12* (7), 1225.

(117) Willke, T.; Vorlop, K.-D. Biotechnological Production of Itaconic Acid. *Appl. Microbiol. Biotechnol.* **2001**, *56* (3–4), 289–295.

(118) Hocking, M. B. Vanillin : Synthetic Flavoring from Spent Sulfite Liquor. *J. Chem. Educ.* **1997**, *74* (9), 1055–1059.

(119) Bjorsvik, H.; Liguori, L. Organic Processes to Pharmaceutical Chemicals Based on Fine Chemicals from Lignosulfonates. *Oranic Process Res. Dev.* **2002**, *6* (3), 279–290.

(120) Fache, M.; Auvergne, R.; Boutevin, B.; Caillol, S. New Vanillin-Derived Diepoxy Monomers for the Synthesis of Biobased Thermosets. *Eur. Polym. J.* **2015**, *67*, 527–538.

(121) Pang, C.; Zhang, J.; Wu, G.; Wang, Y.; Gao, H.; Ma, J. Renewable Polyesters Derived from 10-Undecenoic Acid and Vanillic Acid with Versatile Properties. *Polym. Chem.* **2014**, *5* (8), 2843–2853.

(122) Jagadish, R. S.; Divyashree, K. N.; Viswanath, P.; Srinivas, P.; Raj, B. Preparation of N-Vanillyl Chitosan and 4-Hydroxybenzyl Chitosan and Their Physico-Mechanical, Optical, Barrier, and Antimicrobial Properties. *Carbohydr. Polym.* **2012**, *87* (1), 110–116.

(123) Marin, L.; Stoica, I.; Mares, M.; Dinu, V.; Simionescu, B. C.; Barboiu, M. Antifungal Vanillin-Imino-Chitosan Biodynameric Films. *J. Mater. Chem. B* **2013**, *1* (27), 3353–3358.

(124) Marin, L.; Simionescu, B.; Barboiu, M. Imino-Chitosan Biodynamers. *Chem. Commun.* **2012**, *48* (70), 8778–8780.

(125) Azadi, P.; Inderwildi, O. R.; Farnood, R.; King, D. A. Liquid Fuels, Hydrogen and Chemicals from Lignin: A Critical Review. *Renew. Sustain. Energy Rev.*

2013, *21*, 506–523.

(126) Fache, M.; Darroman, E.; Besse, V.; Auvergne, R.; Caillol, S.; Boutevin, B. Vanillin, a Promising Biobased Building-Block for Monomer Synthesis. *Green Chem.* **2014**, *16* (4), 1987.

(127) Zhao, C.; Huang, C.; Chen, Q.; Ingram, I. D. V; Zeng, X.; Ren, T.; Xie, H. Sustainable Aromatic Aliphatic Polyesters and Polyurethanes Prepared from Vanillin-Derived Diols via Green Catalysis. *Polymers (Basel).* **2020**, *12*, 1–15.

(128) Aouf, C.; Lecomte, J.; Villeneuve, P.; Dubreucq, E.; Fulcrand, H. Chemo-Enzymatic Functionalization of Gallic and Vanillic Acids: Synthesis of Bio-Based Epoxy Resins Prepolymers. *Green Chem.* **2012**, *14* (8), 2328–2336.

(129) Wang, S.; Ma, S.; Xu, C.; Liu, Y.; Dai, J.; Wang, Z.; Liu, X.; Chen, J.; Shen, X.; Wei, J.; et al. Vanillin-Derived High-Performance Flame Retardant Epoxy Resins: Facile Synthesis and Properties. *Macromolecules* **2017**, *50* (5), 1892–1901.

(130) Tao, Y.; Zhou, J.; Fang, L.; Wang, Y.; Chen, X.; Chen, X.; Hou, J.; Sun, J.; Fang, Q. Fluoro-Containing Polysiloxane Thermoset with Good Thermostability and Acid Resistance Based on the Renewable Multifunctional Vanillin. *ACS Sustain. Chem. Eng.* **2019**, *7* (7), 7304–7311.

(131) Yuan, W.; Ma, S.; Wang, S.; Li, Q.; Wang, B.; Xu, X.; Huang, K.; Chen, J.; You, S.; Zhu, J. Synthesis of Fully Bio-Based Diepoxy Monomer with Dicyclo Diacetal for High-Performance, Readily Degradable Thermosets. *Eur. Polym. J.* **2019**, *117* (February), 200–207.

(132) Firdaus, M.; Meier, M. A. R. Renewable Co-Polymers Derived from Vanillin and Fatty Acid Derivatives. *Eur. Polym. J.* **2013**, *49* (1), 156–166.

(133) Bai, D.; Chen, Q.; Chai, Y.; Ren, T.; Huang, C.; Ingram, I. D. V.; North, M.; Zheng, Q.; Xie, H. Vanillin Derived a Carbonate Dialdehyde and a Carbonate Diol: Novel Platform Monomers for Sustainable Polymers Synthesis. *RSC Adv.* **2018**, *8* (60), 34297–34303.

(134) Llevot, A.; Grau, E.; Carlotti, S.; Grelier, S.; Cramail, H. Renewable (Semi)Aromatic Polyesters from Symmetrical Vanillin-Based Dimers. *Polym.*

Chem. **2015**, *6* (33), 6058–6066.

(135) Amarasekara, A. S.; Wiredu, B.; Razzaq, A. Vanillin Based Polymers: I. An Electrochemical Route to Polyvanillin. *Green Chem.* **2012**, *14* (9), 2395.

(136) Amarasekara, A. S.; Razzaq, A. Vanillin-Based Polymers—Part II: Synthesis of Schiff Base Polymers of Divanillin and Their Chelation with Metal Ions. *ISRN Polym. Sci.* **2012**, *2012*, 1–5.

(137) Renbutsu, E.; Okabe, S.; Omura, Y.; Nakatsubo, F.; Minami, S.; Saimoto, H.; Shigemasa, Y. Synthesis of UV-Curable Chitosan Derivatives and Palladium (II) Adsorption Behavior on Their UV-Exposed Films. *Carbohydr. Polym.* **2007**, *69* (4), 697–706.

(138) Class, G. O. F.; Compounds, O. F. O. Commission on Nomenclature of Organic Chemistry (. *Pure Appl. Chem.* **1995**, *67*, 1307–1375.

(139) Zhang, J.-L.; Zhang, S.-B.; Zhang, Y.-P.; Kitajima, K. Effects of Phylogeny and Climate on Seed Oil Fatty Acid Composition across 747 Plant Species in China. *Ind. Crops Prod.* **2015**, *63*, 1–8.

(140) Requejo-Tapia. Seasonal Changes of Lipid Content in the Leaves of Some Ferns. *Physiol. Plant.* **2001**, *113* (1), 59–63.

(141) Harwood, H. J. Reactions of the Hydrocarbon Chain of Fatty Acids. *Chem. Rev.* **1962**, *62* (2), 99–154.

(142) Guschina, I. A.; Harwood, J. L. Mechanisms of Temperature Adaptation in Poikilotherms. *FEBS Lett.* **2006**, *580* (23), 5477–5483.

(143) Gunstone, F. D. *The Chemistry of Oils and Fats: Sources, Composition and Uses*; Blackwell Pub.: Oxford, UK, 2004.

(144) Andjelkovic, D. D.; Valverde, M.; Henna, P.; Li, F.; Larock, R. C. Novel Thermosets Prepared by Cationic Copolymerization of Various Vegetable Oils—Synthesis and Their Structure–Property Relationships. *Polymer (Guildf).* **2005**, *46* (23), 9674–9685.

(145) The Statistics Portal website, accessed 27/03/2020. https://www.statista.com/statistics/263978/global-vegetable-oil-production-since-2000-2001/.

(146) The Statistics Portal website, accessed 27/03/2020. https://www.statista.com/statistics/263933/production-of-vegetable-oils-worldwide-since-2000/.

(147) Holman, R. T.; Elmer, O. C. The Rates of Oxidation of Unsaturated Fatty Acids and Esters. *J. Am. Oil Chem. Soc.* **1947**, *24* (4), 127–129.

(148) Mallégol, J.; Gardette, J.-L.; Lemaire, J. Long-Term Behavior of Oil-Based Varnishes and Paints I. Spectroscopic Analysis of Curing Drying Oils. *J. Am. Oil Chem. Soc.* **1999**, *76* (8), 967–976.

(149) Chintareddy, V. R.; Oshel, R. E.; Doll, K. M.; Yu, Z.; Wu, W.; Zhang, G.; Verkade, J. G. Investigation of Conjugated Soybean Oil as Drying Oils and CLA Sources. *JAOCS, J. Am. Oil Chem. Soc.* **2012**, *89* (9), 1749–1762.

(150) Soucek, M. D.; Khattab, T.; Wu, J. Review of Autoxidation and Driers. *Prog. Org. Coatings* **2012**, *73* (4), 435–454.

(151) de Espinosa, L. M.; Ronda, J. C.; Galià, M.; Cádiz, V. A New Route to Acrylate Oils: Crosslinking and Properties of Acrylate Triglycerides from High Oleic Sunflower Oil. *J. Polym. Sci. Part A Polym. Chem.* **2009**, *47* (4), 1159–1167.

(152) De Espinosa, L. M.; Ronda, J. C.; GaliÀ, M.; Cádiz, V. A Straightforward Strategy for the Efficient Synthesis of Acrylate and Phosphine Oxide-Containing Vegetable Oils and Their Crosslinked Materials. *J. Polym. Sci. Part A Polym. Chem.* **2009**, *47* (16), 4051–4063.

(153) Çaylı, G.; Küsefoğlu, S. Isothiocyanate Derivatives of Soybean Oil Triglycerides: Synthesis, Characterization, and Polymerization with Polyols and Polyamines. *J. Appl. Polym. Sci.* **2010**, *116* (1), 125–131.

(154) Çaylı, G.; Küsefoğlu, S. Biobased Polyisocyanates from Plant Oil Triglycerides: Synthesis, Polymerization, and Characterization. *J. Appl. Polym. Sci.* **2008**, *109* (5), 2948–2955.

(155) Winkler, M.; Steinbiß, M.; Meier, M. A. R. A More Sustainable Wohl-Ziegler Bromination: Versatile Derivatization of Unsaturated FAMEs and Synthesis of Renewable Polyamides. *Eur. J. Lipid Sci. Technol.* **2014**, *116* (1), 44–51.

(156) Norman, W. Process for Converting Unsaturated Fatty Acids or Their

Glycerides into Saturated Compounds. GBD190301515 19030121, 1902.

(157) Montero de Espinosa, L.; Meier, M. A. R. Plant Oils: The Perfect Renewable Resource for Polymer Science?! *Eur. Polym. J.* **2011**, *47* (5), 837–852.

(158) Erhan, S. Z.; Bagby, M. O.; Nelsen, T. C. Drying Properties of Metathesized Soybean Oil. *J. Am. Oil Chem. Soc.* **1997**, *74* (6), 703–706.

(159) Aguilera, A. F.; Tolvanen, P.; Heredia, S.; Muñoz, M. G.; Samson, T.; Oger, A.; Verove, A.; Eränen, K.; Leveneur, S.; Mikkola, J.-P.; et al. Epoxidation of Fatty Acids and Vegetable Oils Assisted by Microwaves Catalyzed by a Cation Exchange Resin. *Ind. Eng. Chem. Res.* **2018**, *57* (11), 3876–3886.

(160) Chen, J.; de Liedekerke Beaufort, M.; Gyurik, L.; Dorresteijn, J.; Otte, M.; Klein Gebbink, R. J. M. Highly Efficient Epoxidation of Vegetable Oils Catalyzed by a Manganese Complex with Hydrogen Peroxide and Acetic Acid. *Green Chem.* **2019**, *21* (9), 2436–2447.

(161) Kumar, S.; Samal, S. K.; Mohanty, S.; Nayak, S. K. Recent Development of Biobased Epoxy Resins: A Review. *Polym. Plast. Technol. Eng.* **2018**, *57* (3), 133–155.

(162) Fernandes, F. C.; Kirwan, K.; Lehane, D.; Coles, S. R. Epoxy Resin Blends and Composites from Waste Vegetable Oil. *Eur. Polym. J.* **2017**, *89* (February), 449–460.

(163) Abdullah, B.; Salimon, J. Epoxidation of Veg Oils and Fatty Acids. *J. Appl. Sci.* **2010**, *10*, 1545–1553.

(164) Saurabh, T.; Patnaik, M.; Bhagt, S.; Renge, V. Epoxidation of Vegetable Oils: A Review. *Int. J. Adv. Eng. Technol* **2011**, *2*, 491–501.

(165) Campanella, A.; Baltanas, M. A.; Capel-Sanchez, M. C.; Campos-Martin, J. M.; Fierro, J. L. G. Soybean Oil Epoxidation with Hydrogen Peroxide Using an Amorphous Ti/SiO2 Catalyst. *Green Chem.* **2004**, *6* (7), 330–334.

(166) Törnvall, U.; Orellana-Coca, C.; Hatti-Kaul, R.; Adlercreutz, D. Stability of Immobilized Candida Antarctica Lipase B during Chemo-Enzymatic Epoxidation of Fatty Acids. *Enzyme Microb. Technol.* **2007**, *40* (3), 447–451.

(167) Lligadas, G.; Ronda, J. C.; Galià, M.; Cádiz, V. Oleic and Undecylenic Acids

as Renewable Feedstocks in the Synthesis of Polyols and Polyurethanes. *Polymers (Basel).* **2010**, *2* (4), 440–453.

(168) Coles, S. R.; Barker, G.; Clark, A. J.; Kirwan, K.; Jacobs, D.; Makenji, K.; Pink, D. Synthetic Mimicking of Plant Oils and Comparison with Naturally Grown Products in Polyurethane Synthesis. *Macromol. Biosci.* **2008**, *8* (6), 526–532.

(169) Guo, A.; Javni, I.; Petrovic, Z. Rigid Polyurethane Foams Based on Soybean Oil. *J. Appl. Polym. Sci.* **1999**, *77* (467), 467–473.

(170) Lligadas, G.; Ronda, J. C.; Galià, M.; Cádiz, V. Plant Oils as Platform Chemicals for Polyurethane Synthesis: Current State-of-the-Art. *Biomacromolecules* **2010**, *11* (11), 2825–2835.

(171) Pfister, D. P.; Xia, Y.; Larock, R. C. Recent Advances in Vegetable Oil-Based Polyurethanes. *ChemSusChem* **2011**, *4* (6), 703–717.

(172) Singh, I.; Samal, S. K.; Mohanty, S.; Nayak, S. K. Recent Advancement in Plant Oil Derived Polyol-Based Polyurethane Foam for Future Perspective: A Review. *Eur. J. Lipid Sci. Technol.* **2020**, *122* (3), 1–23.

(173) Clark, A. J.; Ross, A. H.; Bon, S. A. F. Synthesis and Properties of Polyesters from Waste Grapeseed Oil: Comparison with Soybean and Rapeseed Oils. *J. Polym. Environ.* **2017**, *25* (1), 1–10.

(174) Clark, A. J.; Hoong, S. S. Copolymers of Tetrahydrofuran and Epoxidized Vegetable Oils: Application to Elastomeric Polyurethanes. *Polym. Chem.* **2014**, *5* (9), 3238–3244.

(175) Lligadas, G.; Ronda, J. C.; Galià, M.; Biermann, U.; Metzger, J. O. Synthesis and Characterization of Polyurethanes from Epoxidized Methyl Oleate Based Polyether Polyols as Renewable Resources. *J. Polym. Sci. Part A Polym. Chem.* **2006**, *44* (1), 634–645.

(176) Tan, S. G.; Chow, W. S. Biobased Epoxidized Vegetable Oils and Its Greener Epoxy Blends: A Review. *Polym. Plast. Technol. Eng.* **2010**, *49* (15), 1581–1590.

(177) Jérmôe, F.; Pouilloux, Y.; Barrault, J. Rational Design of Solid Catalysts for the Selective Use of Glycerol as a Natural Organic Building Block. *ChemSusChem*

2008, *1* (7), 586–613.

(178) Foley, P.; Kermanshahi pour, A.; Beach, E.; Zimmerman, J. Derivation and Synthesis of Renewable Surfactants. *Chem. Soc. Rev.* **2012**, *41* (4), 1452–1461.

(179) Ackelsberg, O. J.; Drew, E. F. Fat Splitting. *J. Am. Chem. Soc.* **1958**, *35*, 635–640.

(180) Pryde, E. H.; Cowan, J. C. Industrial Chemical Uses of Polyunsaturated Fatty Acids. *J. Am. Oil Chem. Soc.* **1971**, *48* (7), 349–354.

(181) Holliday, R. L.; King, J. W.; List, G. R. Hydrolysis of Vegetable Oils in Sub- and Supercritical Water. *Ind. Eng. Chem. Res.* **1997**, *36* (3), 932–935.

(182) Ngaosuwan, K.; Lotero, E.; Suwannakarn, K.; Goodwin, J. G.; Praserthdam, P. Hydrolysis of Triglycerides Using Solid Acid Catalysts. *Ind. Eng. Chem. Res.* **2009**, *48* (10), 4757–4767.

(183) Mahlia, T. M. I.; Syazmi, Z. A. H. S.; Mofijur, M.; Abas, A. E. P.; Bilad, M. R.; Ong, H. C.; Silitonga, A. S. Patent Landscape Review on Biodiesel Production: Technology Updates. *Renew. Sustain. Energy Rev.* **2020**, *118* (October 2019), 109526.

(184) Li, Y. Y.; Luo, X.; Hu, S. Bio-Based Polyols and Polyurethanes. *Bio-based Polyols and Polyurethanes* **2015**, 1–79.

(185) Williams, C. K.; Hillmyer, M. A. Polymers from Renewable Resources: A Perspective for a Special Issue of Polymer Reviews. *Polym. Rev.* **2008**, *48* (1), 1–10.

(186) Campanella, A.; Zhan, M.; Watt, P.; Grous, A. T.; Shen, C.; Wool, R. P. Triglyceride-Based Thermosetting Resins with Different Reactive Diluents and Fiber Reinforced Composite Applications. *Compos. Part A Appl. Sci. Manuf.* **2015**, *72*, 192–199.

(187) The Statistics Portal website, accessed 23/04/2020. https://www.statista.com/statistics/271472/biodiesel-production-in-selected-countries/.

(188) Srivastava, A.; Prasad, R. Triglycerides-Based Diesel Fuels. *Renew. Sustain. Energy Rev.* **2000**, *4* (2), 111–133.

(189) Meher, L. C.; Vidya Sagar, D.; Naik, S. N. Technical Aspects of Biodiesel Production by Transesterification - A Review. *Renew. Sustain. Energy Rev.* **2006**, *10* (3), 248–268.

(190) Hammond, E. G.; Lee, I.; Johnson, L. a. Use of Branched-Chain Esters to Reduce the Crystallization Temperature of Biodiesel. *J. Am. Oil Chem. Soc.* **1995**, *72* (10), 1155–1160.

(191) Noureddini, H.; Medikonduru, V. Glycerolysis of Fats and Methyl Esters. *J. Am. Oil Chem. Soc.* **1997**, *74* (4), 419–425.

(192) Gast, L. E.; Schneider, W. J.; Cowan, J. C. Polyester Amides from Linseed Oil for Protective Coatings. *J. Am. Oil Chem. Soc.* **1966**, *43* (6), 418–421.

(193) Jamil, M. A. R.; Siddiki, S. M. A. H.; Touchy, A. S.; Rashed, M. N.; Poly, S. S.; Jing, Y.; Ting, K. W.; Toyao, T.; Maeno, Z.; Shimizu, K. ichi. Selective Transformations of Triglycerides into Fatty Amines, Amides, and Nitriles by Using Heterogeneous Catalysis. *ChemSusChem* **2019**, *12* (13), 3115–3125.

(194) De Zoete, M. C.; Kock-Van Dalen, A. C.; Van Rantwijk, F.; Sheldon, R. A. Lipase-Catalysed Ammoniolysis of Lipids. A Facile Synthesis of Fatty Acid Amides. *J. Mol. Catal. B Enzym.* **1996**, *1* (3–6), 109–113.

(195) Awasthi, N. P.; Singh, R. P. Microwave-Assisted Facile and Convenient Synthesis of Fatty Acid Amide (Erucamide): Chemical-Catalyzed Rapid Method. *Eur. J. Lipid Sci. Technol.* **2009**, *111* (2), 202–206.

(196) Van Pelt, S.; Teeuwen, R. L. M.; Janssen, M. H. A.; Sheldon, R. A.; Dunn, P. J.; Howard, R. M.; Kumar, R.; Martínez, I.; Wong, J. W. Pseudomonas Stutzeri Lipase: A Useful Biocatalyst for Aminolysis Reactions. *Green Chem.* **2011**, *13* (7), 1791–1798.

(197) Perreux, L.; Loupy, A.; Volatron, F. Solvent-Free Preparation of Amides from Acids and Primary Amines under Microwave Irradiation. *Tetrahedron* **2002**, *58* (11), 2155–2162.

(198) De Almeida, C. G.; De Souza, I. F.; Sousa, R. A.; Le Hyaric, M. Direct Aminolysis of Triglycerides: A Novel Use for Heterogeneous Catalysts. *Catal. Commun.* **2013**, *42*, 25–29.

(199) Kumar, D.; Kim, S. M.; Ali, A. One Step Synthesis of Fatty Acid Diethanolamides and Methyl Esters from Triglycerides Using Sodium Doped Calcium Hydroxide as a Nanocrystalline Heterogeneous Catalyst. *New J. Chem.* **2015**, *39* (9), 7097–7104.

(200) Araújo, P. H. F.; Barata, P. H. S.; Araújo, I. F.; Curti, J. M.; Amaral, R. R.; Bereau, D.; Carvalho, J. C. T.; Ferreira, I. M. Direct and Solvent-Free Aminolysis of Triglyceride from Oenocarpus Bataua (Patawa) Oil Catalyzed by Al2O3. *Catal. Letters* **2018**, *148* (3), 843–851.

(201) Guan, L. P.; Zhao, D. H.; Xiu, J. H.; Sui, X.; Piao, H. R.; Quan, Z. S. Synthesis and Anticonvulsant Activity of N-(2-Hydroxyethyl)Amide Derivatives. *Arch. Pharm. (Weinheim).* **2009**, *342* (1), 34–40.

(202) Adewuyi, A. Synthesis and Surface-Active Property of Diethanolamide and Epoxidised Diethanolamide Surfactant from the Seed Oil of Baphia Nitida. *Arab. J. Chem.* **2014**, 1–7.

(203) Guan, L. P.; Sui, X.; Deng, X. Q.; Zhao, D. H.; Qu, Y. Le; Quan, Z. S. N-Palmitoylethanolamide Derivatives: Synthesis and Studies on Anticonvulsant and Antidepressant Activities. *Med. Chem. Res.* **2011**, *20* (5), 601–606.

(204) Karak, N.; Konwarh, R.; Voit, B. Catalytically Active Vegetable-Oil-Based Thermoplastic Hyperbranched Polyurethane/ Silver Nanocomposites. *Macromol. Mater. Eng.* **2010**, *295* (2), 159–169.

(205) Dutta, S.; Karak, N. Effect of the NCO/OH Ratio on the Properties of Mesua Ferrea L. Seed Oil-Modified Polyurethane Resins. *Polym. Int.* **2006**, *55* (1), 49–56.

(206) Deka, H.; Karak, N. Bio-Based Hyperbranched Polyurethanes for Surface Coating Applications. *Prog. Org. Coatings* **2009**, *66* (3), 192–198.

(207) Stirna, U.; Cabulis, U.; Beverte, I. Water-Blown Polyisocyanurate Foams from Vegetable Oil Polyols. *J. Cell. Plast.* **2008**, *44* (2), 139–160.

(208) Palanisamy, A.; Karuna, M. S. L.; Satyavani, T.; Rohini Kumar, D. B. Development and Characterization of Water-Blown Polyurethane Foams from Diethanolamides of Karanja Oil. *J. Am. Oil Chem. Soc.* **2011**, *88* (4), 541–549.

(209) Palanisamy, A.; Rao, B. S.; Mehazabeen, S. Diethanolamides of Castor Oil as Polyols for the Development of Water-Blown Polyurethane Foam. *J. Polym. Environ.* **2011**, *19* (3), 698–705.

(210) Huisgen, R. Kinetics and Mechanism of 1,3-Dipolar Cycloadditions. *Angew. Chem. Int. Ed.* **1963**, *2* (11), 633–645.

(211) Huisgen, R. 1,3-Dipolar Cycloadditions: Past & Future. *Angew. Chem., Int. Ed.* **1963**, *2* (10), 565–598.

(212) Firestone, R. A. On the Mechanism of 1,3-Dipolar Cycloadditions. *J. Org. Chem.* **1968**, *33* (6), 2285–2290.

(213) Houk, K. N.; Gonzalez, J.; Li, Y. Pericyclic Reaction Transition States: Passions and Punctilios, 1935-1995. *Acc. Chem. Res.* **1995**, *28* (2), 81–90.

(214) Gothelf, K. V.; Jørgensen, K. A. Asymmetric 1,3-Dipolar Cycloaddition Reactions. *Chem. Rev.* **1998**, *98* (2), 863–910.

(215) Sustmann, R. A Simple Model for Substituent Effects in Cycloaddition Reactions. I. 1,3-Dipolar Cycloadditions. *Tetrahedron Lett.* **1971**, *12* (29), 2717–2720.

(216) Sustmann, R. Orbital Energy Control of Cycloaddition Reactivity. *Pure Appl. Chem.* **1974**, *40* (4), 569–593.

(217) Torssell, K. *Nitrile Oxides, Nitrones, and Nitronates in Organic Synthesis*; VCH Publishers, Inc.: New York, 1998.

(218) Kolb, H. C.; Finn, M. G.; Sharpless, K. B. Click Chemistry: Diverse Chemical Function from a Few Good Reactions. *Angew. Chem. Int. Ed. Engl.* **2001**, *40* (11), 2004–2021.

(219) Kolb, H. C.; Sharpless, K. B. The Growing Impact of Click Chemistry on Drug Discovery. *Drug Discov. Today* **2003**, *8* (24), 1128–1137.

(220) Rostovtsev, V. V; Green, L. G.; Fokin, V. V; Sharpless, K. B. A Stepwise Huisgen Cycloaddition Process: Copper(I)-Catalyzed Regioselective "Ligation" of Azides and Terminal Alkynes. *Angew. Chem. Int. Ed. Engl.* **2002**, *41* (14), 2596–2599.

(221) Zhang, L.; Chen, X.; Xue, P.; Sun, H. H. Y.; Williams, I. D.; Sharpless, K. B.; Fokin, V. V.; Jia, G. Ruthenium-Catalyzed Cycloaddition of Alkynes and Organic Azides. *J. Am. Chem. Soc.* **2005**, *127* (46), 15998–15999.

(222) Johansson, J. R.; Beke-Somfai, T.; Said Stålsmeden, A.; Kann, N. Ruthenium-Catalyzed Azide Alkyne Cycloaddition Reaction: Scope, Mechanism, and Applications. *Chem. Rev.* **2016**, *116* (23), 14726–14768.

(223) Singh, M. S.; Chowdhury, S.; Koley, S. Advances of Azide-Alkyne Cycloaddition-Click Chemistry over the Recent Decade. *Tetrahedron* **2016**, *72* (35), 5257–5283.

(224) Rostovtsev, V. V.; Green, L. G.; Fokin, V. V.; Sharpless, K. B. A Stepwise Huisgen Cycloaddition Process: Copper(I)-Catalyzed Regioselective "Ligation" of Azides and Terminal Alkynes. *Angew. Chemie Int. Ed.* **2002**, *41* (14), 2596–2599.

(225) Worrell, B. T.; Malik, J. A.; Fokin, V. V. Direct Evidence of a Dinuclear Copper Intermediate in Cu(I)-Catalyzed Azide-Alkyne Cycloadditions. *Science (80-.).* **2013**, *340* (6131), 457–460.

(226) Gaetke, L. M.; Chow, C. K. Copper Toxicity, Oxidative Stress, and Antioxidant Nutrients. *Toxicology* **2003**, *189* (1–2), 147–163.

(227) Lutz, J.-F. Copper-Free Azide-Alkyne Cycloadditions: New Insights and Perspectives. *Angew. Chem. Int. Ed. Engl.* **2008**, *47* (12), 2182–2184.

(228) Wang, Q.; Chan, T. R.; Hilgraf, R.; Fokin, V. V.; Sharpless, K. B.; Finn, M. Bioconjugation by Copper (I)-Catalyzed Azide-Alkyne [3+ 2] Cycloaddition. *J. Am. Chem. Soc* **2003**, *125* (I), 3192–3193.

(229) Gierlich, J.; Burley, G. a.; Gramlich, P. M. E.; Hammond, D. M.; Carell, T. Click Chemistry as a Reliable Method for the High-Density Functionalisation of Alkyne-Modified Oligodeoxyribonucleotides. *Org. Lett.* **2006**, *8* (17), 3639–3642.

(230) Becer, C. R.; Hoogenboom, R.; Schubert, U. S. Click Chemistry beyond Metal-Catalyzed Cycloaddition. *Angew. Chem. Int. Ed. Engl.* **2009**, *48* (27), 4900–4908.

(231) Lallana, E.; Fernandez-Megia, E.; Riguera, R. Surpassing the Use of Copper in the Click Functionalization of Polymeric Nanostructures: A Strain-Promoted Approach. *J. Am. Chem. Soc.* **2009**, *131* (16), 5748–5750.

(232) Handrick, G. R. T H E RELATIOKSHIP BETWEEN PERFORMANCE AND COMPOUNDS. *Chem. Rev* **1948**, *44*, 419–445.

(233) Moses, J. E.; Moorhouse, A. D. The Growing Applications of Click Chemistry. *Chem. Soc. Rev.* **2007**, *36* (8), 1249–1262.

(234) Golas, P. L.; Matyjaszewski, K. Marrying Click Chemistry with Polymerization: Expanding the Scope of Polymeric Materials. *Chem. Soc. Rev.* **2010**, *39* (4), 1338–1354.

(235) Wu, D.; Song, X.; Tang, T.; Zhao, H. Macromolecular Brushes Synthesized by "Grafting from" Approach Based on "Click Chemistry" and RAFT Polymerization. *J. Polym. Sci. Part A Polym. Chem.* **2010**, *48* (2), 443–453.

(236) Huo, J.; Hu, H.; Zhang, M.; Hu, X.; Chen, M.; Chen, D.; Liu, J.; Xiao, G.; Wang, Y.; Wen, Z. A Mini Review of the Synthesis of Poly-1,2,3-Triazole-Based Functional Materials. *RSC Adv.* **2017**, *7* (4), 2281–2287.

(237) Liu, L.; He, S.; Zhang, S.; Zhang, M.; Guiver, M. D.; Li, N. 1,2,3-Triazolium-Based Poly(2,6-Dimethyl Phenylene Oxide) Copolymers as Anion Exchange Membranes. *ACS Appl. Mater. Interfaces* **2016**, *8* (7), 4651–4660.

(238) Marrocchi, A.; Facchetti, A.; Lanari, D.; Santoro, S.; Vaccaro, L. Click-Chemistry Approaches to π-Conjugated Polymers for Organic Electronics Applications. *Chem. Sci.* **2016**, *7* (10), 6298–6308.

(239) Wu, J.; Chen, J.; Wang, J.; Liao, X.; Xie, M.; Sun, R. Synthesis and Conductivity of Hyperbranched Poly(Triazolium)s with Various End-Capping Groups. *Polym. Chem.* **2016**, *7* (3), 633–642.

(240) Montagnat, O. D.; Lessene, G.; Hughes, A. B. Synthesis of Azide-Alkyne Fragments for "Click" Chemical Applications. Part 2. Formation of Oligomers from Orthogonally Protected Chiral Trialkylsilylhomopropargyl Azides and Homopropargyl Alcohols. *J. Org. Chem.* **2010**, *75* (2), 390–398.

(241) Chow, H.-F.; Lau, K.-N.; Ke, Z.; Liang, Y.; Lo, C.-M. Conformational and

Supramolecular Properties of Main Chain and Cyclic Click Oligotriazoles and Polytriazoles. *Chem. Commun.* **2010**, *46* (20), 3437.

(242) Binauld, S.; Damiron, D.; Connal, L. A.; Hawker, C. J.; Drockenmuller, E. Precise Synthesis of Molecularly Defined Oligomers and Polymers by Orthogonal Iterative Divergent/Convergent Approaches. *Macromol. Rapid Commun.* **2011**, *32* (2), 147–168.

(243) Hong, J.; Luo, Q.; Shah, B. K. Catalyst- and Solvent-Free "Click" Chemistry: A Facile Approach to Obtain Cross-Linked Biopolymers from Soybean Oil. *Biomacromolecules* **2010**, *11*, 2960–2965.

(244) Hong, J.; Luo, Q.; Wan, X.; Petrović, Z. S.; Shah, B. K. Biopolymers from Vegetable Oils via Catalyst- and Solvent-Free "Click" Chemistry: Effects of Cross-Linking Density. *Biomacromolecules* **2012**, *13* (1), 261–266.

(245) Floros, M. C.; Leão, A. L.; Narine, S. S. Vegetable Oil Derived Solvent, and Catalyst Free "Click Chemistry" Thermoplastic Polytriazoles. *Biomed Res. Int.* **2014**, *2014*, 1–14.

(246) Floros, M. C.; Bortolatto, J. F.; Oliveira, O. B.; Salvador, S. L.; Narine, S. S. Antimicrobial Activity of Amphiphilic Triazole-Linked Polymers Derived from Renewable Sources. *ACS Biomater. Sci. Eng.* **2016**, *2* (3), 336–343.

(247) Qin, A.; Lam, J. W. Y.; Tang, B. Z. Click Polymerization. *Chem. Soc. Rev.* **2010**, *39* (7), 2522.

(248) Xi, W.; Scott, T. F.; Kloxin, C. J.; Bowman, C. N. Click Chemistry in Materials Science. *Adv. Funct. Mater.* **2014**, *24* (18), 2572–2590.

(249) Wong, E. H. H.; Junkers, T.; Barner-Kowollik, C. Nitrones in Synthetic Polymer Chemistry. *Polym. Chem.* **2011**, *2* (5), 1008–1017.

(250) Liu, X.; Xiang, L.; Li, J.; Wu, Y.; Zhang, K. Stoichiometric Imbalance-Promoted Step-Growth Polymerization Based on Self-Accelerating 1,3-Dipolar Cycloaddition Click Reactions. *Polym. Chem.* **2019**, *11* (1), 125–134.

(251) Vretik, L.; Ritter, H. 1,3-Dipolar Cycloaddition in Polymer Synthesis. 1. Polyadducts with Flexible Spacers Derived from Bis(N-Methylnitrone)s and Bis(N-Phenylmaleimide)S. *Macromolecules* **2003**, *36* (17), 6340–6345.

(252) Padwa, A.; Koehler, K. F.; Rodriguez, A. Nitrone Cycloaddition. A New Approach to β-Lactams. *J. Am. Chem. Soc.* **1981**, *103* (16), 4974–4975.

(253) Lothrop, W. C.; Richard Handrick, G. The Relationship between Performance and Constitution of Pure Organic Explosive Compounds. *Chem. Rev.* **1949**, *44* (3), 419–445.

(254) Delaittre, G.; Guimard, N. K.; Barner-Kowollik, C. Cycloadditions in Modern Polymer Chemistry. *Acc. Chem. Res.* **2015**, *48* (5), 1296–1307.

(255) Coutouli-Argyropoulou, E.; Lianis, P.; Mitakou, M.; Giannoulis, A.; Nowak, J. 1,3-Dipolar Cycloaddition Approach to Isoxazole, Isoxazoline and Isoxazolidine Analogues of C-Nucleosides Related to Pseudouridine. *Tetrahedron* **2006**, *62* (7), 1494–1501.

(256) Heaney, F. Nitrile Oxide/Alkyne Cycloadditions - A Credible Platform for Synthesis of Bioinspired Molecules by Metal-Free Molecular Clicking. *European J. Org. Chem.* **2012**, *2012* (16), 3043–3058.

(257) Goodall, G. W.; Hayes, W. Advances in Cycloaddition Polymerizations. *Chem. Soc. Rev.* **2006**, *35* (3), 280–312.

(258) Grundmann, C.; Grunanger, P. *The Nitrile Oxides*; Springer-Verlag: Berlin, 1971.

(259) Pasinszki, T.; Hajgató, B.; Havasi, B.; Westwood, N. P. C. Dimerisation of Nitrile Oxides: A Quantum-Chemical Study. *Phys. Chem. Chem. Phys.* **2009**, *11* (26), 5263–5272.

(260) Grundmann, C.; Dean, J. M. Nitrile Oxides. V. Stable Aromatic Nitrile Oxides. *J. Org. Chem.* **1965**, *30* (8), 2809–2812.

(261) Taylor, G. a. The Nitrile Oxide–Isocyanate Rearrangement. *J. Chem. Soc., Perkin Trans. 1* **1985**, 1181–1184.

(262) Dondoni, A.; Mangini, A.; Ghersetti, S. Kinetics of Dimerization of Benzonitrile N-Oxides. *Tetrahedron Lett.* **1966**, *7* (39), 4789–4791.

(263) Beltrame, P.; Comotti, A.; Veglio, C. Kinetic Evidence for a Two-Step 1,3-Cycloaddition. *Chem. Commun.* **1967**, *0* (19), 996.

(264) Curran, D. P.; Fenk, C. J. Thermolysis of Bis[2-[(Trimethylsilyl)Oxy]Propyl]Furoxan (TOP-Furoxan). The First Practical Method for Intermolecular Cycloaddition of an in Situ Generated Nitrile Oxide with 1,2-Di- and Trisubstituted Olefins. *J. Am. Chem. Soc.* **1985**, *107* (21), 6023–6028.

(265) Kulikov, A. S.; Epishina, M. A.; Ovchinnikov, I. V.; Makhova, N. N. Thermolysis of Furoxans Annulated with Five Membered Carbocycles in the Presence of Dipolarophiles *. *Russ. Chem. Bull. Int. Ed.* **2007**, *56* (8), 1580–1587.

(266) Mitchell, W. R.; Paton, R. M. Isolation of Nitrile Oxides from the Thermal Fragmentation of Furazan -Oxides. *Tetrahedron Lett.* **1979**, *20* (26), 2443–2446.

(267) Whitney, R. A.; Nicholas, E. S. Furoxans as Nitrile Oxide Precursors: Cycloaddition Reactions of Bis(Benzenesulfonyl)Furoxan. *Tetrahedron Lett.* **1981**, *22* (35), 3371–3374.

(268) Brittelli, D. R.; Boswell, G. A. New Furoxan Chemistry. 2. Chemistry of Acyl Nitrile Oxides Generated in Situ by Thermolysis of Diacylfuroxans. *J. Org. Chem.* **1981**, *46* (2), 316–320.

(269) Chapman, J. A.; Crosby, J.; Cummings, C. A.; Rennie, R. A. C.; Paton, R. M. Furazan N-Oxides: A Convenient Source of Both Nitrile Oxides and Isocyanates. *J. Chem. Soc. Chem. Commun.* **1976**, No. 7, 240.

(270) Minakata, S.; Okumura, S.; Nagamachi, T.; Takeda, Y. Generation of Nitrile Oxides from Oximes Using t -BuOI and Their Cycloaddition. *Org. Lett.* **2011**, *13* (11), 2966–2969.

(271) Chiang, H. U. I. Chlorination of Oximes. *J. Org. Chem.* **1971**, *36* (15), 2146–2155.

(272) Liu, K.-C.; Shelton, B. R.; Howe, R. K. A Particularly Convenient Preparation of Benzohydroximinoyl Chlorides (Nitrile Oxide Precursors). *J. Org. Chem.* **1980**, *45* (19), 3916–3918.

(273) Kim, J. N.; Ryu, B. K. A Convenient Synthesis of Benzohydroximoyl Chlorides

as Nitrile Oxide Precursors by HCl/N,N-Dimethylformamide/Oxone System. *J. Org. Chem.* **1992**, *57* (24), 6649–6650.

(274) Hegarty, A. F.; Mullane, M. Large Stereoelectronic Effect in 1,3-Dehydrohalogenation to Form a 1 ,S-Dipole. *J. Chem. Soc., Chem. Commun.* **1984**, 229–230.

(275) Sutharchanadevi, M.; Murugan, R. Isoxazoles. In *Comprehensive Heterocyclic Chemistry II*; Elsevier, 1996; Vol. 3, pp 221–260.

(276) Donati, D.; Fusi, S.; Ponticelli, F. Photochemical Synthesis of a 4,5-Dihydrofuroazetidinone, a Novel β-Lactam System. *ChemInform* **2004**, *35* (14), 9247–9250.

(277) Das, N. B.; Torssell, K. B. G. Silyl Nitronates, Nitrile Oxides, and Derived 2-Isoxazolines in Organic Synthesis. Functionalization of Butadiene, a Novel Route to Furans and 2-Isoxazolines as an Alternative to Aldol-Type Condensations. *Tetrahedron* **1983**, *39* (13), 2247–2253.

(278) Khurana, A. L.; Unrau, A. M. Reduction of Some Alkylisoxazoles with Lithium Aluminum-Hydride. *Can. J. Chem.* **1975**, *53* (20), 3011–3013.

(279) Nitta, M.; Kobayashi, T. Reductive Ring Opening of Isoxazoles with Mo(CO)6 and Water. *J. Chem. Soc., Chem. Commun.* **1982**, *529* (15), 877–878.

(280) Evans, D. A.; Ripin, D. H. B.; Halstead, D. P.; Campos, K. R. Synthesis and Absolute Stereochemical Assignment of (+)-Miyakolide. *J. Am. Chem. Soc.* **1999**, *121* (29), 6816–6826.

(281) Caplan, J. F.; Zheng, R.; Blanchard, J. S.; Vederas, J. C. Vinylogous Amide Analogues of Diaminopimelic Acid (DAP) as Inhibitors of Enzymes Involved in Bacterial Lysine Biosynthesis. *Org. Lett.* **2000**, *2* (24), 3857–3860.

(282) Jiang, D.; Chen, Y. Reduction of Δ 2 -Isoxazolines to β-Hydroxy Ketones with Iron and Ammonium Chloride as Reducing Agent. *J. Org. Chem.* **2008**, *73* (22), 9181–9183.

(283) Ho, I. T.; Haung, K. C.; Chung, W. S. 1,3-Alternate Calix[4]Arene as a Homobinuclear Ditopic Fluorescent Chemosensor for Ag+ Ions. *Chem. - An Asian J.* **2011**, *6* (10), 2738–2746.

(284) Han, B.; Yang, X. L.; Fang, R.; Yu, W.; Wang, C.; Duan, X. Y.; Liu, S. Oxime Radical Promoted Dioxygenation, Oxyamination, and Diamination of Alkenes: Synthesis of Isoxazolines and Cyclic Nitrones. *Angew. Chemie - Int. Ed.* **2012**, *51* (35), 8816–8820.

(285) Klier, L.; Diène, C. R.; Schickinger, M.; Metzger, A.; Wagner, A. J.; Karaghiosoff, K.; Marek, I.; Knochel, P. Isoxazole-Embedded Allylic Zinc Reagent for the Diastereoselective Preparation of Highly Functionalized Aldol-Type Derivatives Bearing a Stereocontrolled Quaternary Center. *Chem. - A Eur. J.* **2014**, *20* (43), 14096–14101.

(286) Natale, N. R. Selective Reduction of Isoxazoles with Samarium Diiodide. *Tetrahedron Lett.* **1982**, *23* (48), 5009–5012.

(287) Kijima, M.; Nambu, Y.; Endo, T. Reduction of Cyclic Compounds Having an N-O Linkage by Dihydrolipoamide-Iron(II). *J. Org. Chem.* **1985**, *50* (7), 1140–1142.

(288) Gothelf, K.; Torssell, K. Synthesis of 2,8-Diarylpyrano[3,2-g]Chromene-4,6-Diones. *Acta. Chem. Scand.* **1994**, *48*, 165–168.

(289) Gothelf, K.; Torssell, K. Synthesis of Flavones via Application of the Nitile Oxide and the Reactions. *Acta. Chem. Scand.* **1994**, *48*, 61–67.

(290) Jensen, S.; Torssek, K. Sythesis of 4-Quinolone Derivatives. *Acta. Chem. Scand.* **1995**, *49*, 53–56.

(291) Félix, C. P.; Khatimi, N.; Laurent, A. J. Reduction of 5-(Trifluoromethyl)Isoxazoles with Lithium Aluminum Hydride: Synthesis of (2,2,2-Trifluoroethyl)Aziridines. *J. Org. Chem.* **1995**, *60* (12), 3907–3909.

(292) Auricchio, S.; Bini, A.; Pastormerlo, E.; Truscello, A. M. Iron Dichloride Induced Isomerization or Reductive Cleavage of Isoxazoles: A Facile Synthesis of 2-Carboxy-Azirines. *Tetrahedron* **1997**, *53* (31), 10911–10920.

(293) Fraenkel, G.; Duncan, J. H.; Wang, J. Restricted Stereochemistry of Solvation of Allylic Lithium Compounds: Structural and Dynamic Consequences. *J. Am. Chem. Soc.* **1999**, *121* (2), 432–443.

(294) King, G. S.; Magnus, P. D.; Rzepa, H. S. Reductive and Oxidative Cleavage of

5-Phenyl-Δ 2 -Isoxazoline-3-Carboxylic Acid. *J. Chem. Soc., Perkin Trans. 1* **1972**, *53* (9), 437–443.

(295) Morita, T.; Yugandar, S.; Fuse, S.; Nakamura, H. Recent Progresses in the Synthesis of Functionalized Isoxazoles. *Tetrahedron Lett.* **2018**, *59* (13), 1159–1171.

(296) Kaur, K.; Kumar, V.; Sharma, A. K.; Gupta, G. K. Isoxazoline Containing Natural Products as Anticancer Agents: A Review. *Eur. J. Med. Chem.* **2014**, *77*, 121–133.

(297) Overberger, C. G.; Fujimoto, S. Polycycloaddition of Terephthalonitrile Oxide. *J. Polym. Sci. Part B Polym. Lett.* **1965**, *3* (9), 735–738.

(298) Iwakura, Y.; Akiyama, M.; Shiraishi, S. A Polymerization of Isophthalonitrile Di- N -Oxide by 1,3-Dipolar Cycloaddition Reaction. *Bull. Chem. Soc. Jpn.* **1965**, *38* (2), 335–336.

(299) Fujimoto, S. A Topochemical Study of the Polymerization of Terephthalonitrile Oxide. *J. Polym. Sci. Part B Polym. Lett.* **1967**, *5* (4), 301–305.

(300) Overberger, C. G.; Fujimoto, S. Polycycloaddition of Terephthalonitrile Oxide. *J. Polym. Sci. Part C Polym. Symp.* **1967**, *16* (7), 4161–4168.

(301) Iwakura, Y.; Shiraishi, S.; Akiyama, M.; Yuyama, M. Polymerizations by 1,3-Dipolar Cycloaddition Reactions. V. The 1,3-Dipolar Polycycloadditions of Dinitrile N -Oxides with Diolefins. *Bull. Chem. Soc. Jpn.* **1968**, *41* (7), 1648–1653.

(302) Hong, S. .; Iwakura, Y.; Uno, K. ESR and Crystallinity of Polyphenyleneisoxazole. *Polymer (Guildf).* **1971**, *12* (8), 521–523.

(303) Iwakura, Y.; Uno, K.; Hong, S.-J.; Tatsuhiko, H. A Novel Synthesis of Polyisoxazoline and Polyisoxazole. The Reaction of Terephthalohydroxamoyl Chloride with Bisdipolarophiles. *Polym. J.* **1971**, *2* (1), 36–42.

(304) Hong, S.-J. Electrical Properties of Polymers Containing Isoxazoline and Isoxazole Heterocycles. *Polymer (Guildf).* **1973**, *14* (6), 286–287.

(305) Mahrous, S. Study of Hopping Conduction in Polyisoxazoline. *Int. J. Polym. Mater.* **2003**, *52* (7), 587–597.

(306) Mahrous, S. Study of Cooperative Motions in Polyisoxazoline by Thermally Stimulated Currents. *Phys. Status Solidi Appl. Res.* **2003**, *199* (2), 360–365.

(307) Mahrous, S. Dielectric Breakdown of Polyisoxazoline-Polyvinyl Chloride Polyblend. *Polym. Test.* **2005**, *24* (2), 253–255.

(308) Mahrous, S. Dielectric Breakdown of Polyisoxazoline. *Int. J. Polym. Mater. Polym. Biomater.* **2005**, *54* (1), 37–42.

(309) Mahrous, S. Influence of Magnetic Field on the Resisitivity of Polyisoxazoline. *Int. J. Polym. Mater.* **1997**, *36*, 19–22.

(310) Moriya, O.; Endo, T. Synthesis of Polyisoxazolines via 1,3-Dipolar Cycloaddition Using O,O′-Bis(Tributylstannyl)Ether of Isophthalaldoxime. *Polym. J.* **1997**, *29* (5), 467–470.

(311) Kurth, M. J.; Ahlberg Randall, L. A.; Takenouchi, K. Solid-Phase Combinatorial Synthesis of Polyisoxazolines: A Two-Reaction Iterative Protocol. *J. Org. Chem.* **1996**, *61* (25), 8755–8761.

(312) Li, Y.; Cheng, B. One-Pot Synthesis of Precise Polyisoxazoles by Click Polymerization: Copper (I)-Catalyzed 1,3-Dipolar Cycloaddition of Nitrile Oxides with Alkynes. *J. Polym. Sci. Part A Polym. Chem.* **2013**, *51* (7), 1645–1650.

(313) Pindur, U.; Lutz, G.; Otto, C. Acceleration and Selectivity Enhancement of Diels-Alder Reactions by Special and Catalytic Methods. *Chem. Rev.* **1993**, *93* (2), 741–761.

(314) Sen, S. E.; Smith, S. M.; Sullivan, K. A. Organic Transformations Using Zeolites and Zeotype Materials. *Tetrahedron*. 1999.

(315) Matsuura, T.; Bode, J. W.; Hachisu, Y.; Suzuki, K. Molecular Sieve (MS 4A) Promoted Cyclocondensation of Hindered, Aromatic Nitrile Oxides and Cyclic Diketones under Mild Conditions. *Synlett* **2003**, No. 11, 1746–1748.

(316) Kim, N.; Ryu, E. K. 1,3-Dipolar Cycloaddition: Molecular Sieves Assisted Generation of Nitrile Oxides from Hydroximoyl Chlorides. *Heterocycles* **1990**, *31* (9), 1693.

(317) Koyama, Y.; Yonekawa, M.; Takata, T. New Click Chemistry: Click

Polymerization via 1,3-Dipolar Addition of Homo-Ditopic Aromatic Nitrile Oxides Formed In Situ. *Chem. Lett.* **2008**, *37* (9), 918–919.

(318) Lee, Y.-G.; Koyama, Y.; Yonekawa, M.; Takata, T. New Click Chemistry: Polymerization Based on 1,3-Dipolar Cycloaddition of a Homo Ditopic Nitrile N -Oxide and Transformation of the Resulting Polymers into Reactive Polymers. *Macromolecules* **2009**, *42* (20), 7709–7717.

(319) Espeel, P.; Du Prez, F. E. "click"-Inspired Chemistry in Macromolecular Science: Matching Recent Progress and User Expectations. *Macromolecules* **2015**, *48* (1), 2–14.

(320) Qin, A.; Lam, J. W. Y.; Tang, B. Z. Click Polymerization: Progresses, Challenges, and Opportunities. *Macromolecules* **2010**, *43* (21), 8693–8702.

(321) Heaney, F. Nitrile Oxide/Alkyne Cycloadditions - A Credible Platform for Synthesis of Bioinspired Molecules by Metal-Free Molecular Clicking. *European J. Org. Chem.* **2012**, No. 16, 3043–3058.

(322) Huang, D.; Qin, A.; Zhong, B. *Click Polymerization*; The Royal Society of Chemistry, 2018.

(323) Houk, K. N.; Sims, J.; Watts, C. R.; Luskus, L. J. The Origin of Reactivity, Regioselectivity, and Periselectivity in 1,3-Dipolar Cycloadditions. *J. Am. Chem. Soc* **1968**, *553*, 7301–7315.

(324) Declercq, J. P.; Germain, G.; Van Meerssche, M. Chlorure de 4-Nitrobenzohydroxamoyle. *Acta Crystallogr. Sect. B Struct. Crystallogr. Cryst. Chem.* **1975**, *31* (12), 2894–2895.

(325) Liu, X. G.; Feng, Y. Q.; Liu, D. Q.; Zhao, Y. 1,4-Bis[Chloro(Hydroxyimino)Methyl]Benzene N,N′-Dimethylformamide Disolvate. *Acta Crystallogr. Sect. E Struct. Reports Online* **2005**, *61* (7), 1970–1972.

(326) Vilsmeier, A.; Haack, A. Über Die Einwirkung von Halogenphosphor Auf Alkyl-Formanilide. Eine Neue Methode Zur Darstellung Sekundärer Und Tertiärer p -Alkylamino-Benzaldehyde. *Berichte der Dtsch. Chem. Gesellschaft (A B Ser.* **1927**, *60* (1), 119–122.

(327) Andrade, D.; Moya, C.; Olate, F.; Gatica, N.; Sanchez, S.; Díaz, E.; Elgueta, E.; Parra, M.; Dahrouch, M. Soft Amphiphilic Polyesters Obtained from PEGs and Silicon Fatty Compounds: Structural Characterizations and Self-Assembly Studies. *RSC Adv.* **2016**, *6* (45), 38505–38514.

(328) Han, S.; Kim, C.; Kwon, D. Thermal Degradation of Poly(Ethyleneglycol). *Polym. Degrad. Stab.* **1995**, *47* (2), 203–208.

(329) Yu, Z. X.; Caramella, P.; Houk, K. N. Dimerizations of Nitrile Oxides to Furoxans Are Stepwise via Dinitrosoalkene Diradicals: A Density Functional Theory Study. *J. Am. Chem. Soc.* **2003**, *125* (50), 15420–15425.

(330) Koyama, Y.; Yonekawa, M.; Takata, T. Supporting Info: New Click Chemistry : Click Polymerization via 1 , 3-Dipolar Addition of Homo Ditopic Aromatic Nitrile Oxides Formed In Situ. *Chem. Lett.* **2008**, *37* (9), 918–919.

(331) Bilyk, A.; Bistline, R. G.; Piazza, G. J.; Feairheller, S. H.; Haas, M. J. A Novel Technique for the Preparation of Secondary Fatty Amides. *J. Am. Oil Chem. Soc.* **1992**, *69* (5), 488–491.

(332) Pfrang, C.; Sebastiani, F.; Lucas, C. O. M.; King, M. D.; Hoare, I. D.; Chang, D.; Campbell, R. A. Ozonolysis of Methyl Oleate Monolayers at the Air–Water Interface: Oxidation Kinetics, Reaction Products and Atmospheric Implications. *Phys. Chem. Chem. Phys.* **2014**, *16* (26), 13220–13228.

(333) Math M. C. and; N., C. K. Optimization of Alkali Catalyzed Transesterification of Safflower Oil for Production of Biodiesel. *J. Eng.* **2016**, *2016*, 7.

(334) Stewart, W. .; Siddall, T. H. Nuclear Magnetic Resonance Studies Of Amides. *Chem. Rev.* **1970**, *70*, 517–551.

(335) Kemnitz, C. R.; Loewen, M. J. “Amide Resonance” Correlates with a Breadth of C-N Rotation Barriers. *J. Am. Chem. Soc.* **2007**, *129* (9), 2521–2528.

(336) Clark, A. J.; Curran, D. P.; Fox, D. J.; Ghelfi, F.; Guy, C. S.; Hay, B.; James, N.; Phillips, J. M.; Roncaglia, F.; Sellars, P. B.; et al. Axially Chiral Enamides: Substituent Effects, Rotation Barriers, and Implications for Their Cyclization Reactions. *J. Org. Chem.* **2016**, *81* (13), 5547–5565.

(337) Fulmer, G. R.; Miller, A. J. M.; Sherden, N. H.; Gottlieb, H. E.; Nudelman, A.;

Stoltz, B. M.; Bercaw, J. E.; Goldberg, K. I. NMR Chemical Shifts of Trace Impurities: Common Laboratory Solvents, Organics, and Gases in Deuterated Solvents Relevant to the Organometallic Chemist. *Organometallics* **2010**, *29* (9), 2176–2179.

(338) Aitken, R. A.; Smith, M. H.; Wilson, H. S. Variable Temperature 1H and 13C NMR Study of Restricted Rotation in N,N-Bis(2-Hydroxyethyl)Acetamide. *J. Mol. Struct.* **2016**, *1113*, 171–173.

(339) Meth-Cohn, O.; Stanforth, S. P. The Vilsmeier–Haack Reaction. In *Comprehensive Organic Synthesis*; Trost, B. M., Fleming, I. B. T.-C. O. S., Eds.; Elsevier: Oxford, 1991; pp 777–794.

(340) Califano, S.; Piacenti, F.; Speroni, G. Infra-Red and Raman Spectra of Isoxazole : The Vibiational Assignment. *Spectrochim. Acta.* **1959**, *15*, 86–94.

(341) Dissanayake, A. A.; Odom, A. L. Regioselective Conversion of Alkynes to 4-Substituted and 3,4-Disubstituted Isoxazoles Using Titanium-Catalyzed Multicomponent Coupling Reactions. *Tetrahedron* **2012**, *68* (3), 807–812.

(342) Pinho e Melo, T. Recent Advances on the Synthesis and Reactivity of Isoxazoles. *Curr. Org. Chem.* **2005**, *9* (10), 925–958.

(343) Siadati, S. A. An Example of a Stepwise Mechanism for the Catalyst-Free 1,3-Dipolar Cycloaddition between a Nitrile Oxide and an Electron Rich Alkene. *Tetrahedron Lett.* **2015**, *56* (34), 4857–4863.

(344) Soltani Rad, M. N.; Behrouz, S.; Faghihi, M. A. Copper-Doped Silica Cuprous Sulfate (CDSCS) as a Highly Efficient Heterogeneous Nano Catalyst for Synthesis of 3,5-Disubstituted Isoxazoles. *J. Iran. Chem. Soc.* **2014**, *11* (2), 361–367.

(345) Tanaka, M.; Haino, T.; Ideta, K.; Kubo, K.; Mori, A.; Fukazawa, Y. Combinatorial Synthesis of Isoxazole Library and Their Liquid Crystalline Properties. *Tetrahedron* **2007**, *63* (3), 652–665.

(346) Tang, S.; He, J.; Sun, Y.; He, L.; She, X. Efficient and Regioselective One-Pot Synthesis of 3-Substituted and 3 , 5-Disubstituted Isoxazoles. *Org. Lett.* **2009**, *11*, 3982–3985.

(347) Galenko, A. V; Khlebnikov, A. F.; Novikov, M. S.; Pakalnis, V. V; Rostovskii, N. V. Recent Advances in Isoxazole Chemistry. *Russ. Chem. Rev.* **2015**, *84* (4), 335–377.

(348) Habashy, M. M.; Youseef, A. S. A. 1 , 3-Dipolar Cycloaddition of Arylnitrile-N-Oxides with Methyl 3-Aryl-Prop-2-Yn-Oates And. **1987**, 1116–1122.

(349) Han, L.; Zhang, B.; Zhu, M.; Yan, J. An Environmentally Benign Synthesis of Isoxazolines and Isoxazoles Mediated by Potassium Chloride in Water. *Tetrahedron Lett.* **2014**, *55* (14), 2308–2311.

(350) Hansen, T. V.; Wu, P.; Fokin, V. V. One-Pot Copper(I)-Catalyzed Synthesis of 3,5-Disubstituted Isoxazoles. *J. Org. Chem.* **2005**, *70* (19), 7761–7764.

(351) Hashimoto, T.; Maruoka, K. Recent Advances of Catalytic Asymmetric 1,3-Dipolar Cycloadditions. *Chem. Rev.* **2015**, *115* (11), 5366–5412.

(352) Hu, F.; Szostak, M. Recent Developments in the Synthesis and Reactivity of Isoxazoles: Metal Catalysis and Beyond. *Adv. Synth. Catal.* **2015**, *357* (12), 2583–2614.

(353) Kaiser, T. M.; Huang, J.; Yang, J. Regiochemistry Discoveries in the Use of Isoxazole as a Handle for the Rapid Construction of an All-Carbon Macrocyclic Precursor in the Synthetic Studies of Celastrol. *J. Org. Chem.* **2013**, *78* (12), 6297–6302.

(354) Lai, Z.; Li, Z.; Liu, Y.; Yang, P.; Fang, X.; Zhang, W.; Liu, B.; Chang, H.; Xu, H.; Xu, Y. Iron-Mediated Synthesis of Isoxazoles from Alkynes: Using Iron(III) Nitrate as a Nitration and Cyclization Reagent. *J. Org. Chem.* **2018**, *83* (1).

(355) King, T. A.; Stewart, H. L.; Mortensen, K. T.; North, A. J. P.; Sore, H. F.; Spring, D. R. Cycloaddition Strategies for the Synthesis of Diverse Heterocyclic Spirocycles for Fragment-Based Drug Discovery. *European J. Org. Chem.* **2019**, *2019* (31–32), 5219–5229.

(356) Ho, T. C.; Kamimura, H.; Ohmori, K.; Suzuki, K. Total Synthesis of (+)-Vicenin-2. *Org. Lett.* **2016**, *18* (18), 4488–4490.

(357) Sun, W.; Silva, W. G. D. P.; Van Wijngaarden, J. Rotational Spectra and Structures of Phenyl Isocyanate and Phenyl Isothiocyanate. *J. Phys. Chem. A*

2019, *123* (12), 2351–2360.

(358) Tillet, G.; Boutevin, B.; Ameduri, B. Chemical Reactions of Polymer Crosslinking and Post-Crosslinking at Room and Medium Temperature. *Prog. Polym. Sci.* **2011**, *36* (2), 191–217.

(359) Gleede, T.; Reisman, L.; Rieger, E.; Mbarushimana, P. C.; Rupar, P. A.; Wurm, F. R. Aziridines and Azetidines: Building Blocks for Polyamines by Anionic and Cationic Ring-Opening Polymerization. *Polym. Chem.* **2019**, *10* (24), 3257–3283.

(360) Liu, X.; Hong, D.; Sapir, N. G.; Yang, W.; Hersh, W. H.; Leung, P.-H.; Yang, D.; Chen, Y. Iron-Catalyzed Transfer Hydrogenation in Aged N -Methyl-2-Pyrrolidone: Reductive Ring-Opening of 3,5-Disubstituted Isoxazoles and Isoxazolines. *J. Org. Chem.* **2019**, *84* (24), 16204–16213.

(361) Beltrame, P.; Gelli, G.; Loi, A. 1,3-Cycloaddition of Substituted Benzonitrile Oxides to Aliphatic Nitriles. The Kinetic Effect of Substituents. *J. Heterocycl. Chem.* **1983**, *20* (6), 1609–1612.

(362) Beltrame, P.; Gelli, G. 3,3′-diaryl-5-morpholino-4,5,4′,5′-tetrahydro-4,5′-spirobi[Isoxazoles]. Synthesis by Cycloaddition Reactions and Substituent Effect on the Cycloaddition Kinetics. *J. Heterocycl. Chem.* **1986**, *23* (5), 1539–1543.

(363) Gozzo, F. C.; Fernandes, S. A.; Rodrigues, D. C.; Eberlin, M. N.; Marsaioli, A. J. Regioselectivity in Aromatic Claisen Rearrangements. *J. Org. Chem.* **2003**, *68* (14), 5493–5499.

(364) Lee, Y.-G.; Yonekawa, M.; Koyama, Y.; Takata, T. Synthesis of a Kinetically Stabilized Homoditopic Nitrile N-Oxide Directed toward Catalyst-Free Click Polymerization. *Chem. Lett.* **2010**, *39* (4), 420–421.

(365) Autenrieth, B.; Frey, W.; Buchmeiser, M. R. A Dicationic Ruthenium Alkylidene Complex for Continuous Biphasic Metathesis Using Monolith-Supported Ionic Liquids. *Chem. - A Eur. J.* **2012**, *18* (44), 14069–14078.

(366) Sanders, B. C.; Friscourt, F.; Ledin, P. A.; Mbua, N. E.; Arumugam, S.; Guo, J.; Boltje, T. J.; Popik, V. V.; Boons, G.-J. Metal-Free Sequential [3 + 2]-

Dipolar Cycloadditions Using Cyclooctynes and 1,3-Dipoles of Different Reactivity. *J. Am. Chem. Soc.* **2011**, *133* (4), 949–957.

(367) Kelly, D. R.; Baker, S. C.; King, D. S.; De Silva, D. S.; Lord, G.; Taylor, J. P. Studies of Nitrile Oxide Cycloadditions, and the Phenolic Oxidative Coupling of Vanillin Aldoxime by Geobacillus Sp. DDS012 from Italian Rye Grass Silage. *Org. Biomol. Chem.* **2008**, *6* (4), 787–796.

(368) Sagnella, S. M.; Conn, C. E.; Krodkiewska, I.; Drummond, C. J. Nonionic Diethanolamide Amphiphiles with Saturated Hydrocarbon Chains: Neat Crystalline and Lyotropic Liquid Crystalline Phase Behavior. *Phys. Chem. Chem. Phys.* **2011**, *13*, 13370–13381.

(369) Méndez-Sánchez, D.; Lavandera, I.; Gotor, V.; Gotor-Fernández, V. Novel Chemoenzymatic Oxidation of Amines into Oximes Based on Hydrolase-Catalysed Peracid Formation. *Org. Biomol. Chem.* **2017**, *15* (15), 3196–3201.

(370) Di Nunno, L.; Vitale, P.; Scilimati, A.; Simone, L.; Capitelli, F. Stereoselective Dimerization of 3-Arylisoxazoles to Cage-Shaped Bis-β-Lactams Syn 2,6-Diaryl-3,7-Diazatricyclo[4.2.0.02,5]Octan-4,8-Diones Induced by Hindered Lithium Amides. *Tetrahedron* **2007**, *63* (50), 12388–12395.

(371) Vo, Q. V.; Trenerry, C.; Rochfort, S.; Wadeson, J.; Leyton, C.; Hughes, A. B. Synthesis and Anti-Inflammatory Activity of Aromatic Glucosinolates. *Bioorg. Med. Chem.* **2013**, *21* (19), 5945–5954.

(372) Kamal, A.; Shaheer Malik, M.; Bajee, S.; Azeeza, S.; Faazil, S.; Ramakrishna, S.; Naidu, V. G. M.; Vishnuwardhan, M. V. P. S. Synthesis and Biological Evaluation of Conformationally Flexible as Well as Restricted Dimers of Monastrol and Related Dihydropyrimidones. *Eur. J. Med. Chem.* **2011**, *46* (8), 3274–3281.

(373) Dikusar, E. A.; Kozlov, N. G. Esters Derived from Vanillin and Vanillal and Aromatic and Functionalized Aliphatic Carboxylic Acids. *Russ. J. Org. Chem.* **2005**, *41* (7), 992–996.

(374) da Silva, V. D.; de Faria, B. M.; Colombo, E.; Ascari, L.; Freitas, G. P. A.; Flores, L. S.; Cordeiro, Y.; Romão, L.; Buarque, C. D. Design, Synthesis,

Structural Characterization and in Vitro Evaluation of New 1,4-Disubstituted-1,2,3-Triazole Derivatives against Glioblastoma Cells. *Bioorg. Chem.* **2019**, *83*, 87–97.